APPENDIX C

1.4 Test: Dr95FF (PT1)-Dynamic Response

1.4.1 Motion 10 (M10)

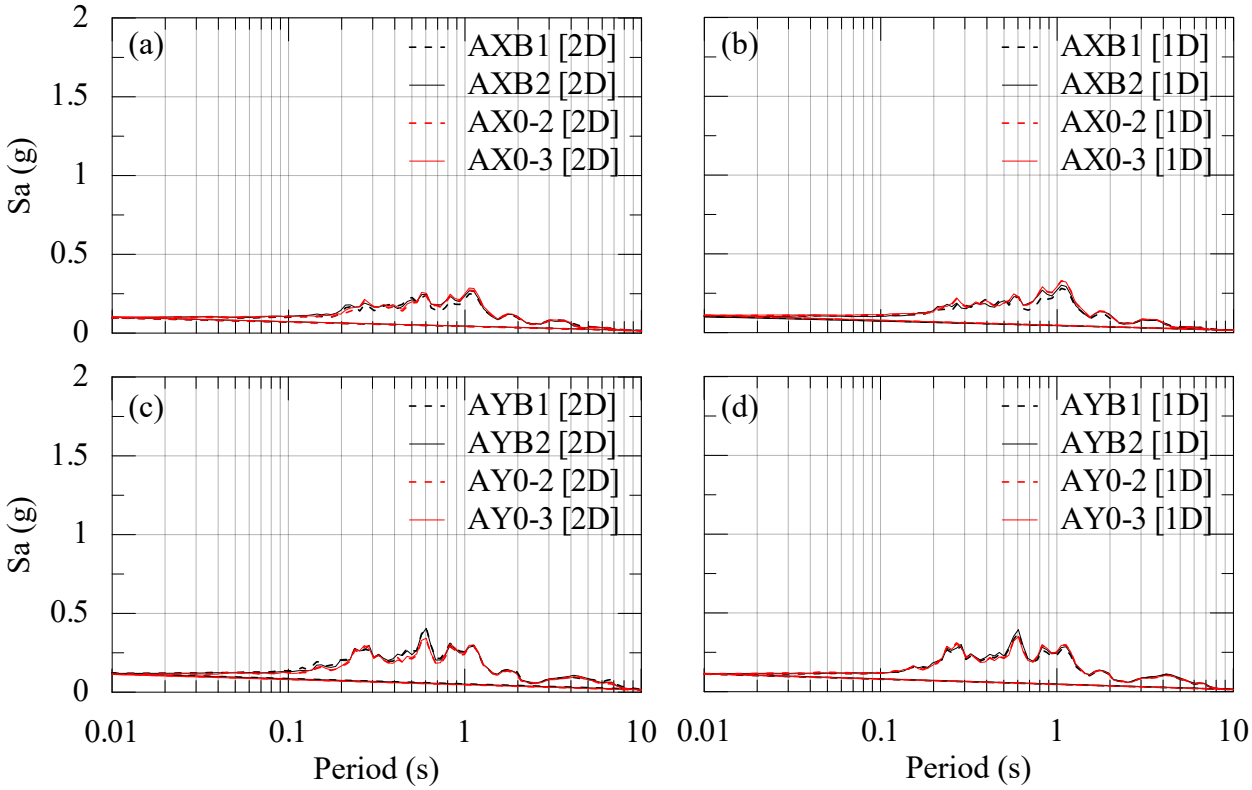

Figure C-219 Comparison of response spectra of 2D laminar container table and within model base input motion for motions (M10-X, Y and 2D).

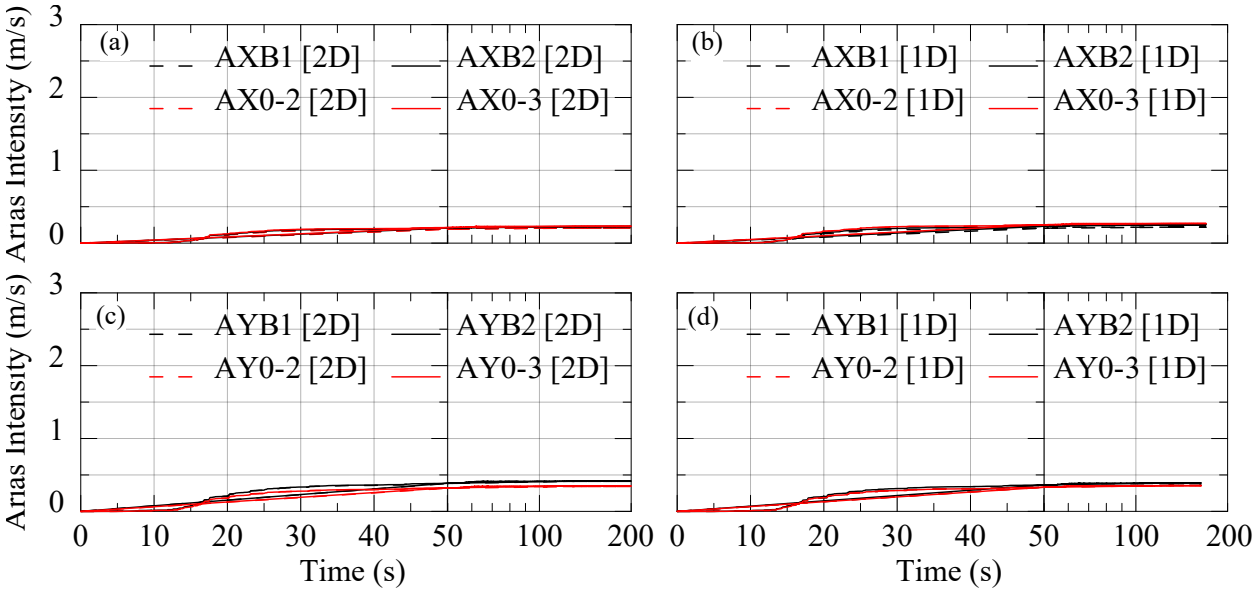

Figure C-220 Comparison of Arias Intensity of 2D laminar container table and within model base input motion for motions (a) M10-2D [X]; (b) M10-2D [Y]; (c) M10-1D [X] and (d) M10-1D [Y]

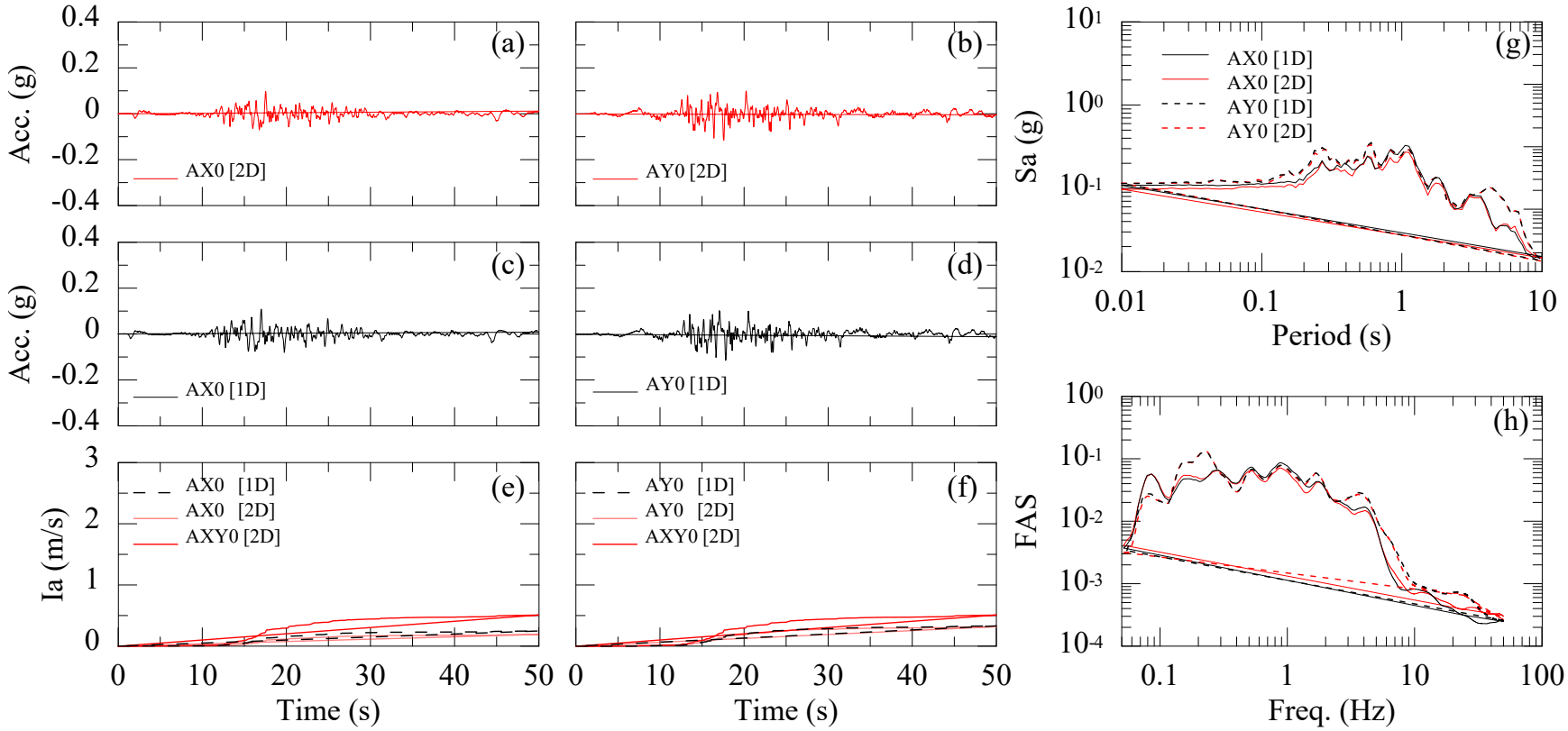

Figure C-221 Recorded input (2D) and 1D (X or Y) ground motions for: (a) M10-2D [X]; (b) M10-2D [Y]; (c) M10-1D [X]; and (d) M10-1D [Y]. Arias Intensity M10 (1D and 2D) for: (e) X direction; and (f) Y direction. Response Spectra (g) M10-2D [X]; M10-2D [Y]; M10-1D [X]; and M10-1D [Y]. Smoothed Fourier amplitude spectra (FAS) (h) M10-2D [X]; M10-2D [Y]; M10-1D [X]; and M10-1D [Y].

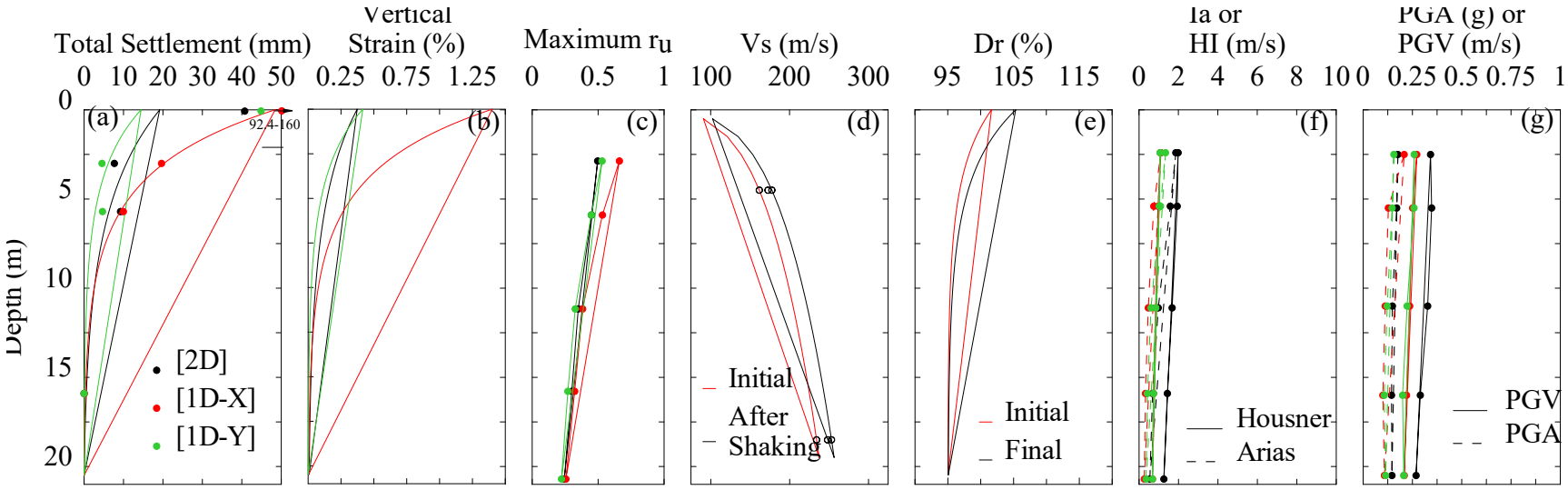

Figure C-222 Recorded or computed profiles for input motion M10-X, Y, and 2D. (a) Settlement; (b) total strain; (c) excess pore water pressure ratio; (d) shear wave velocity; (e) relative density; (f) Arias and Housner intensities; and (g) PGA and PGV.

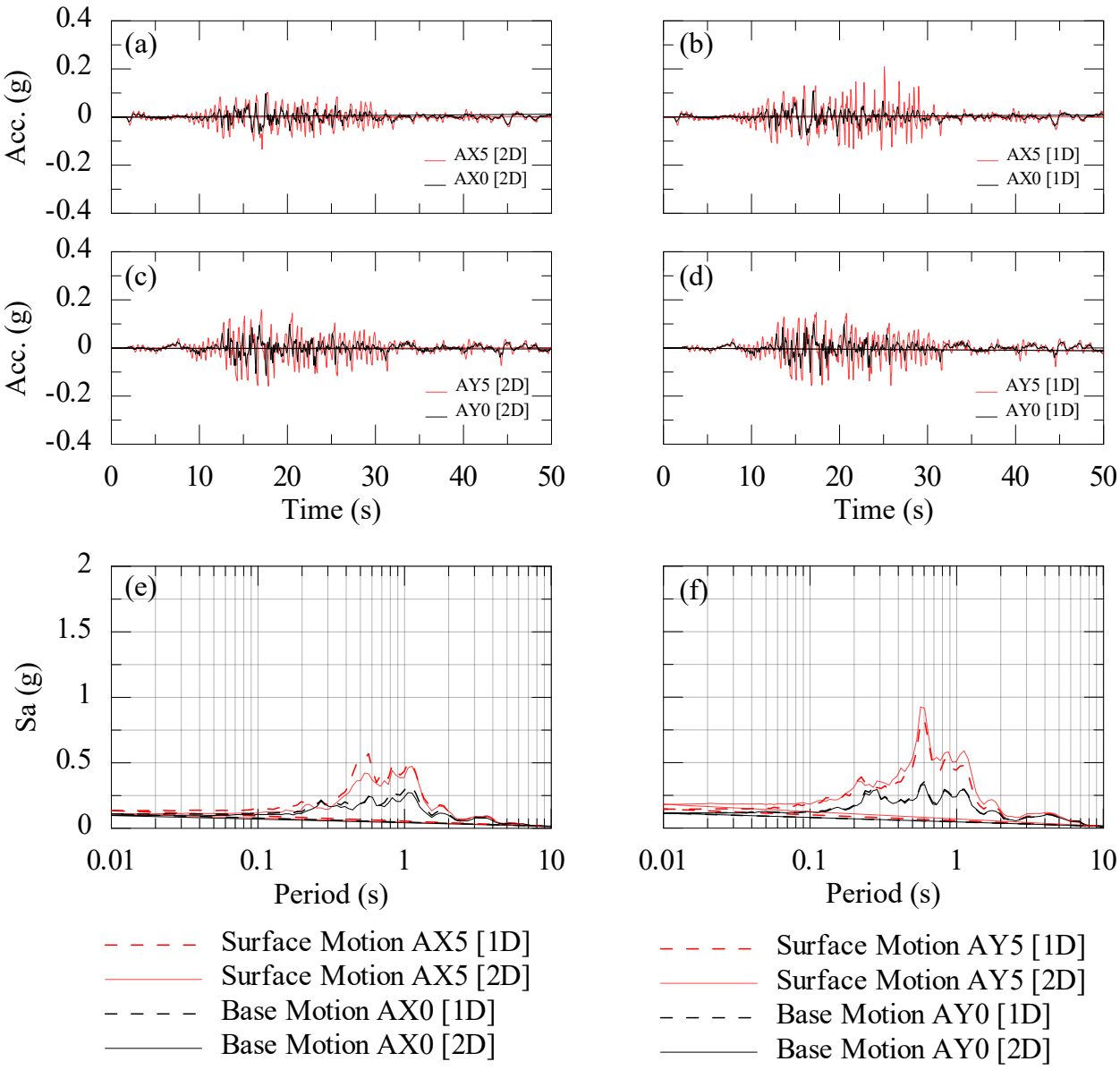

Figure C-223 Recorded input and surface ground motion: (a) M10-2D [X]; (b) M10-1D [X]; (c) M10-2D [Y]; and (d) M10-1D [Y]. Computed response spectra from Free Field Test [PT2] for motions M10 (1D and 2D) for: (e) X direction; and (f) Y direction.

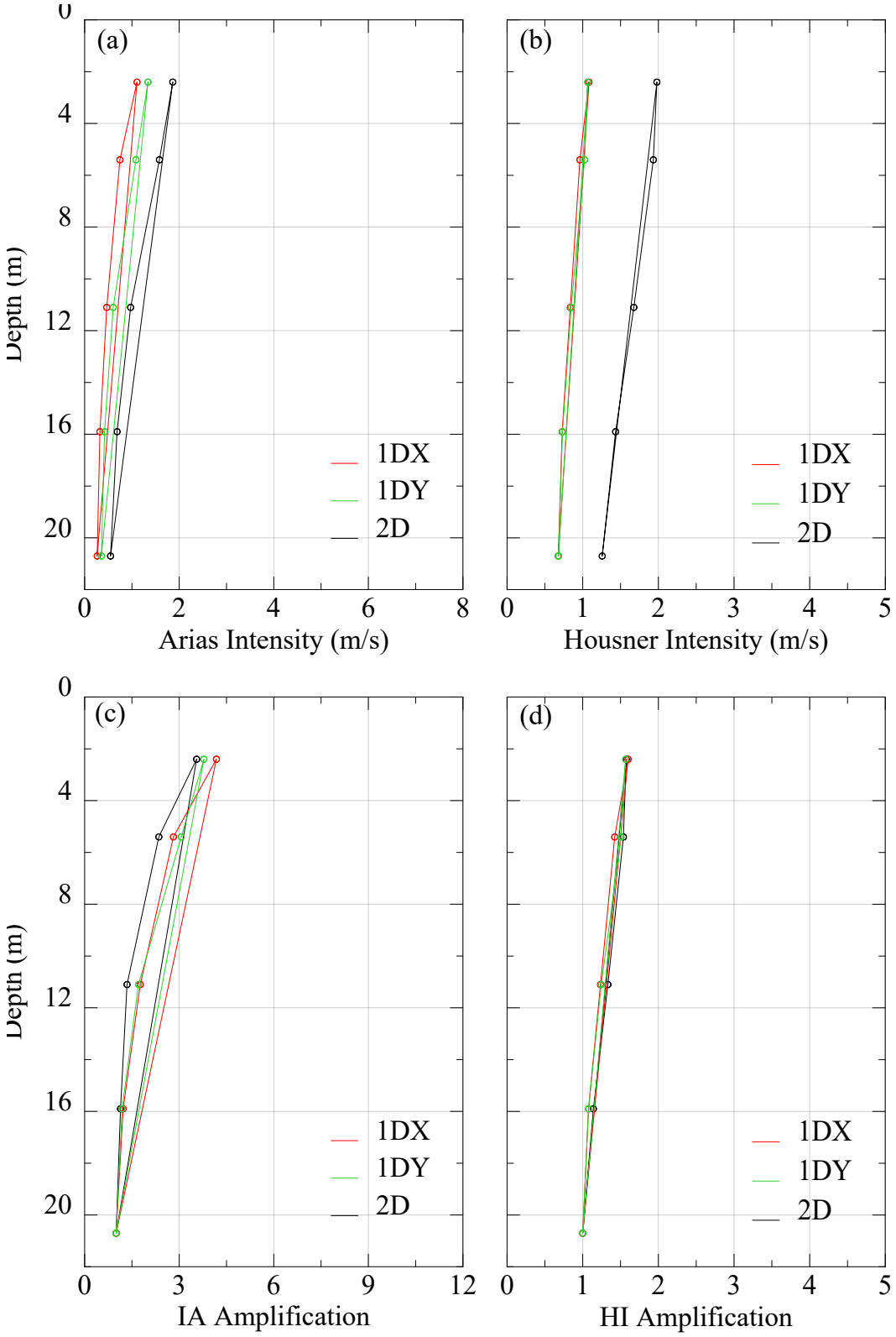

Figure C-224 Variation of total (a) Arias Intensity (M10-X,Y and 2D) ; (b) Housner Intensity (M10-X,Y and 2D) (c) Arias Intensity Amplification Factor (M10-X,Y and 2D); and (d) Housner Intensity Amplification Factor (M10-X,Y and 2D).

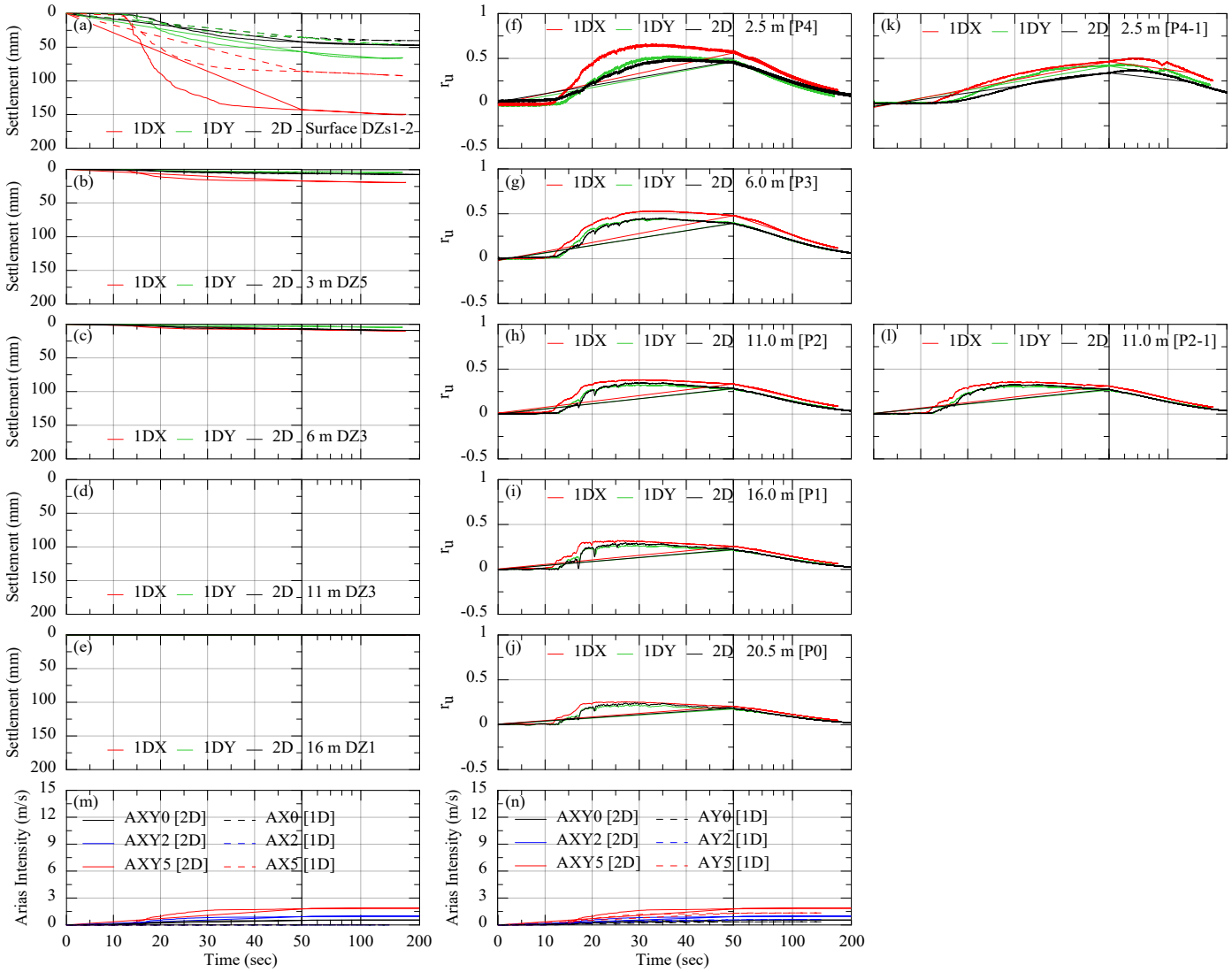

Figure C-225 Variation of total (a) to (e) Settlement with depth (M10-X,Y and 2D) ; (f) to (l) Excess pore water pressure ratio (ru) (M10-X,Y and 2D) (m) and (n) Arias Intensity along model (M10-X,Y and 2D).

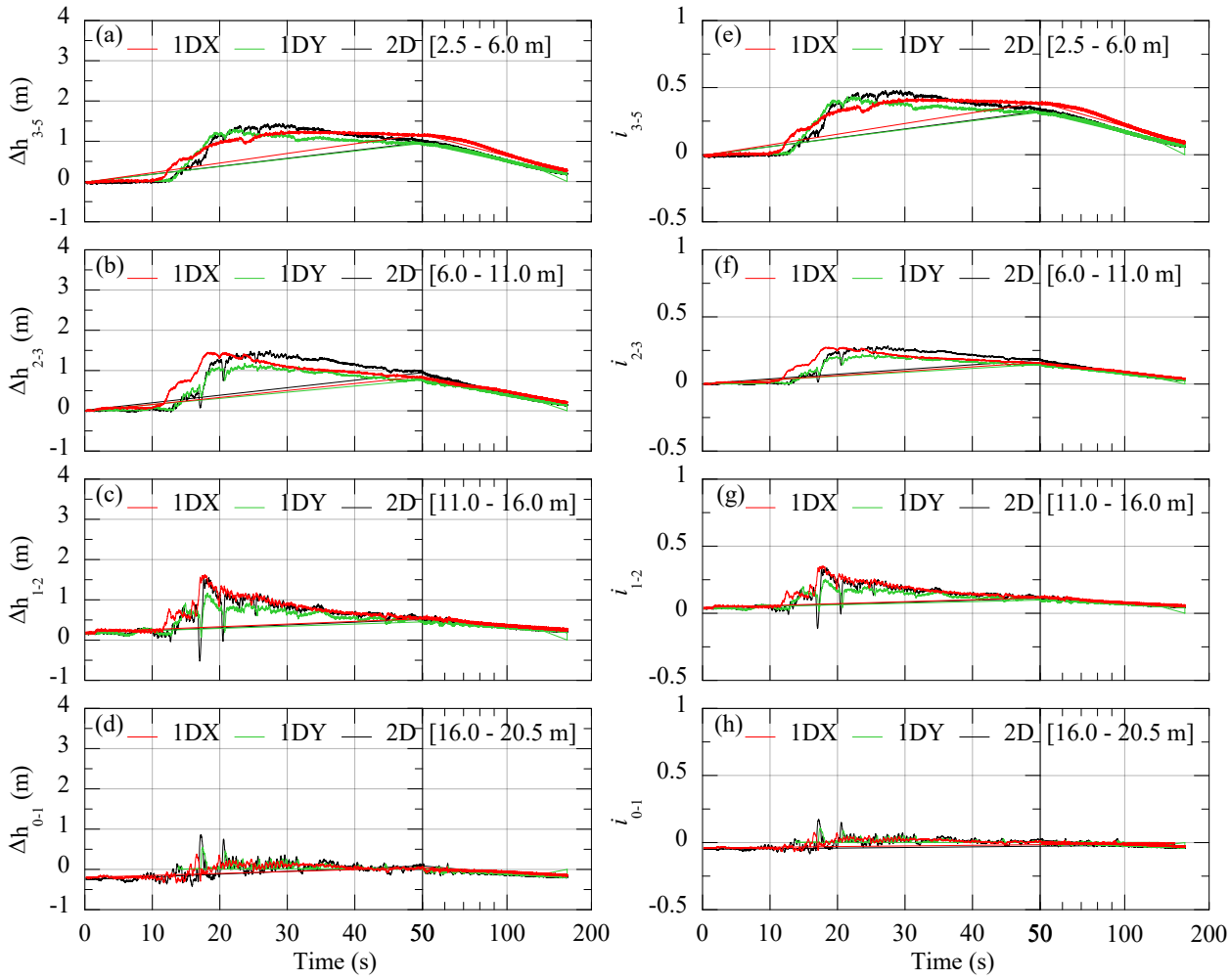

Figure C-226 Variation of total (a) to (d) Total Head Loss with depth (M10-X, Y and 2D); (e) to (h) Shaking induced Hydraulic Gradient (M10-X, Y and 2D)

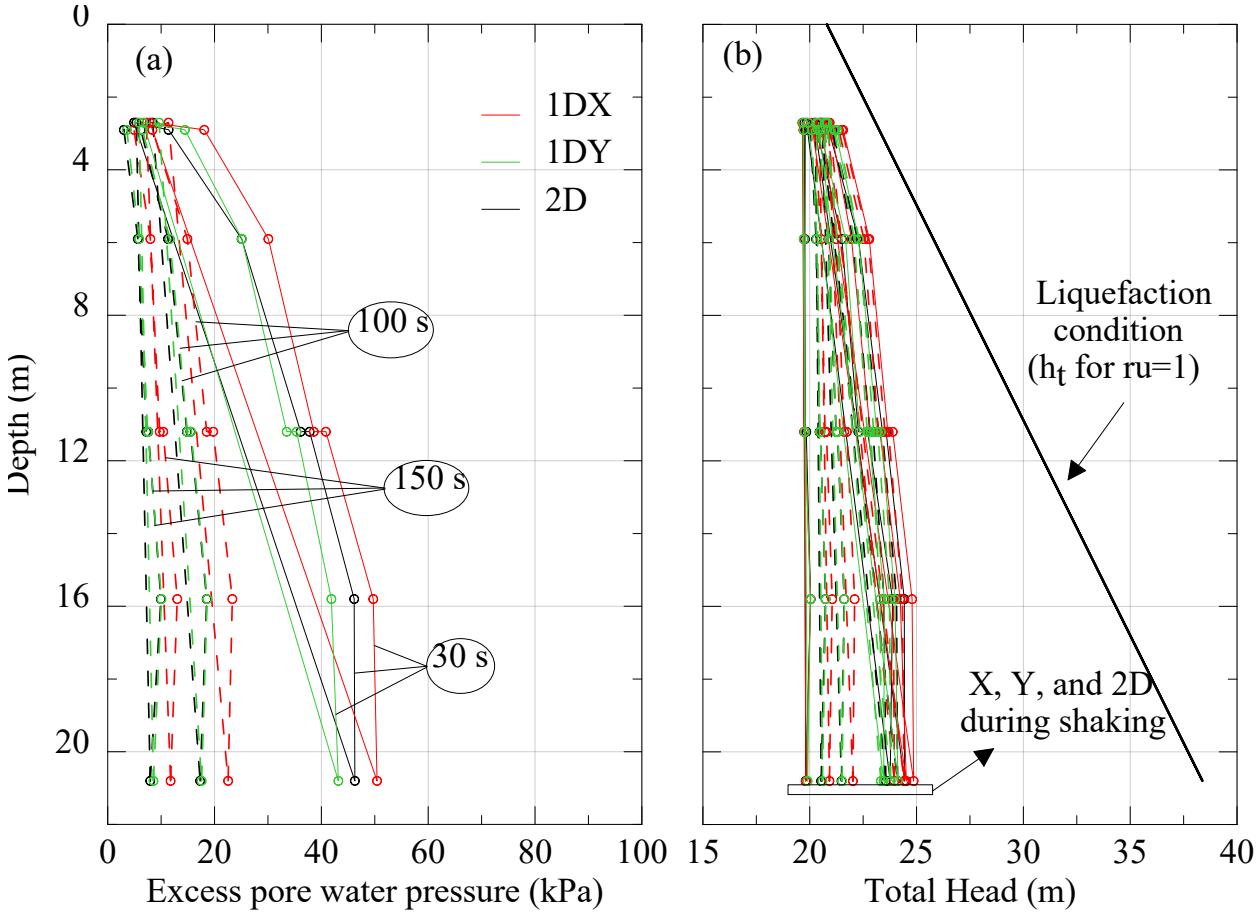

Figure C-227 Variation of total (a) Excess pore water pressure ratio (ru) with depth (M10-X,Y and 2D); (e) to (b) Total Head Loss with depth (M10-X,Y and 2D)

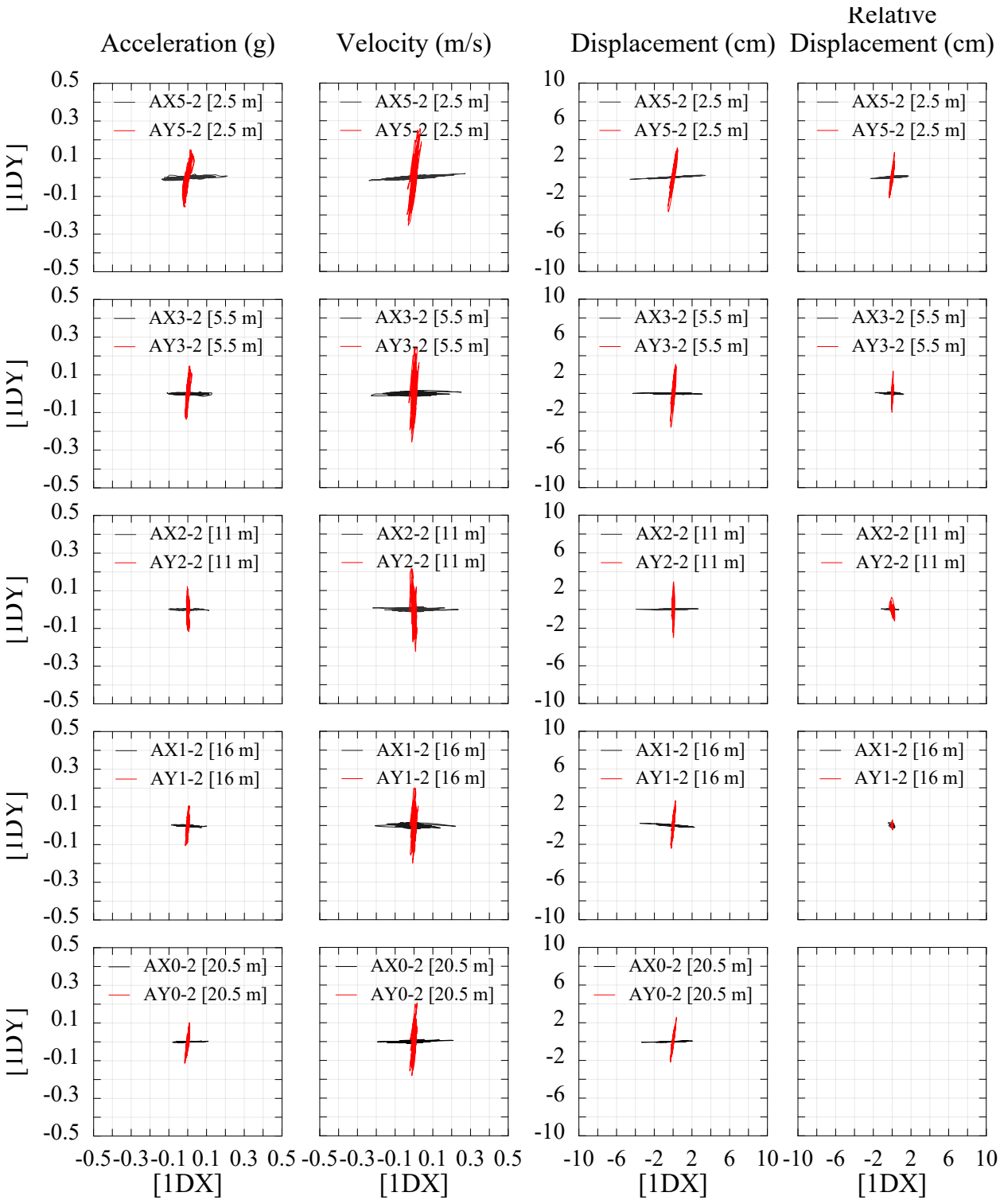

Figure C-228 Recorded input and within model ground motions for acceleration, velocity, displacement and relative displacement for M10-1D [X] and M10-1D [Y]

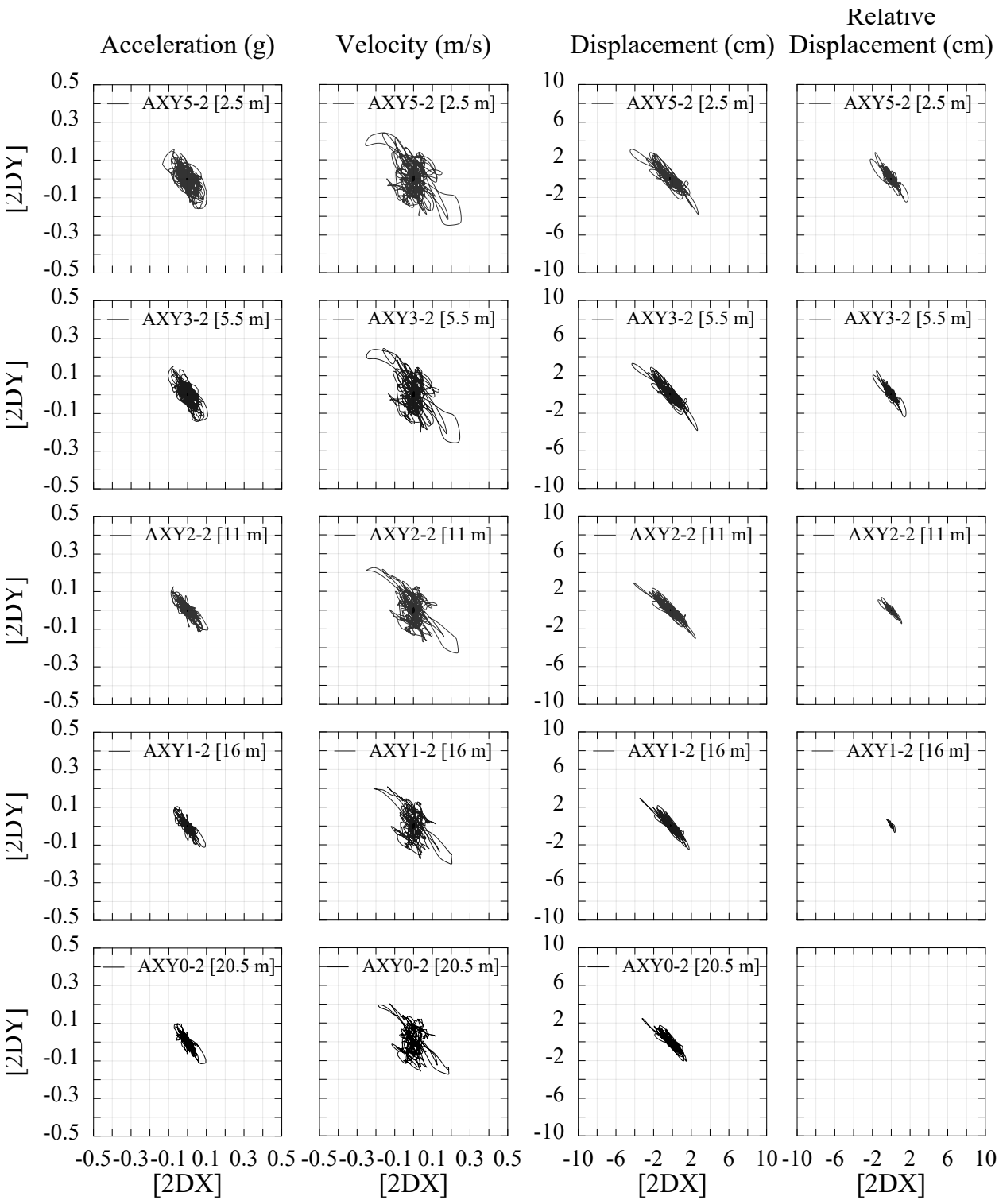

Figure C-229 Recorded input and within model ground motions for acceleration, velocity, displacement and relative displacement for M10-2D

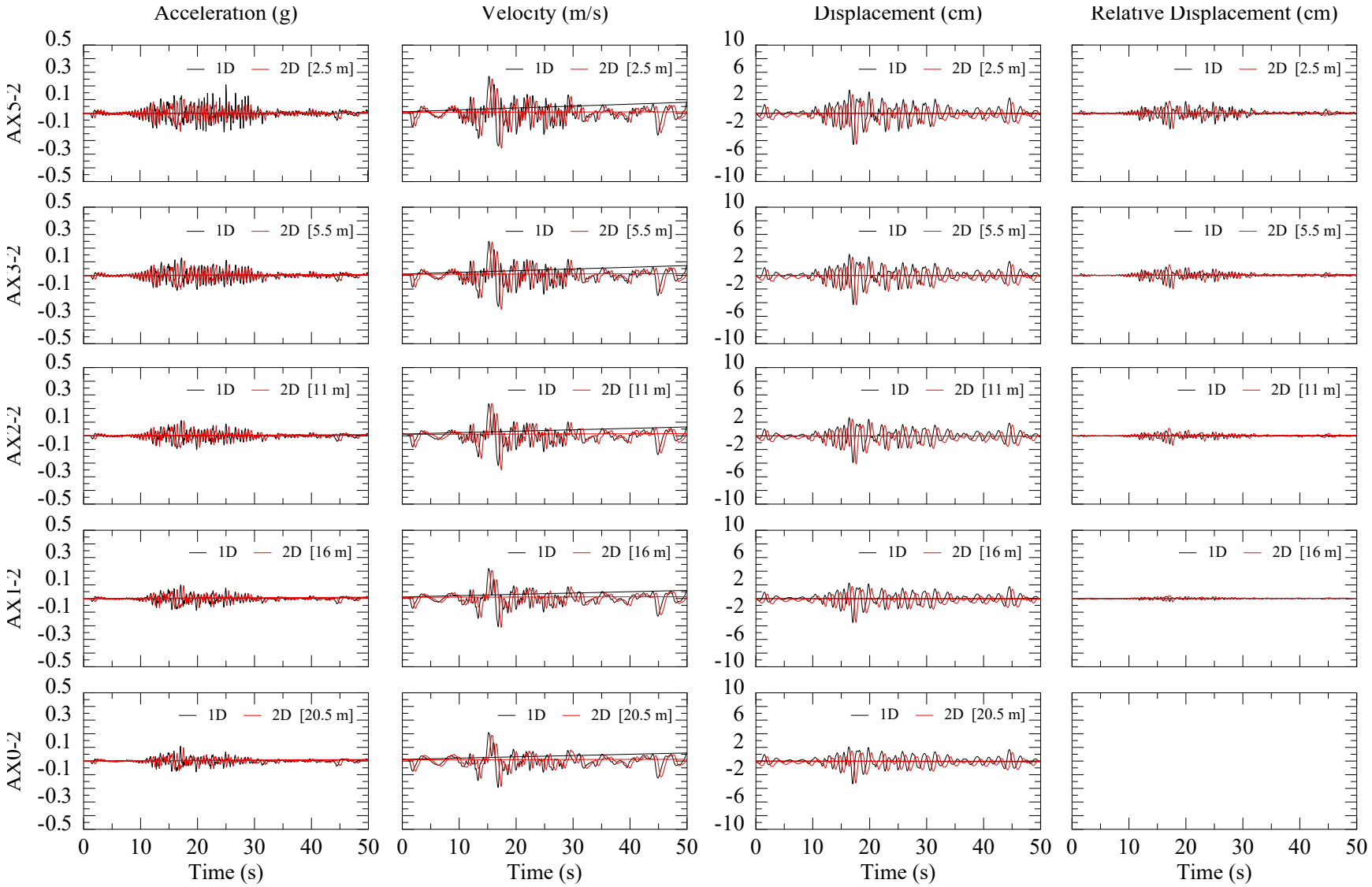

Figure C-230 Recorded input and within model ground motions time histories for acceleration, velocity, displacement and relative displacement for M10-2D [X] and M10-1D [X]

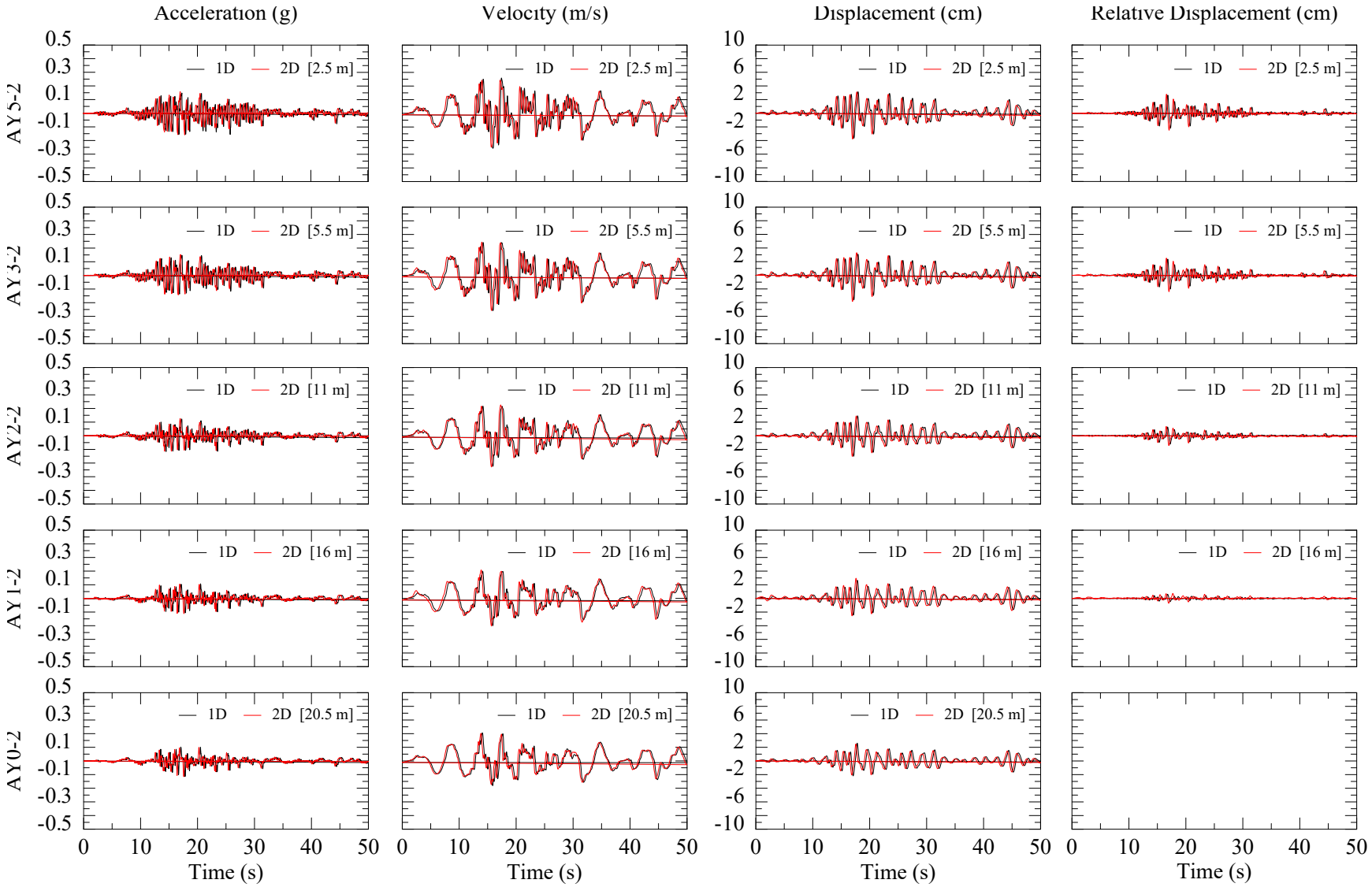

Figure C-231 Recorded input and within model ground motions time histories for acceleration, velocity, displacement and relative displacement for M10-2D [Y] and M10-1D [Y]

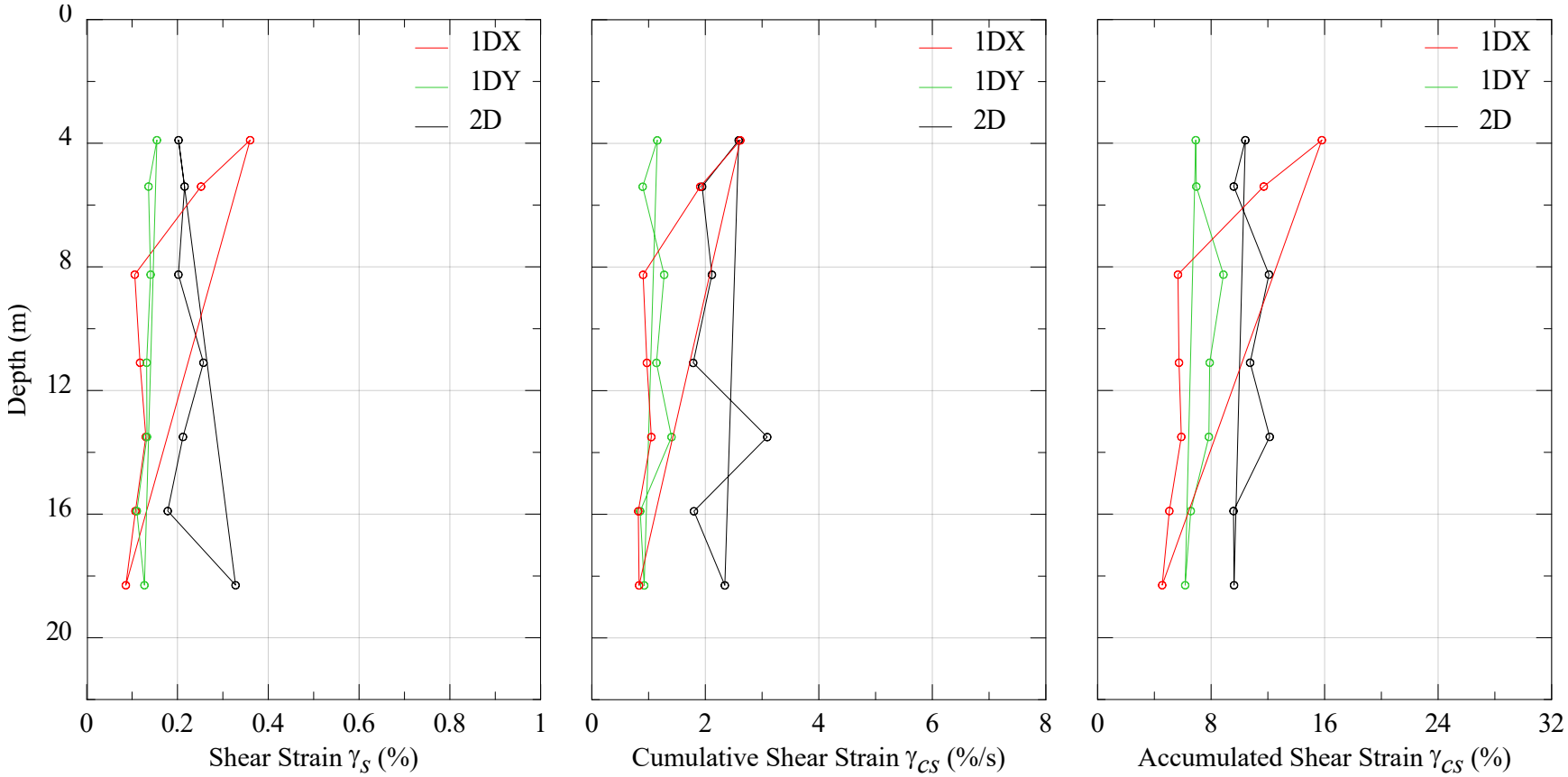

Figure C-232 Estimated (a) maximum shear strain; (b) cumulative shear strain; and (c) accumulated shear strain for M10-2D [X] and M10-1D [X]

1.4.2 Motion 11 (M11)

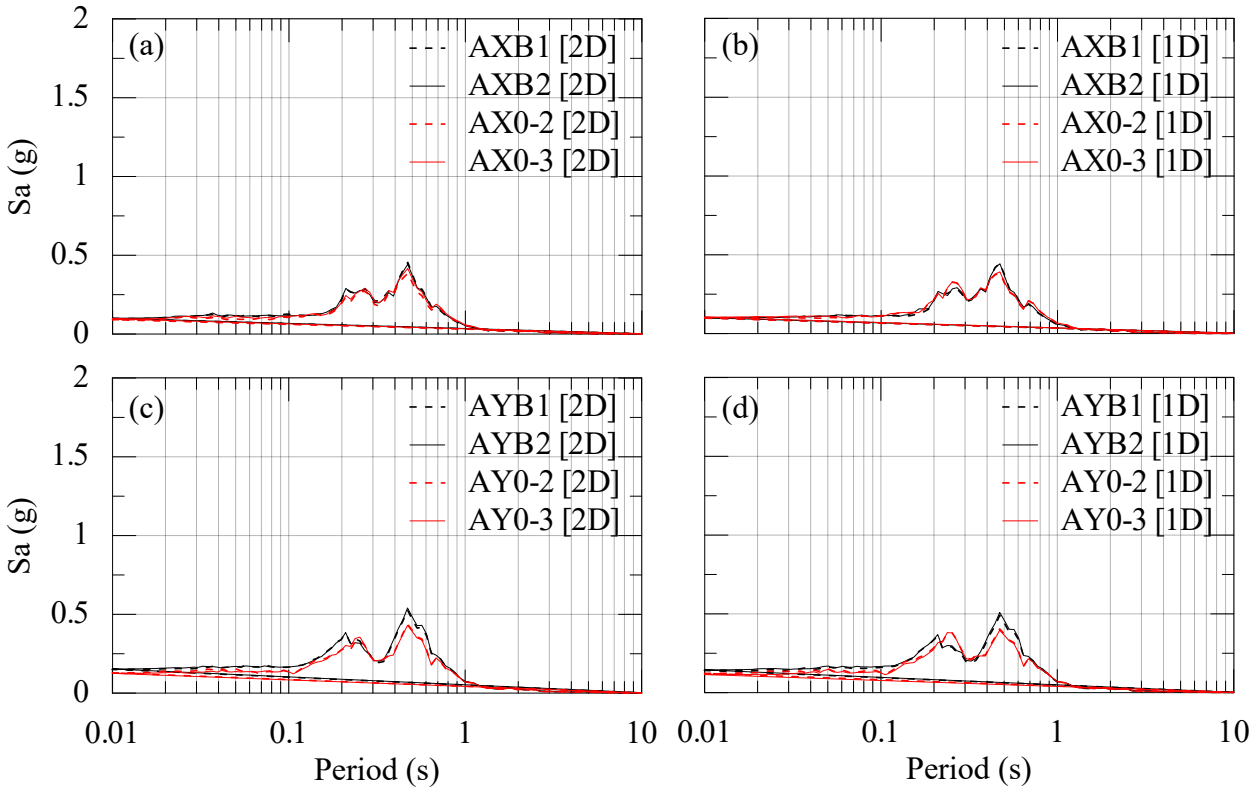

Figure C-233 Comparison of response spectra of 2D laminar container table and within model base input motion for motions (M11-X, Y and 2D).

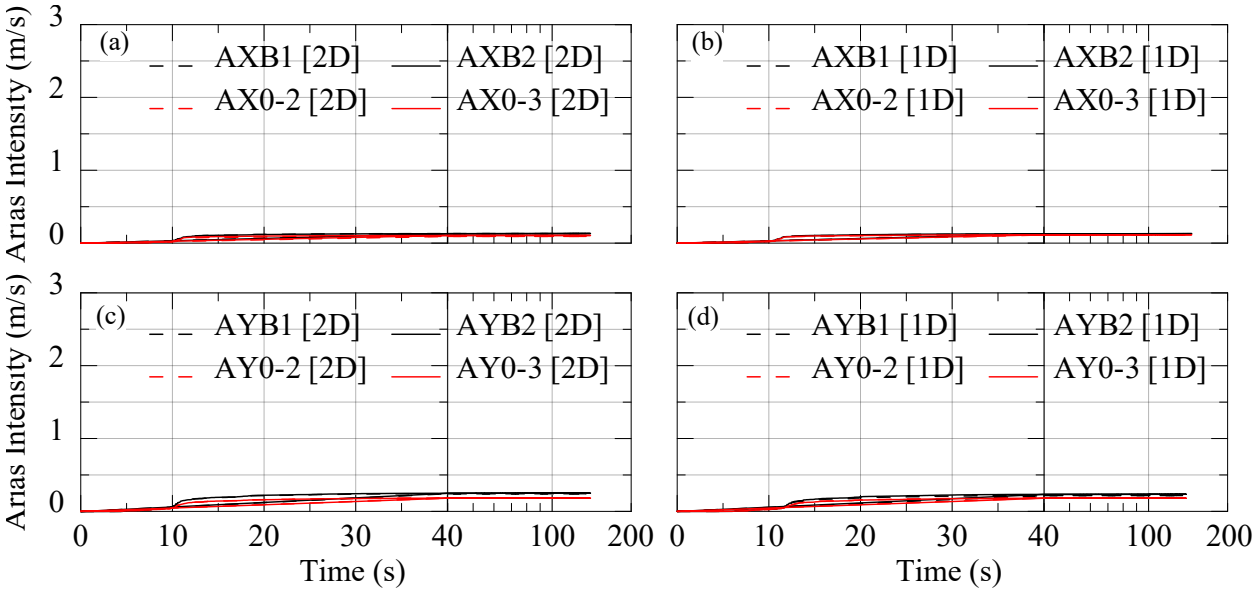

Figure C-234 Comparison of Arias Intensity of 2D laminar container table and within model base input motion for motions (a) M11-2D [X]; (b) M11-2D [Y]; (c) M11-1D [X] and (d) M11-1D [Y]

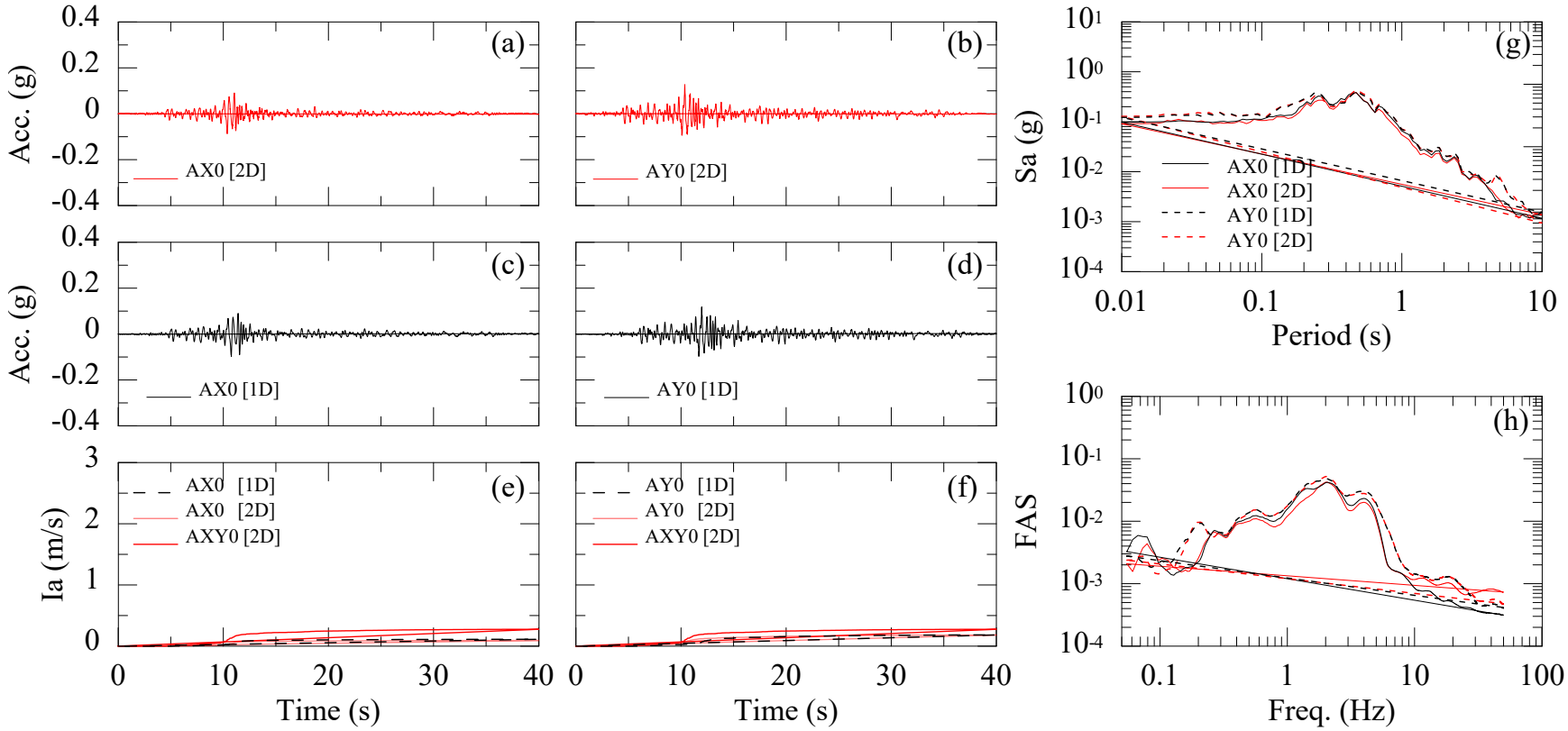

Figure C-235 Recorded input (2D) and 1D (X or Y) ground motions for: (a) M11-2D [X]; (b) M11-2D [Y]; (c) M11-1D [X]; and (d) M11-1D [Y]. Arias Intensity M11 (1D and 2D) for: (e) X direction; and (f) Y direction. Response Spectra (g) M11-2D [X]; M11-2D [Y]; M11-1D [X]; and M11-1D [Y]. Smoothed Fourier amplitude spectra (FAS) (h) M11-2D [X]; M11-2D [Y]; M11-1D [X]; and M11-1D [Y].

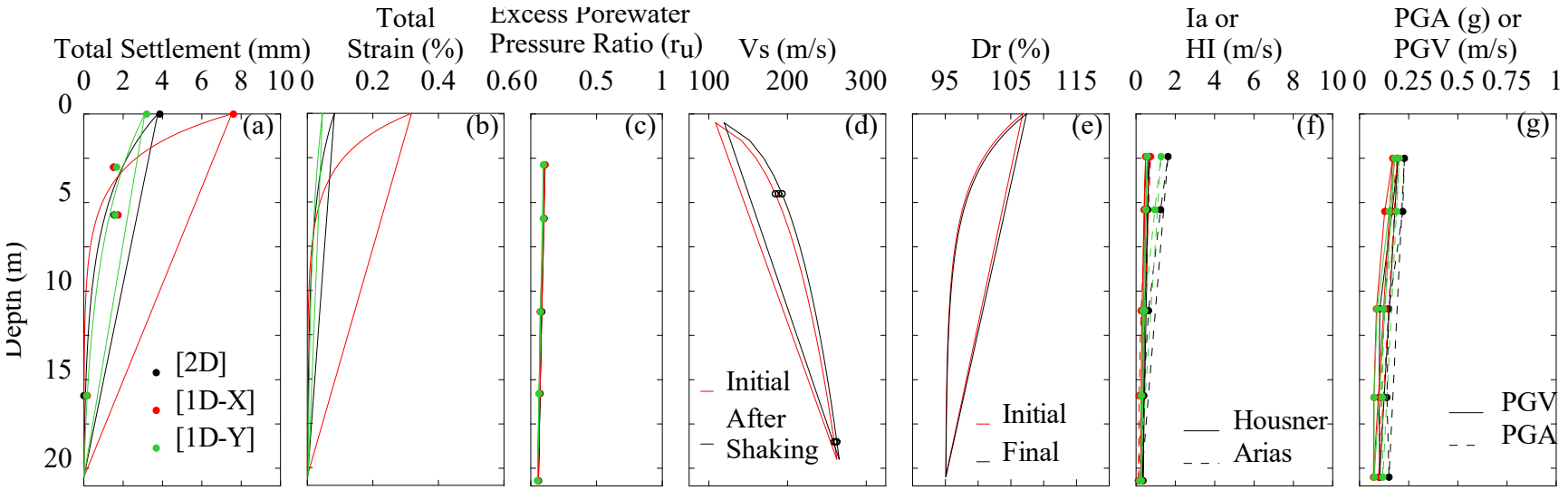

Figure C-236 Recorded or computed profiles for input motion M11-X, Y, and 2D. (a) Settlement; (b) total strain; (c) excess pore water pressure ratio; (d) shear wave velocity; (e) relative density; (f) Arias and Housner intensities; and (g) PGA and PGV.

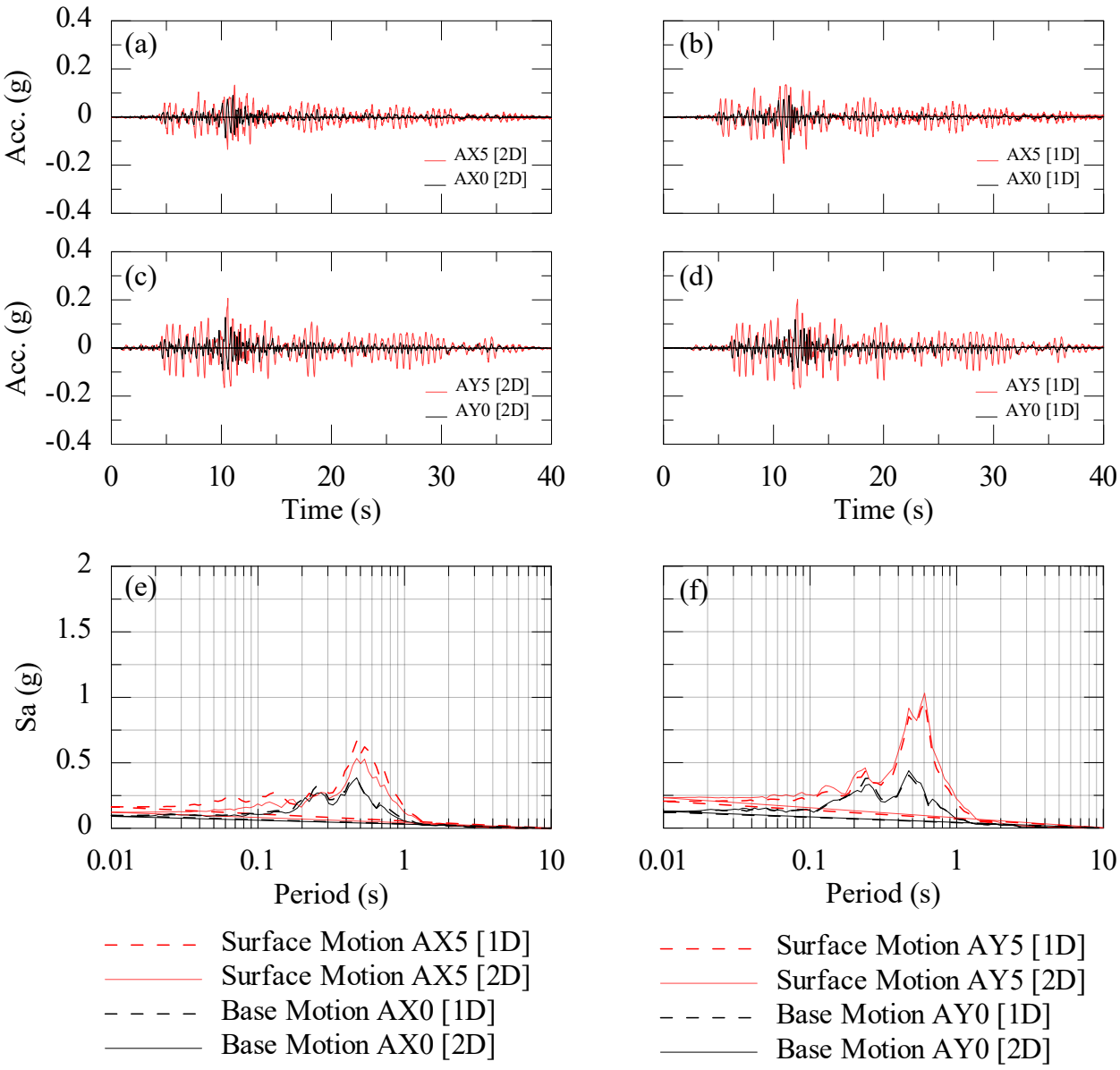

Figure C-237 Recorded input and surface ground motion: (a) M11-2D [X]; (b) M11-1D [X]; (c) M11-2D [Y]; and (d) M11-1D [Y]. Computed response spectra from Free Field Test [PT2] for motions M11 (1D and 2D) for: (e) X direction; and (f) Y direction.

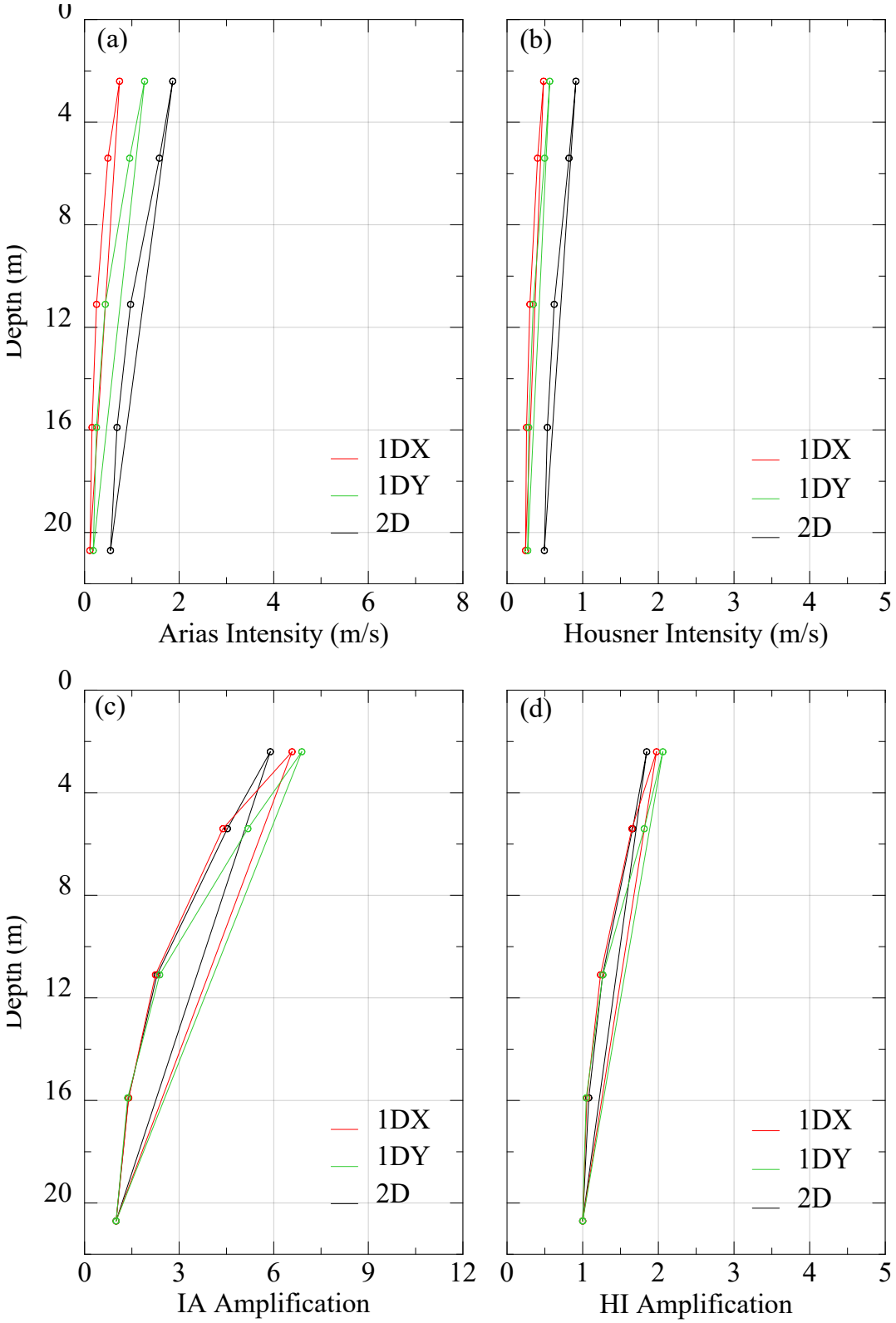

Figure C-238 Variation of total (a) Arias Intensity (M11-X,Y and 2D) ; (b) Housner Intensity (M11-X,Y and 2D) (c) Arias Intensity Amplification Factor (M11-X,Y and 2D); and (d) Housner Intensity Amplification Factor (M11-X,Y and 2D).

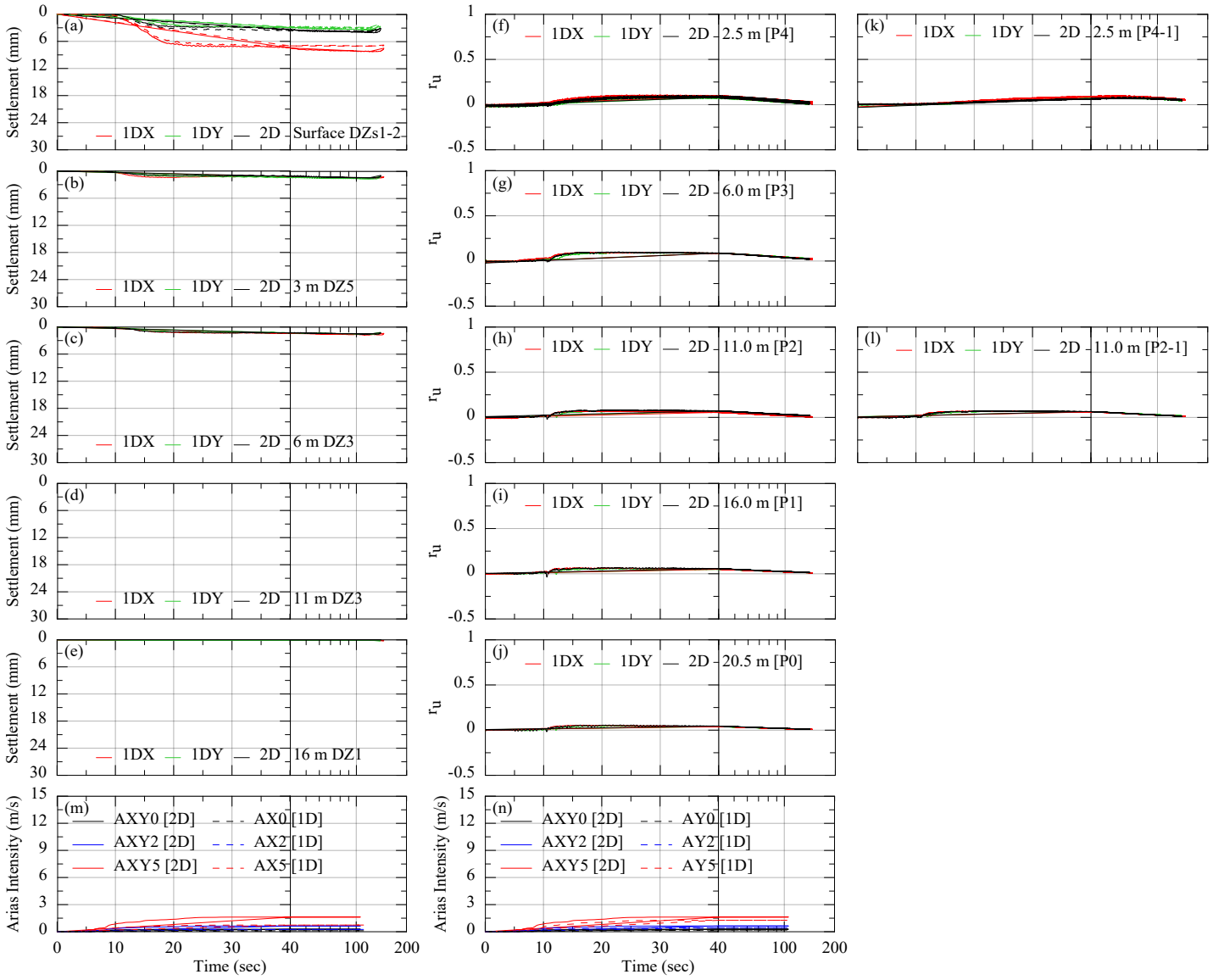

Figure C-239 Variation of total (a) to (e) Settlement with depth (M11-X,Y and 2D) ; (f) to (l) Excess pore water pressure ratio (ru) (M11-X,Y and 2D) (m) and (n) Arias Intensity along model (M11-X,Y and 2D).

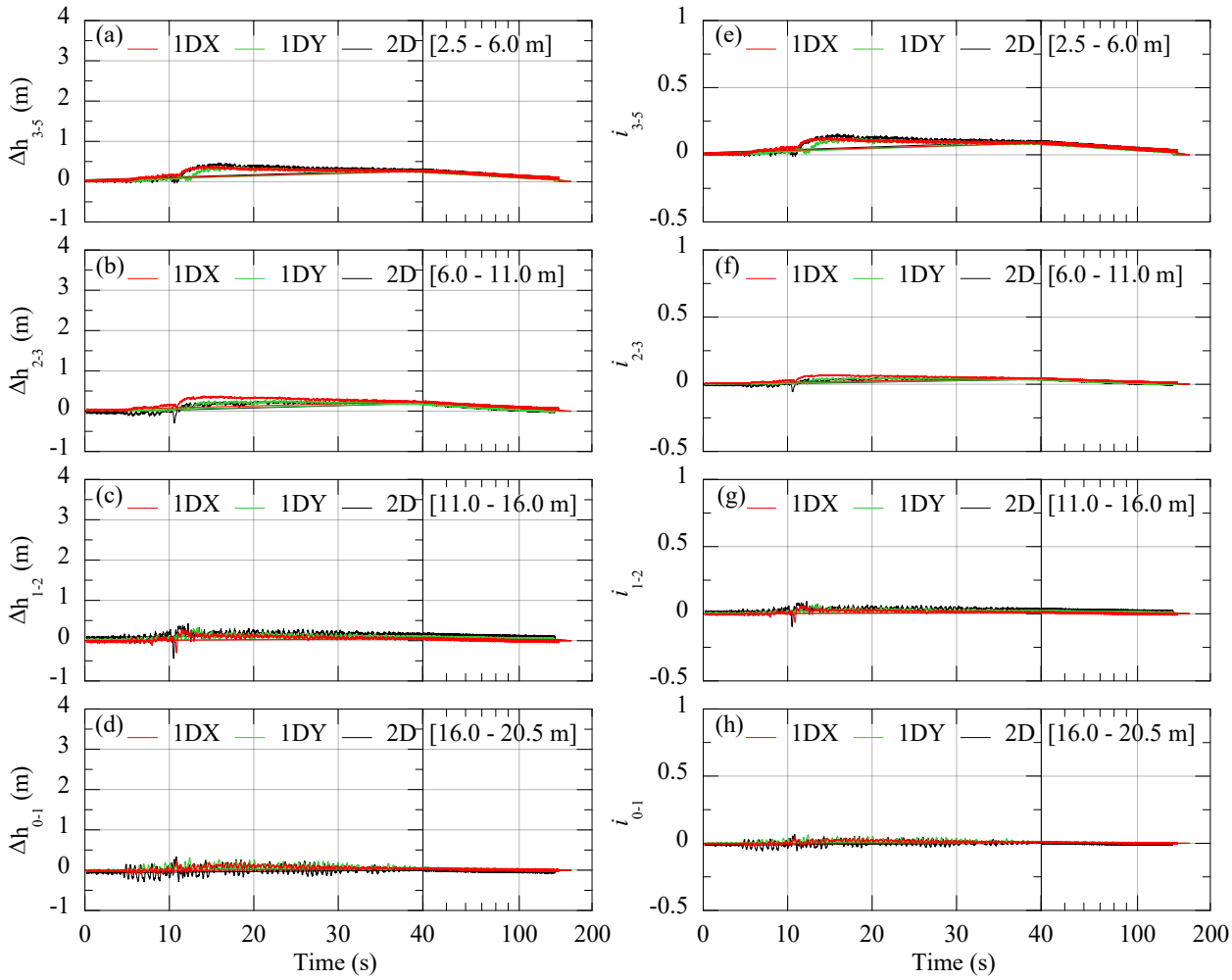

Figure C-240 Variation of total (a) to (d) Total Head Loss with depth (M11-X, Y and 2D); (e) to (h) Shaking induced Hydraulic Gradient (M11-X, Y and 2D)

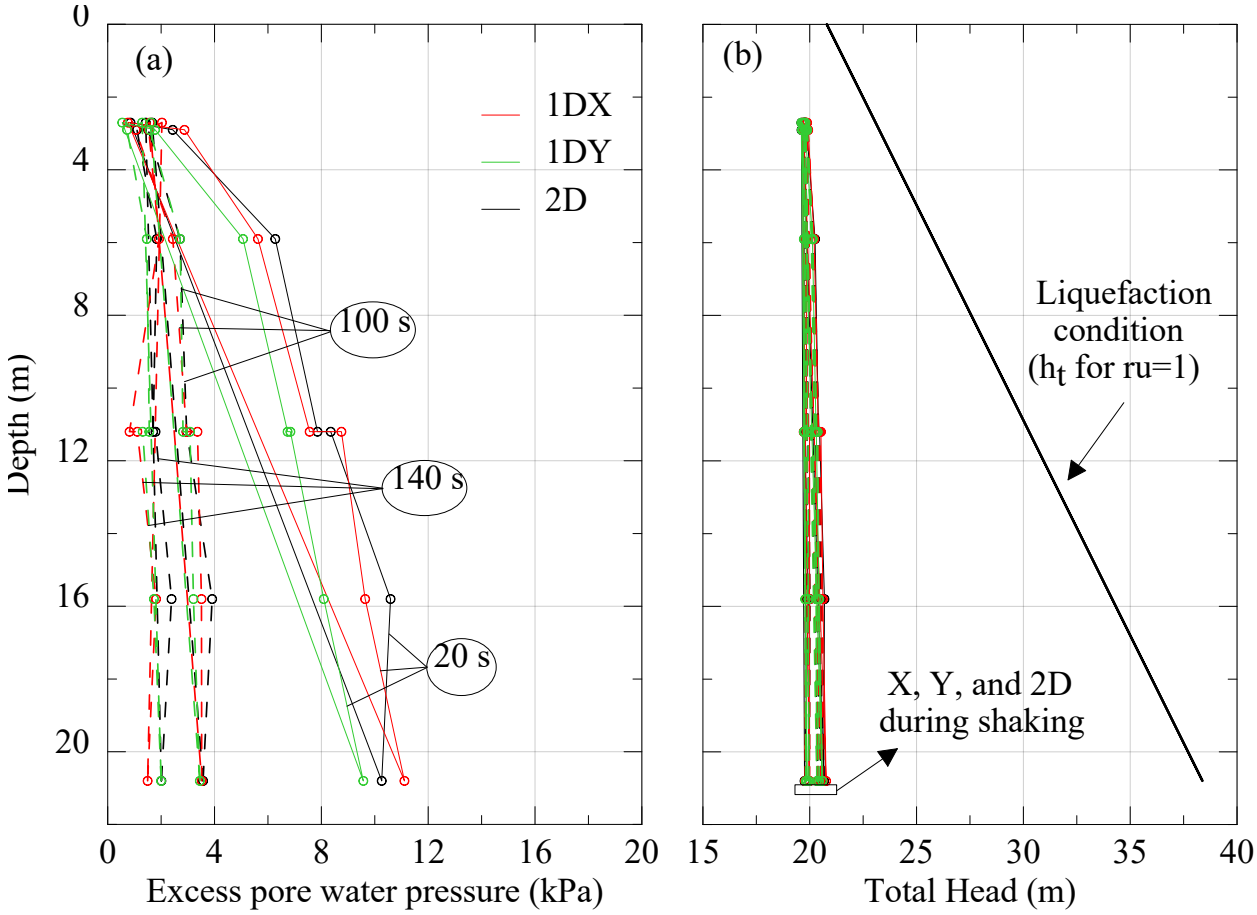

Figure C-241 Variation of total (a) Excess pore water pressure ratio (ru) with depth (M11-X,Y and 2D); (e) to (b) Total Head Loss with depth (M11-X,Y and 2D)

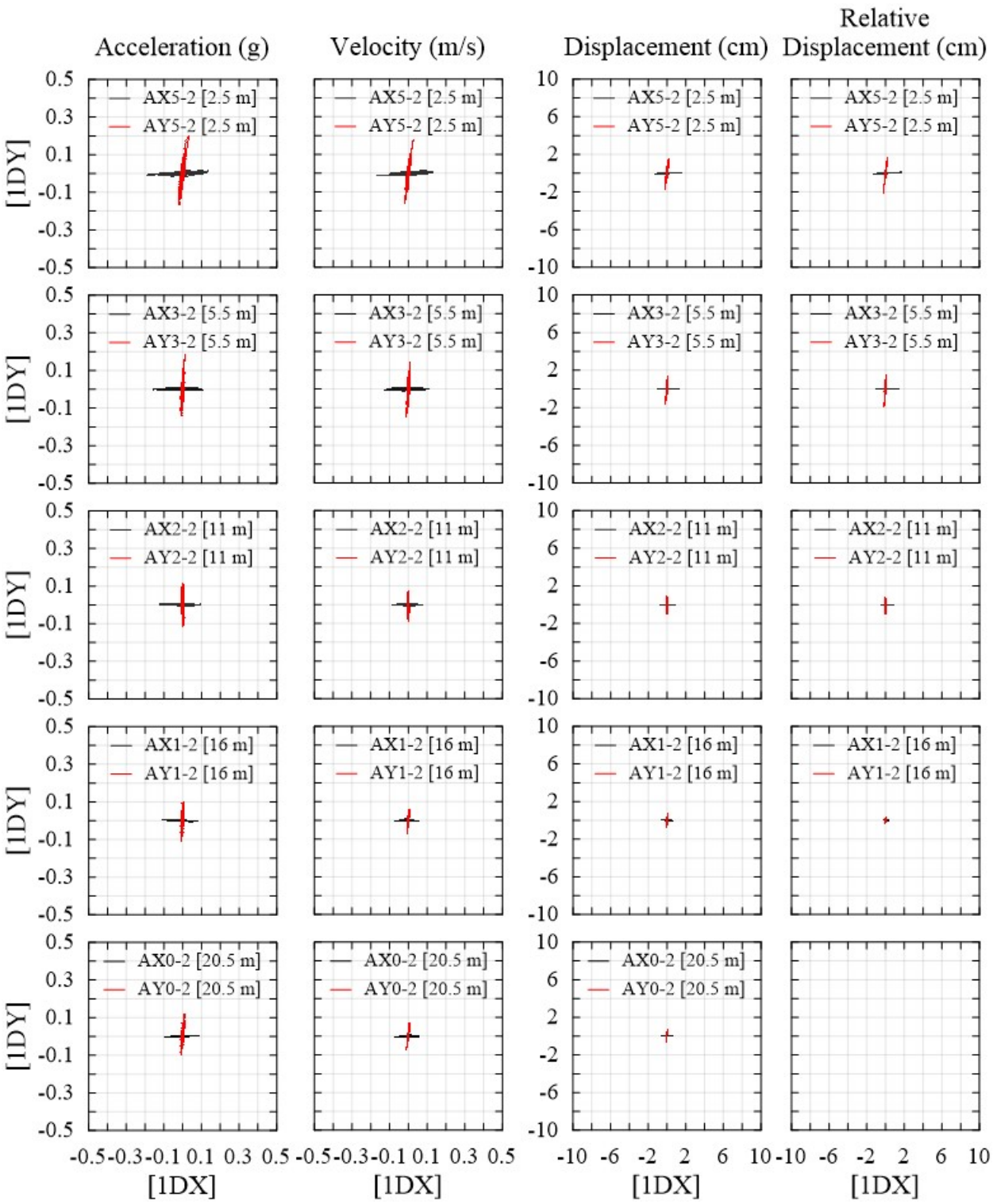

Figure C-242 Recorded input and within model ground motions for acceleration, velocity, displacement and relative displacement for M11-1D [X] and M11-1D [Y]

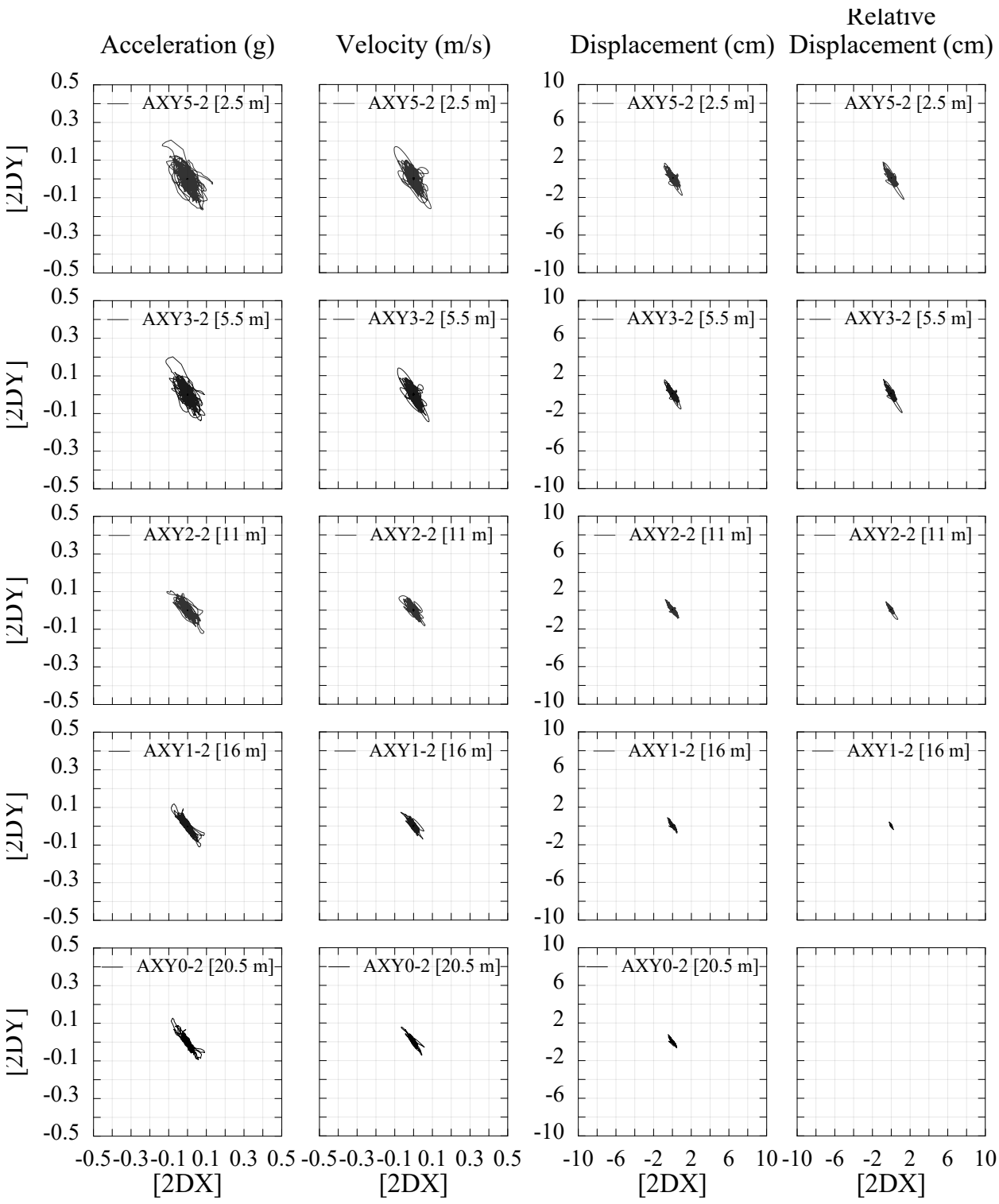

Figure C-243 Recorded input and within model ground motions for acceleration, velocity, displacement and relative displacement for M11-2D

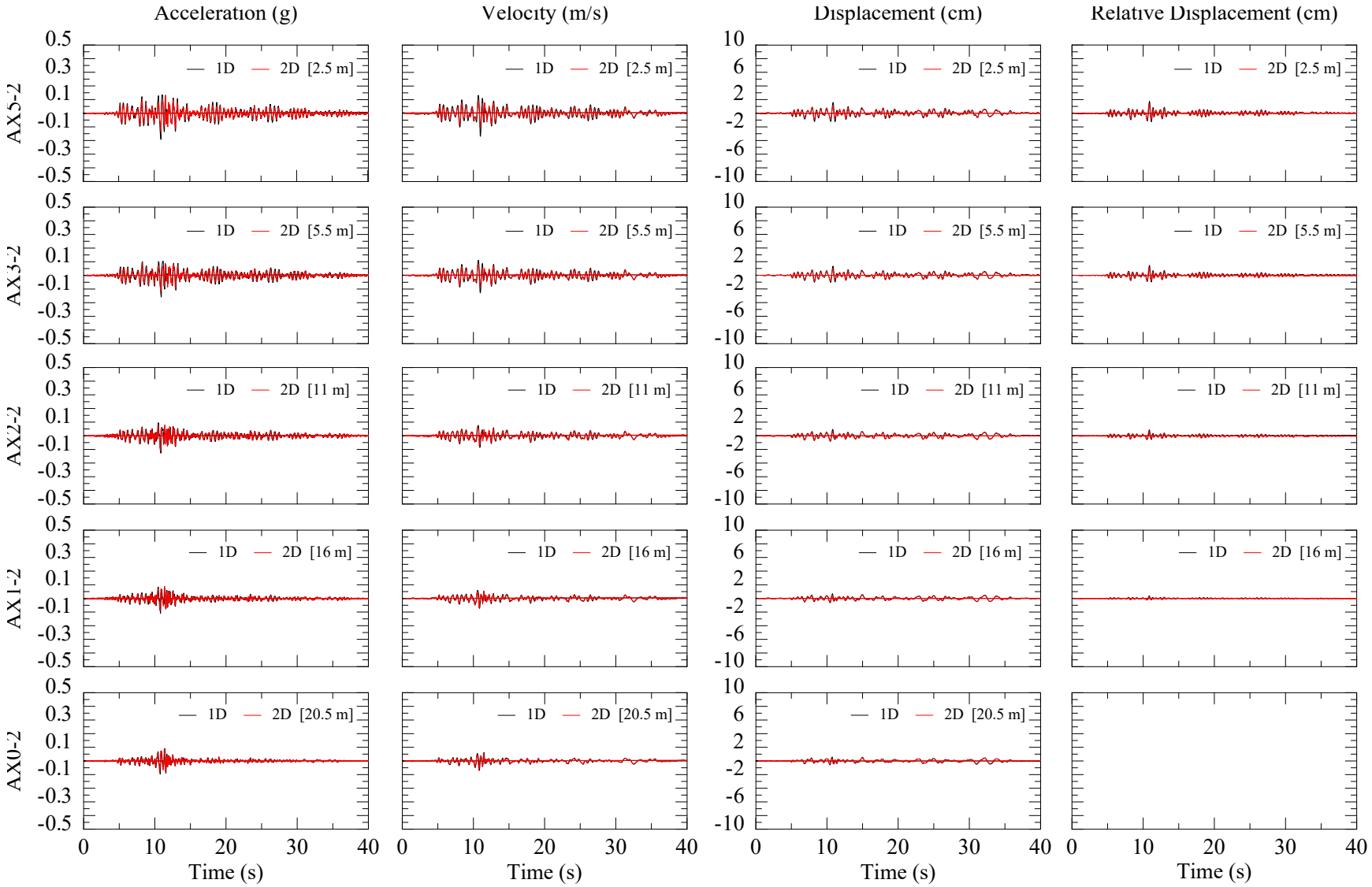

Figure C-244 Recorded input and within model ground motions time histories for acceleration, velocity, displacement and relative displacement for M11-2D [X] and M11-1D [X]

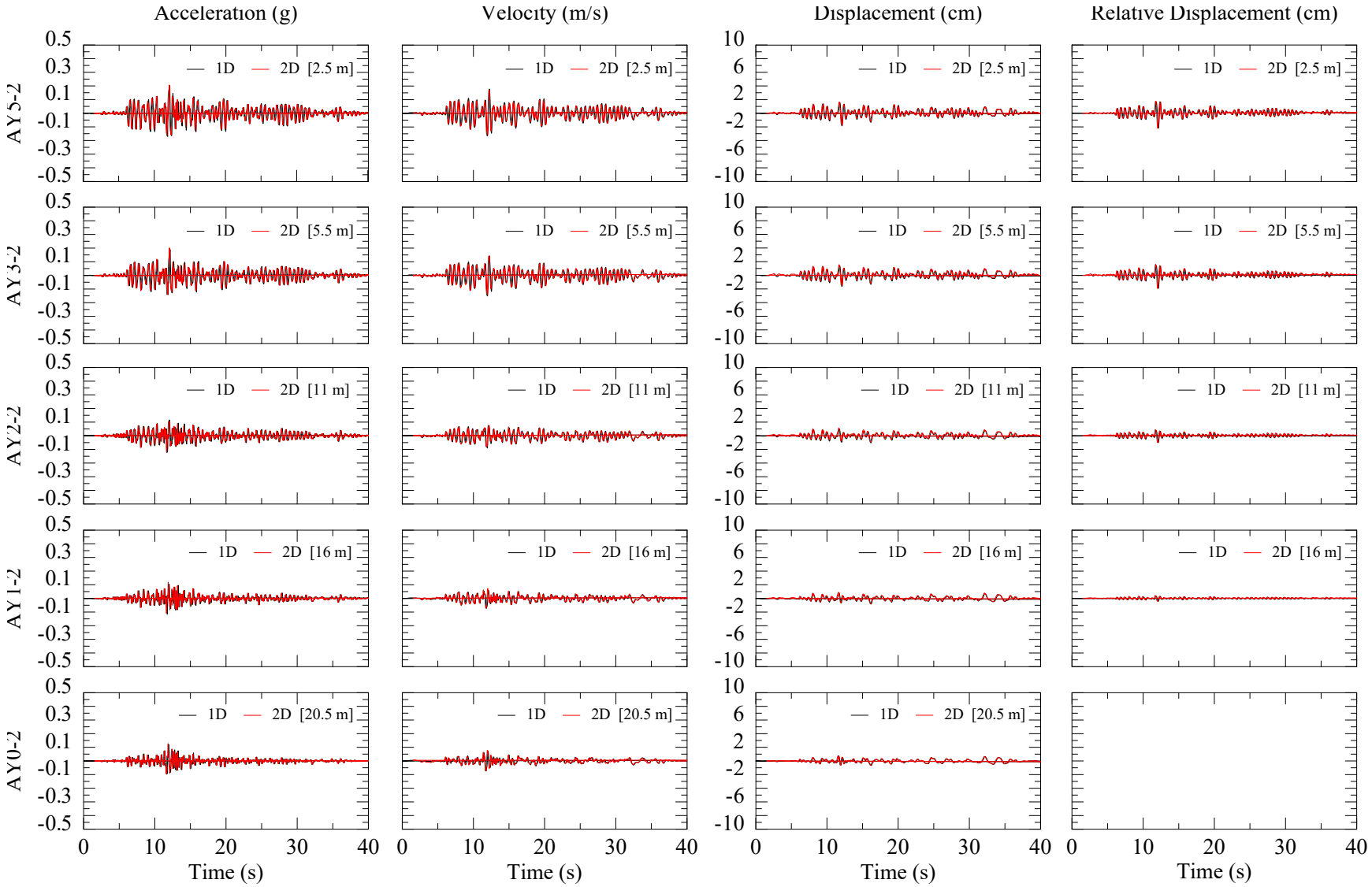

Figure C-245 Recorded input and within model ground motions time histories for acceleration, velocity, displacement and relative displacement for M11-2D [Y] and M11-1D [Y]

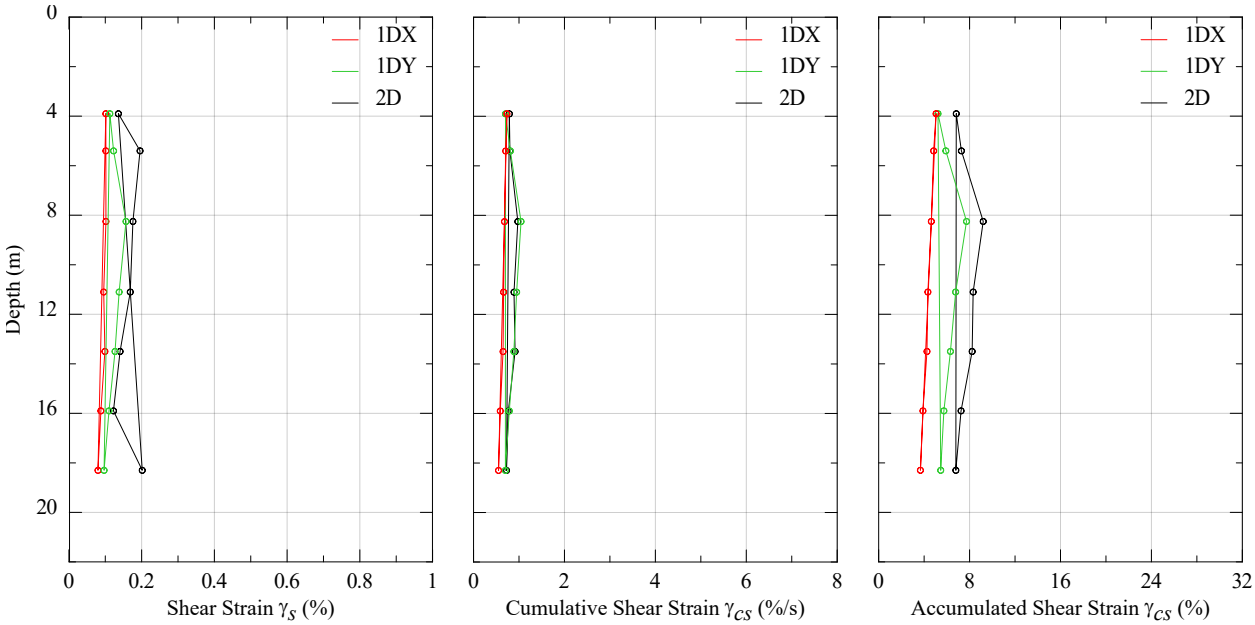

Figure C-246 Estimated (a) maximum shear strain; (b) cumulative shear strain; and (c) accumulated shear strain for M11-2D [X] and M11-1D [X]

1.4.3 Motion 1 (M1)

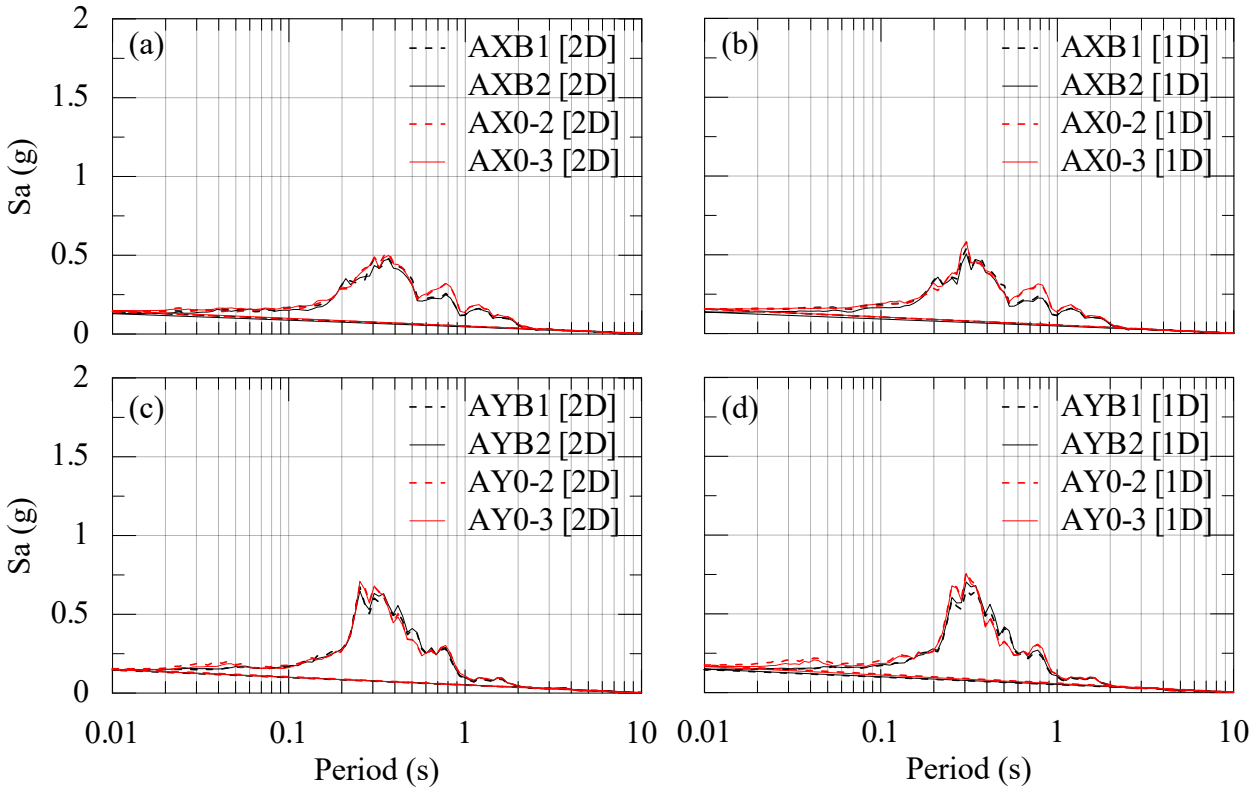

Figure C-247 Comparison of response spectra of 2D laminar container table and within model base input motion for motions (M1-X, Y and 2D).

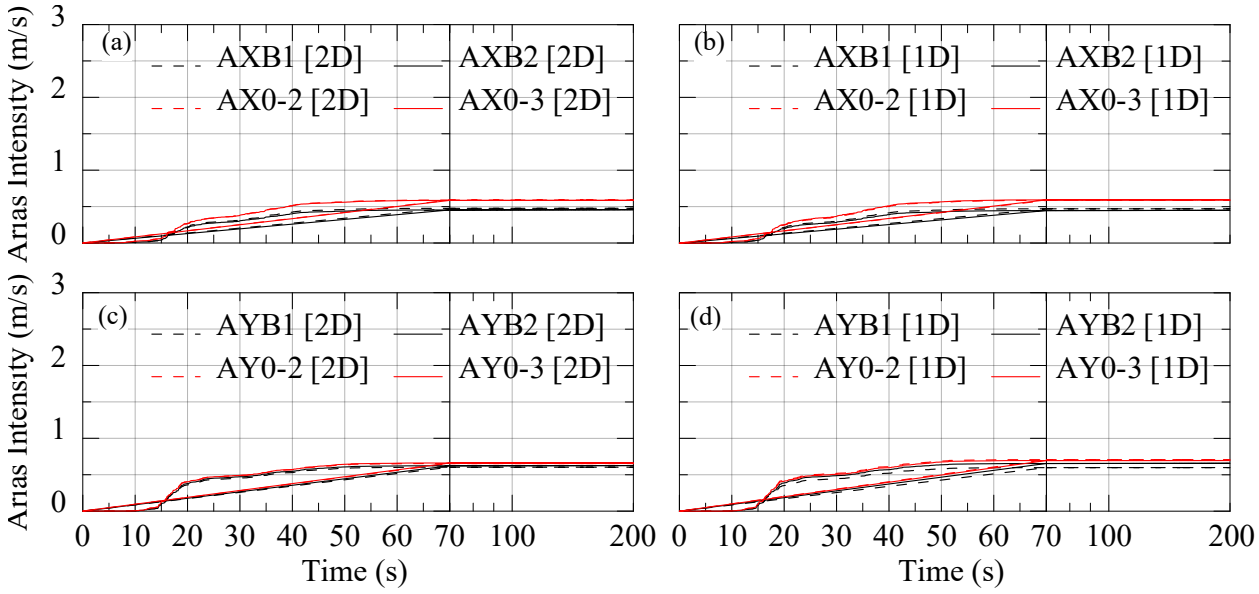

Figure C-248 Comparison of Arias Intensity of 2D laminar container table and within model base input motion for motions (a) M1-2D [X]; (b) M1-2D [Y]; (c) M1-1D [X] and (d) M1-1D [Y]

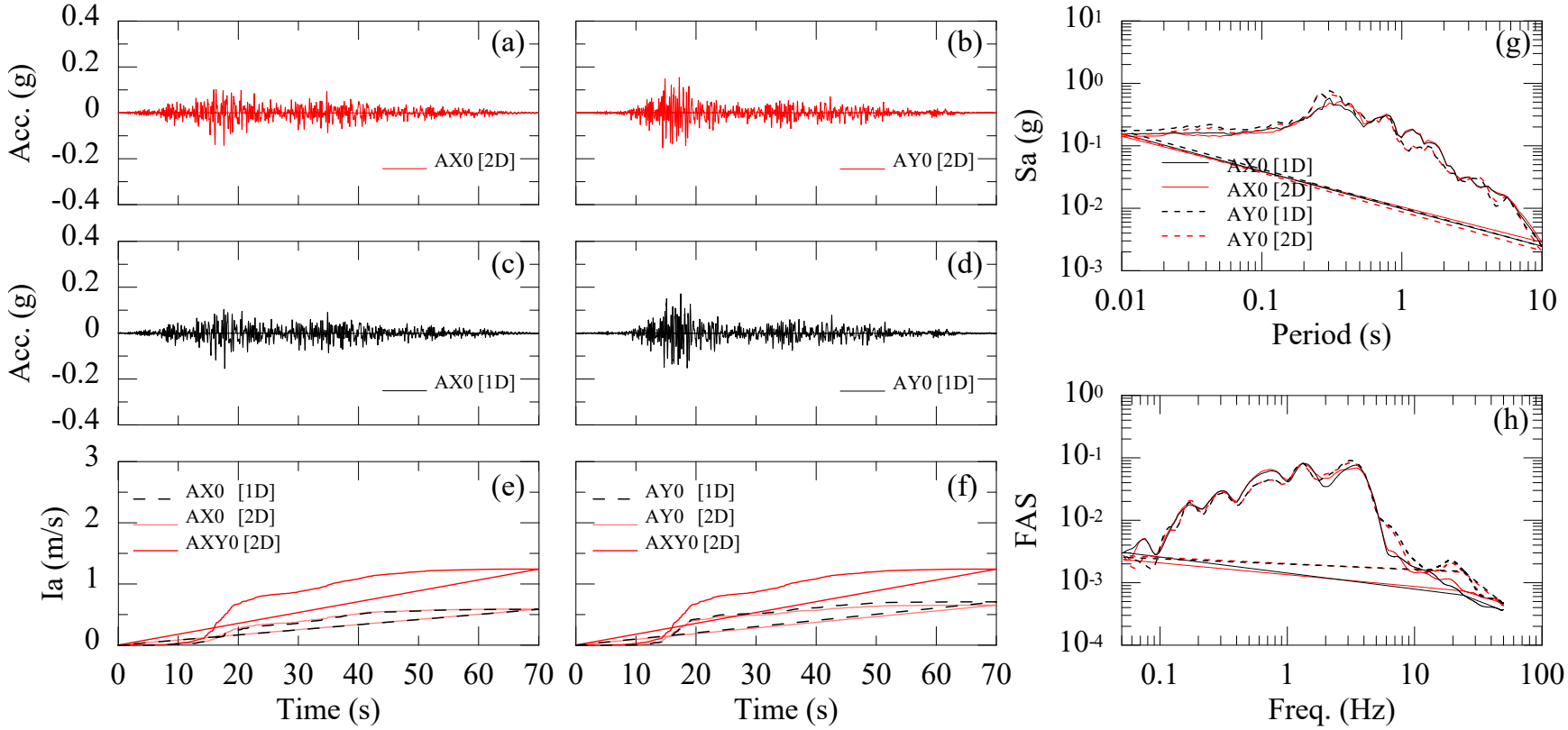

Figure C-249 Recorded input (2D) and 1D (X or Y) ground motions for: (a) M1-2D [X]; (b) M1-2D [Y]; (c) M1-1D [X]; and (d) M1-1D [Y]. Arias Intensity M1 (1D and 2D) for: (e) X direction; and (f) Y direction. Response Spectra (g) M1-2D [X]; M1-2D [Y]; M1-1D [X]; and M1-1D [Y]. Smoothed Fourier amplitude spectra (FAS) (h) M1-2D [X]; M1-2D [Y]; M1-1D [X]; and M1-1D [Y].

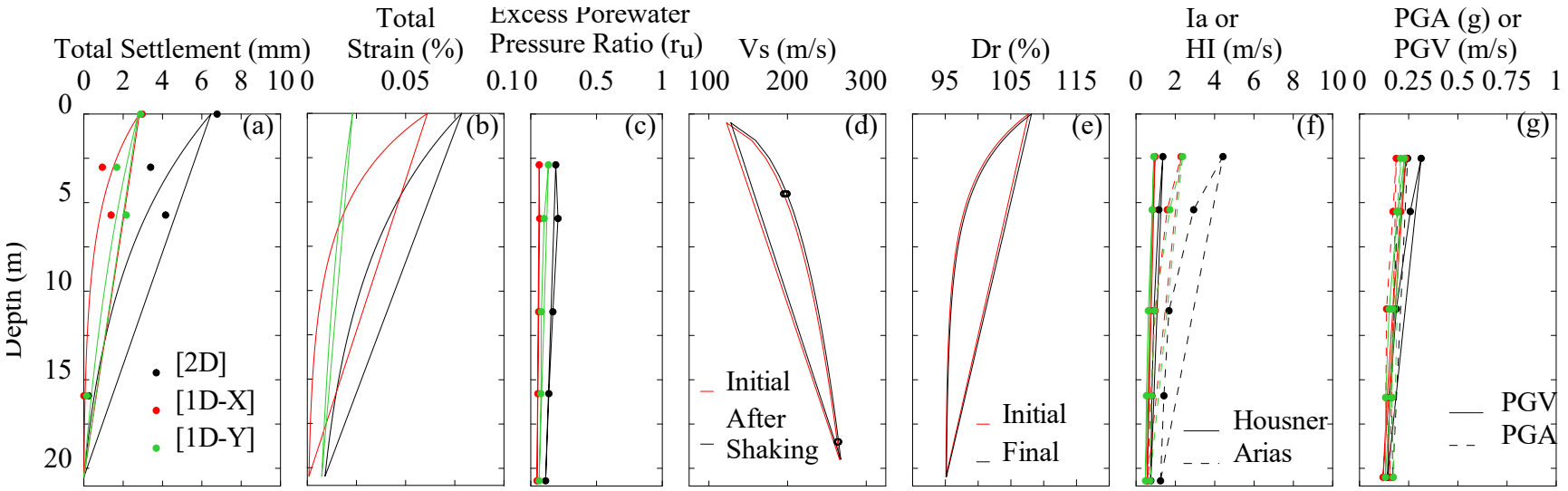

Figure C-250 Recorded or computed profiles for input motion M1-X, Y, and 2D. (a) Settlement; (b) total strain; (c) excess pore water pressure ratio; (d) shear wave velocity; (e) relative density; (f) Arias and Housner intensities; and (g) PGA and PGV.

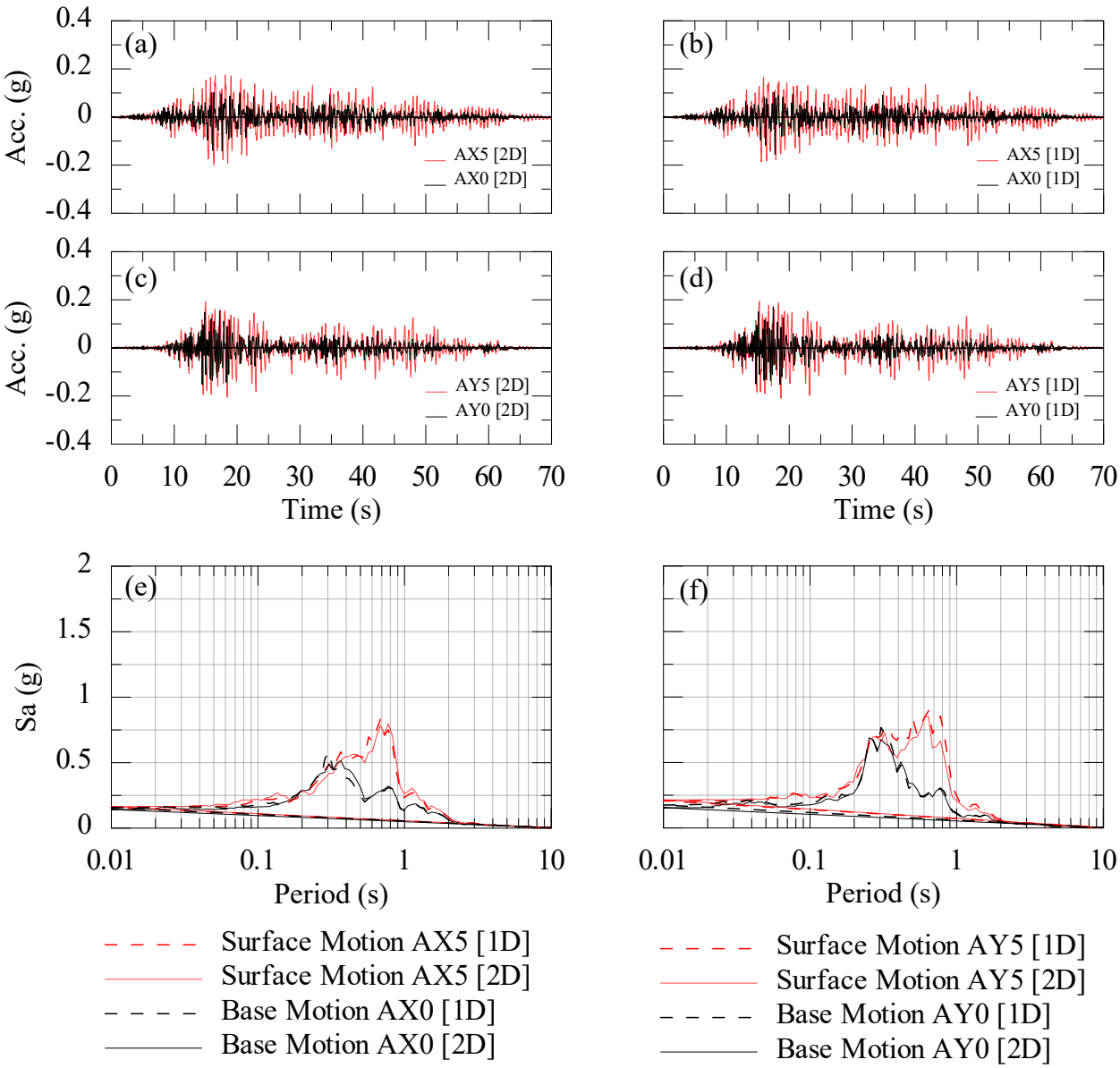

Figure C-251 Recorded input and surface ground motion: (a) M1-2D [X]; (b) M1-1D [X]; (c) M1-2D [Y]; and (d) M1-1D [Y]. Computed response spectra from Free Field Test [PT2] for motions M1 (1D and 2D) for: (e) X direction; and (f) Y direction.

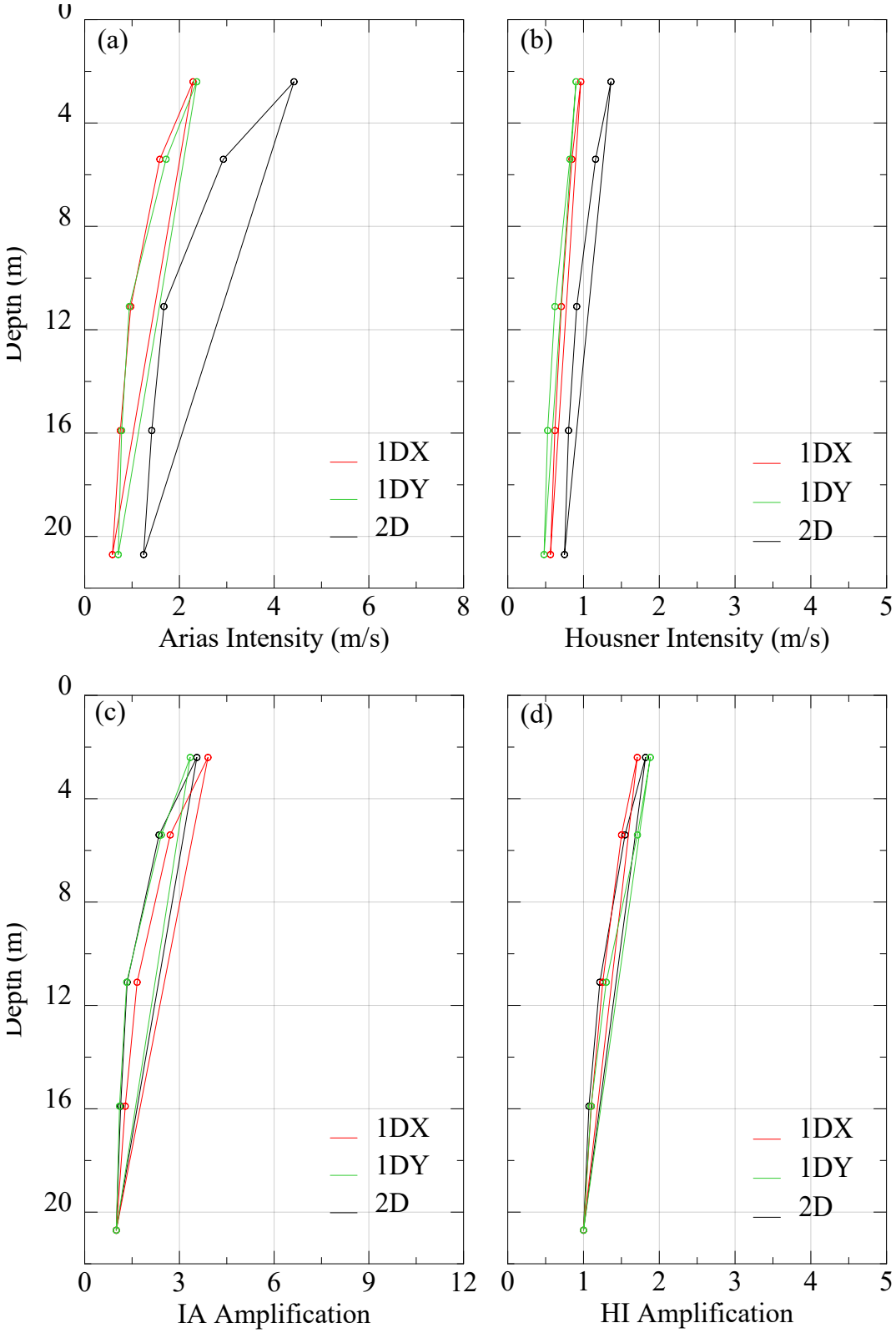

Figure C-252 Variation of total (a) Arias Intensity (M1-X,Y and 2D) ; (b) Housner Intensity (M1-X,Y and 2D) (c) Arias Intensity Amplification Factor (M1-X,Y and 2D); and (d) Housner Intensity Amplification Factor (M1-X,Y and 2D).

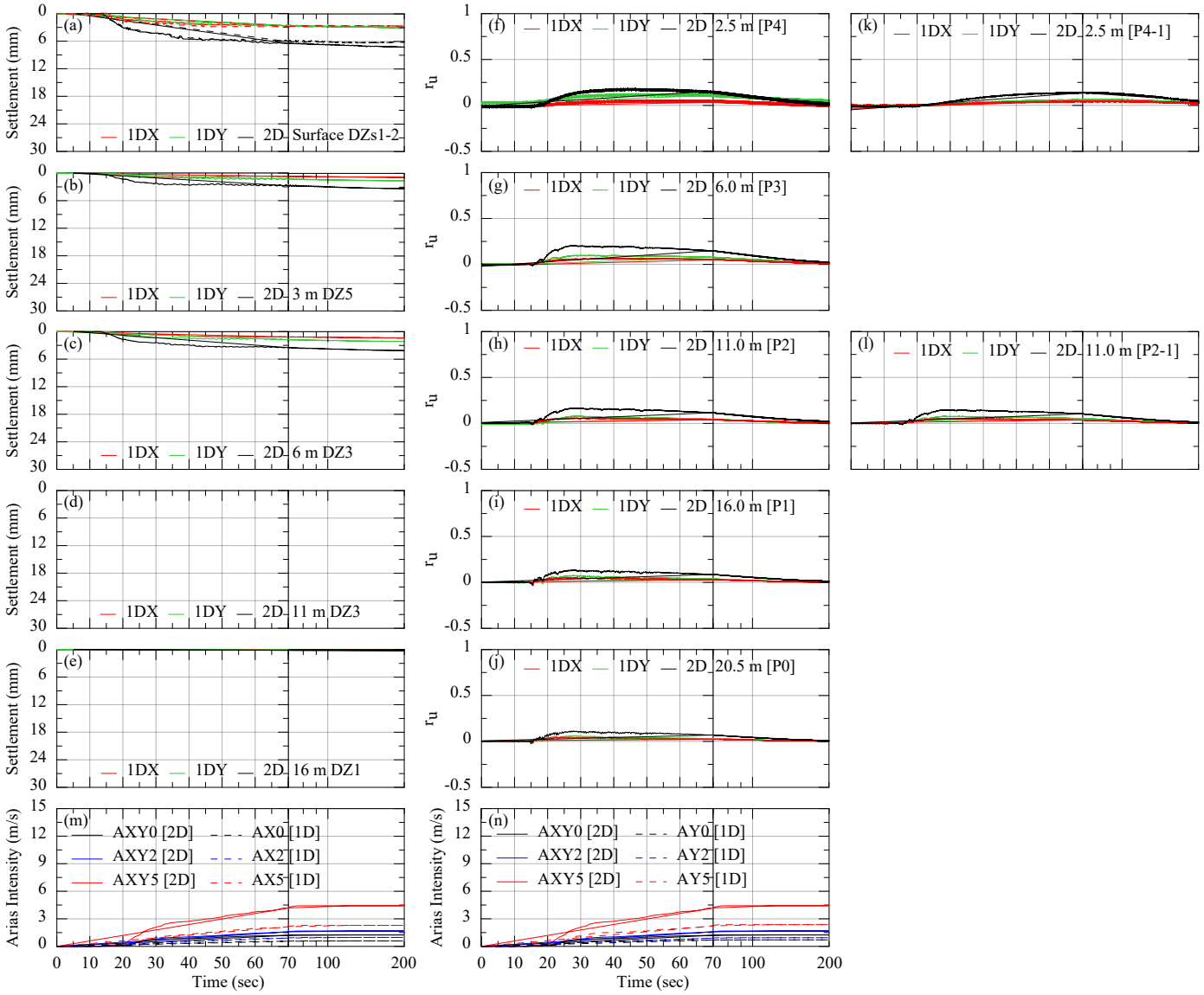

Figure C-253 Variation of total (a) to (e) Settlement with depth (M1-X,Y and 2D) ; (f) to (l) Excess pore water pressure ratio (ru) (M1-X,Y and 2D) (m) and (n) Arias Intensity along model (M1-X,Y and 2D).

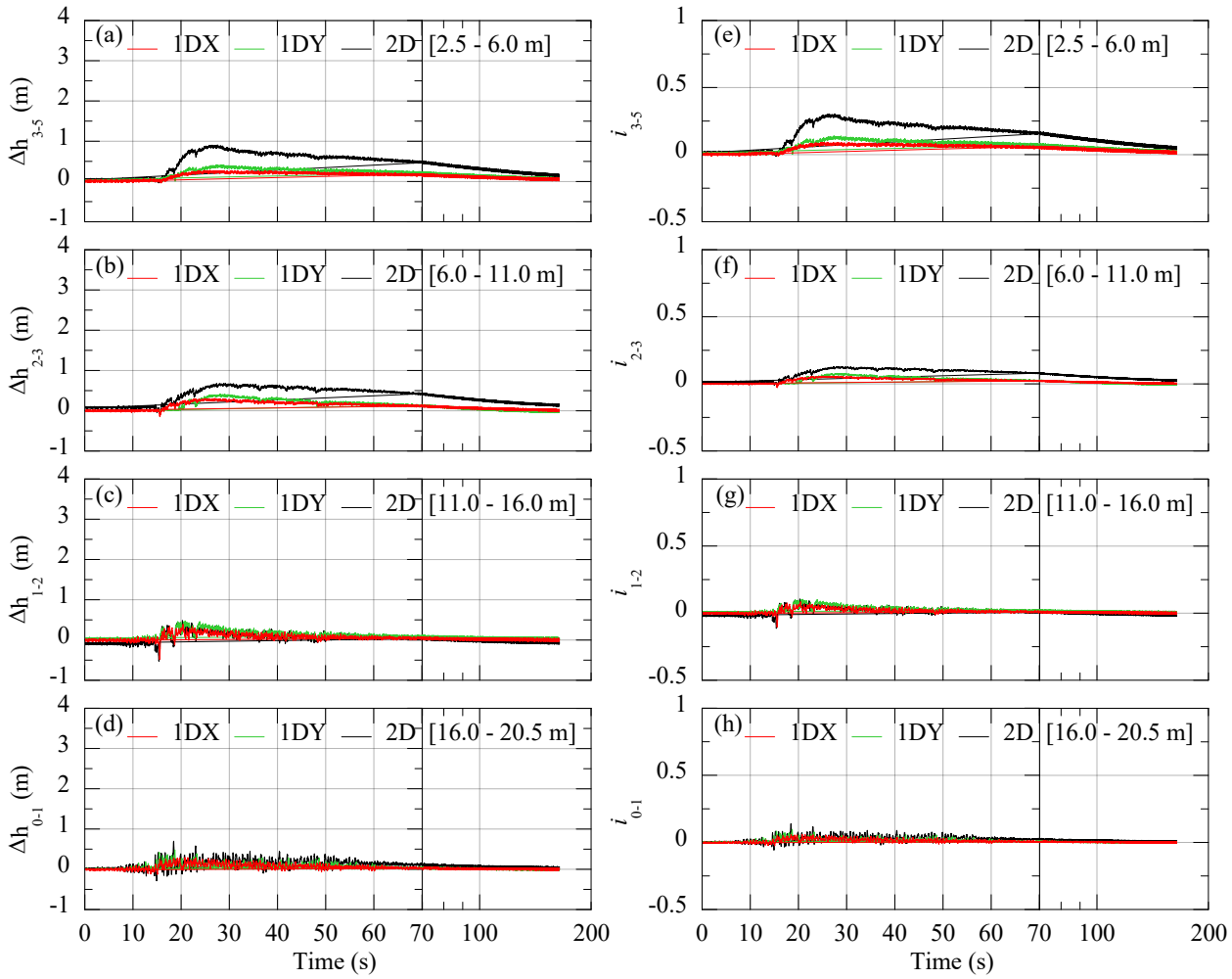

Figure C-254 Variation of total (a) to (d) Total Head Loss with depth (M1-X, Y and 2D); (e) to (h) Shaking induced Hydraulic Gradient (M1-X, Y and 2D)

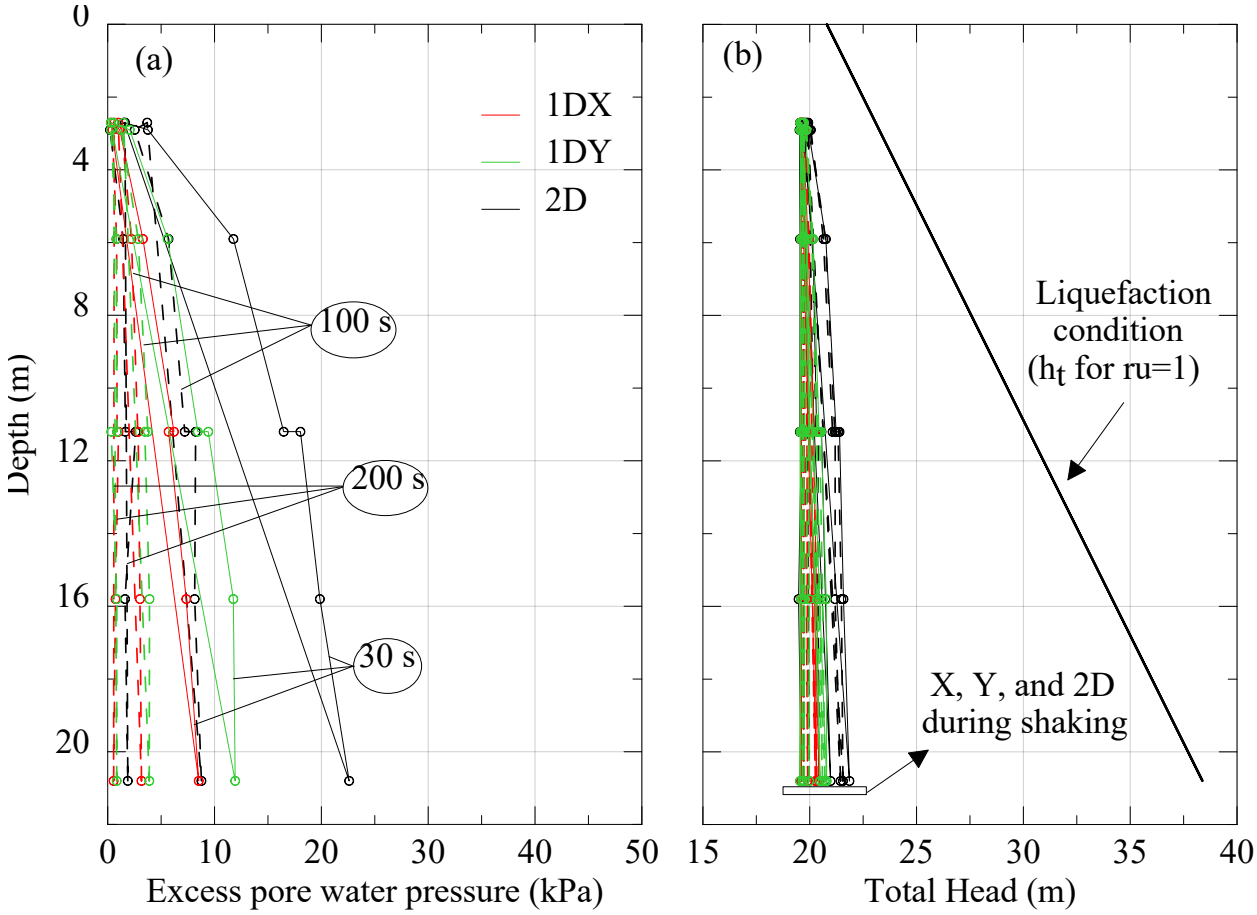

Figure C-255 Variation of total (a) Excess pore water pressure ratio (ru) with depth (M1-X,Y and 2D); (e) to (b) Total Head Loss with depth (M1-X,Y and 2D)

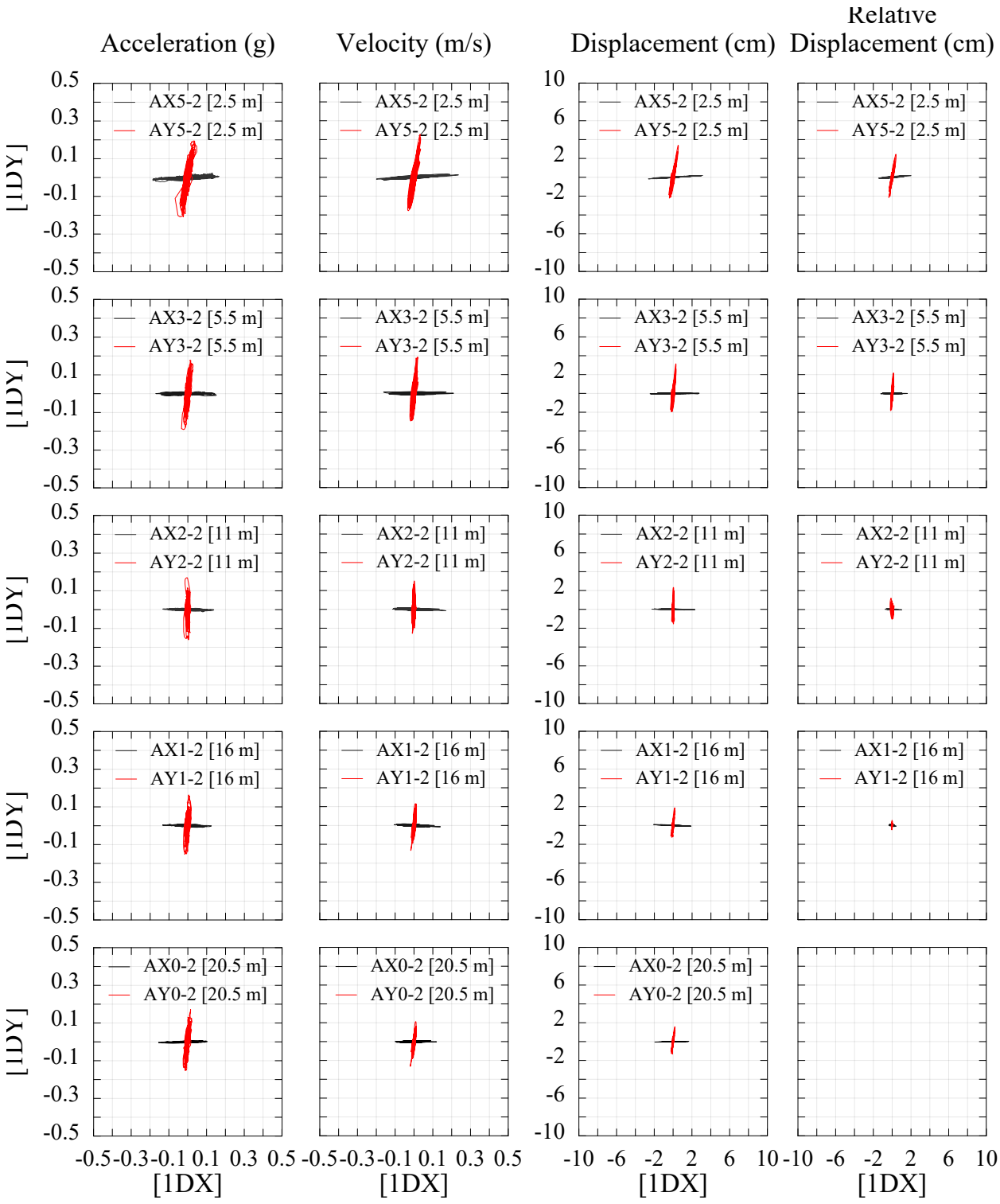

Figure C-256 Recorded input and within model ground motions for acceleration, velocity, displacement and relative displacement for M1-1D [X] and M1-1D [Y]

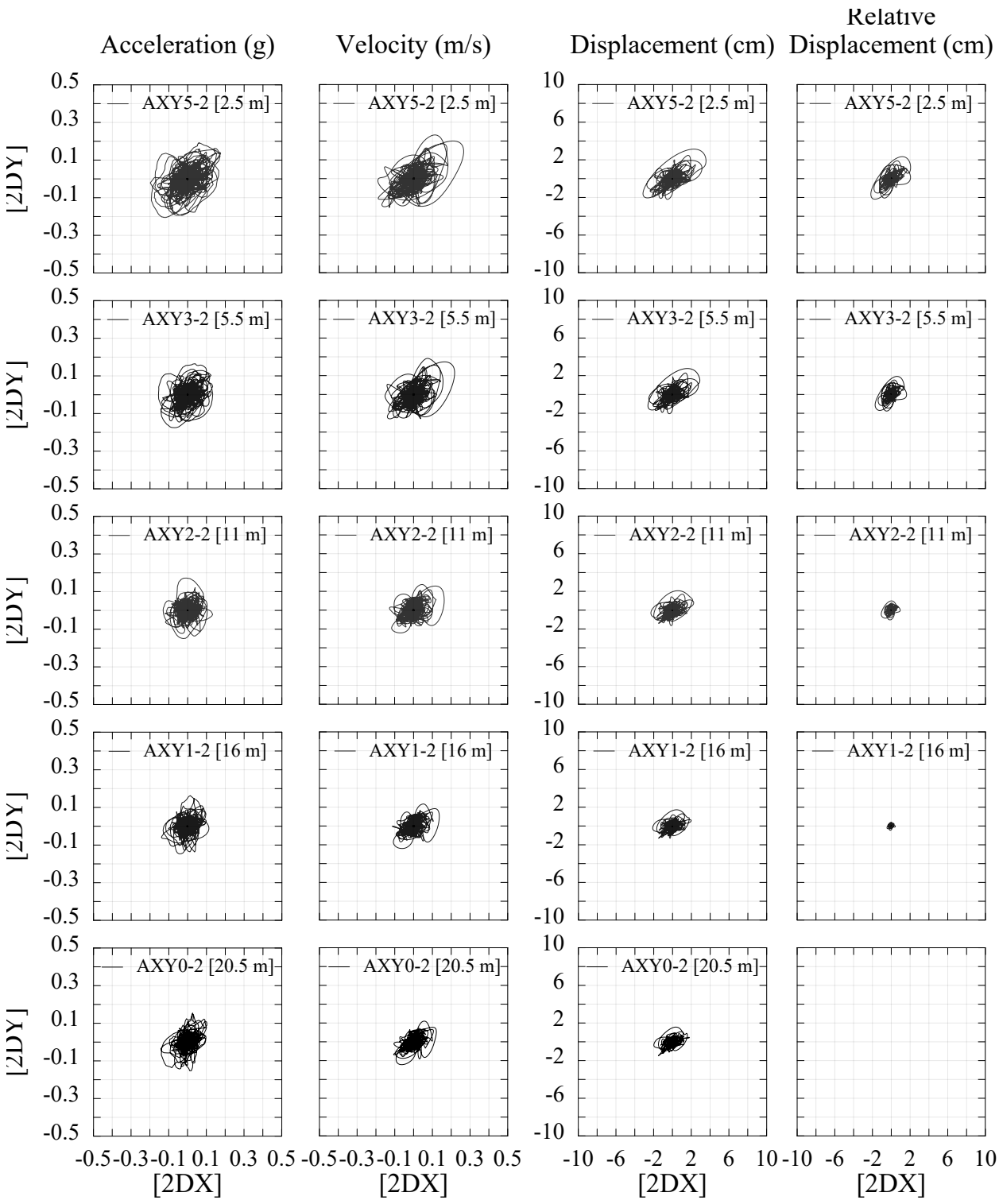

Figure C-257 Recorded input and within model ground motions for acceleration, velocity, displacement and relative displacement for M1-2D

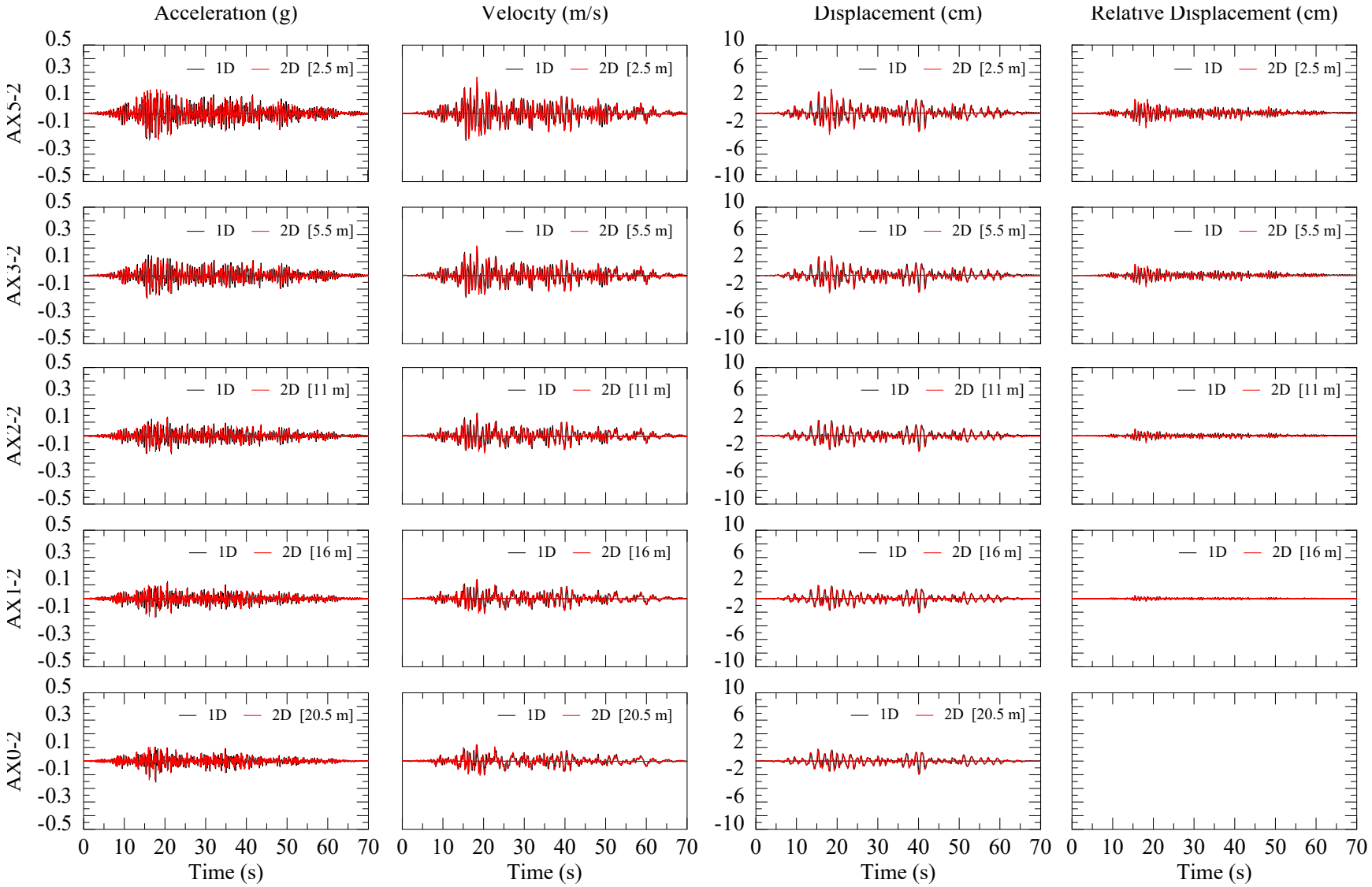

Figure C-258 Recorded input and within model ground motions time histories for acceleration, velocity, displacement and relative displacement for M1-2D [X] and M1-1D [X]

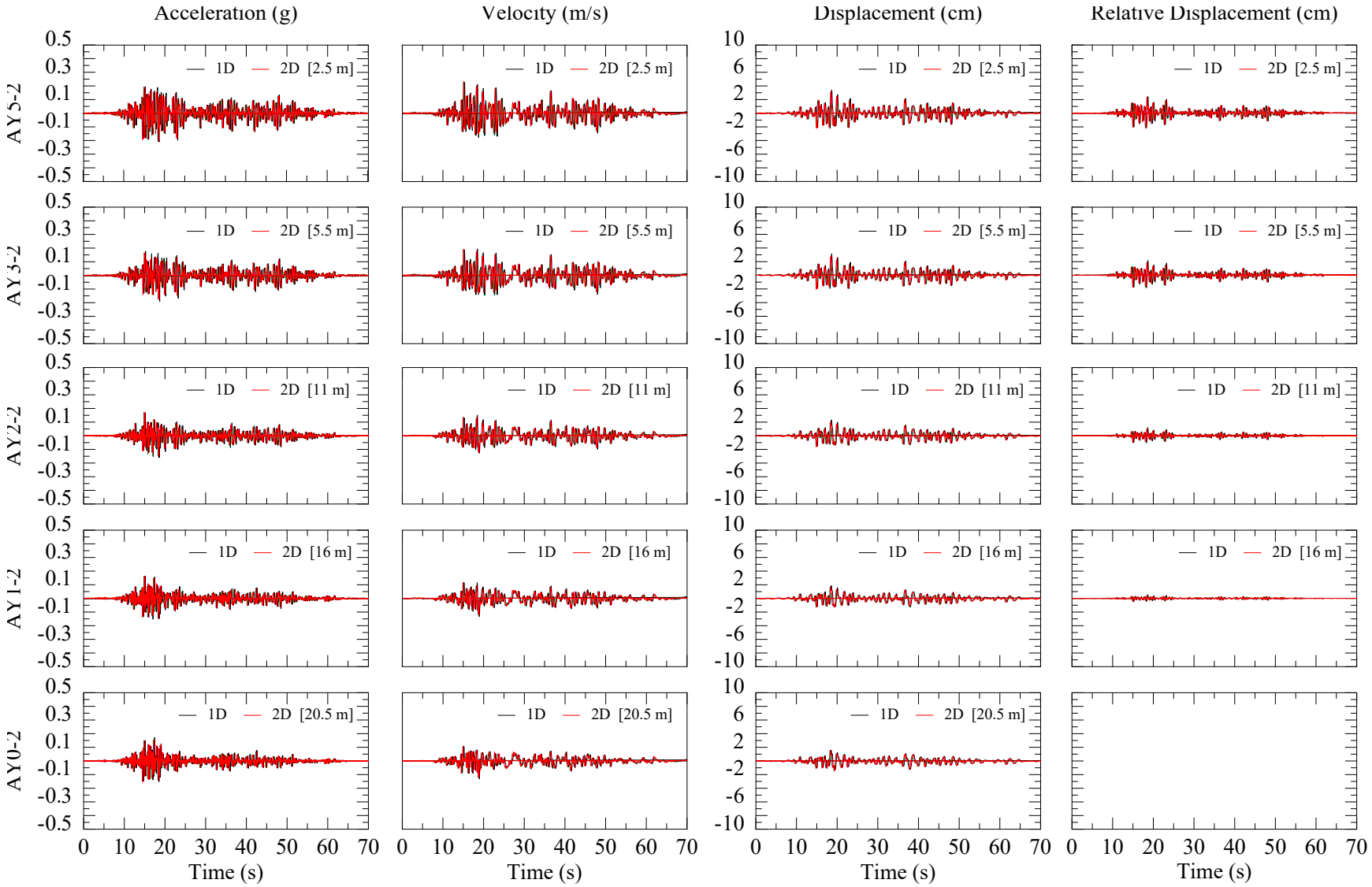

Figure C-259 Recorded input and within model ground motions time histories for acceleration, velocity, displacement and relative displacement for M1-2D [Y] and M1-1D [Y]

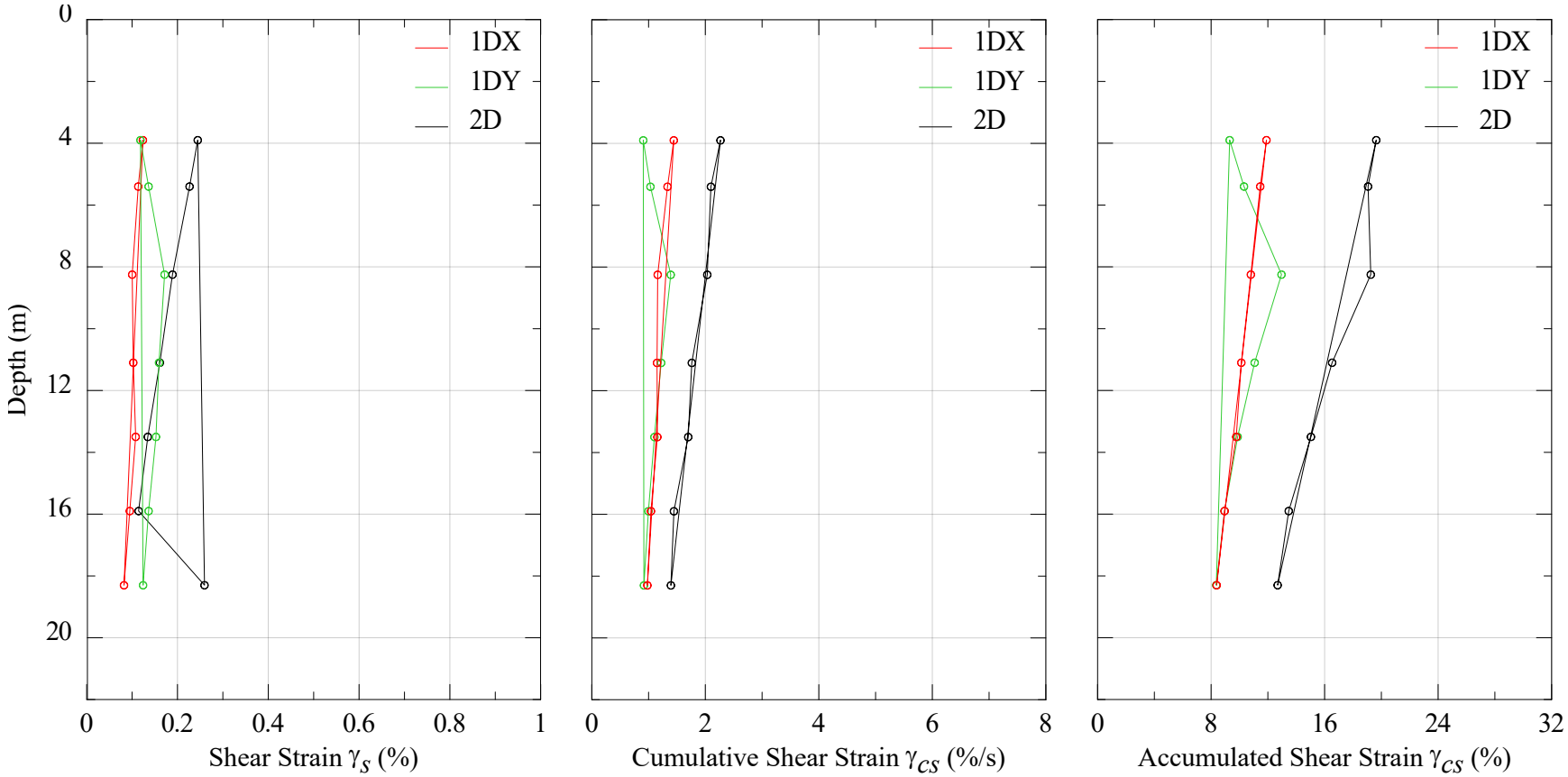

Figure C-260 Estimated (a) maximum shear strain; (b) cumulative shear strain; and (c) accumulated shear strain for M1-2D [X] and M1-1D [X]

1.4.4 Motion 12 (M12)

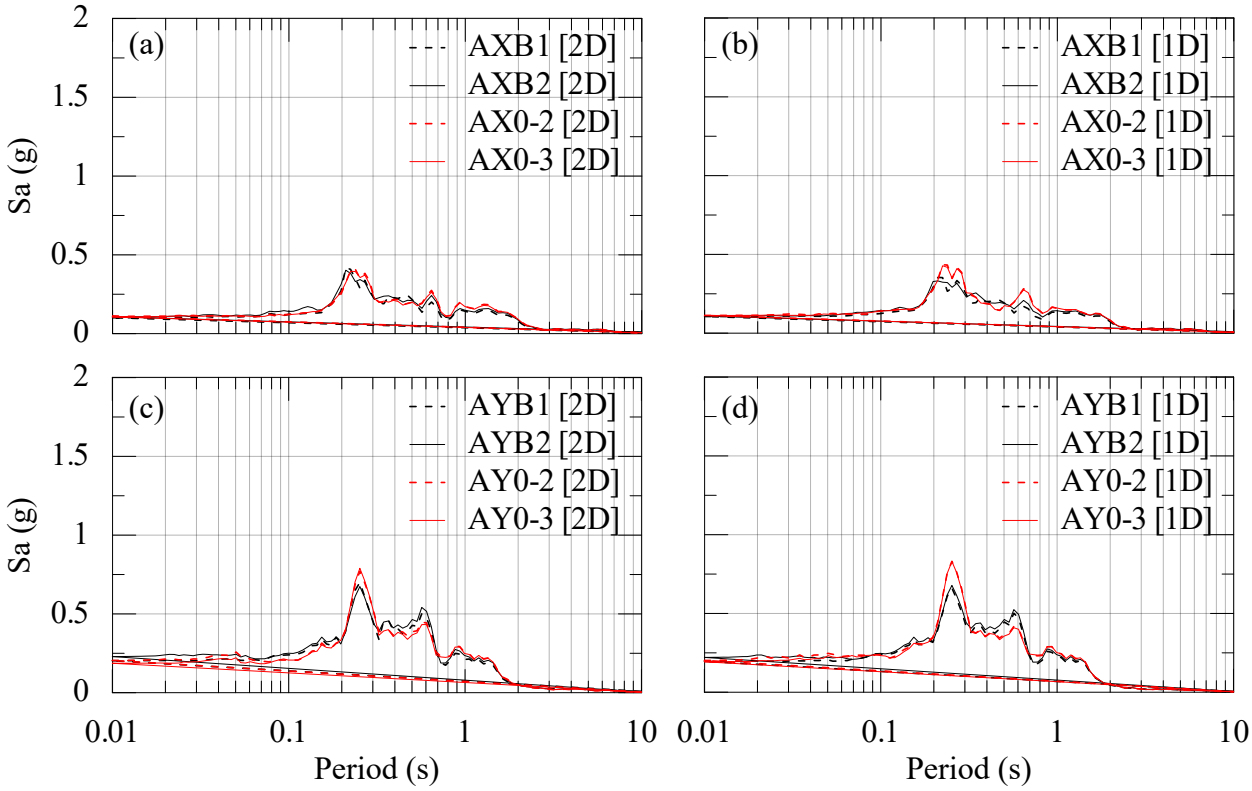

Figure C-261 Comparison of response spectra of 2D laminar container table and within model base input motion for motions (M12-X, Y and 2D).

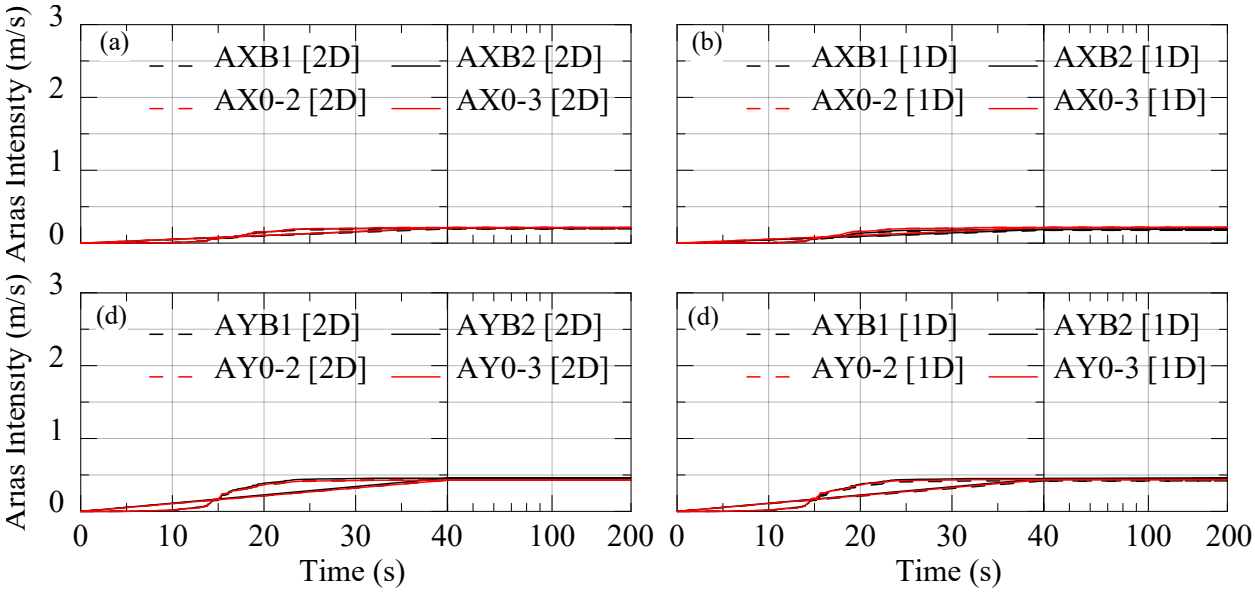

Figure C-262 Comparison of Arias Intensity of 2D laminar container table and within model base input motion for motions (a) M12-2D [X]; (b) M12-2D [Y]; (c) M12-1D [X] and (d) M12-1D [Y]

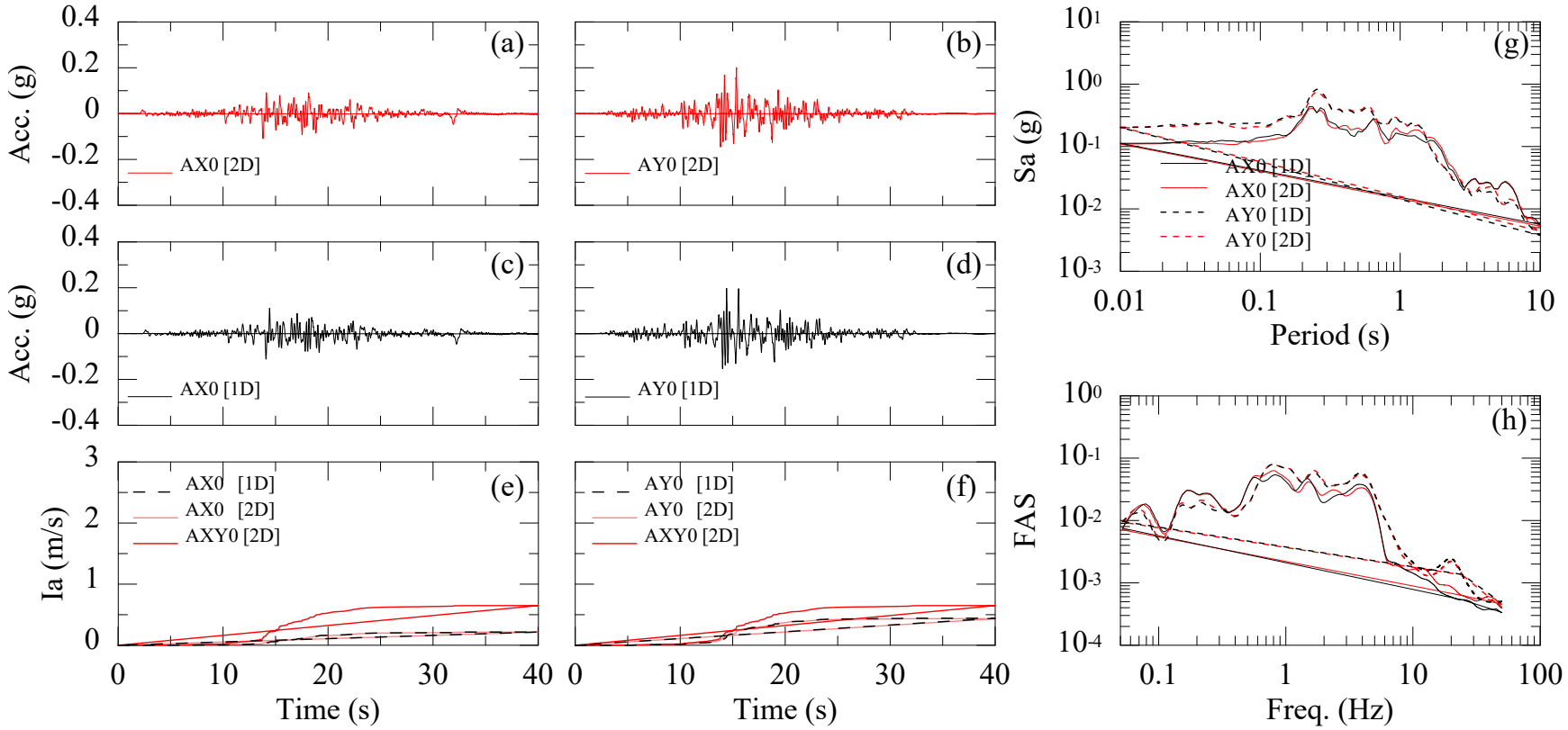

Figure C-263 Recorded input (2D) and 1D (X or Y) ground motions for: (a) M12-2D [X]; (b) M12-2D [Y]; (c) M12-1D [X]; and (d) M12-1D [Y]. Arias Intensity M12 (1D and 2D) for: (e) X direction; and (f) Y direction. Response Spectra (g) M12-2D [X]; M12-2D [Y]; M12-1D [X]; and M12-1D [Y]. Smoothed Fourier amplitude spectra (FAS) (h) M12-2D [X]; M12-2D [Y]; M12-1D [X]; and M12-1D [Y].

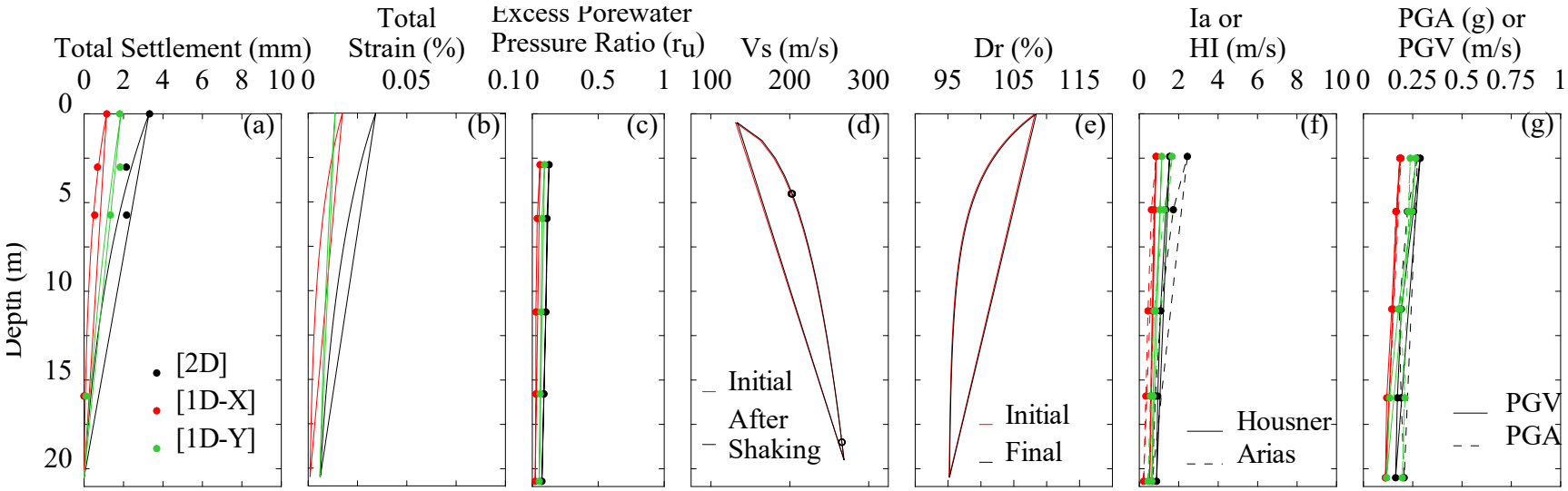

Figure C-264 Recorded or computed profiles for input motion M12-X, Y, and 2D. (a) Settlement; (b) total strain; (c) excess pore water pressure ratio; (d) shear wave velocity; (e) relative density; (f) Arias and Housner intensities; and (g) PGA and PGV.

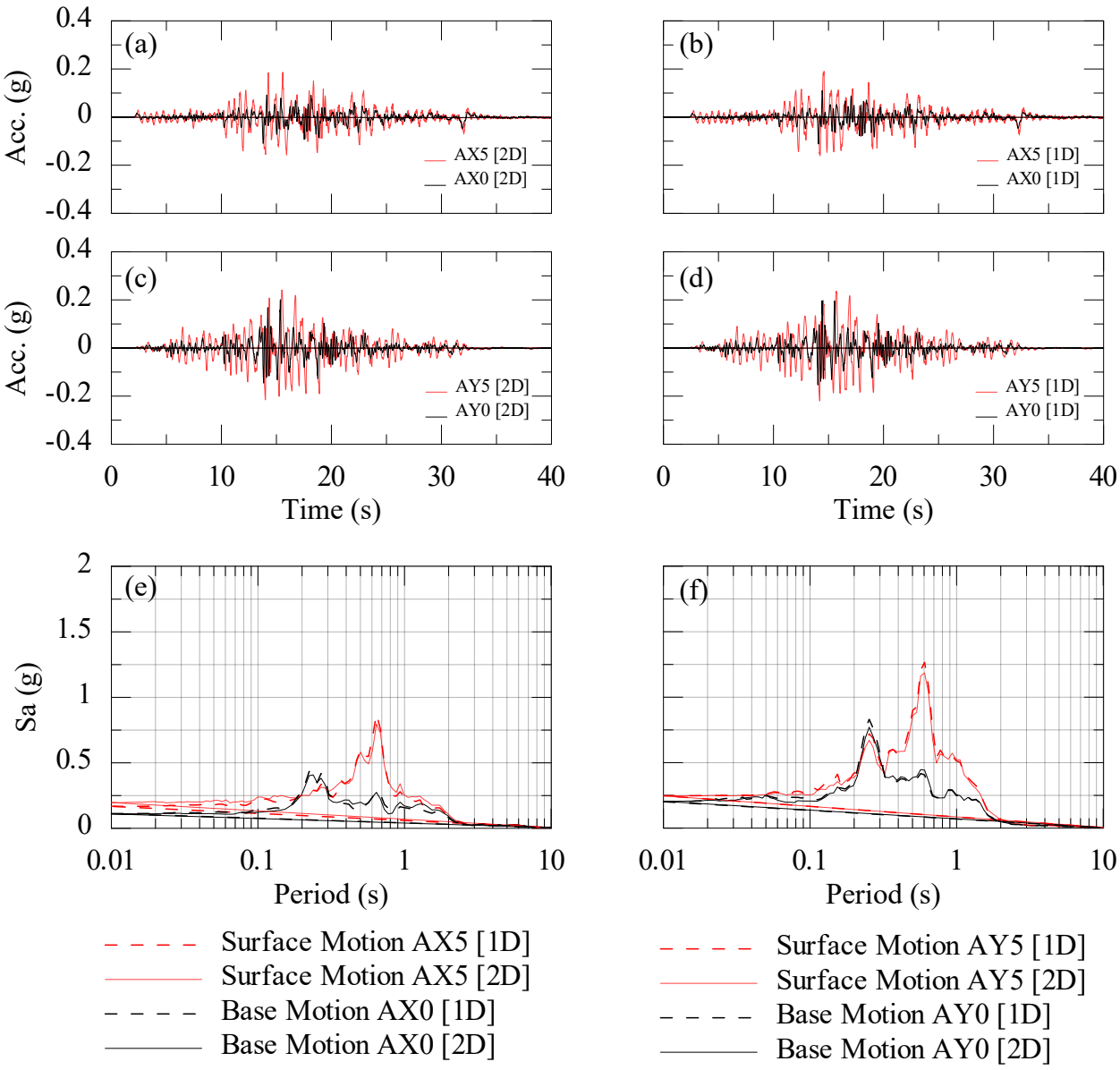

Figure C-265 Recorded input and surface ground motion: (a) M12-2D [X]; (b) M12-1D [X]; (c) M12-2D [Y]; and (d) M12-1D [Y]. Computed response spectra from Free Field Test [PT2] for motions M12 (1D and 2D) for: (e) X direction; and (f) Y direction.

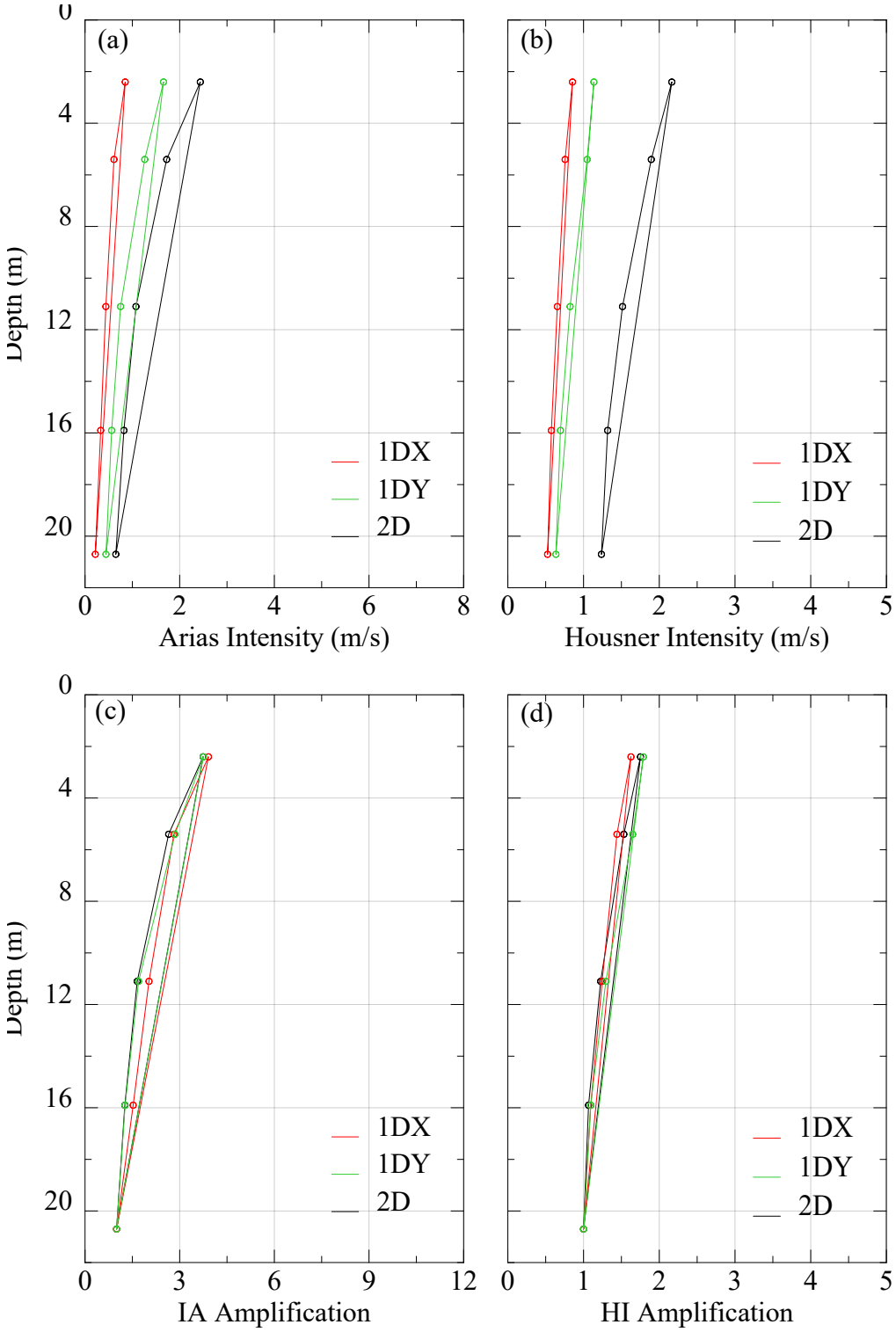

Figure C-266 Variation of total (a) Arias Intensity (M12-X,Y and 2D) ; (b) Housner Intensity (M12-X,Y and 2D) (c) Arias Intensity Amplification Factor (M12-X,Y and 2D); and (d) Housner Intensity Amplification Factor (M12-X,Y and 2D).

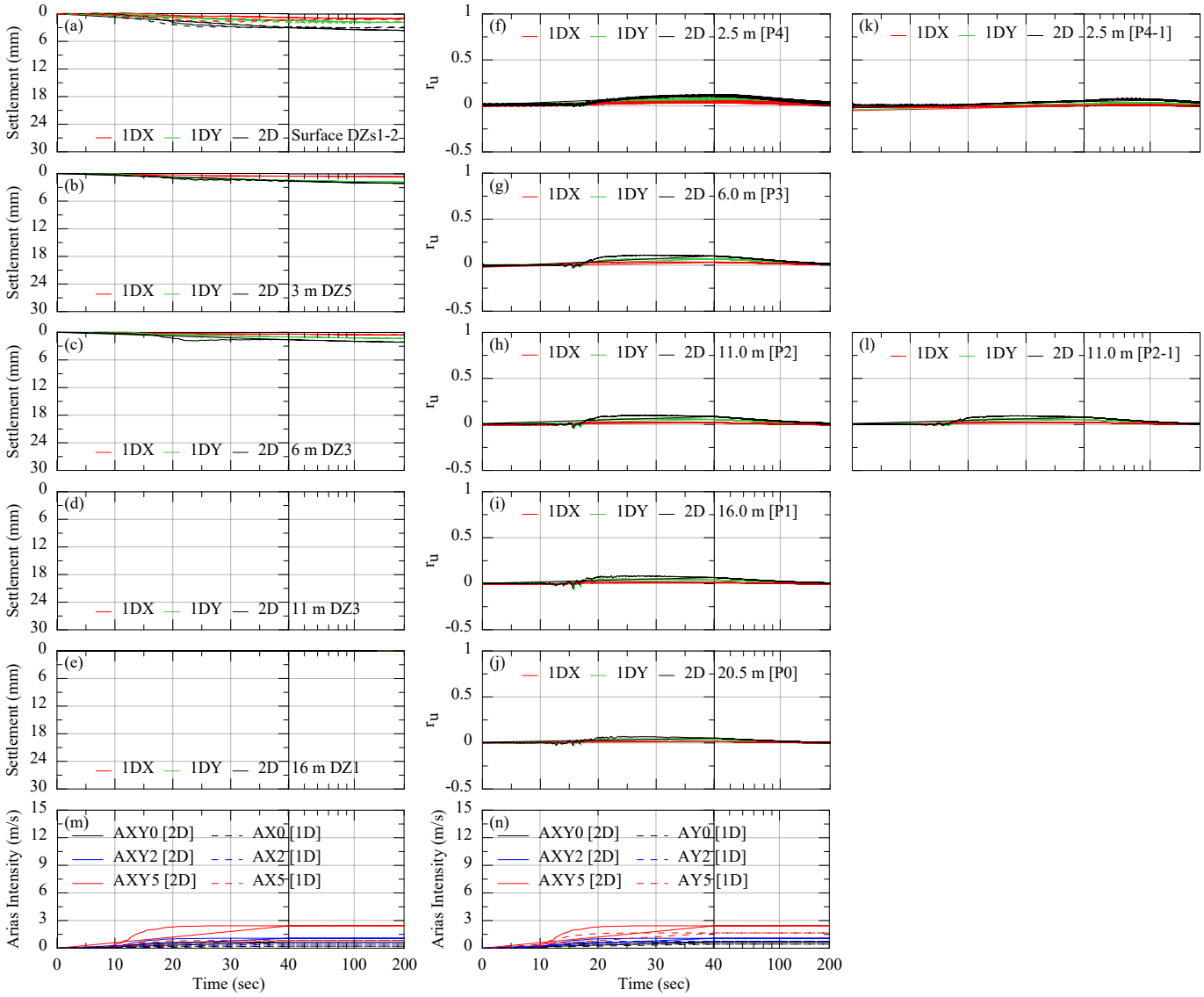

Figure C-267 Variation of total (a) to (e) Settlement with depth (M12-X,Y and 2D) ; (f) to (l) Excess pore water pressure ratio (ru) (M12-X,Y and 2D) (m) and (n) Arias Intensity along model (M12-X,Y and 2D).

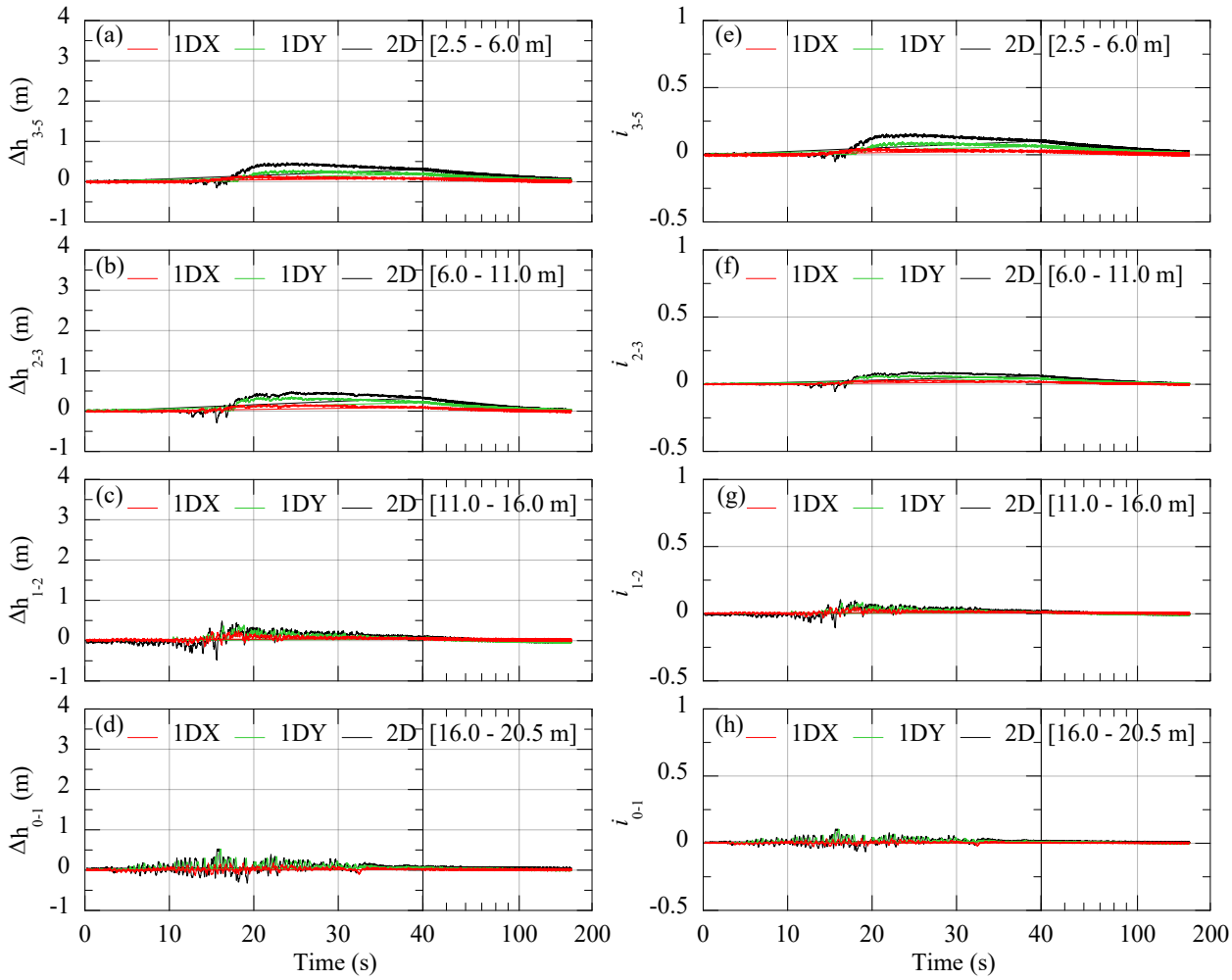

Figure C-268 Variation of total (a) to (d) Total Head Loss with depth (M12-X, Y and 2D); (e) to (h) Shaking induced Hydraulic Gradient (M12-X, Y and 2D)

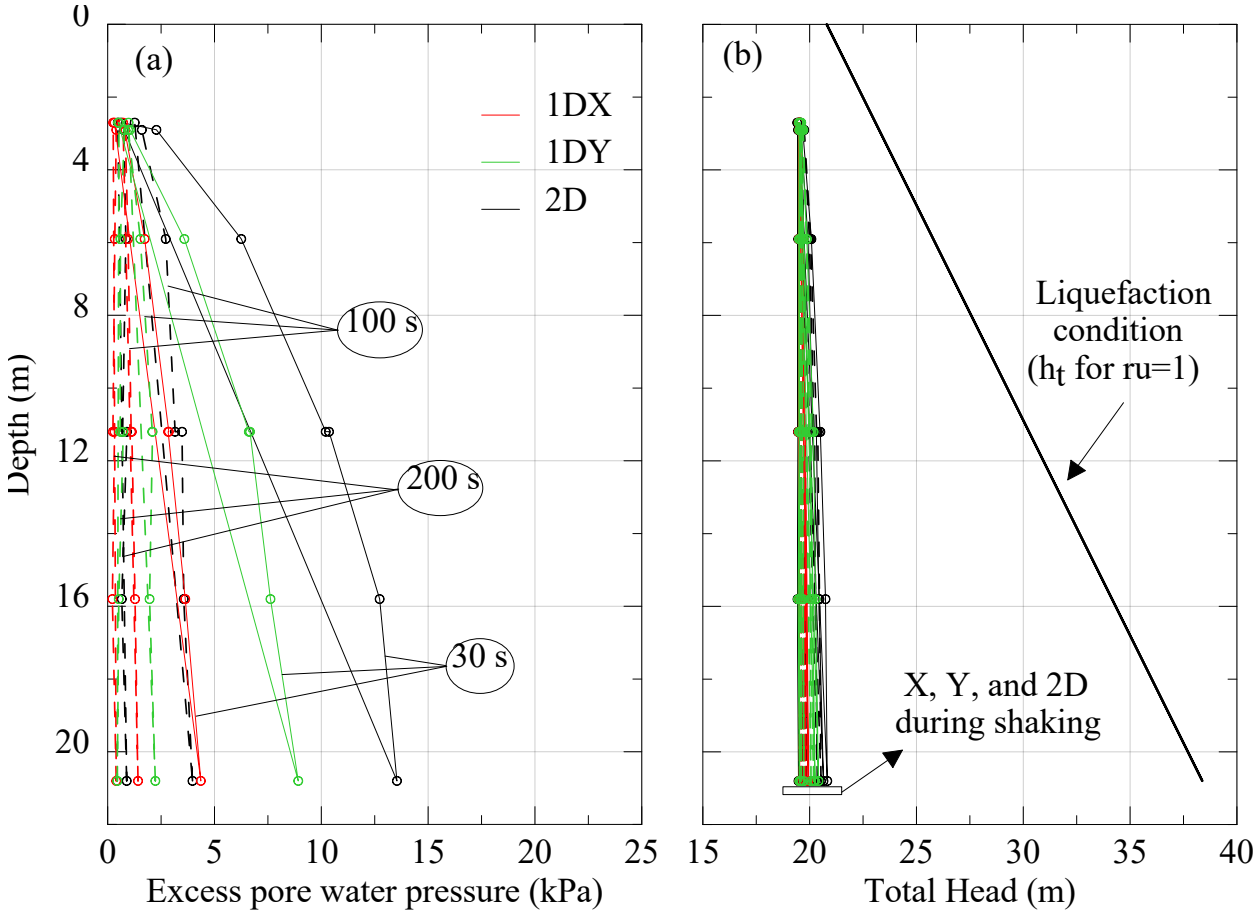

Figure C-269 Variation of total (a) Excess pore water pressure ratio (ru) with depth (M12-X,Y and 2D); (e) to (b) Total Head Loss with depth (M12-X,Y and 2D)

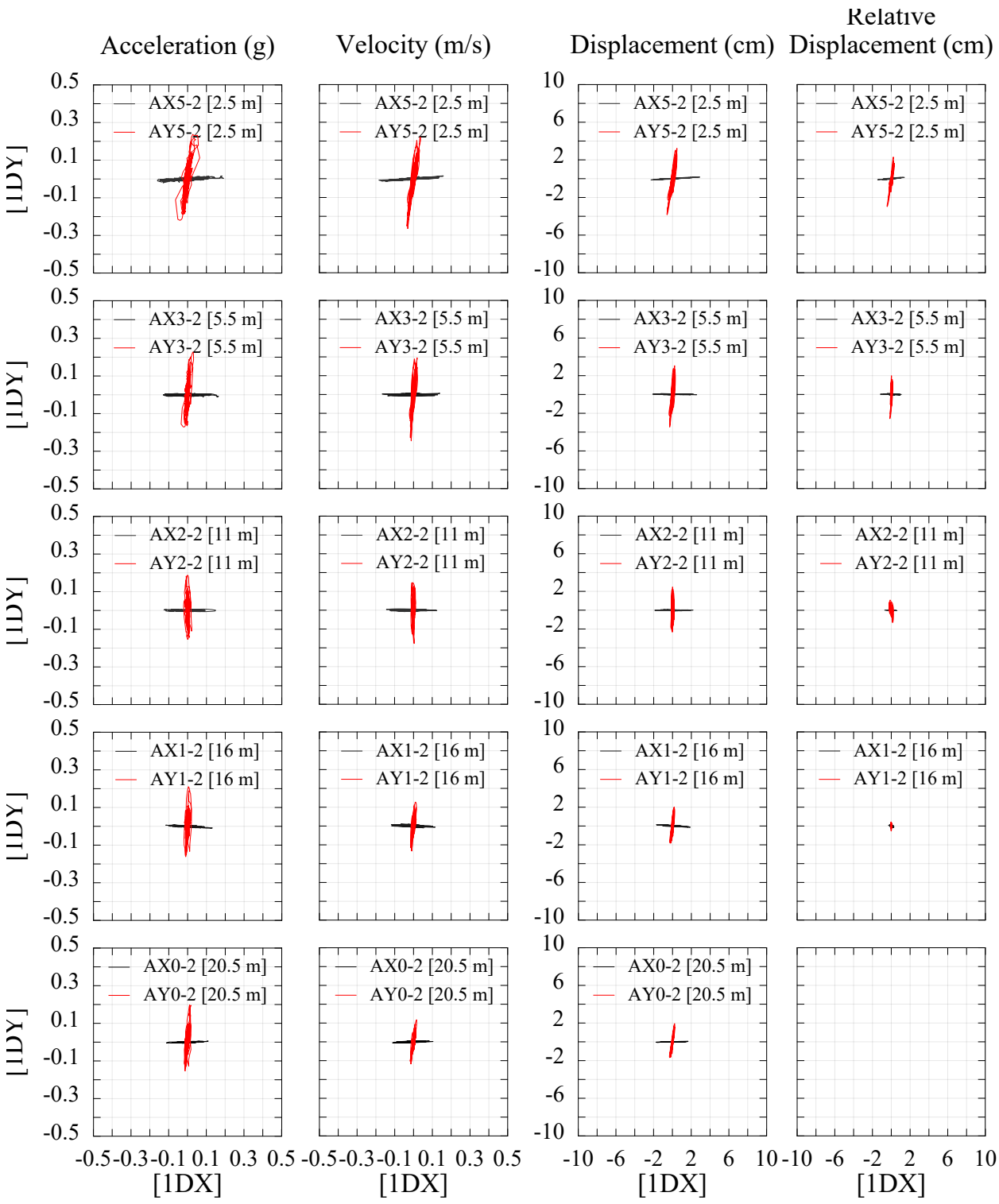

Figure C-270 Recorded input and within model ground motions for acceleration, velocity, displacement and relative displacement for M12-1D [X] and M12-1D [Y]

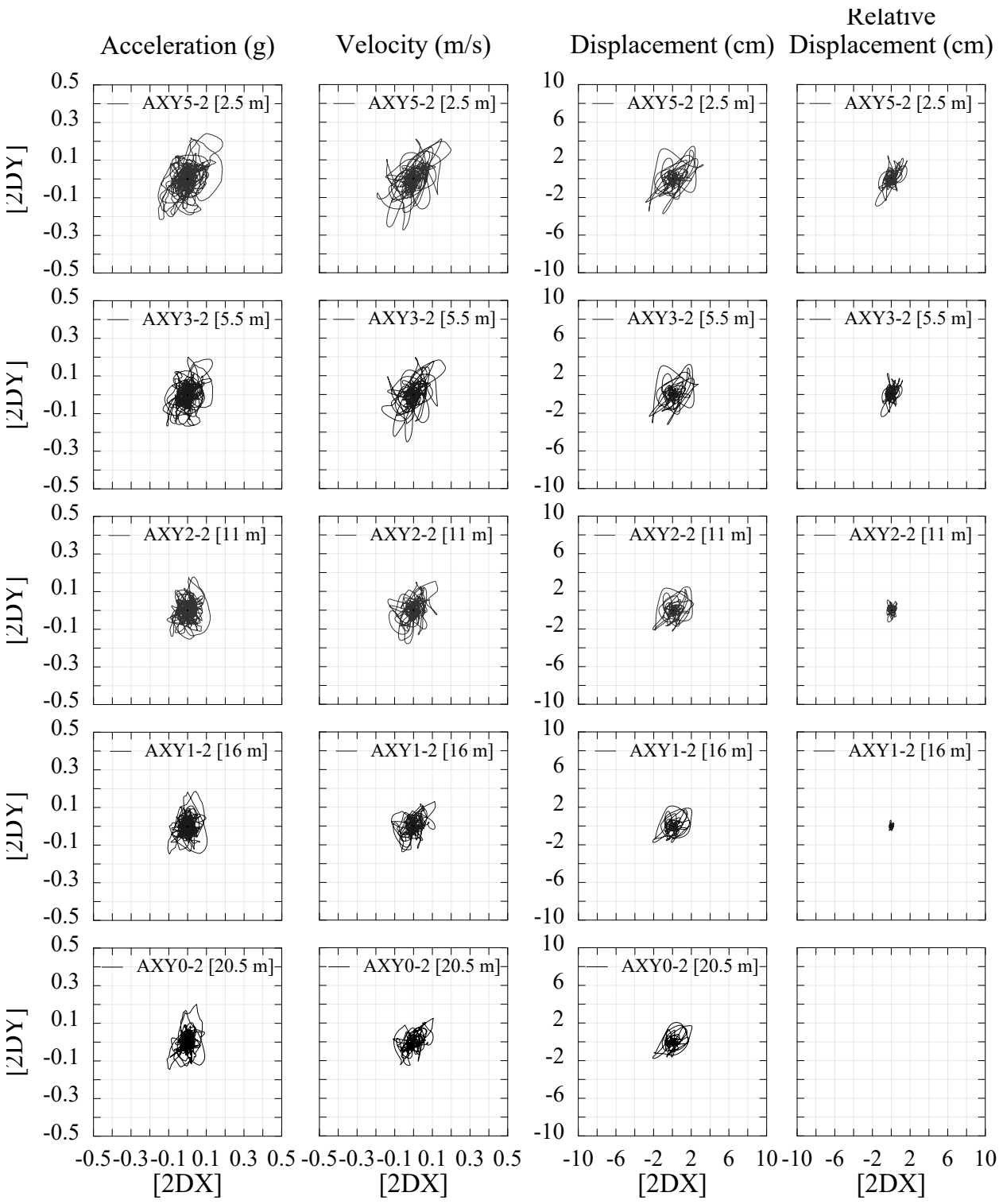

Figure C-271 Recorded input and within model ground motions for acceleration, velocity, displacement and relative displacement for M12-2D

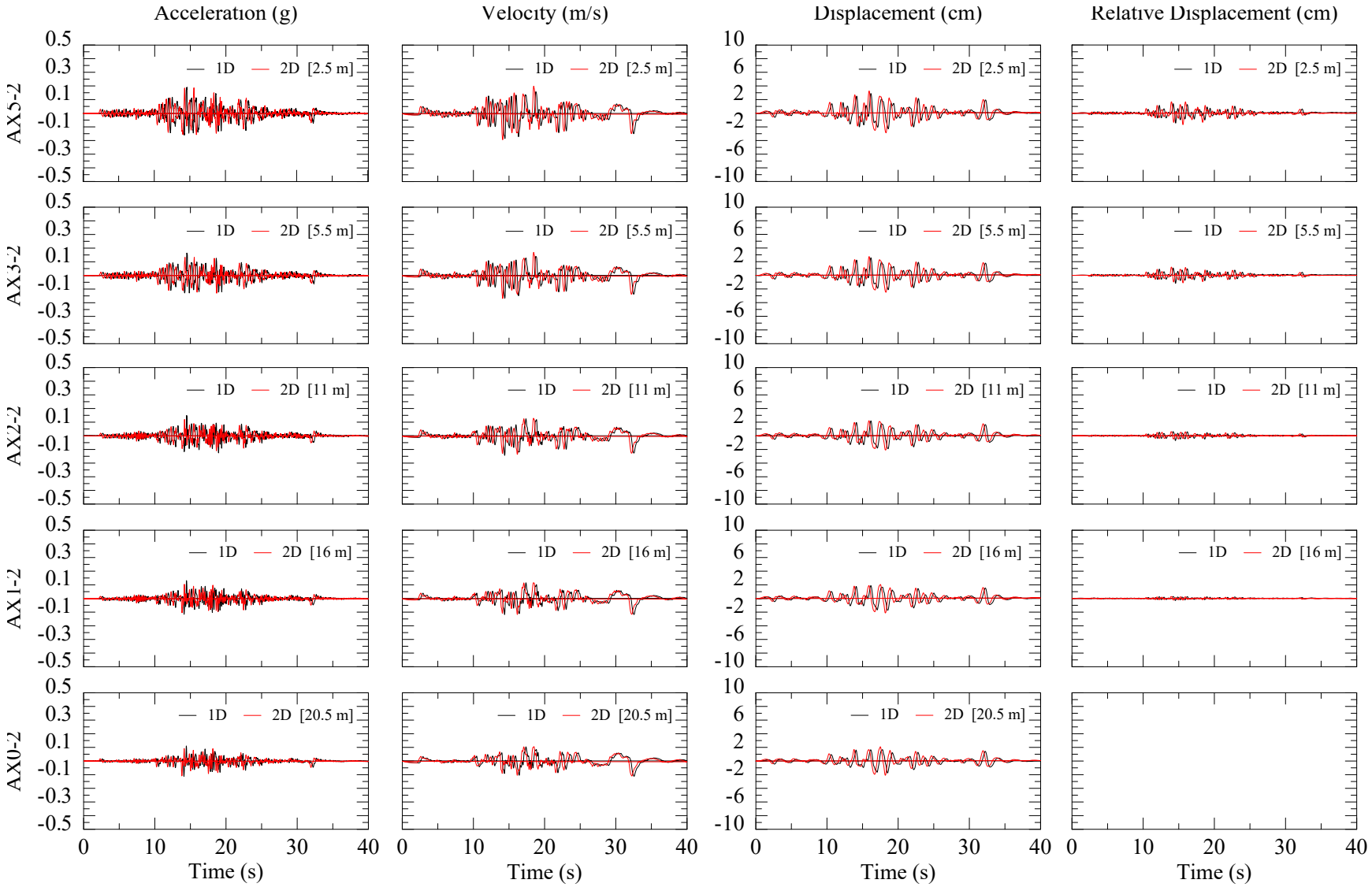

Figure C-272 Recorded input and within model ground motions time histories for acceleration, velocity, displacement and relative displacement for M12-2D [X] and M12-1D [X]

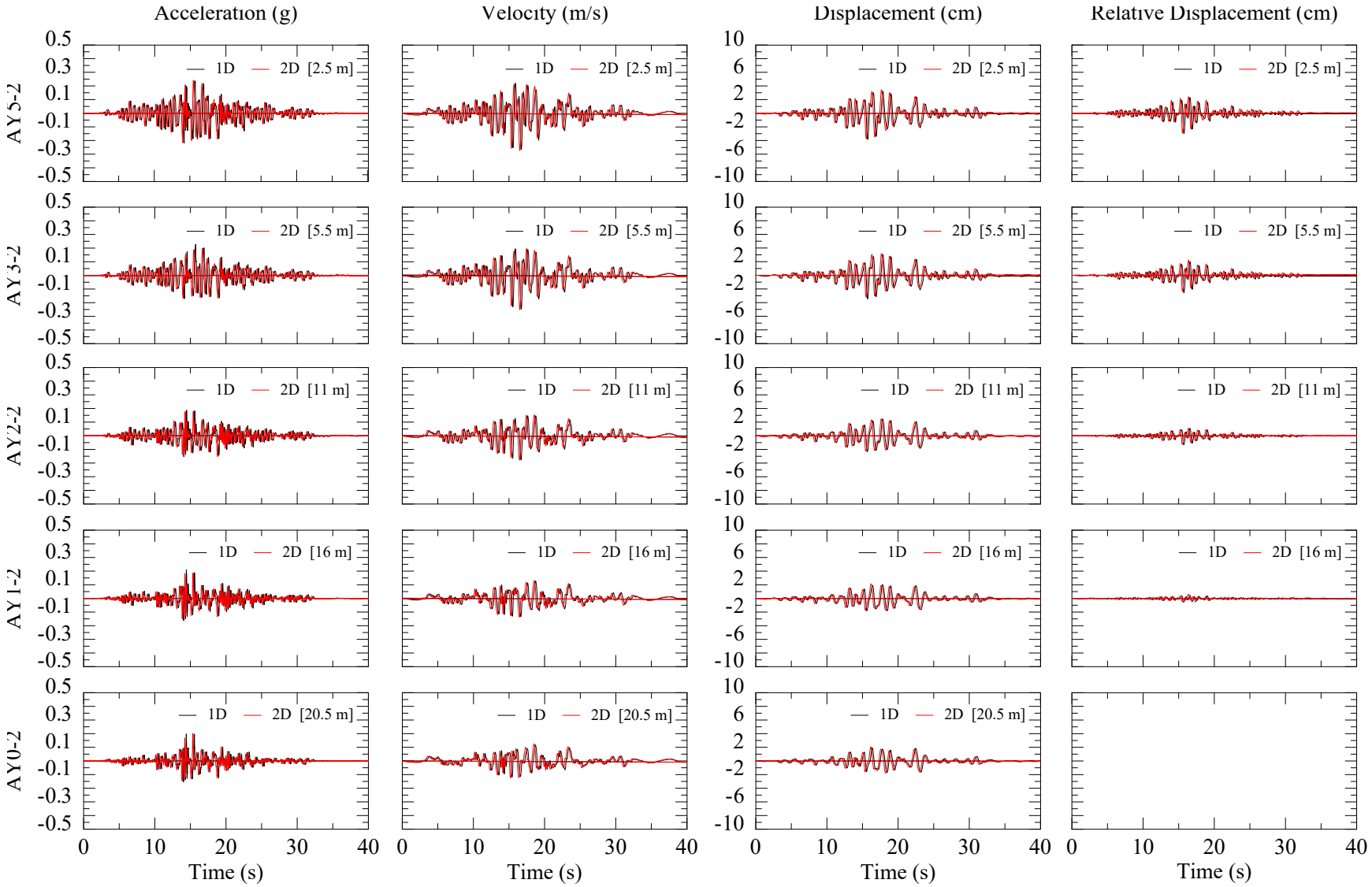

Figure C-273 Recorded input and within model ground motions time histories for acceleration, velocity, displacement and relative displacement for M12-2D [Y] and M12-1D [Y]

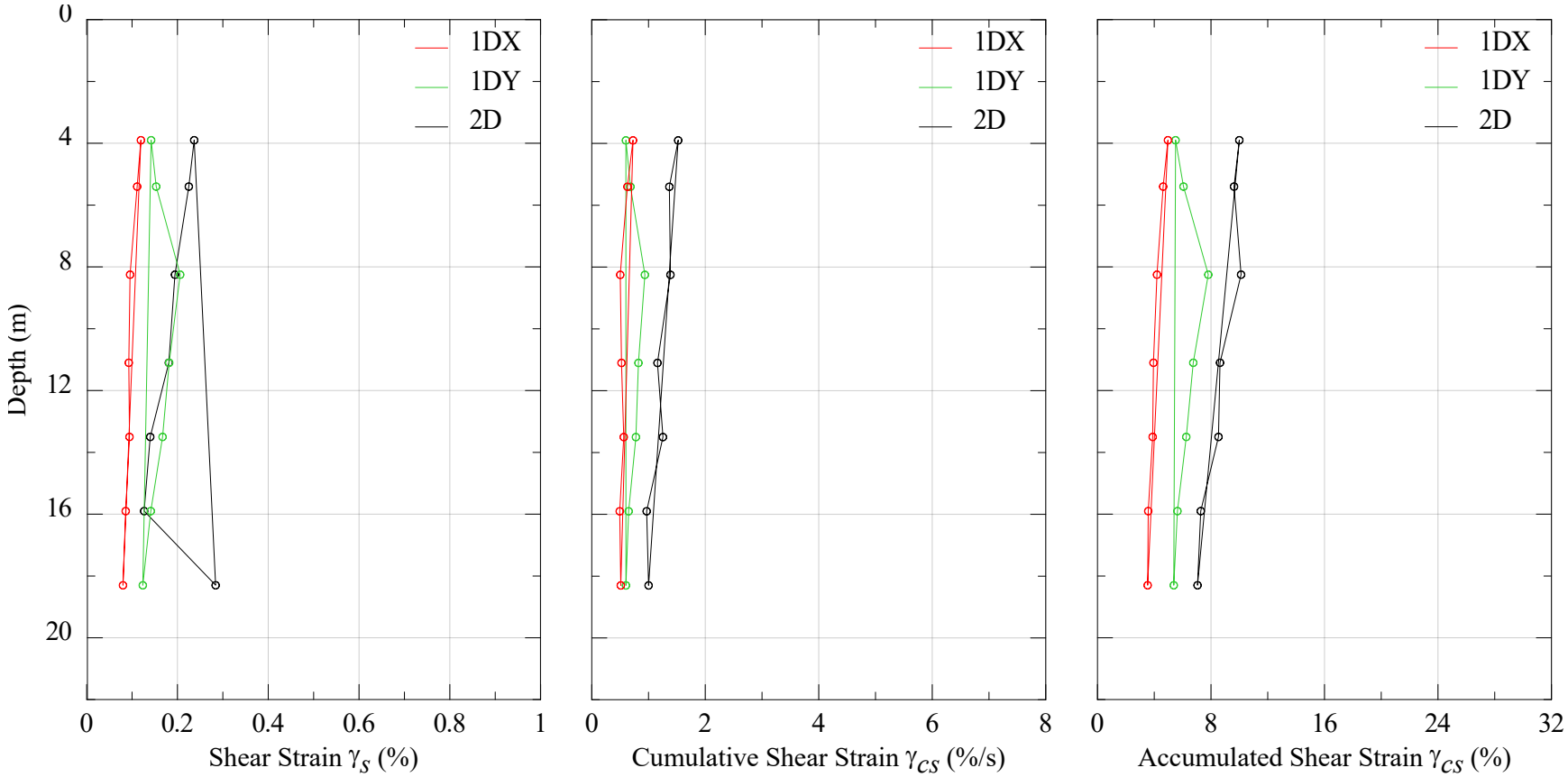

Figure C-274 Estimated (a) maximum shear strain; (b) cumulative shear strain; and (c) accumulated shear strain for M12-2D [X] and M12-1D [X]

1.4.5 Motion 13 (M13)

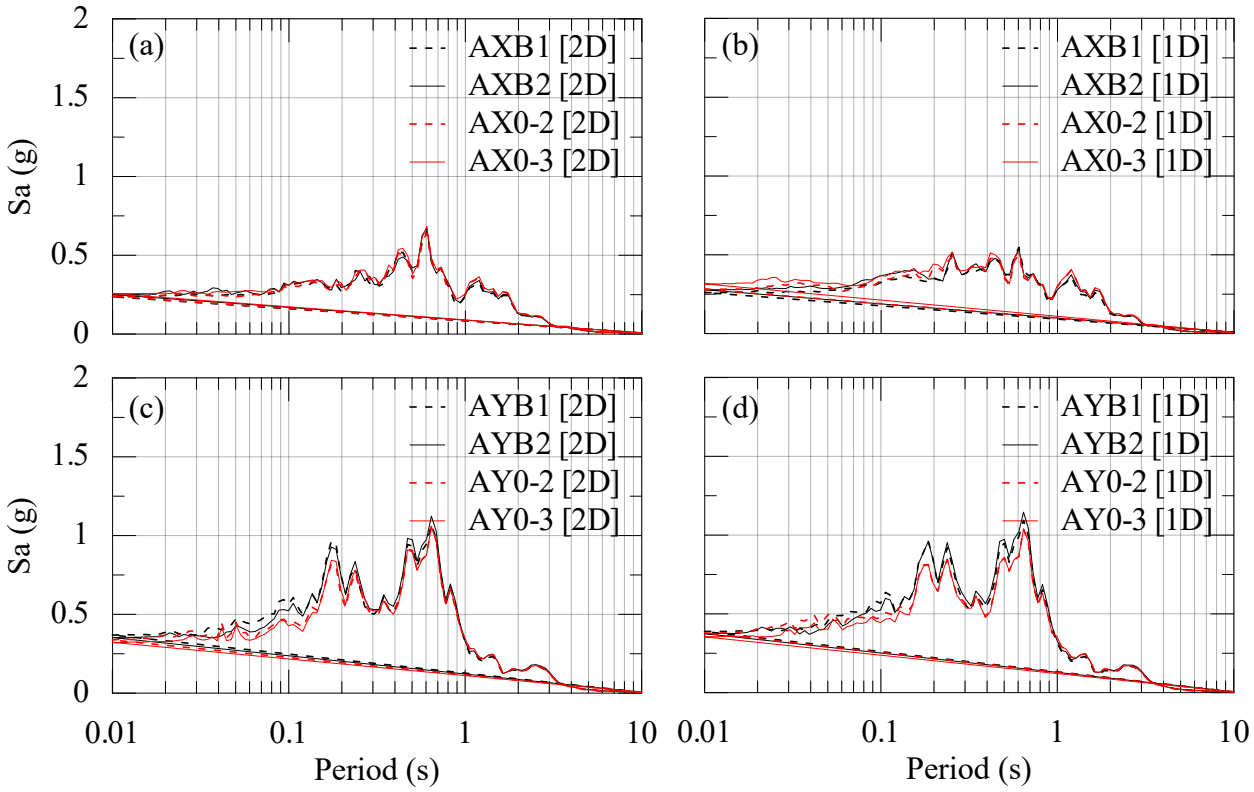

Figure C-275 Comparison of response spectra of 2D laminar container table and within model base input motion for motions (M13-X, Y and 2D).

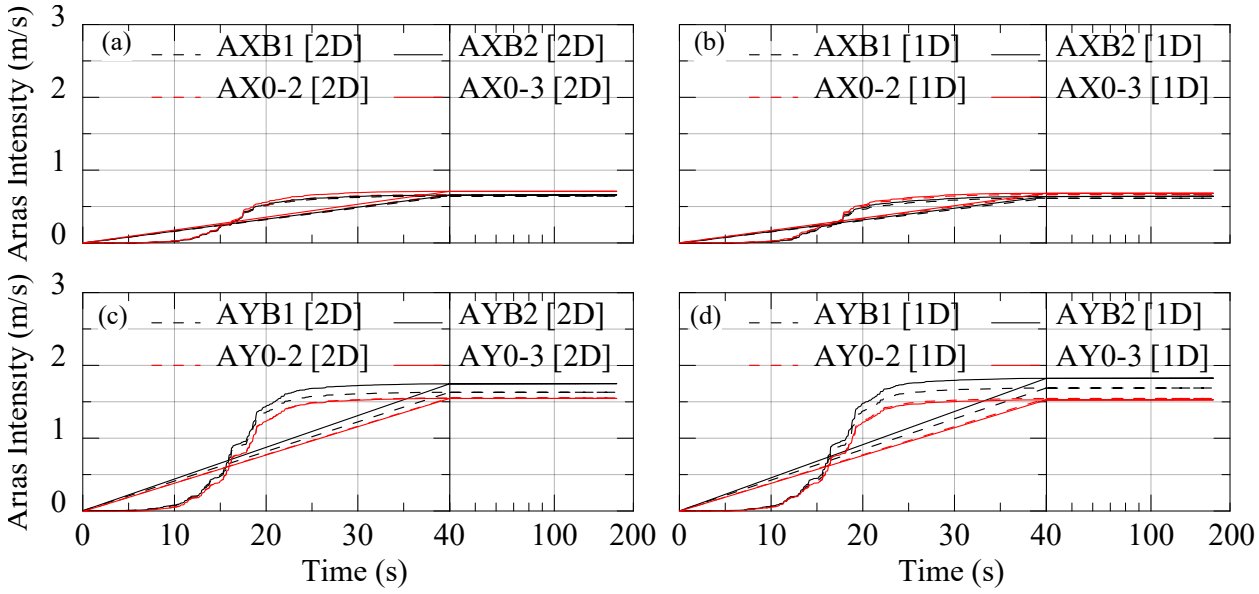

Figure C-276 Comparison of Arias Intensity of 2D laminar container table and within model base input motion for motions (a) M13-2D [X]; (b) M13-2D [Y]; (c) M13-1D [X] and (d) M13-1D [Y]

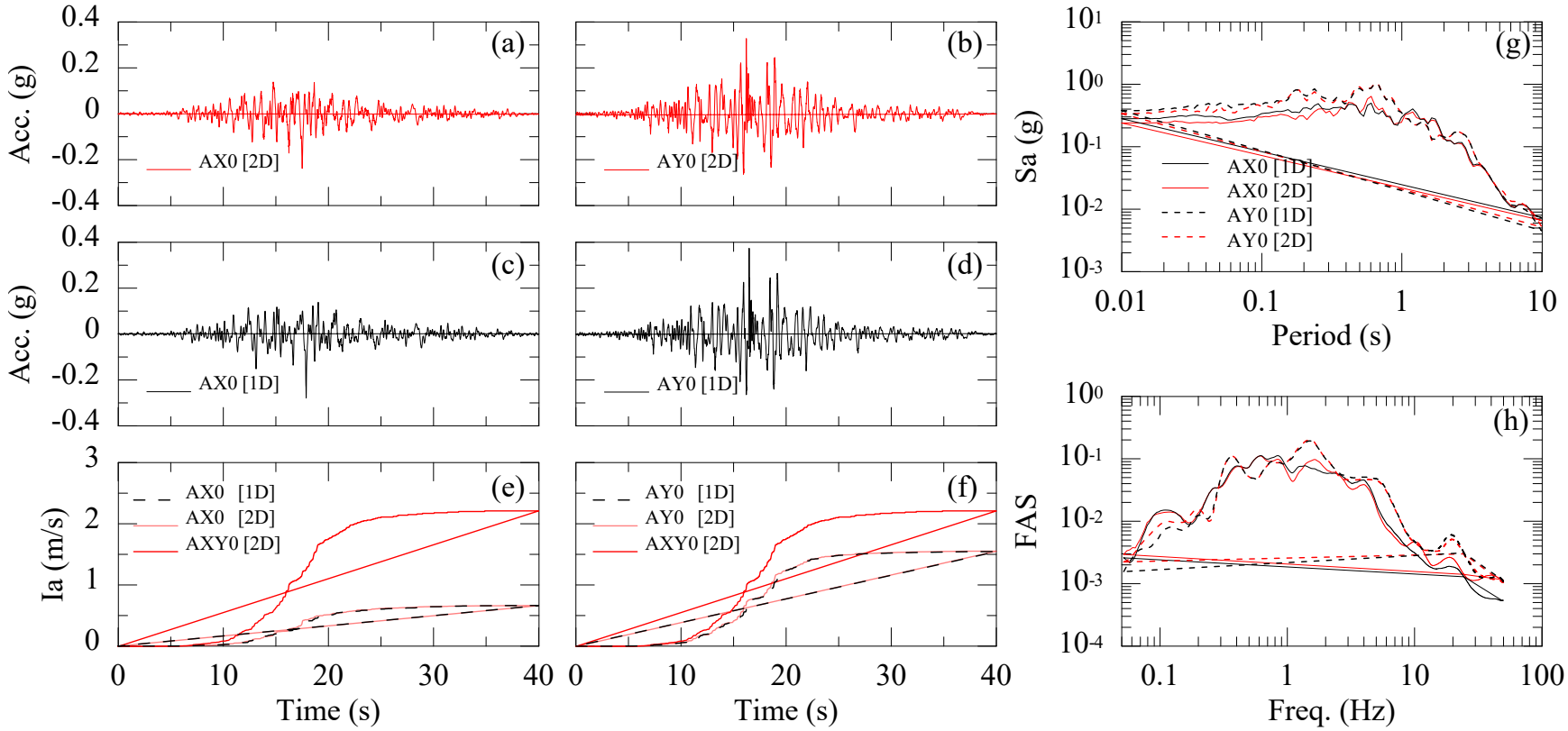

Figure C-277 Recorded input (2D) and 1D (X or Y) ground motions for: (a) M13-2D [X]; (b) M13-2D [Y]; (c) M13-1D [X]; and (d) M13-1D [Y]. Arias Intensity M13 (1D and 2D) for: (e) X direction; and (f) Y direction. Response Spectra (g) M13-2D [X]; M13-2D [Y]; M13-1D [X]; and M13-1D [Y]. Smoothed Fourier amplitude spectra (FAS) (h) M13-2D [X]; M13-2D [Y]; M13-1D [X]; and M13-1D [Y].

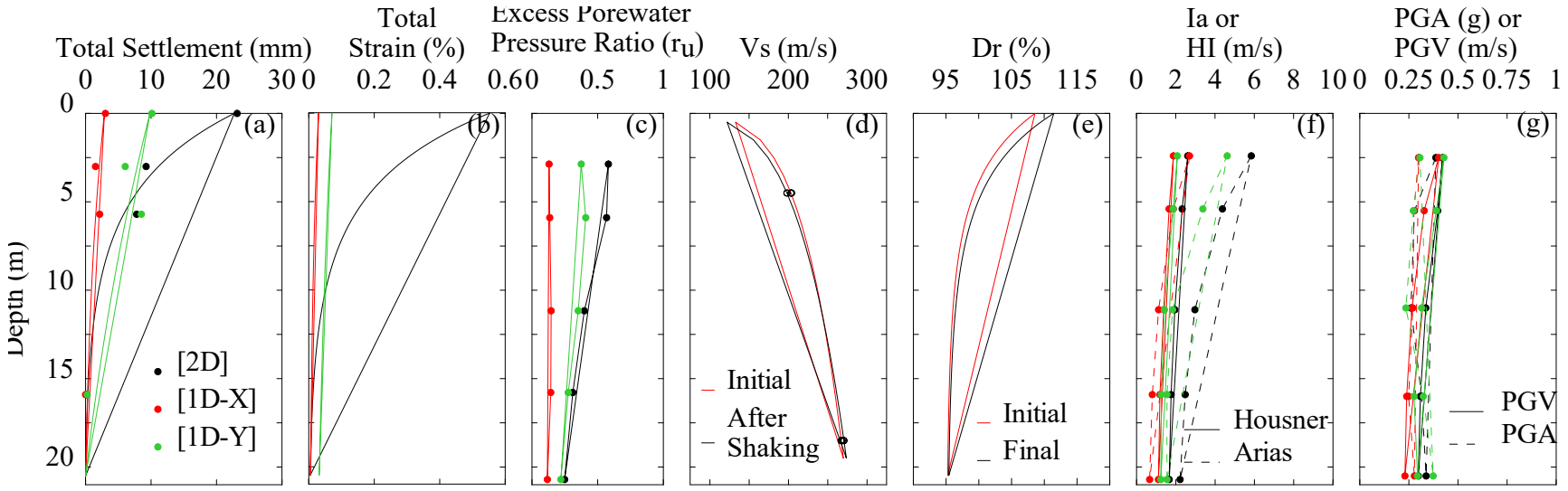

Figure C-278 Recorded or computed profiles for input motion M13-X, Y, and 2D. (a) Settlement; (b) total strain; (c) excess pore water pressure ratio; (d) shear wave velocity; (e) relative density; (f) Arias and Housner intensities; and (g) PGA and PGV.

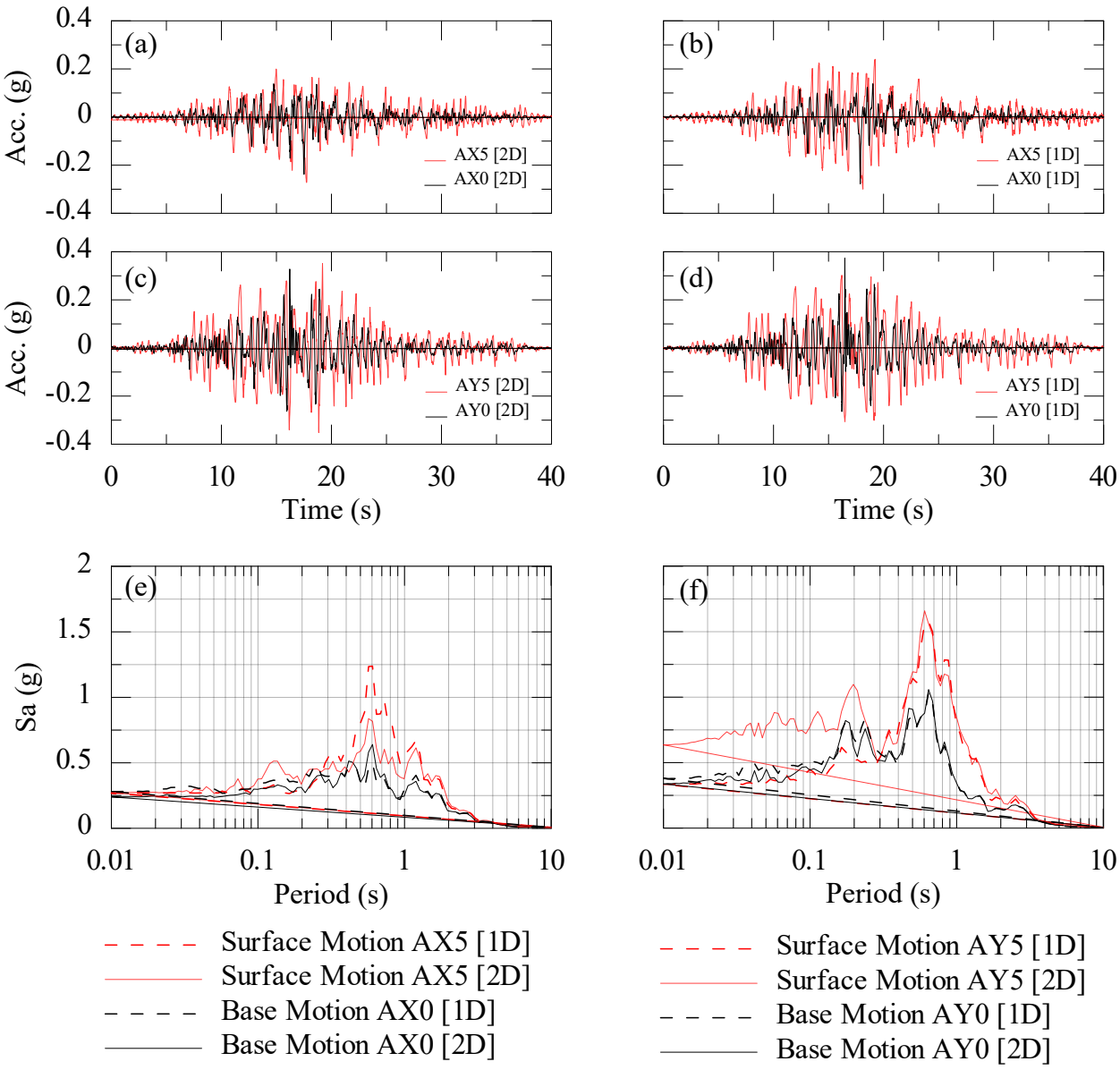

Figure C-279 Recorded input and surface ground motion: (a) M13-2D [X]; (b) M13-1D [X]; (c) M13-2D [Y]; and (d) M13-1D [Y]. Computed response spectra from Free Field Test [PT2] for motions M13 (1D and 2D) for: (e) X direction; and (f) Y direction.

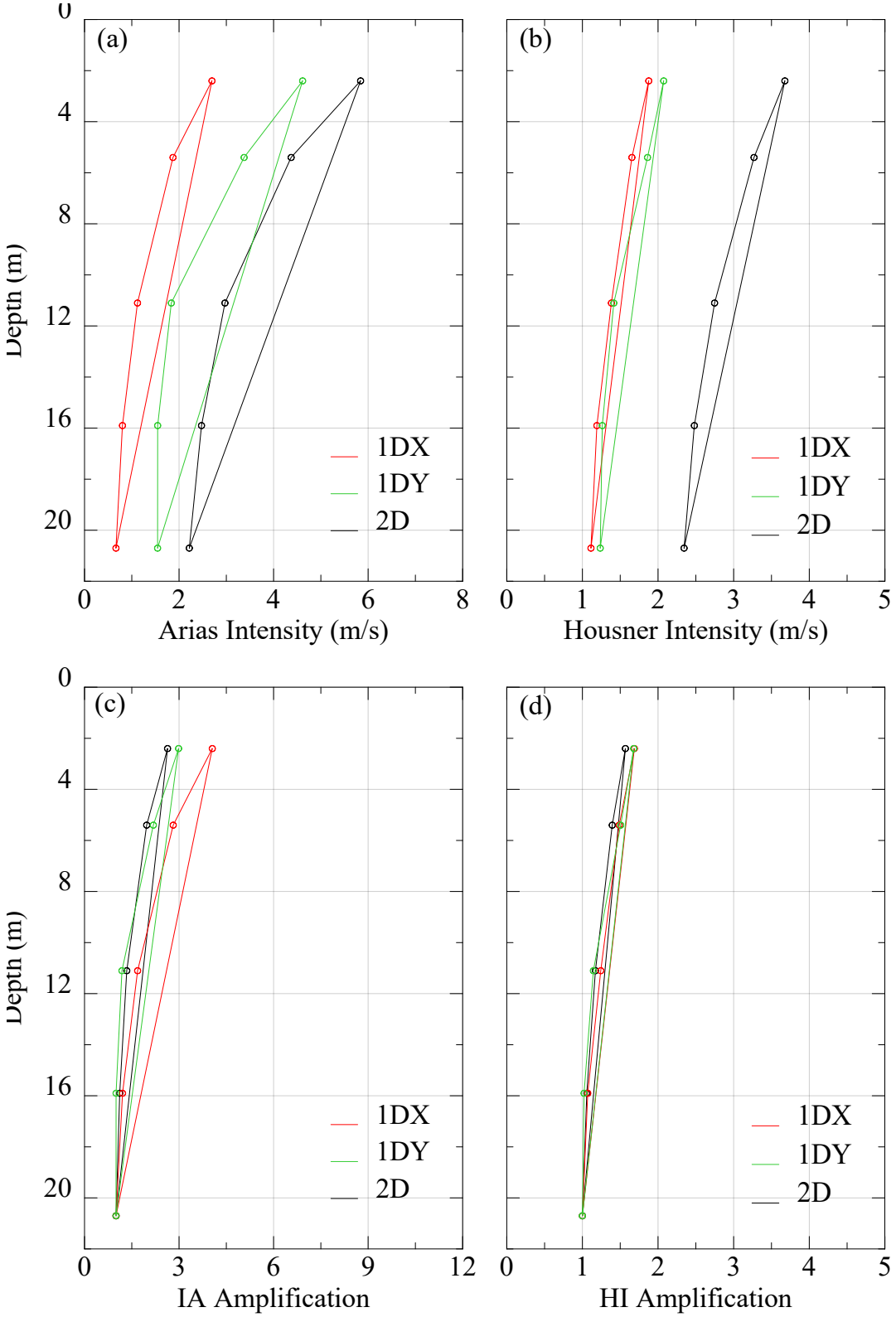

Figure C-280 Variation of total (a) Arias Intensity (M13-X,Y and 2D) ; (b) Housner Intensity (M13-X,Y and 2D) (c) Arias Intensity Amplification Factor (M13-X,Y and 2D); and (d) Housner Intensity Amplification Factor (M13-X,Y and 2D).

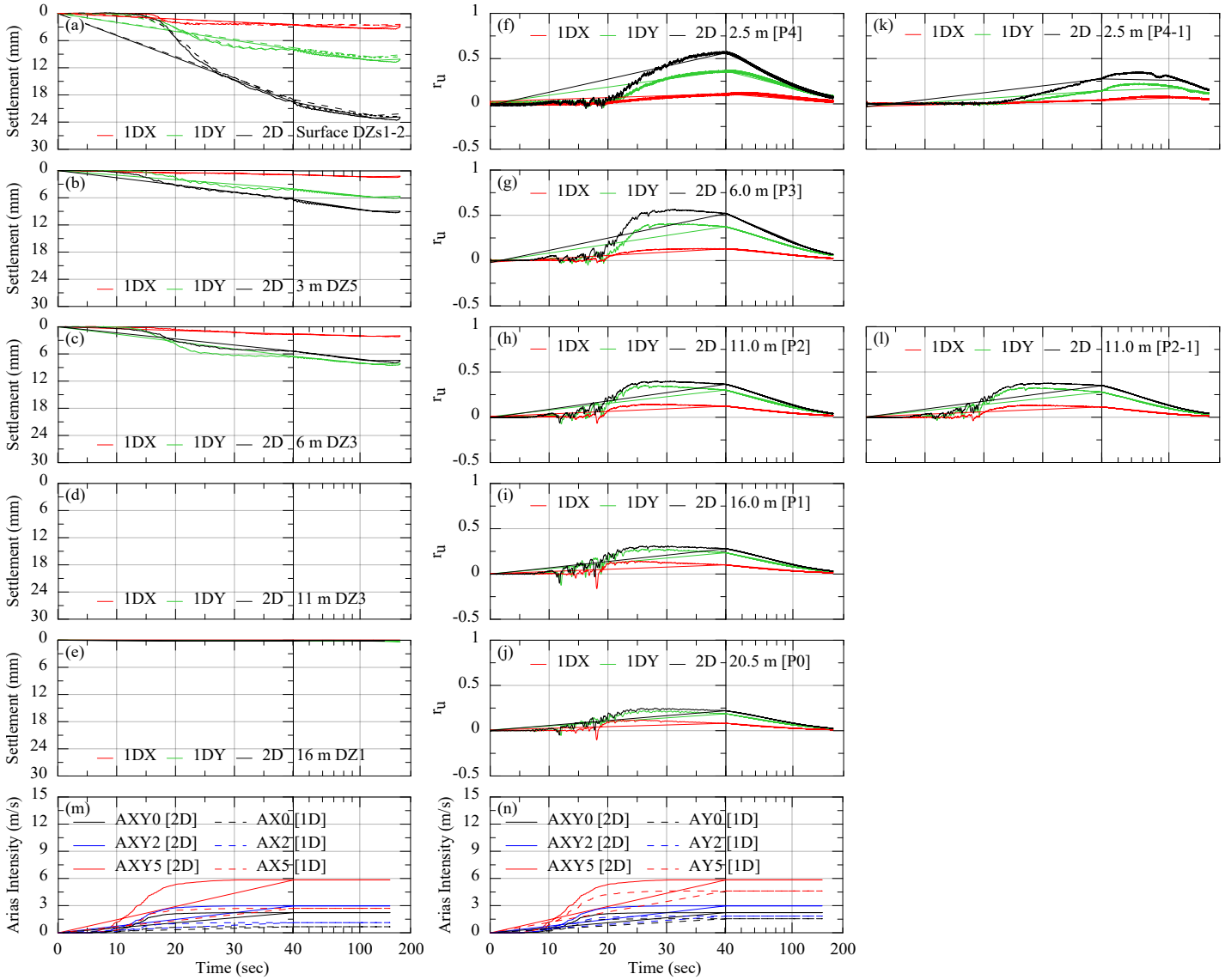

Figure C-281 Variation of total (a) to (e) Settlement with depth (M13-X,Y and 2D) ; (f) to (l) Excess pore water pressure ratio (ru) (M13-X,Y and 2D) (m) and (n) Arias Intensity along model (M13-X,Y and 2D).

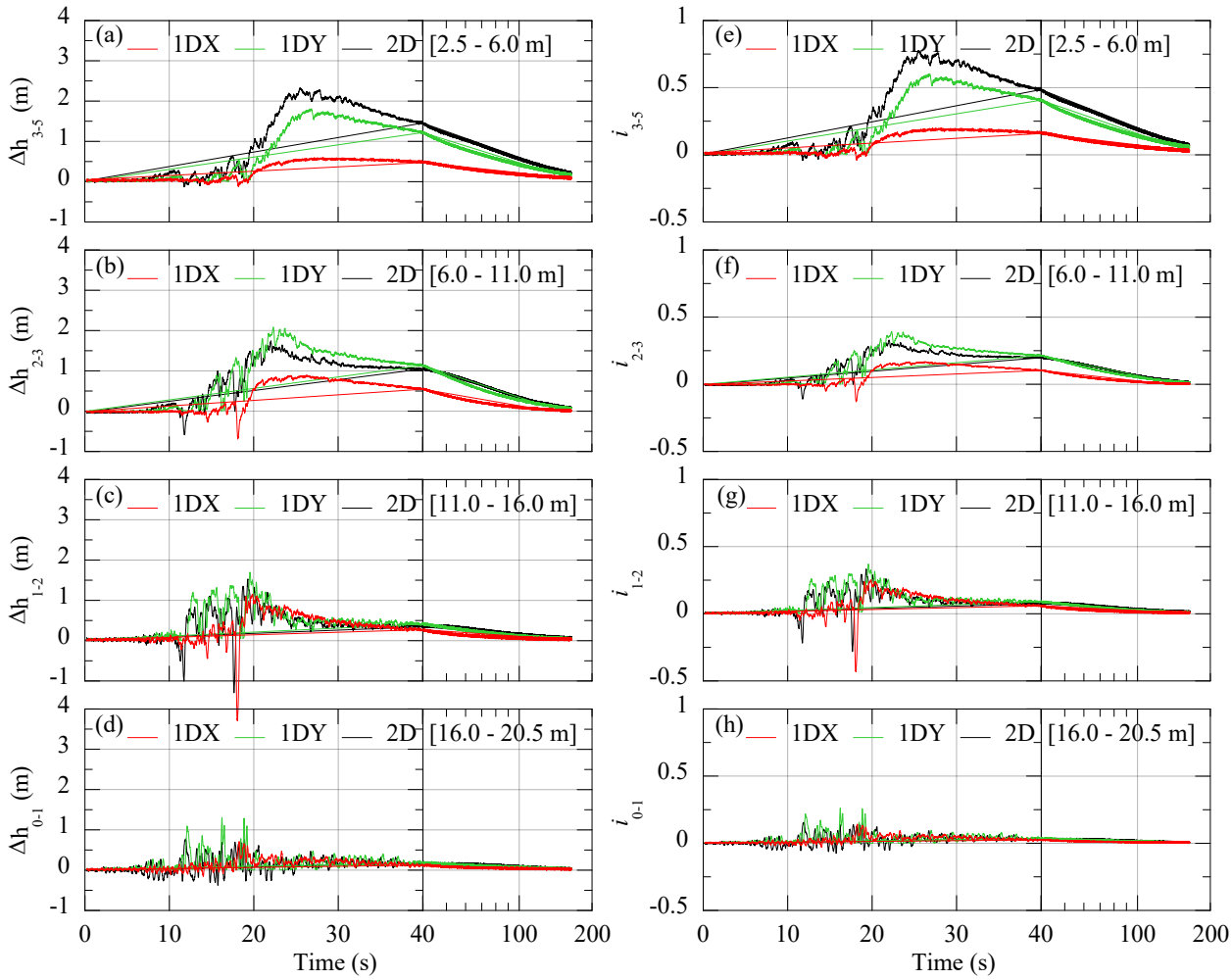

Figure C-282 Variation of total (a) to (d) Total Head Loss with depth (M13-X, Y and 2D); (e) to (h) Shaking induced Hydraulic Gradient (M13-X, Y and 2D)

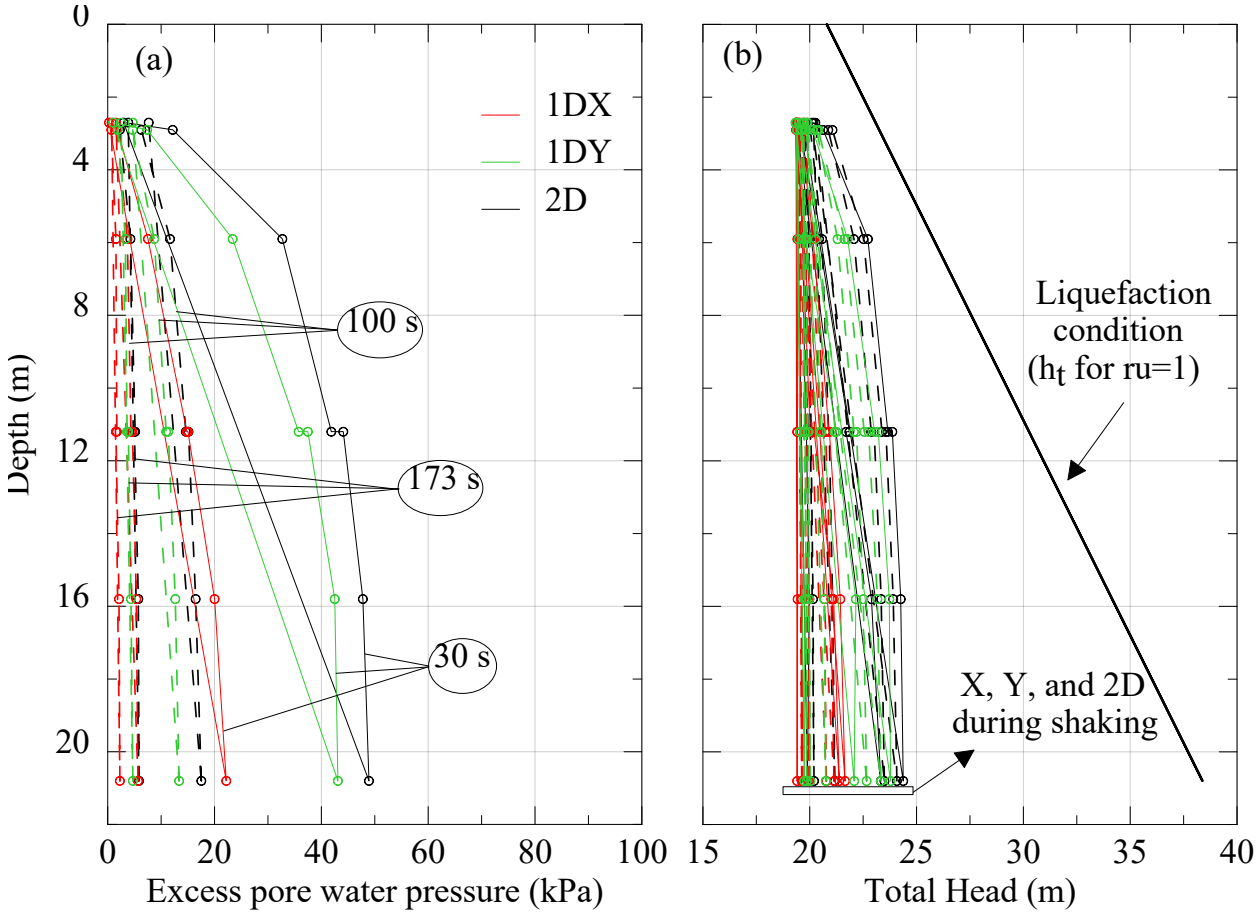

Figure C-283 Variation of total (a) Excess pore water pressure ratio (ru) with depth (M13-X,Y and 2D); (e) to (b) Total Head Loss with depth (M13-X,Y and 2D)

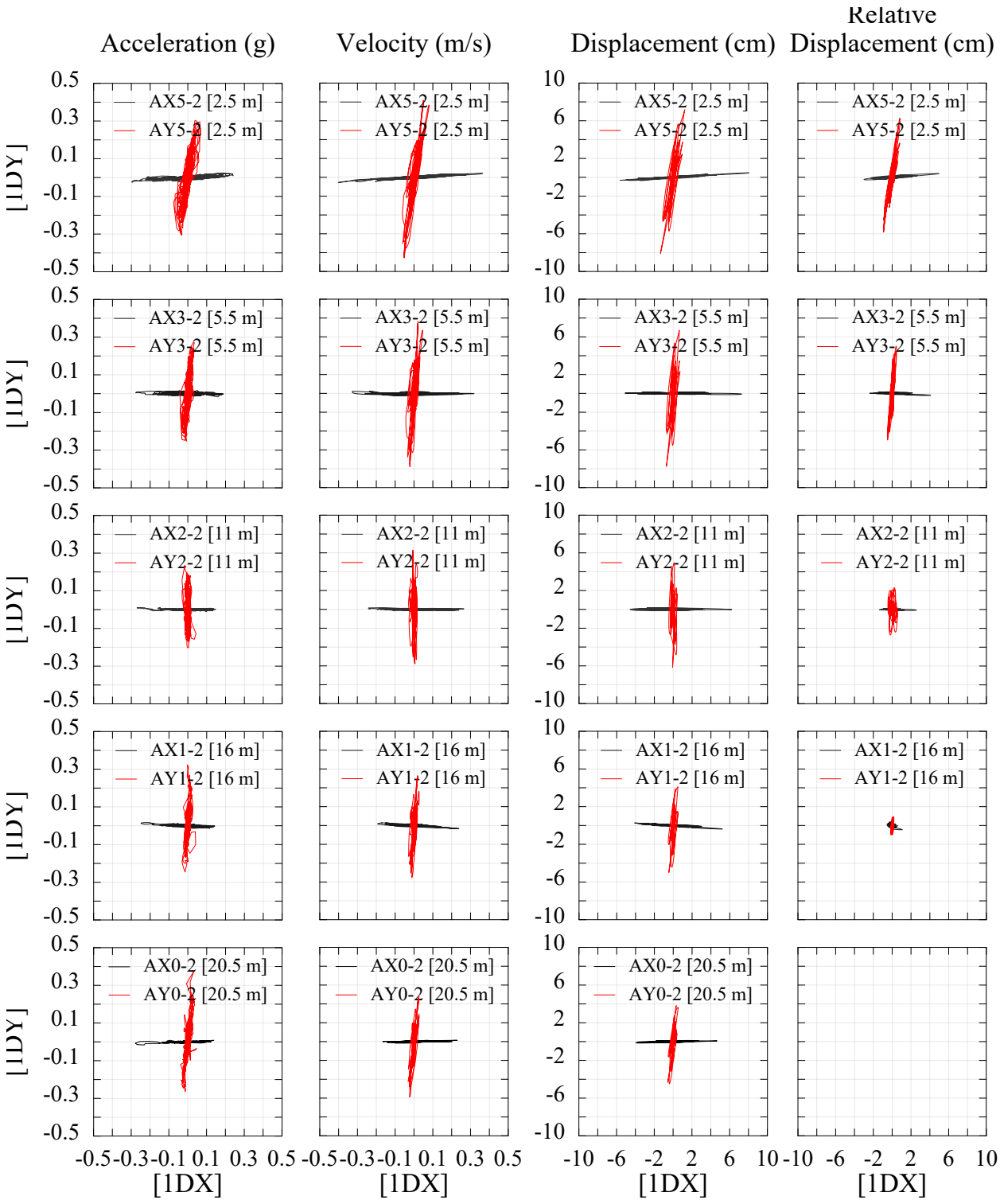

Figure C-284 Recorded input and within model ground motions for acceleration, velocity, displacement and relative displacement for M13-1D [X] and M13-1D [Y]

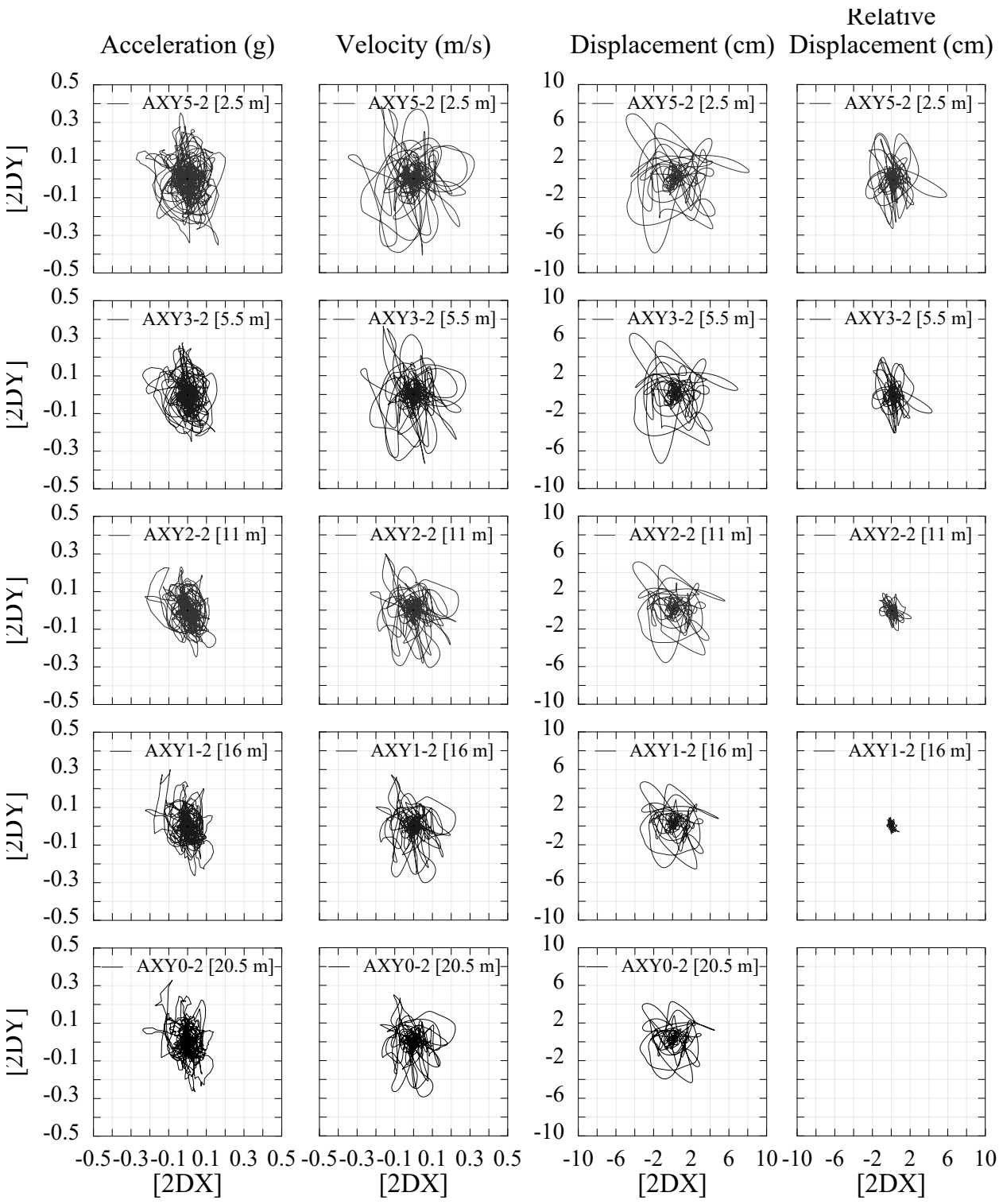

Figure C-285 Recorded input and within model ground motions for acceleration, velocity, displacement and relative displacement for M13-2D

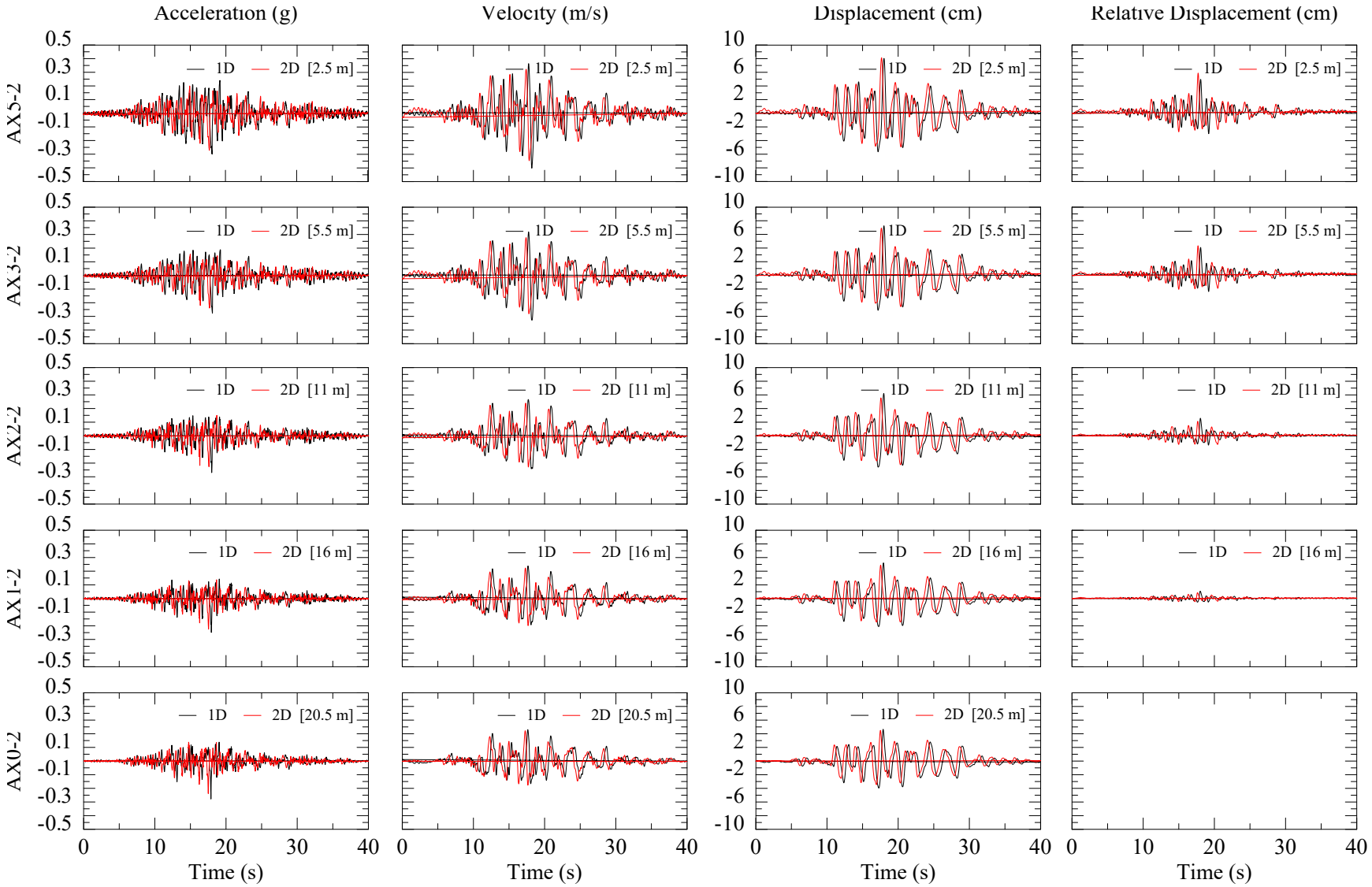

Figure C-286 Recorded input and within model ground motions time histories for acceleration, velocity, displacement and relative displacement for M13-2D [X] and M13-1D [X]

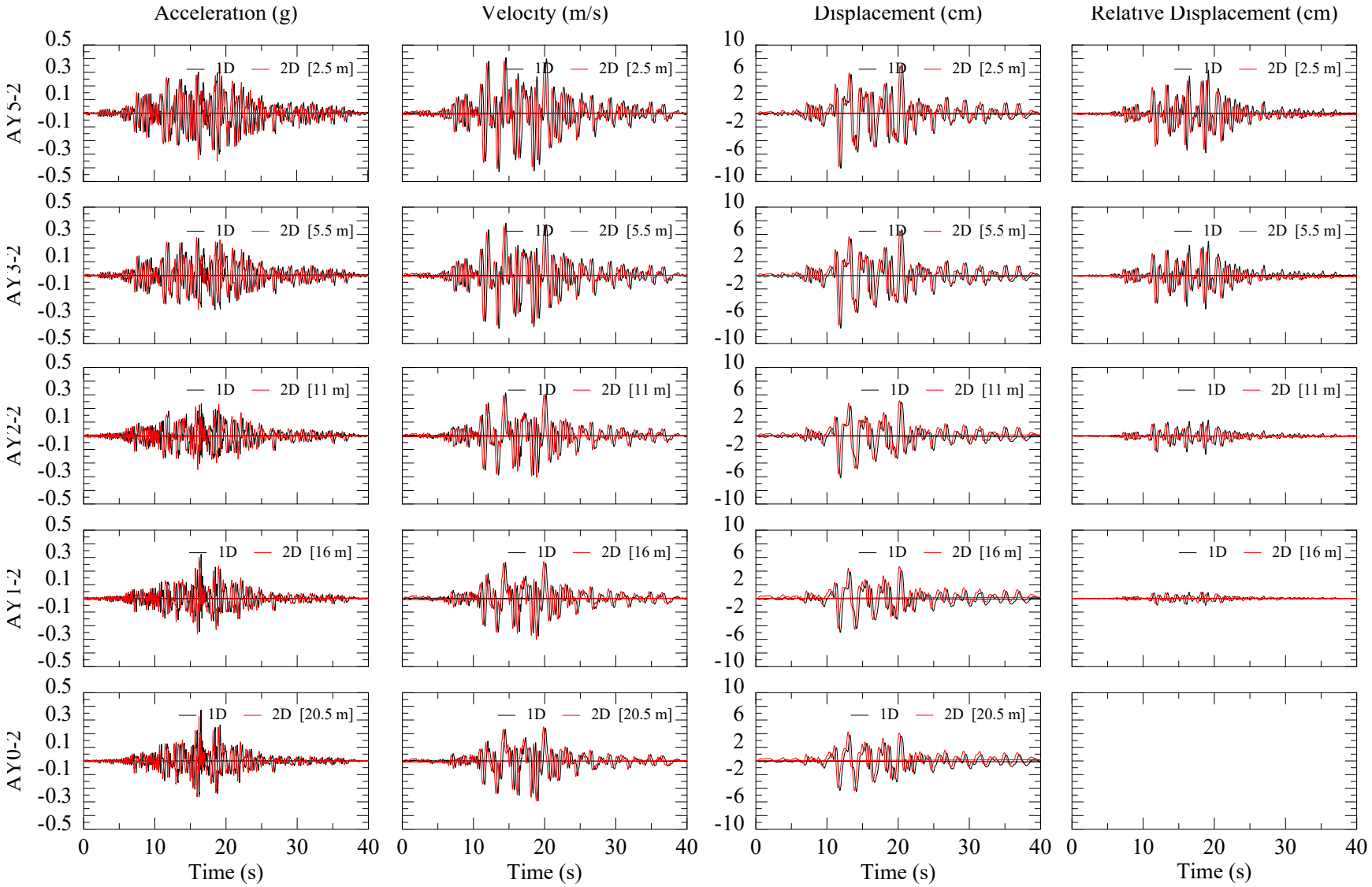

Figure C-287 Recorded input and within model ground motions time histories for acceleration, velocity, displacement and relative displacement for M13-2D [Y] and M13-1D [Y]

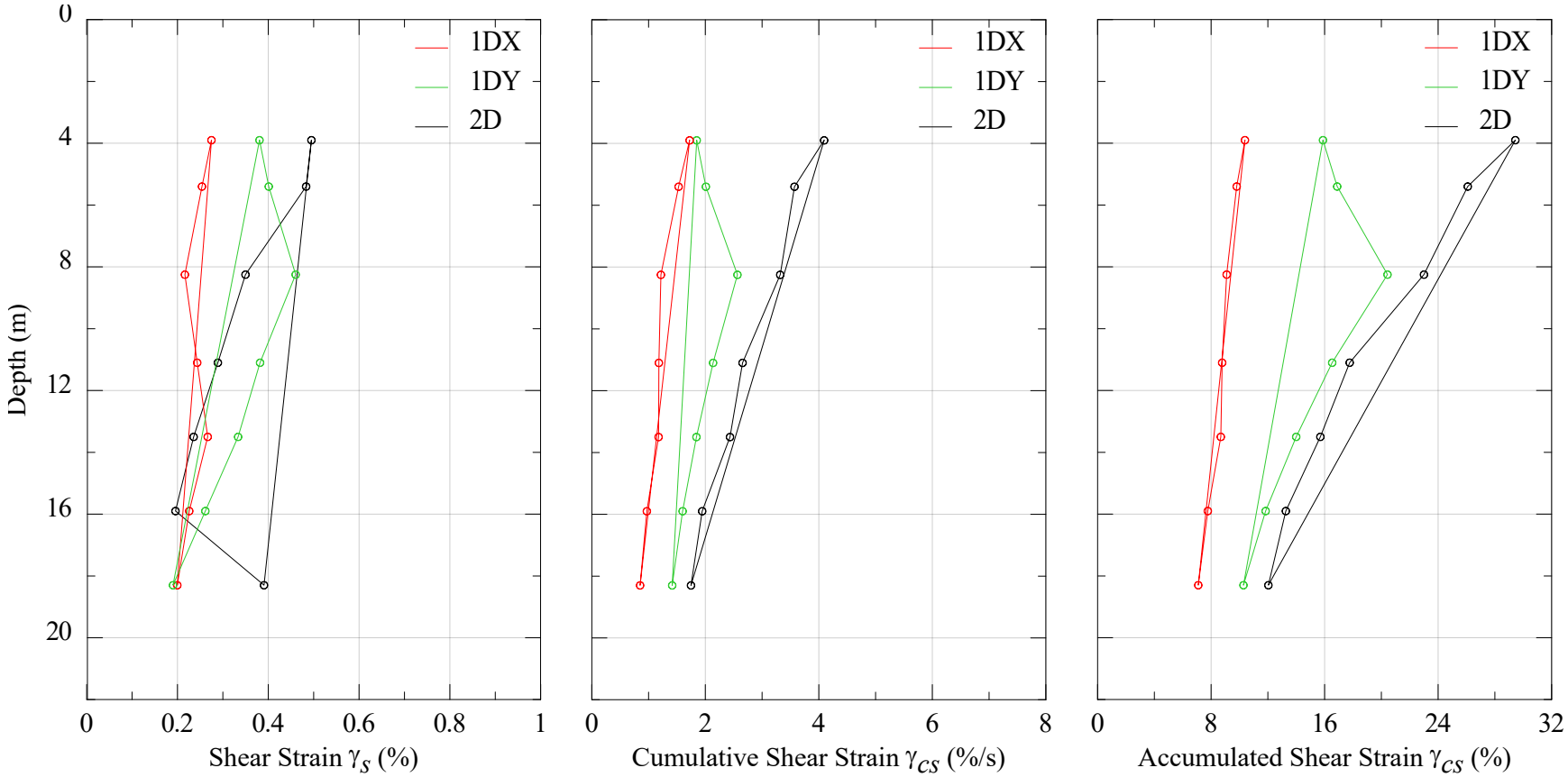

Figure C-288 Estimated (a) maximum shear strain; (b) cumulative shear strain; and (c) accumulated shear strain for M13-2D [X] and M13-1D [X]

1.4.6 Motion 3 (M3)

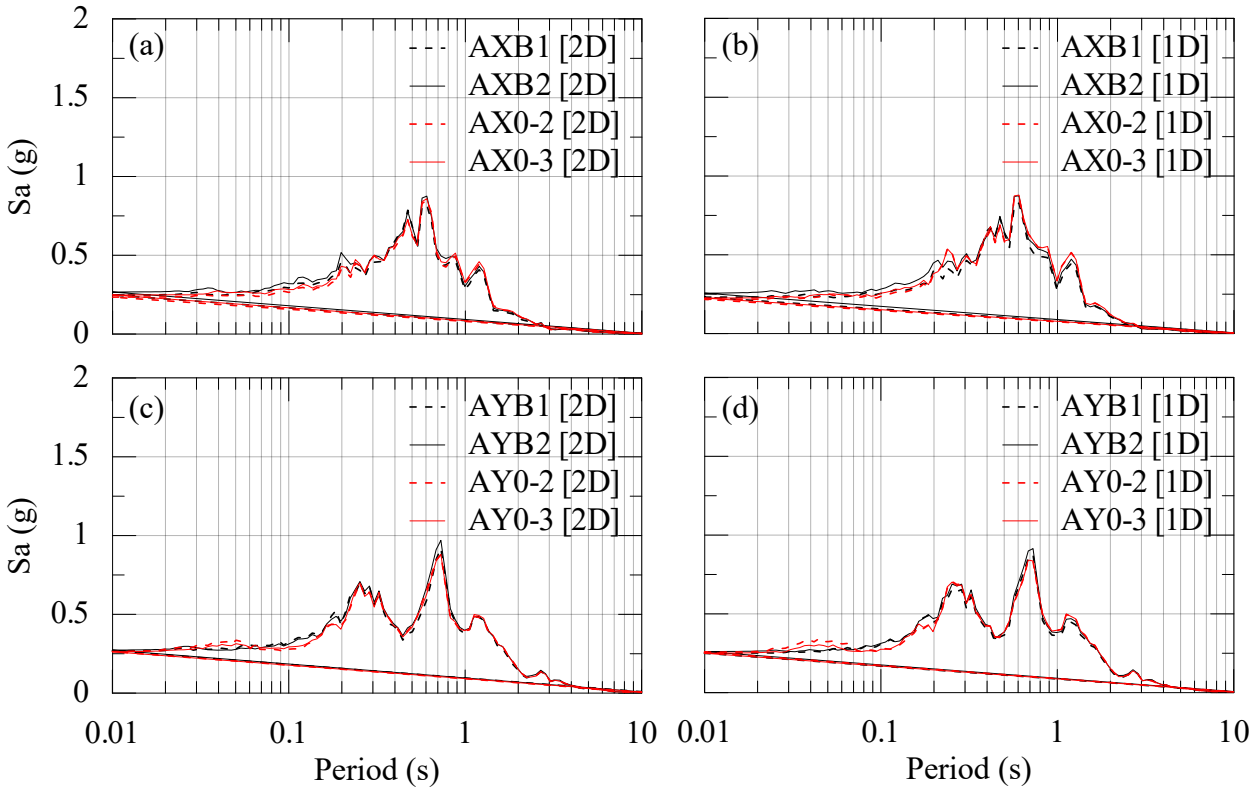

Figure C-289 Comparison of response spectra of 2D laminar container table and within model base input motion for motions (M3-X, Y and 2D).

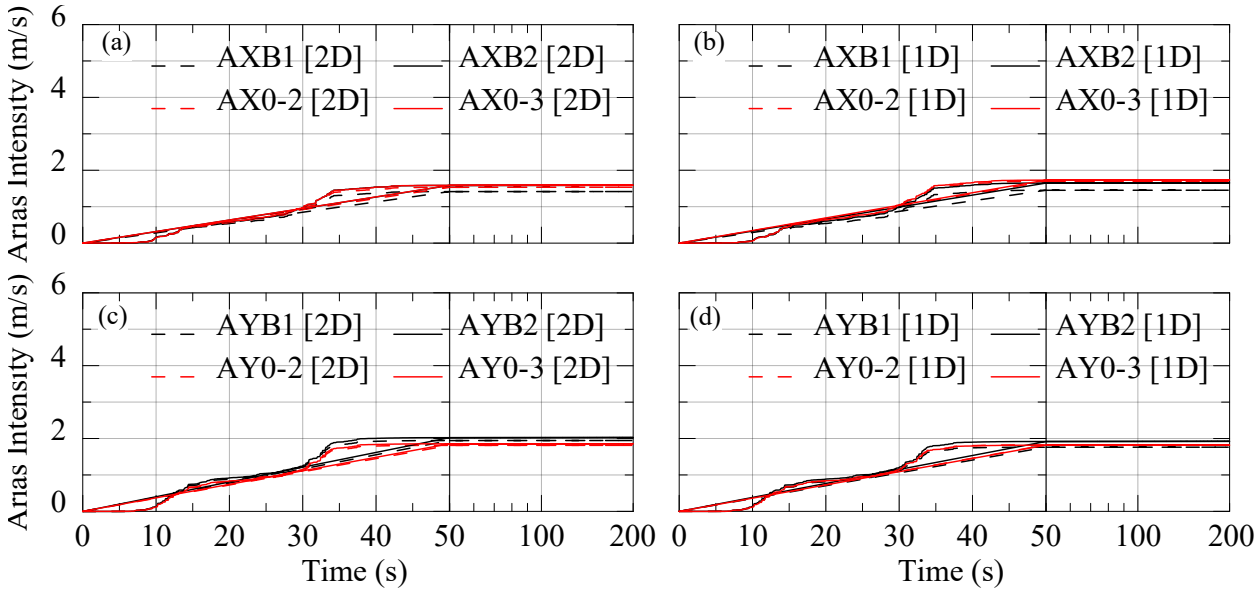

Figure C-290 Comparison of Arias Intensity of 2D laminar container table and within model base input motion for motions (a) M3-2D [X]; (b) M3-2D [Y]; (c) M3-1D [X] and (d) M3-1D [Y]

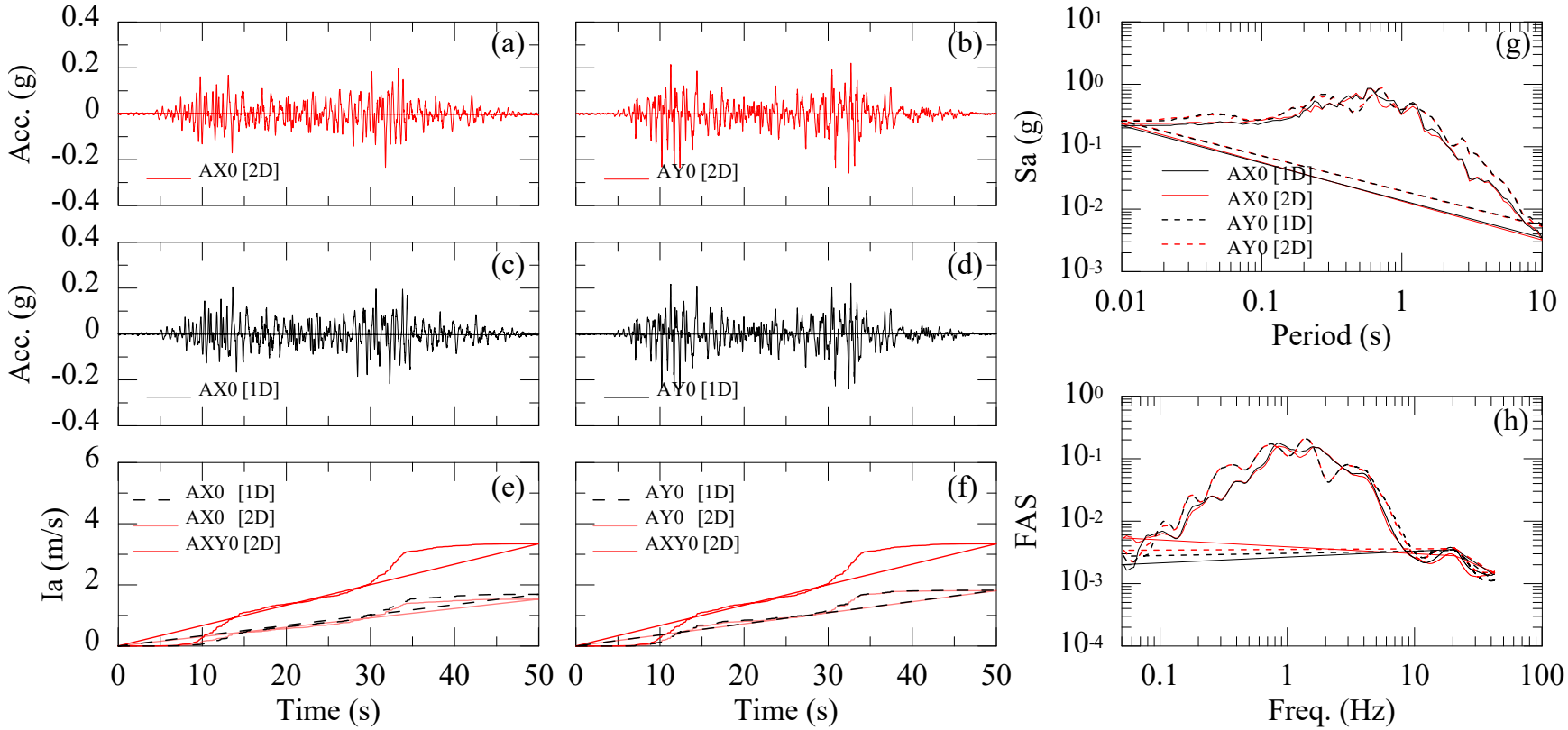

Figure C-291 Recorded input (2D) and 1D (X or Y) ground motions for: (a) M3-2D [X]; (b) M3-2D [Y]; (c) M3-1D [X]; and (d) M3-1D [Y]. Arias Intensity M3 (1D and 2D) for: (e) X direction; and (f) Y direction. Response Spectra (g) M3-2D [X]; M3-2D [Y]; M3-1D [X]; and M3-1D [Y]. Smoothed Fourier amplitude spectra (FAS) (h) M3-2D [X]; M3-2D [Y]; M3-1D [X]; and M3-1D [Y].

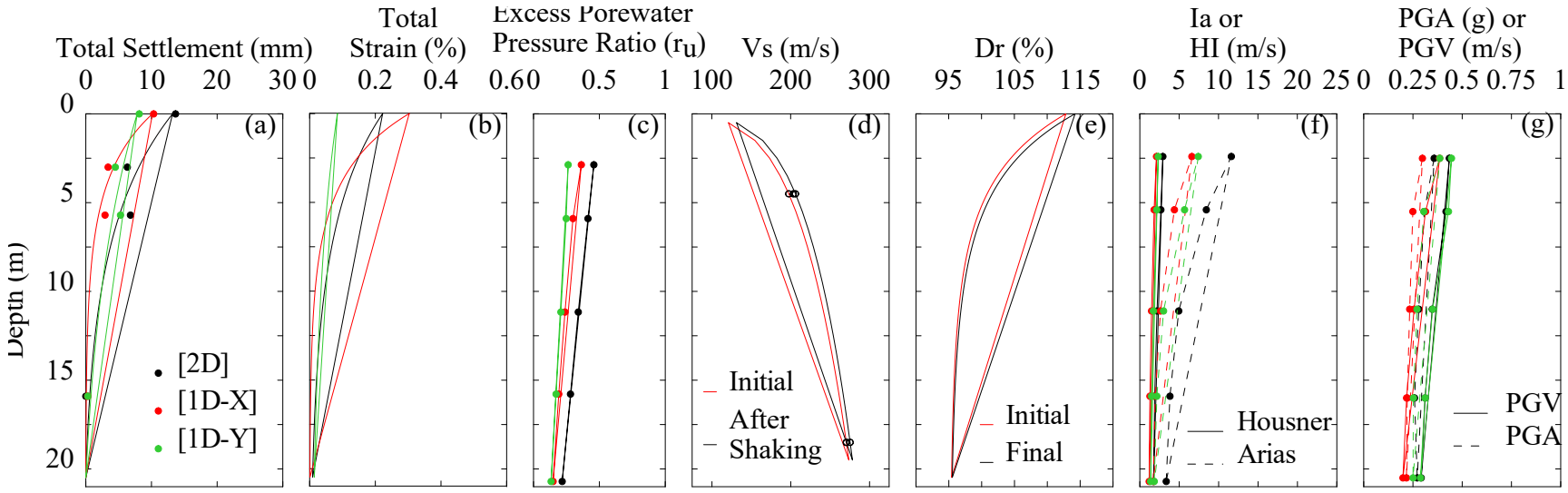

Figure C-292 Recorded or computed profiles for input motion M3-X, Y, and 2D. (a) Settlement; (b) total strain; (c) excess pore water pressure ratio; (d) shear wave velocity; (e) relative density; (f) Arias and Housner intensities; and (g) PGA and PGV.

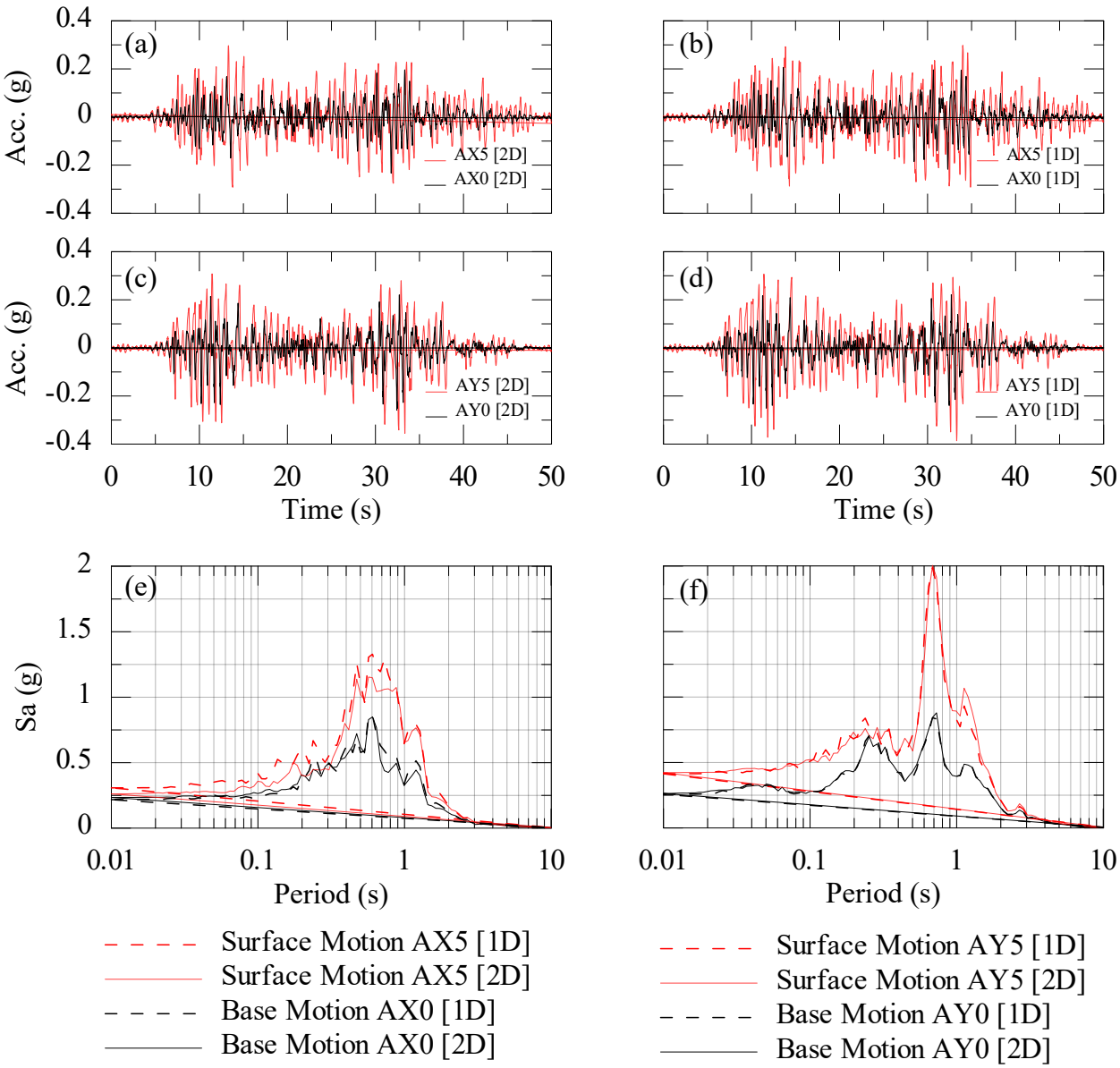

Figure C-293 Recorded input and surface ground motion: (a) M3-2D [X]; (b) M3-1D [X]; (c) M3-2D [Y]; and (d) M3-1D [Y]. Computed response spectra from Free Field Test [PT2] for motions M3 (1D and 2D) for: (e) X direction; and (f) Y direction.

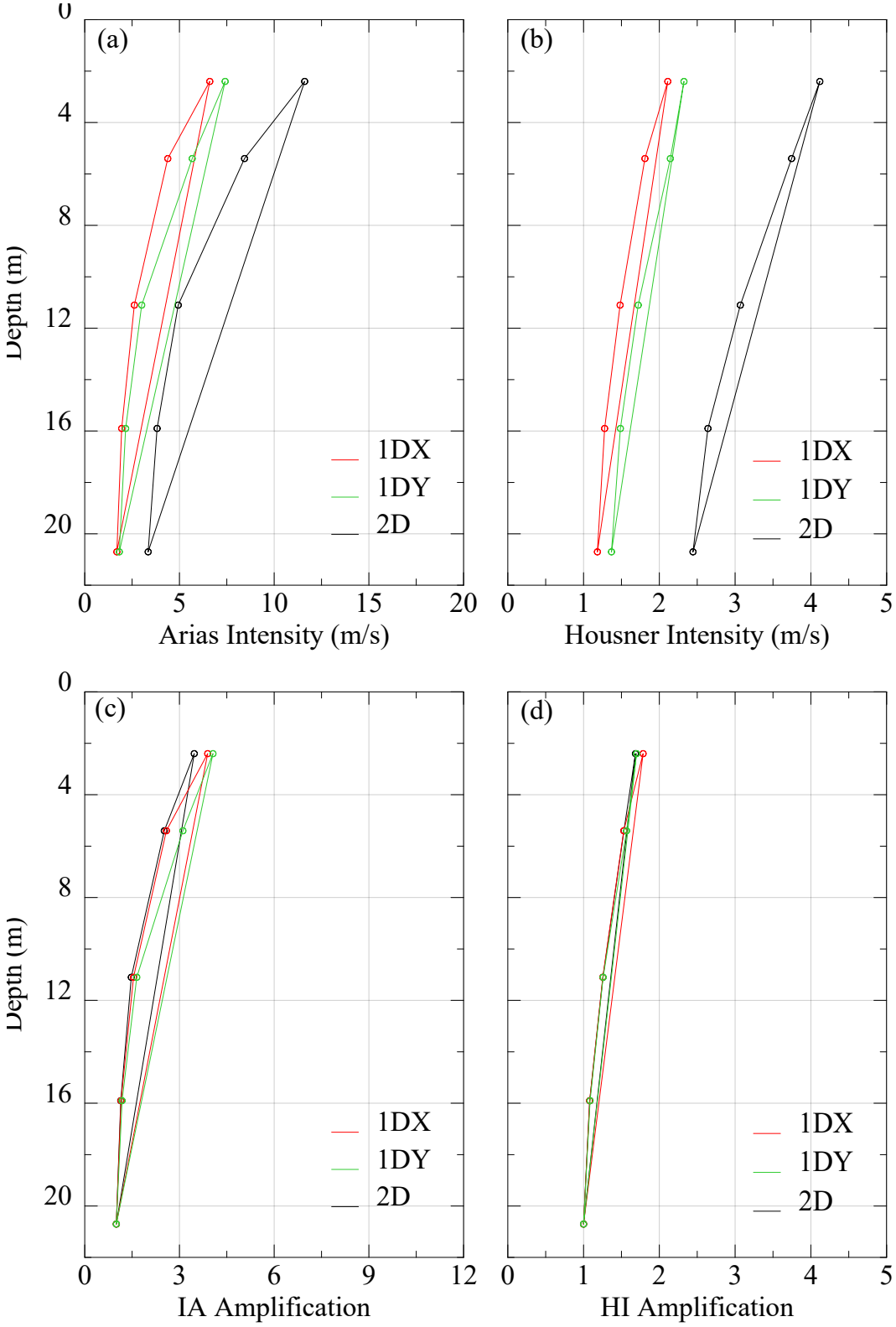

Figure C-294 Variation of total (a) Arias Intensity (M3-X,Y and 2D) ; (b) Housner Intensity (M3-X,Y and 2D) (c) Arias Intensity Amplification Factor (M3-X,Y and 2D); and (d) Housner Intensity Amplification Factor (M3-X,Y and 2D).

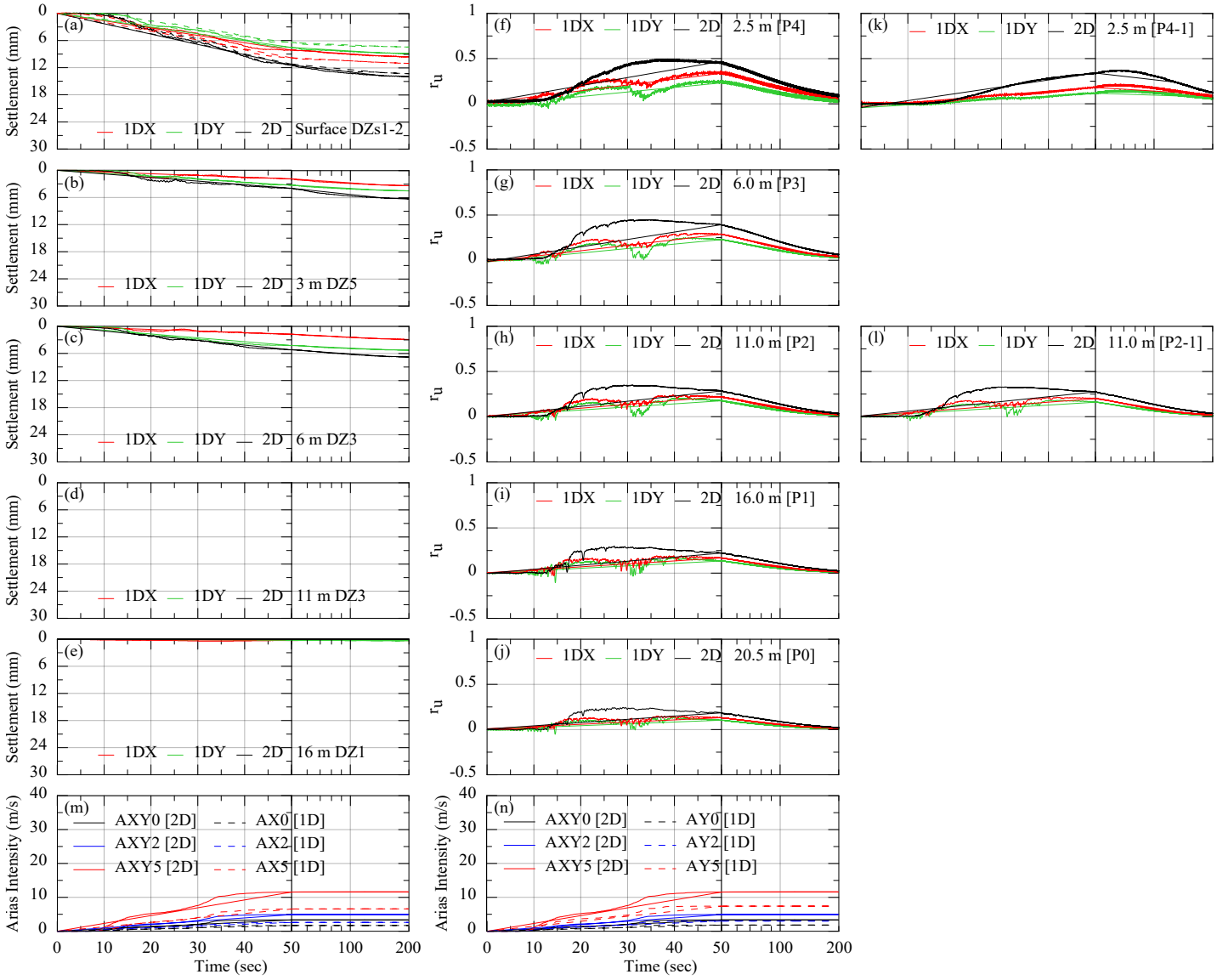

Figure C-295 Variation of total (a) to (e) Settlement with depth (M3-X,Y and 2D) ; (f) to (l) Excess pore water pressure ratio (ru) (M3-X,Y and 2D) (m) and (n) Arias Intensity along model (M3-X,Y and 2D).

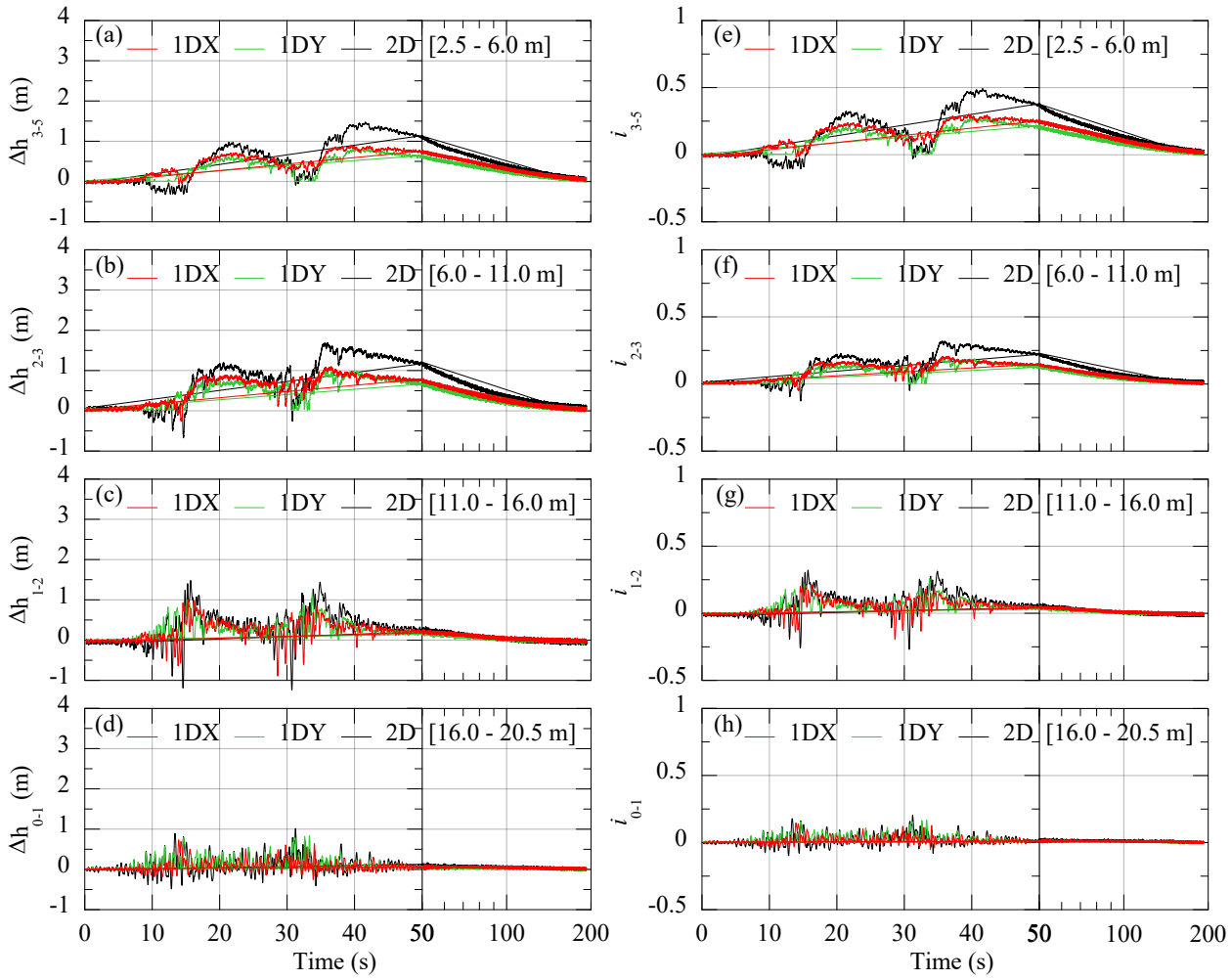

Figure C-296 Variation of total (a) to (d) Total Head Loss with depth (M3-X, Y and 2D); (e) to (h) Shaking induced Hydraulic Gradient (M3-X, Y and 2D)

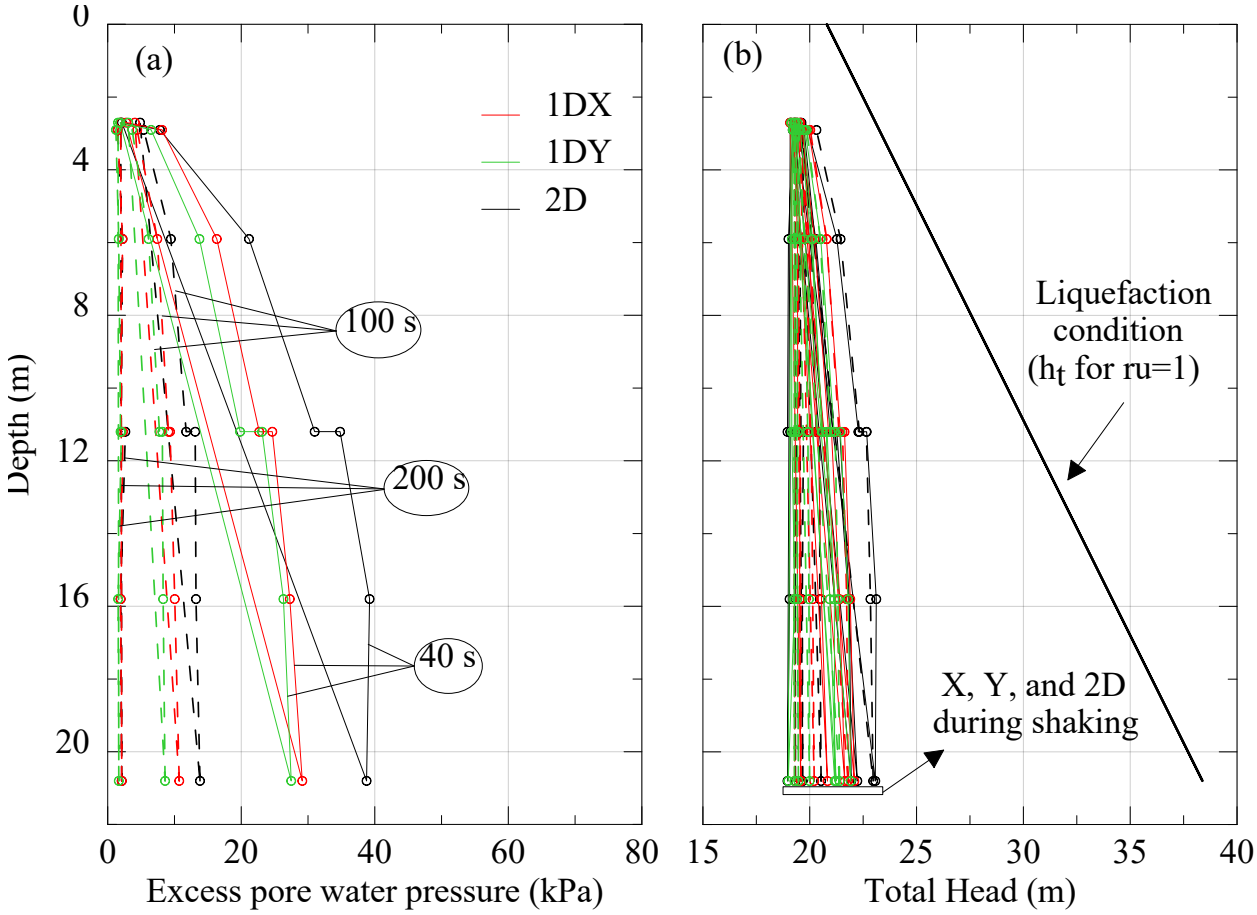

Figure C-297 Variation of total (a) Excess pore water pressure ratio (ru) with depth (M3-X,Y and 2D); (e) to (b) Total Head Loss with depth (M3-X,Y and 2D)

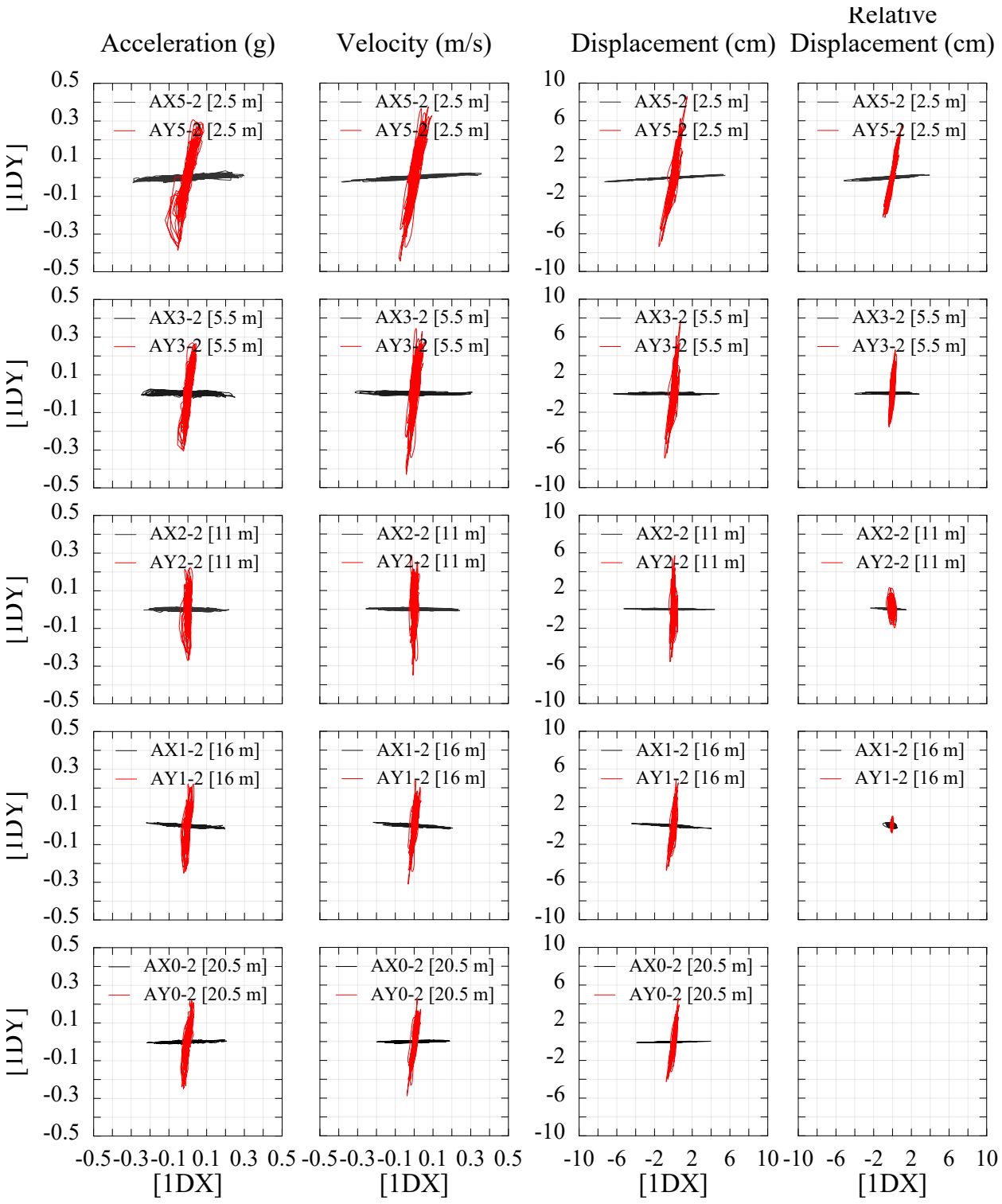

Figure C-298 Recorded input and within model ground motions for acceleration, velocity, displacement and relative displacement for M3-1D [X] and M3-1D [Y]

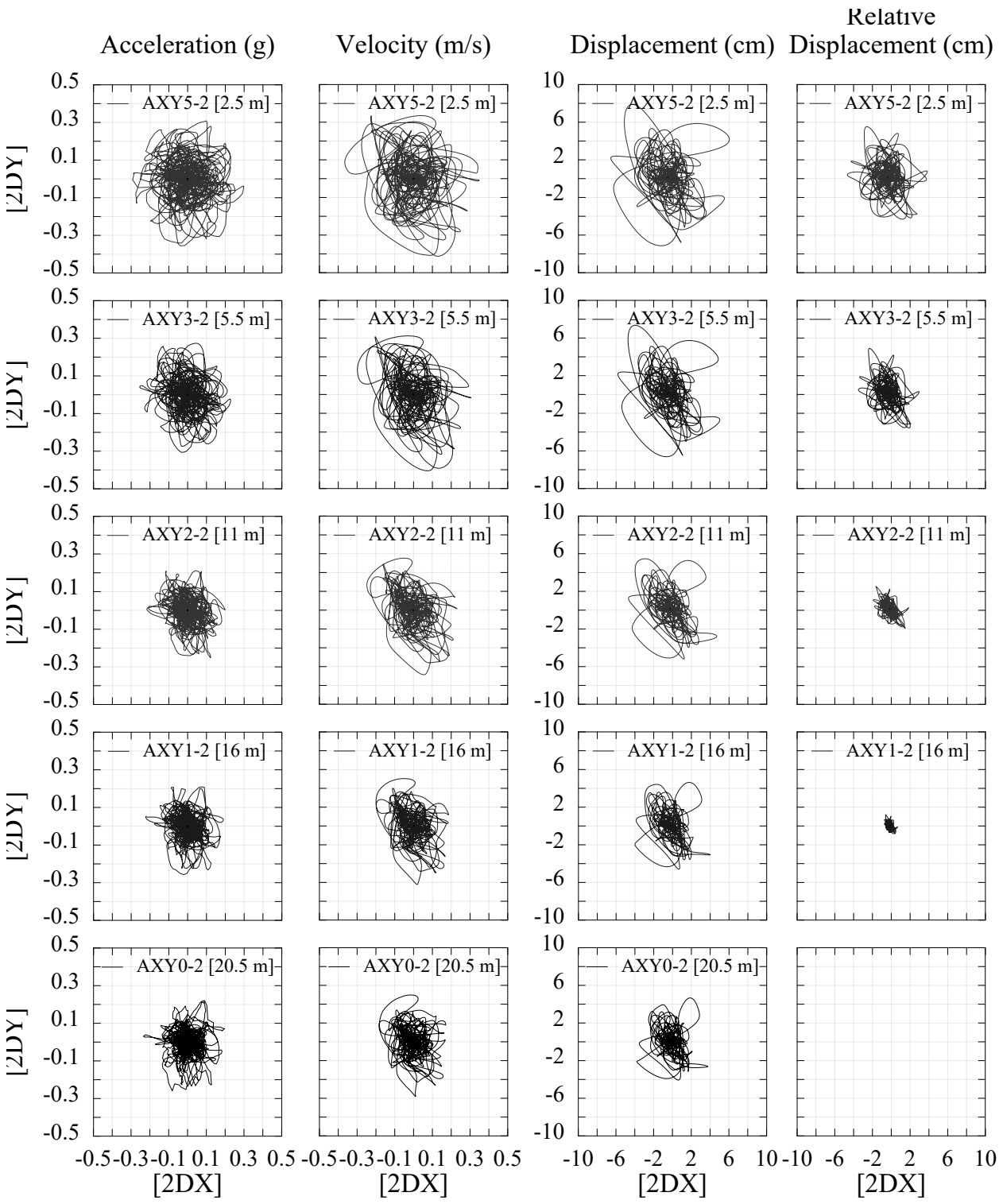

Figure C-299 Recorded input and within model ground motions for acceleration, velocity, displacement and relative displacement for M3-2D

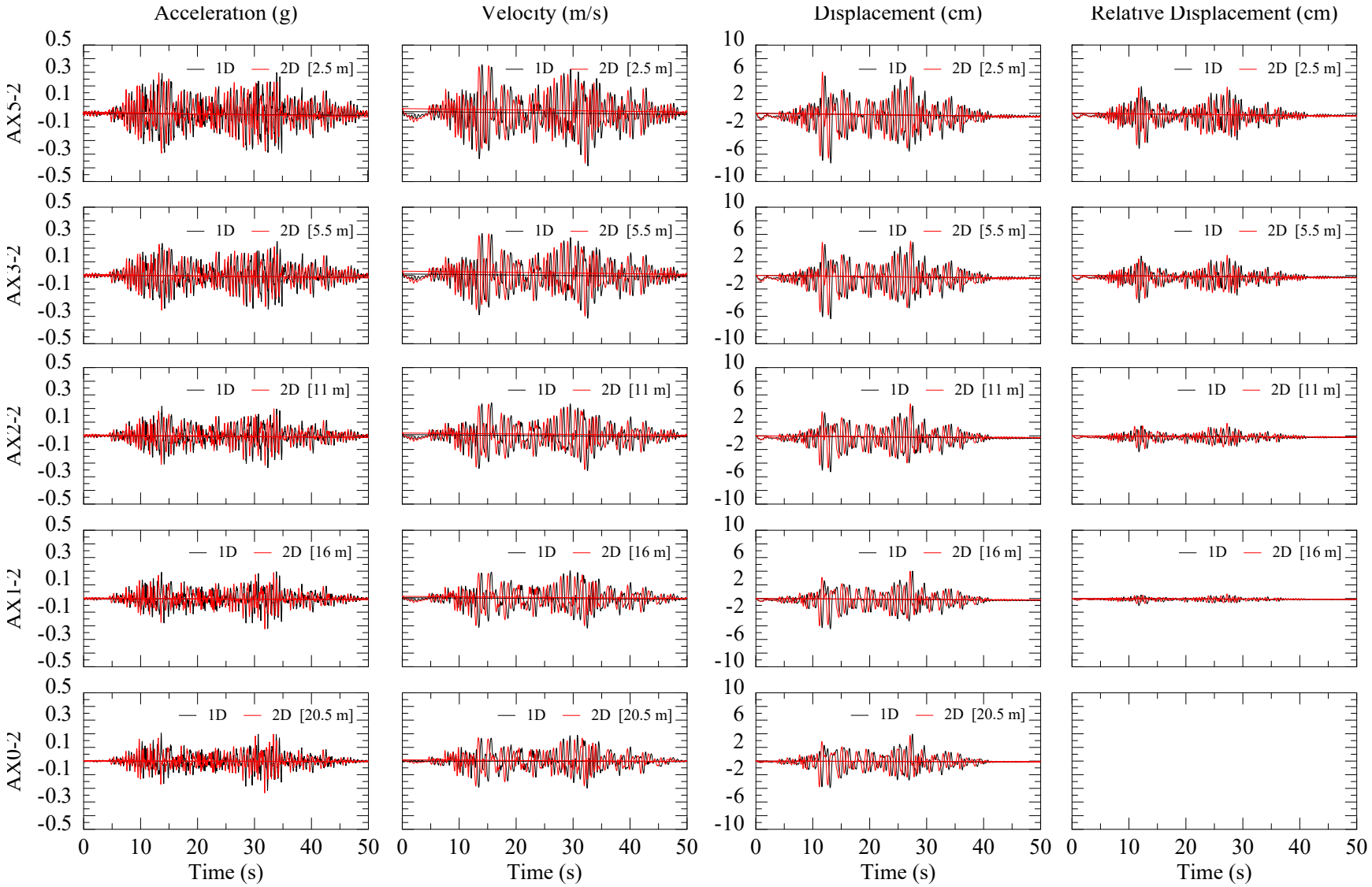

Figure C-300 Recorded input and within model ground motions time histories for acceleration, velocity, displacement and relative displacement for M3-2D [X] and M3-1D [X]

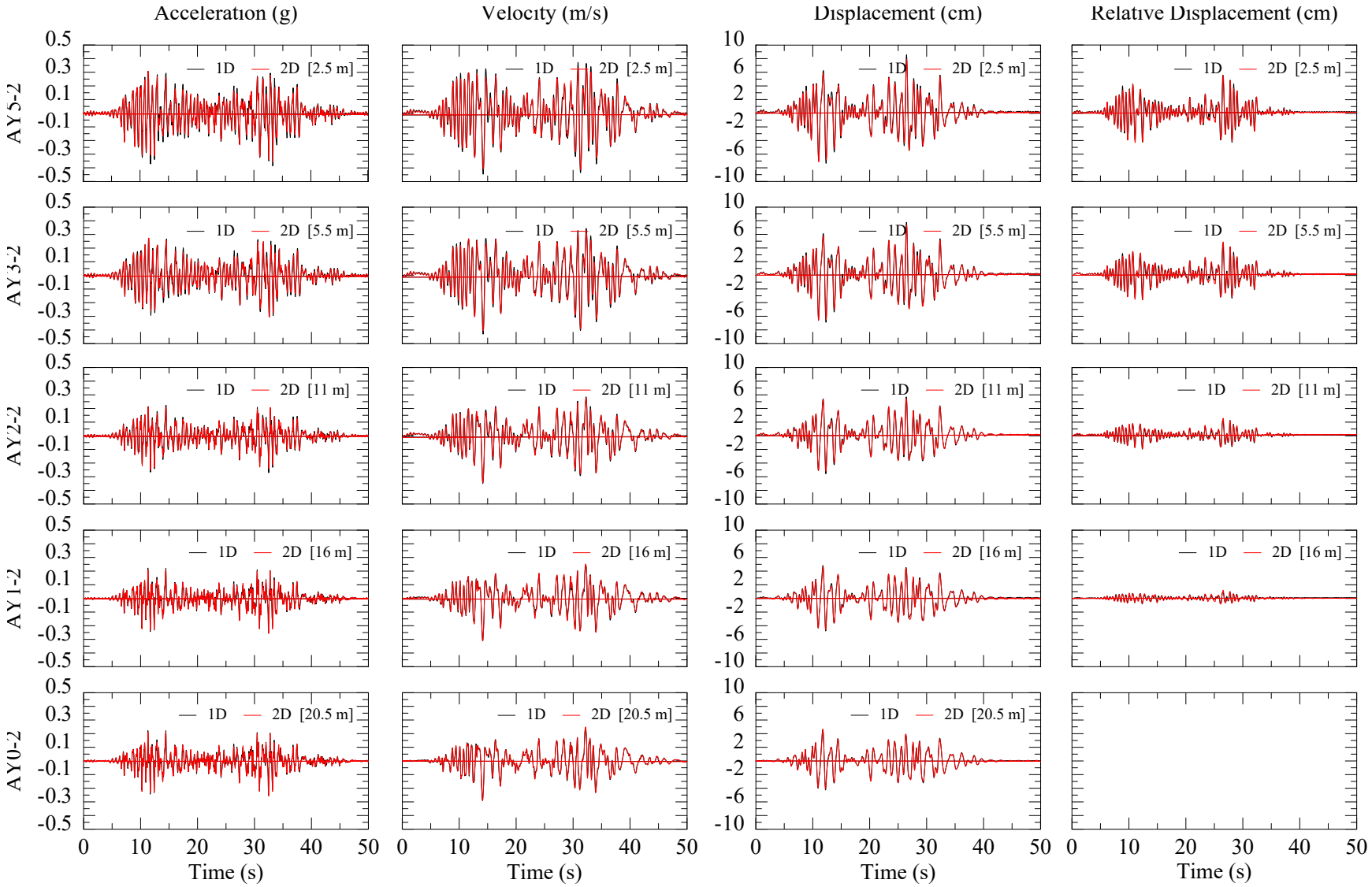

Figure C-301 Recorded input and within model ground motions time histories for acceleration, velocity, displacement and relative displacement for M3-2D [Y] and M3-1D [Y]

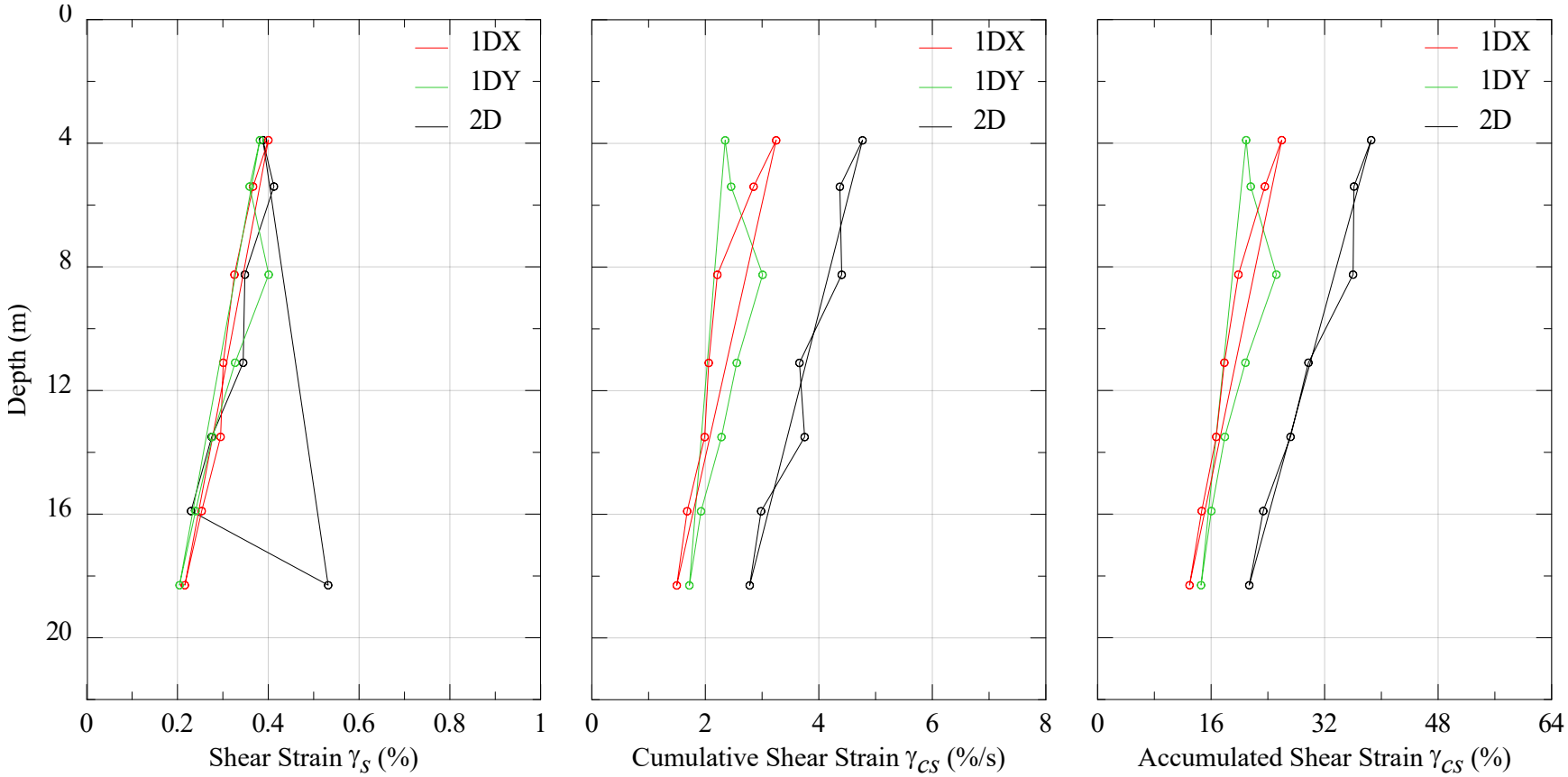

Figure C-302 Estimated (a) maximum shear strain; (b) cumulative shear strain; and (c) accumulated shear strain for M3-2D [X] and M3-1D [X]

1.4.7 Motion 5 (M5)

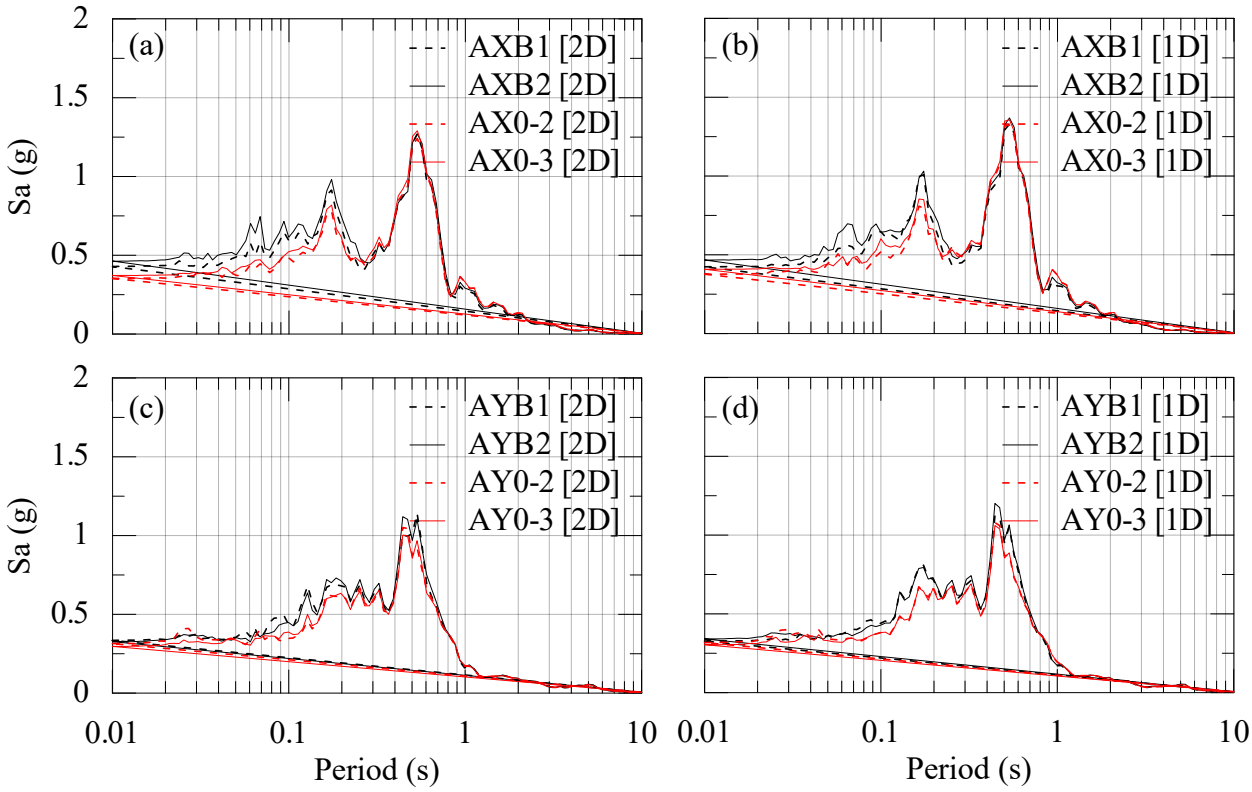

Figure C-303 Comparison of response spectra of 2D laminar container table and within model base input motion for motions (M5-X, Y and 2D).

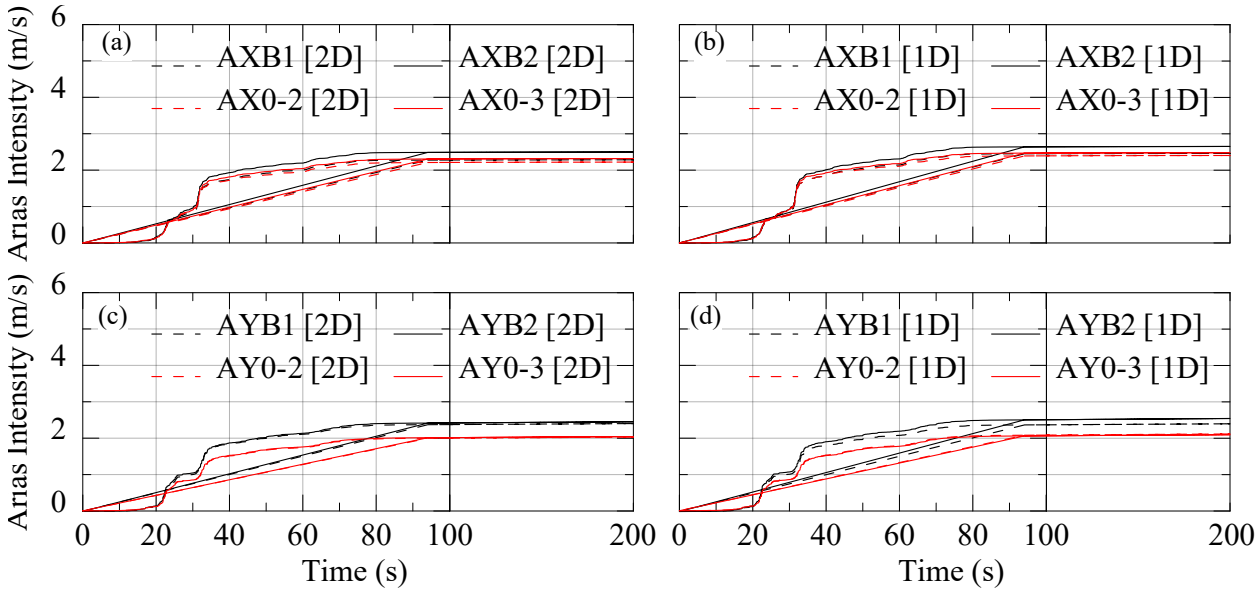

Figure C-304 Comparison of Arias Intensity of 2D laminar container table and within model base input motion for motions (a) M5-2D [X]; (b) M5-2D [Y]; (c) M5-1D [X] and (d) M5-1D [Y]

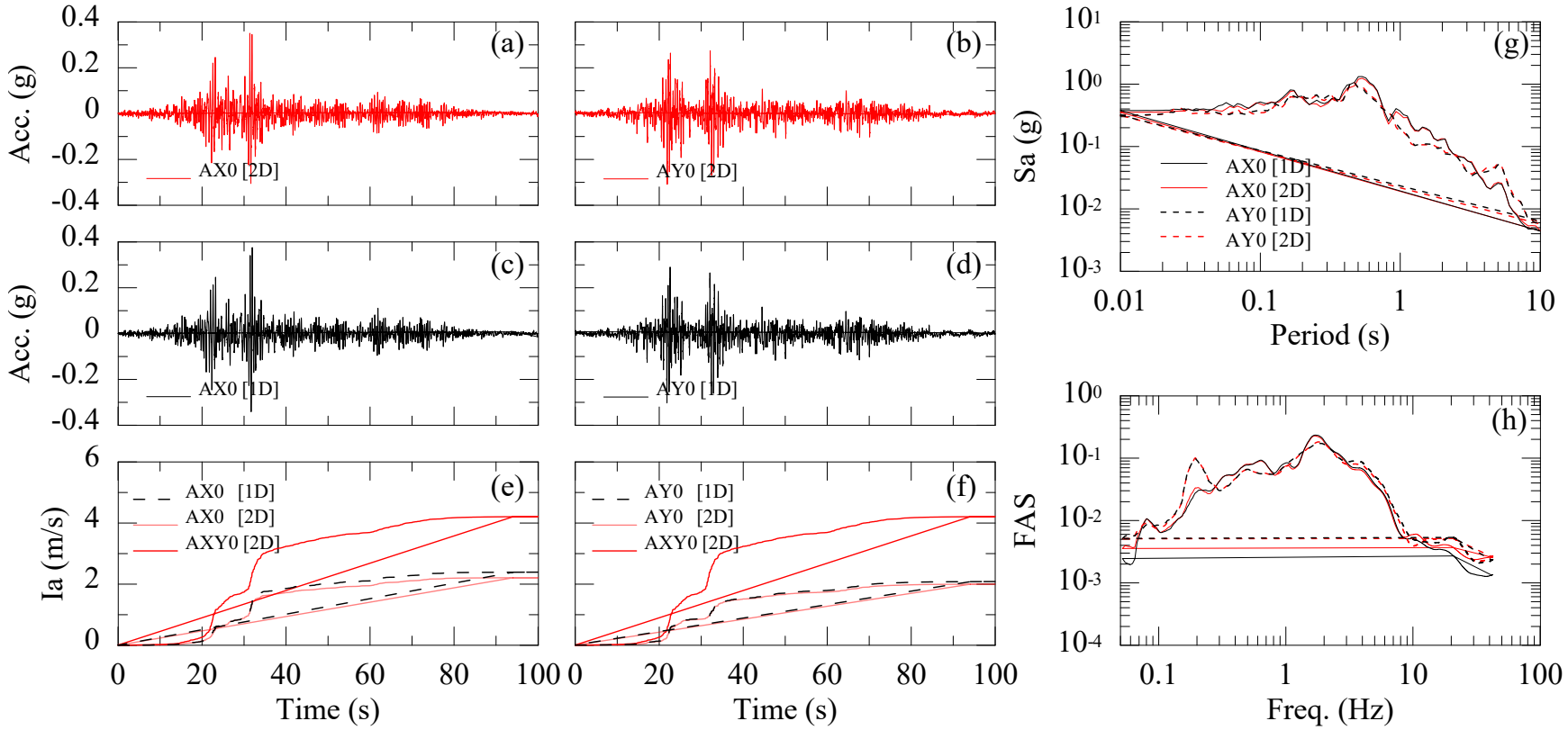

Figure C-305 Recorded input (2D) and 1D (X or Y) ground motions for: (a) M5-2D [X]; (b) M5-2D [Y]; (c) M5-1D [X]; and (d) M5-1D [Y]. Arias Intensity M5 (1D and 2D) for: (e) X direction; and (f) Y direction. Response Spectra (g) M5-2D [X]; M5-2D [Y]; M5-1D [X]; and M5-1D [Y]. Smoothed Fourier amplitude spectra (FAS) (h) M5-2D [X]; M5-2D [Y]; M5-1D [X]; and M5-1D [Y].

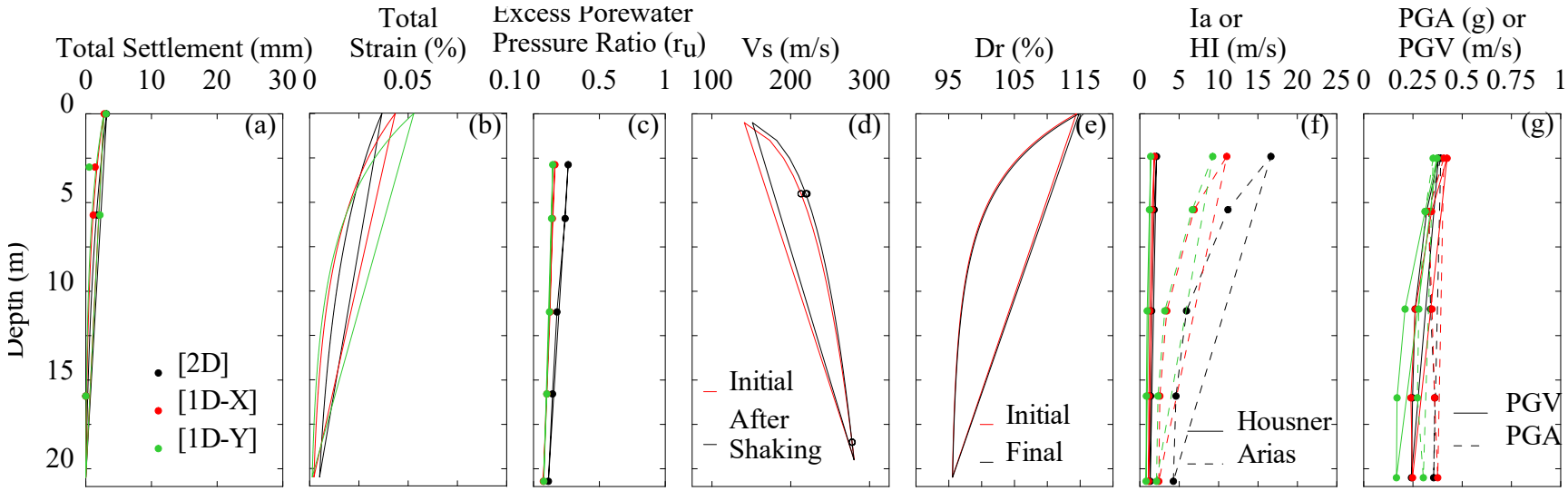

Figure C-306 Recorded or computed profiles for input motion M5-X, Y, and 2D. (a) Settlement; (b) total strain; (c) excess pore water pressure ratio; (d) shear wave velocity; (e) relative density; (f) Arias and Housner intensities; and (g) PGA and PGV.

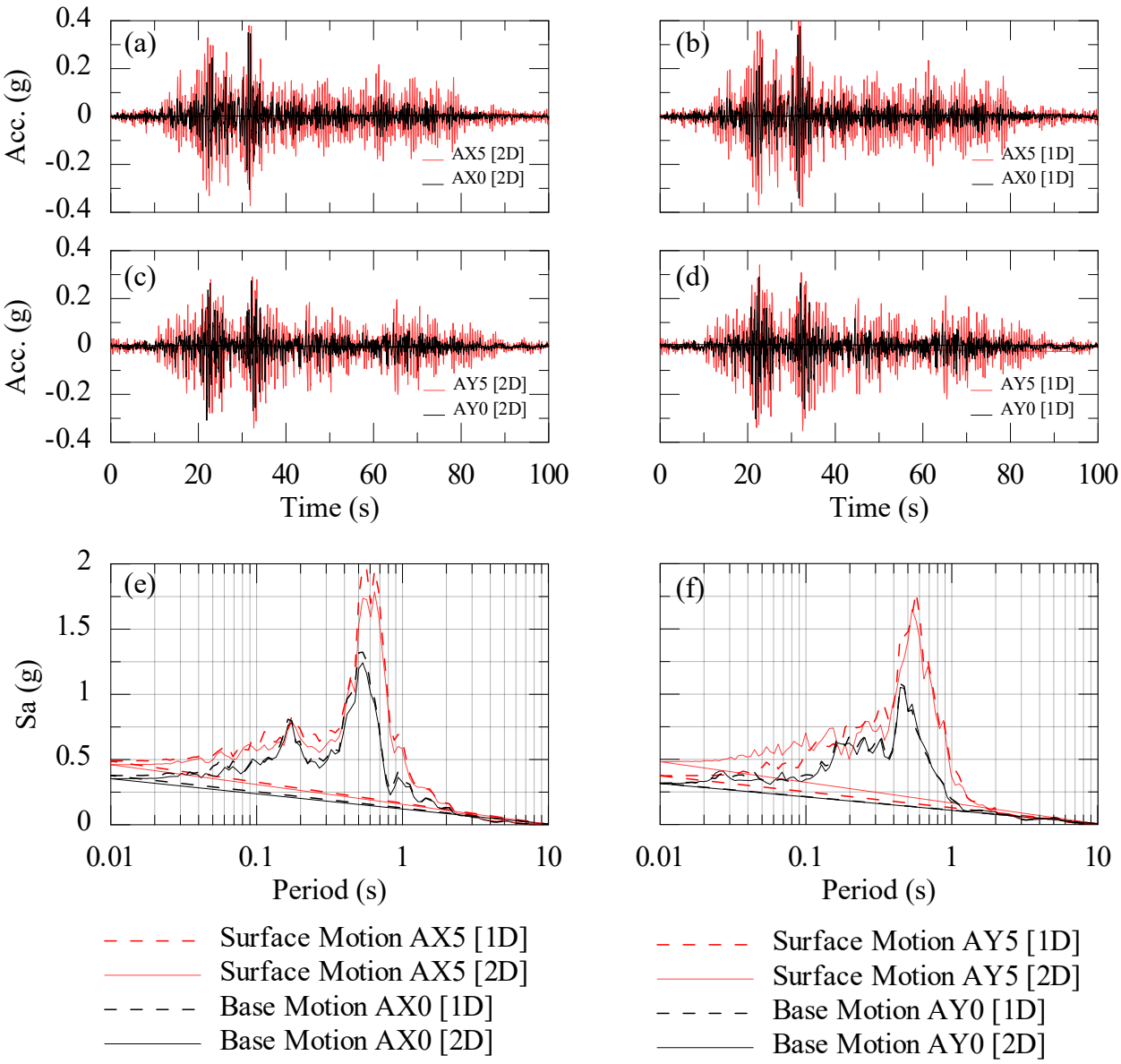

Figure C-307 Recorded input and surface ground motion: (a) M5-2D [X]; (b) M5-1D [X]; (c) M5-2D [Y]; and (d) M5-1D [Y]. Computed response spectra from Free Field Test [PT2] for motions M5 (1D and 2D) for: (e) X direction; and (f) Y direction.

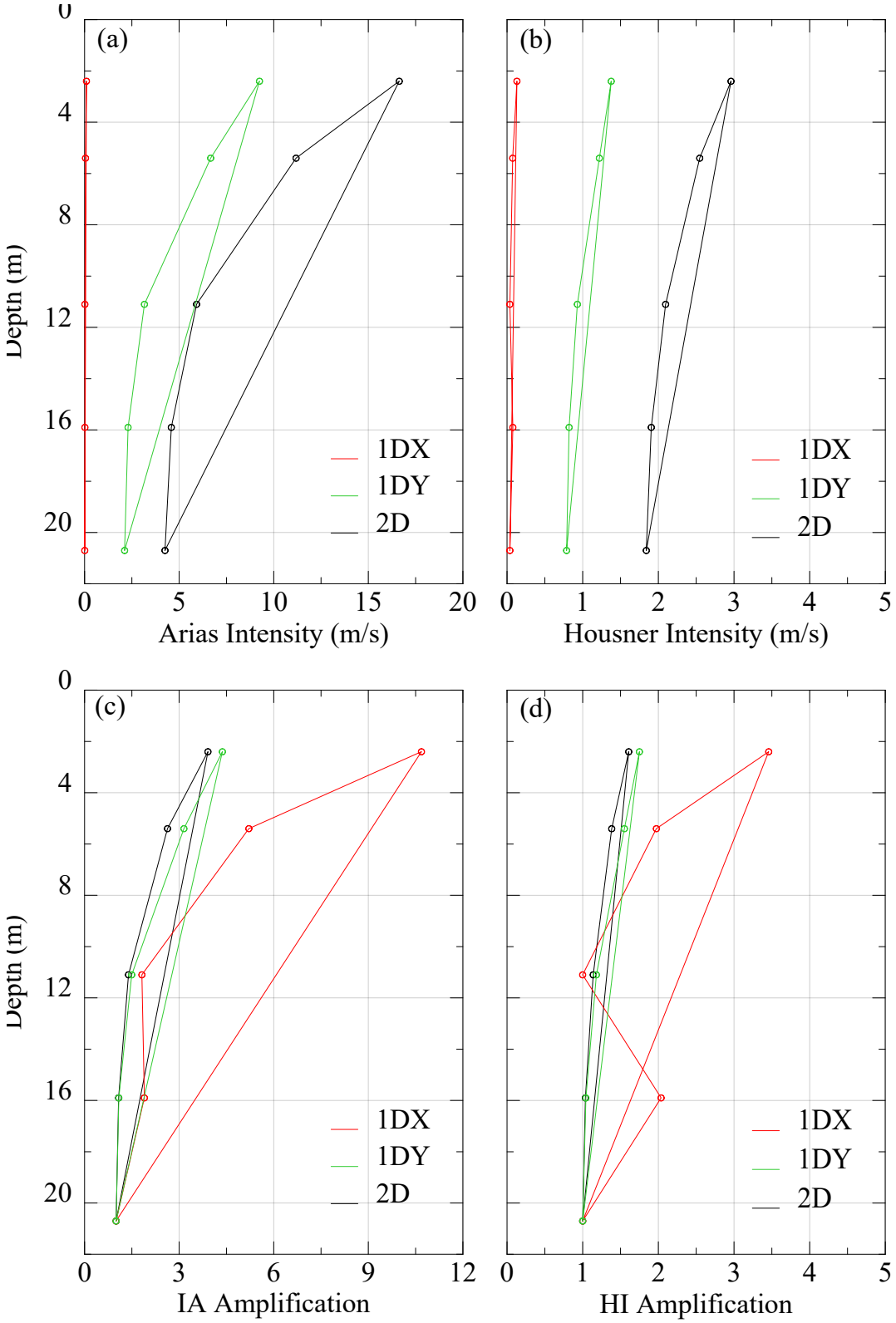

Figure C-308 Variation of total (a) Arias Intensity (M5-X,Y and 2D) ; (b) Housner Intensity (M5-X,Y and 2D) (c) Arias Intensity Amplification Factor (M5-X,Y and 2D); and (d) Housner Intensity Amplification Factor (M5-X,Y and 2D).

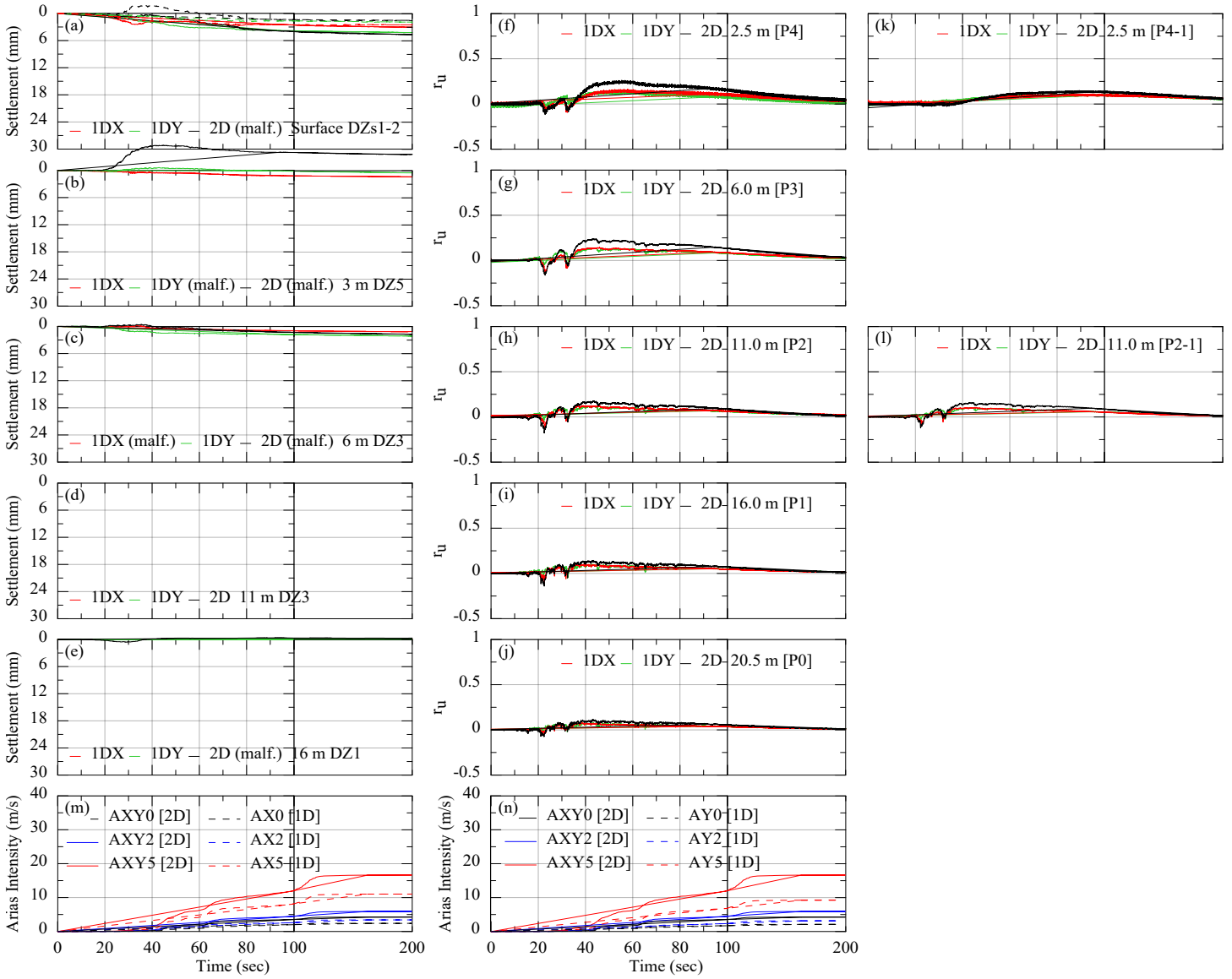

Figure C-309 Variation of total (a) to (e) Settlement with depth (M5-X,Y and 2D) ; (f) to (l) Excess pore water pressure ratio (ru) (M5-X,Y and 2D) (m) and (n) Arias Intensity along model (M5-X,Y and 2D).

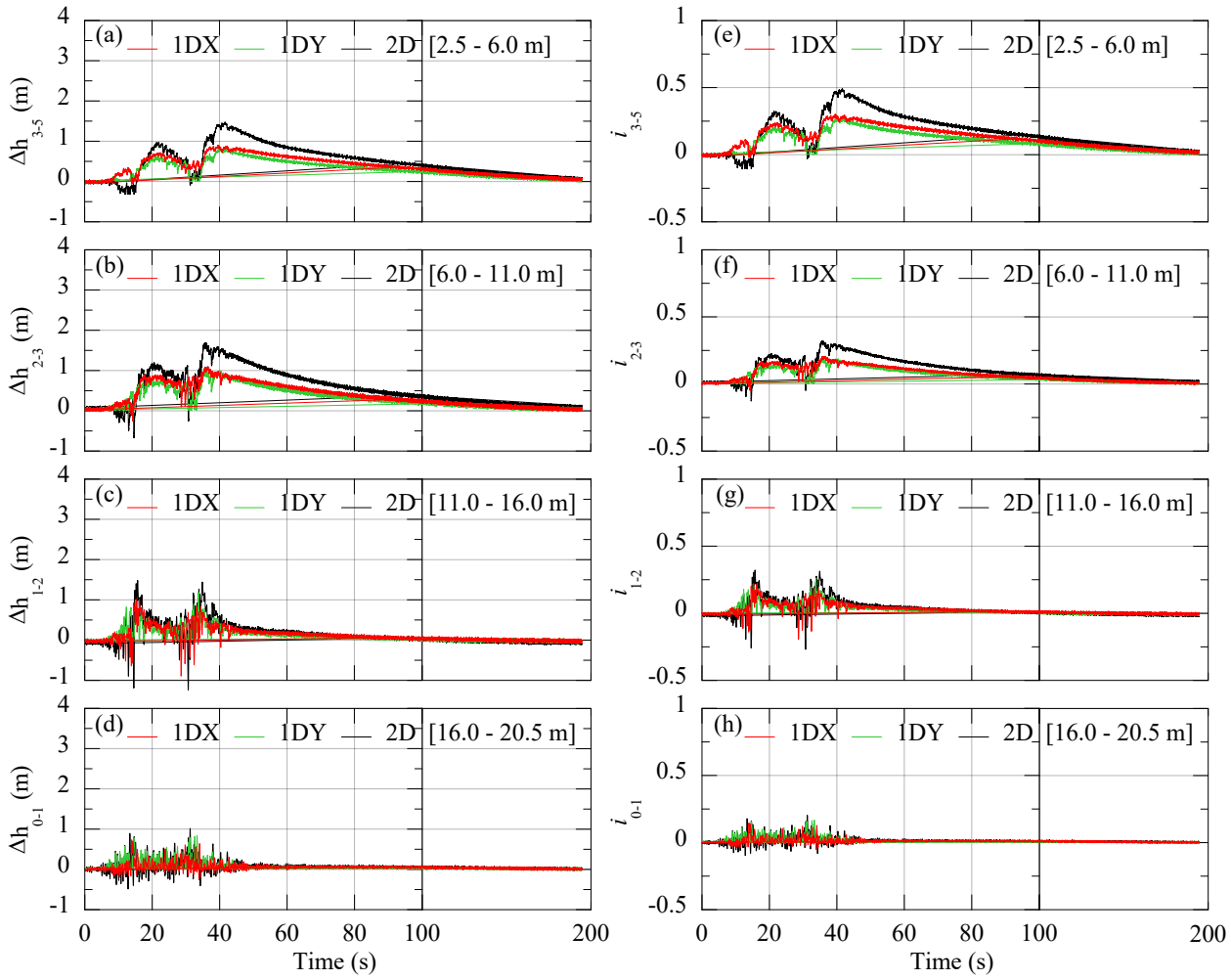

Figure C-310 Variation of total (a) to (d) Total Head Loss with depth (M5-X, Y and 2D); (e) to (h) Shaking induced Hydraulic Gradient (M5-X, Y and 2D)

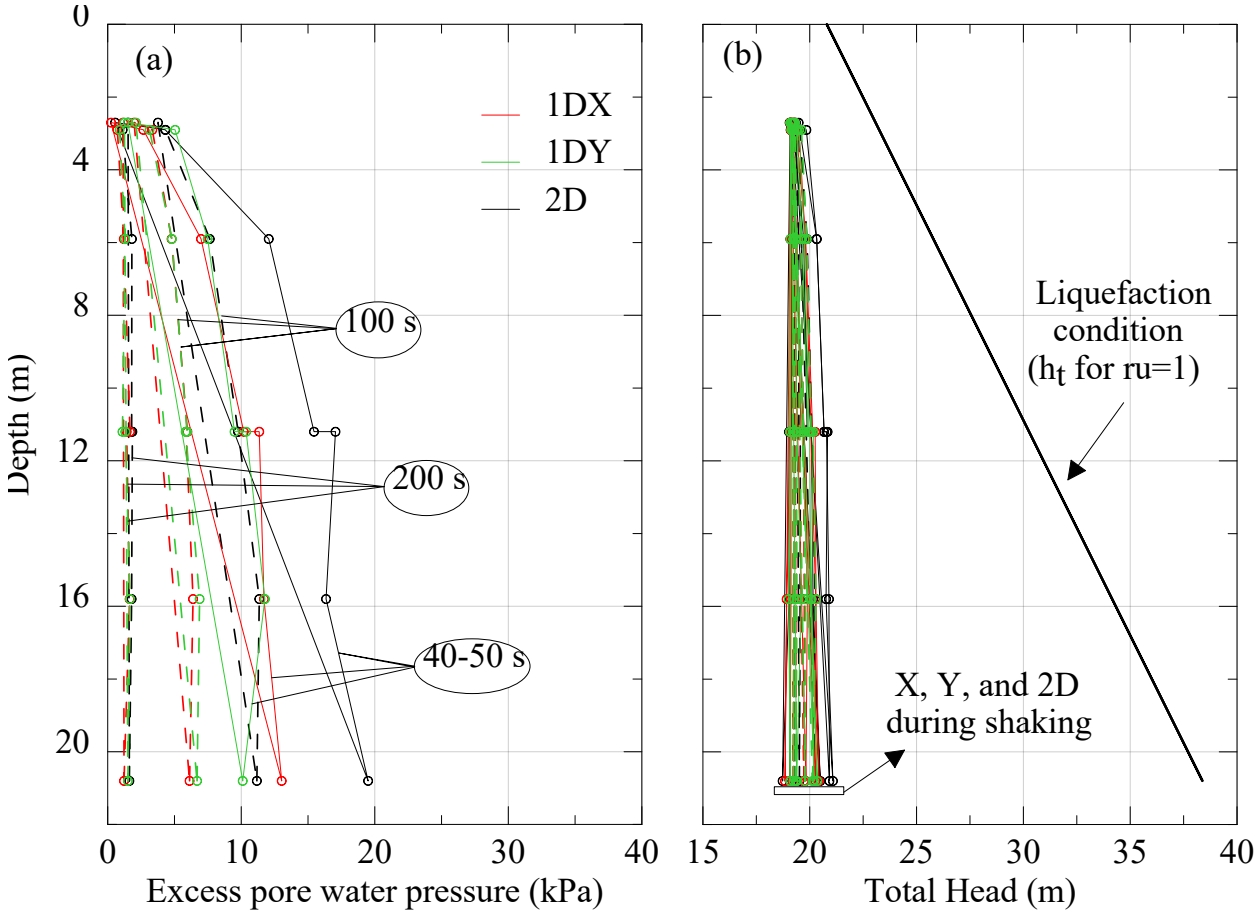

Figure C-311 Variation of total (a) Excess pore water pressure ratio (ru) with depth (M5-X,Y and 2D); (e) to (b) Total Head Loss with depth (M5-X,Y and 2D)

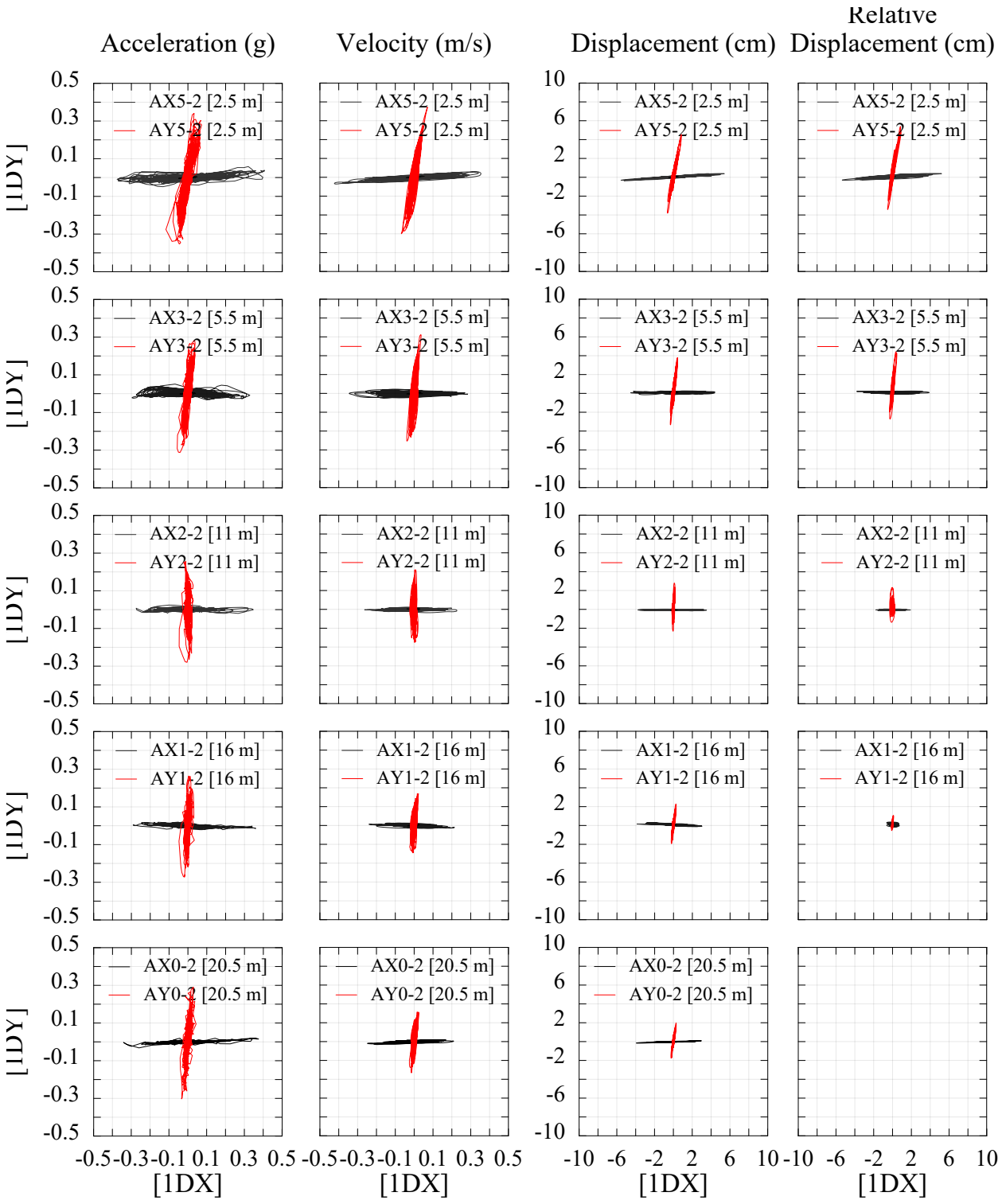

Figure C-312 Recorded input and within model ground motions for acceleration, velocity, displacement and relative displacement for M5-1D [X] and M5-1D [Y]

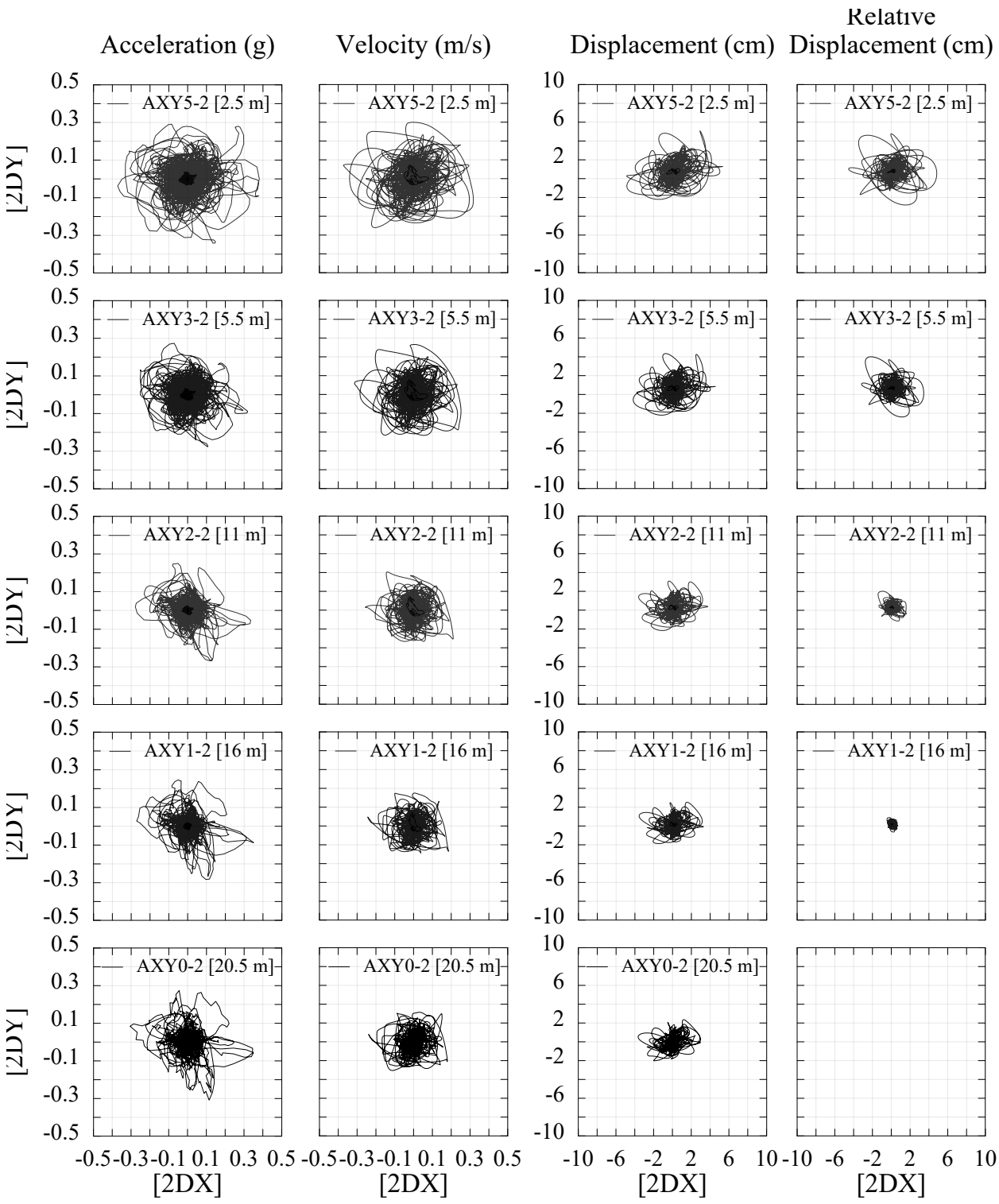

Figure C-313 Recorded input and within model ground motions for acceleration, velocity, displacement and relative displacement for M5-2D

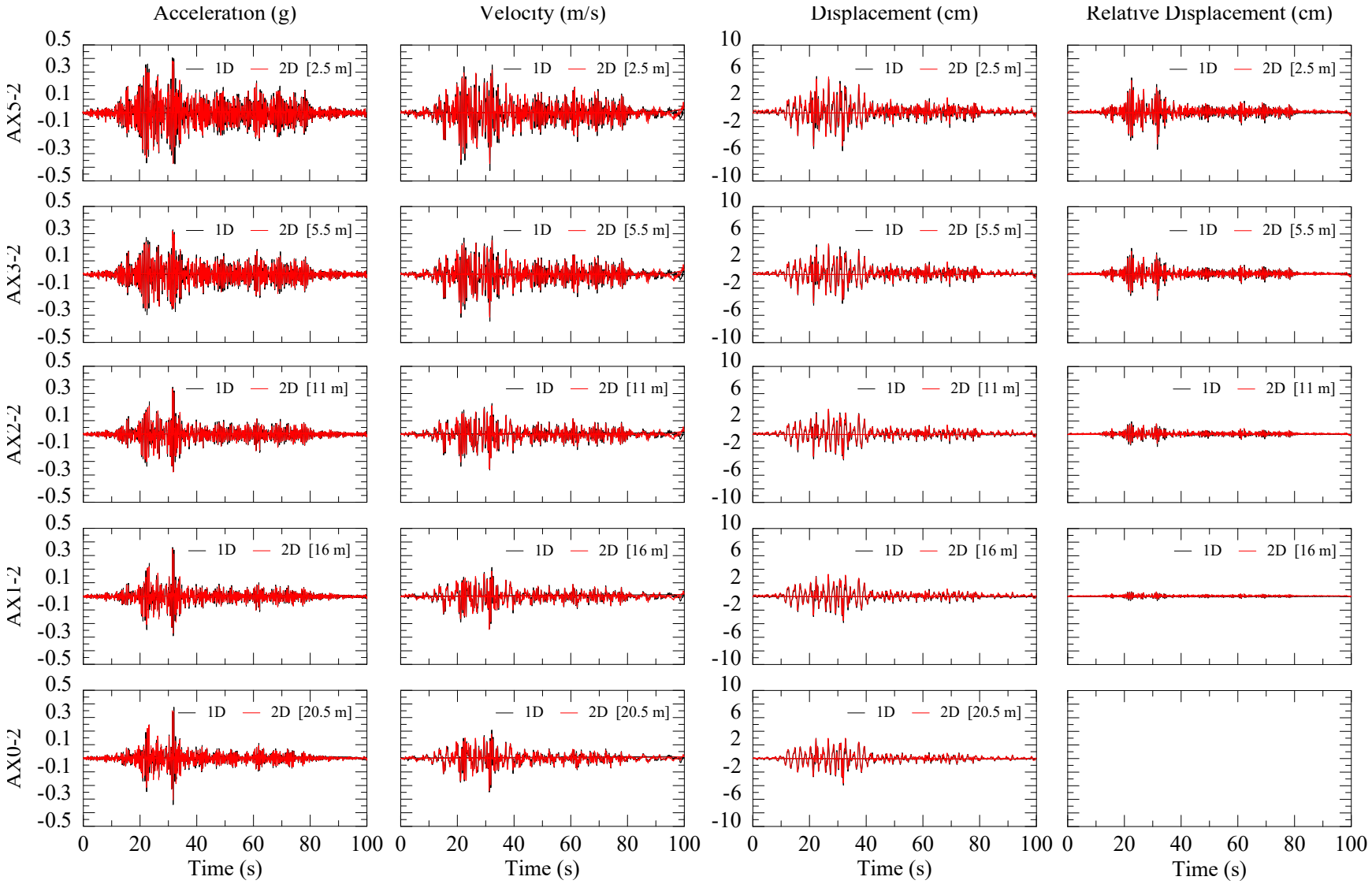

Figure C-314 Recorded input and within model ground motions time histories for acceleration, velocity, displacement and relative displacement for M5-2D [X] and M5-1D [X]

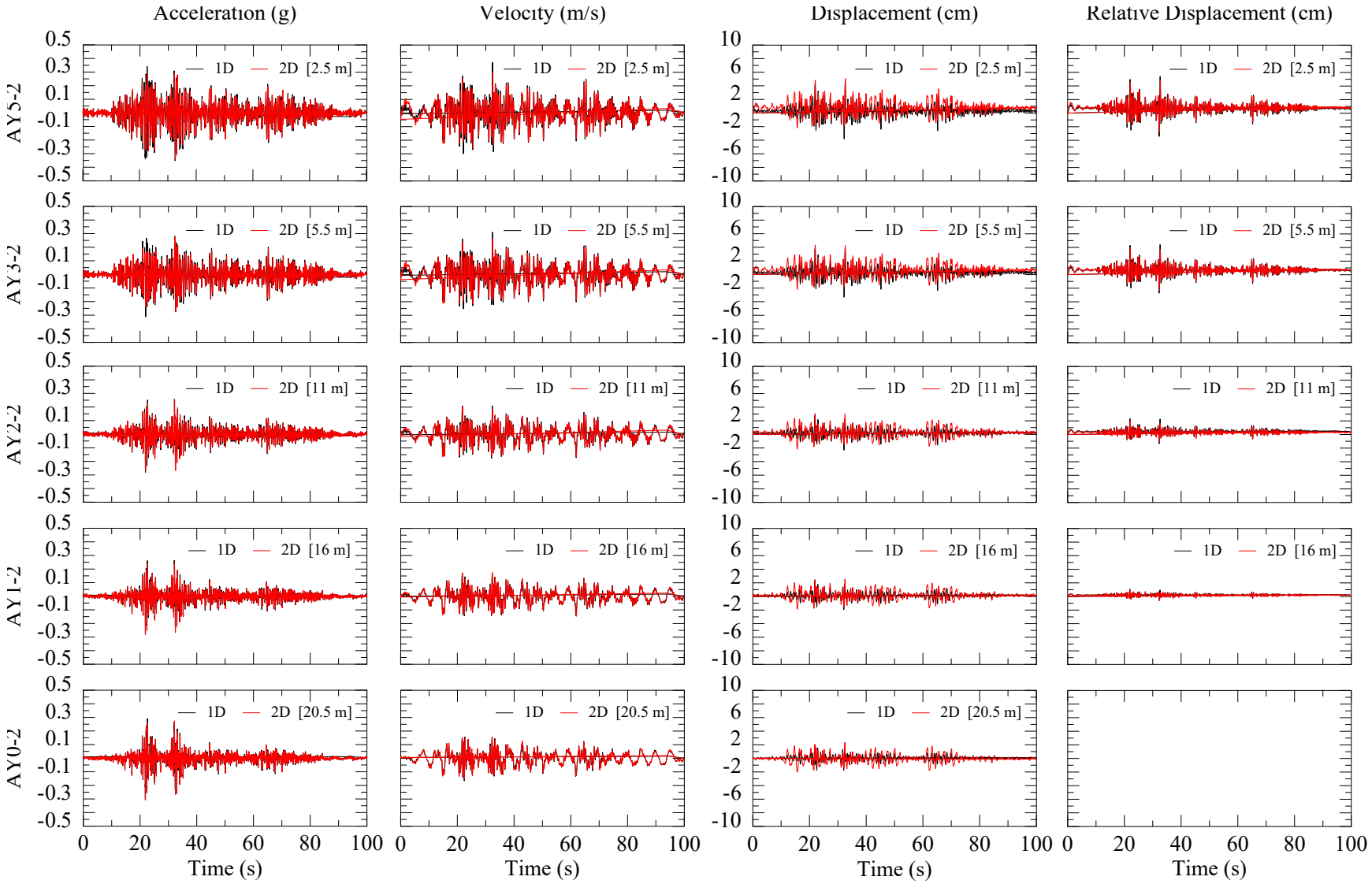

Figure C-315 Recorded input and within model ground motions time histories for acceleration, velocity, displacement and relative displacement for M5-2D [Y] and M5-1D [Y]

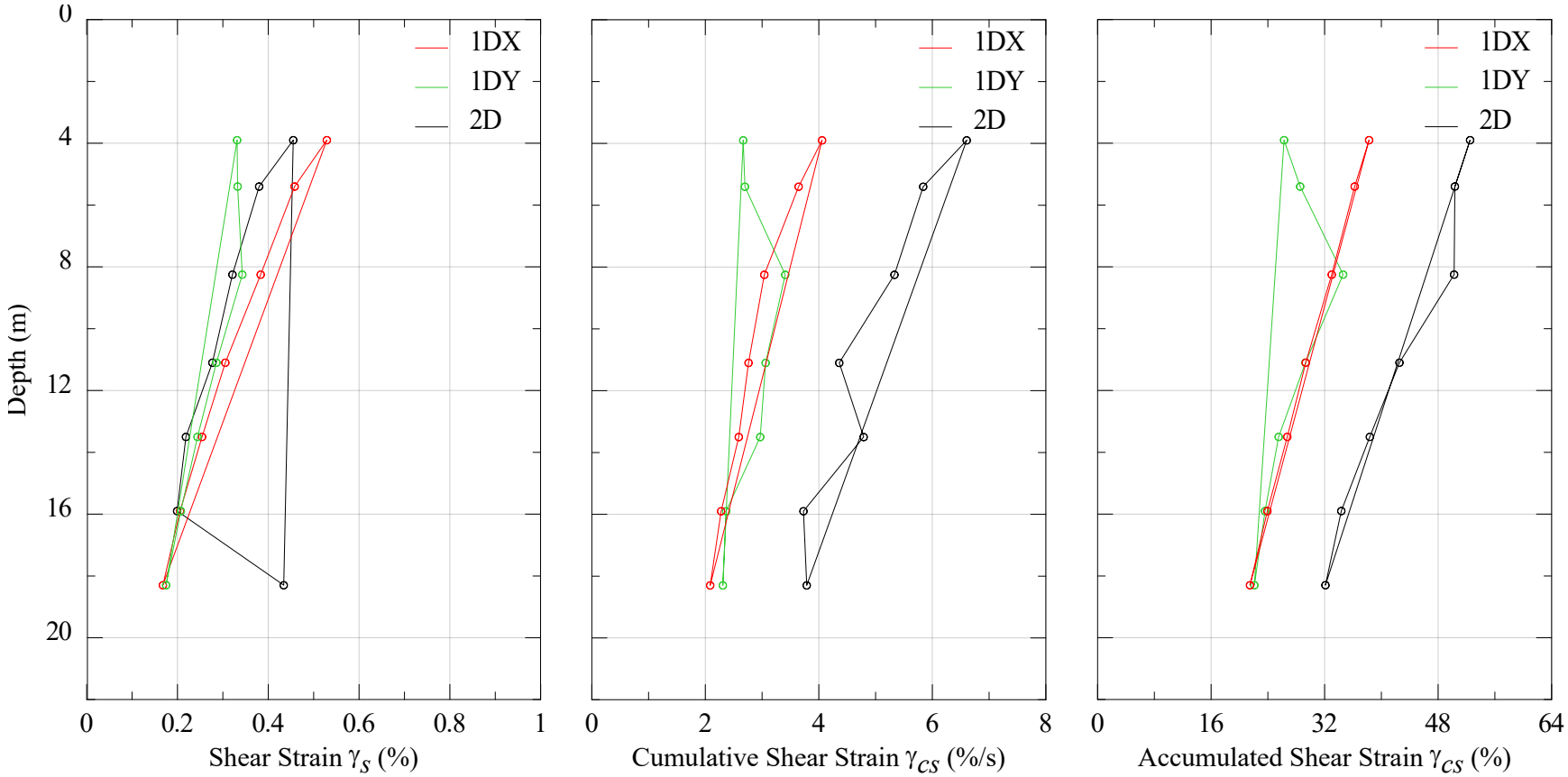

Figure C-316 Estimated (a) maximum shear strain; (b) cumulative shear strain; and (c) accumulated shear strain for M5-2D [X] and M5-1D [X]

1.4.8 Motion 6 (M6)

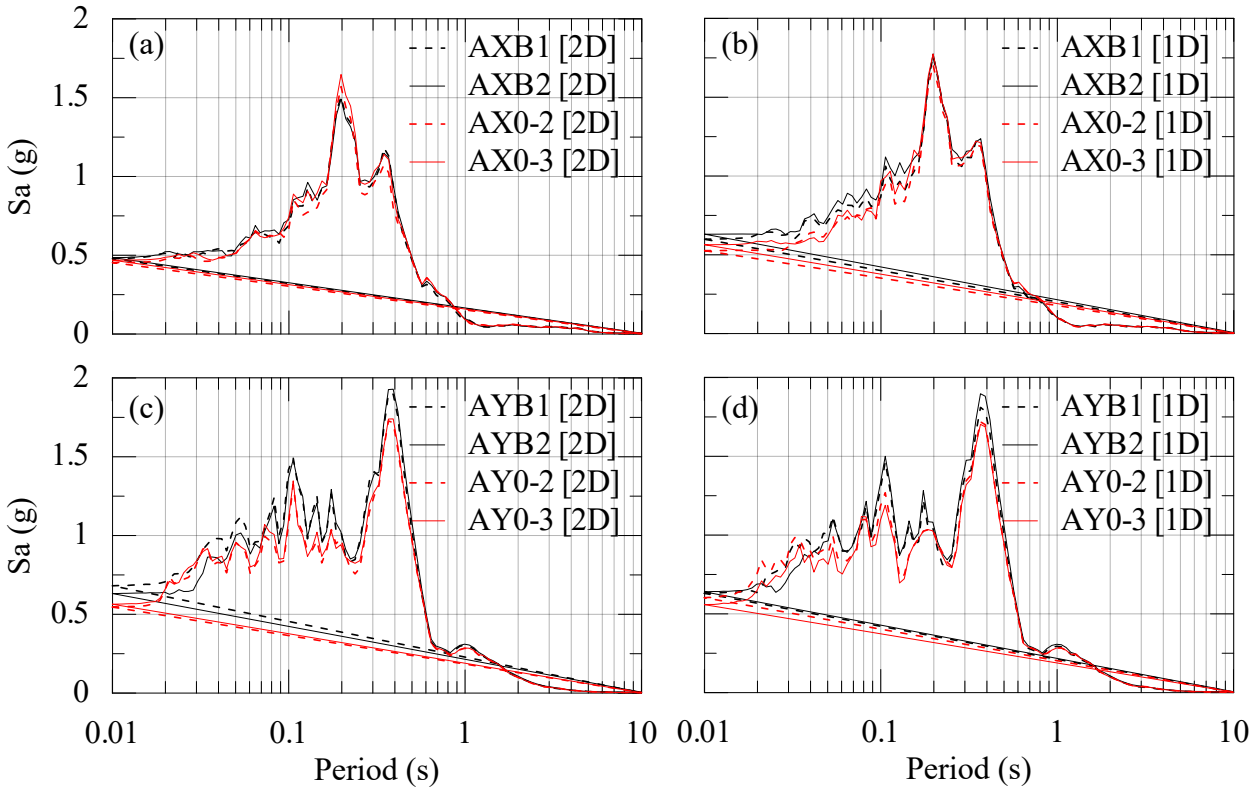

Figure C-317 Comparison of response spectra of 2D laminar container table and within model base input motion for motions (M6-X, Y and 2D).

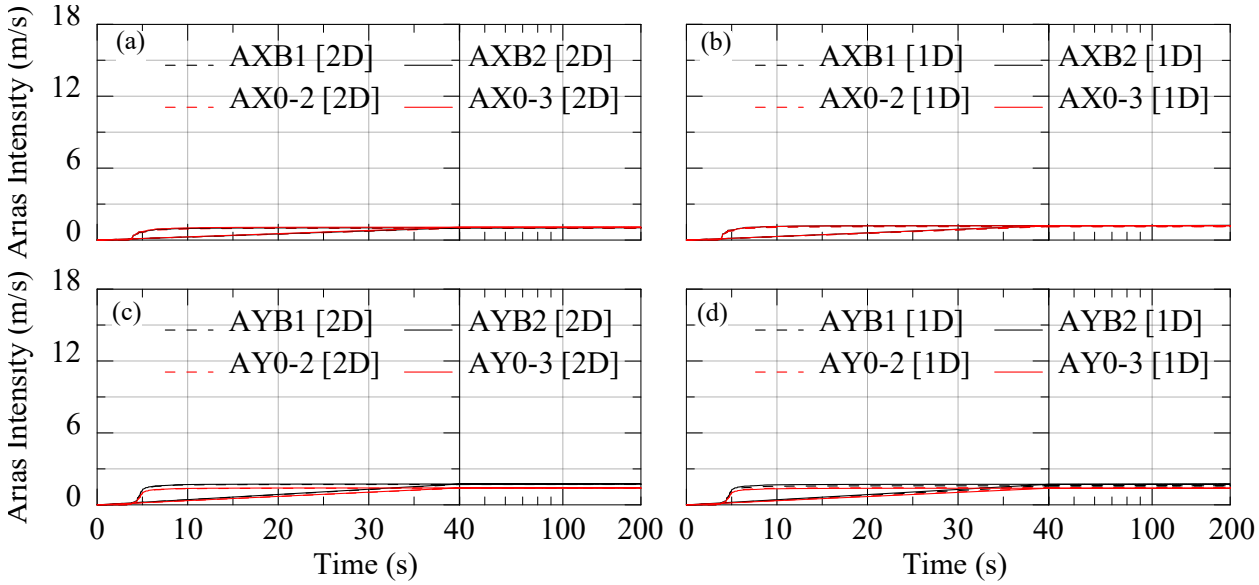

Figure C-318 Comparison of Arias Intensity of 2D laminar container table and within model base input motion for motions (a) M6-2D [X]; (b) M6-2D [Y]; (c) M6-1D [X] and (d) M6-1D [Y]

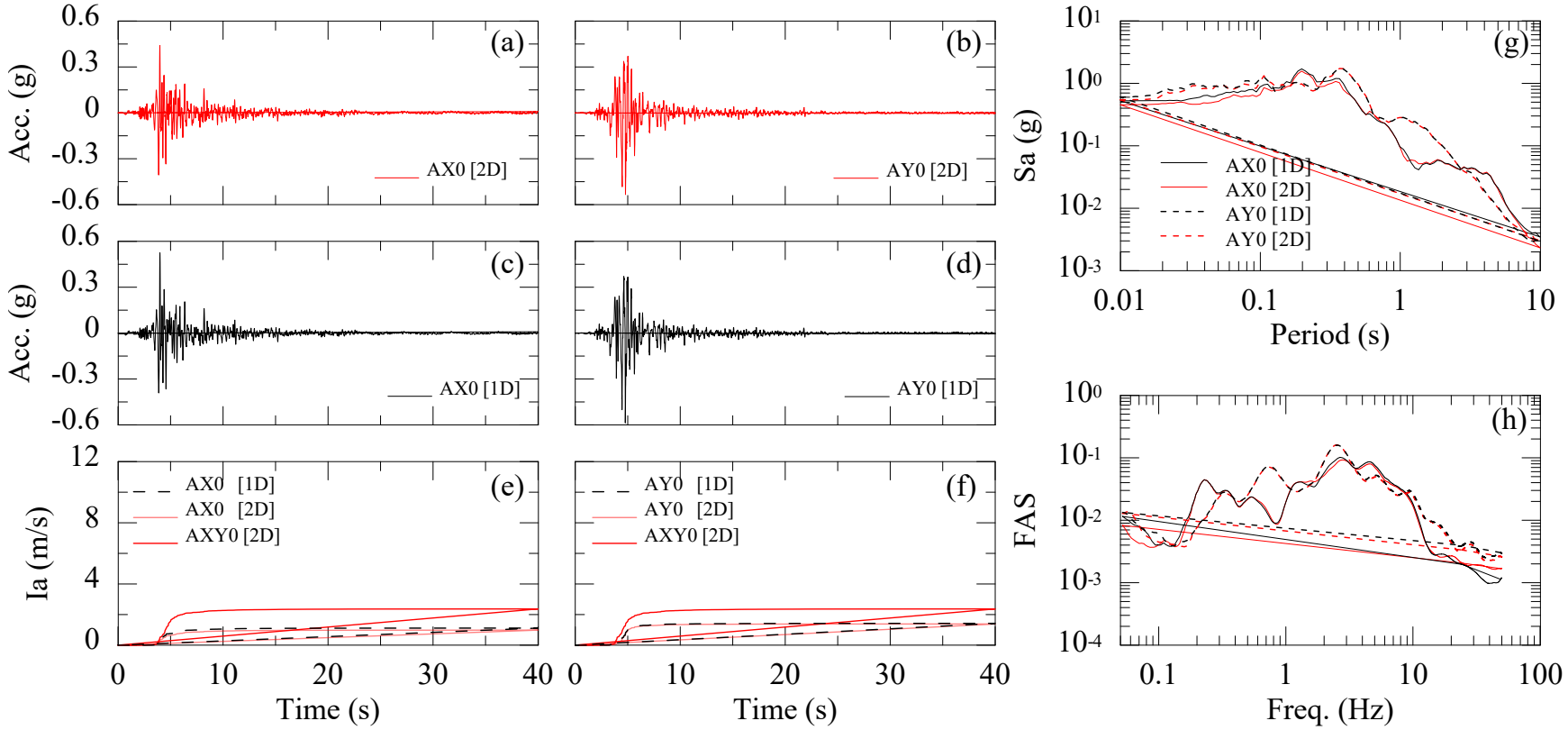

Figure C-319 Recorded input (2D) and 1D (X or Y) ground motions for: (a) M6-2D [X]; (b) M6-2D [Y]; (c) M6-1D [X]; and (d) M6-1D [Y]. Arias Intensity M6 (1D and 2D) for: (e) X direction; and (f) Y direction. Response Spectra (g) M6-2D [X]; M6-2D [Y]; M6-1D [X]; and M6-1D [Y]. Smoothed Fourier amplitude spectra (FAS) (h) M6-2D [X]; M6-2D [Y]; M6-1D [X]; and M6-1D [Y].

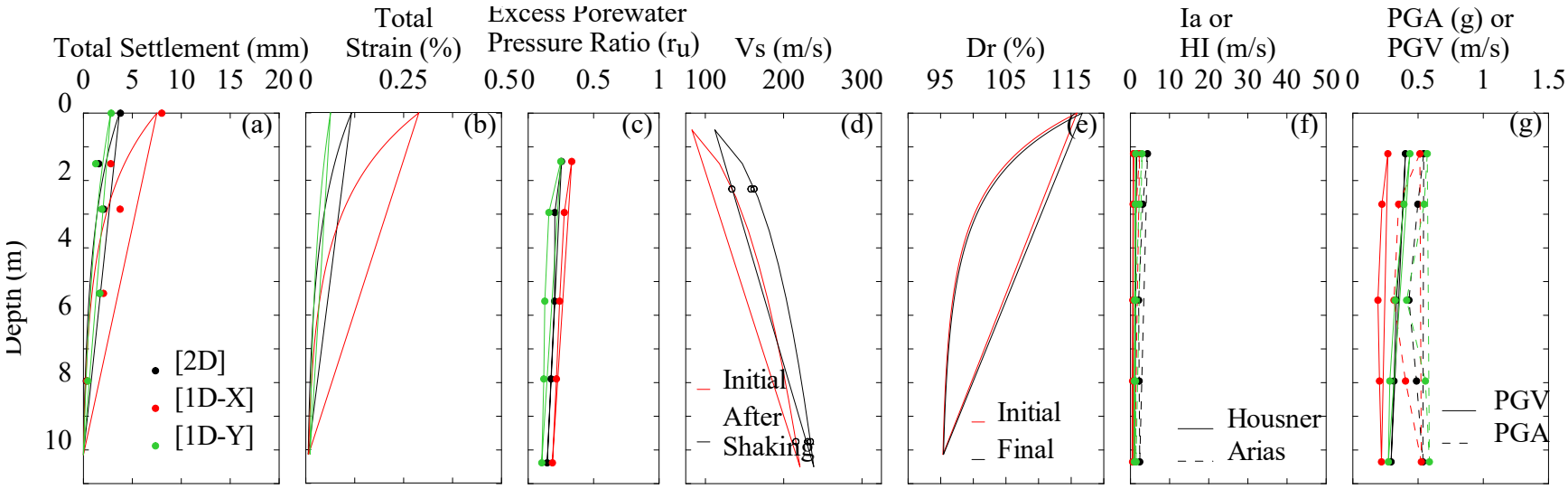

Figure C-320 Recorded or computed profiles for input motion M6-X, Y, and 2D. (a) Settlement; (b) total strain; (c) excess pore water pressure ratio; (d) shear wave velocity; (e) relative density; (f) Arias and Housner intensities; and (g) PGA and PGV.

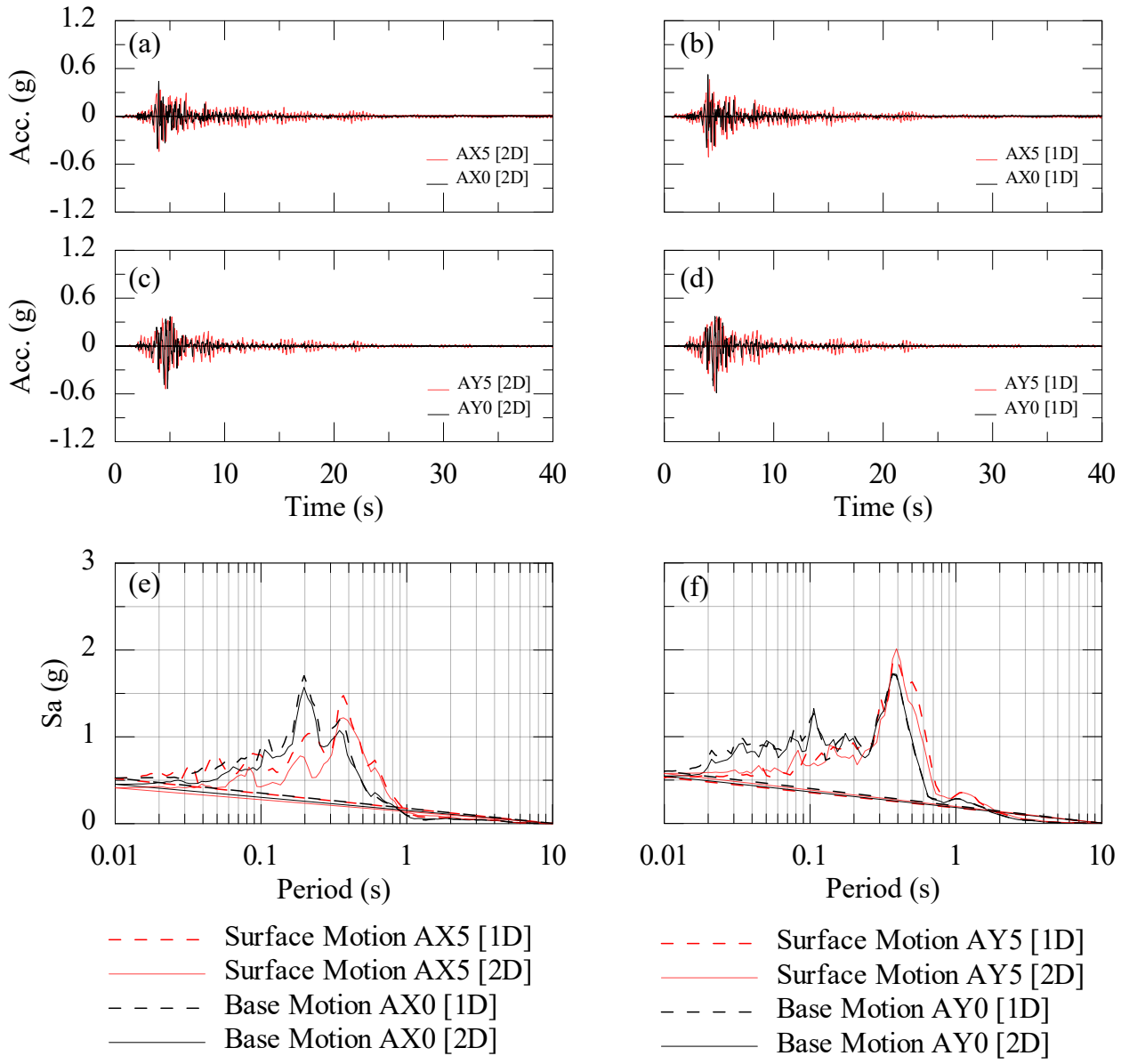

Figure C-321 Recorded input and surface ground motion: (a) M6-2D [X]; (b) M6-1D [X]; (c) M6-2D [Y]; and (d) M6-1D [Y]. Computed response spectra from Free Field Test [PT2] for motions M6 (1D and 2D) for: (e) X direction; and (f) Y direction.

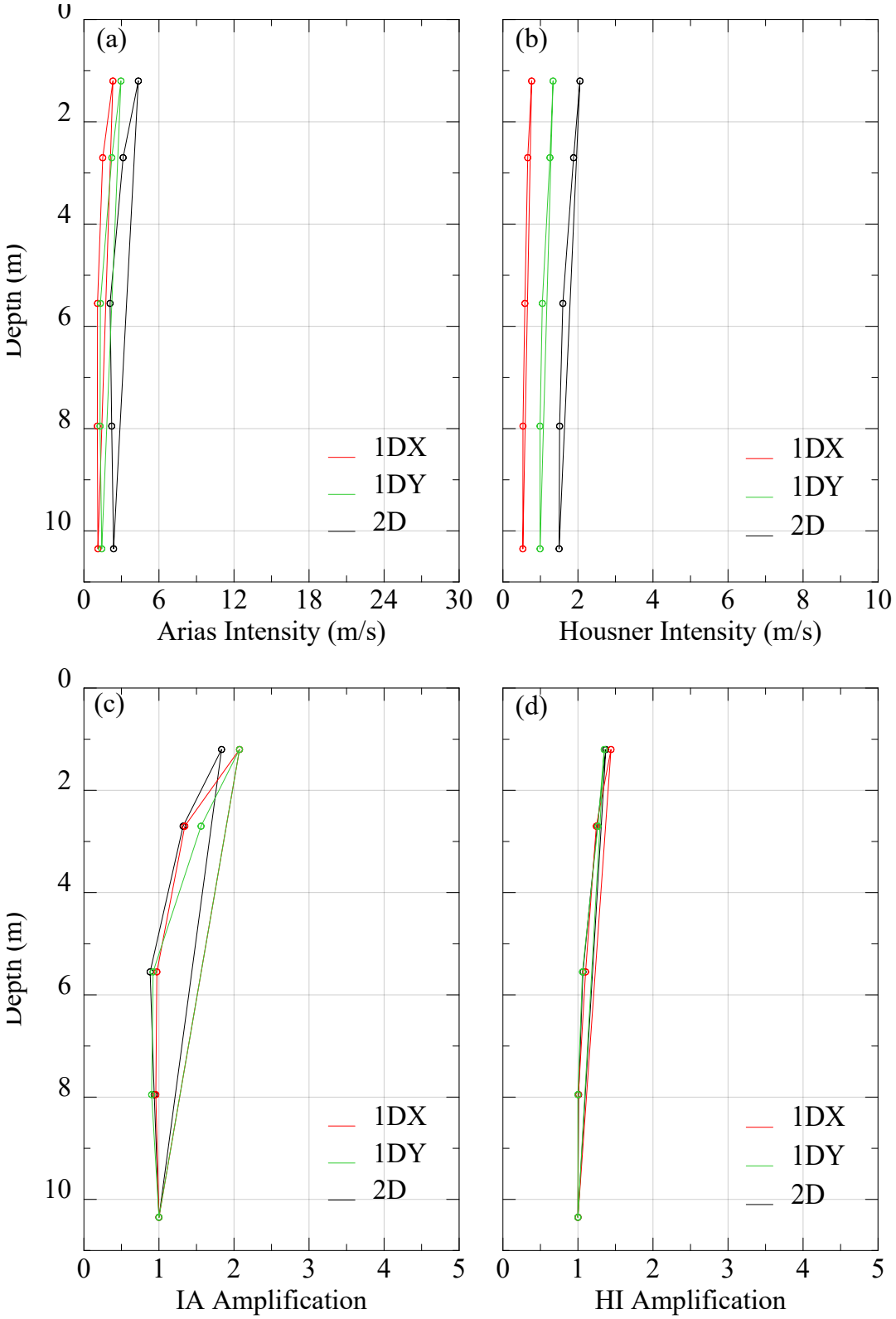

Figure C-322 Variation of total (a) Arias Intensity (M6-X,Y and 2D) ; (b) Housner Intensity (M6-X,Y and 2D) (c) Arias Intensity Amplification Factor (M6-X,Y and 2D); and (d) Housner Intensity Amplification Factor (M6-X,Y and 2D).

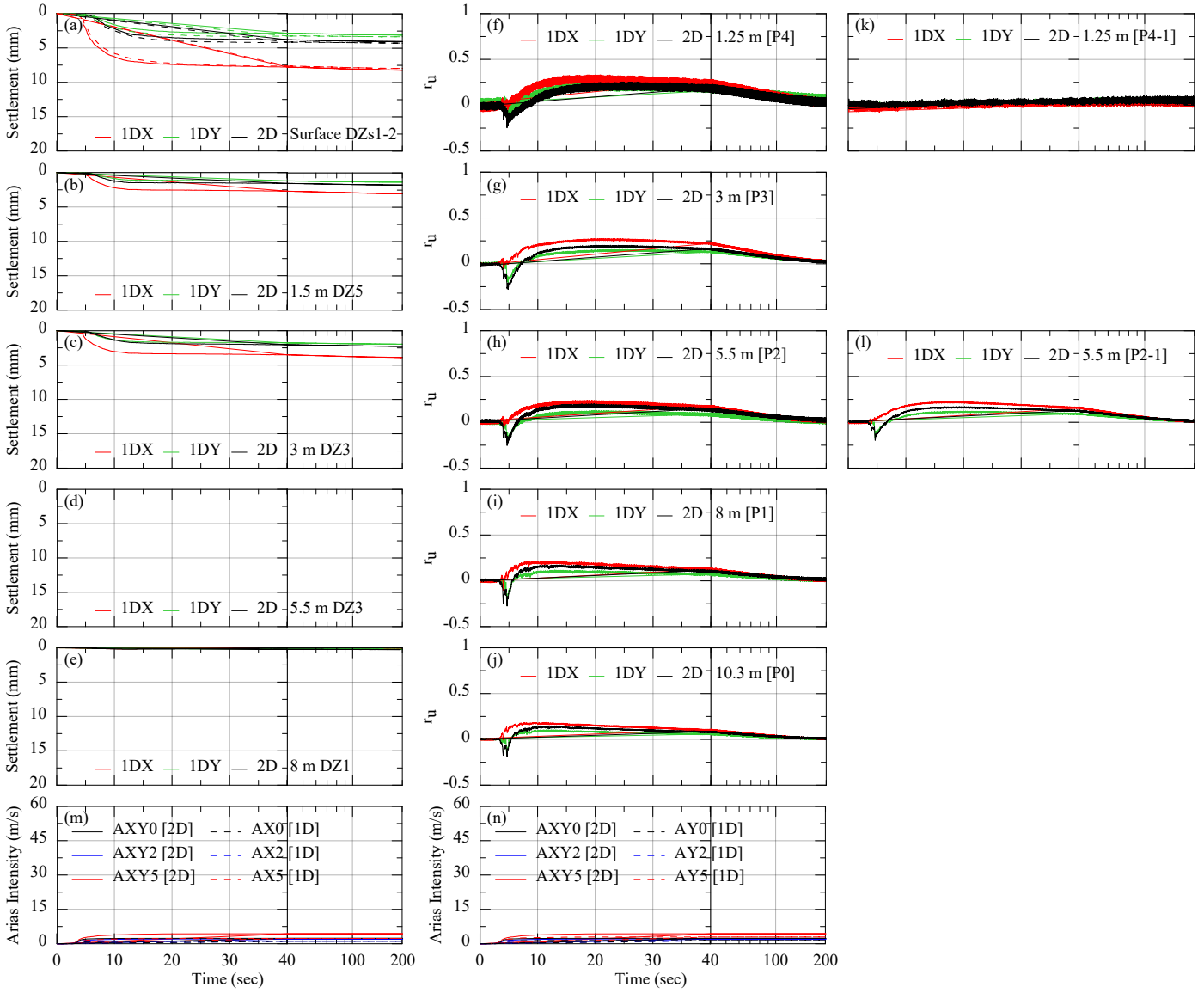

Figure C-323 Variation of total (a) to (e) Settlement with depth (M6-X,Y and 2D) ; (f) to (l) Excess pore water pressure ratio (ru) (M6-X,Y and 2D) (m) and (n) Arias Intensity along model (M6-X,Y and 2D).

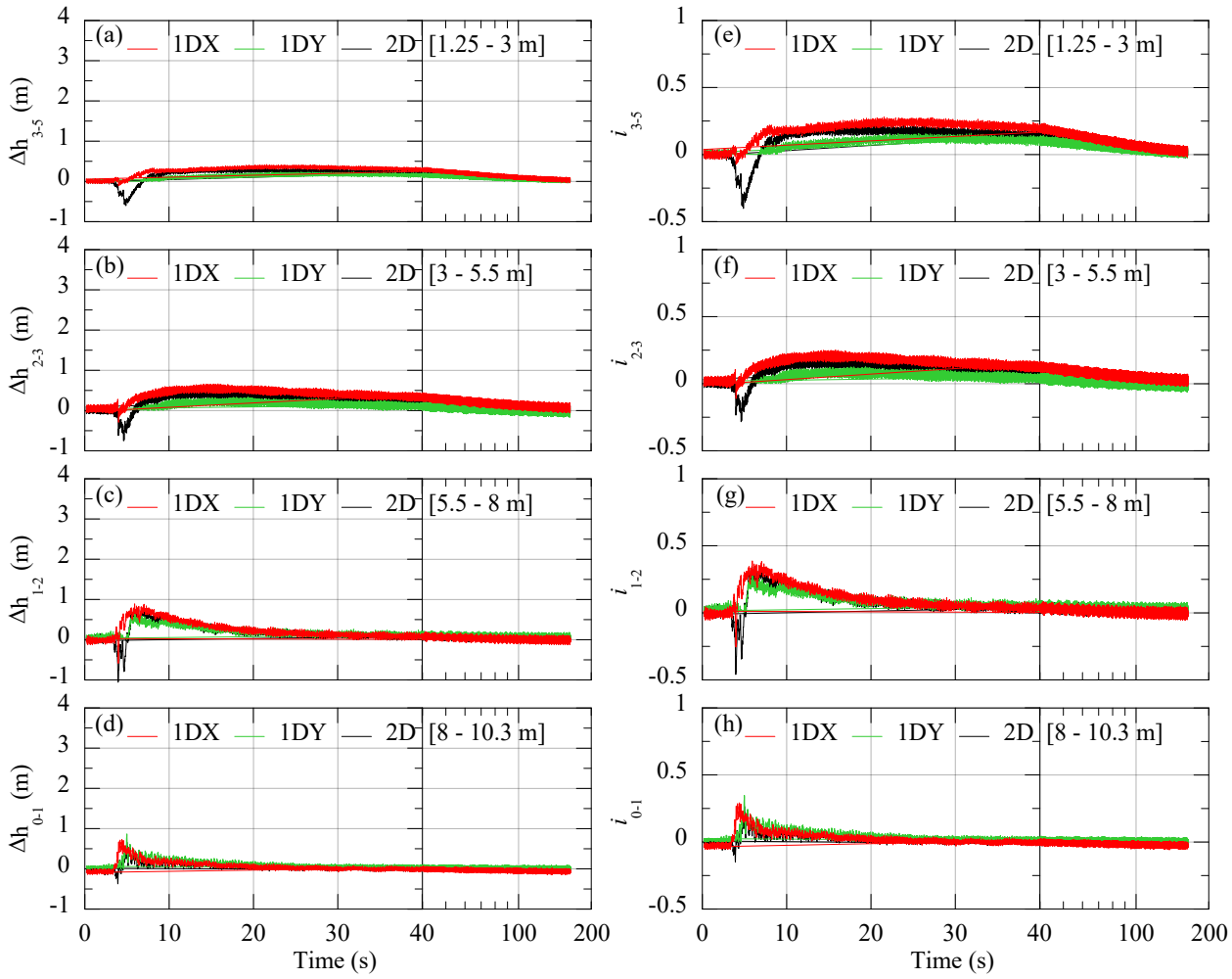

Figure C-324 Variation of total (a) to (d) Total Head Loss with depth (M6-X, Y and 2D); (e) to (h) Shaking induced Hydraulic Gradient (M6-X, Y and 2D)

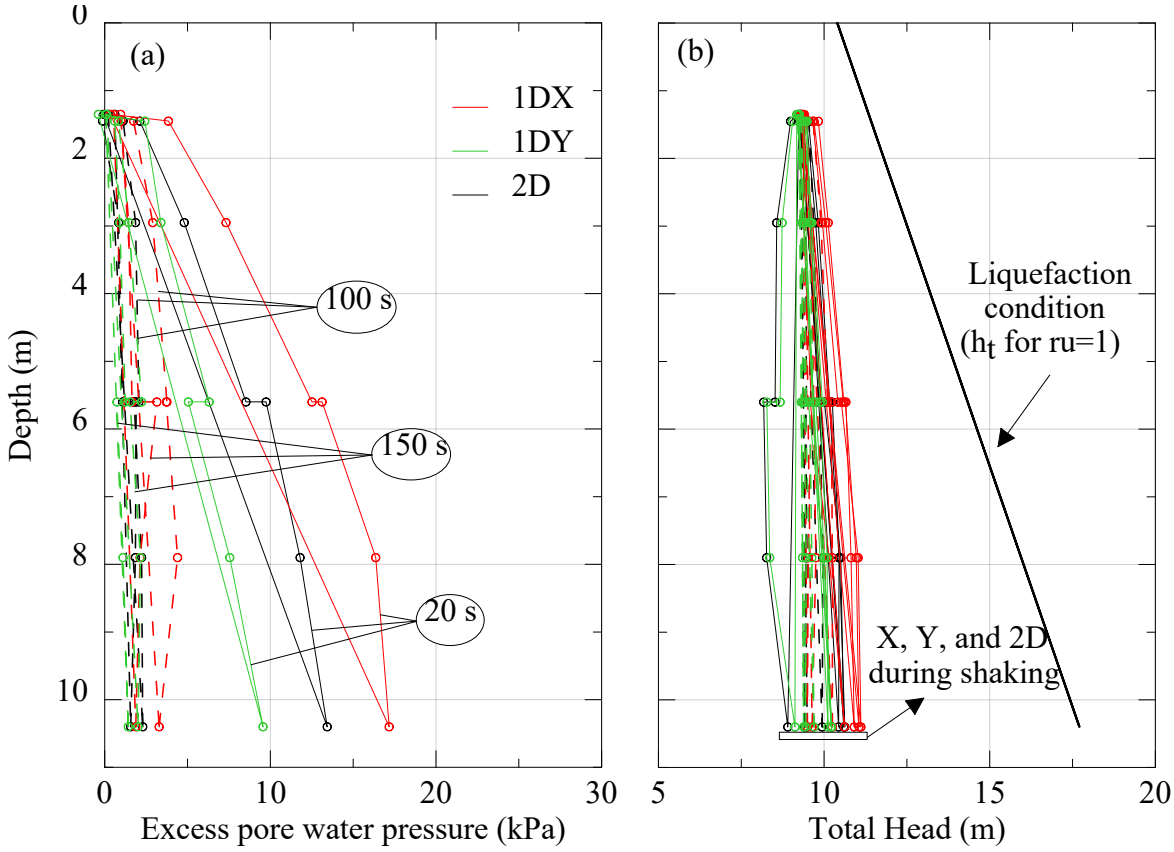

Figure C-325 Variation of total (a) Excess pore water pressure ratio (ru) with depth (M6-X,Y and 2D); (e) to (b) Total Head Loss with depth (M6-X,Y and 2D)

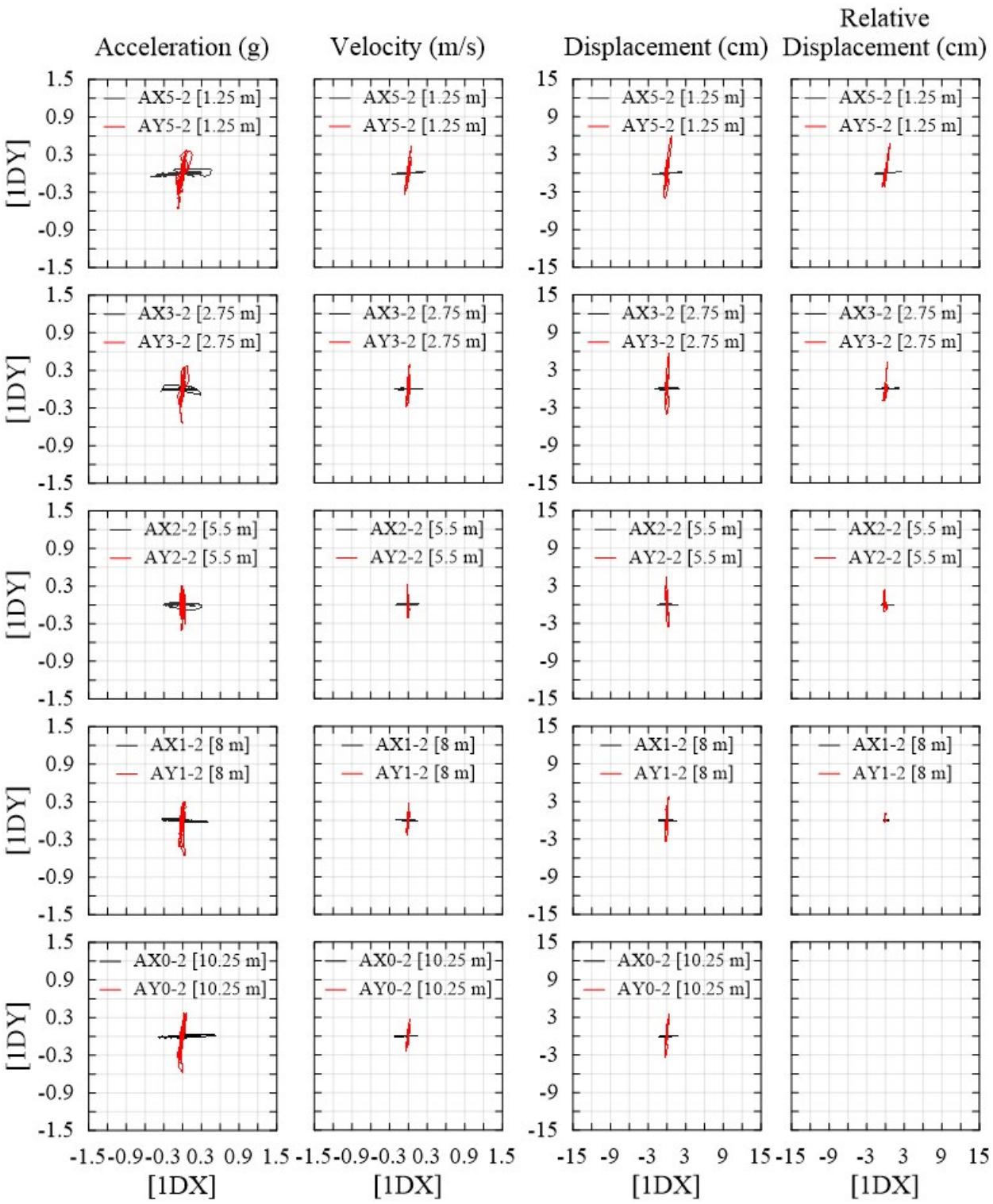

Figure C-326 Recorded input and within model ground motions for acceleration, velocity, displacement and relative displacement for M6-1D [X] and M6-1D [Y]

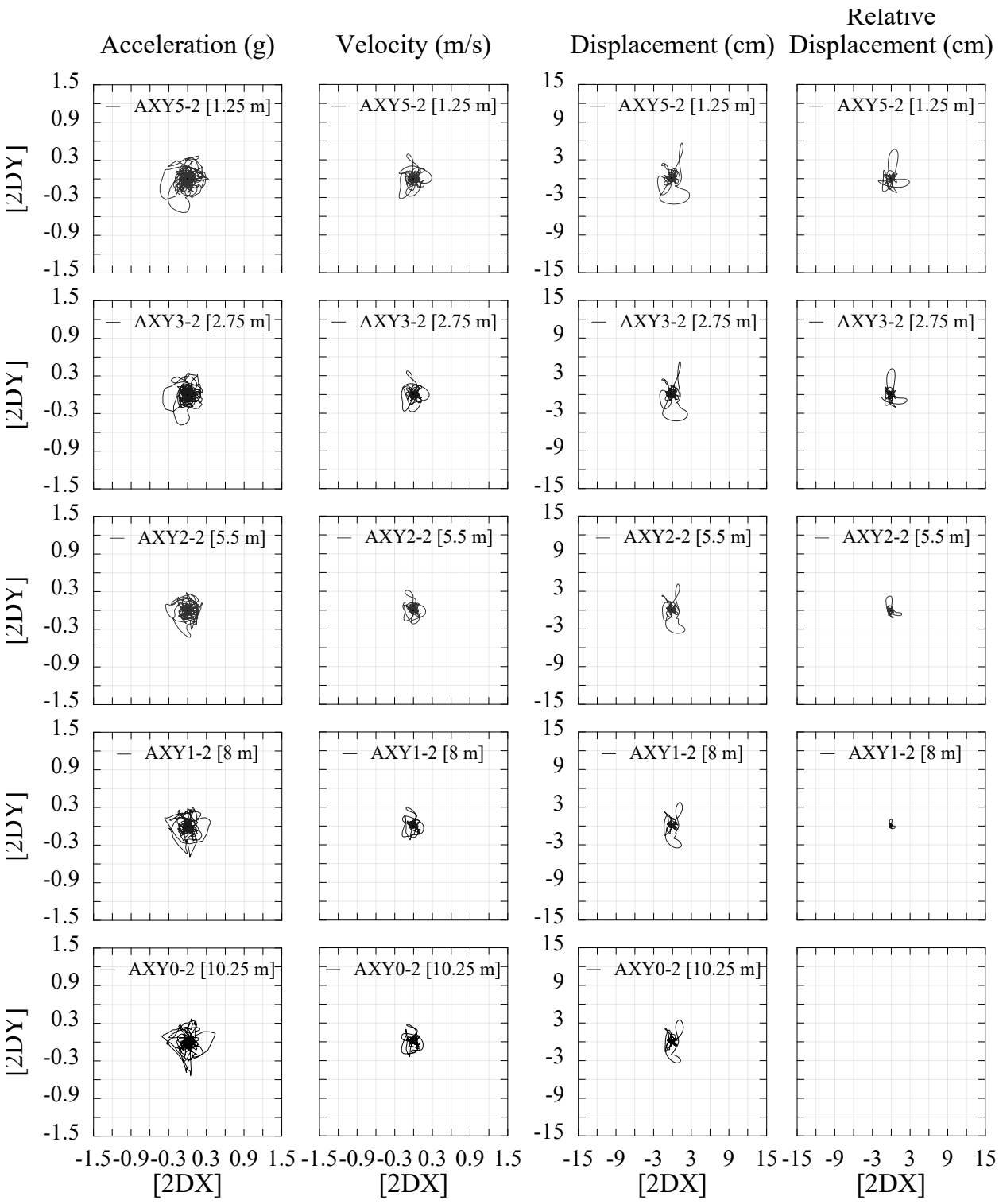

Figure C-327 Recorded input and within model ground motions for acceleration, velocity, displacement and relative displacement for M6-2D

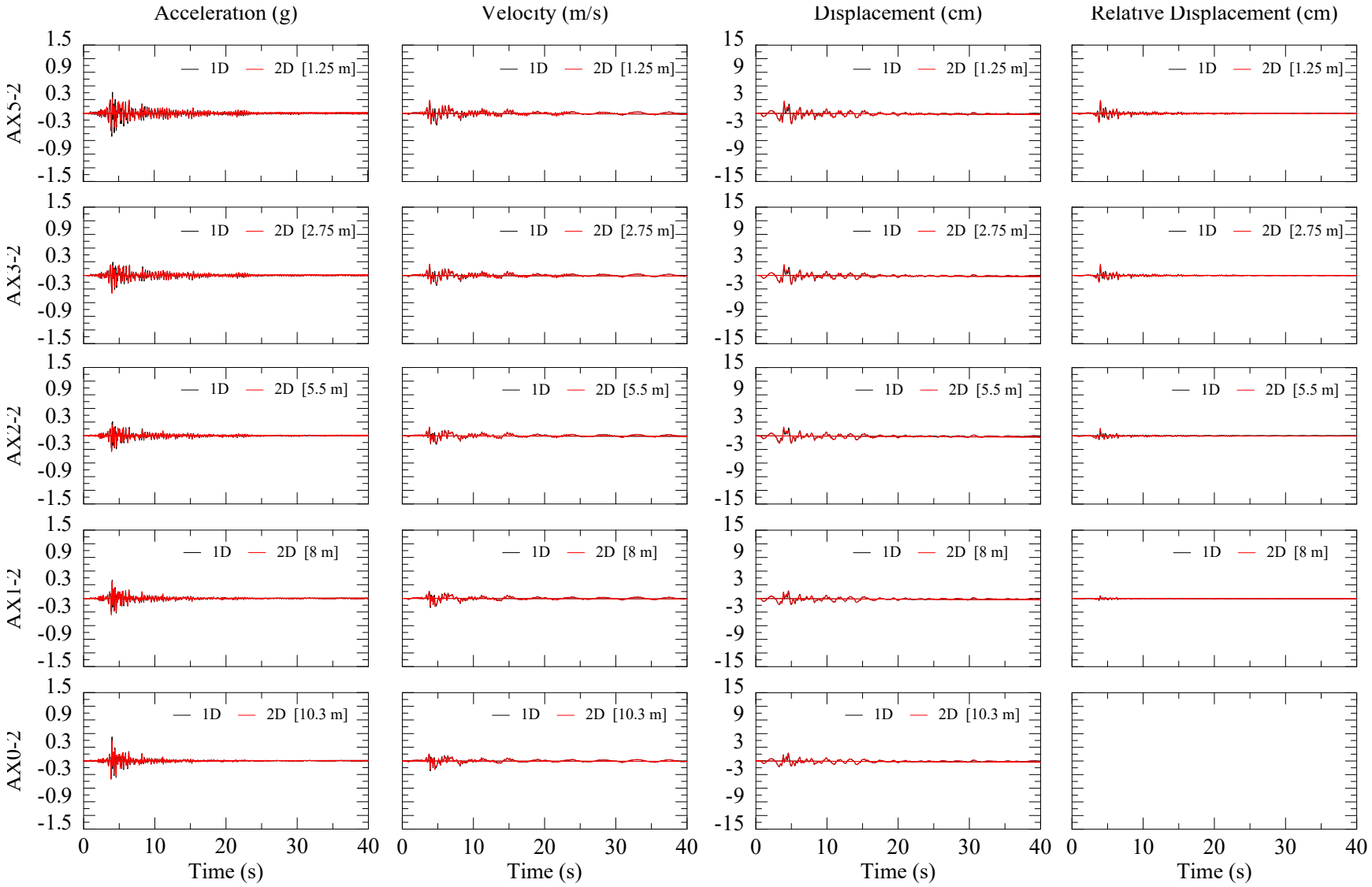

Figure C-328 Recorded input and within model ground motions time histories for acceleration, velocity, displacement and relative displacement for M6-2D [X] and M6-1D [X]

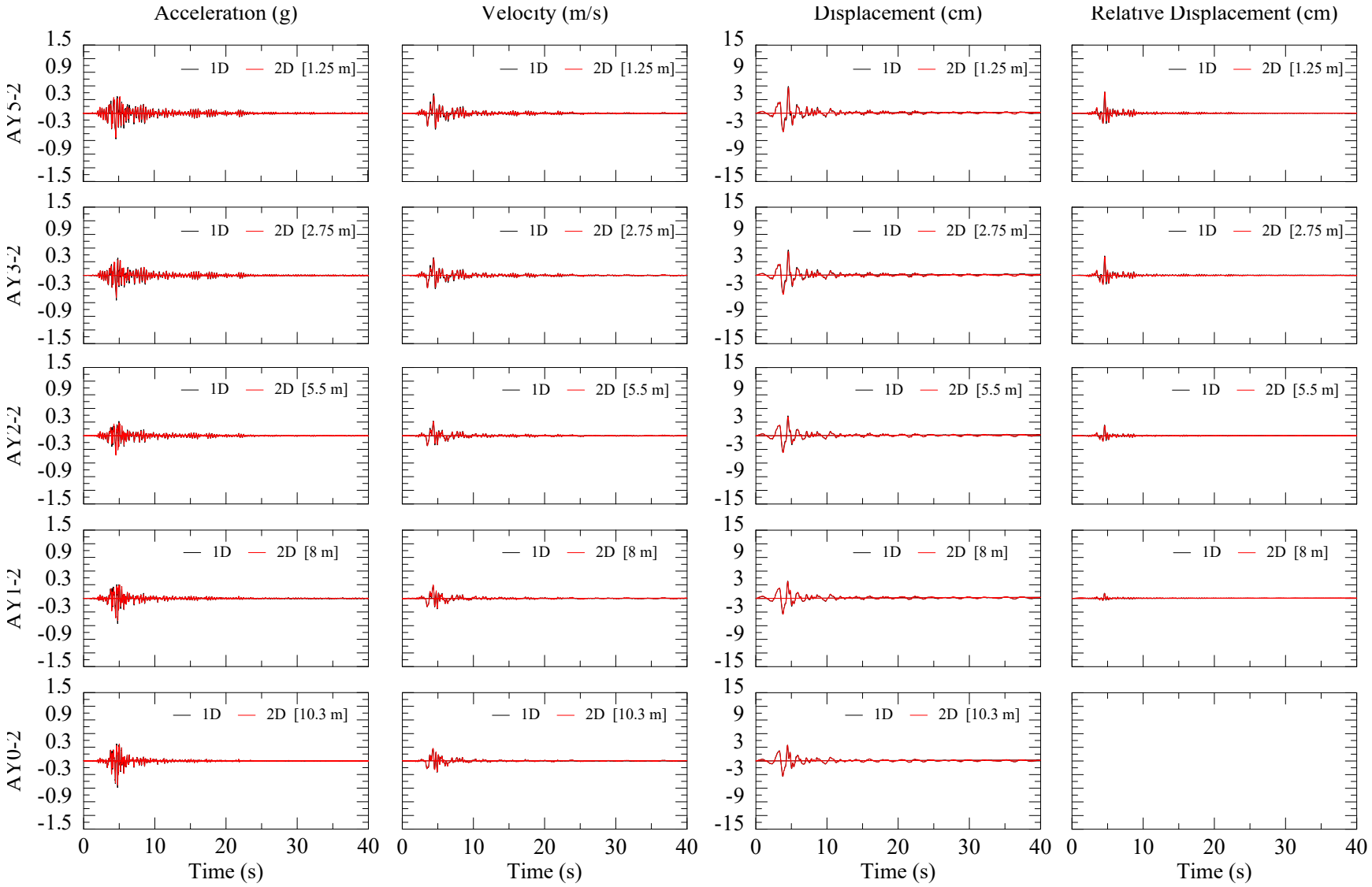

Figure C-329 Recorded input and within model ground motions time histories for acceleration, velocity, displacement and relative displacement for M6-2D [Y] and M6-1D [Y]

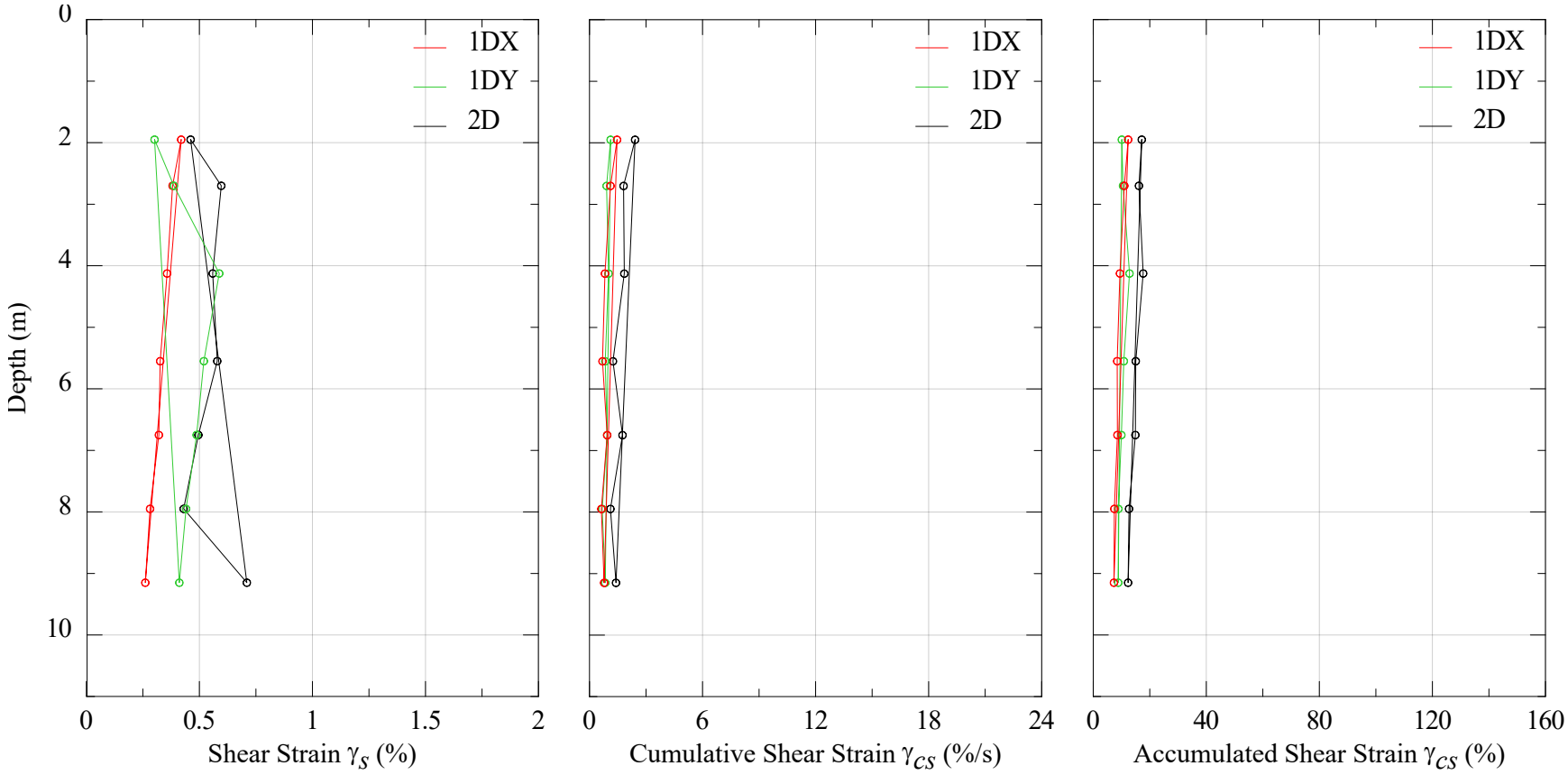

Figure C-330 Estimated (a) maximum shear strain; (b) cumulative shear strain; and (c) accumulated shear strain for M6-2D [X] and M6-1D [X]

1.4.9 Motion 7 (M7)

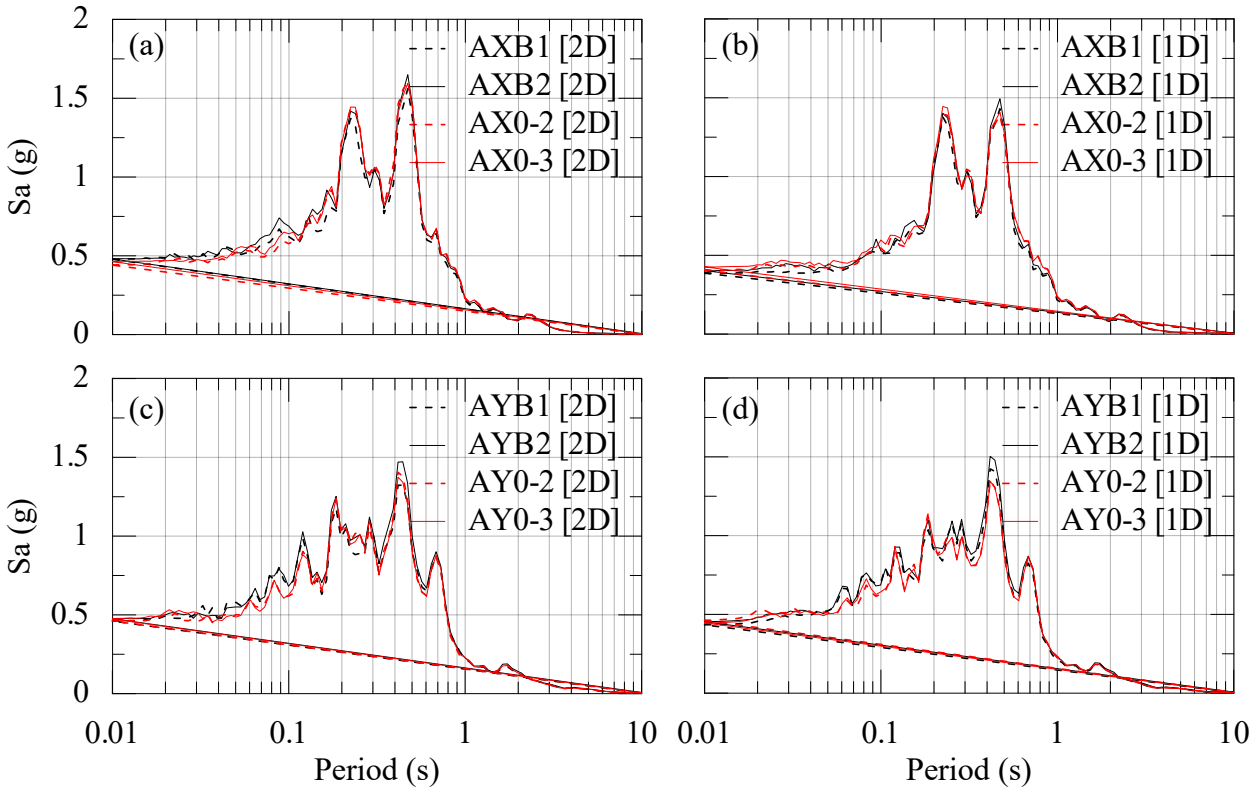

Figure C-331 Comparison of response spectra of 2D laminar container table and within model base input motion for motions (M7-X, Y and 2D).

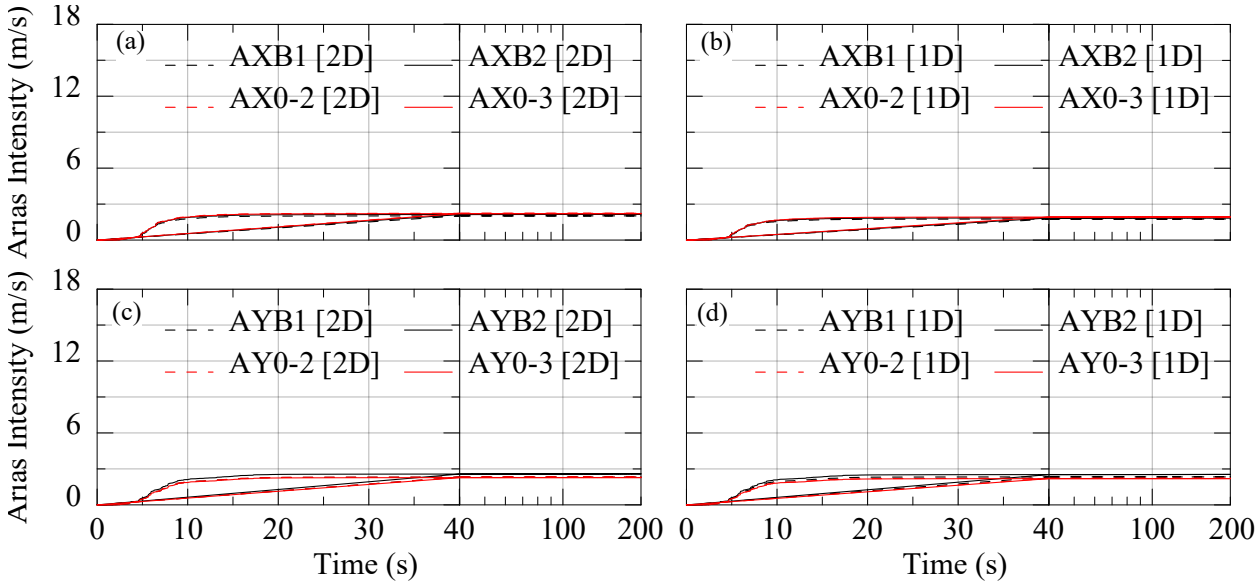

Figure C-332 Comparison of Arias Intensity of 2D laminar container table and within model base input motion for motions (a) M7-2D [X]; (b) M7-2D [Y]; (c) M7-1D [X] and (d) M7-1D [Y]

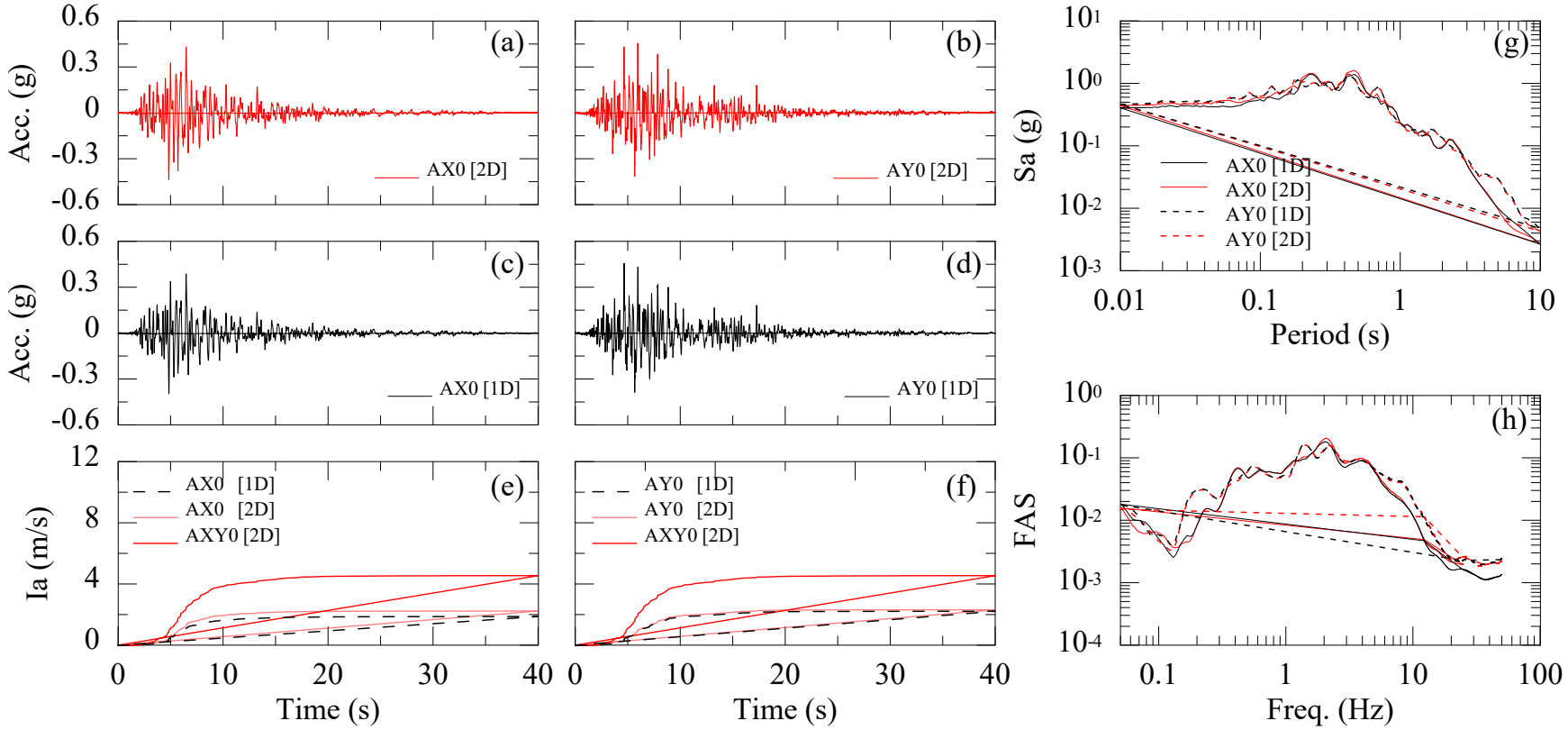

Figure C-333 Recorded input (2D) and 1D (X or Y) ground motions for: (a) M7-2D [X]; (b) M7-2D [Y]; (c) M7-1D [X]; and (d) M7-1D [Y]. Arias Intensity M7 (1D and 2D) for: (e) X direction; and (f) Y direction. Response Spectra (g) M7-2D [X]; M7-2D [Y]; M7-1D [X]; and M7-1D [Y]. Smoothed Fourier amplitude spectra (FAS) (h) M7-2D [X]; M7-2D [Y]; M7-1D [X]; and M7-1D [Y].

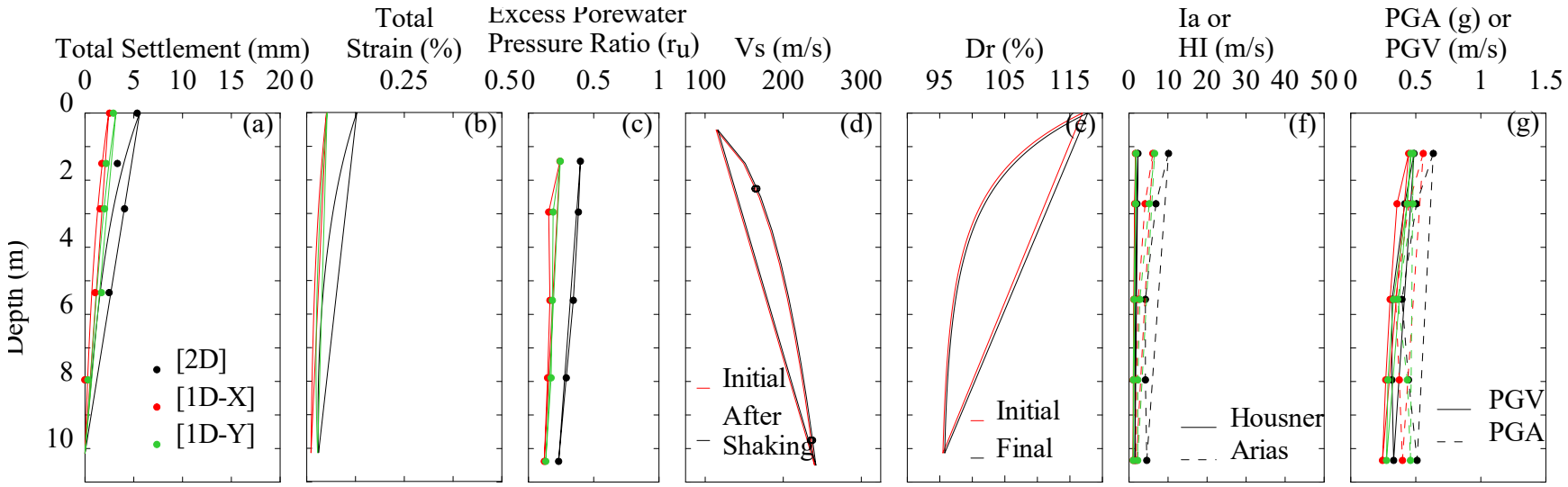

Figure C-334 Recorded or computed profiles for input motion M7-X, Y, and 2D. (a) Settlement; (b) total strain; (c) excess pore water pressure ratio; (d) shear wave velocity; (e) relative density; (f) Arias and Housner intensities; and (g) PGA and PGV.

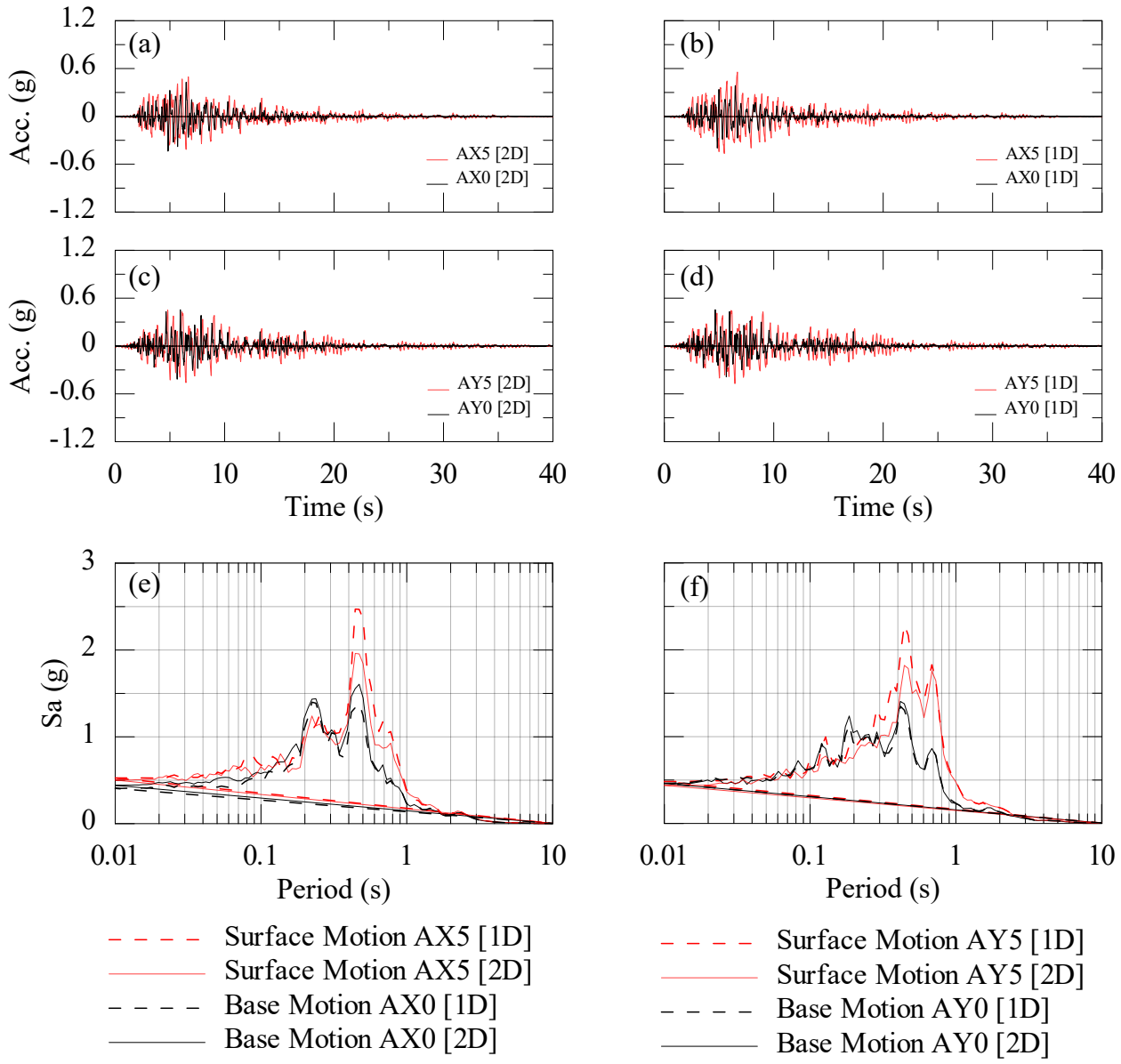

Figure C-335 Recorded input and surface ground motion: (a) M7-2D [X]; (b) M7-1D [X]; (c) M7-2D [Y]; and (d) M7-1D [Y]. Computed response spectra from Free Field Test [PT2] for motions M7 (1D and 2D) for: (e) X direction; and (f) Y direction.

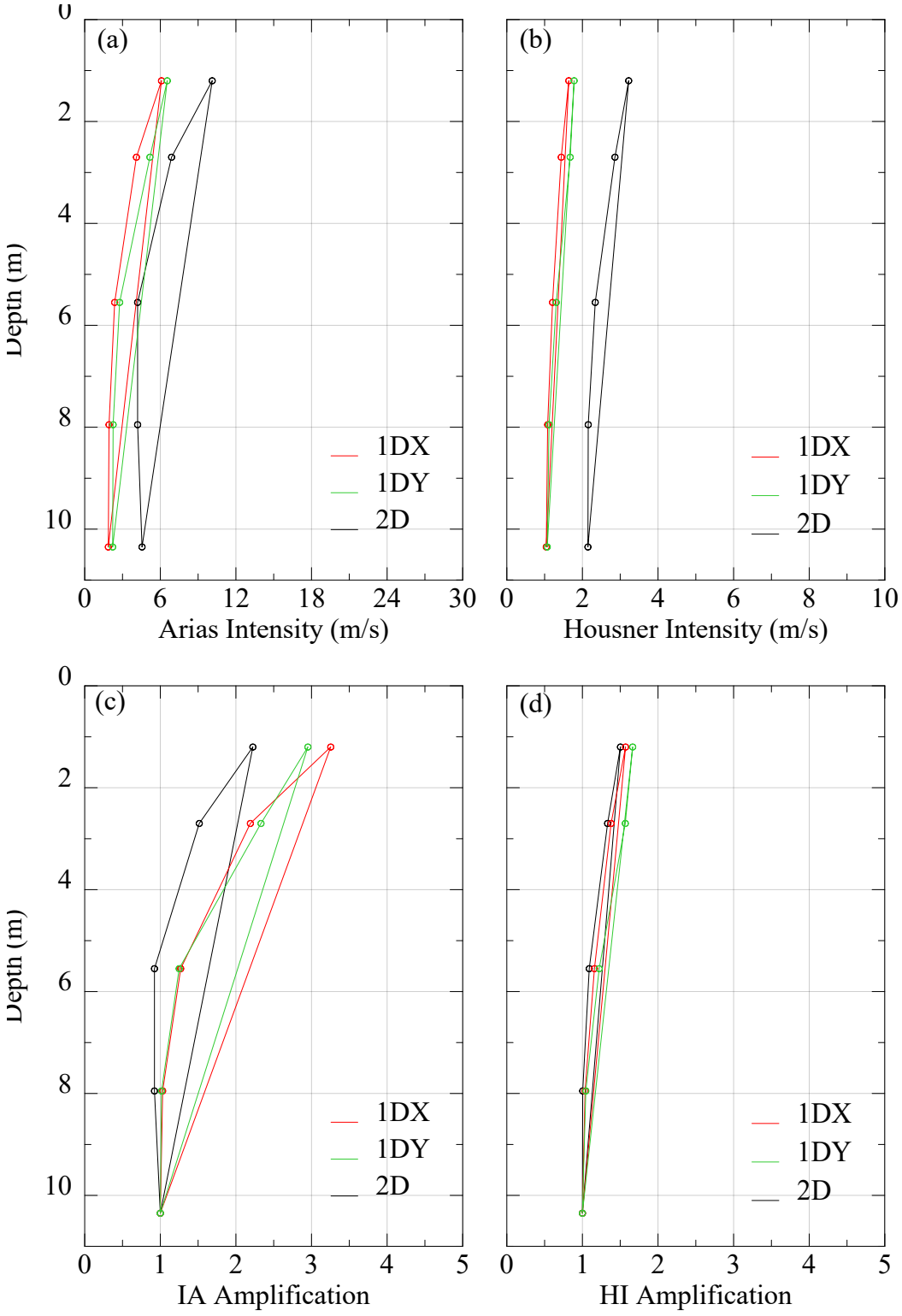

Figure C-336 Variation of total (a) Arias Intensity (M7-X,Y and 2D) ; (b) Housner Intensity (M7-X,Y and 2D) (c) Arias Intensity Amplification Factor (M7-X,Y and 2D); and (d) Housner Intensity Amplification Factor (M7-X,Y and 2D).

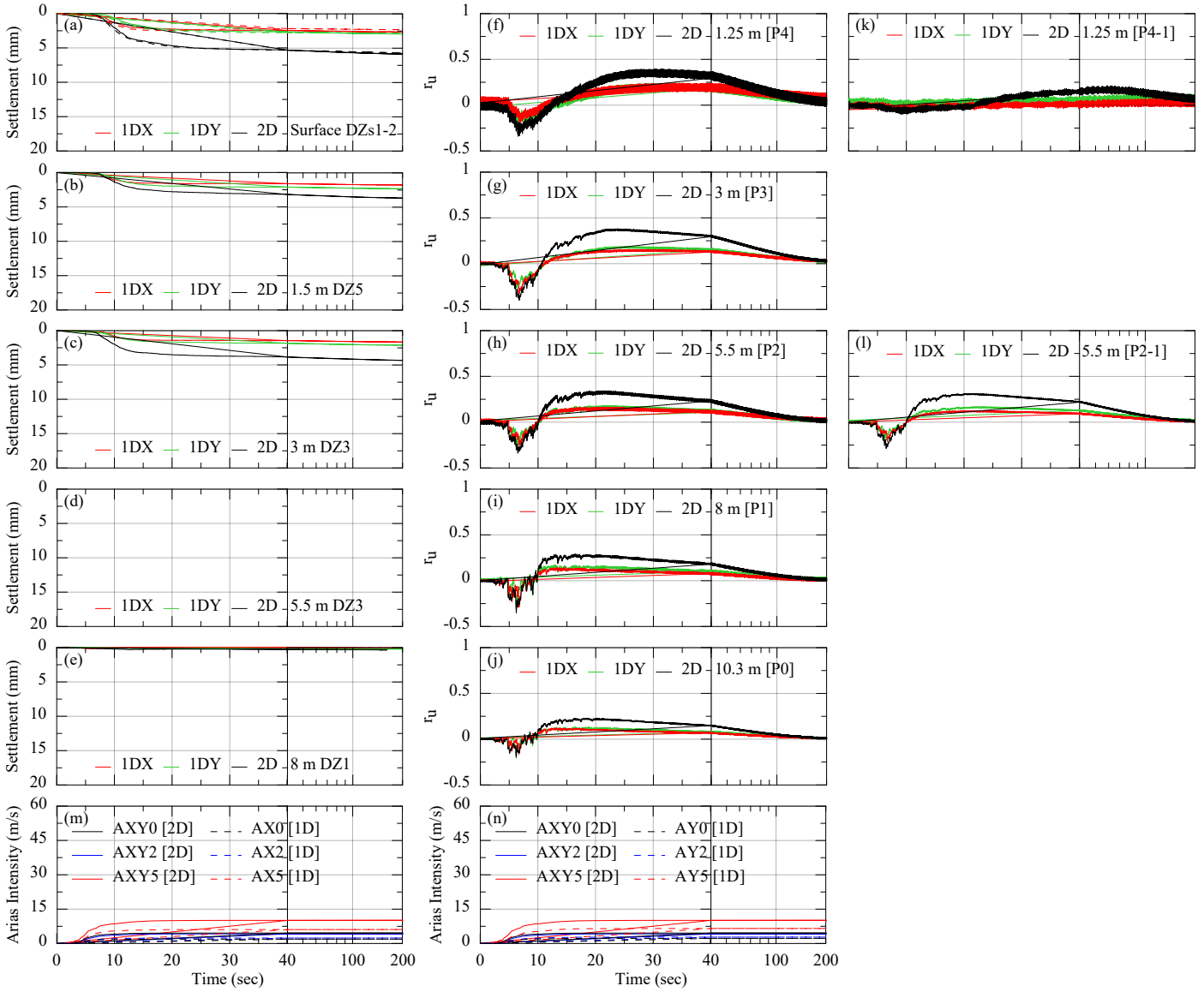

Figure C-337 Variation of total (a) to (e) Settlement with depth (M7-X,Y and 2D) ; (f) to (l) Excess pore water pressure ratio (ru) (M7-X,Y and 2D) (m) and (n) Arias Intensity along model (M7-X,Y and 2D).

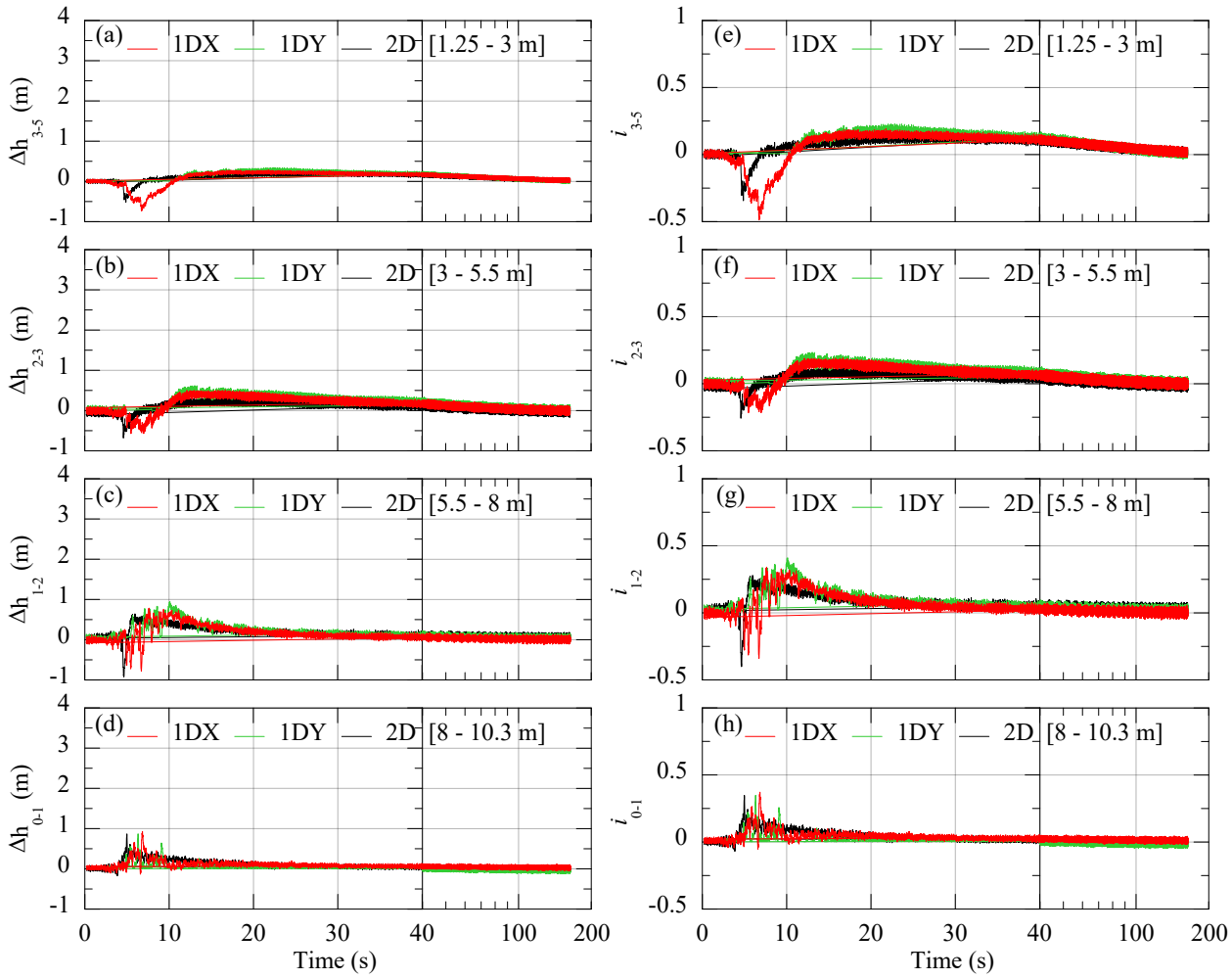

Figure C-338 Variation of total (a) to (d) Total Head Loss with depth (M7-X, Y and 2D); (e) to (h) Shaking induced Hydraulic Gradient (M7-X, Y and 2D)

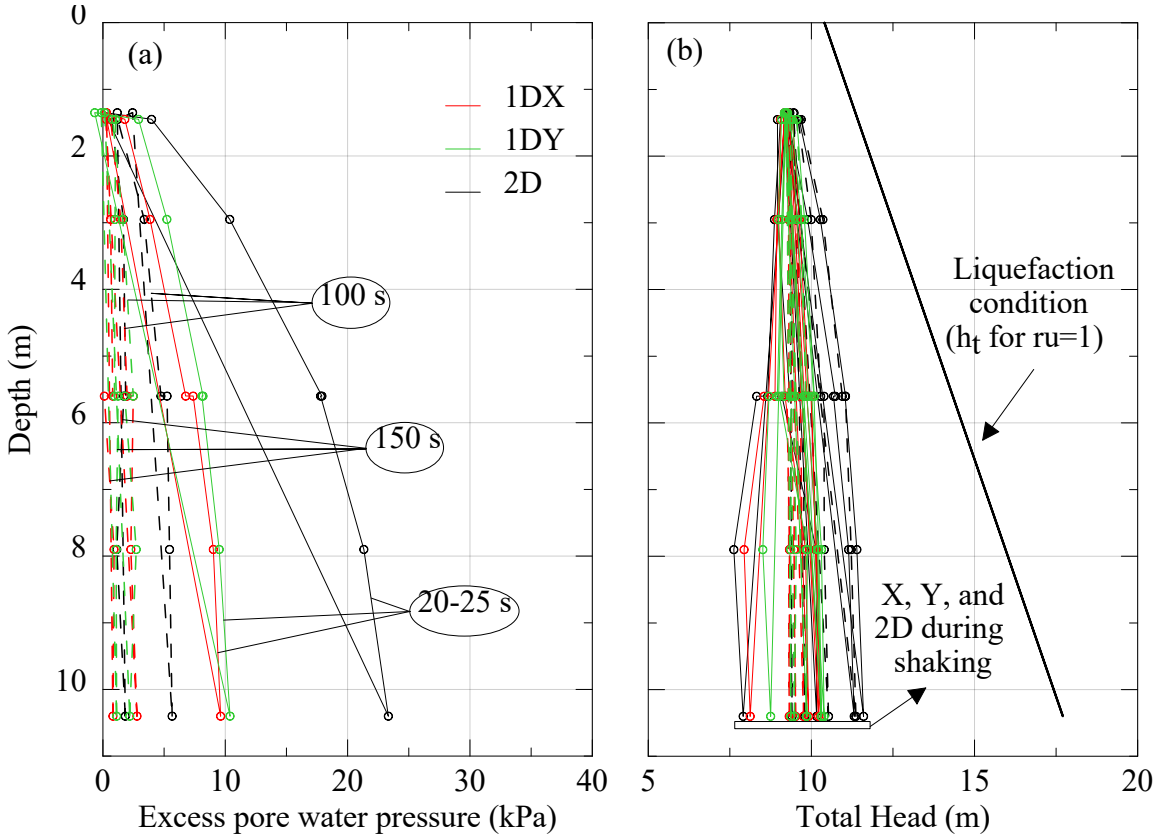

Figure C-339 Variation of total (a) Excess pore water pressure ratio (ru) with depth (M7-X,Y and 2D); (e) to (b) Total Head Loss with depth (M7-X,Y and 2D)

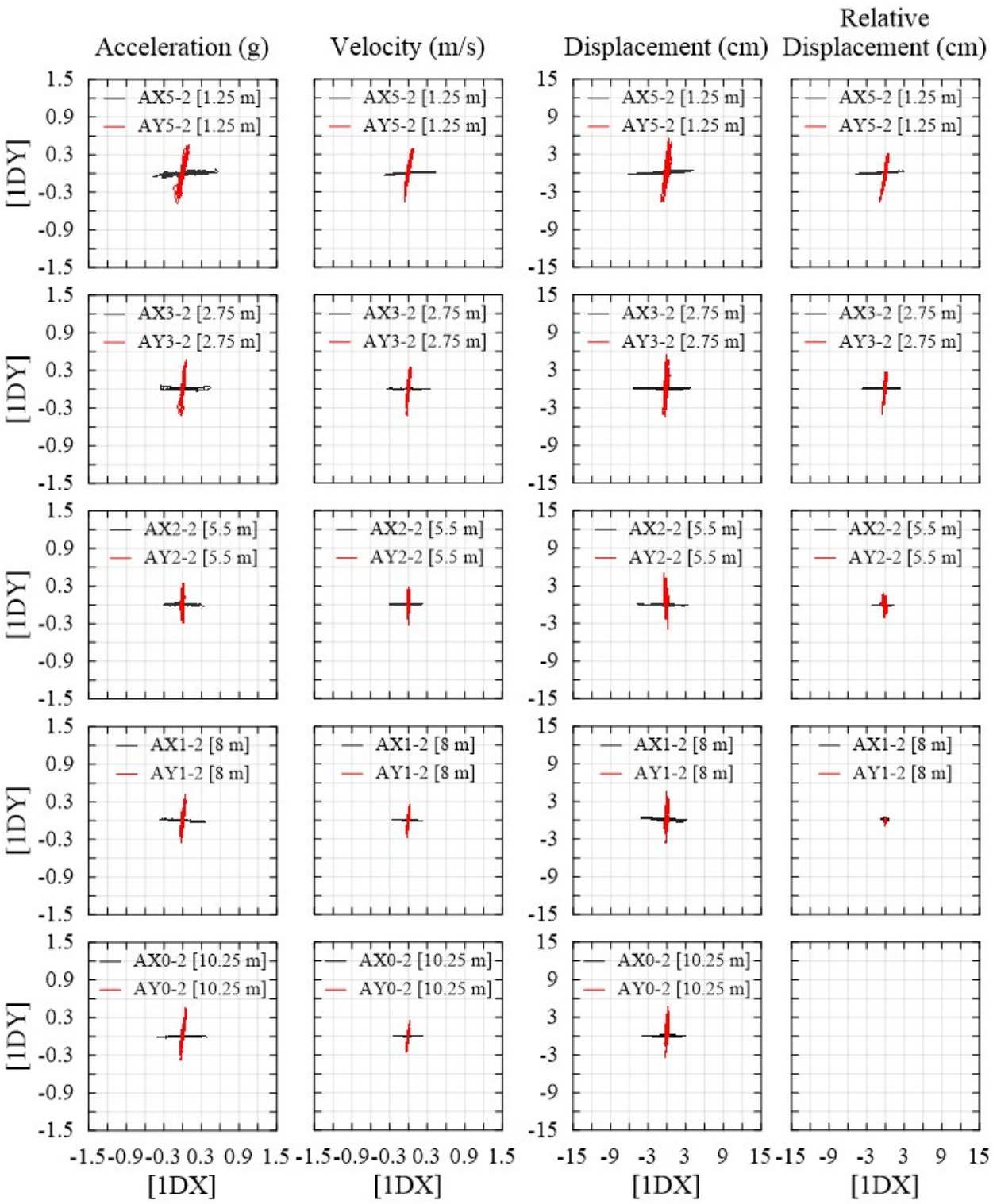

Figure C-340 Recorded input and within model ground motions for acceleration, velocity, displacement and relative displacement for M7-1D [X] and M7-1D [Y]

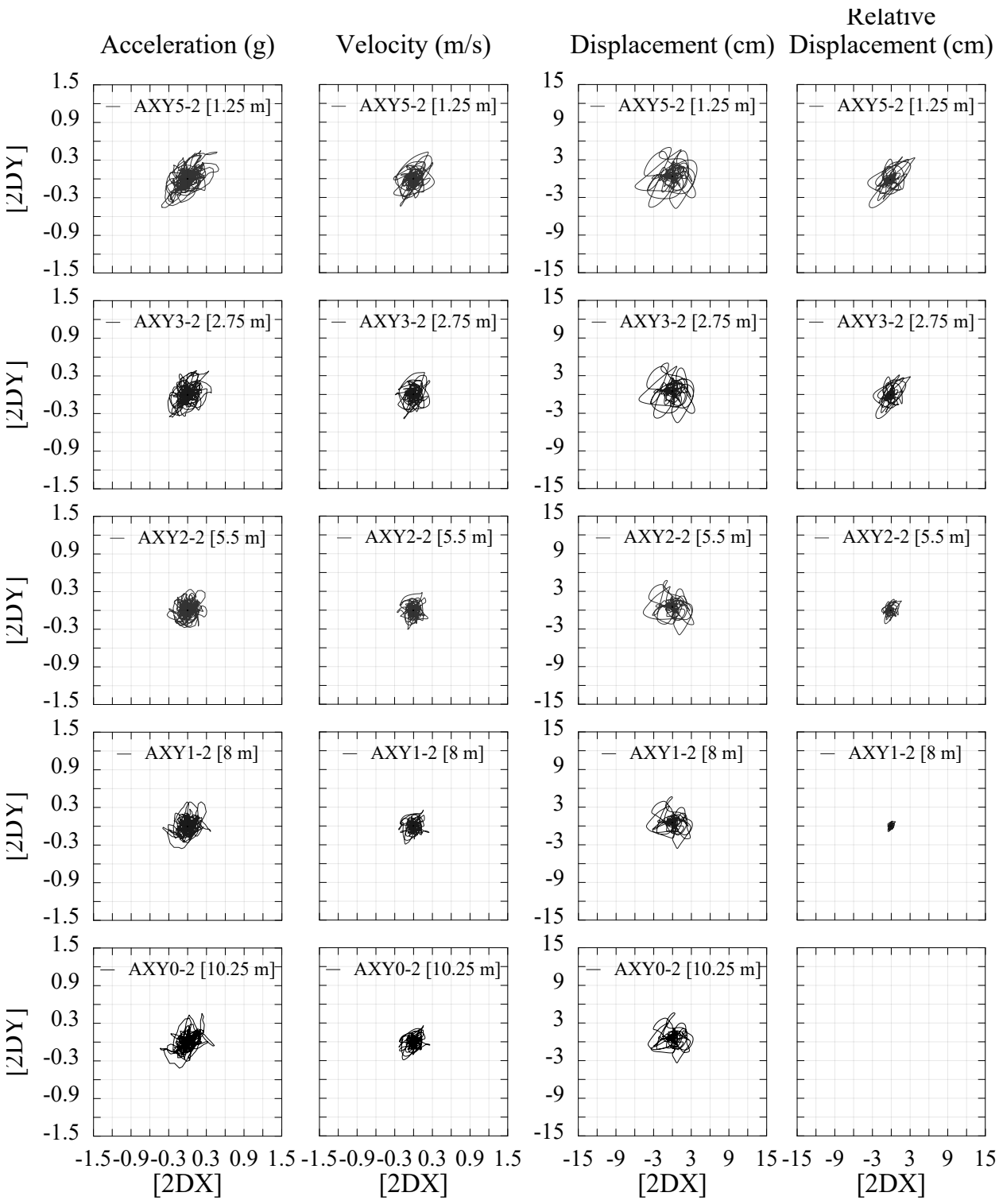

Figure C-341 Recorded input and within model ground motions for acceleration, velocity, displacement and relative displacement for M7-2D

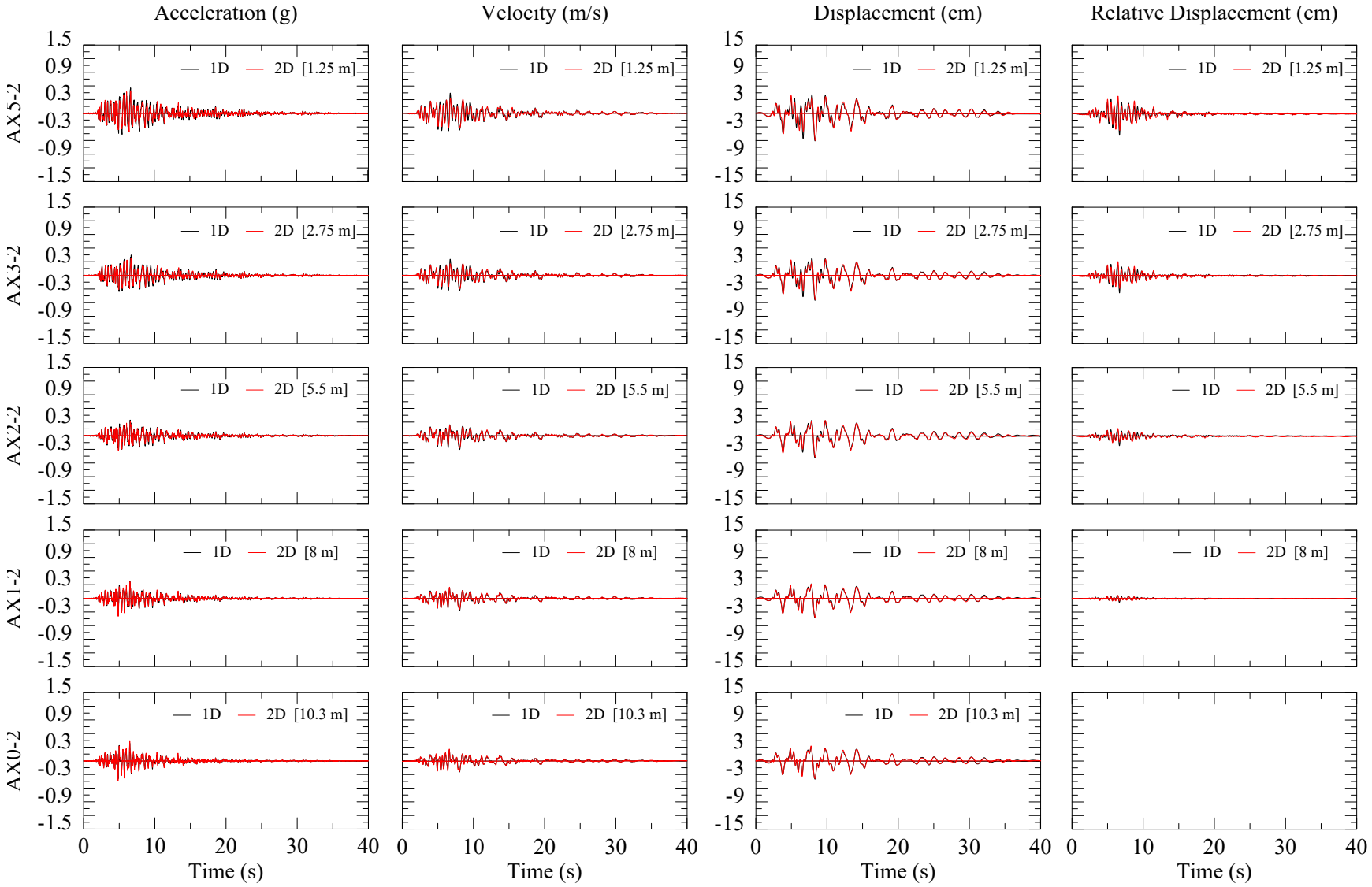

Figure C-342 Recorded input and within model ground motions time histories for acceleration, velocity, displacement and relative displacement for M7-2D [X] and M7-1D [X]

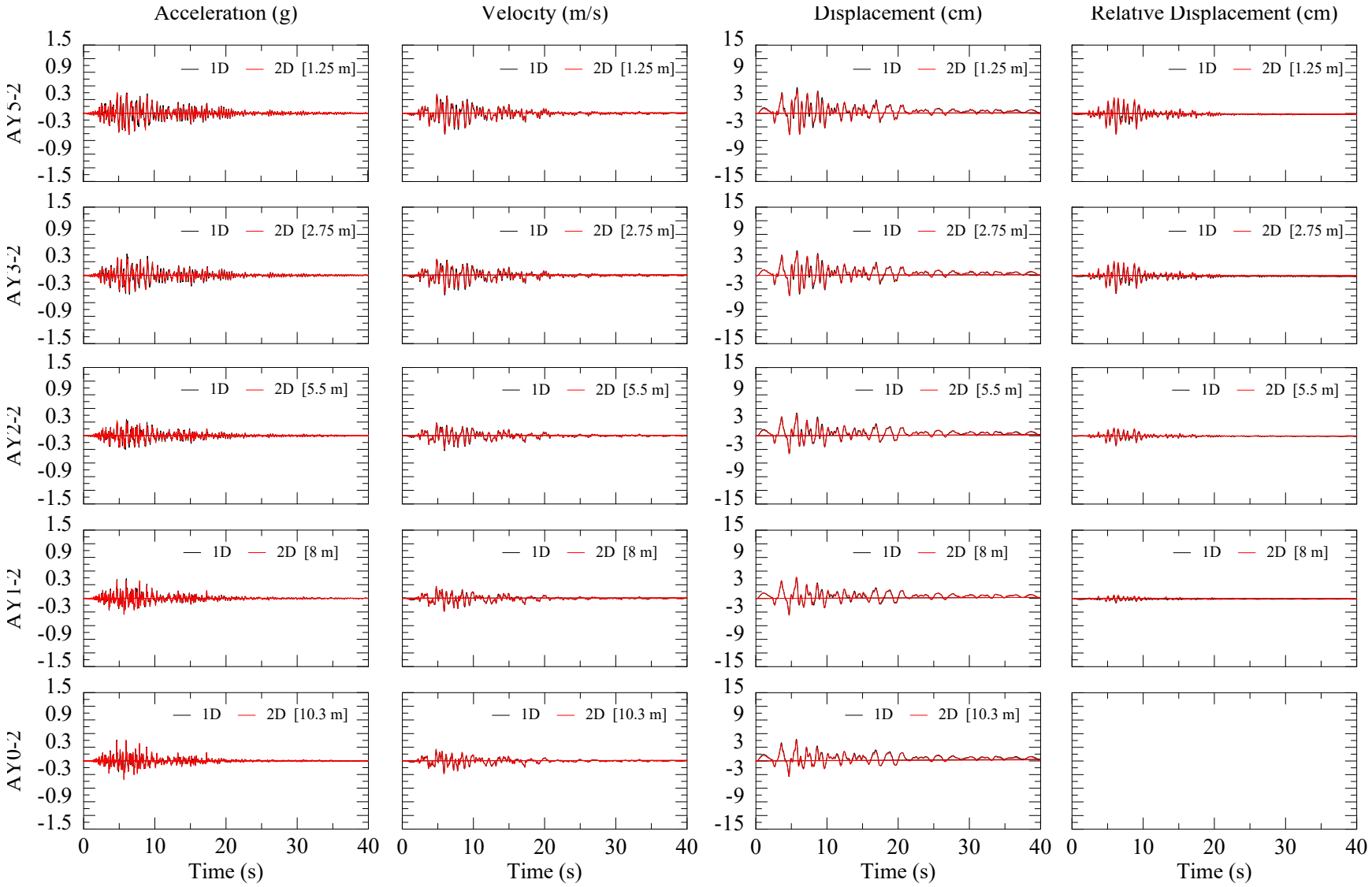

Figure C-343 Recorded input and within model ground motions time histories for acceleration, velocity, displacement and relative displacement for M7-2D [Y] and M7-1D [Y]

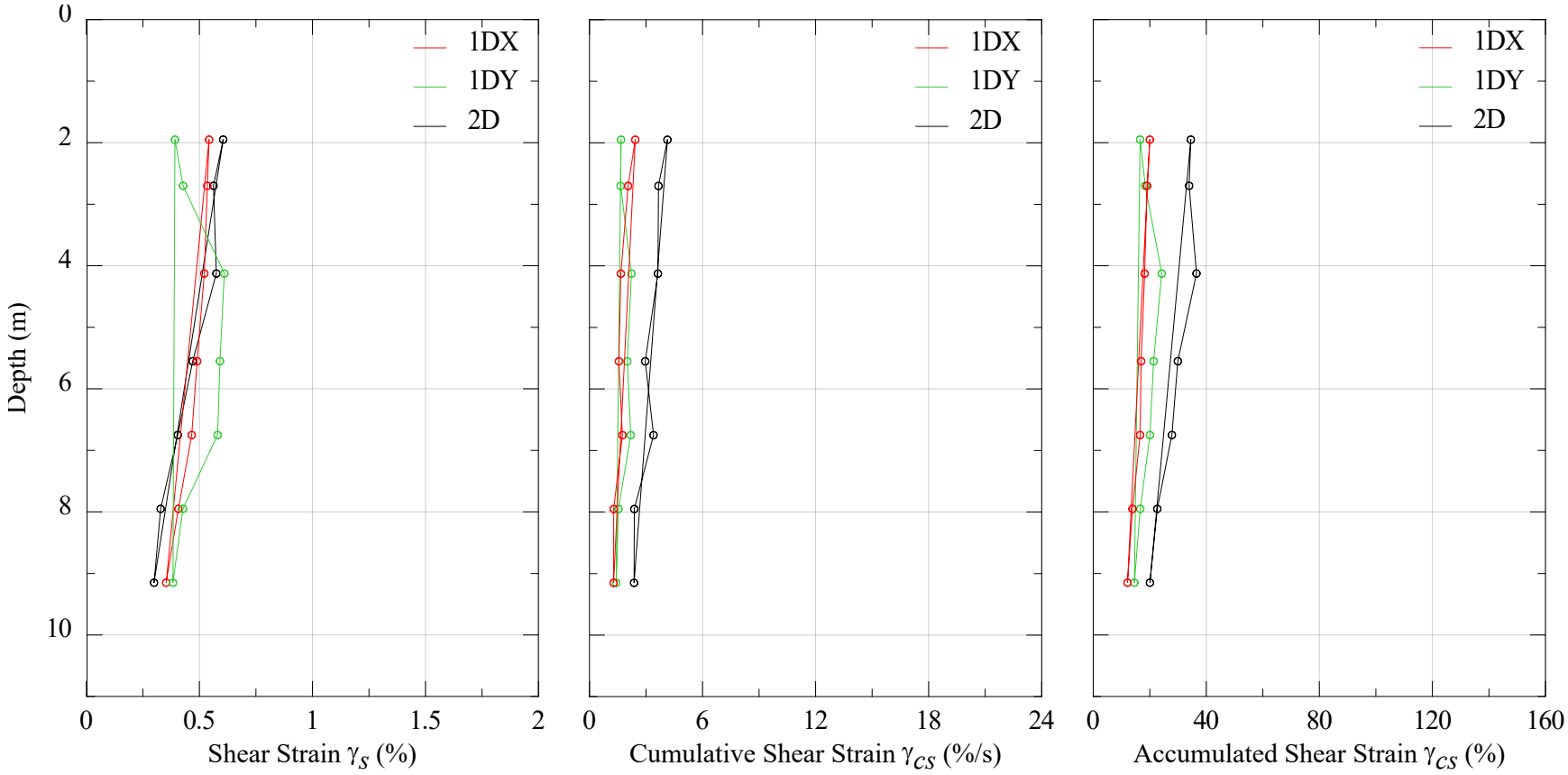

Figure C-344 Estimated (a) maximum shear strain; (b) cumulative shear strain; and (c) accumulated shear strain for M7-2D [X] and M7-1D [X]

1.4.10 Motion 9 (M9)

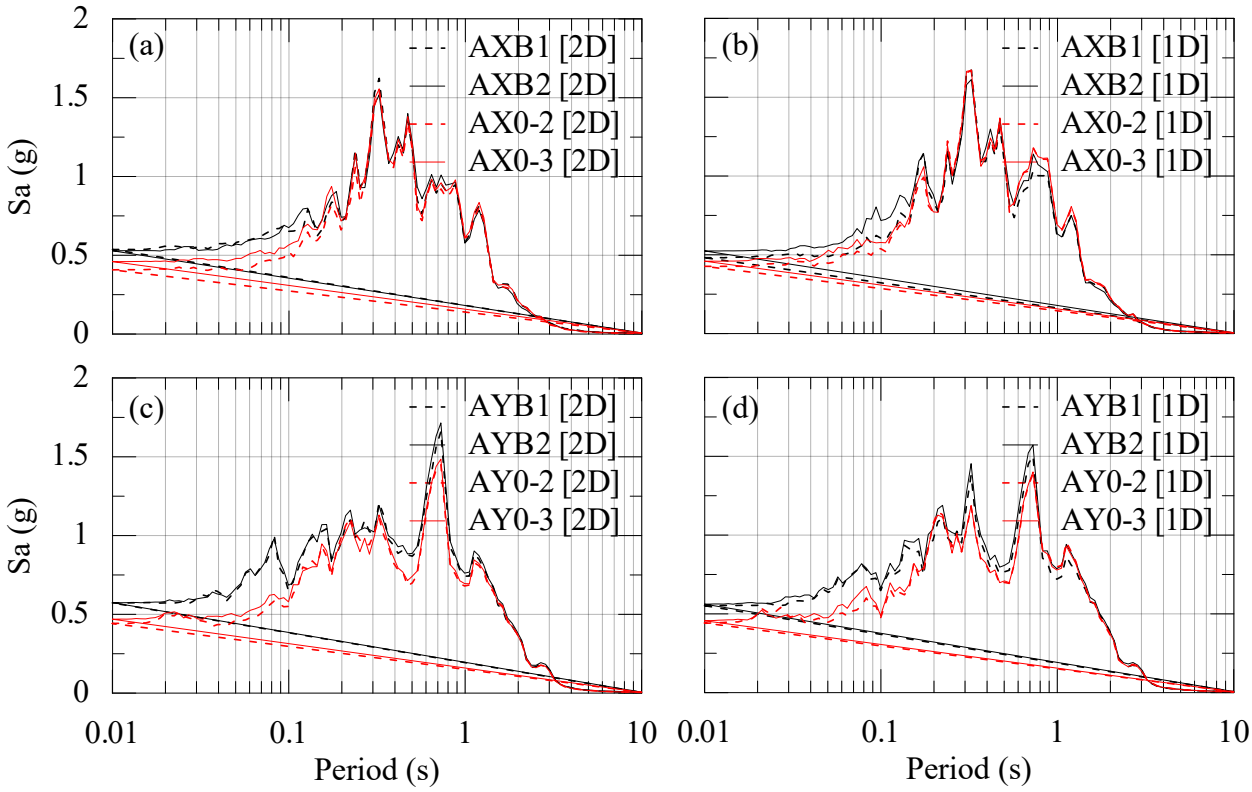

Figure C-345 Comparison of response spectra of 2D laminar container table and within model base input motion for motions (M9-X, Y and 2D).

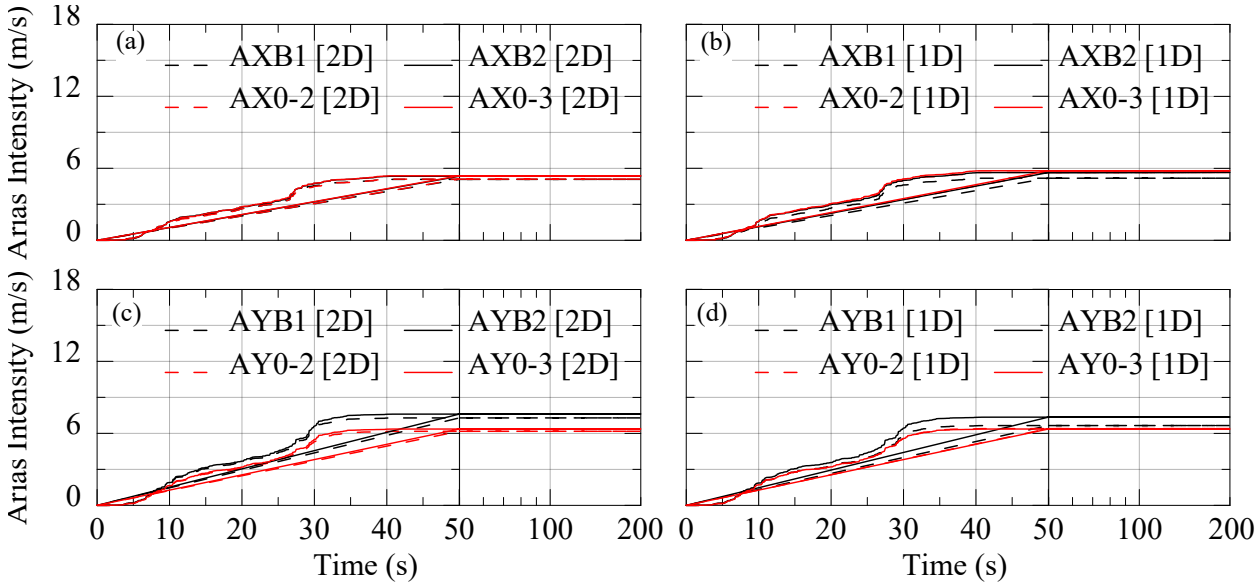

Figure C-346 Comparison of Arias Intensity of 2D laminar container table and within model base input motion for motions (a) M9-2D [X]; (b) M9-2D [Y]; (c) M9-1D [X] and (d) M9-1D [Y]

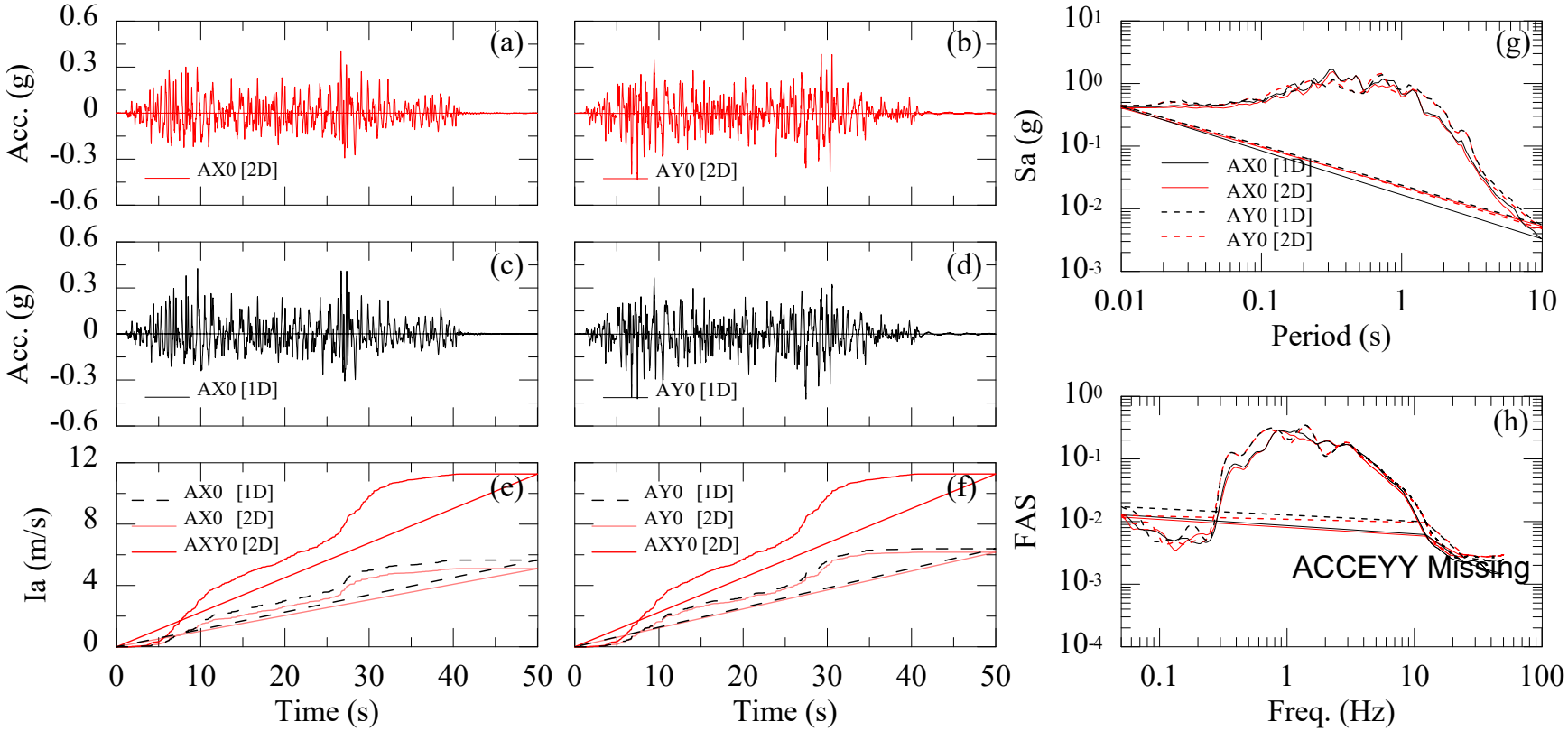

Figure C-347 Recorded input (2D) and 1D (X or Y) ground motions for: (a) M9-2D [X]; (b) M9-2D [Y]; (c) M9-1D [X]; and (d) M9-1D [Y]. Arias Intensity M9 (1D and 2D) for: (e) X direction; and (f) Y direction. Response Spectra (g) M9-2D [X]; M9-2D [Y]; M9-1D [X]; and M9-1D [Y]. Smoothed Fourier amplitude spectra (FAS) (h) M9-2D [X]; M9-2D [Y]; M9-1D [X]; and M9-1D [Y].

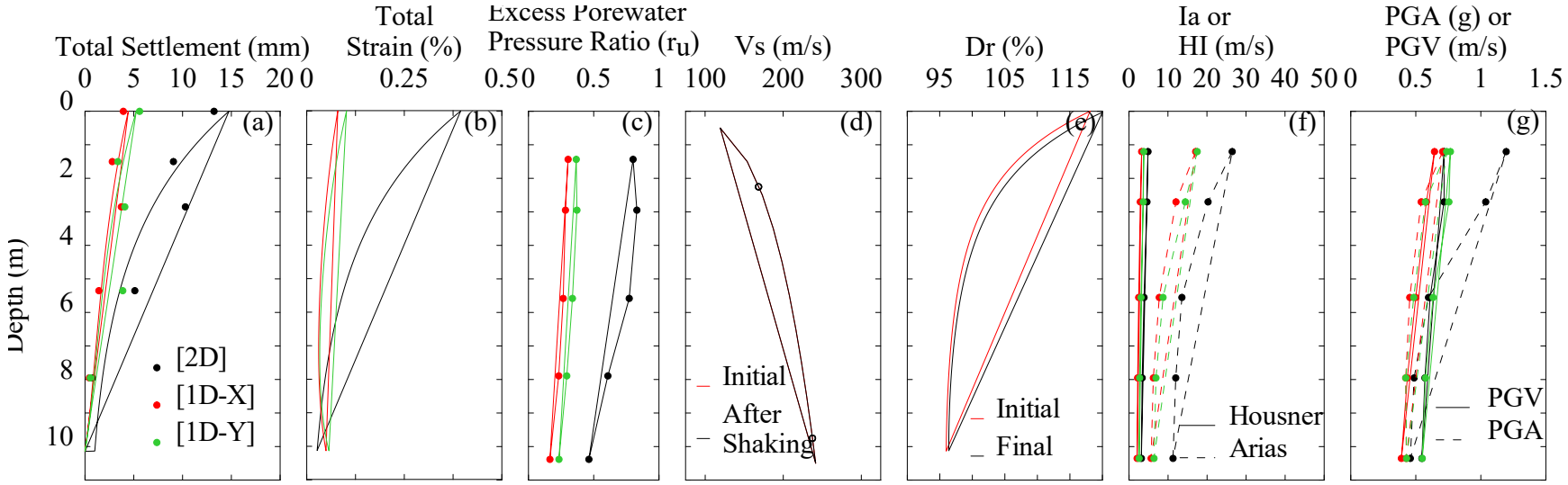

Figure C-348 Recorded or computed profiles for input motion M9-X, Y, and 2D. (a) Settlement; (b) total strain; (c) excess pore water pressure ratio; (d) shear wave velocity; (e) relative density; (f) Arias and Housner intensities; and (g) PGA and PGV.

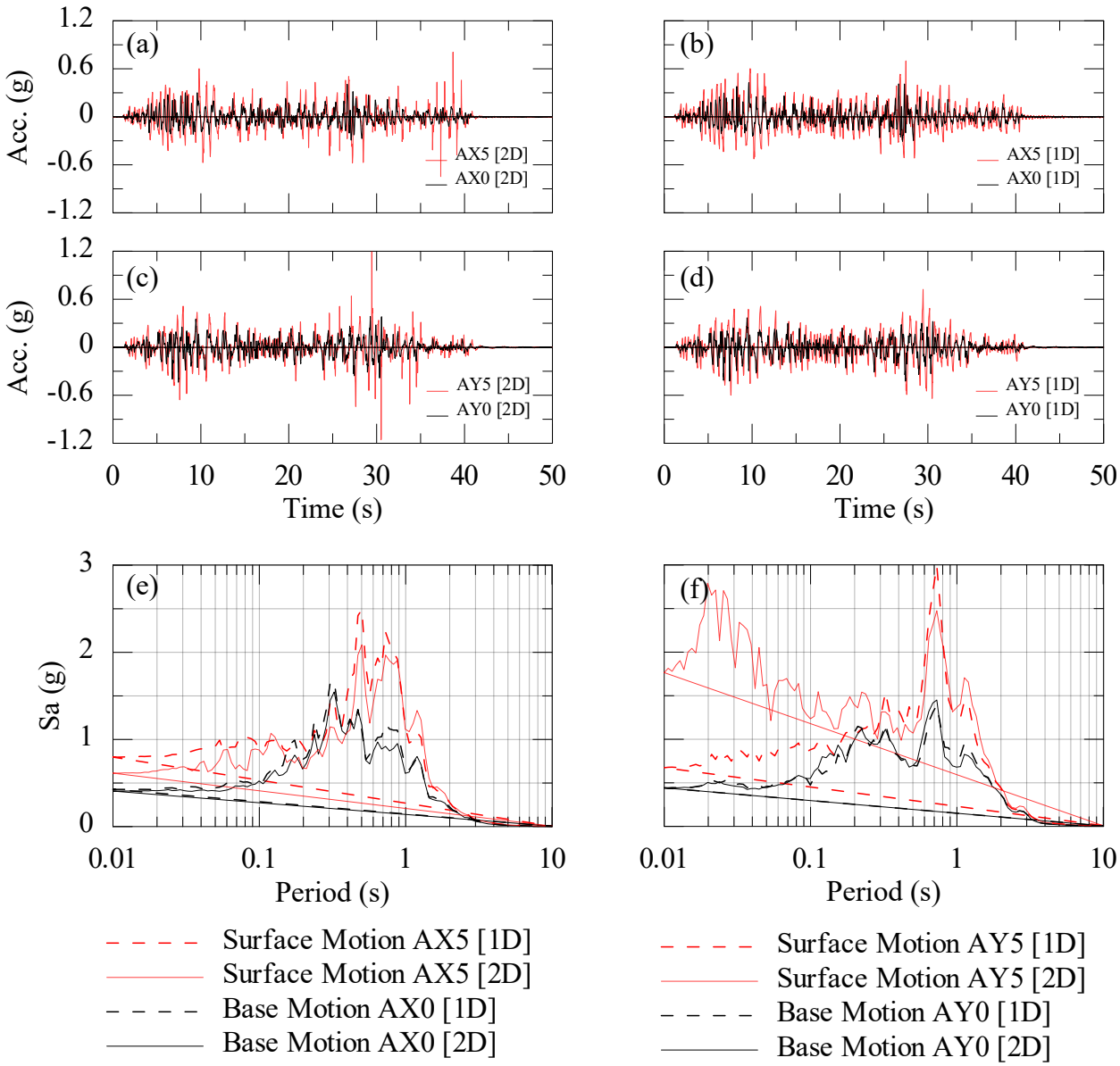

Figure C-349 Recorded input and surface ground motion: (a) M9-2D [X]; (b) M9-1D [X]; (c) M9-2D [Y]; and (d) M9-1D [Y]. Computed response spectra from Free Field Test [PT2] for motions M9 (1D and 2D) for: (e) X direction; and (f) Y direction.

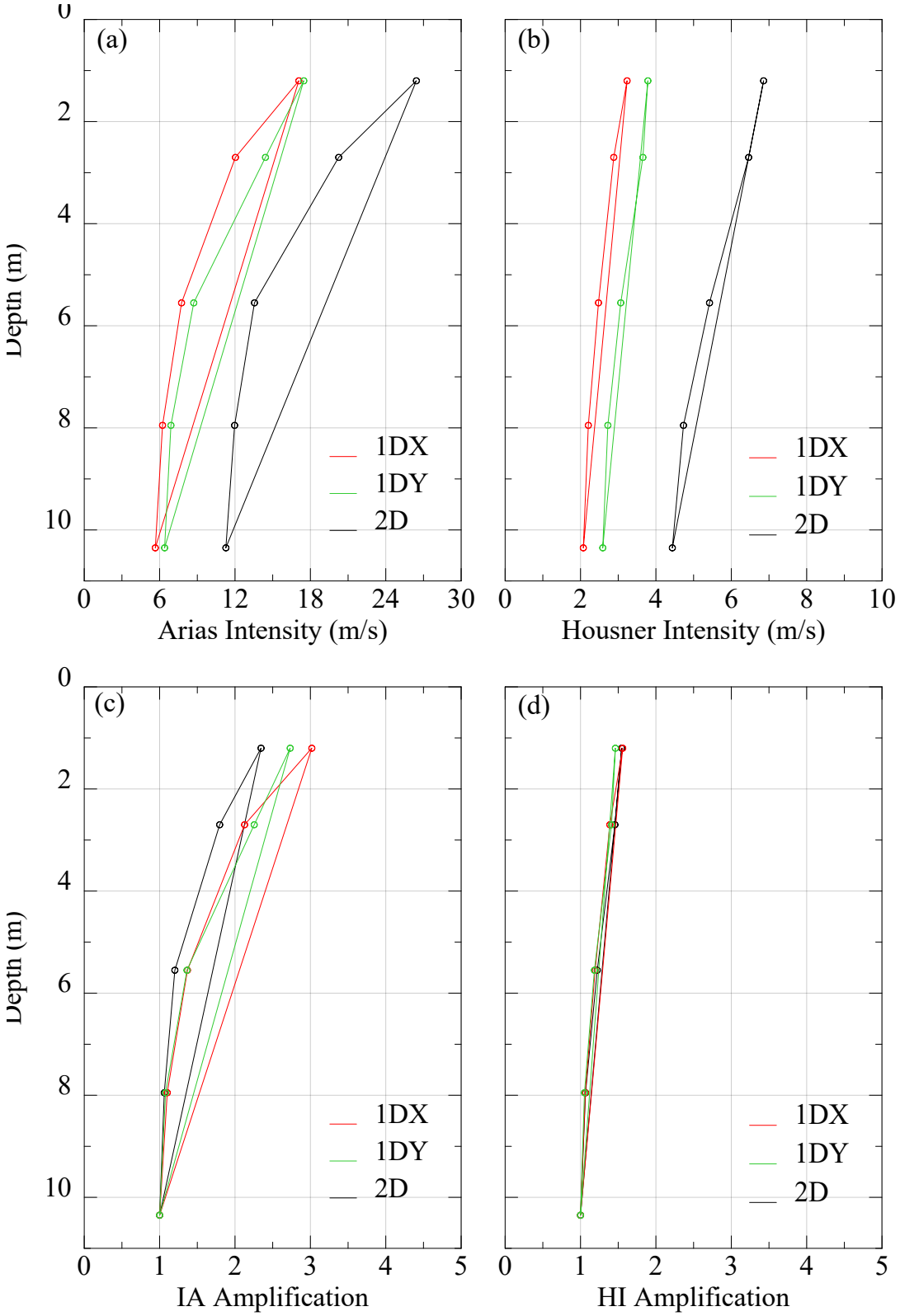

Figure C-350 Variation of total (a) Arias Intensity (M9-X,Y and 2D) ; (b) Housner Intensity (M9-X,Y and 2D) (c) Arias Intensity Amplification Factor (M9-X,Y and 2D); and (d) Housner Intensity Amplification Factor (M9-X,Y and 2D).

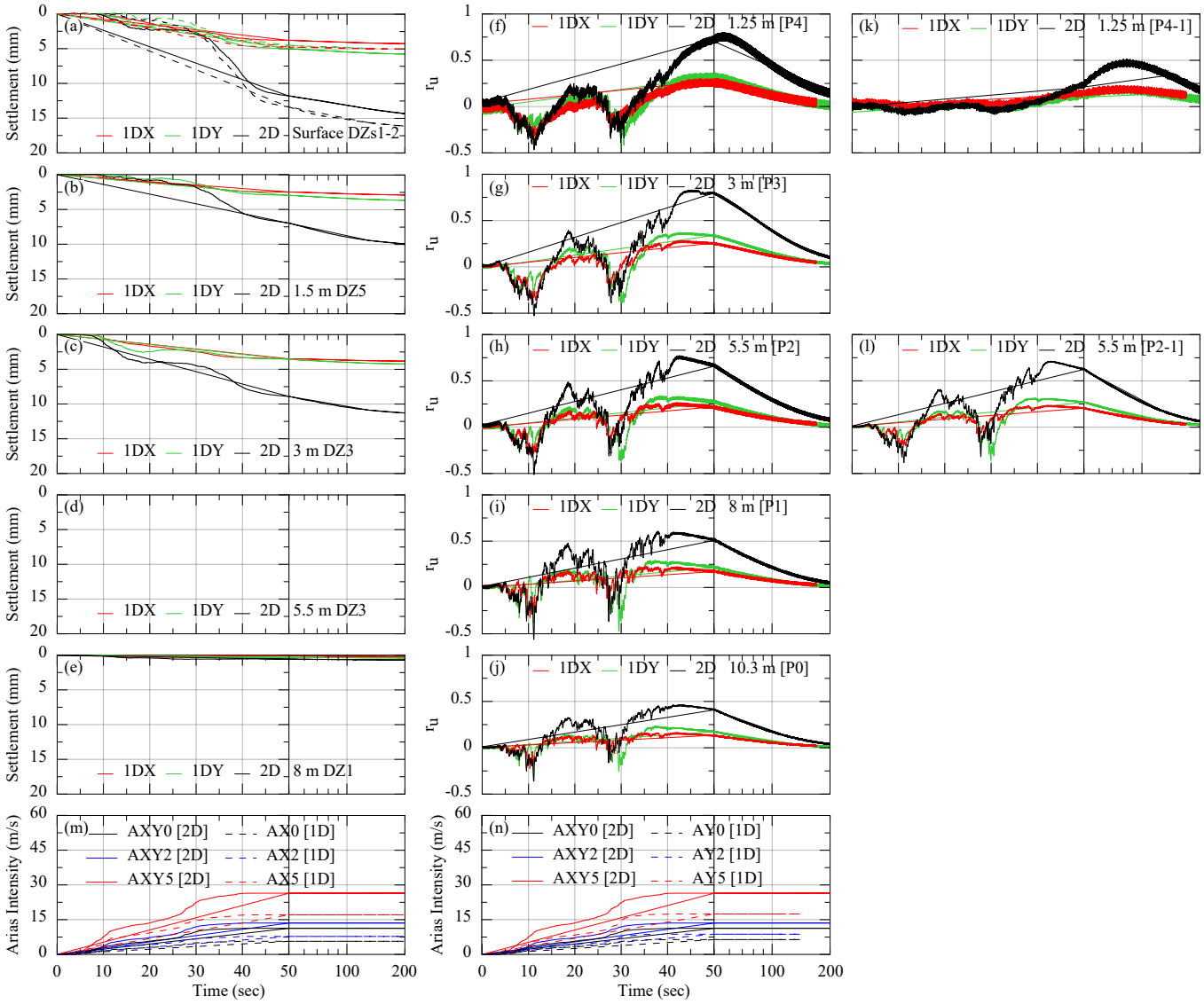

Figure C-351 Variation of total (a) to (e) Settlement with depth (M9-X,Y and 2D) ; (f) to (l) Excess pore water pressure ratio (ru) (M9-X,Y and 2D) (m) and (n) Arias Intensity along model (M9-X,Y and 2D).

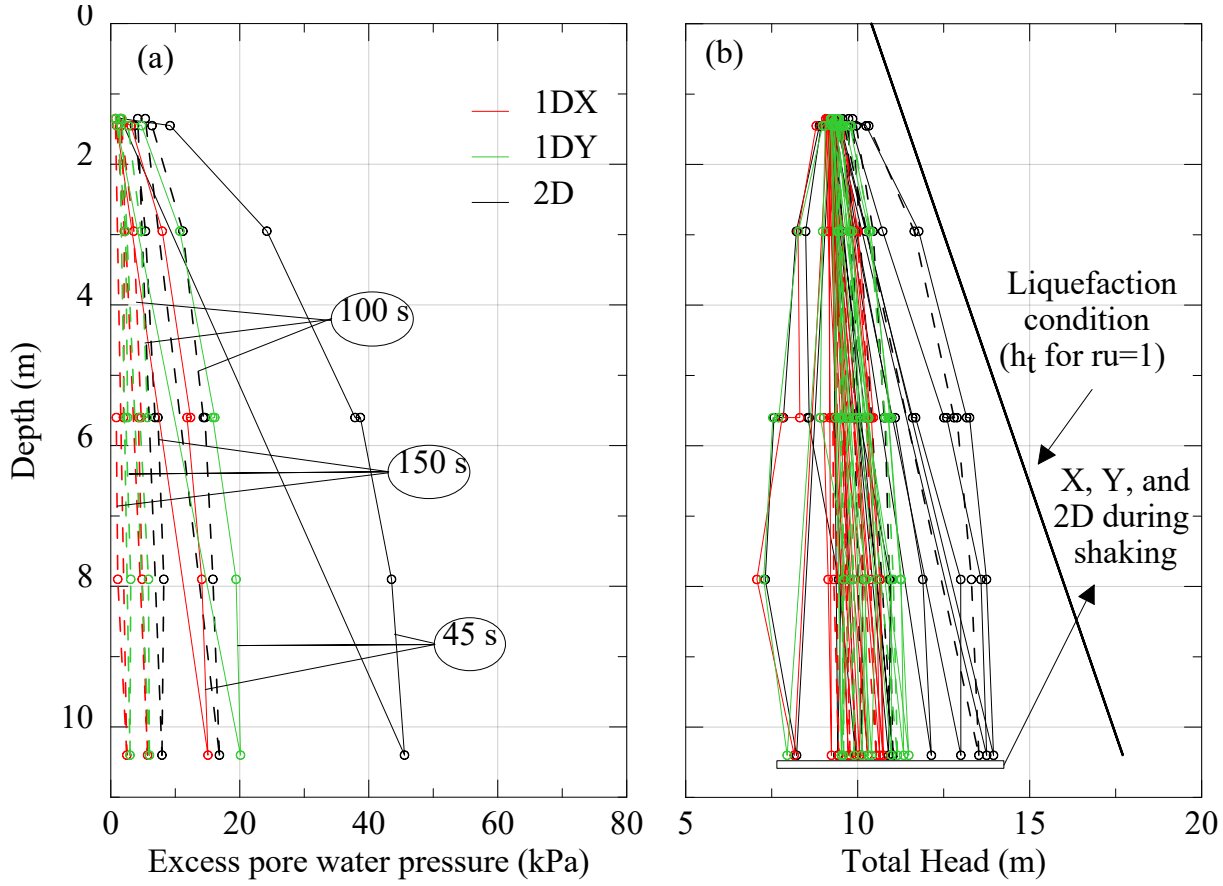

Figure C-352 Variation of total (a) Excess pore water pressure ratio (ru) with depth (M9-X,Y and 2D); (e) to (b) Total Head Loss with depth (M9-X,Y and 2D)

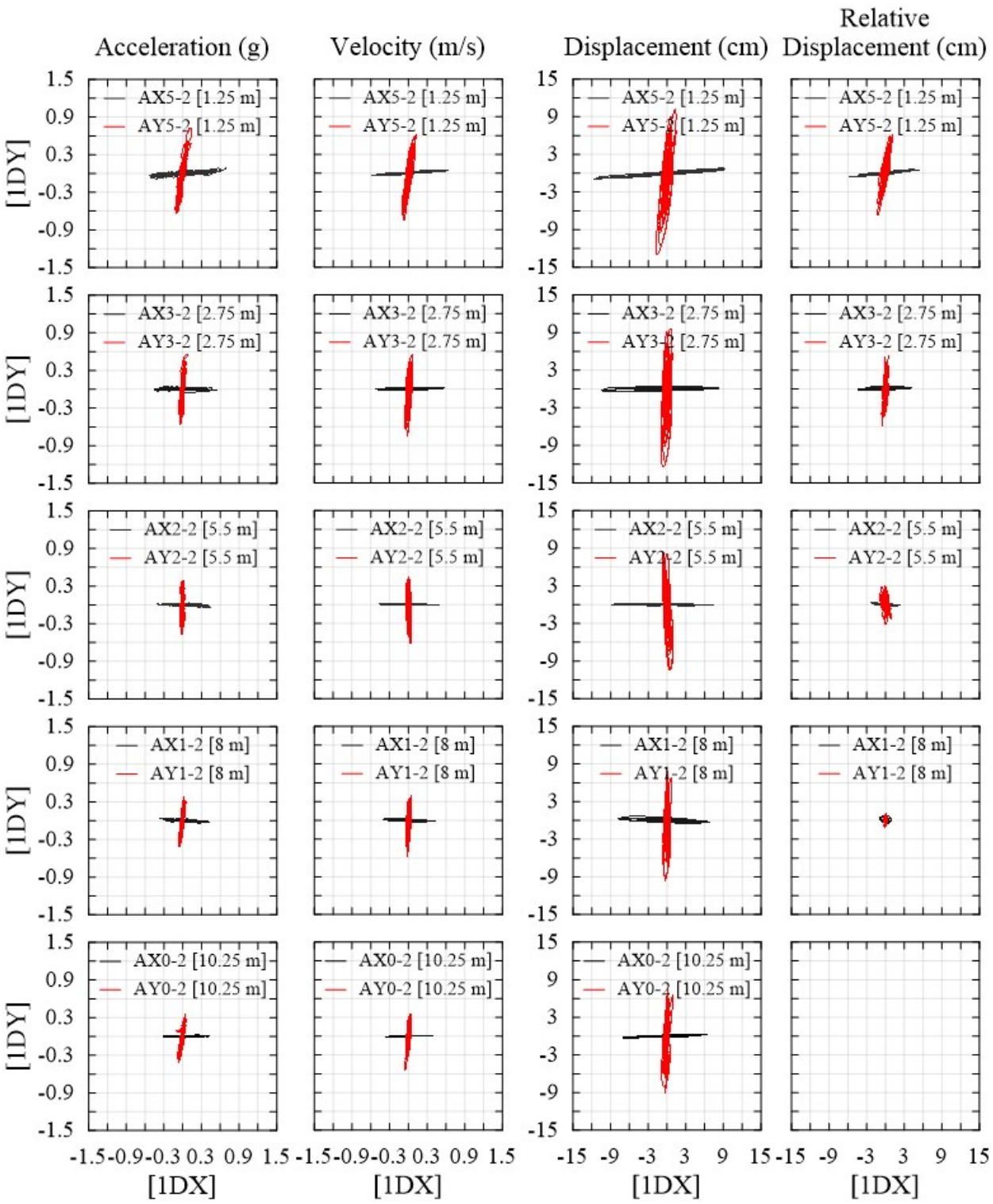

Figure C-353 Recorded input and within model ground motions for acceleration, velocity, displacement and relative displacement for M9-1D [X] and M9-1D [Y]

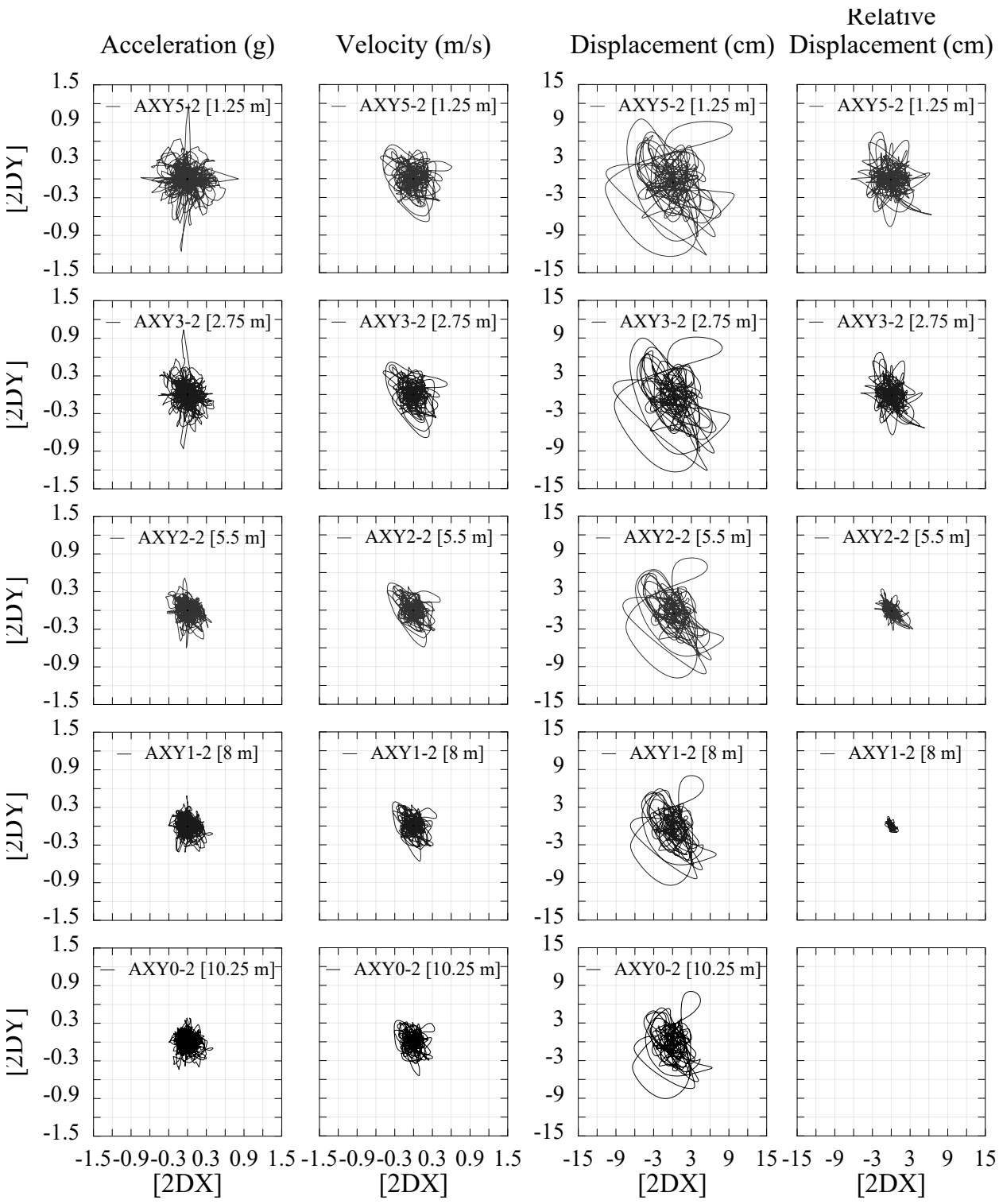

Figure C-354 Recorded input and within model ground motions for acceleration, velocity, displacement and relative displacement for M9-2D

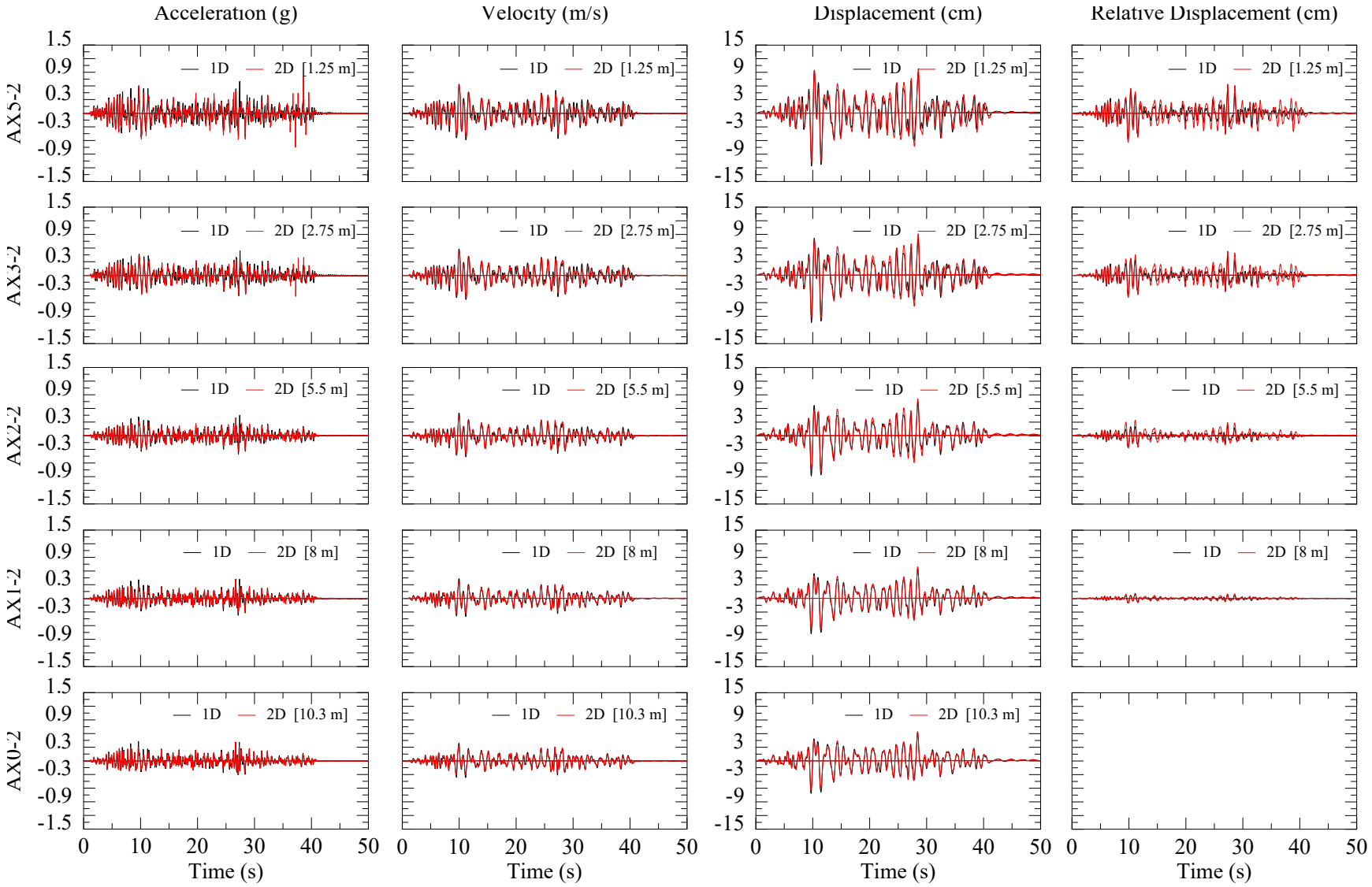

Figure C-355 Recorded input and within model ground motions time histories for acceleration, velocity, displacement and relative displacement for M9-2D [X] and M9-1D [X]

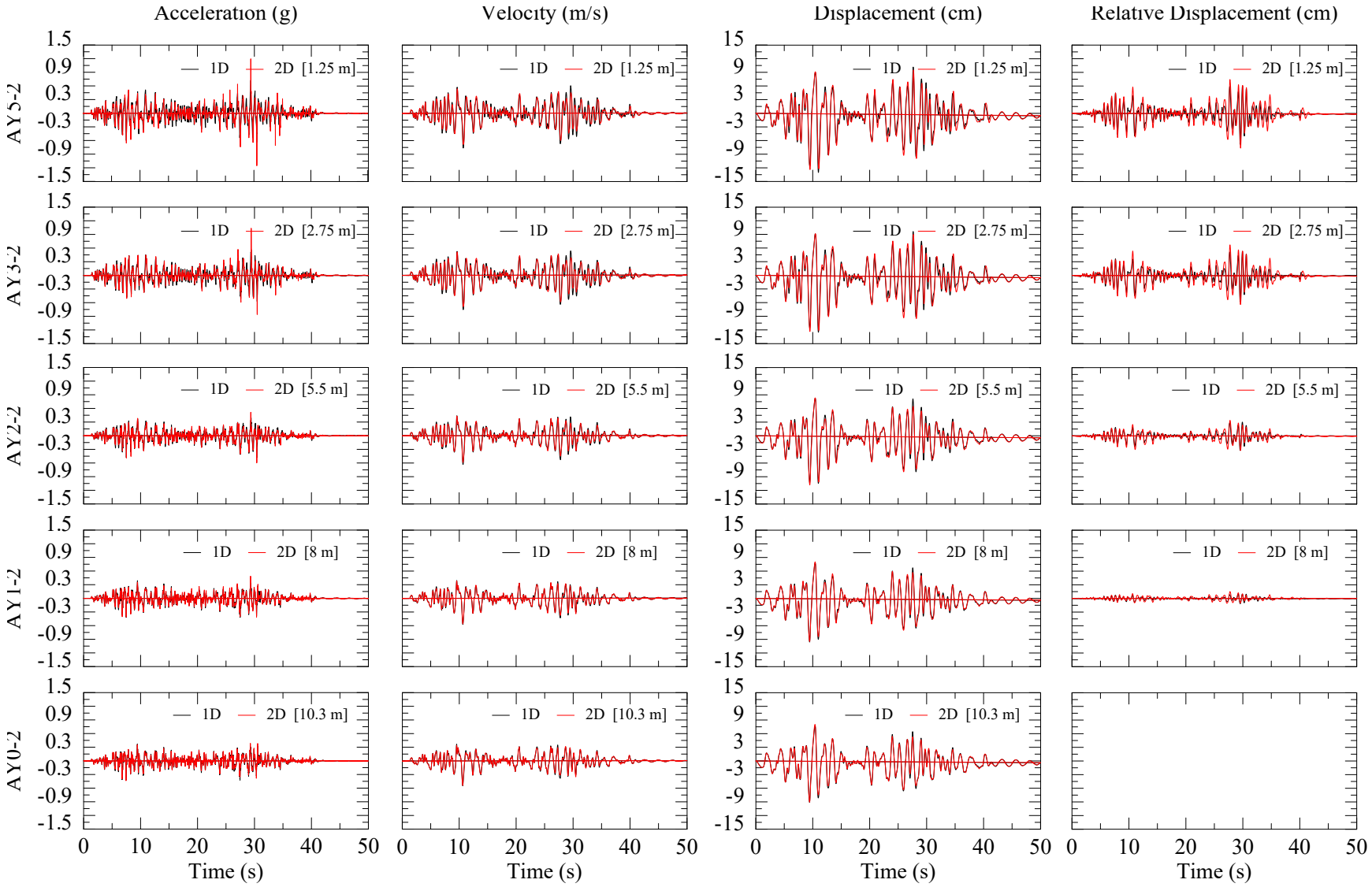

Figure C-356 Recorded input and within model ground motions time histories for acceleration, velocity, displacement and relative displacement for M9-2D [Y] and M9-1D [Y]

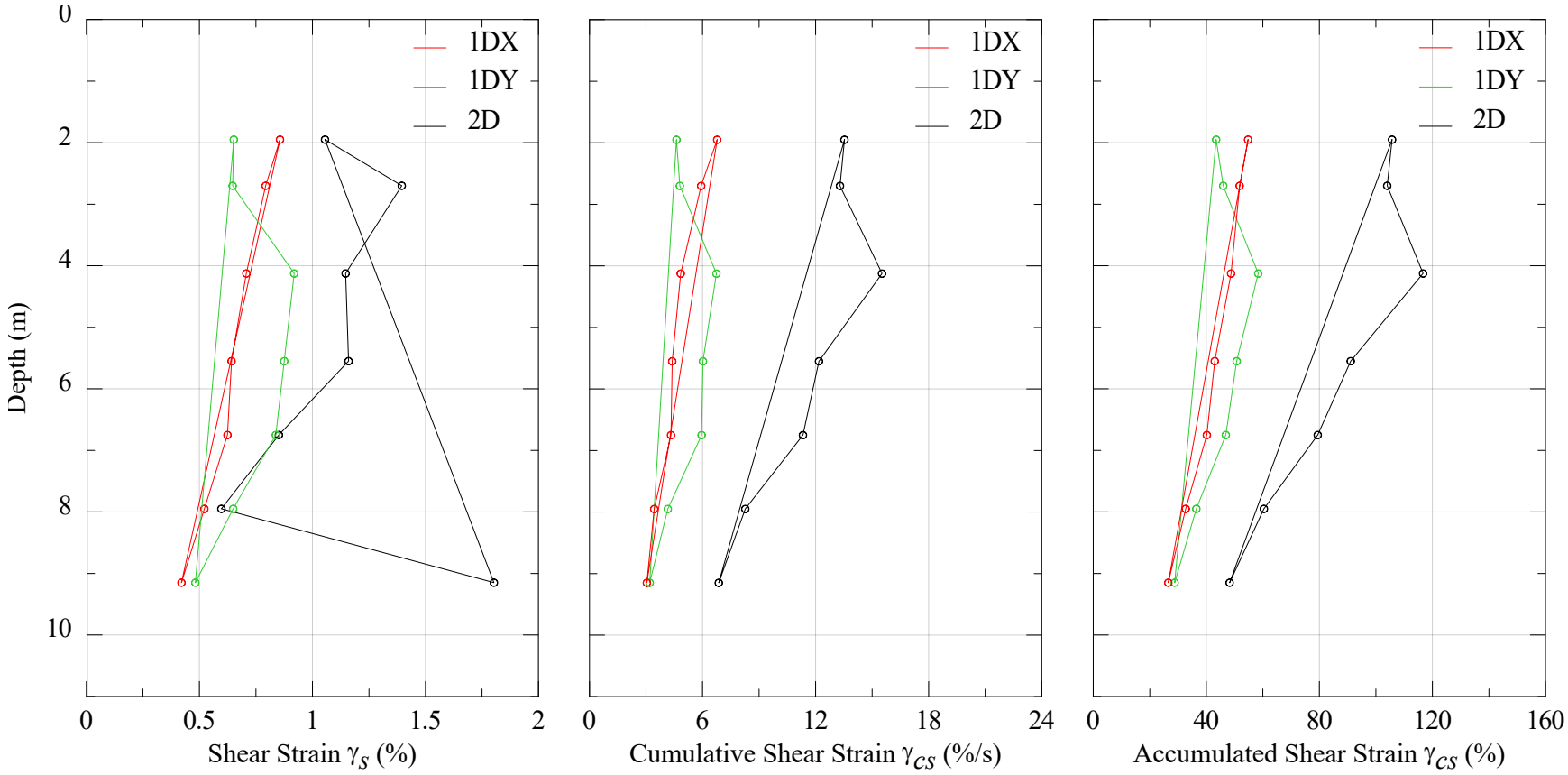

Figure C-357 Estimated (a) maximum shear strain; (b) cumulative shear strain; and (c) accumulated shear strain for M9-2D [X] and M9-1D [X]

1.5 Test: Dr95FF (PT1) - Bender Elements Measurements

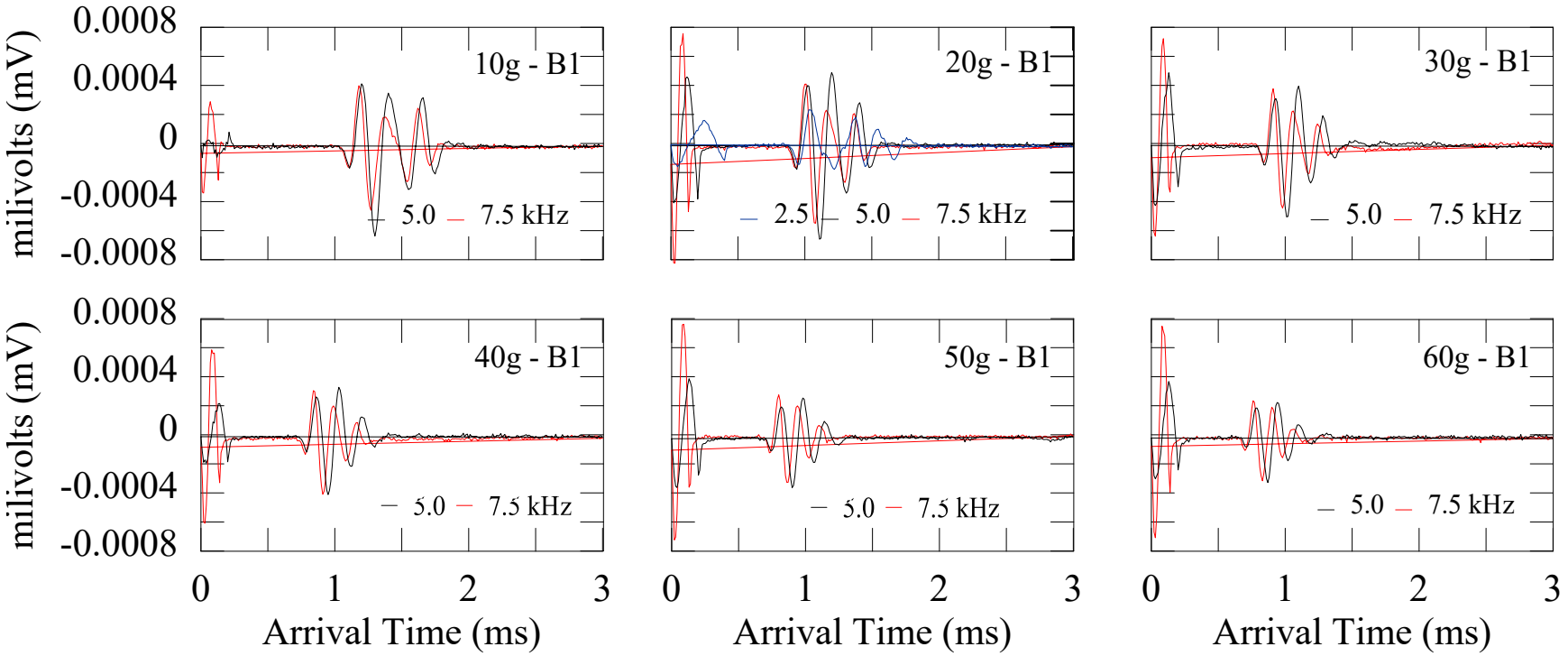

Figure C-358 Bender elements (B1) arrival times at various 'g' levels during spin-up for test Dr95FF.

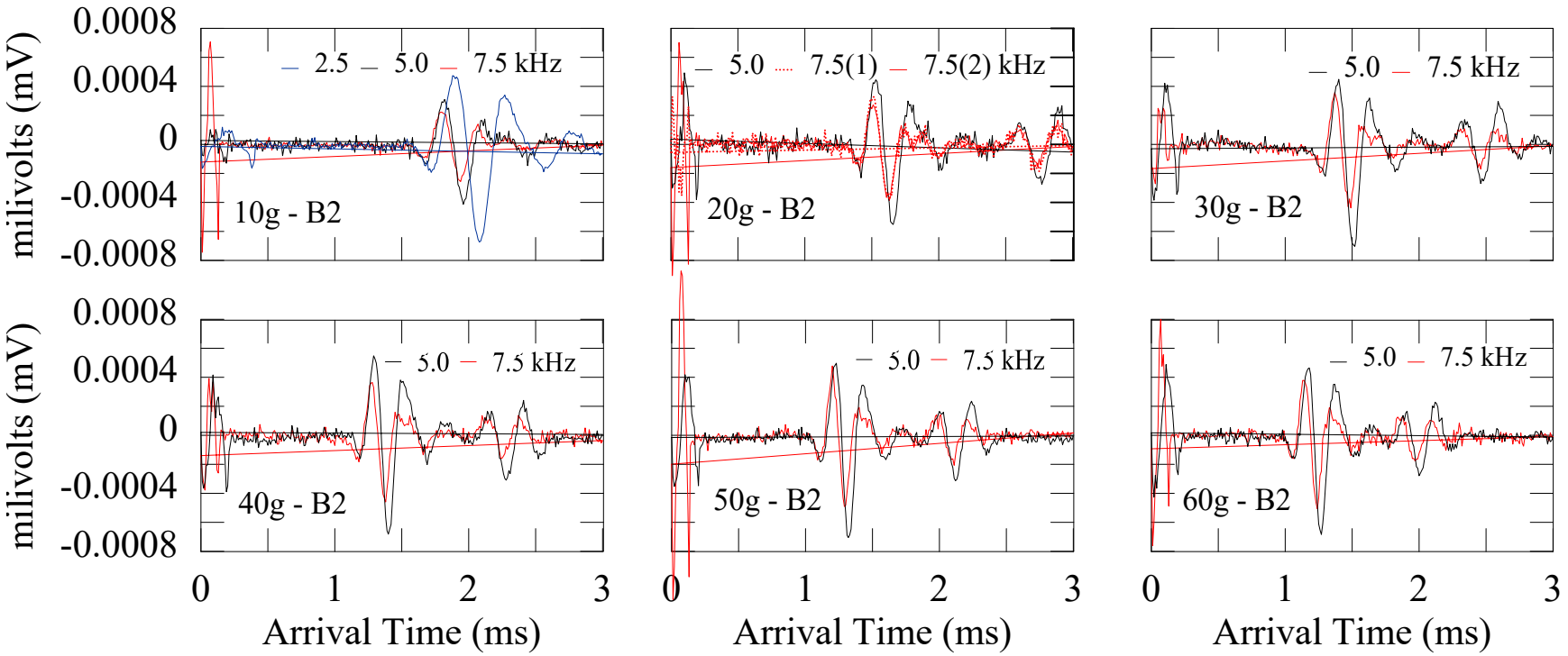

Figure C-359 Bender elements (B2) arrival times at various 'g' levels during spin-up for test Dr95FF.

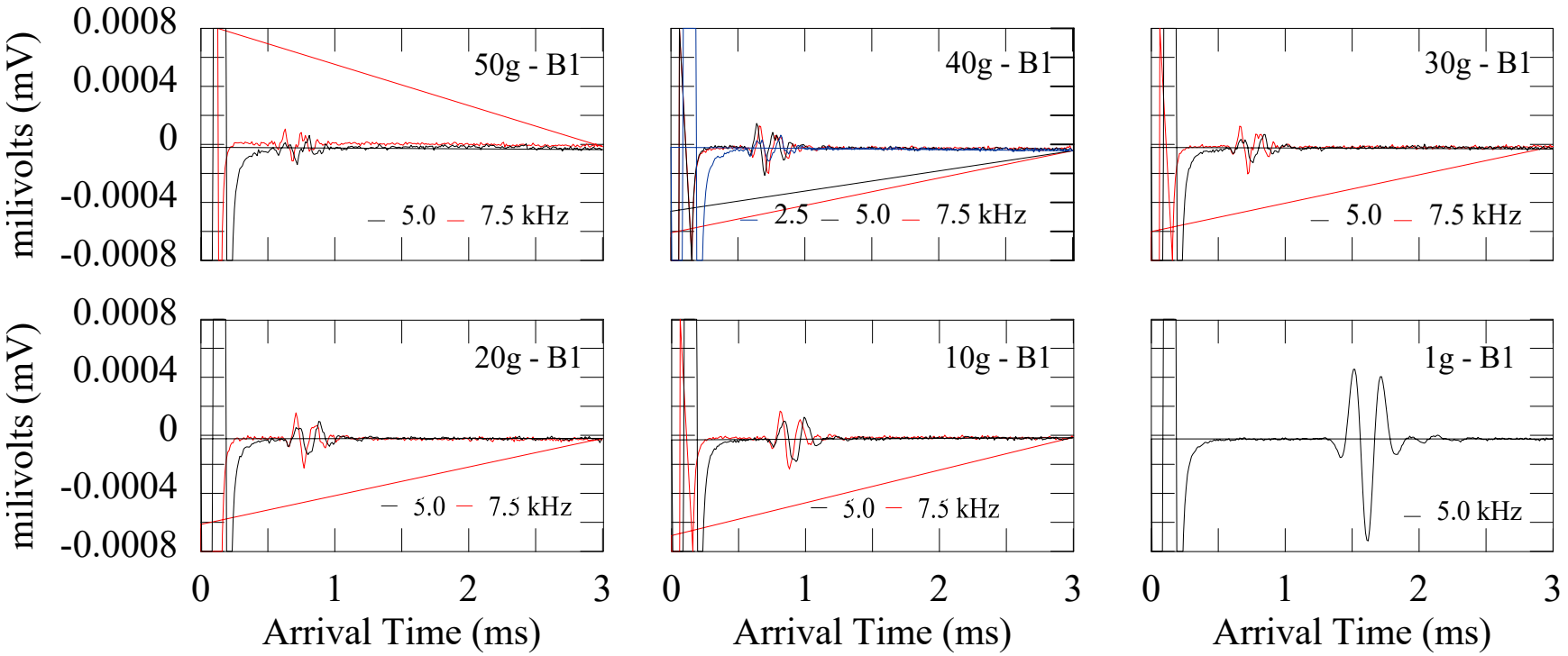

Figure C-360 Bender elements (B1) arrival times at various ‘g’ levels during spin-down for test Dr95FF.

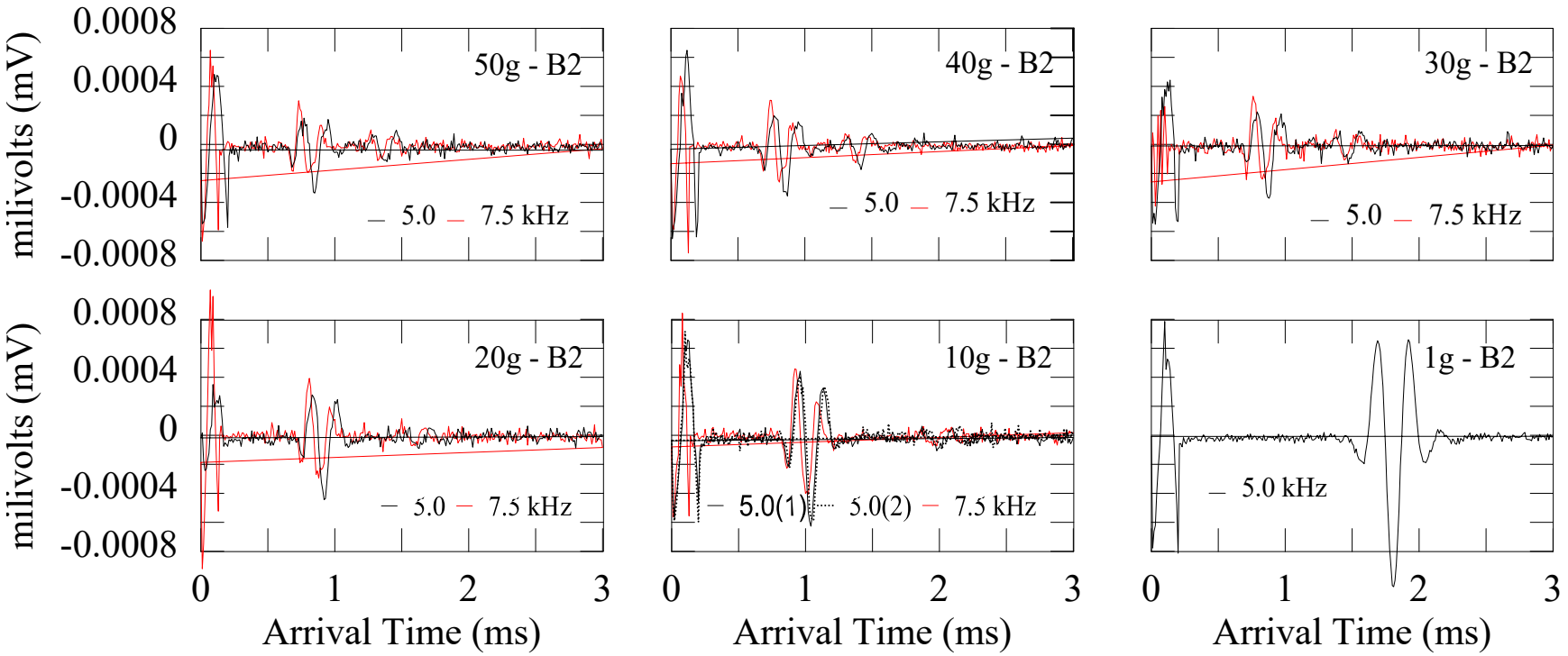

Figure C-361 Bender elements (B2) arrival times at various 'g' levels during spin-down for test Dr95FF.

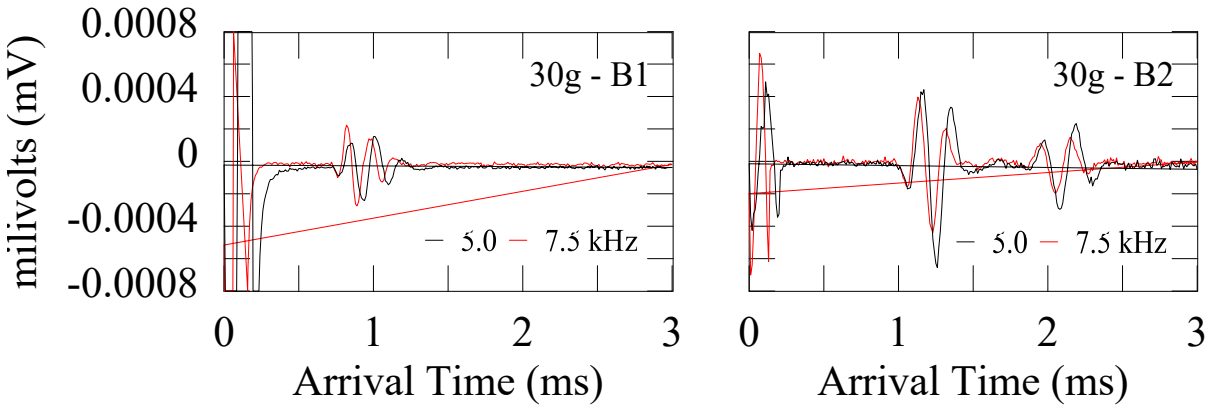

Figure C-362 Bender elements (B2) arrival times at 30g before spin-up 2 for test Dr95FF.

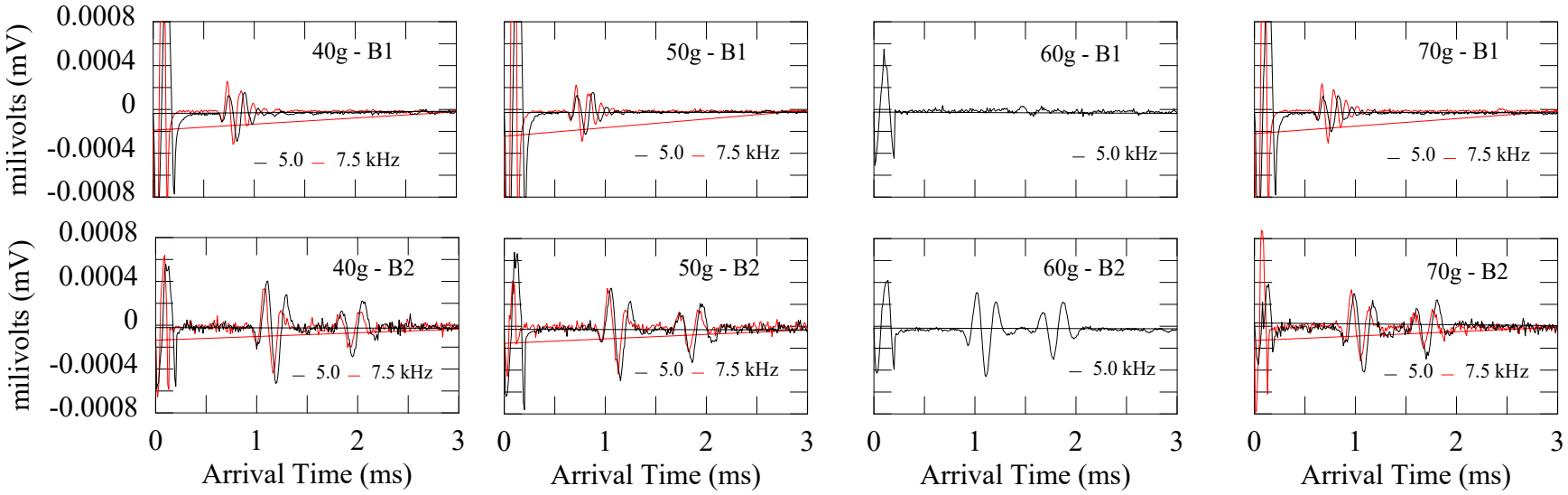

Figure C-363 Bender elements (B2) arrival times at 30g before spin-up 2 for test Dr95FF.

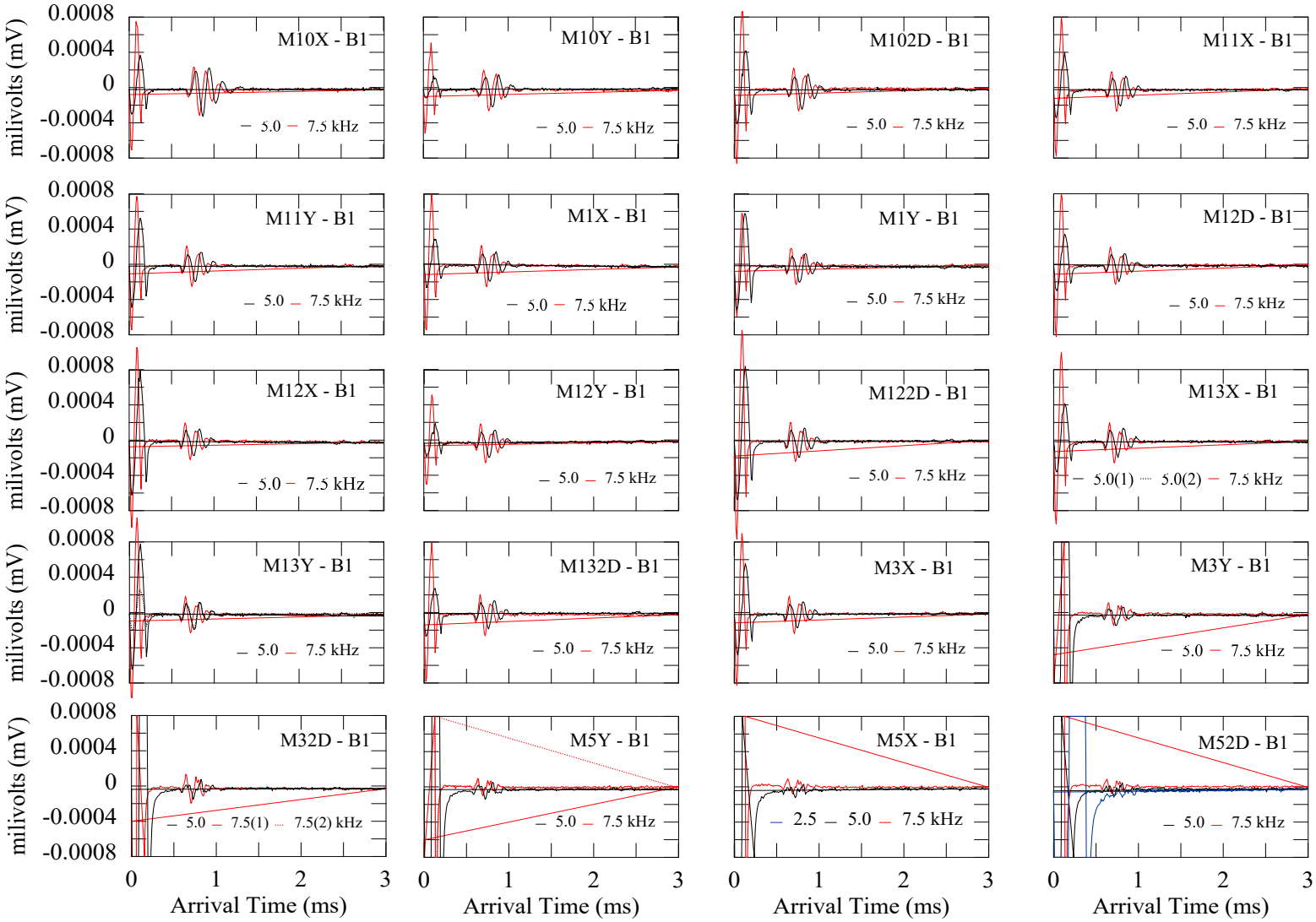

Figure C-364 Bender elements (B1) arrival times in between 60g motions for test Dr95FF.

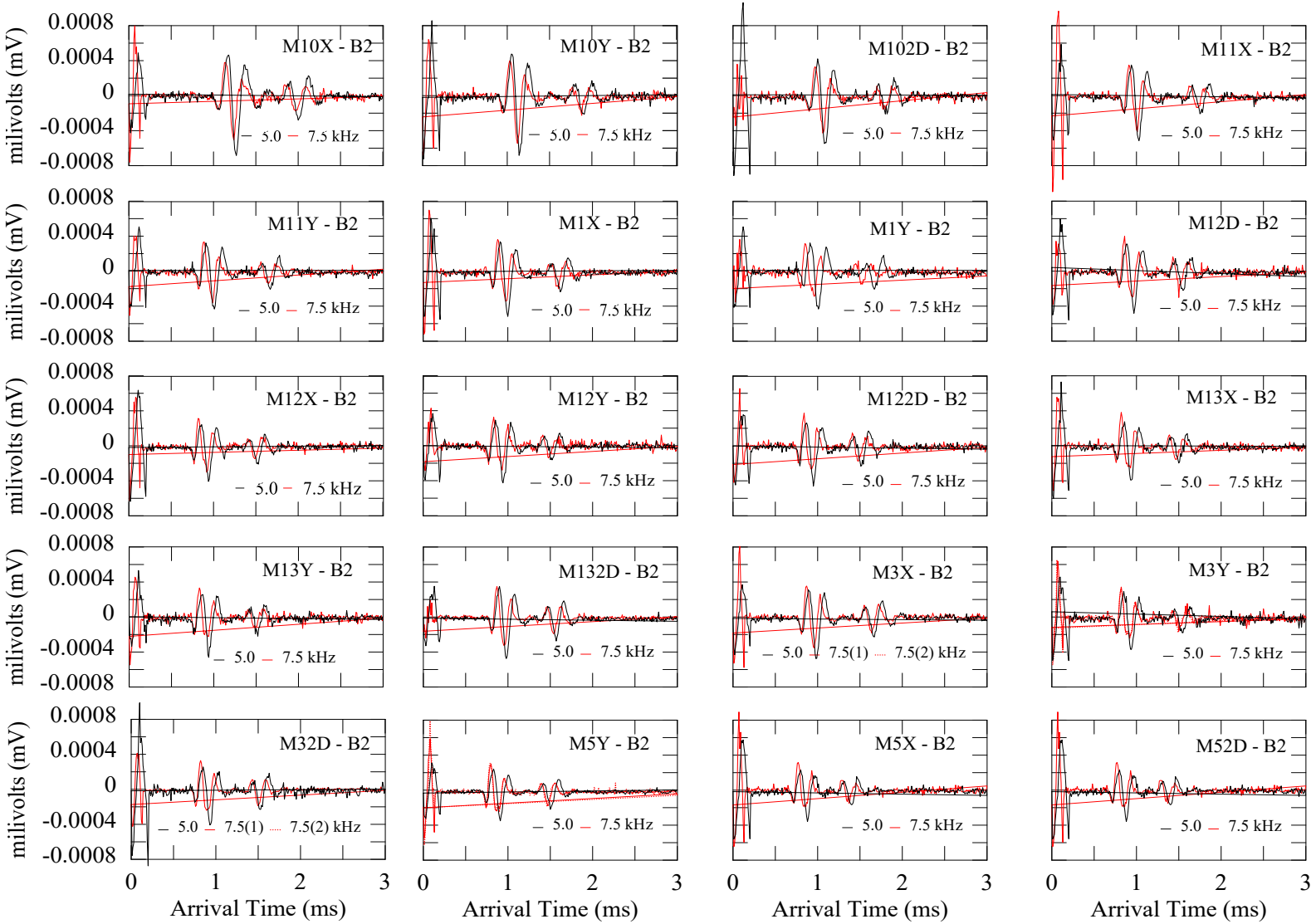

Figure C-365 Bender elements (B2) arrival times in between 60g motions for test Dr95FF.

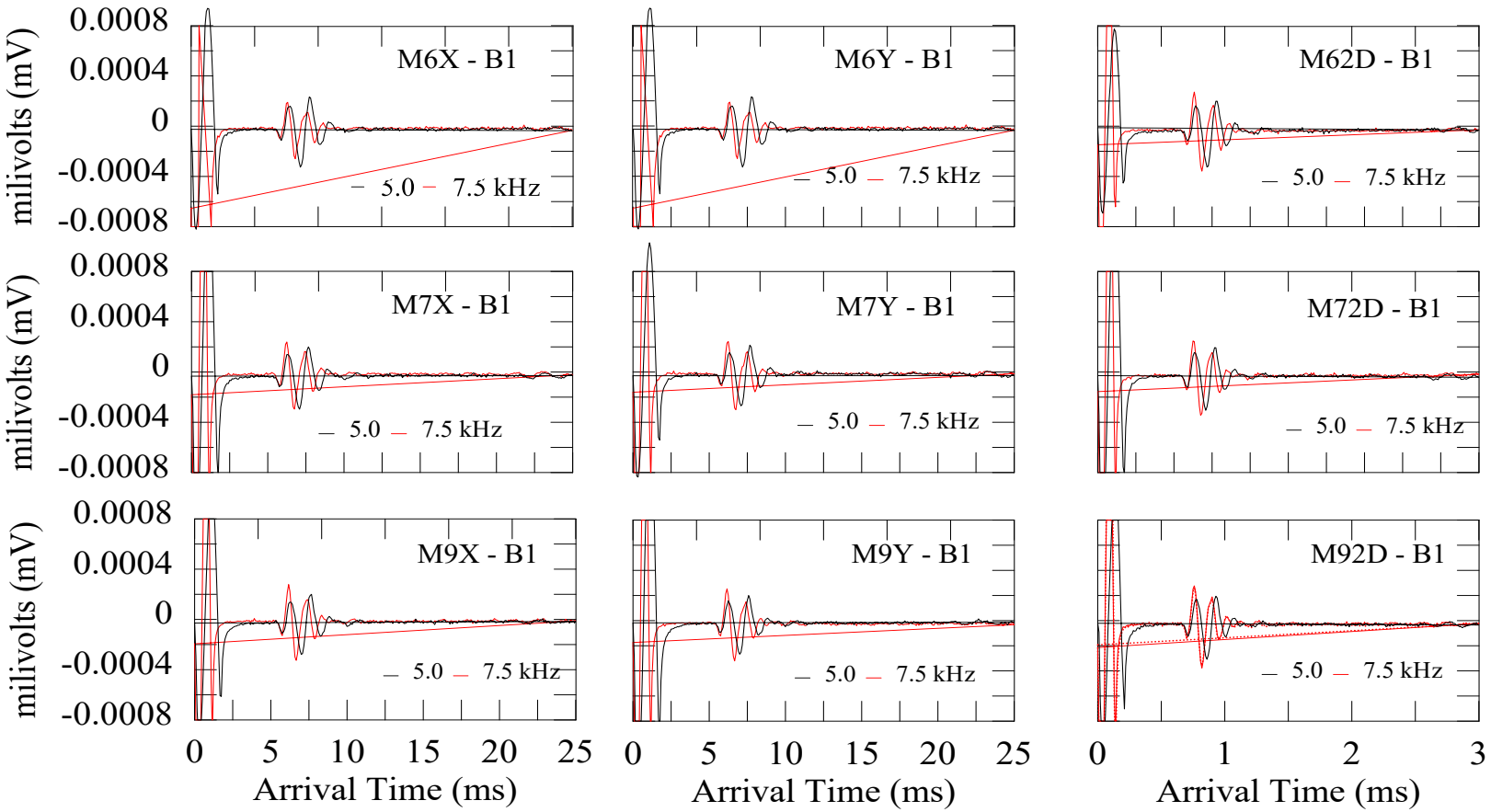

Figure C-366 Bender elements (B1) arrival times in between 30g motions for test Dr95FF.

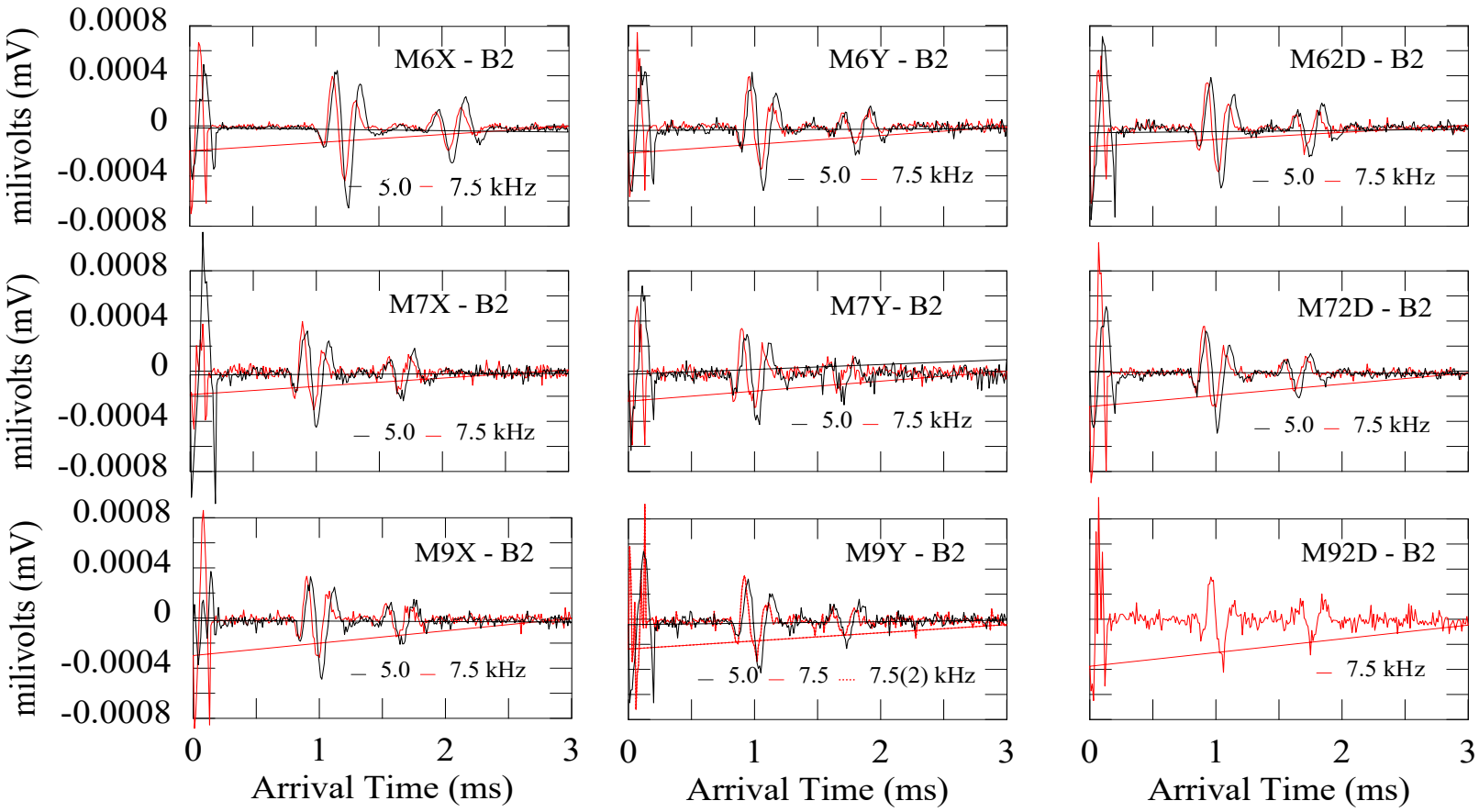

Figure C-367 Bender elements (B2) arrival times in between 30g motions for test Dr95FF.

1.6 Test: Dr95NF (PT2)

1.6.1 Motion 10 (M10)

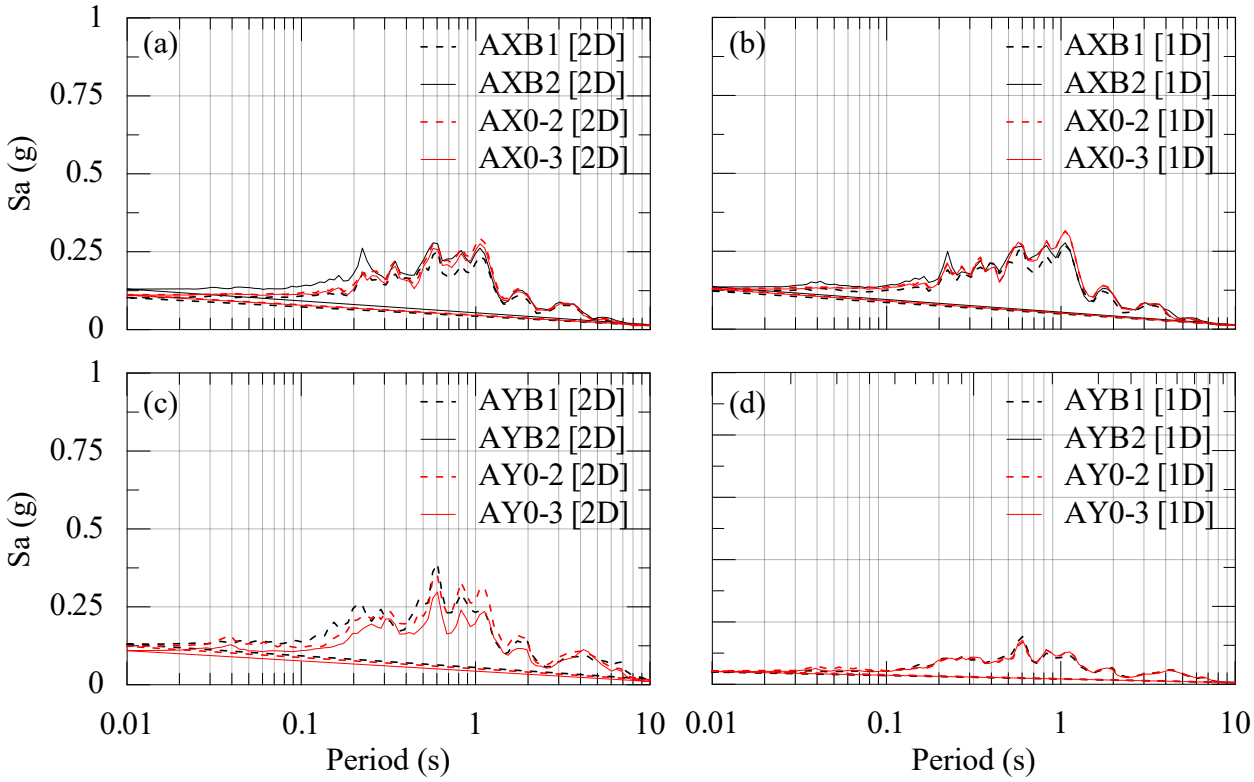

Figure C-368 Comparison of response spectra of 2D laminar container table and within model base input motion for motions (M10-X, Y and 2D).

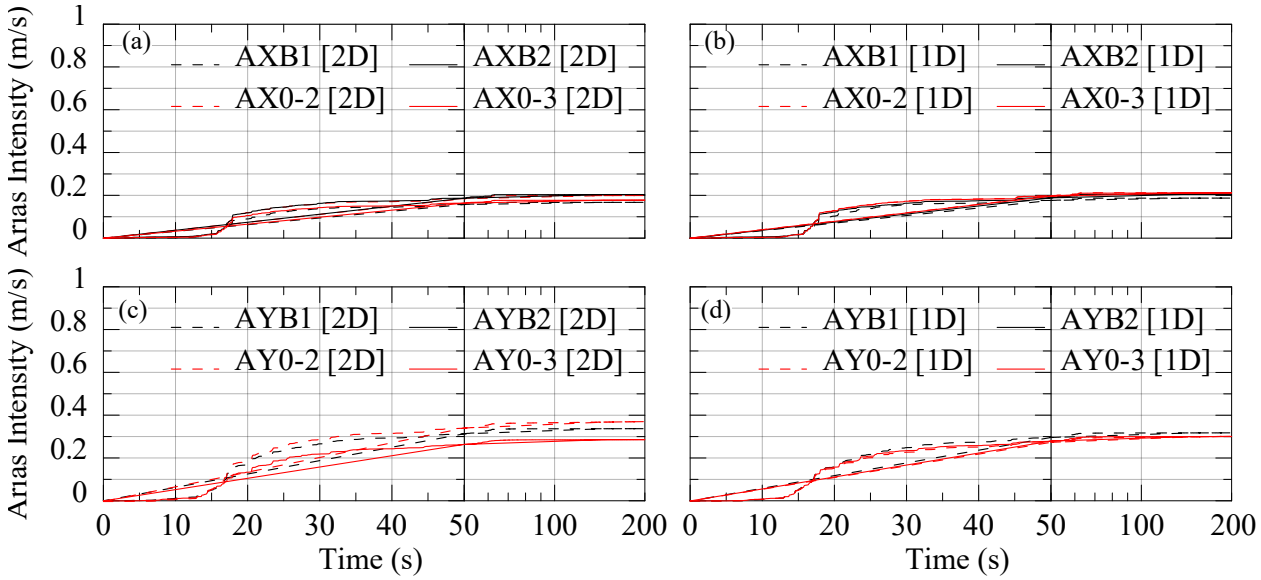

Figure C-369 Comparison of Arias Intensity of 2D laminar container table and within model base input motion for motions (a) M10-2D [X]; (b) M10-2D [Y]; (c) M10-1D [X] and (d) M10-1D [Y]

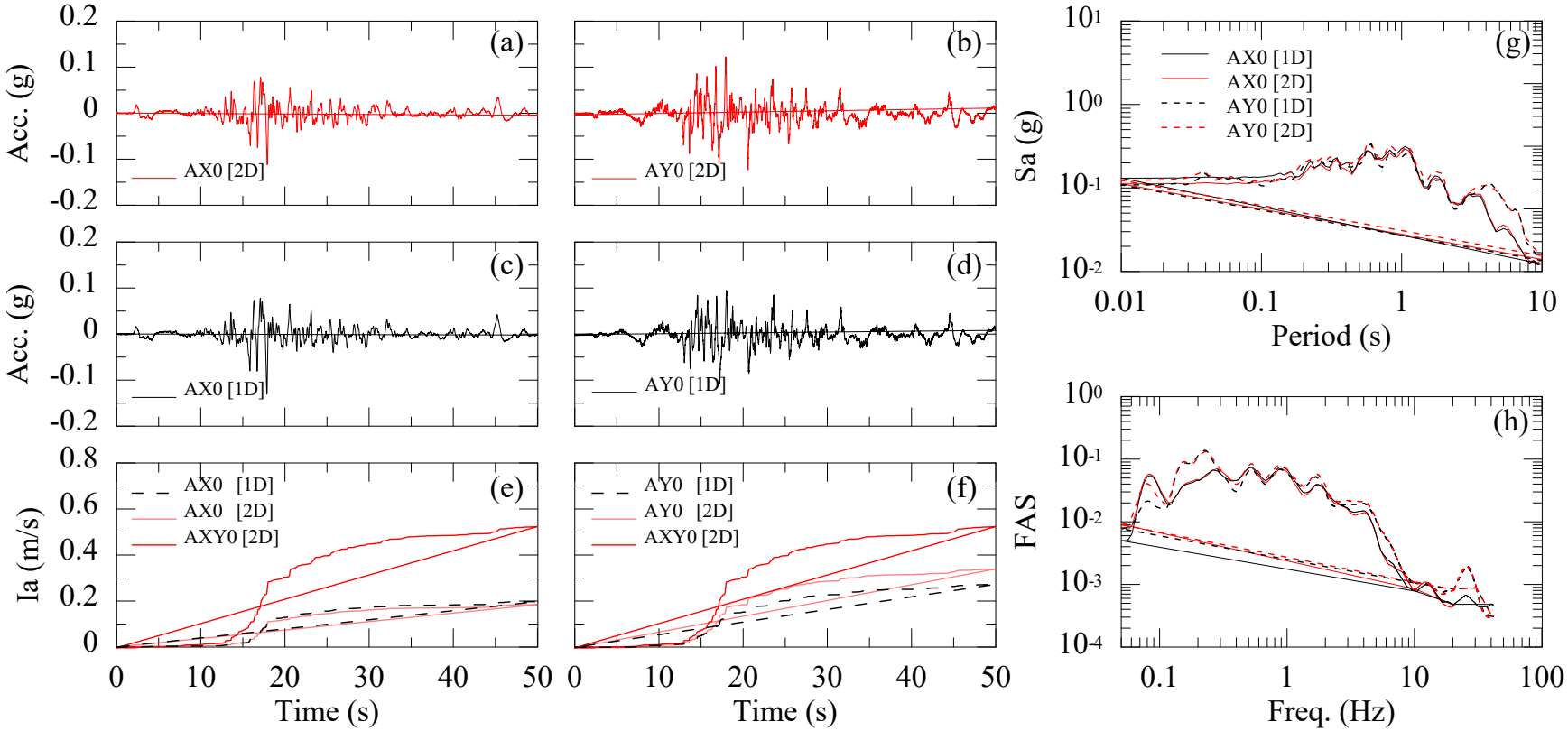

Figure C-370 Recorded input (2D) and 1D (X or Y) ground motions for: (a) M10-2D [X]; (b) M10-2D [Y]; (c) M10-1D [X]; and (d) M10-1D [Y]. Arias Intensity M10 (1D and 2D) for: (e) X direction; and (f) Y direction. Response Spectra (g) M10-2D [X]; M10-2D [Y]; M10-1D [X]; and M10-1D [Y]. Smoothed Fourier amplitude spectra (FAS) (h) M10-2D [X]; M10-2D [Y]; M10-1D [X]; and M10-1D [Y].

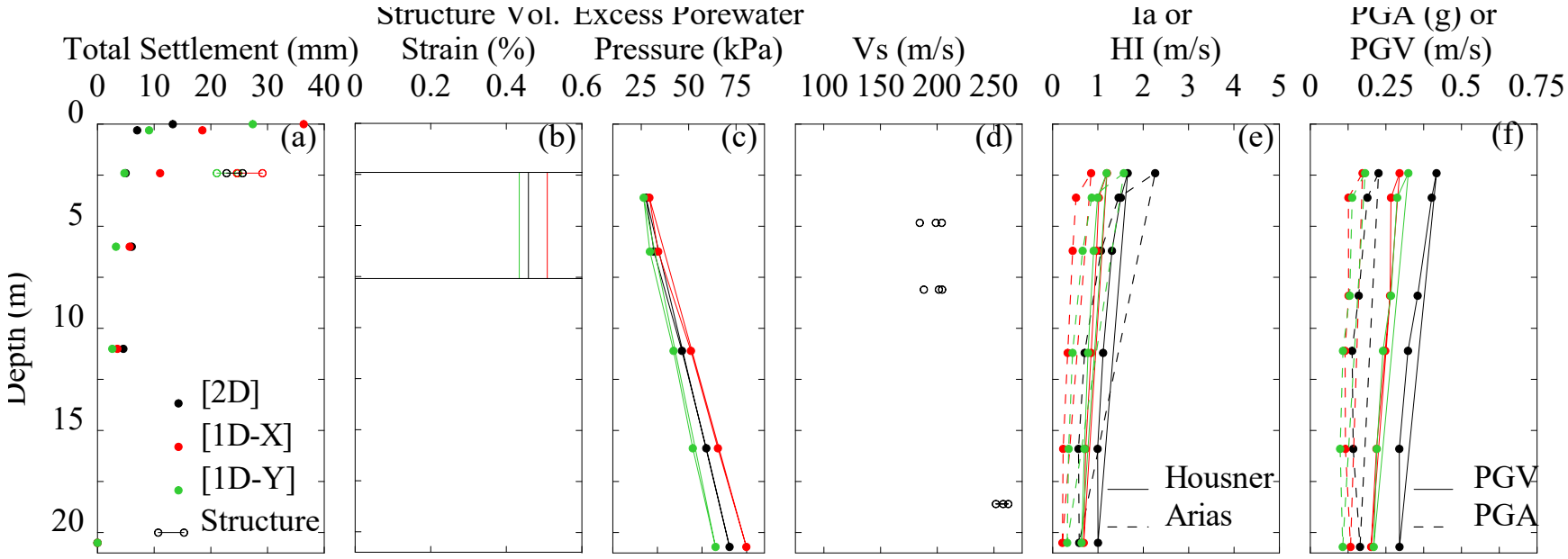

Figure C-371 Recorded or computed profiles for input motion M10-X, Y, and 2D. (a) Total settlement; (b) structure volumetric strain; (c) excess pore water pressure; (d) shear wave velocity; (e) Arias and Housner intensities; and (f) PGA and PGV.

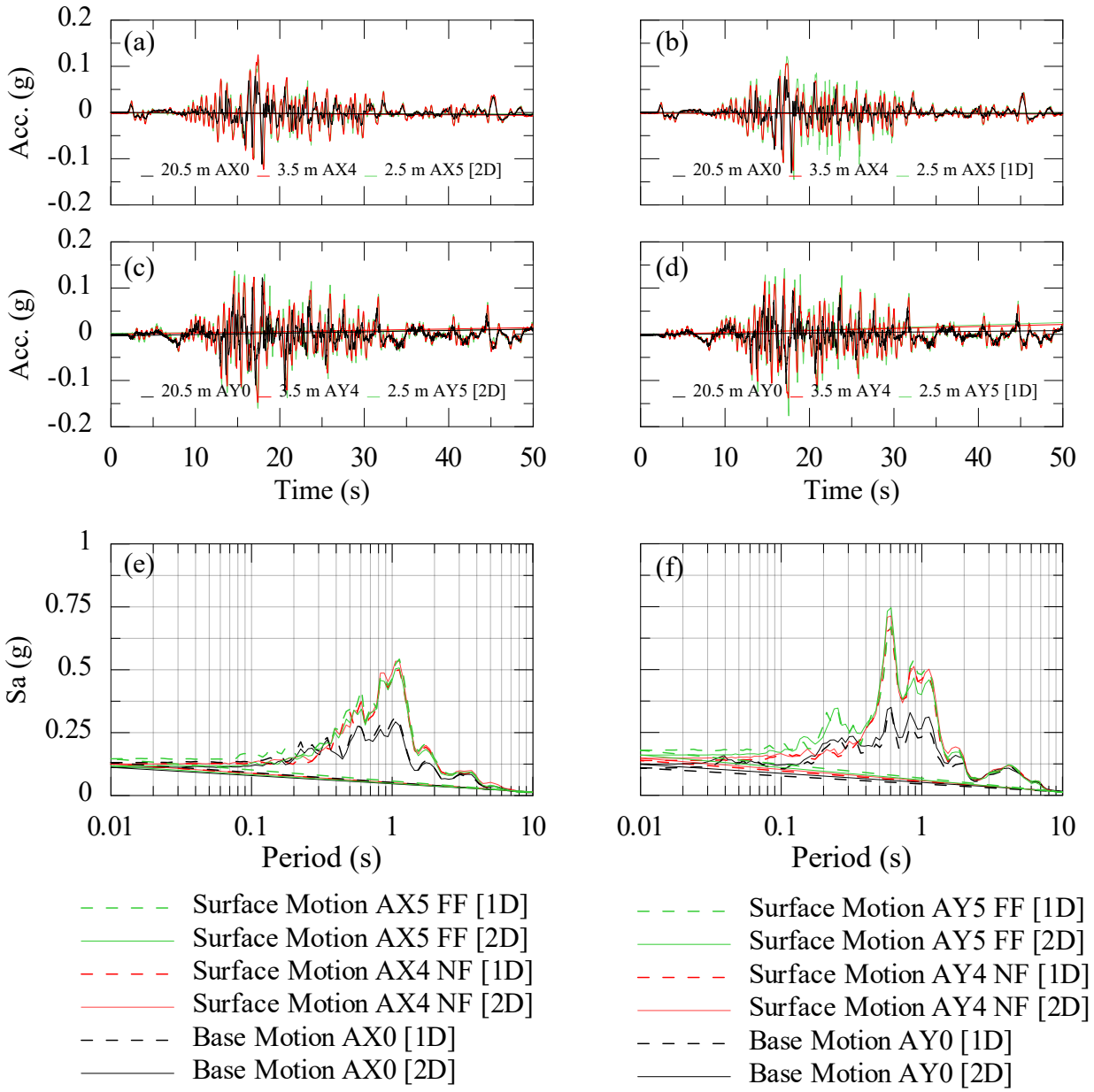

Figure C-372 Recorded input and near surface ground motions: (a) M10-2D [X]; (b) M10-1D [X]; (c) M10-2D [Y]; and (d) M10-1D [Y]. Computed response spectra from Near Field Test [PT3] for motions M10 (1D and 2D) for: (e) X direction; and (f) Y direction.

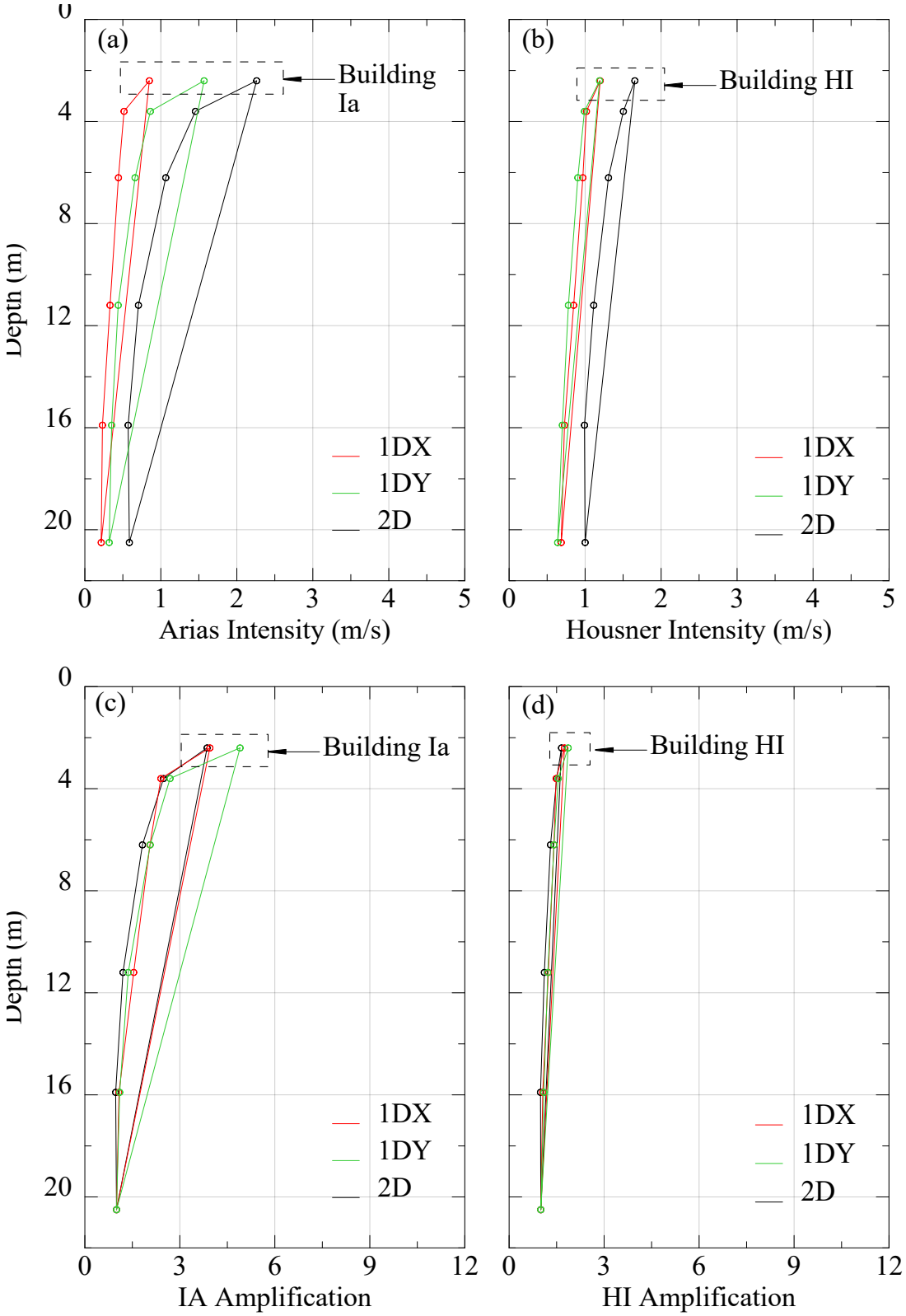

Figure C-373 Variation of total (a) Arias Intensity (M10-X,Y and 2D) ; (b) Housner Intensity (M10-X,Y and 2D) (c) Arias Intensity Amplification Factor (M10-X,Y and 2D); and (d) Housner Intensity Amplification Factor (M10-X,Y and 2D).

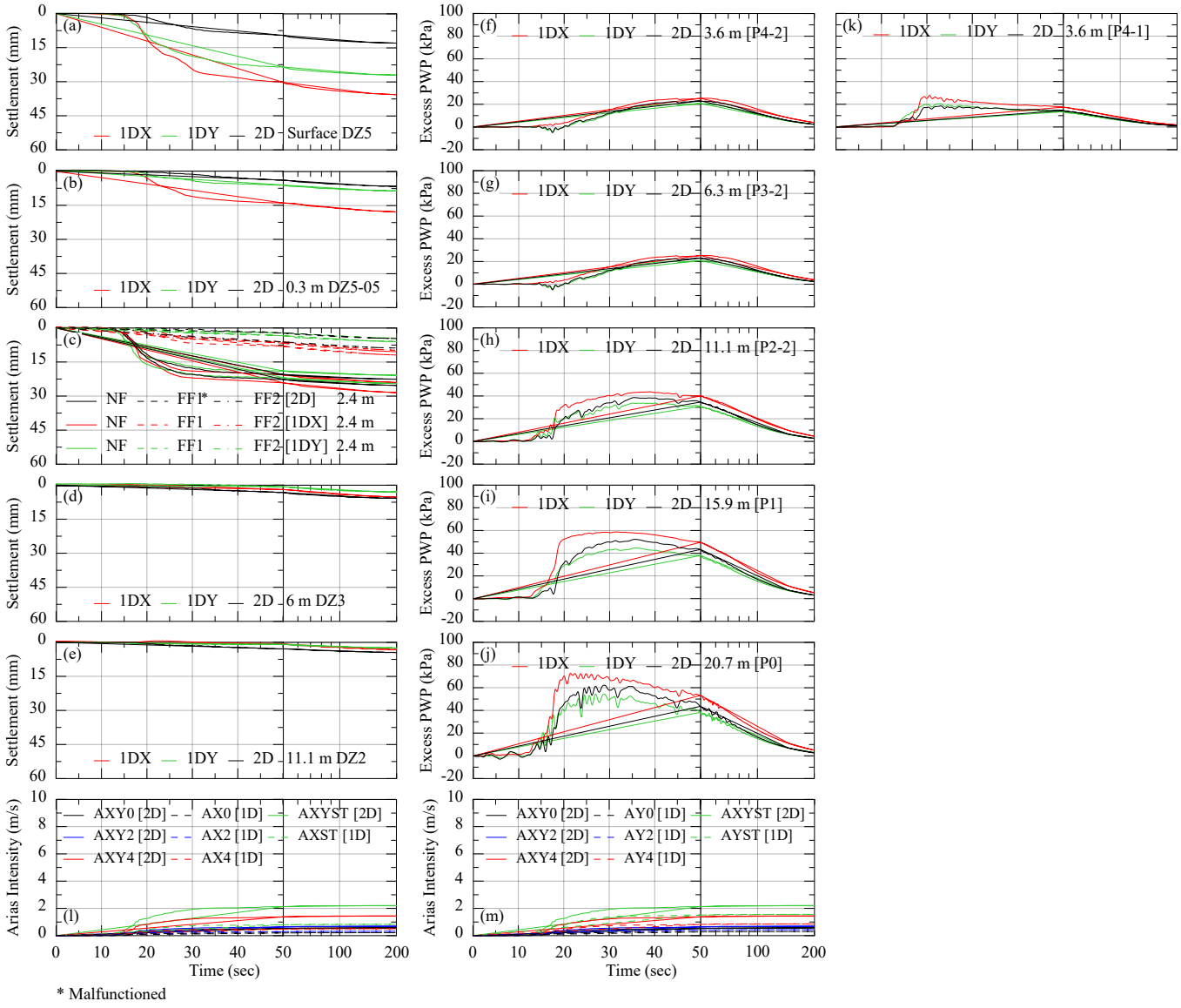

Figure C-374 Variation of total (a) to (e) Settlement with depth (M10-X,Y and 2D) ; (f) to (k) Excess pore water pressure (M10-X,Y and 2D) (l) and (m) Arias Intensity along model (M10-X,Y and 2D).

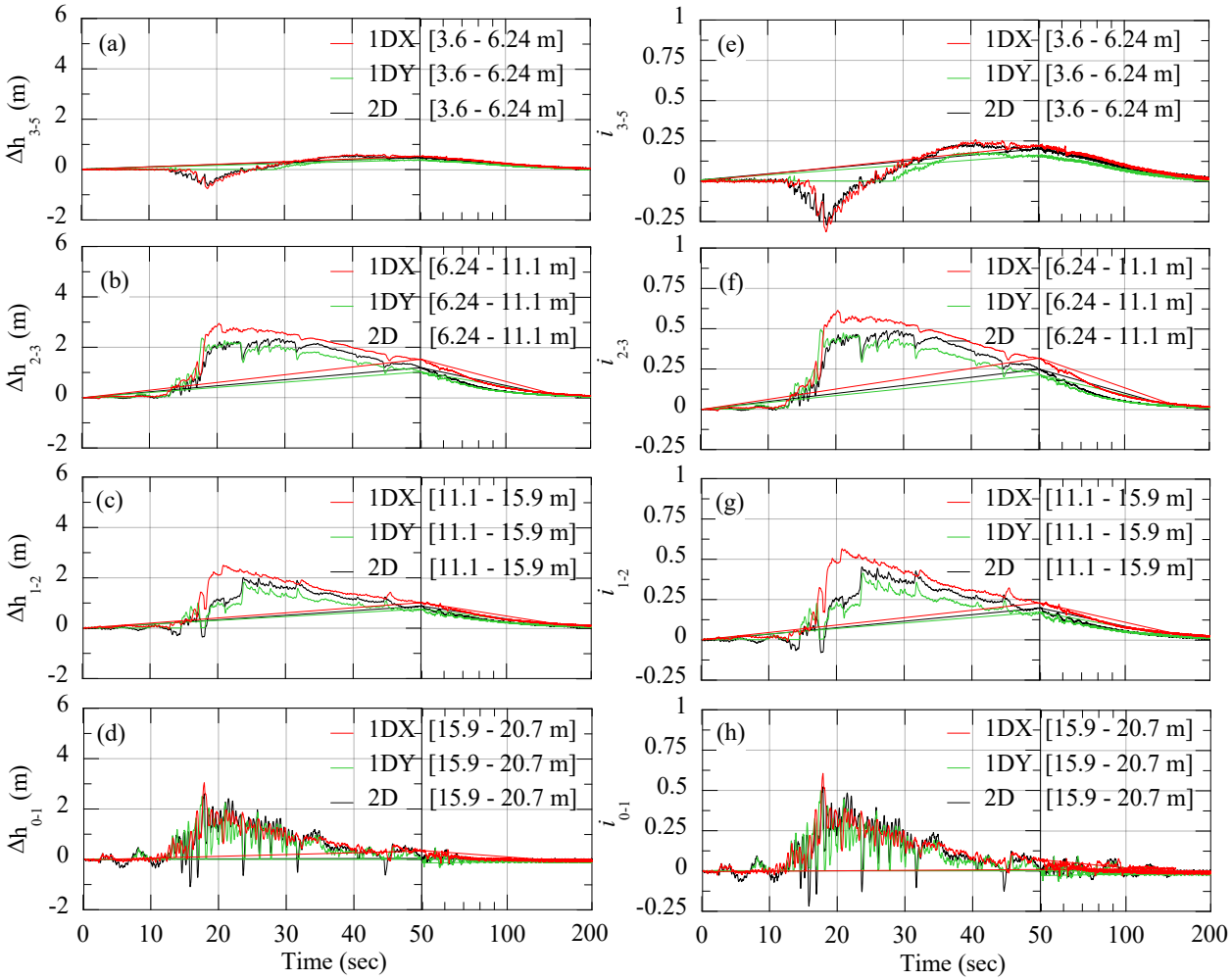

Figure C-375 Variation of total (a) to (d) Total Head Loss with depth (M10-X, Y and 2D); (e) to (h) Shaking induced Hydraulic Gradient (M10-X, Y and 2D)

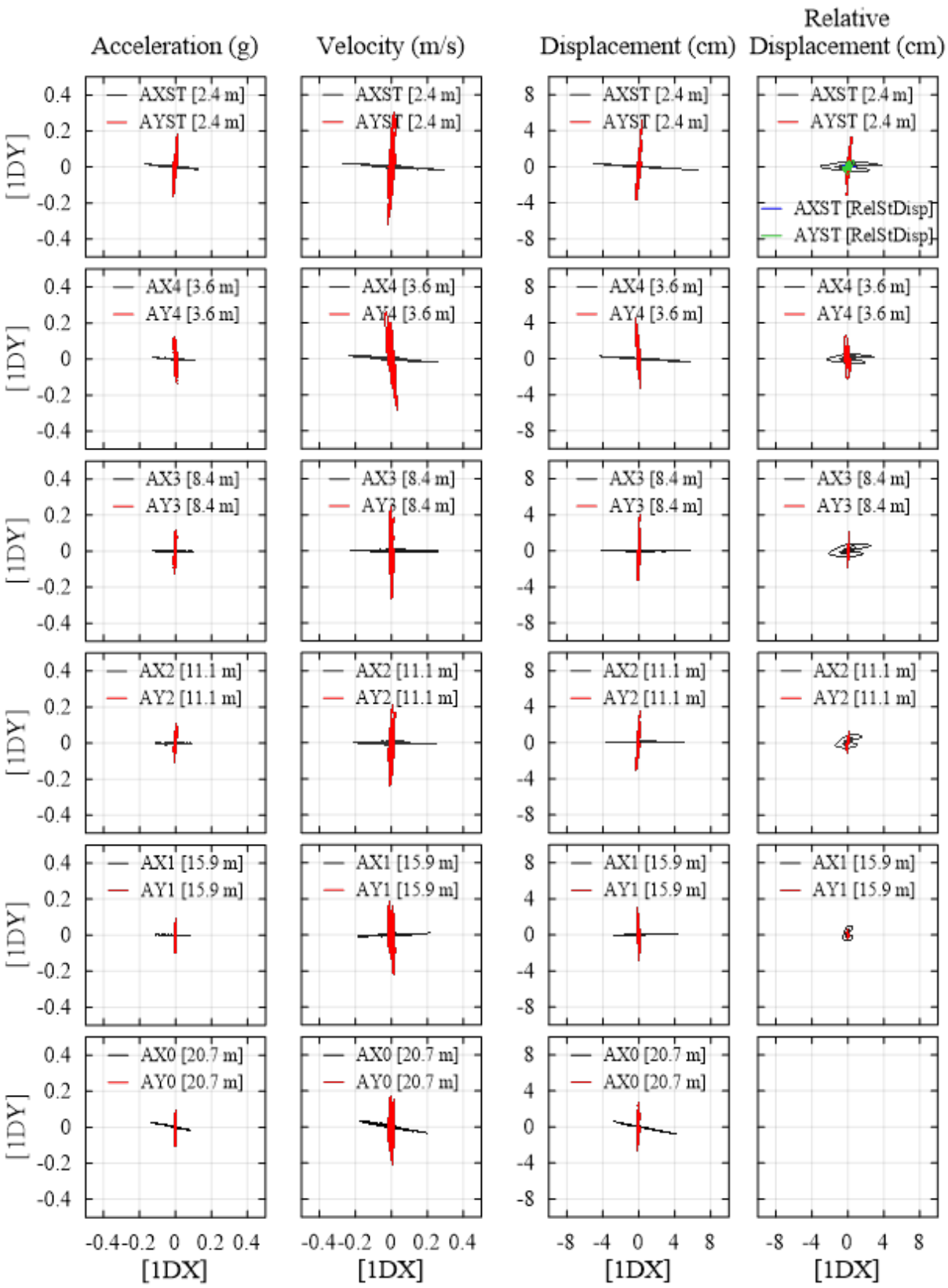

Figure C-376 Recorded input and within model ground motions for acceleration, velocity, displacement and relative displacement for M10-1D [X] and M10-1D [Y]

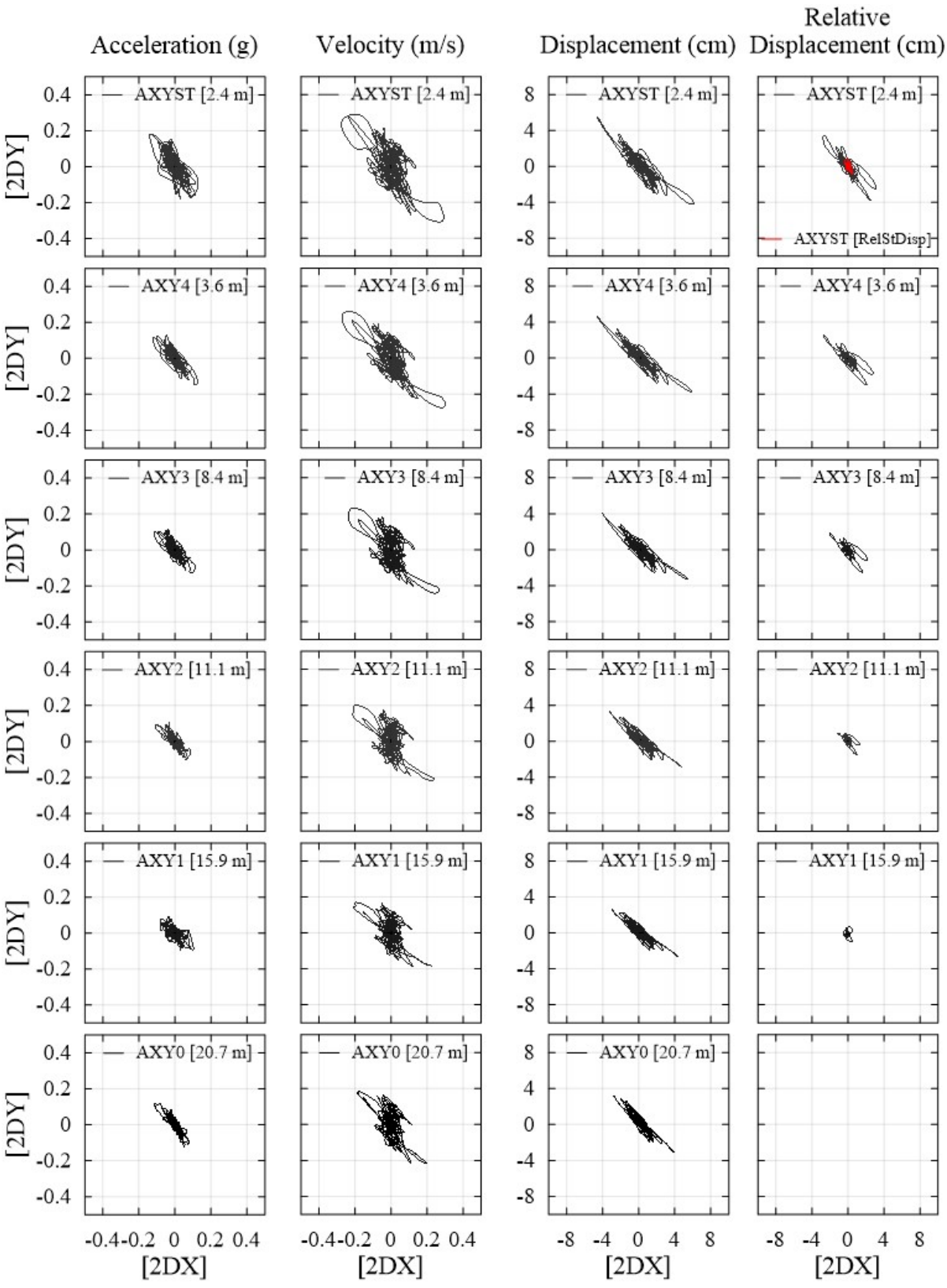

Figure C-377 Recorded input and within model ground motions for acceleration, velocity, displacement and relative displacement for M10-2D

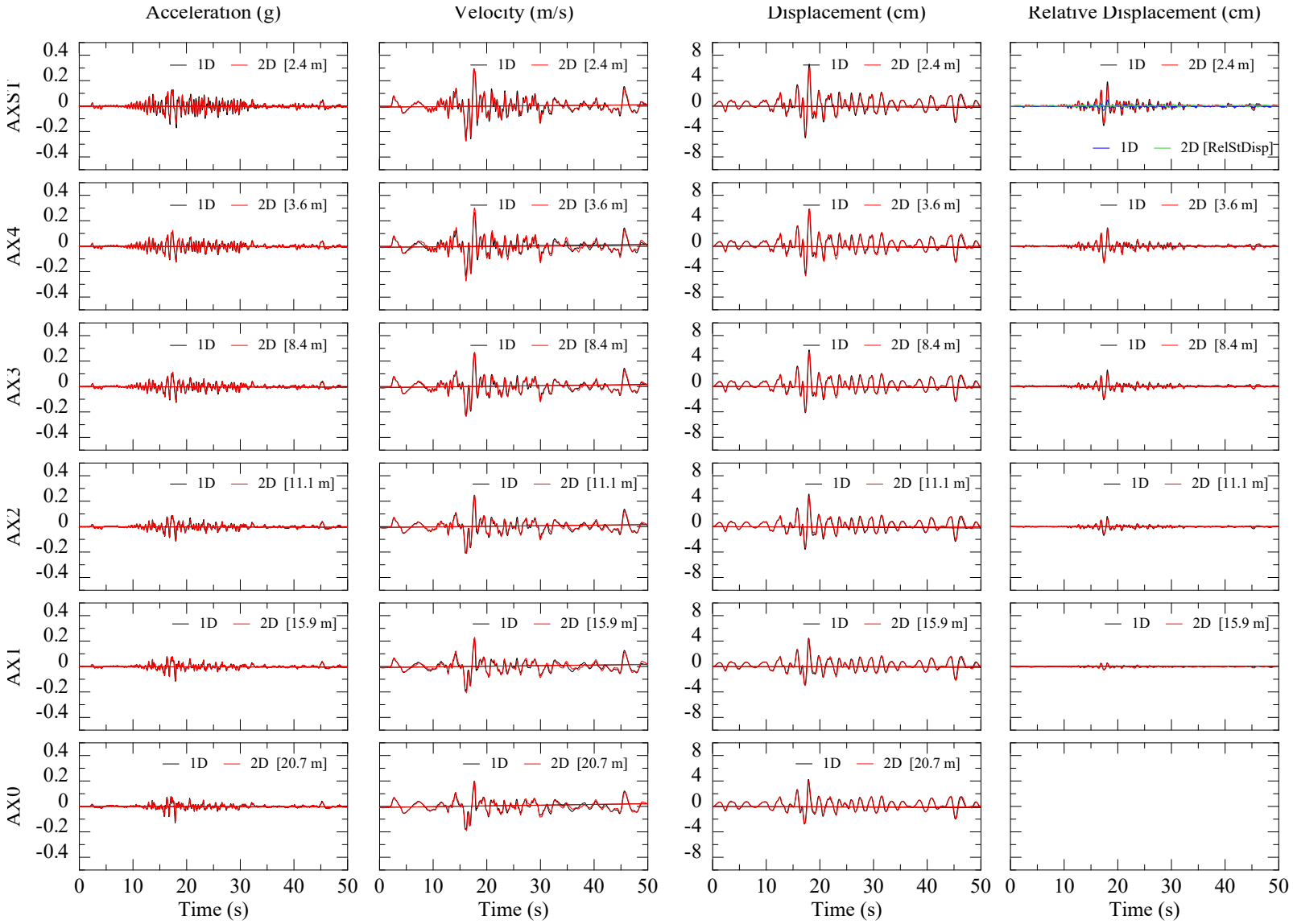

Figure C-378 Recorded input and within model ground motions time histories for acceleration, velocity, displacement and relative displacement for M10-2D [X] and M10-1D [X]

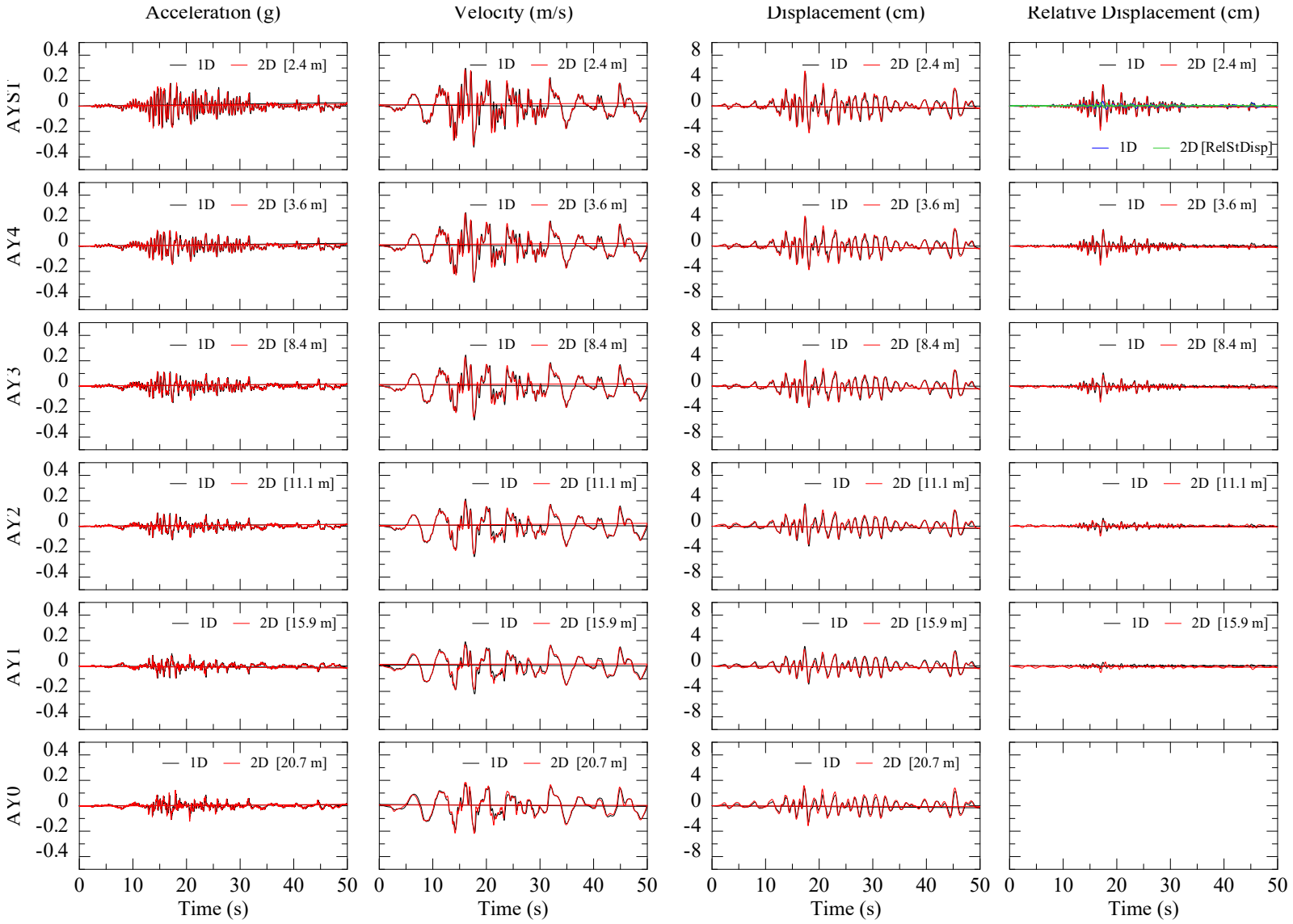

Figure C-379 Recorded input and within model ground motions time histories for acceleration, velocity, displacement and relative displacement for M10-2D [Y] and M10-1D [Y]

1.6.2 Motion 11 (M11)

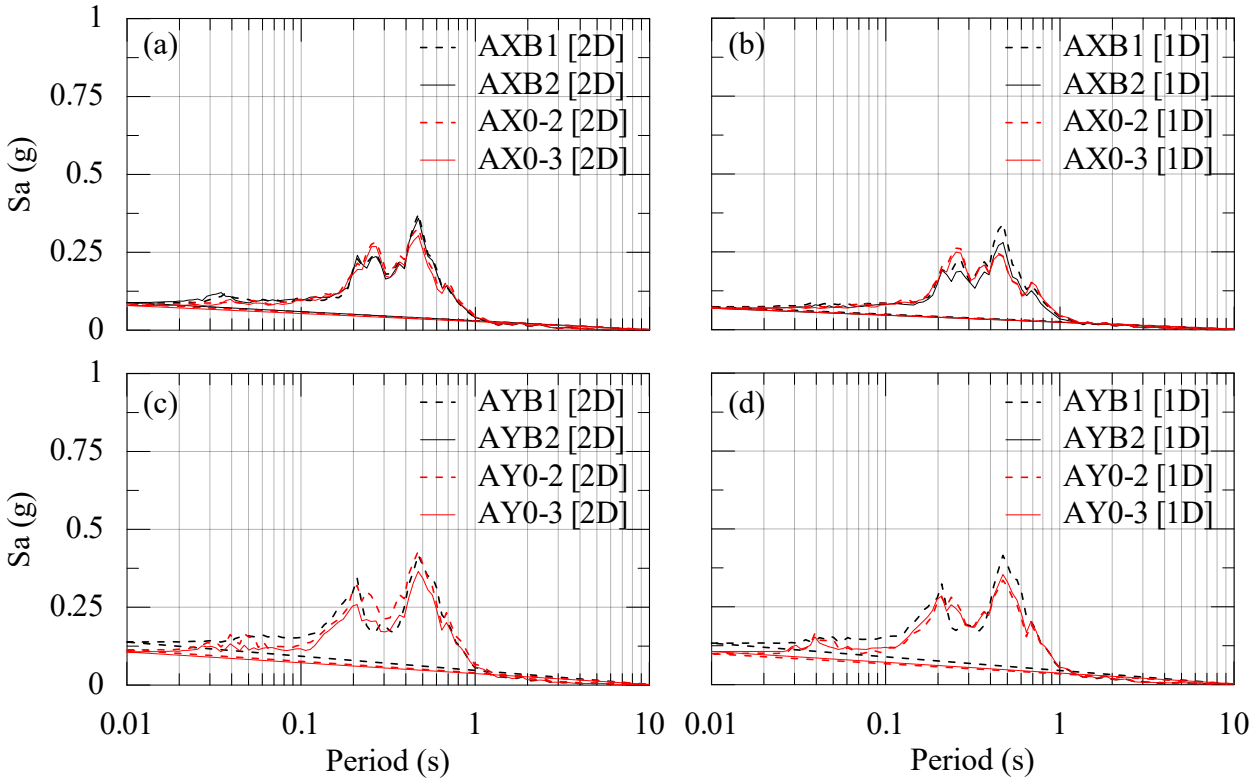

Figure C-380 Comparison of response spectra of 2D laminar container table and within model base input motion for motions (M11-X, Y and 2D).

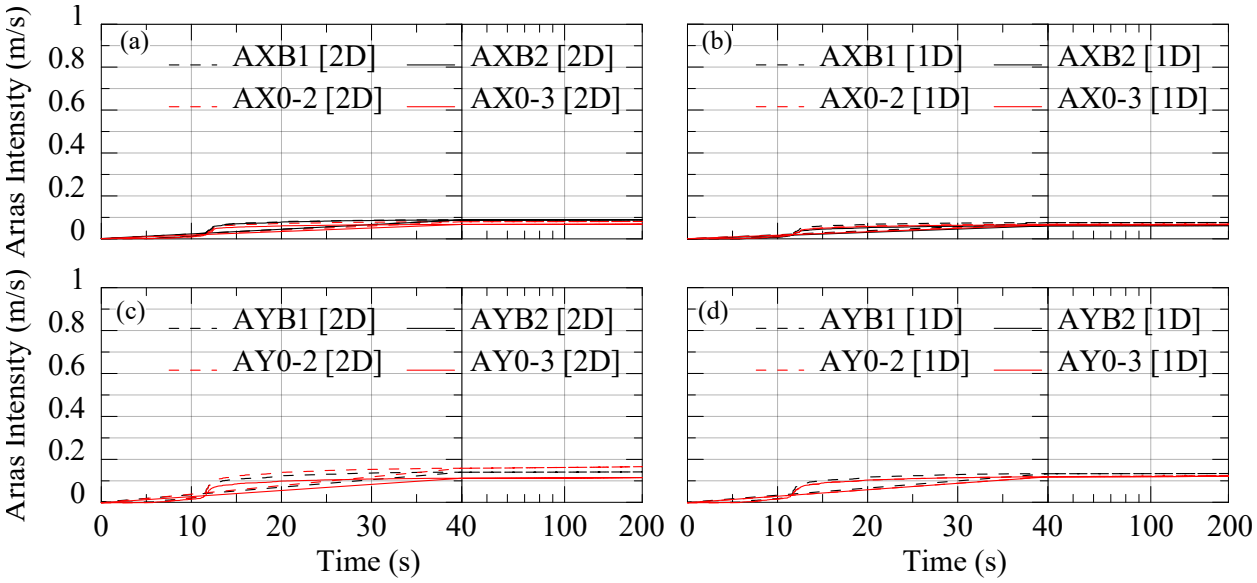

Figure C-381 Comparison of Arias Intensity of 2D laminar container table and within model base input motion for motions (a) M11-2D [X]; (b) M11-2D [Y]; (c) M11-1D [X] and (d) M11-1D [Y]

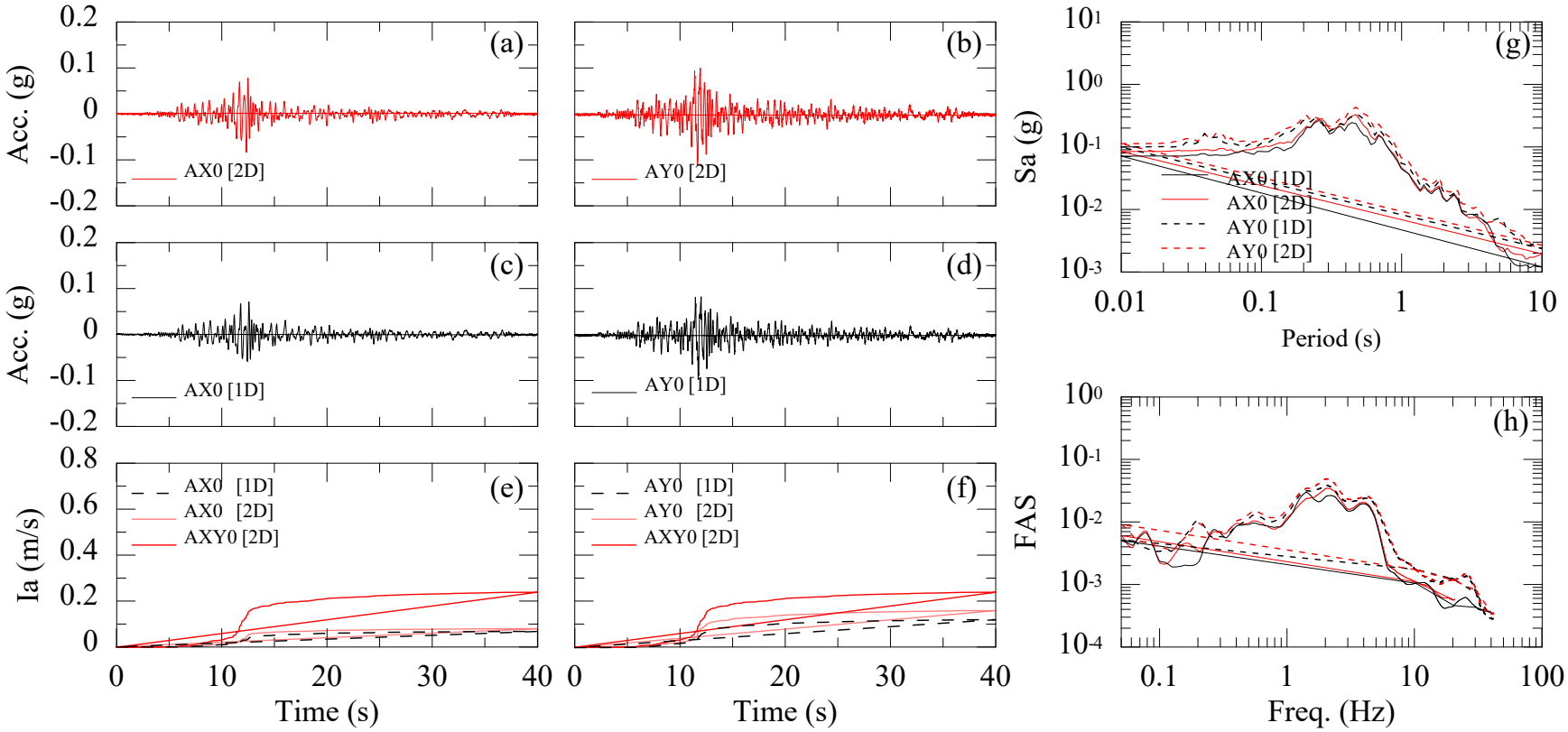

Figure C-382 Recorded input (2D) and 1D (X or Y) ground motions for: (a) M11-2D [X]; (b) M11-2D [Y]; (c) M11-1D [X]; and (d) M11-1D [Y]. Arias Intensity M11 (1D and 2D) for: (e) X direction; and (f) Y direction. Response Spectra (g) M11-2D [X]; M11-2D [Y]; M11-1D [X]; and M11-1D [Y]. Smoothed Fourier amplitude spectra (FAS) (h) M11-2D [X]; M11-2D [Y]; M11-1D [X]; and M11-1D [Y].

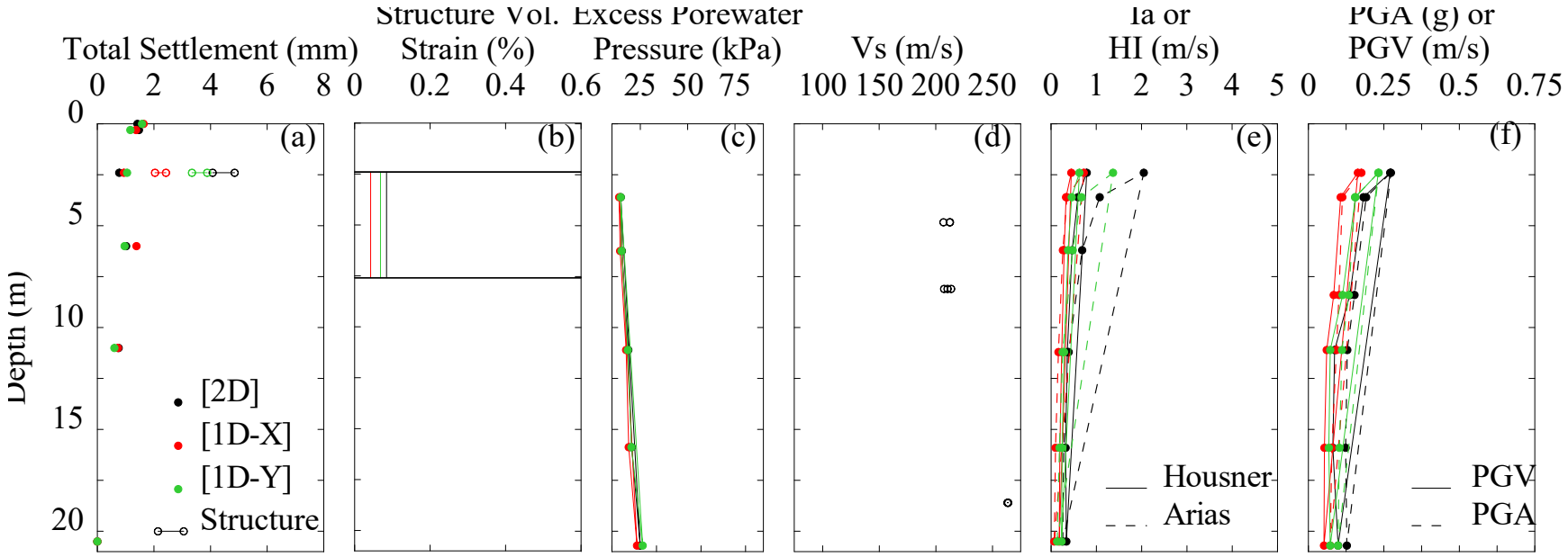

Figure C-383 Recorded or computed profiles for input motion M11-X, Y, and 2D. (a) Total settlement; (b) structure volumetric strain; (c) excess pore water pressure; (d) shear wave velocity; (e) Arias and Housner intensities; and (f) PGA and PGV.

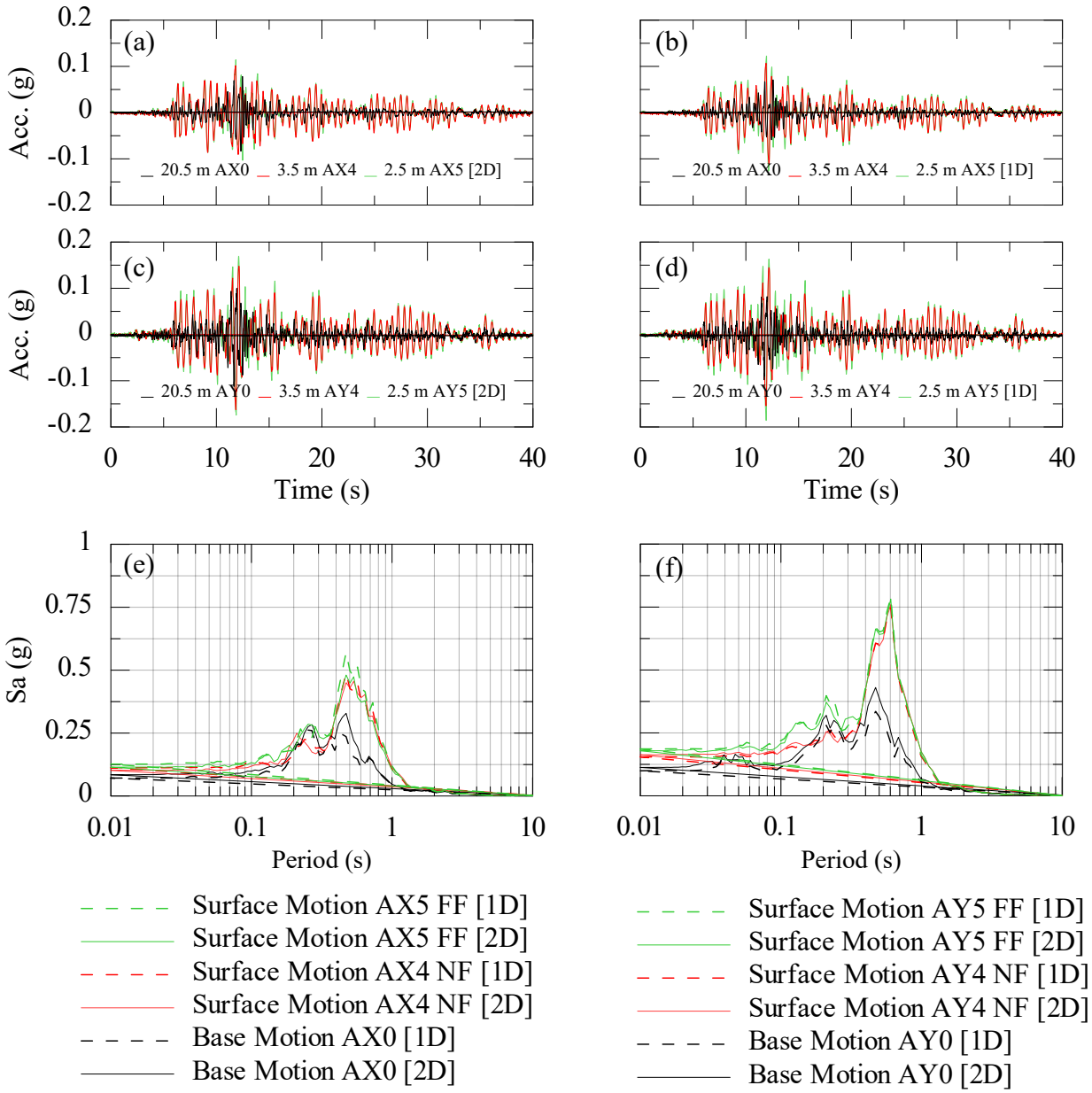

Figure C-384 Recorded input and near surface ground motions: (a) M11-2D [X]; (b) M11-1D [X]; (c) M11-2D [Y]; and (d) M11-1D [Y]. Computed response spectra from Near Field Test [PT3] for motions M11 (1D and 2D) for: (e) X direction; and (f) Y direction.

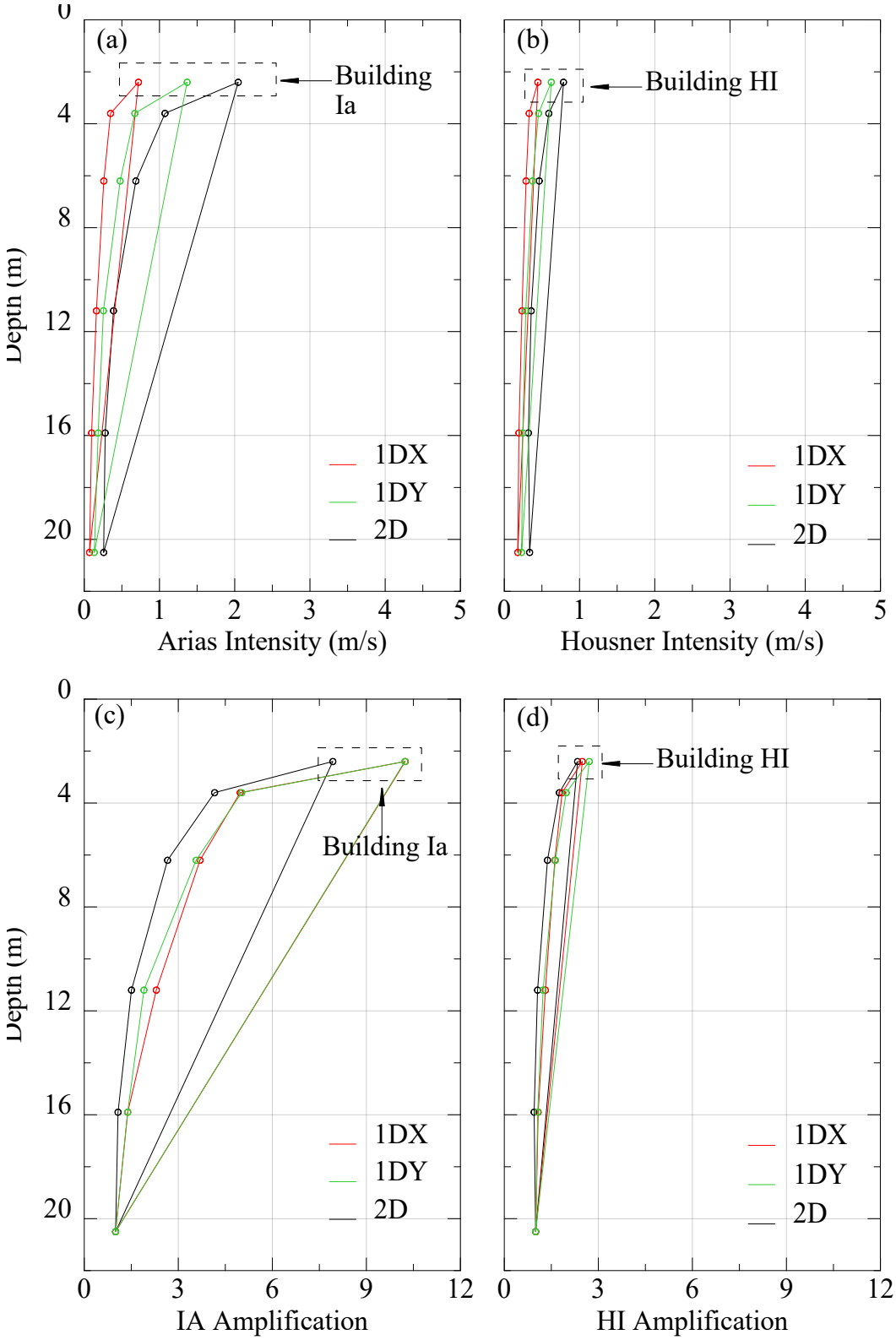

Figure C-385 Variation of total (a) Arias Intensity (M11-X,Y and 2D) ; (b) Housner Intensity (M11-X,Y and 2D) (c) Arias Intensity Amplification Factor (M11-X,Y and 2D); and (d) Housner Intensity Amplification Factor (M11-X,Y and 2D).

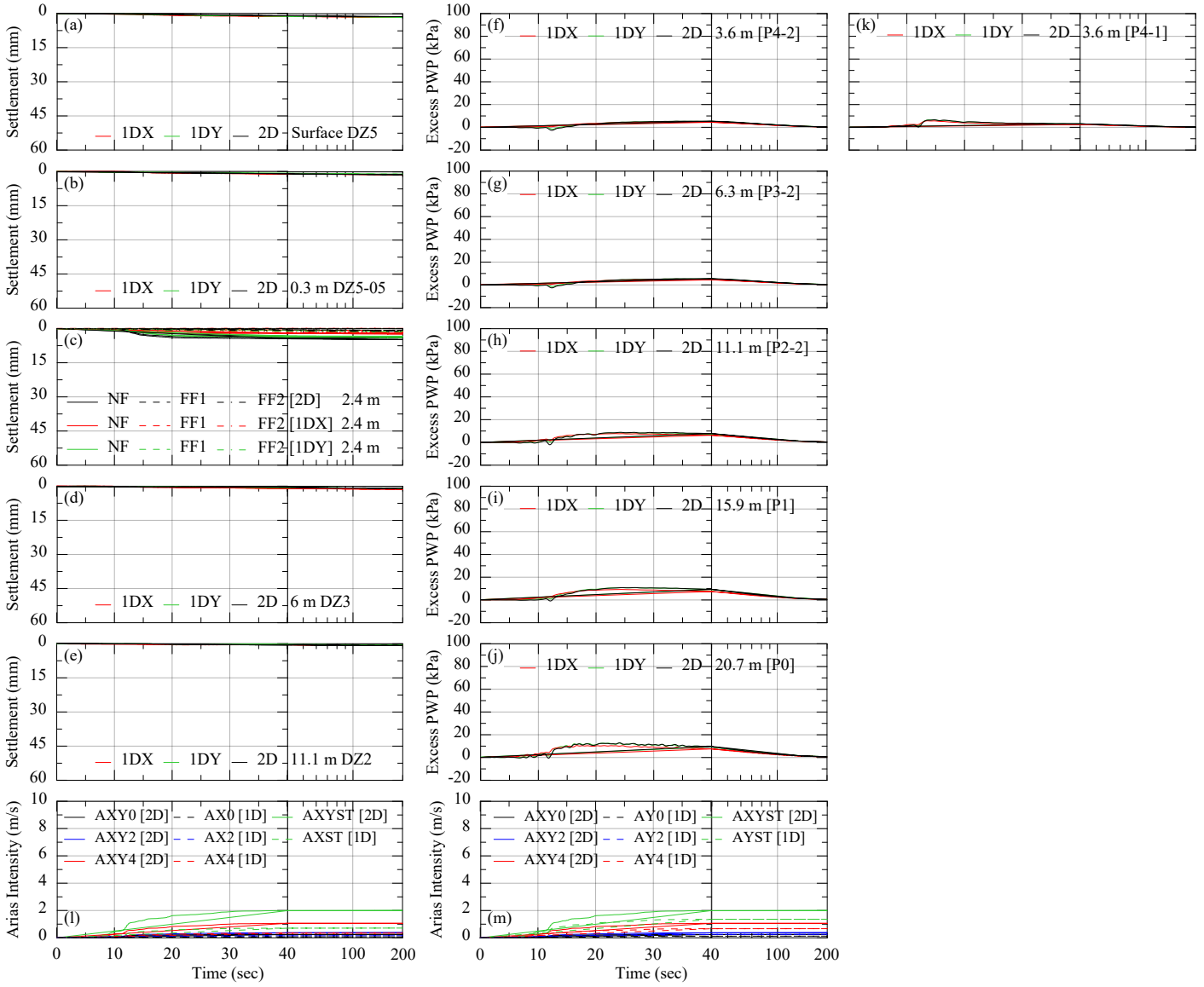

Figure C-386 Variation of total (a) to (e) Settlement with depth (M11-X,Y and 2D) ; (f) to (k) Excess pore water pressure (M11-X,Y and 2D) (l) and (m) Arias Intensity along model (M11-X,Y and 2D).

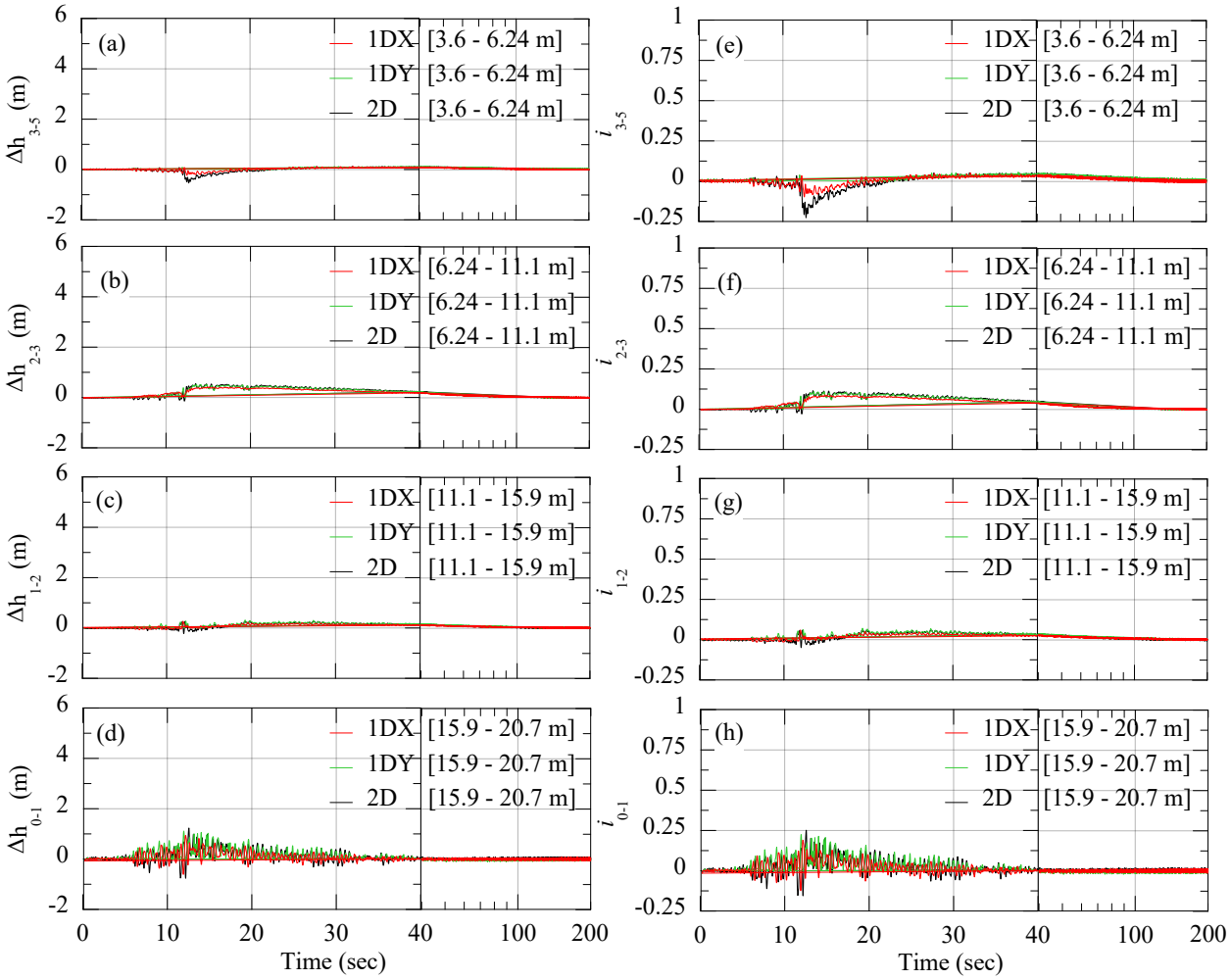

Figure C-387 Variation of total (a) to (d) Total Head Loss with depth (M11-X, Y and 2D); (e) to (h) Shaking induced Hydraulic Gradient (M11-X, Y and 2D)

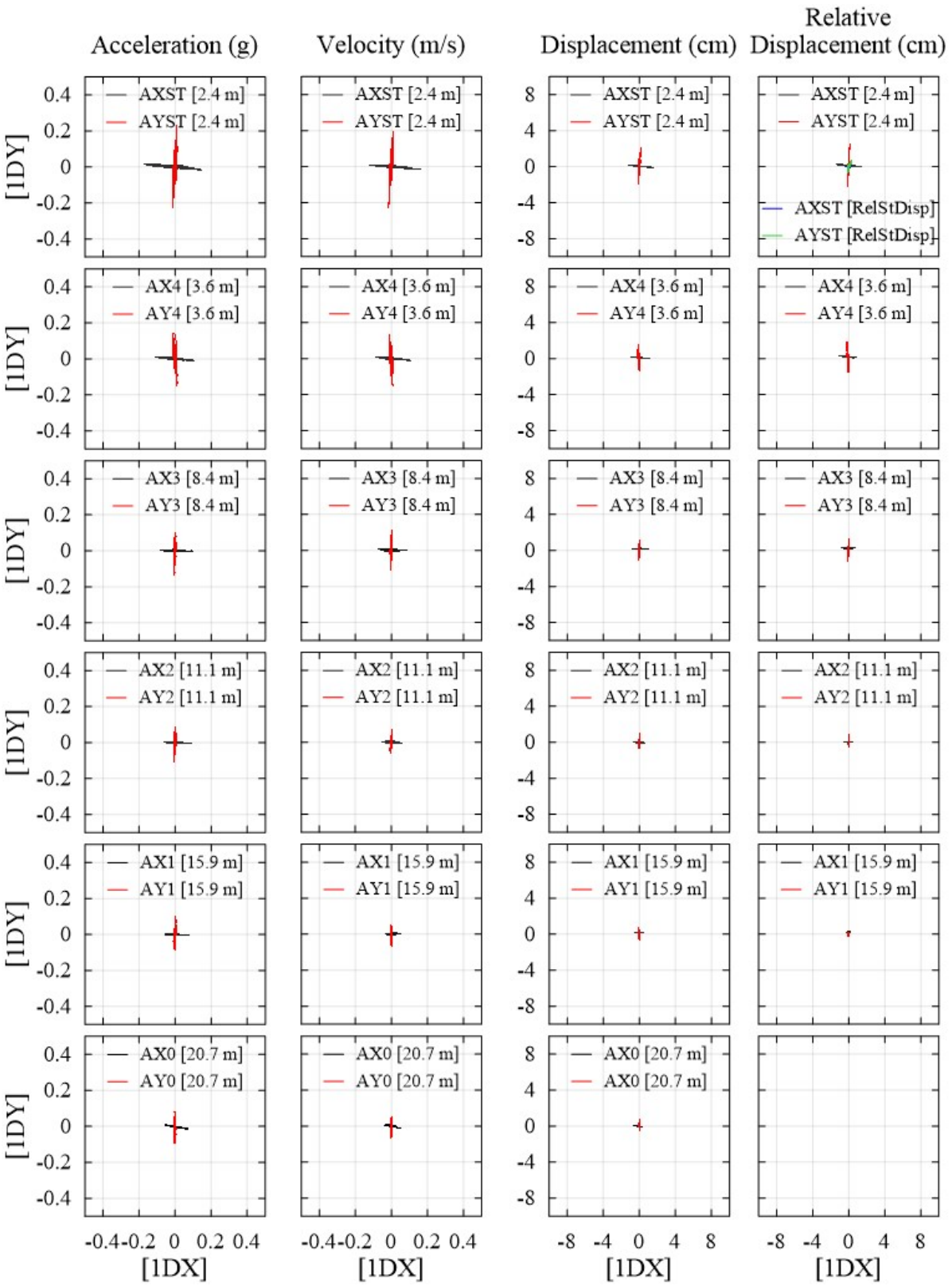

Figure C-388 Recorded input and within model ground motions for acceleration, velocity, displacement and relative displacement for M11-1D [X] and M11-1D [Y]

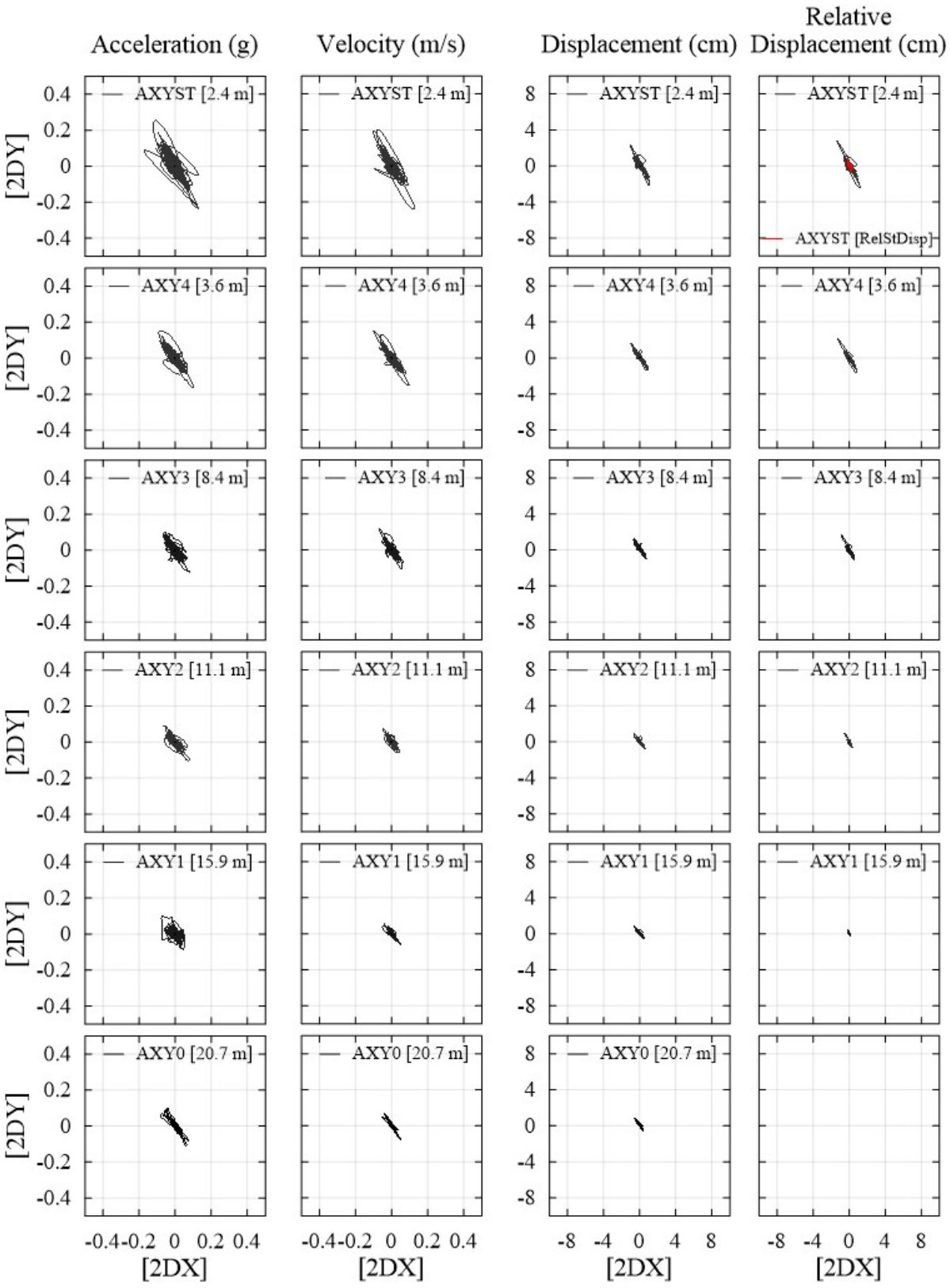

Figure C-389 Recorded input and within model ground motions for acceleration, velocity, displacement and relative displacement for M11-2D

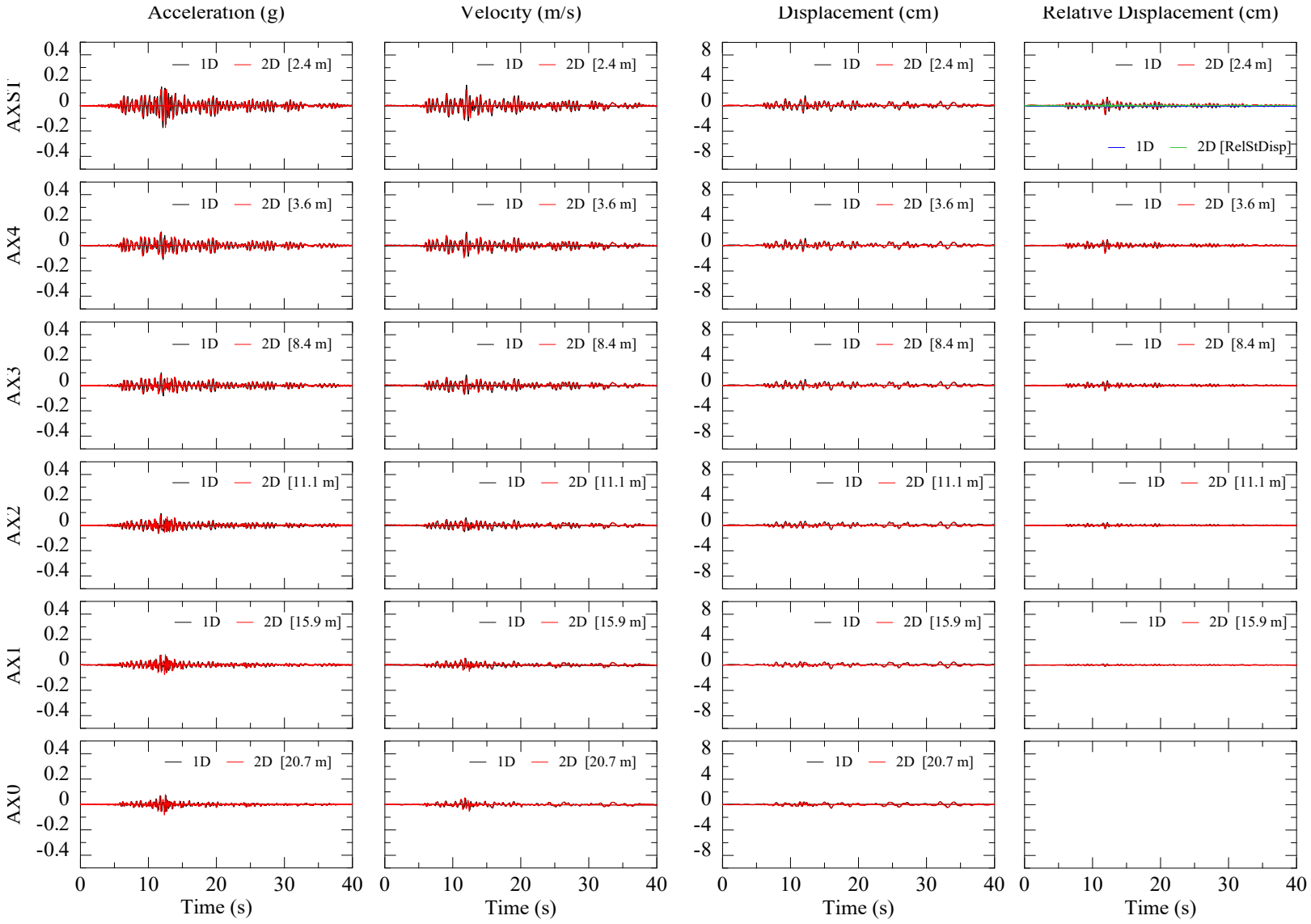

Figure C-390 Recorded input and within model ground motions time histories for acceleration, velocity, displacement and relative displacement for M11-2D [X] and M11-1D [X]

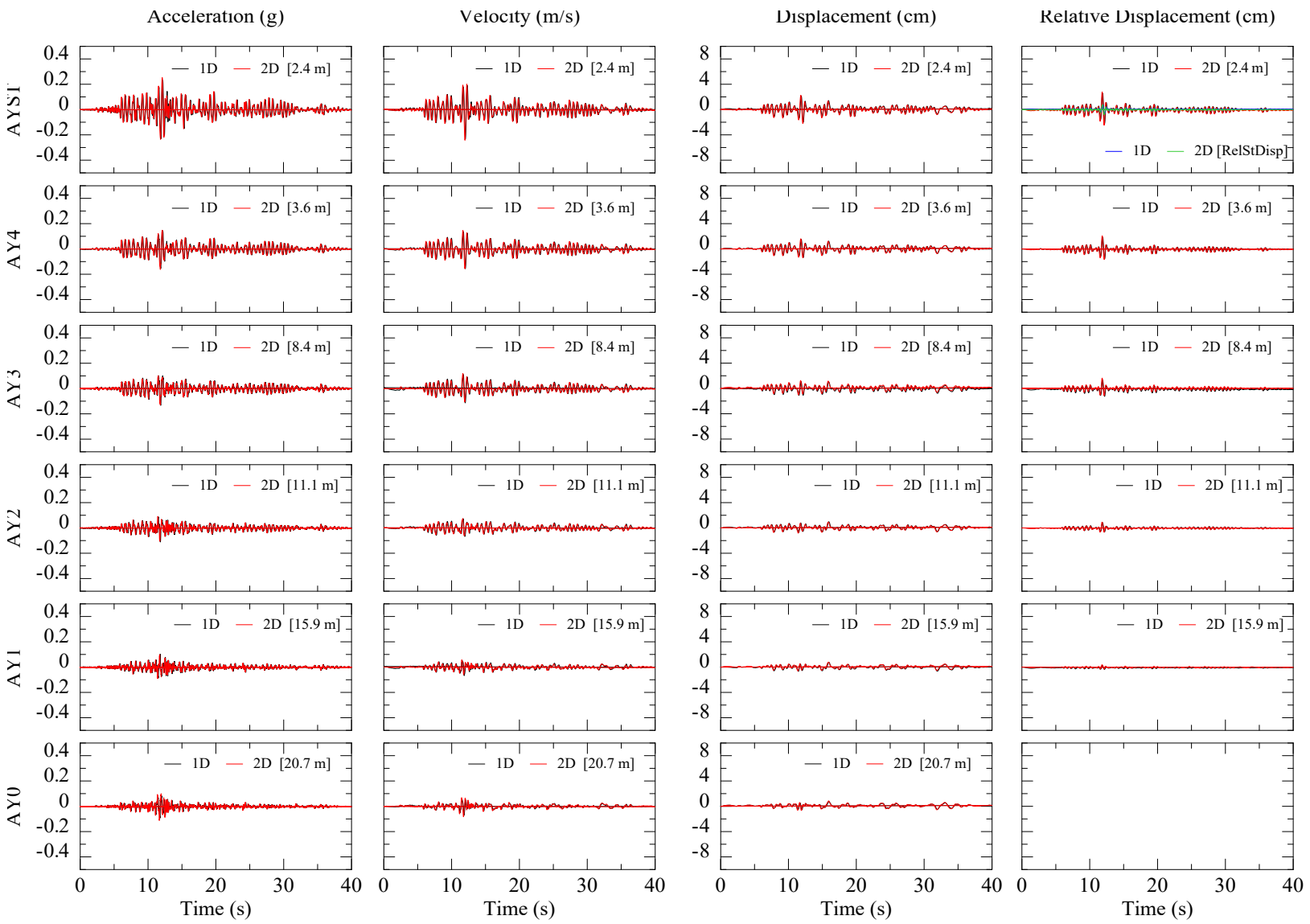

Figure C-391 Recorded input and within model ground motions time histories for acceleration, velocity, displacement and relative displacement for M11-2D [Y] and M11-1D [Y]

1.6.3 Motion 1 (M1)

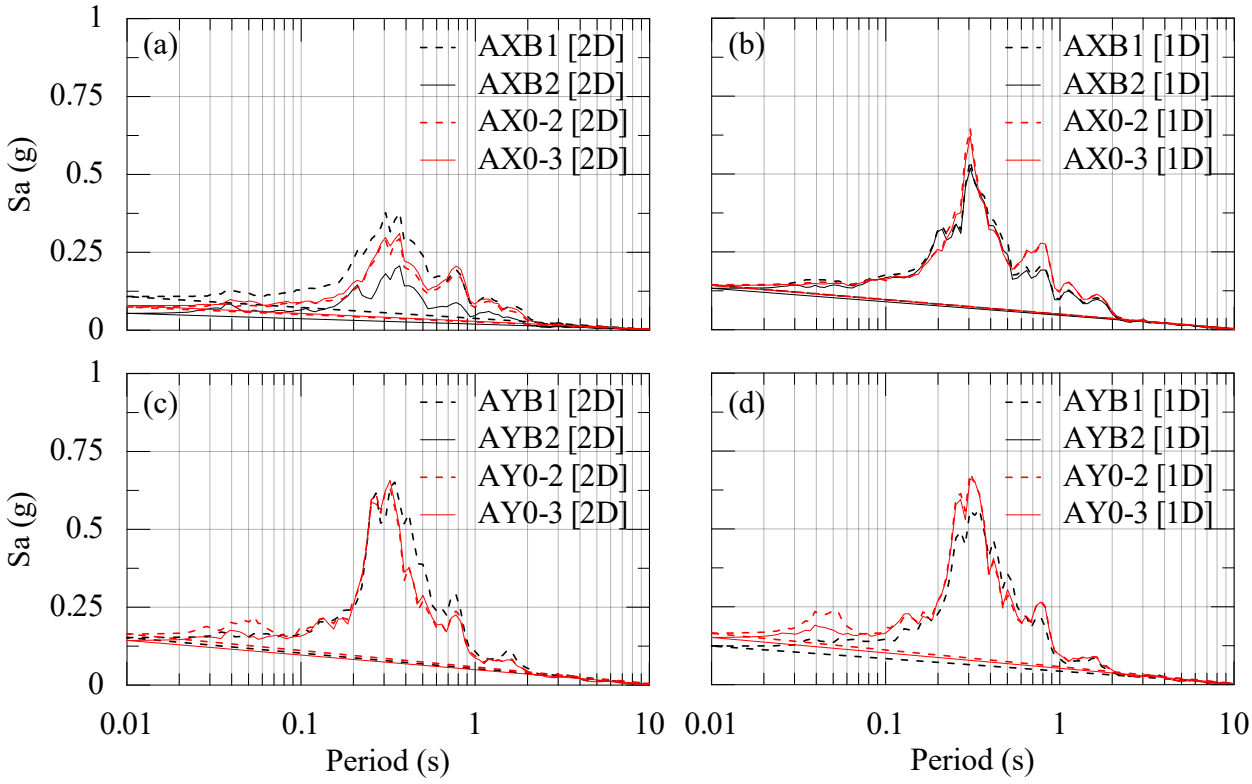

Figure C-392 Comparison of response spectra of 2D laminar container table and within model base input motion for motions (M1-X, Y and 2D).

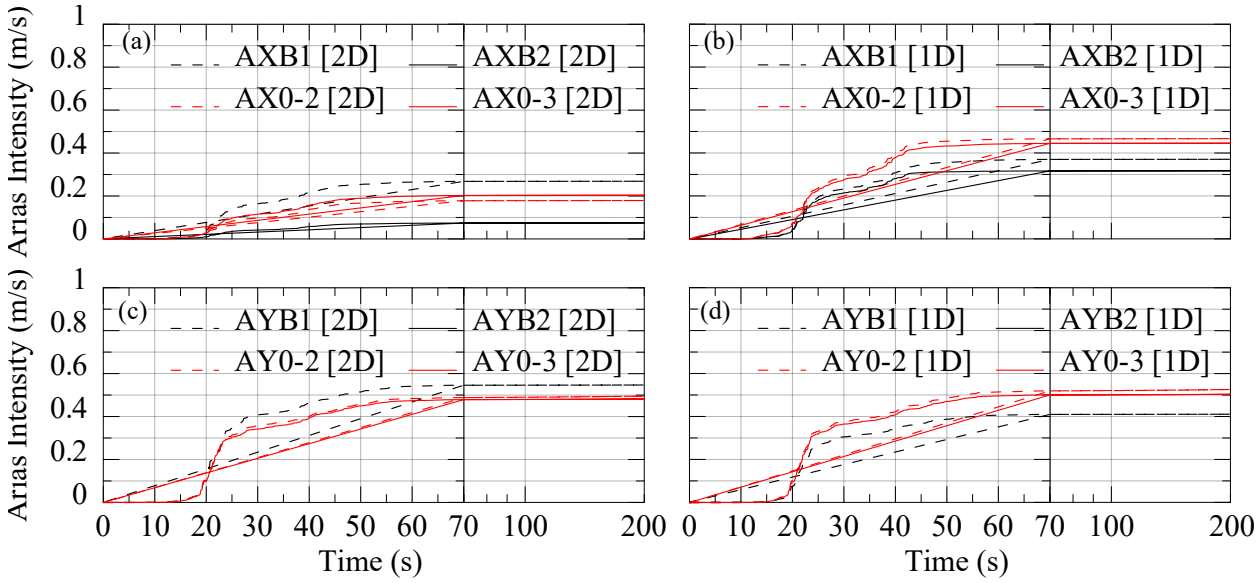

Figure C-393 Comparison of Arias Intensity of 2D laminar container table and within model base input motion for motions (a) M1-2D [X]; (b) M1-2D [Y]; (c) M1-1D [X] and (d) M1-1D [Y]

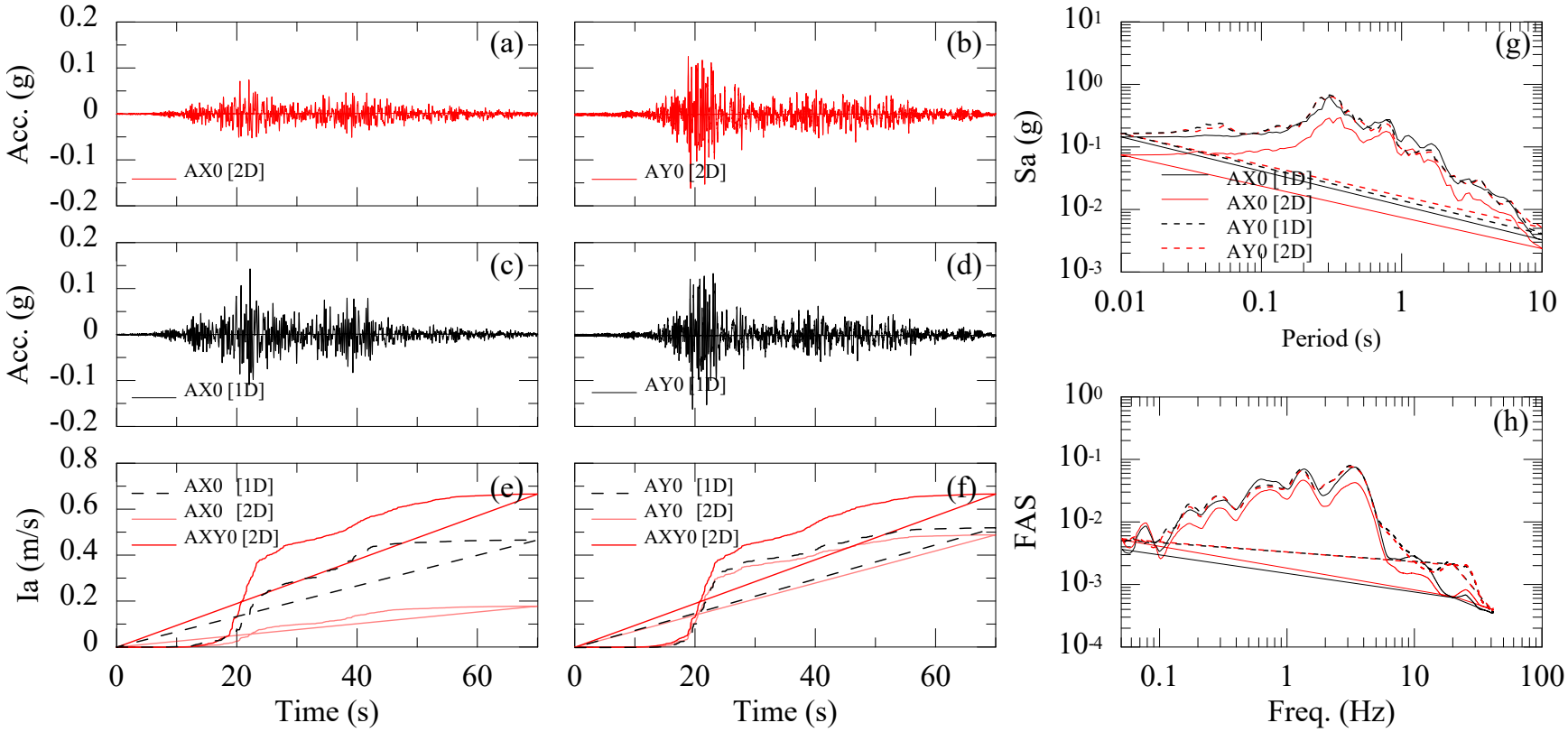

Figure C-394 Recorded input (2D) and 1D (X or Y) ground motions for: (a) M1-2D [X]; (b) M1-2D [Y]; (c) M1-1D [X]; and (d) M1-1D [Y]. Arias Intensity M1 (1D and 2D) for: (e) X direction; and (f) Y direction. Response Spectra (g) M1-2D [X]; M1-2D [Y]; M1-1D [X]; and M1-1D [Y]. Smoothed Fourier amplitude spectra (FAS) (h) M1-2D [X]; M1-2D [Y]; M1-1D [X]; and M1-1D [Y].

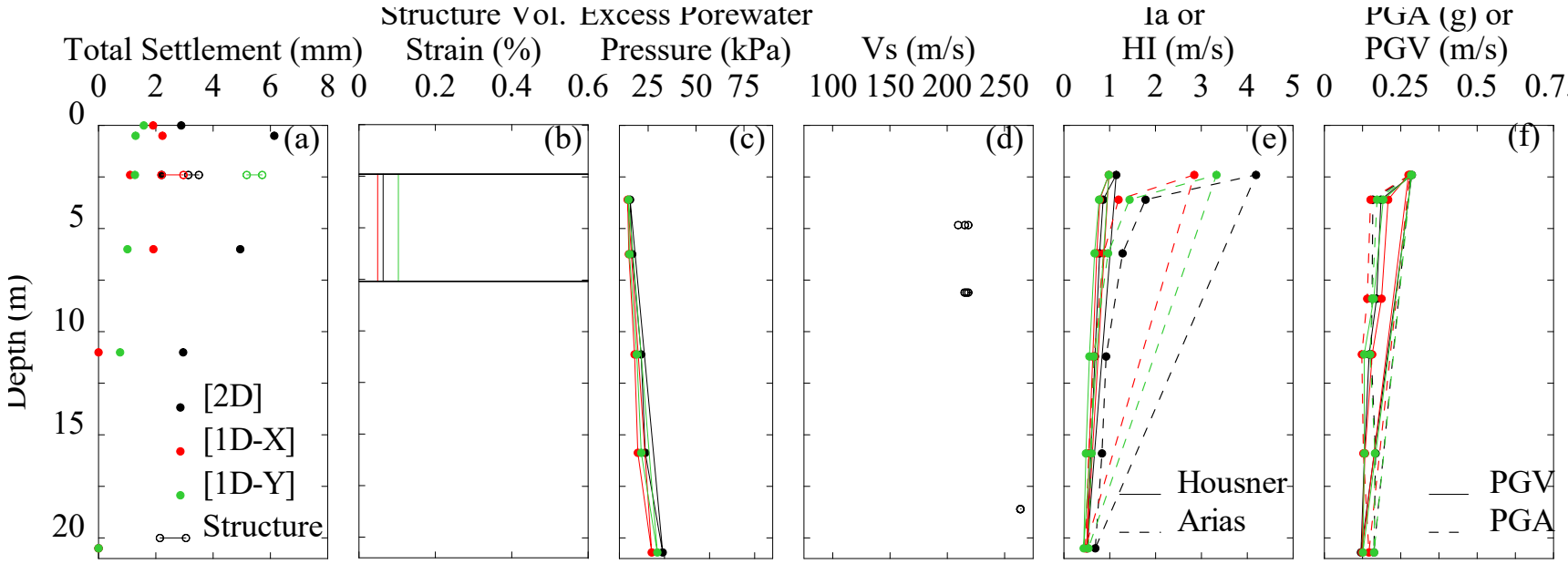

Figure C-395 Recorded or computed profiles for input motion M1-X, Y, and 2D. (a) Total settlement; (b) structure volumetric strain; (c) excess pore water pressure; (d) shear wave velocity; (e) Arias and Housner intensities; and (f) PGA and PGV.

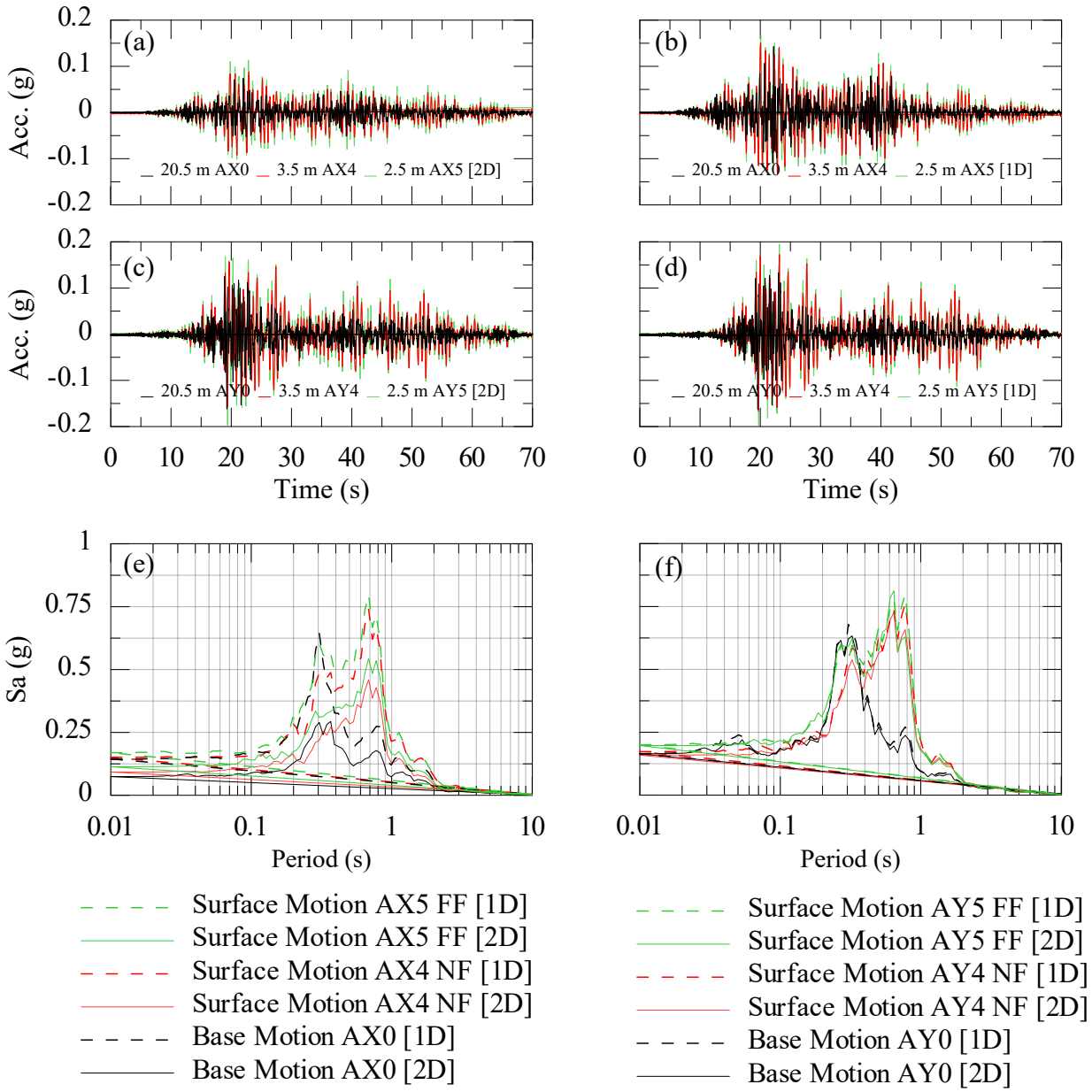

Figure C-396 Recorded input and near surface ground motions: (a) M1-2D [X]; (b) M1-1D [X]; (c) M1-2D [Y]; and (d) M1-1D [Y]. Computed response spectra from Near Field Test [PT3] for motions M1 (1D and 2D) for: (e) X direction; and (f) Y direction.

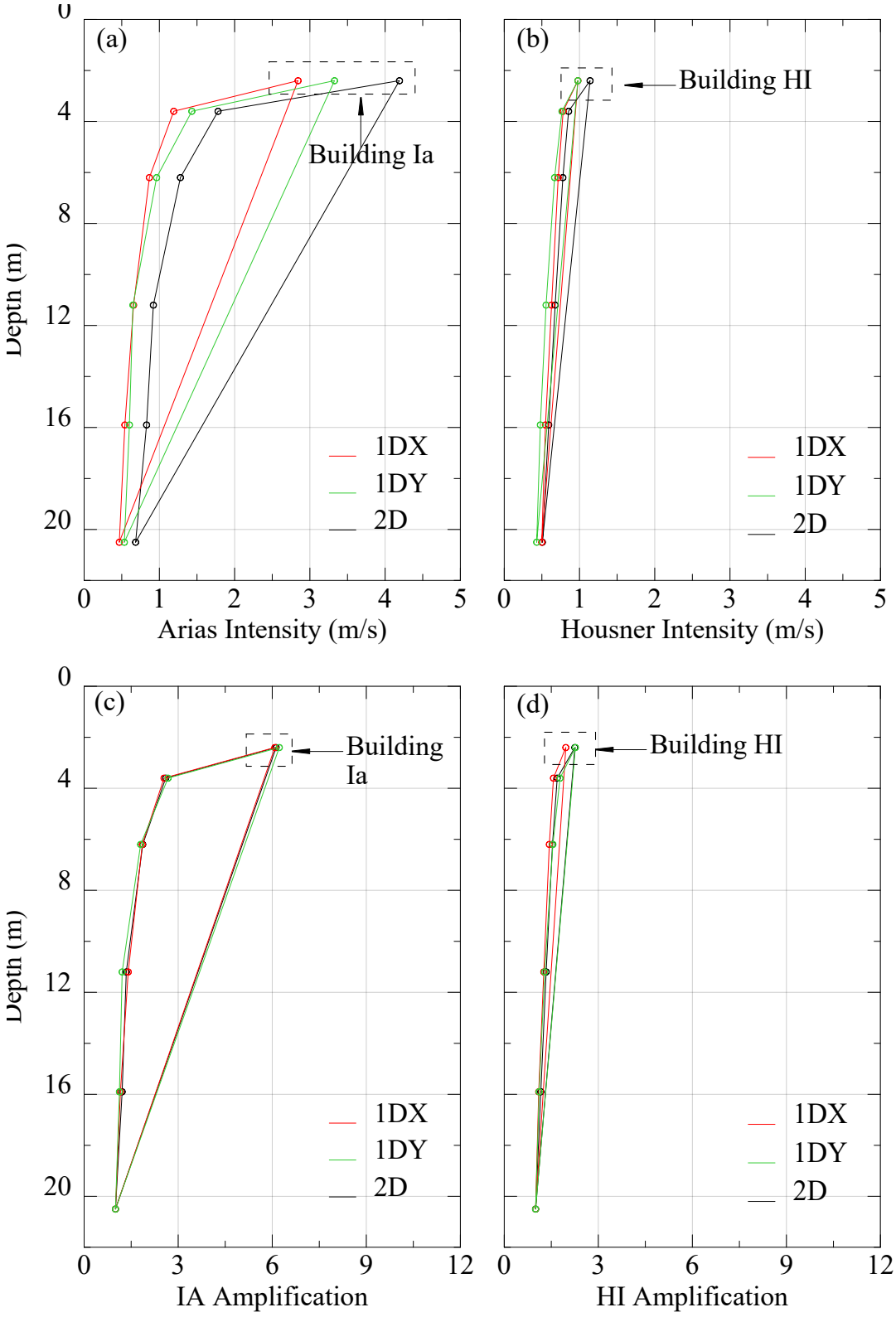

Figure C-397 Variation of total (a) Arias Intensity (M1-X,Y and 2D) ; (b) Housner Intensity (M1-X,Y and 2D) (c) Arias Intensity Amplification Factor (M1-X,Y and 2D); and (d) Housner Intensity Amplification Factor (M1-X,Y and 2D).

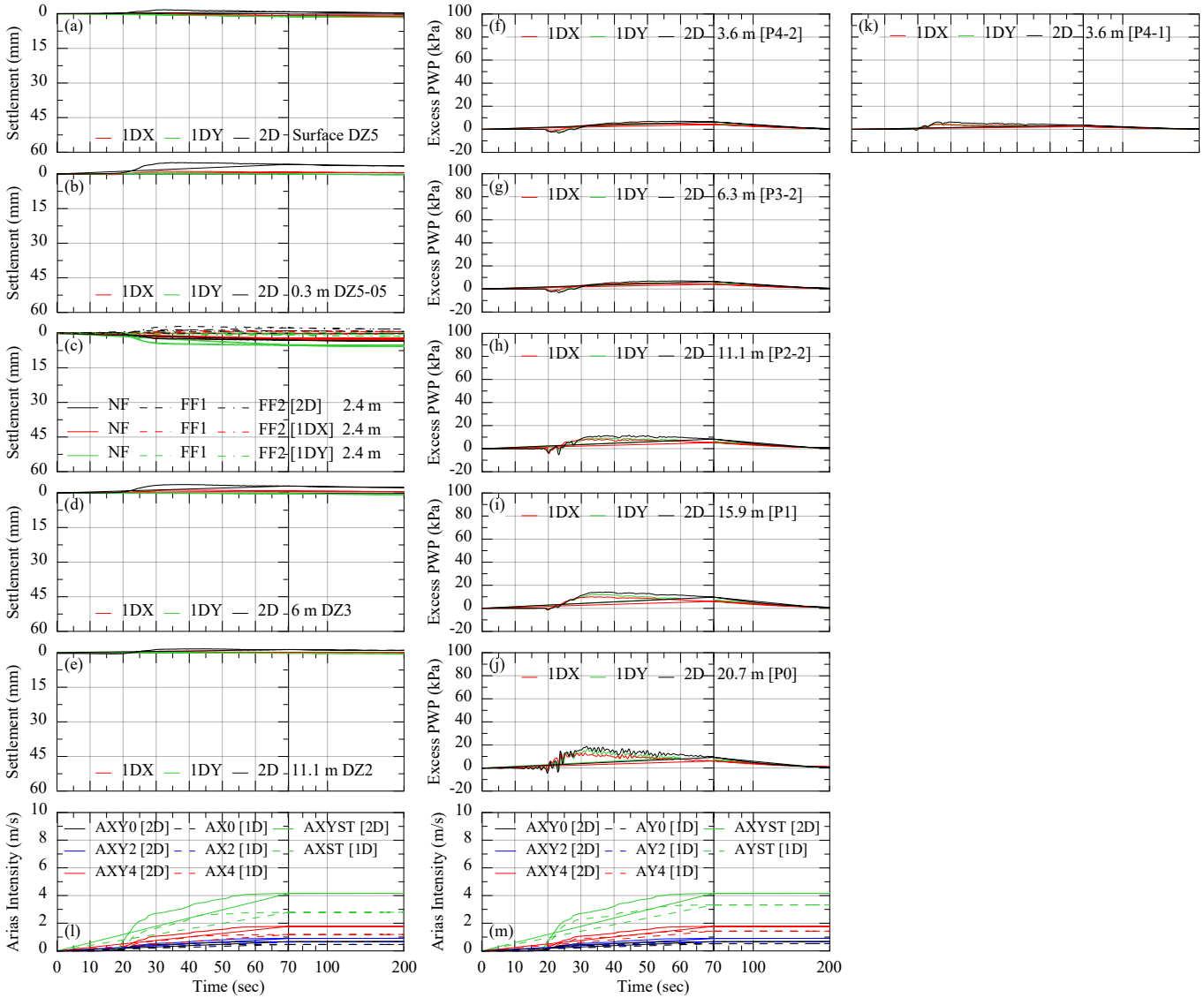

Figure C-398 Variation of total (a) to (e) Settlement with depth (M1-X,Y and 2D) ; (f) to (k) Excess pore water pressure (M1-X,Y and 2D) (l) and (m) Arias Intensity along model (M1-X,Y and 2D).

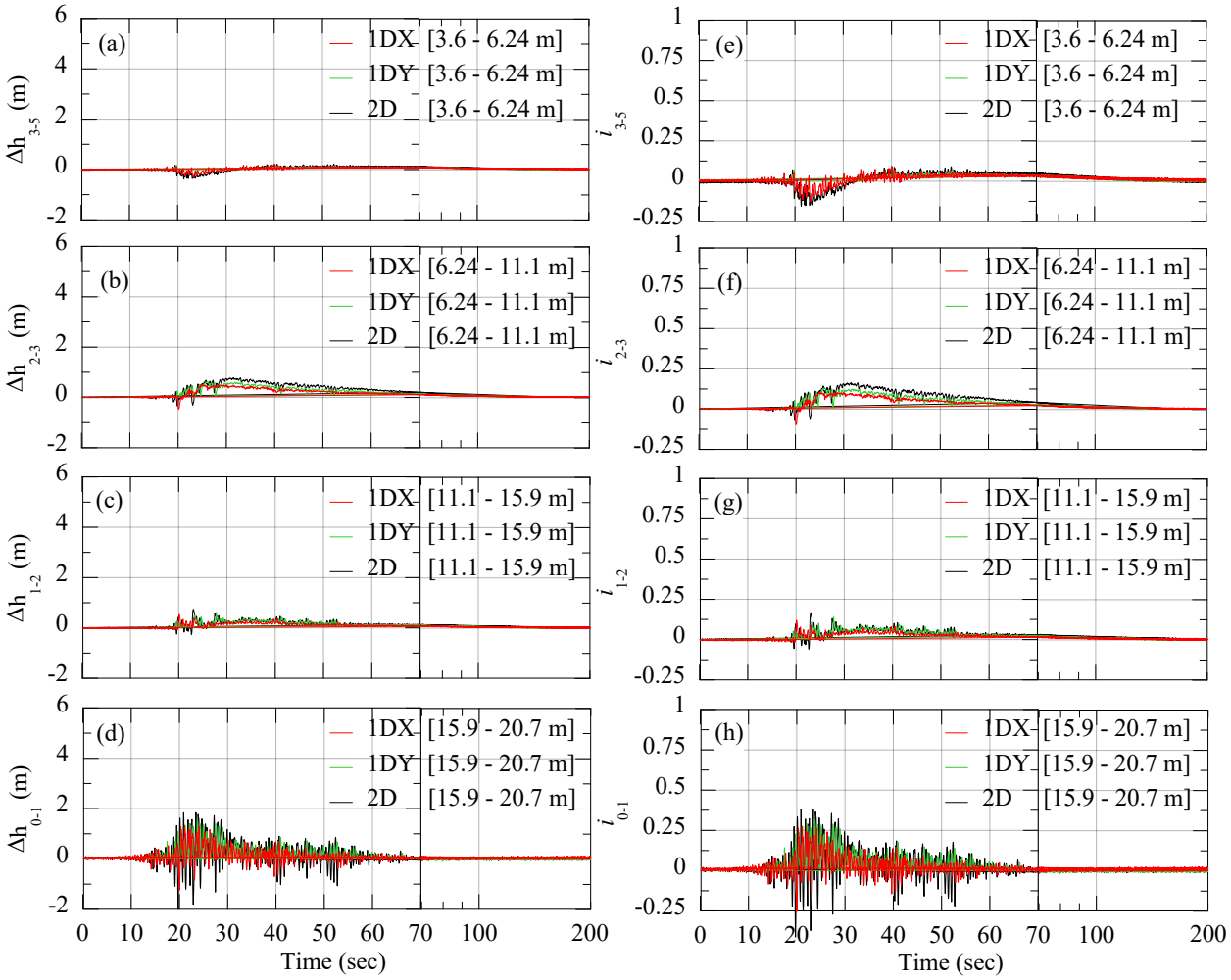

Figure C-399 Variation of total (a) to (d) Total Head Loss with depth (M1-X, Y and 2D); (e) to (h) Shaking induced Hydraulic Gradient (M1-X, Y and 2D)

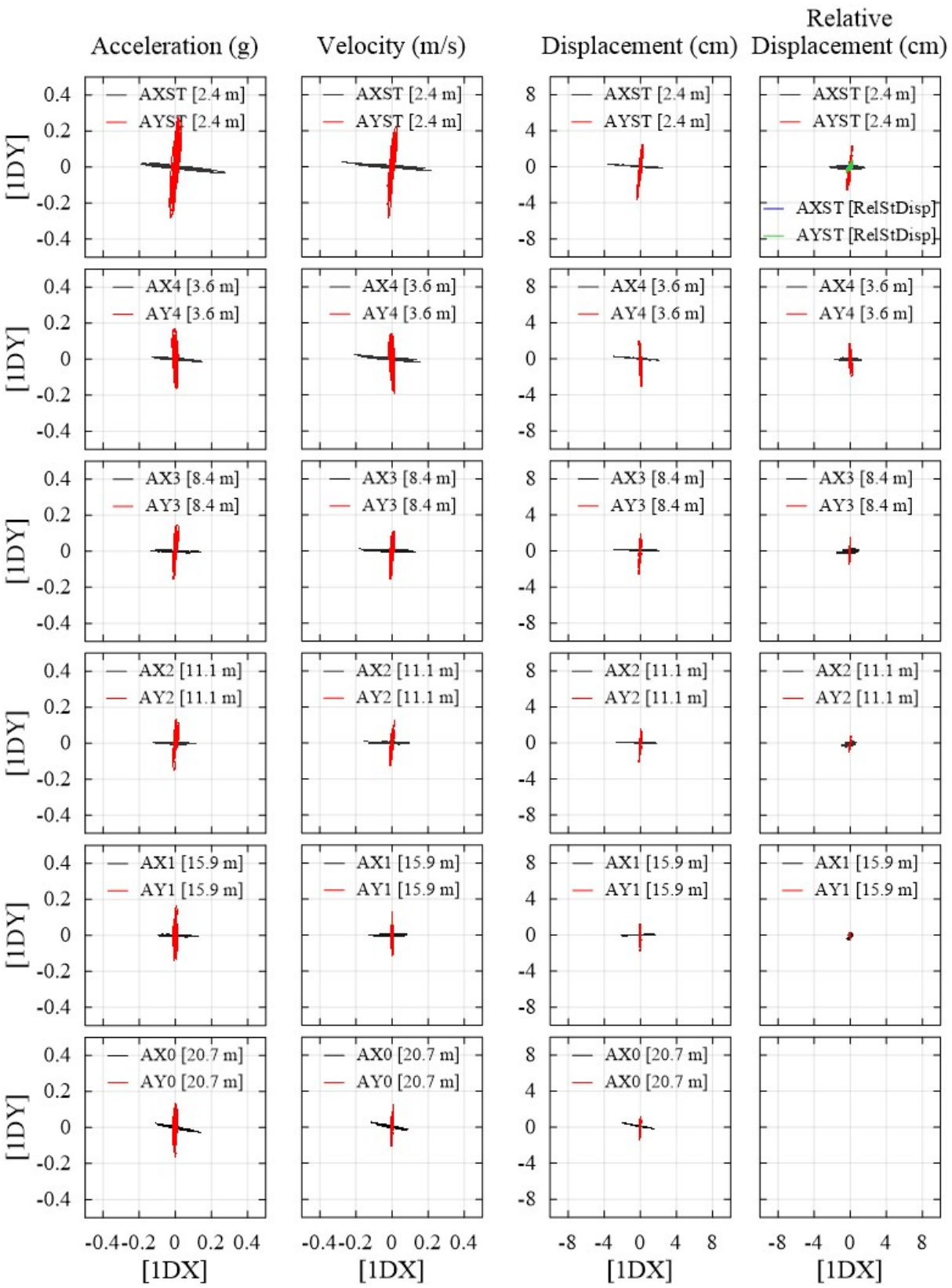

Figure C-400 Recorded input and within model ground motions for acceleration, velocity, displacement and relative displacement for M1-1D [X] and M1-1D [Y]

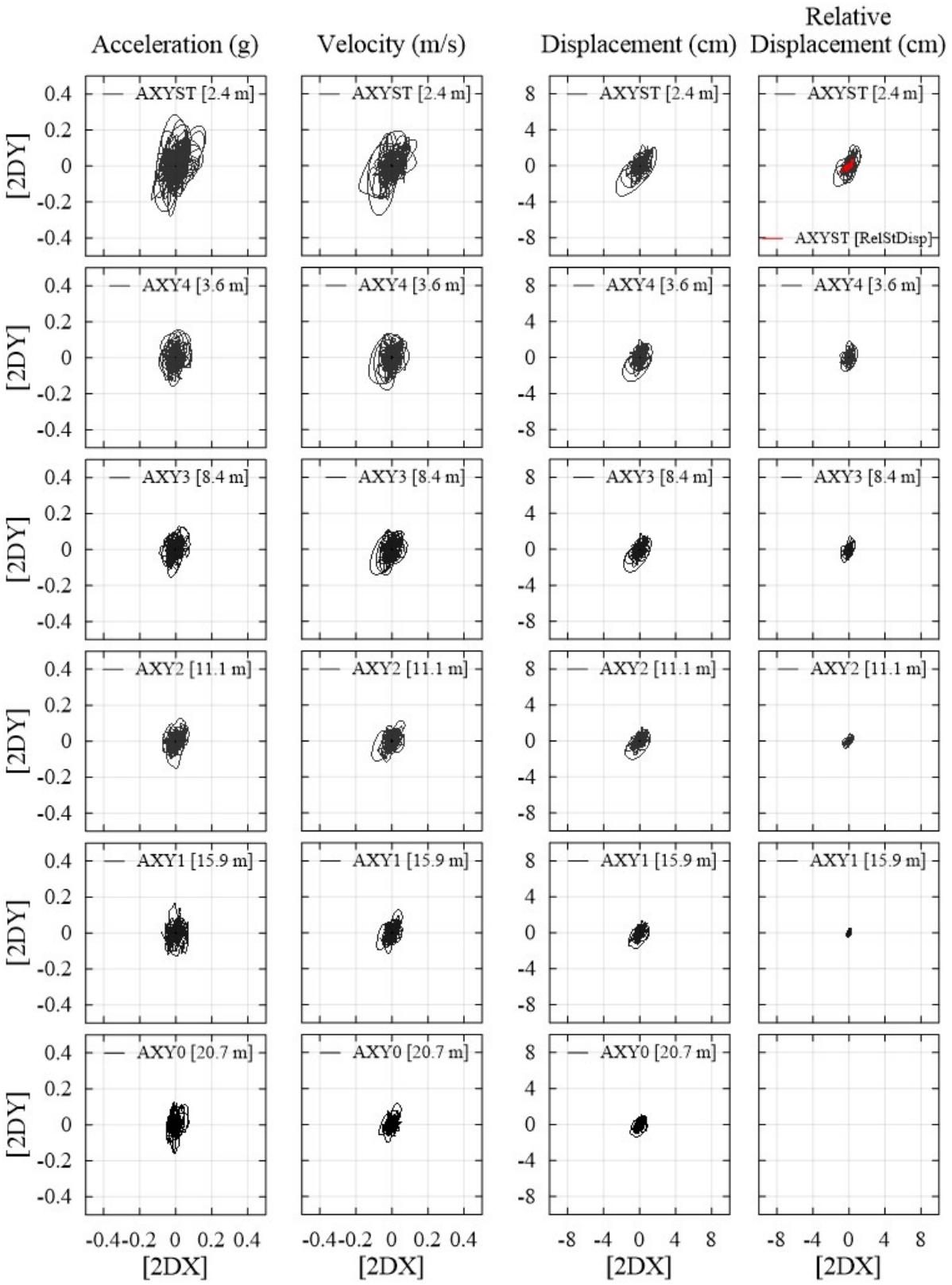

Figure C-401 Recorded input and within model ground motions for acceleration, velocity, displacement and relative displacement for M1-2D

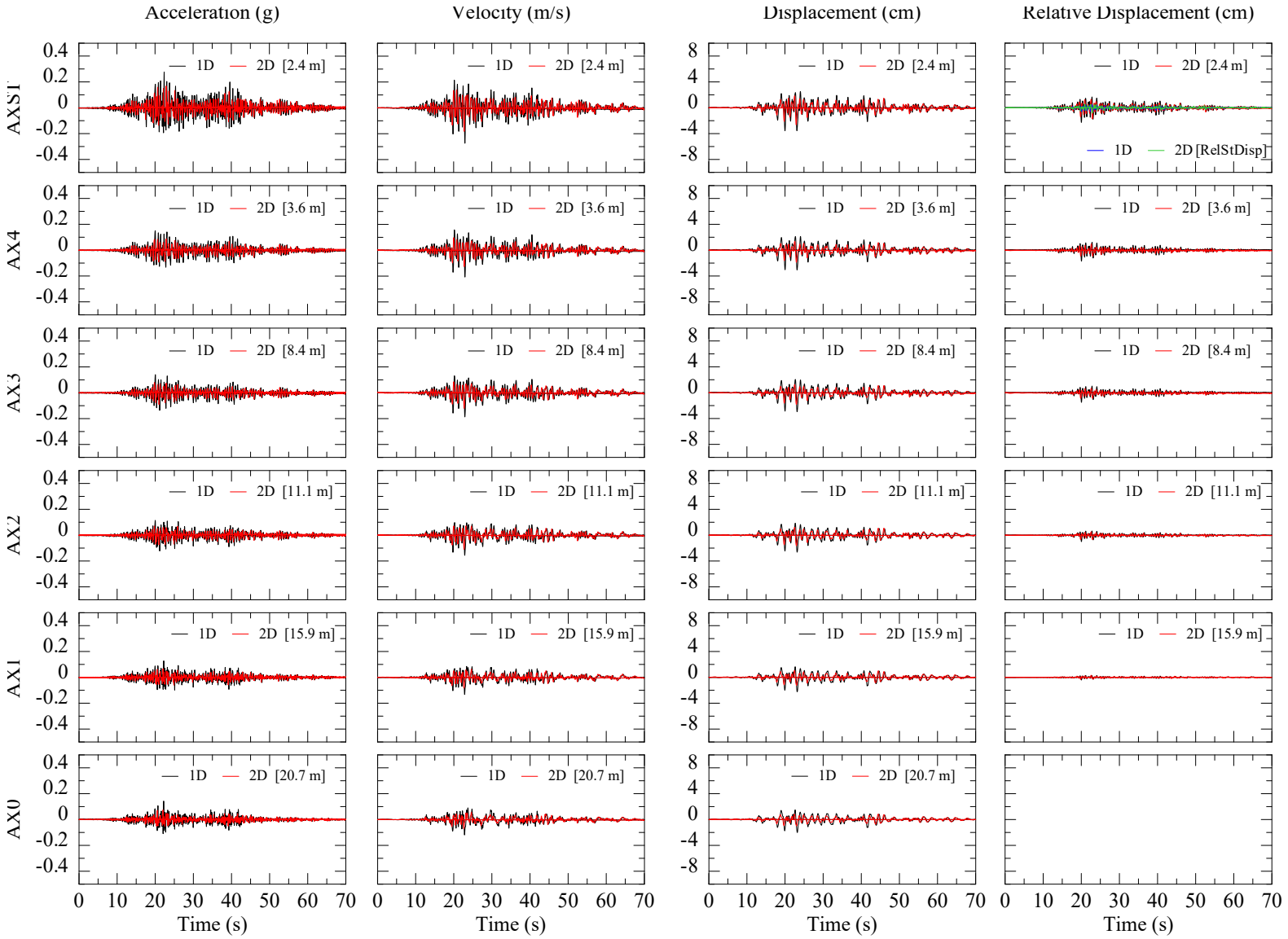

Figure C-402 Recorded input and within model ground motions time histories for acceleration, velocity, displacement and relative displacement for M1-2D [X] and M1-1D [X]

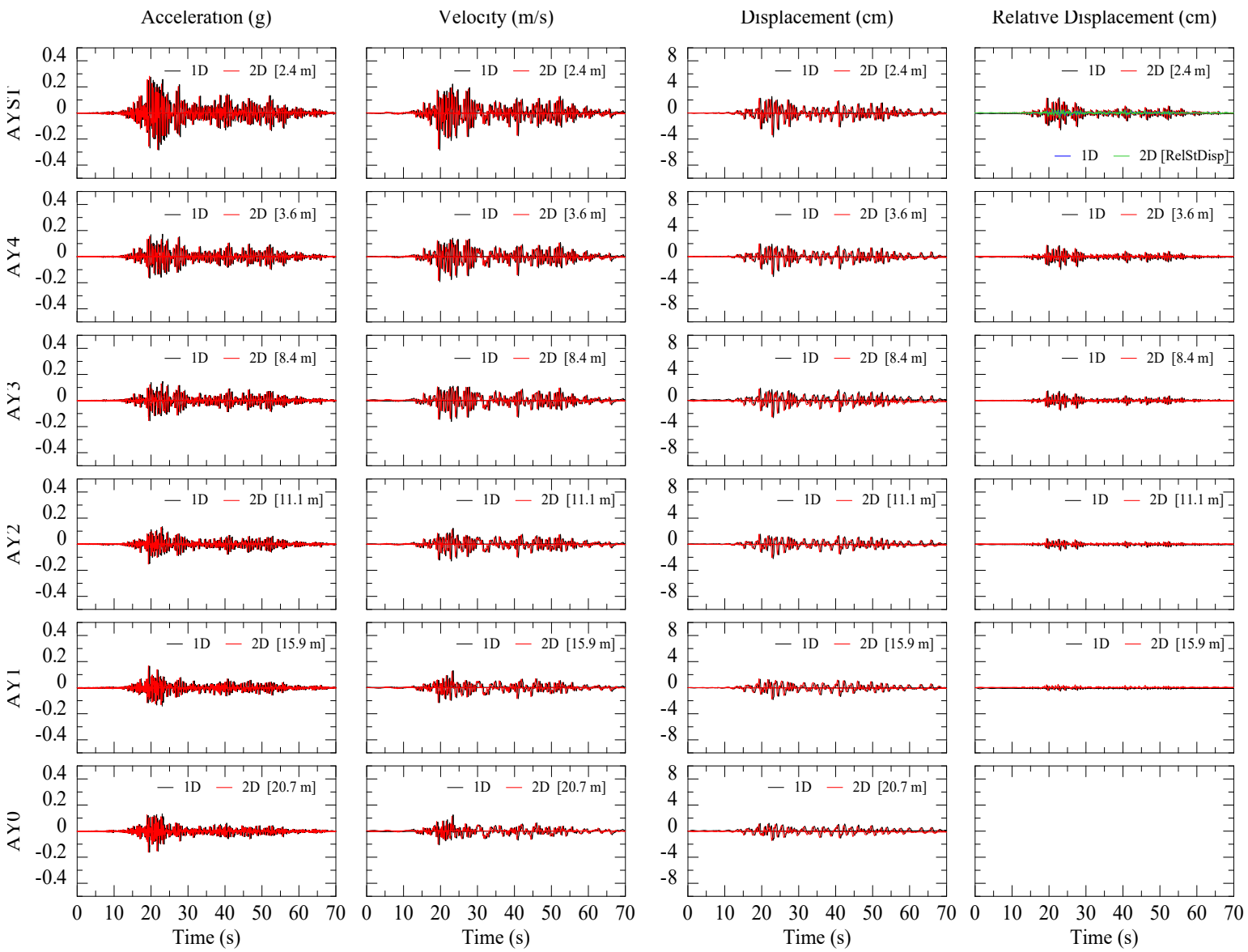

Figure C-403 Recorded input and within model ground motions time histories for acceleration, velocity, displacement and relative displacement for M1-2D [Y] and M1-1D [Y]

1.6.4 Motion 12 (M12)

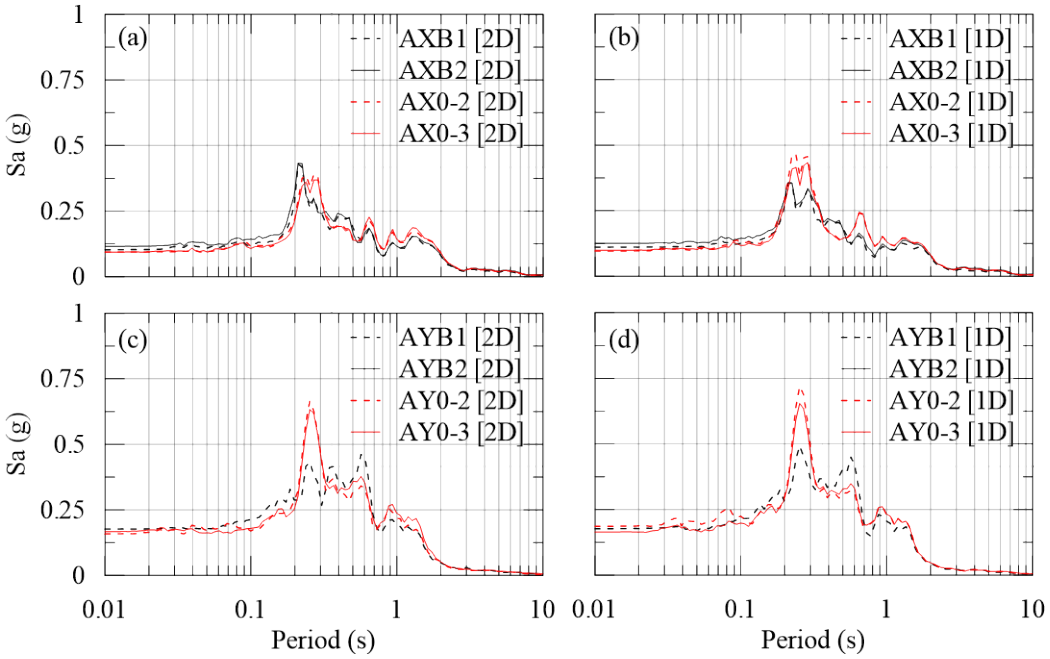

Figure C-404 Comparison of response spectra of 2D laminar container table and within model base input motion for motions (M12-X, Y and 2D).

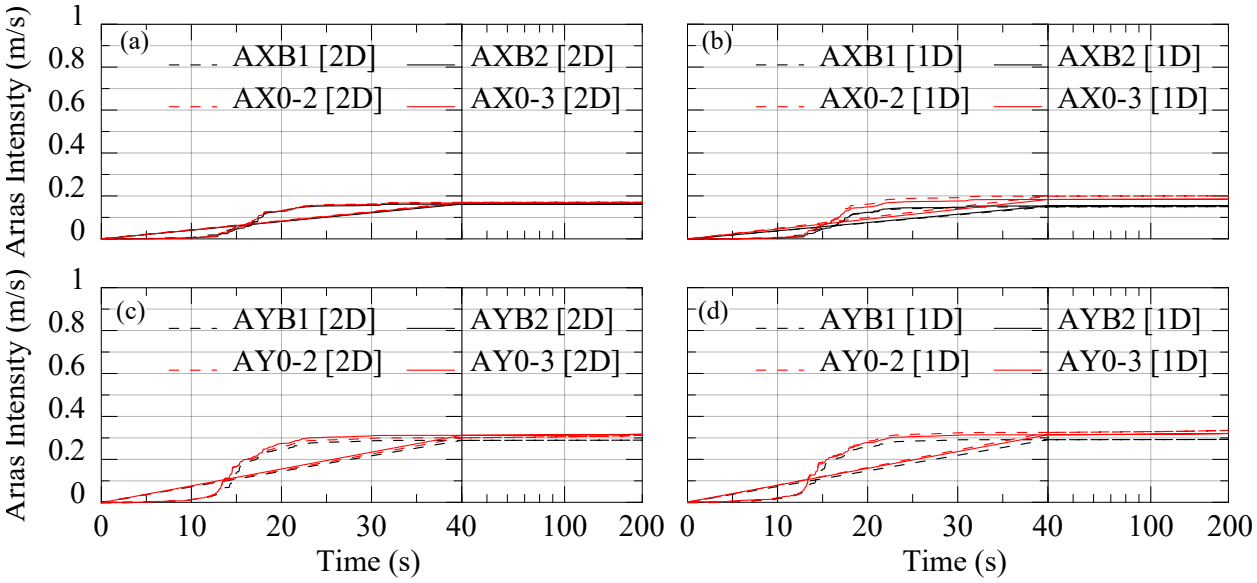

Figure C-405 Comparison of Arias Intensity of 2D laminar container table and within model base input motion for motions (a) M12-2D [X]; (b) M12-2D [Y]; (c) M12-1D [X] and (d) M12-1D [Y]

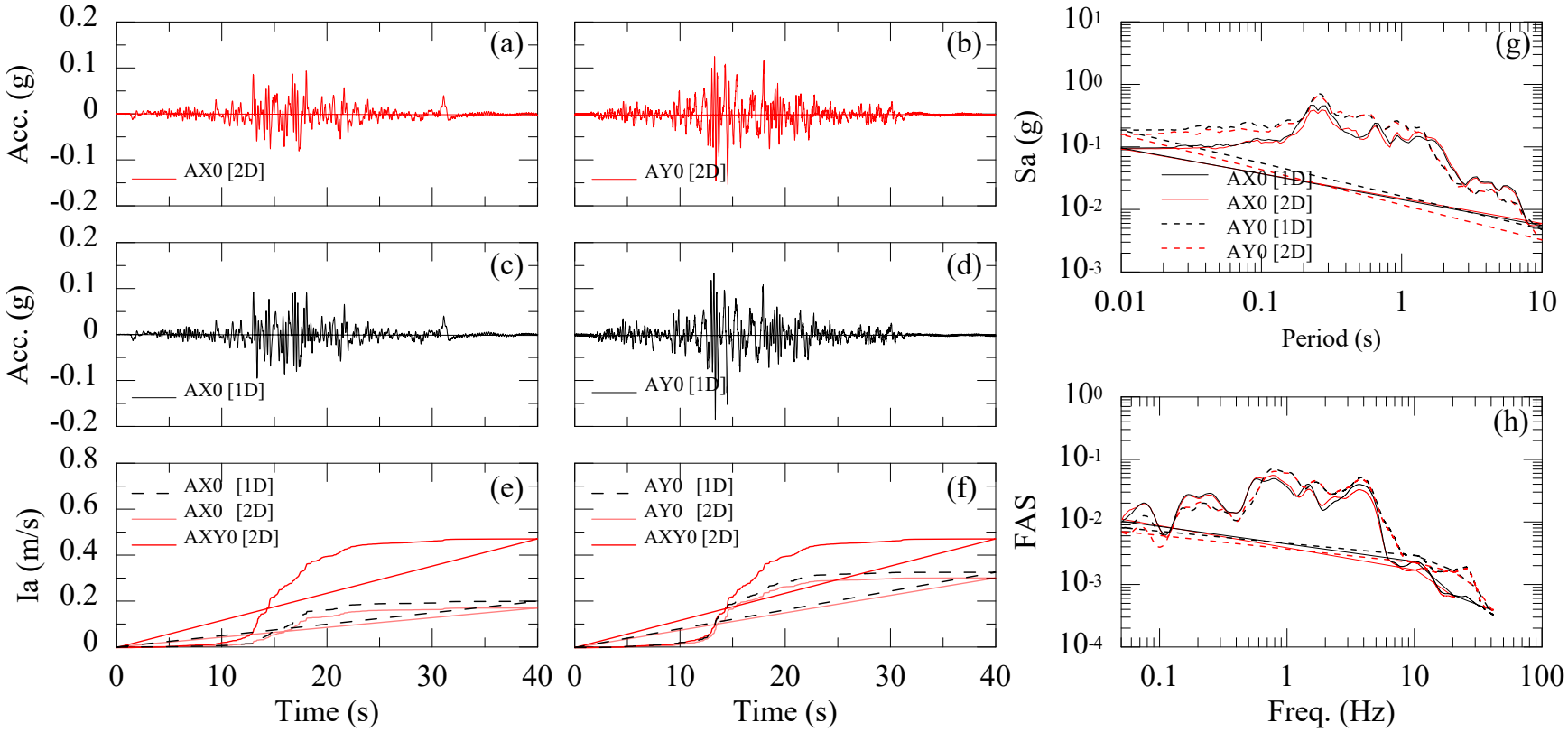

Figure C-406 Recorded input (2D) and 1D (X or Y) ground motions for: (a) M12-2D [X]; (b) M12-2D [Y]; (c) M12-1D [X]; and (d) M12-1D [Y]. Arias Intensity M12 (1D and 2D) for: (e) X direction; and (f) Y direction. Response Spectra (g) M12-2D [X]; M12-2D [Y]; M12-1D [X]; and M12-1D [Y]. Smoothed Fourier amplitude spectra (FAS) (h) M12-2D [X]; M12-2D [Y]; M12-1D [X]; and M12-1D [Y].

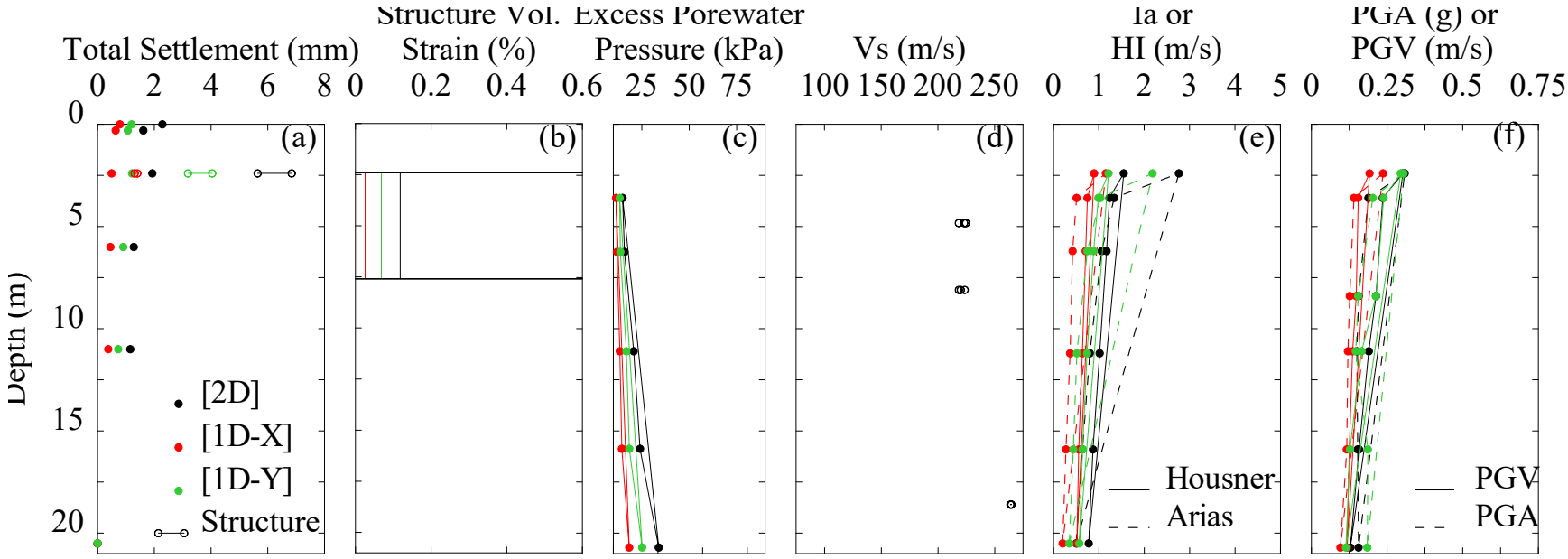

Figure C-407 Recorded or computed profiles for input motion M12-X, Y, and 2D. (a) Total settlement; (b) structure volumetric strain; (c) excess pore water pressure; (d) shear wave velocity; (e) Arias and Housner intensities; and (f) PGA and PGV.

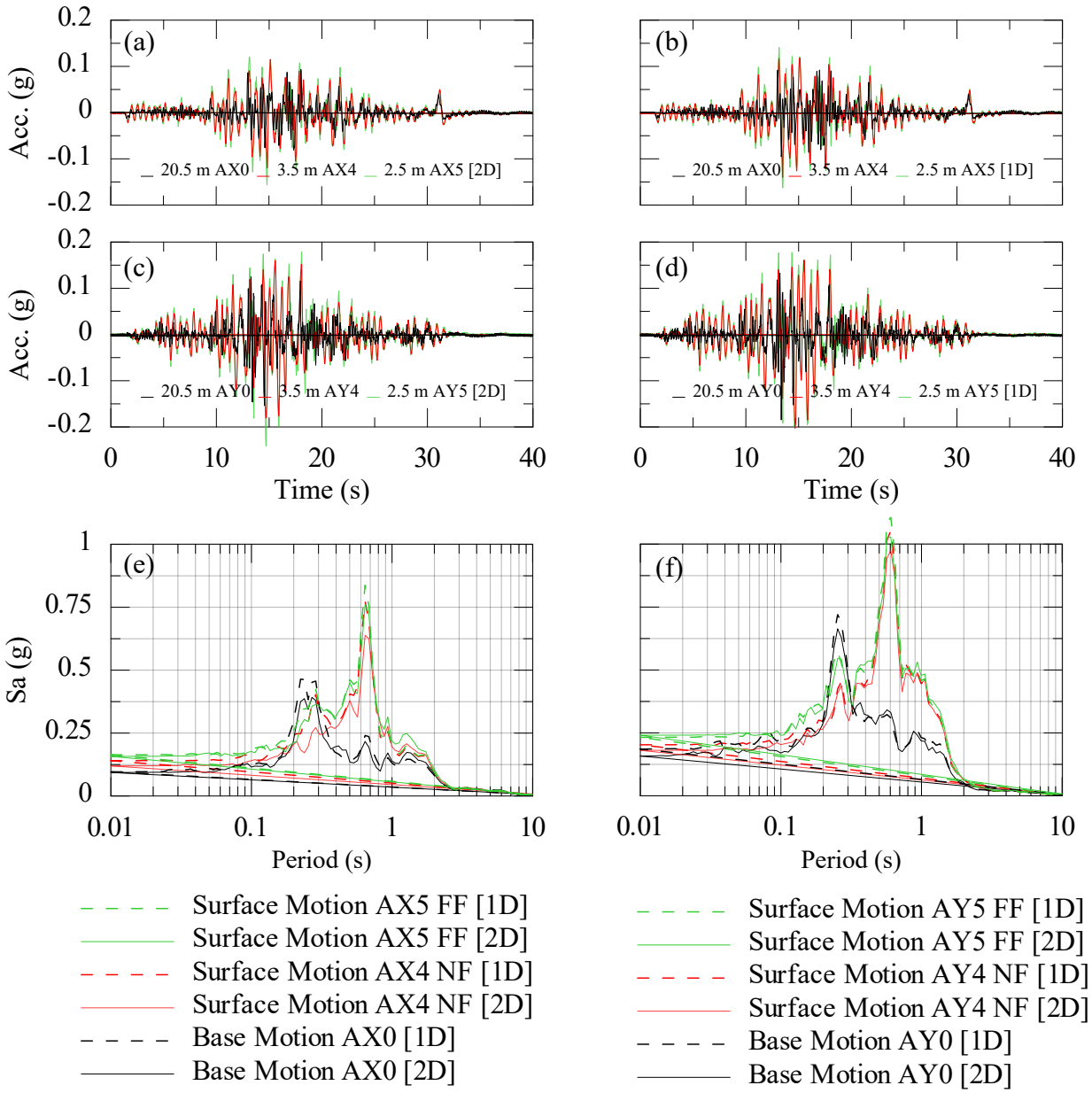

Figure C-408 Recorded input and near surface ground motions: (a) M12-2D [X]; (b) M12-1D [X]; (c) M12-2D [Y]; and (d) M12-1D [Y]. Computed response spectra from Near Field Test [PT3] for motions M12 (1D and 2D) for: (e) X direction; and (f) Y direction.

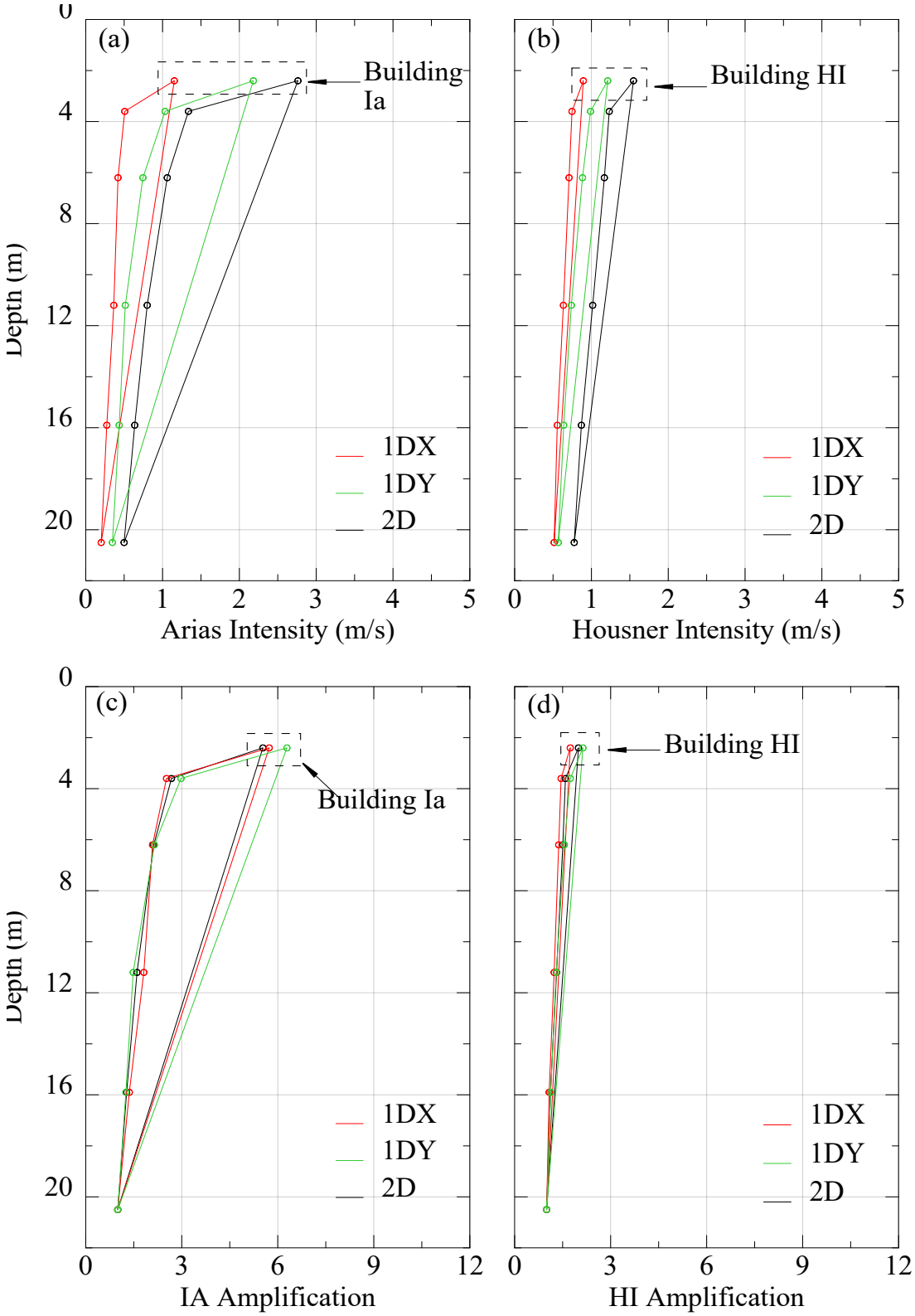

Figure C-409 Variation of total (a) Arias Intensity (M12-X,Y and 2D) ; (b) Housner Intensity (M12-X,Y and 2D) (c) Arias Intensity Amplification Factor (M12-X,Y and 2D); and (d) Housner Intensity Amplification Factor (M12-X,Y and 2D).

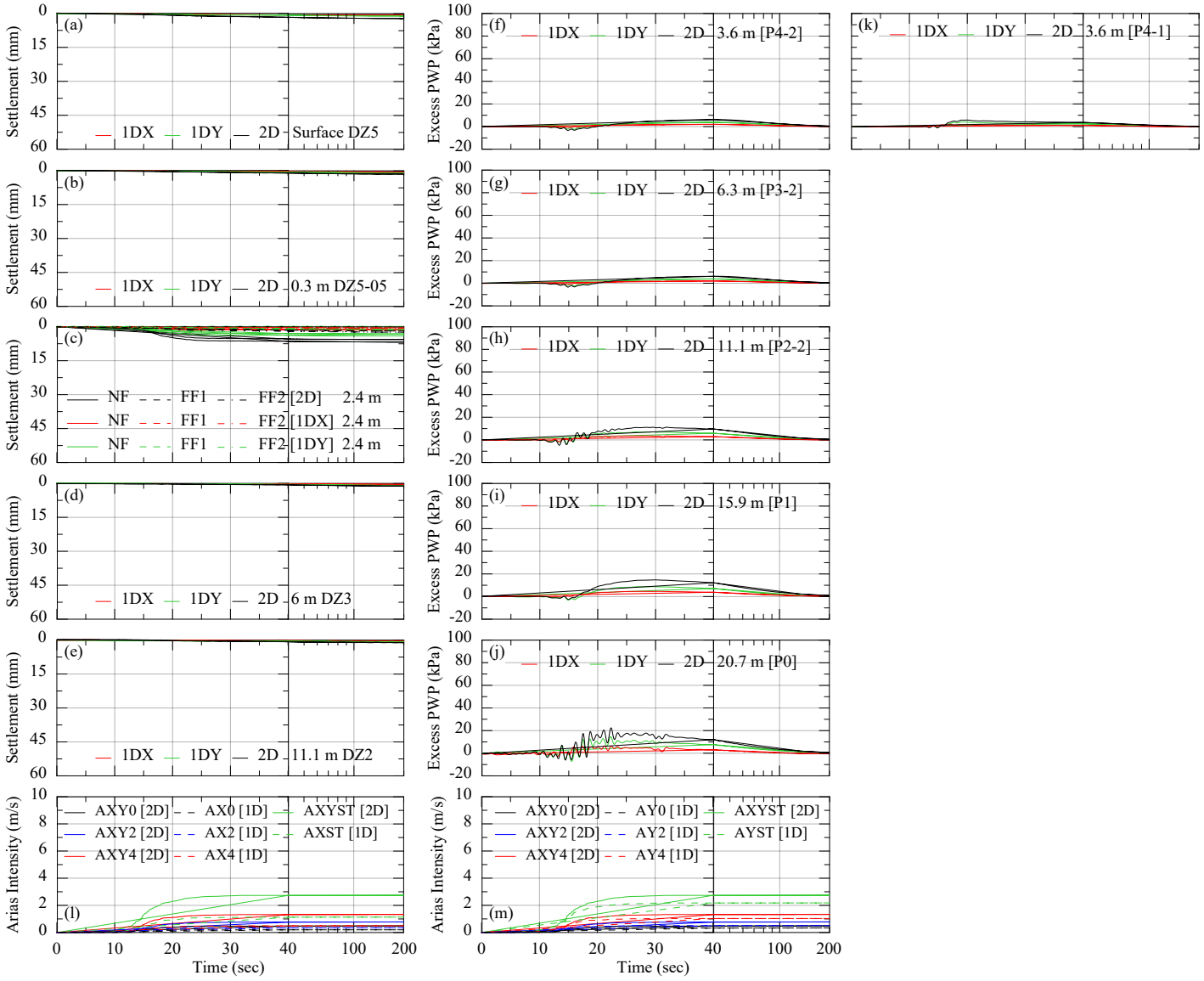

Figure C-410 Variation of total (a) to (e) Settlement with depth (M12-X,Y and 2D) ; (f) to (k) Excess pore water pressure (M12-X,Y and 2D) (l) and (m) Arias Intensity along model (M12-X,Y and 2D).

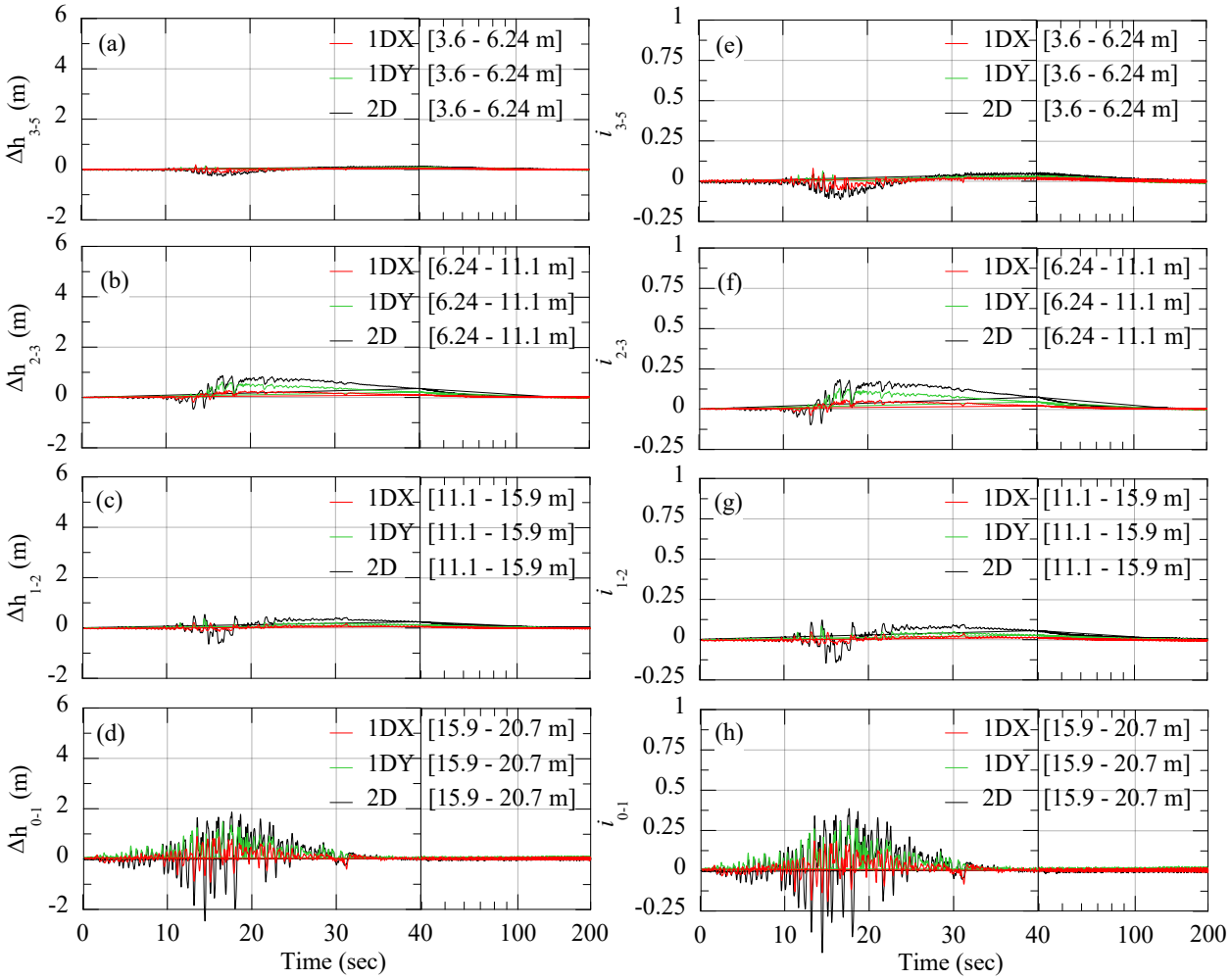

Figure C-411 Variation of total (a) to (d) Total Head Loss with depth (M12-X, Y and 2D); (e) to (h) Shaking induced Hydraulic Gradient (M12-X, Y and 2D)

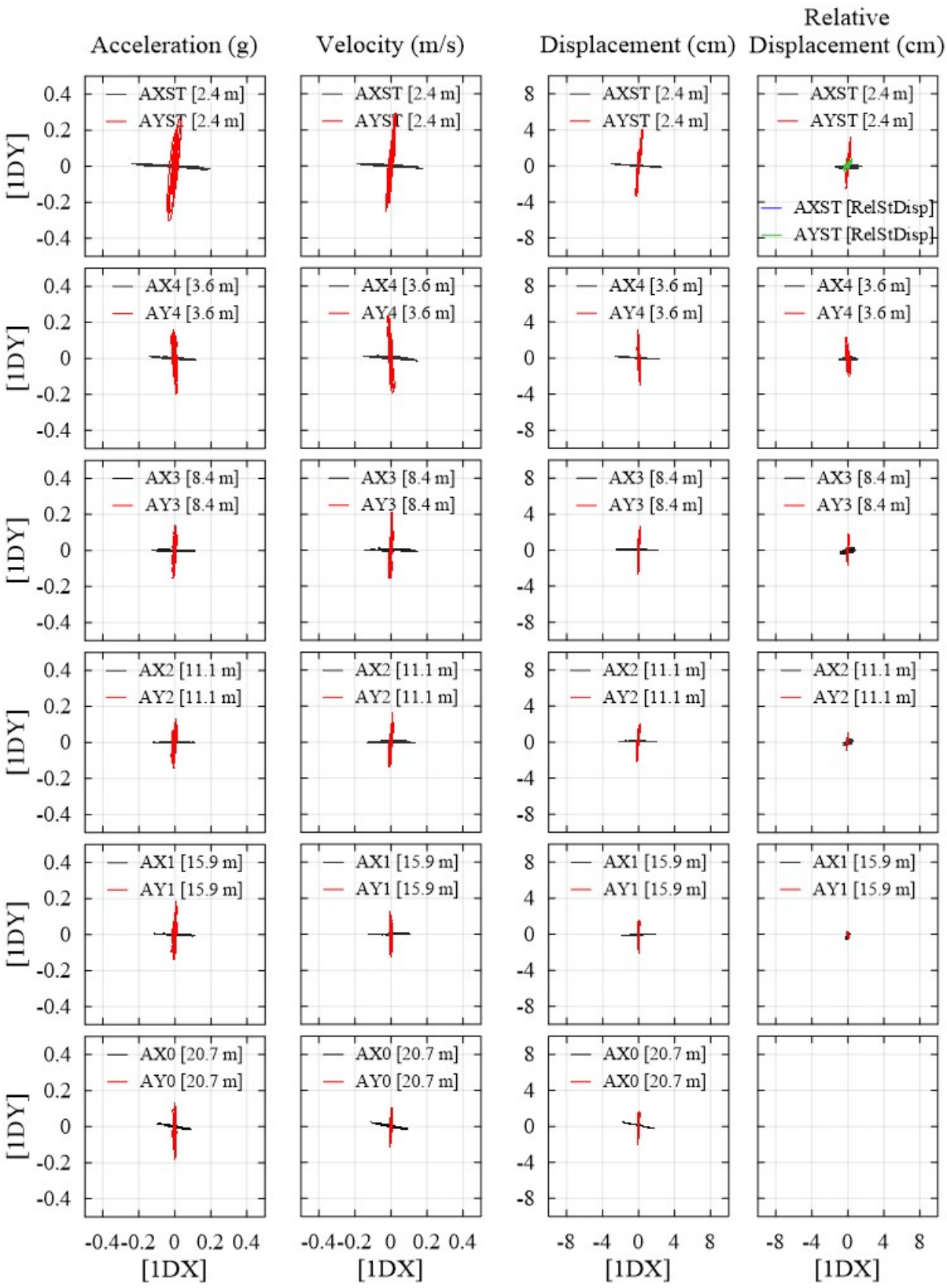

Figure C-412 Recorded input and within model ground motions for acceleration, velocity, displacement and relative displacement for M12-1D [X] and M12-1D [Y]

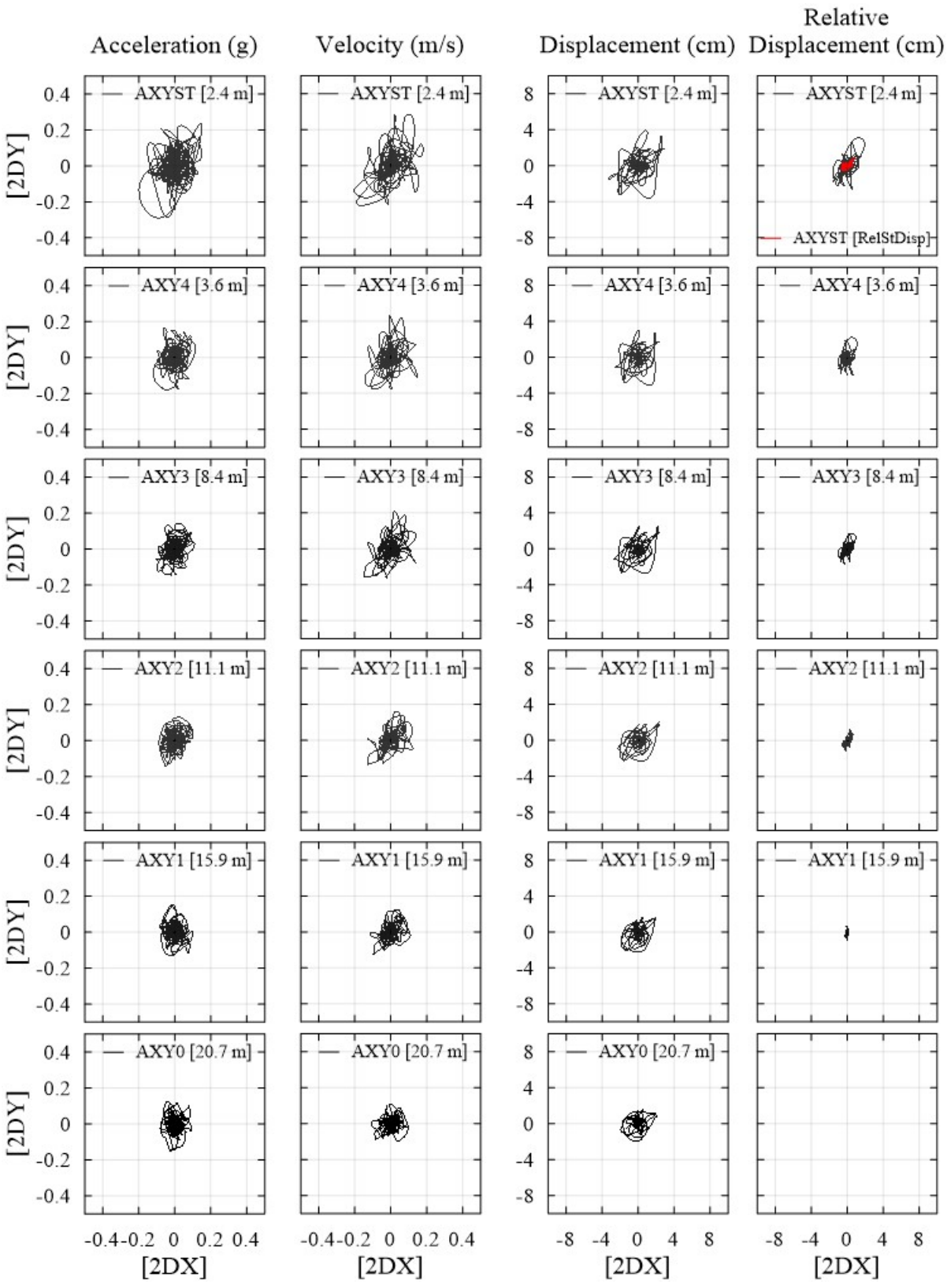

Figure C-413 Recorded input and within model ground motions for acceleration, velocity, displacement and relative displacement for M12-2D

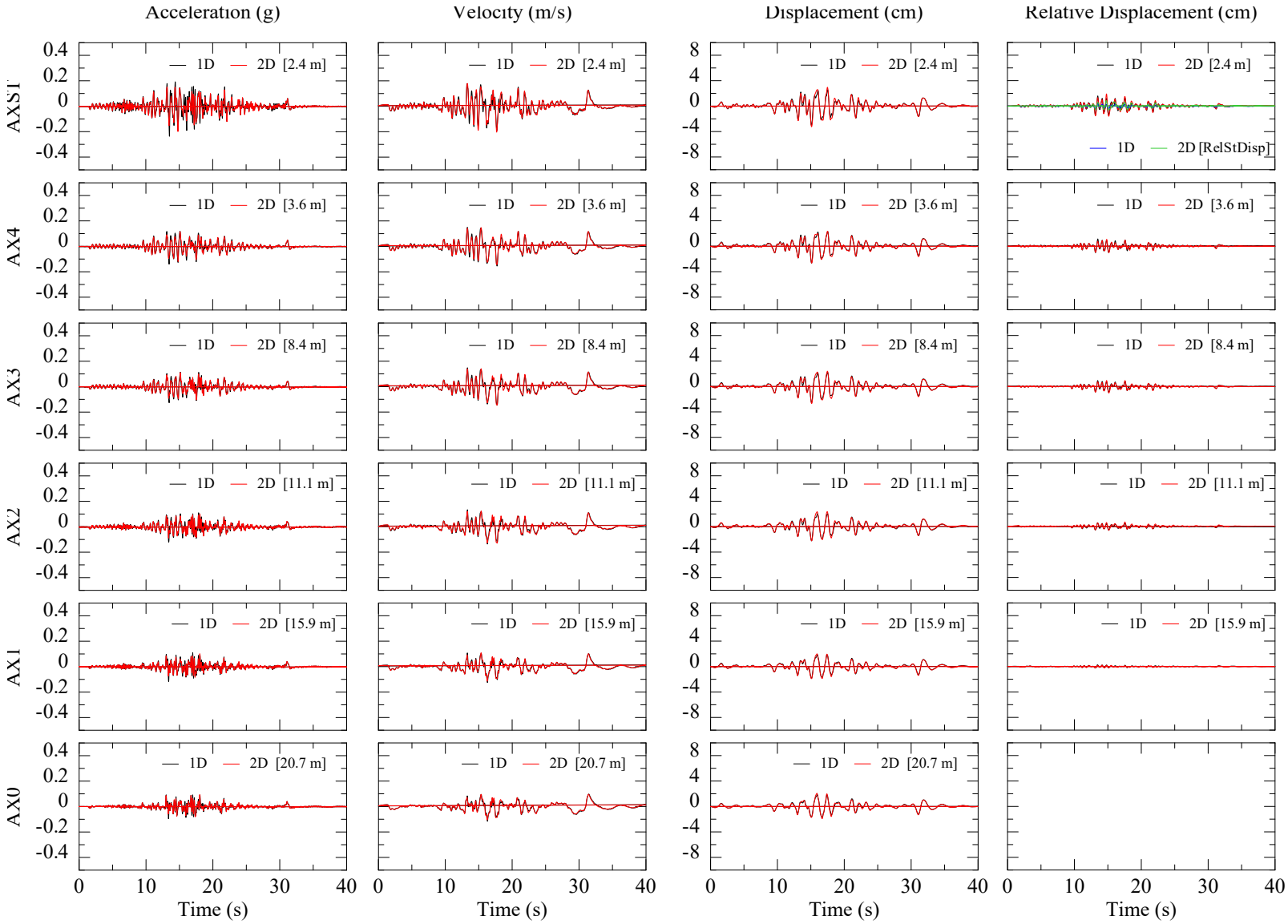

Figure C-414 Recorded input and within model ground motions time histories for acceleration, velocity, displacement and relative displacement for M12-2D [X] and M12-1D [X]

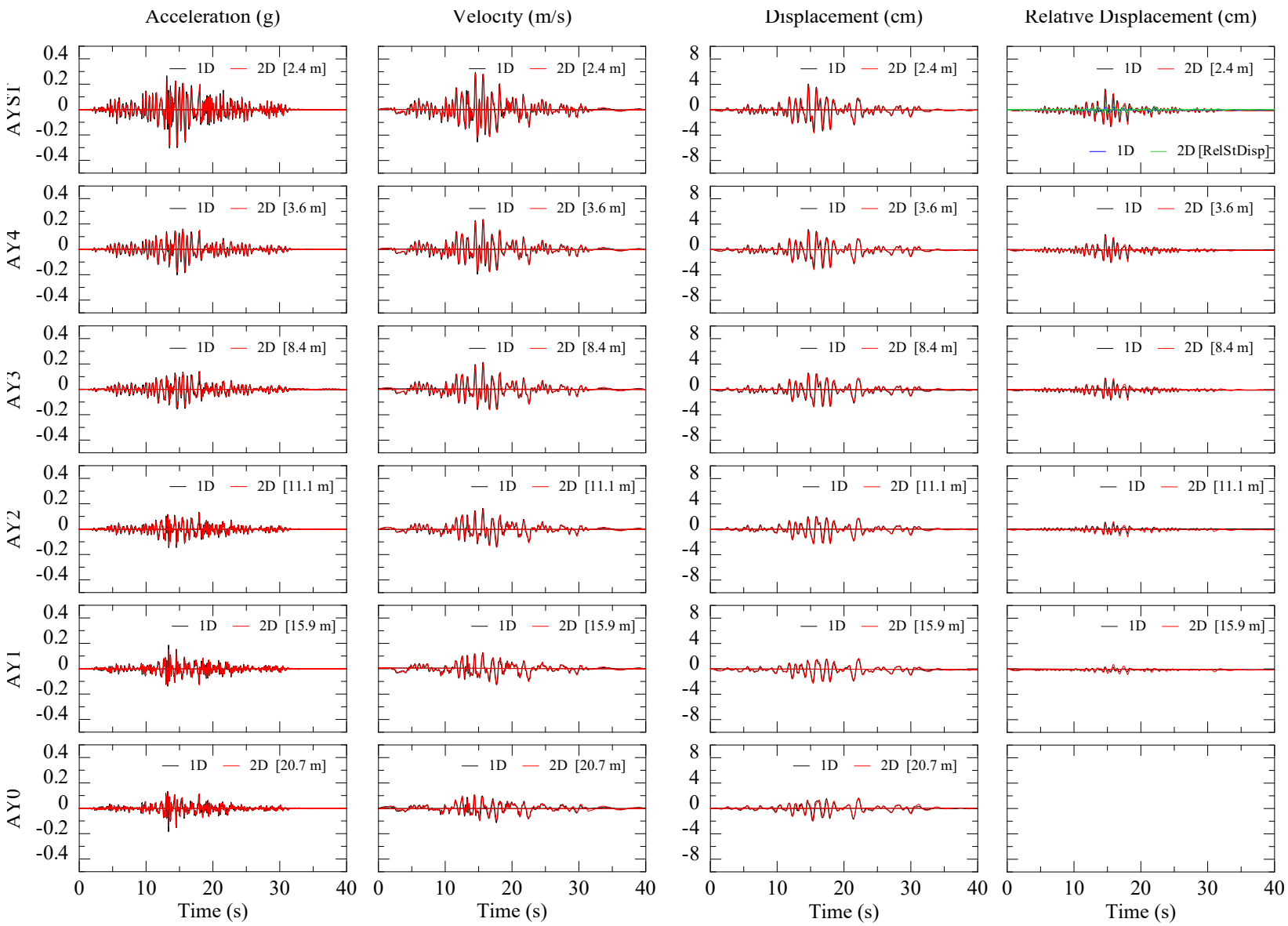

Figure C-415 Recorded input and within model ground motions time histories for acceleration, velocity, displacement and relative displacement for M12-2D [Y] and M12-1D [Y]

1.6.5 Motion 13 (M13)

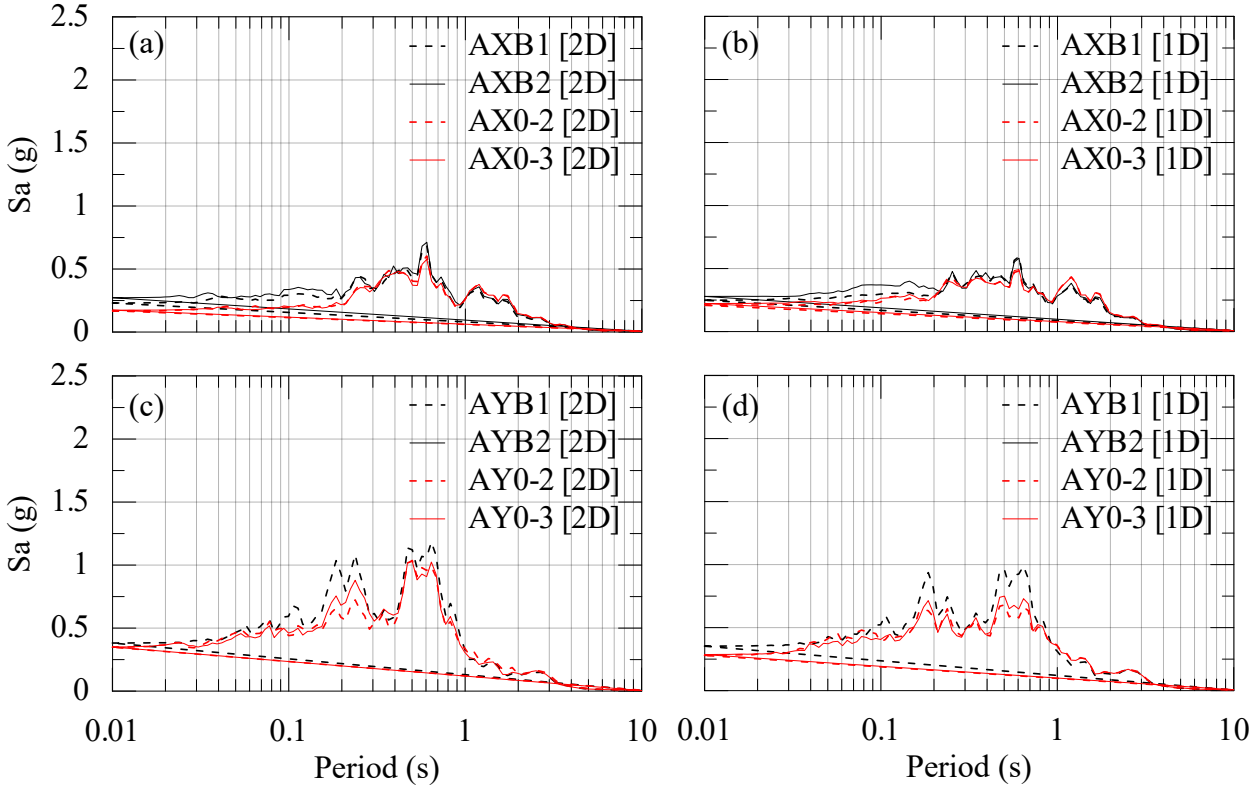

Figure C-416 Comparison of response spectra of 2D laminar container table and within model base input motion for motions (M13-X, Y and 2D).

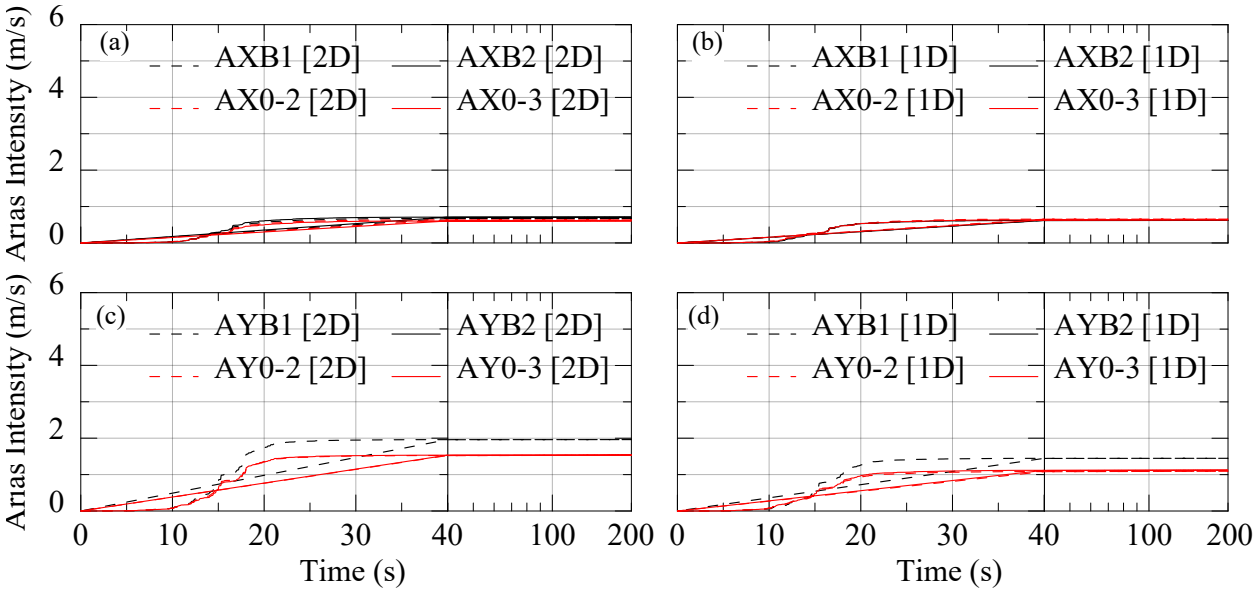

Figure C-417 Comparison of Arias Intensity of 2D laminar container table and within model base input motion for motions (a) M13-2D [X]; (b) M13-2D [Y]; (c) M13-1D [X] and (d) M13-1D [Y]

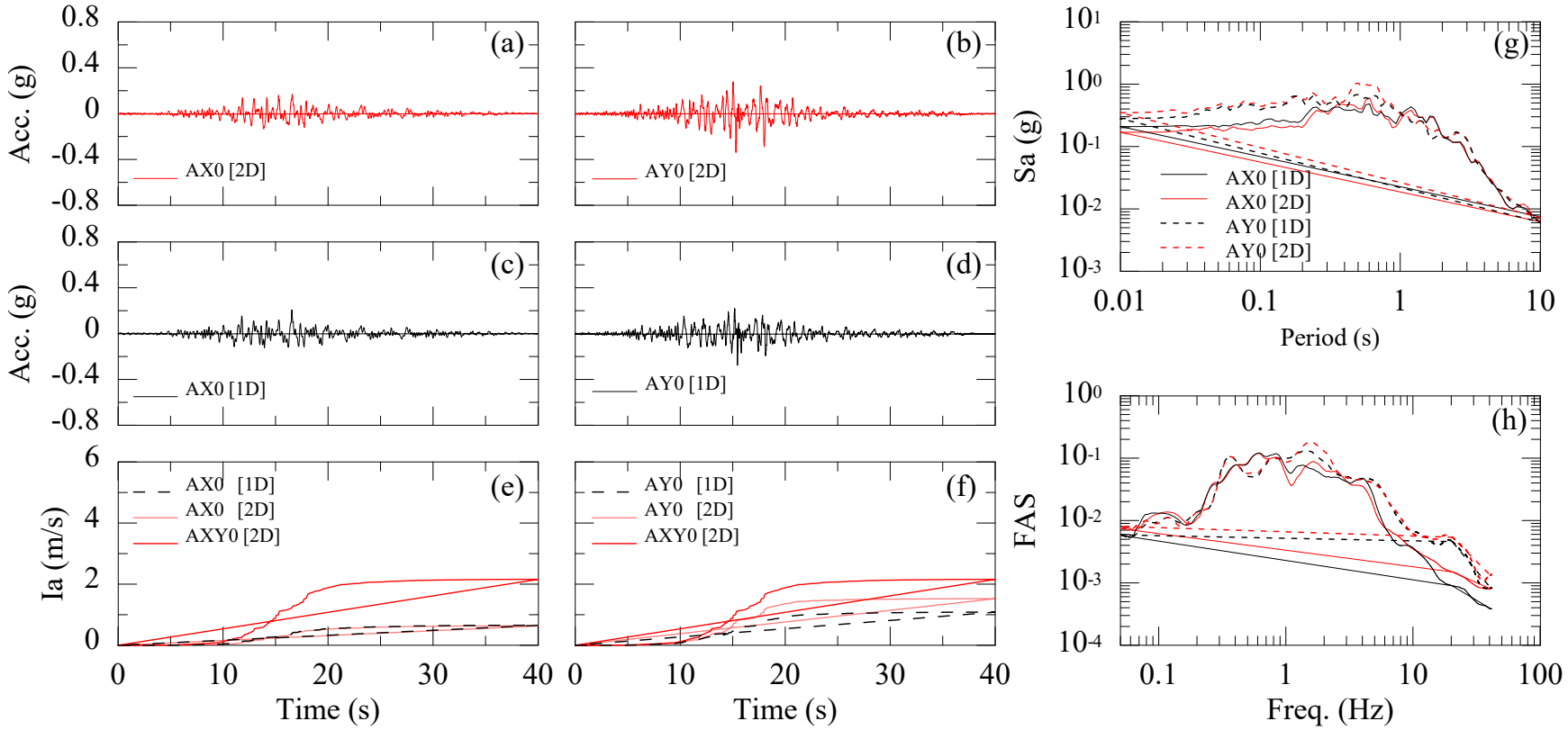

Figure C-418 Recorded input (2D) and 1D (X or Y) ground motions for: (a) M13-2D [X]; (b) M13-2D [Y]; (c) M13-1D [X]; and (d) M13-1D [Y]. Arias Intensity M13 (1D and 2D) for: (e) X direction; and (f) Y direction. Response Spectra (g) M13-2D [X]; M13-2D [Y]; M13-1D [X]; and M13-1D [Y]. Smoothed Fourier amplitude spectra (FAS) (h) M13-2D [X]; M13-2D [Y]; M13-1D [X]; and M13-1D [Y].

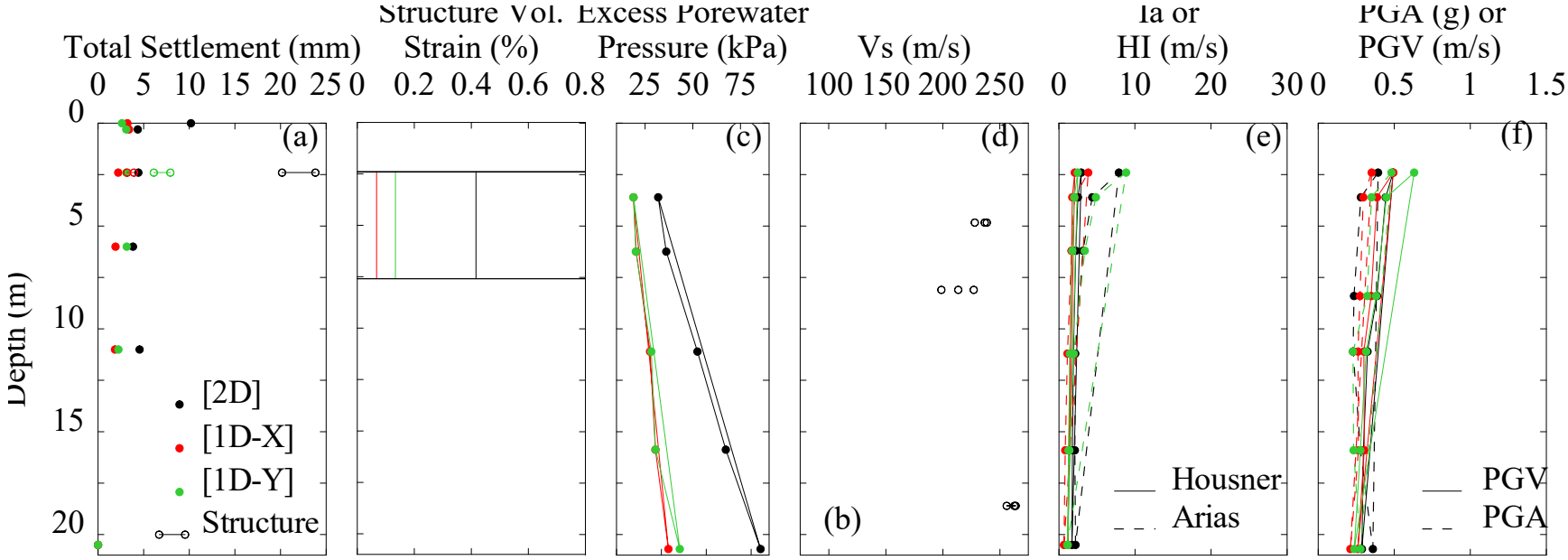

Figure C-419 Recorded or computed profiles for input motion M13-X, Y, and 2D. (a) Total settlement; (b) structure volumetric strain; (c) excess pore water pressure; (d) shear wave velocity; (e) Arias and Housner intensities; and (f) PGA and PGV.

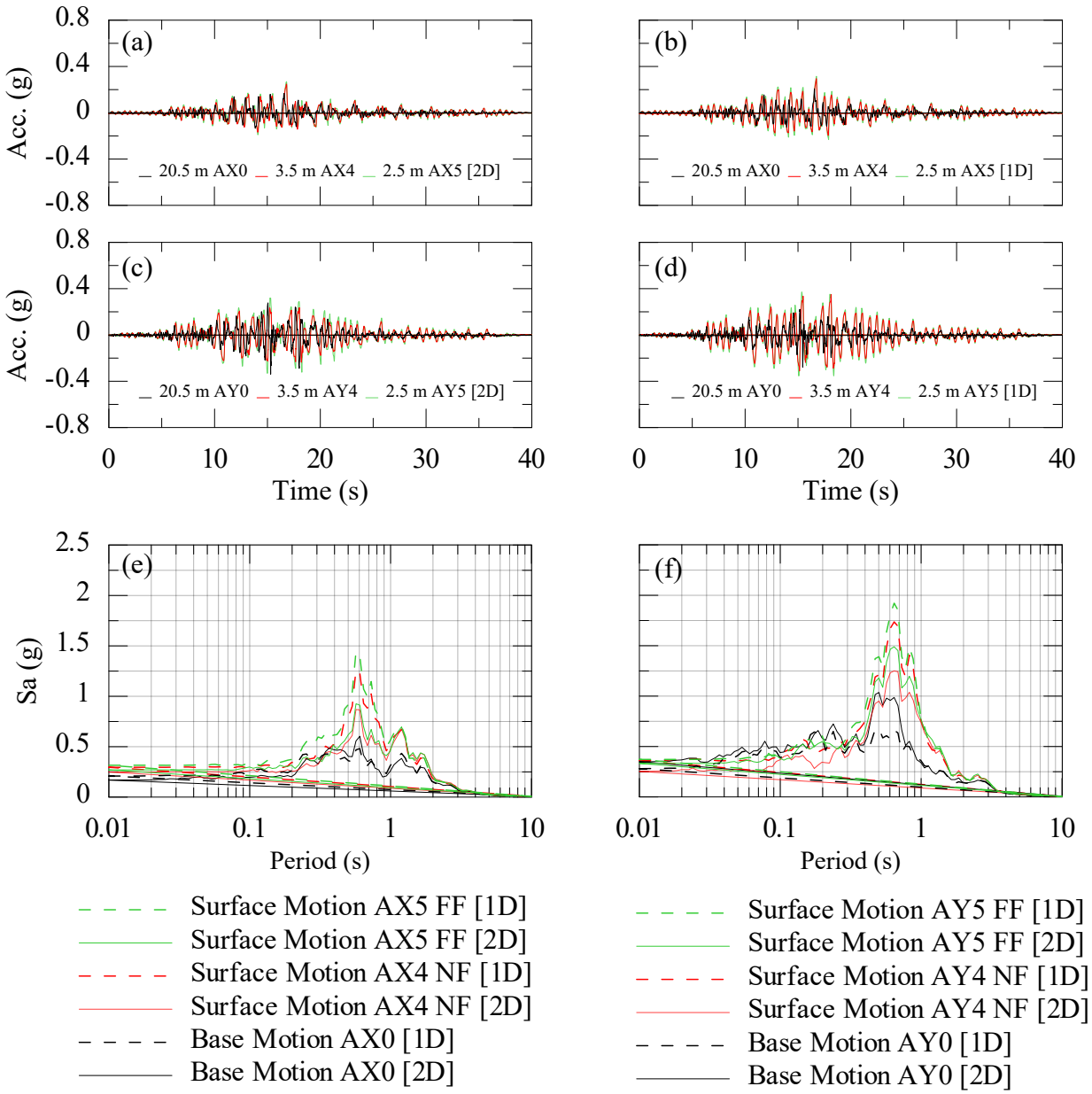

Figure C-420 Recorded input and near surface ground motions: (a) M13-2D [X]; (b) M13-1D [X]; (c) M13-2D [Y]; and (d) M13-1D [Y]. Computed response spectra from Near Field Test [PT3] for motions M13 (1D and 2D) for: (e) X direction; and (f) Y direction.

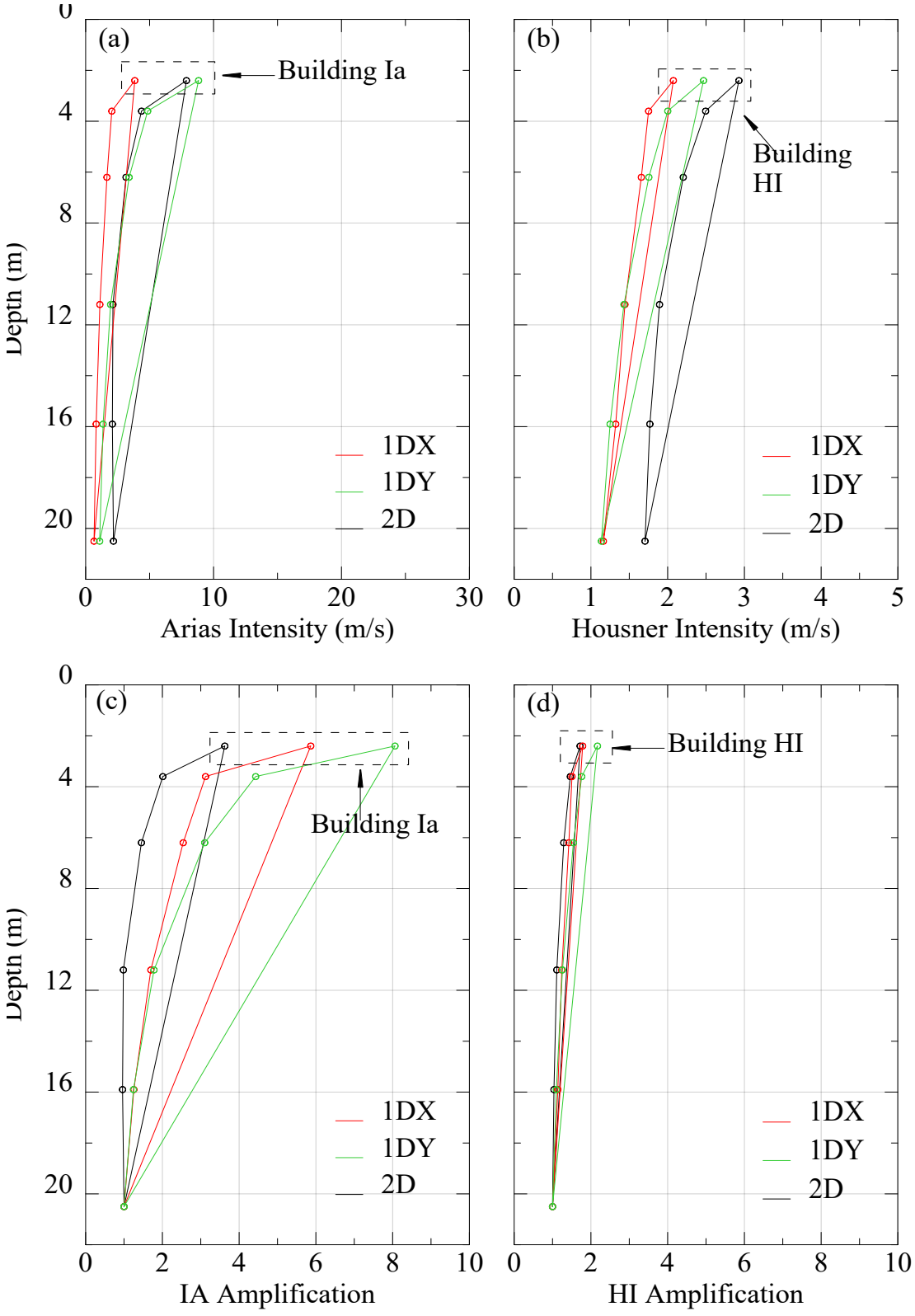

Figure C-421 Variation of total (a) Arias Intensity (M13-X,Y and 2D) ; (b) Housner Intensity (M13-X,Y and 2D) (c) Arias Intensity Amplification Factor (M13-X,Y and 2D); and (d) Housner Intensity Amplification Factor (M13-X,Y and 2D).

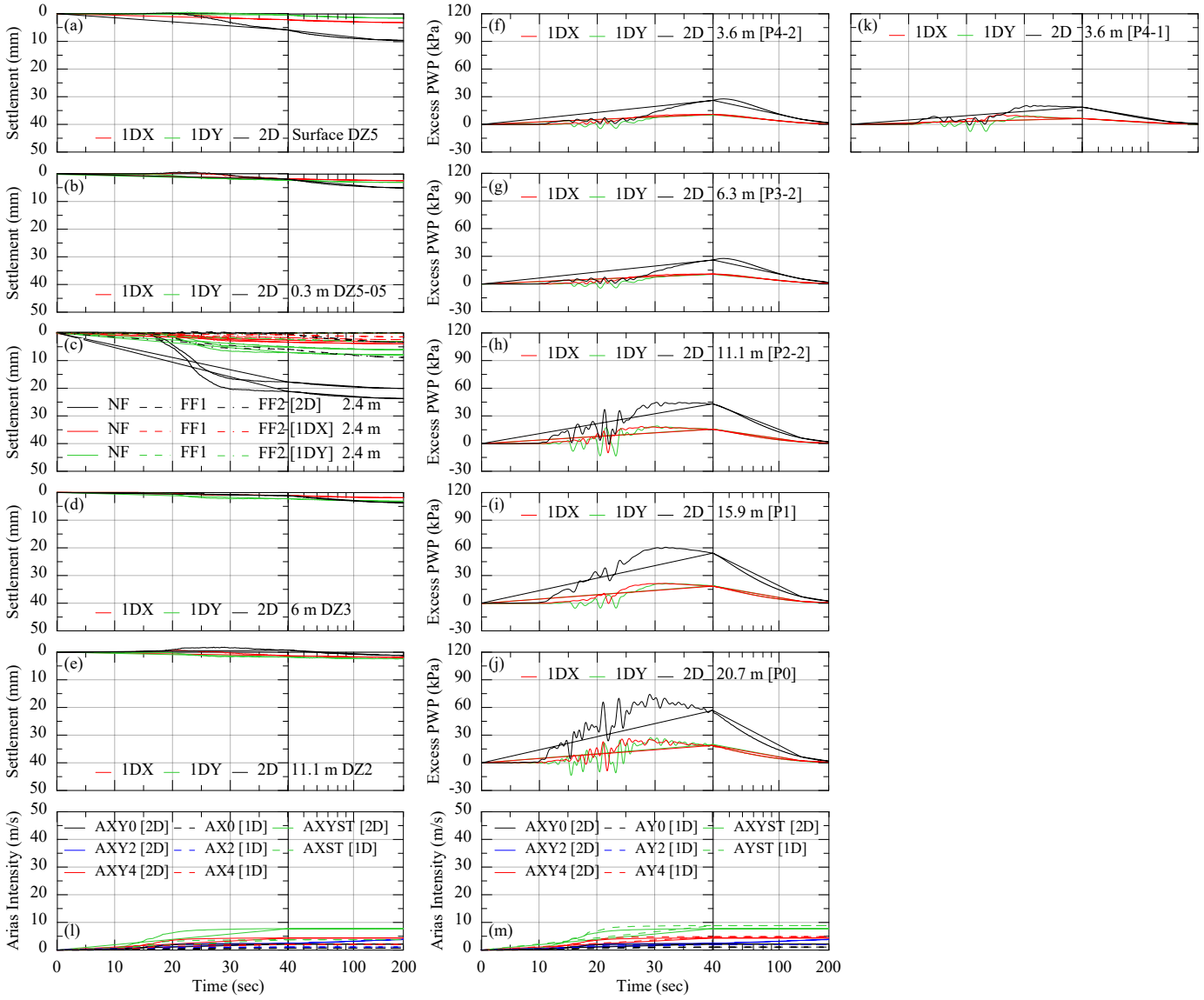

Figure C-422 Variation of total (a) to (e) Settlement with depth (M13-X,Y and 2D) ; (f) to (k) Excess pore water pressure ratio (M13-X,Y and 2D) (l) and (m) Arias Intensity along model (M13-X,Y and 2D).

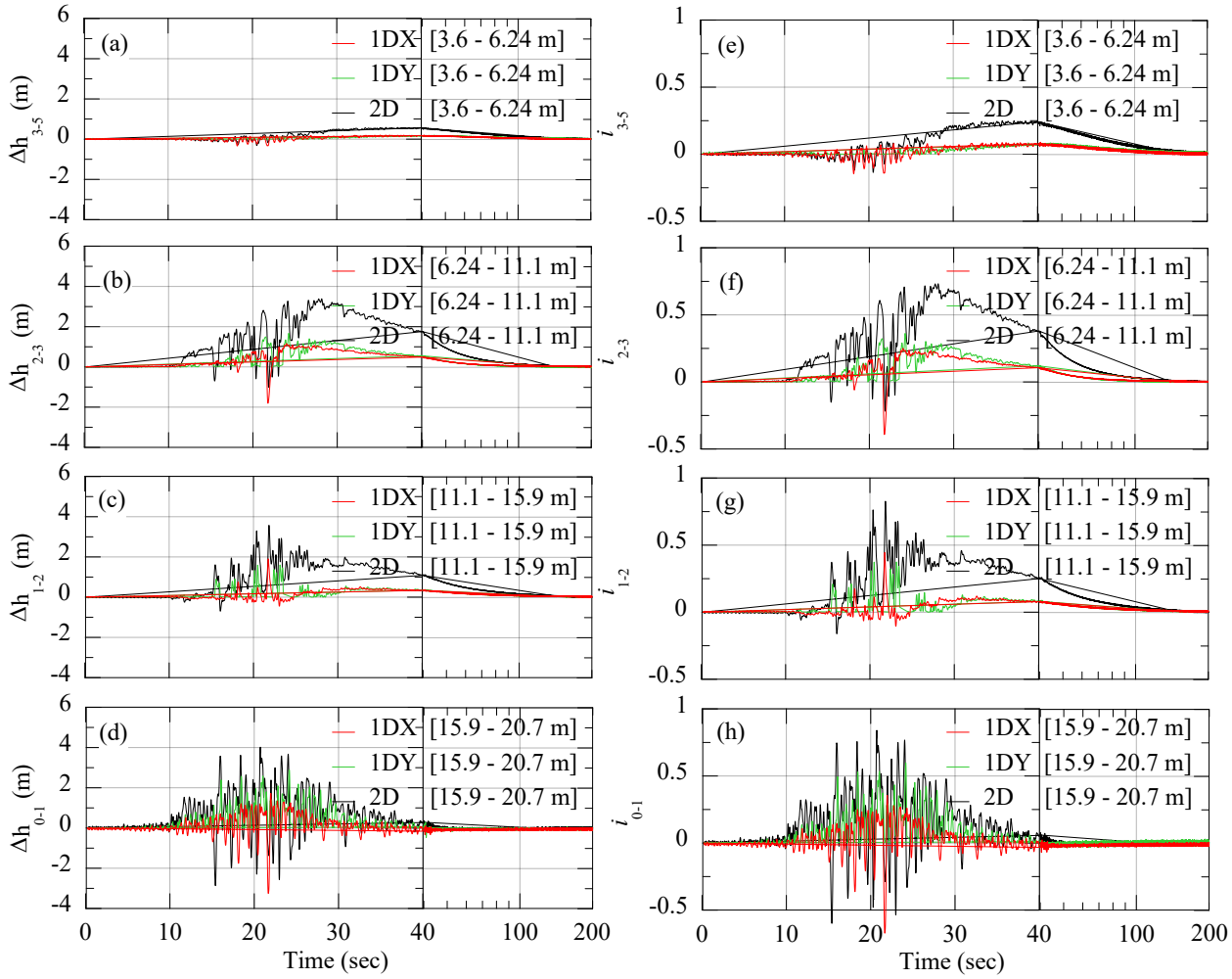

Figure C-423 Variation of total (a) to (d) Total Head Loss with depth (M13-X, Y and 2D); (e) to (h) Shaking induced Hydraulic Gradient (M13-X, Y and 2D)

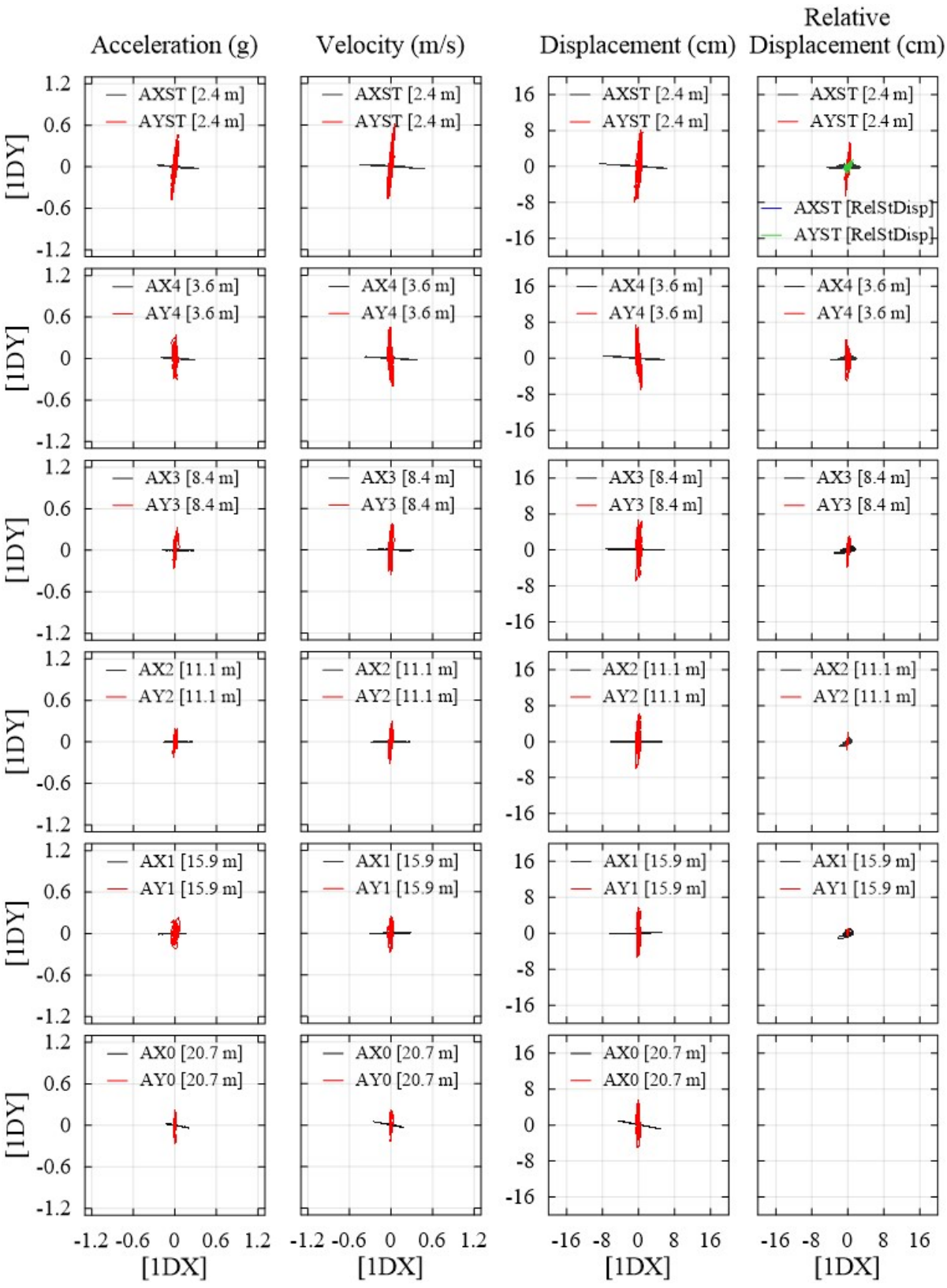

Figure C-424 Recorded input and within model ground motions for acceleration, velocity, displacement and relative displacement for M13-1D [X] and M13-1D [Y]

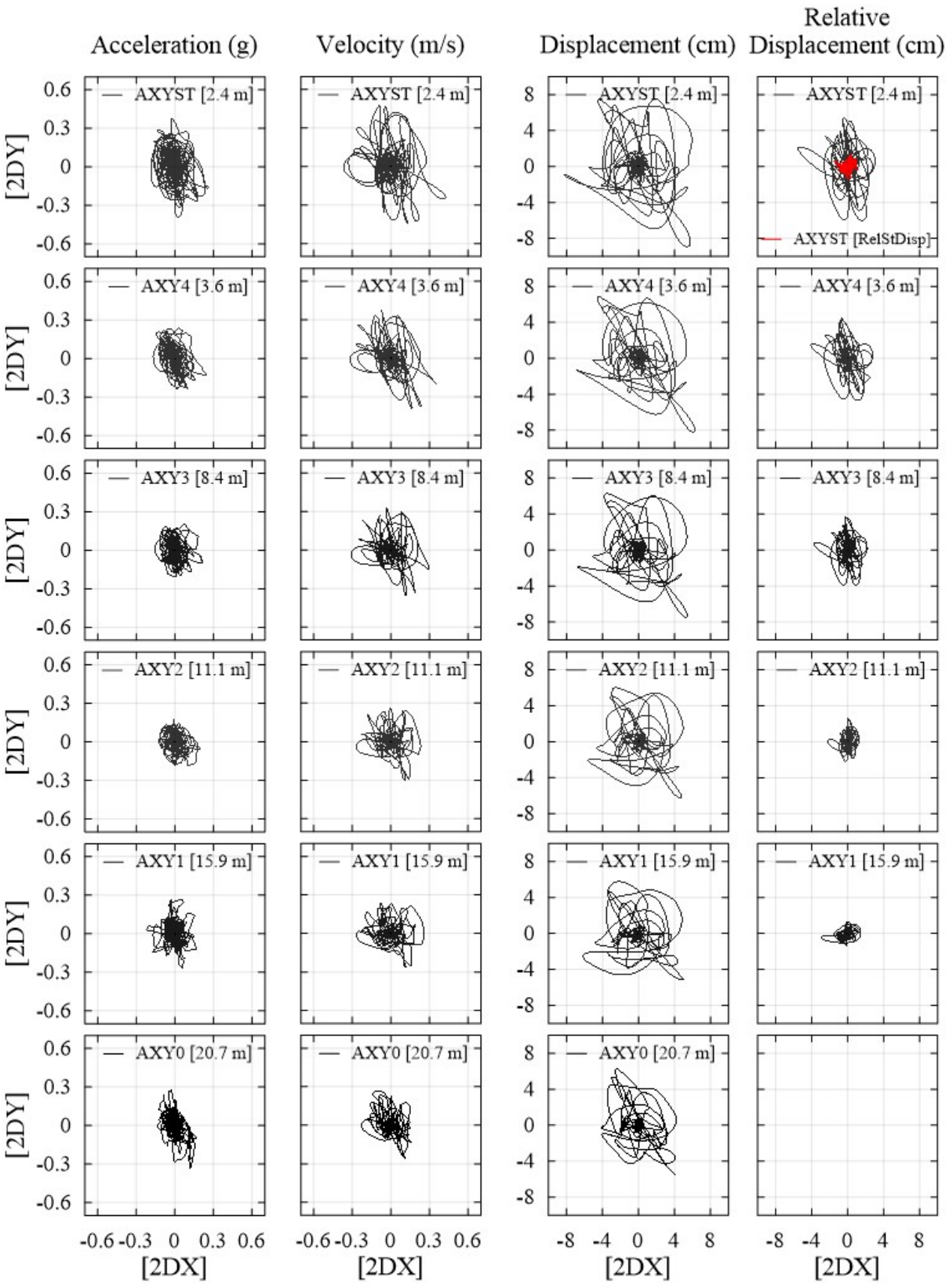

Figure C-425 Recorded input and within model ground motions for acceleration, velocity, displacement and relative displacement for M13-2D

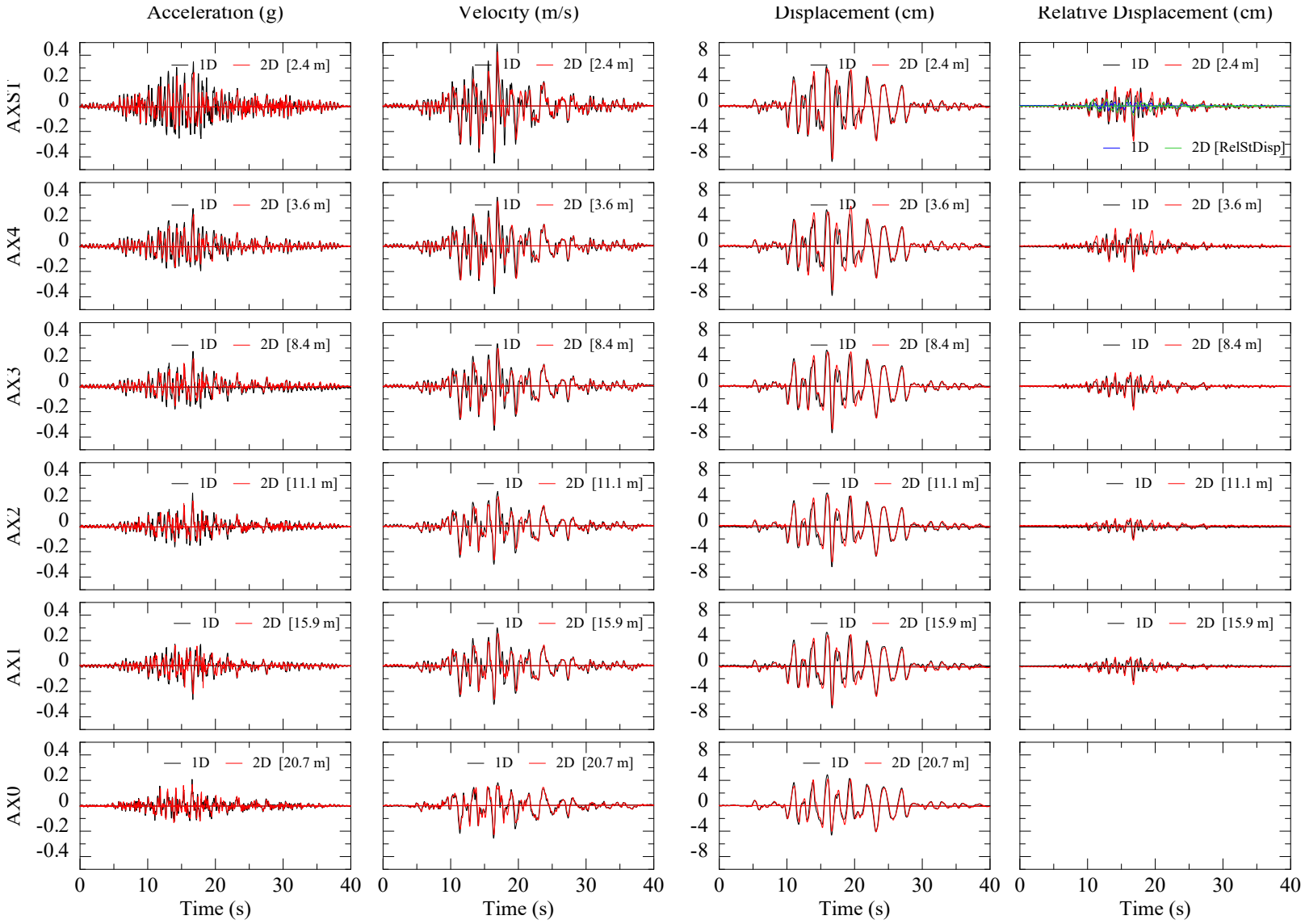

Figure C-426 Recorded input and within model ground motions time histories for acceleration, velocity, displacement and relative displacement for M13-2D [X] and M13-1D [X]

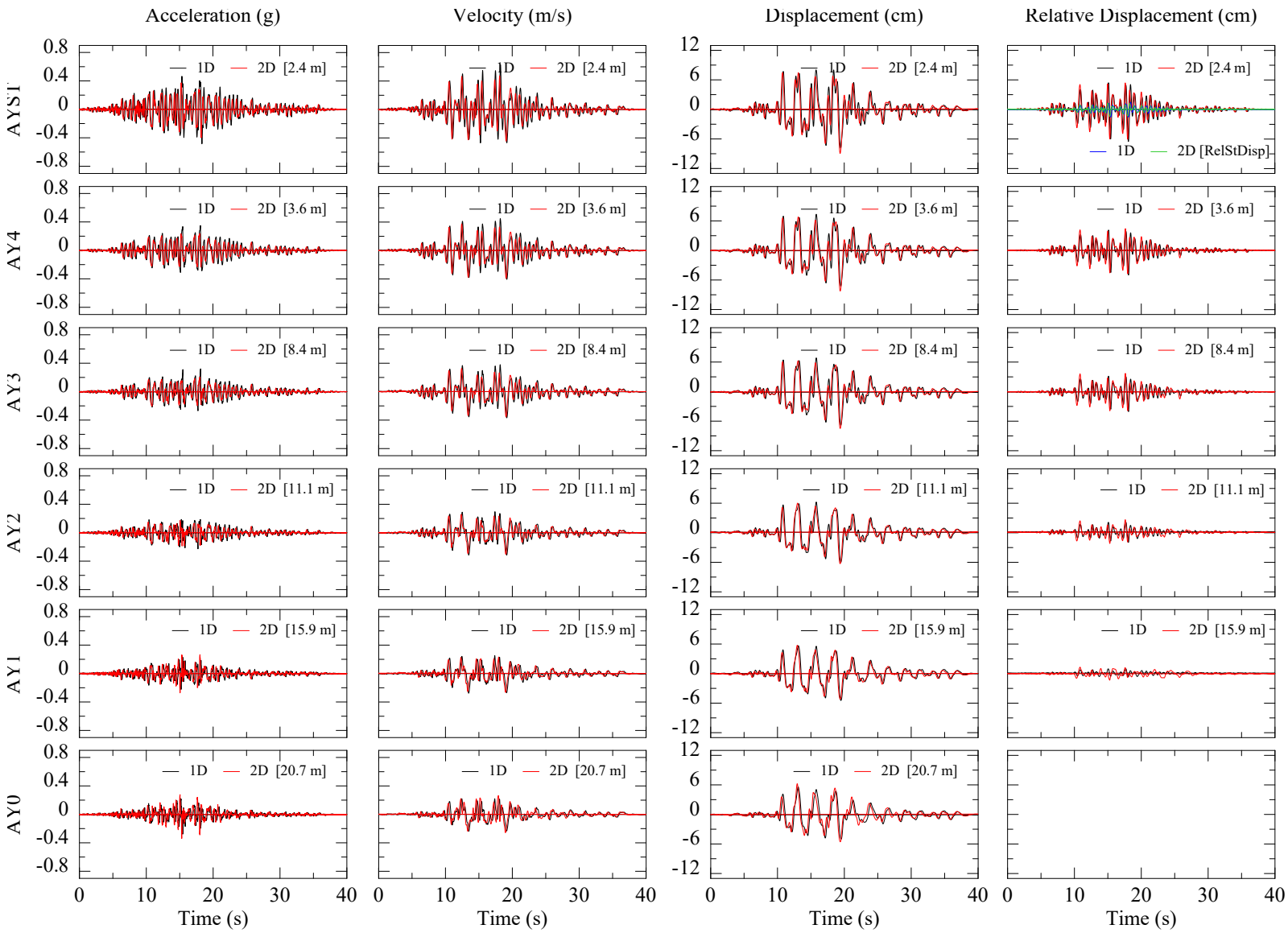

Figure C-427 Recorded input and within model ground motions time histories for acceleration, velocity, displacement and relative displacement for M13-2D [Y] and M13-1D [Y]

1.6.6 Motion 3 (M3)

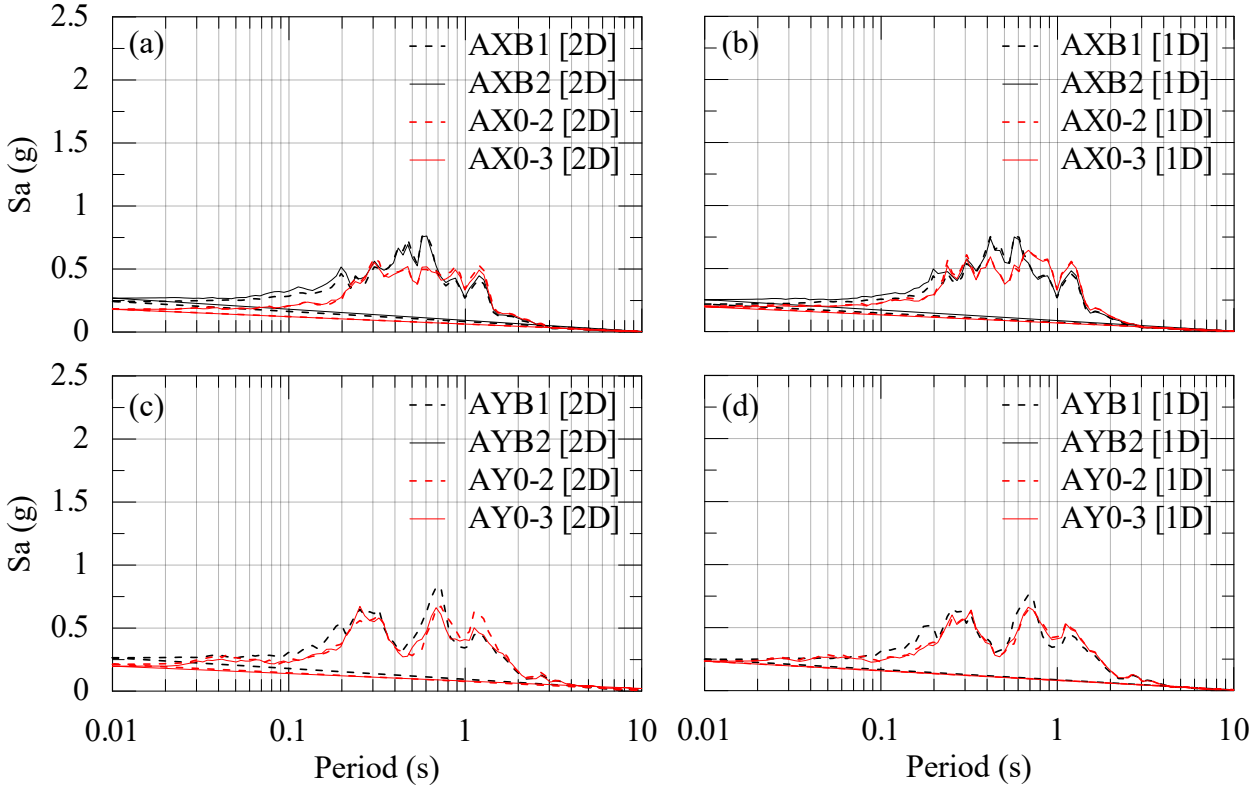

Figure C-428 Comparison of response spectra of 2D laminar container table and within model base input motion for motions (M3-X, Y and 2D).

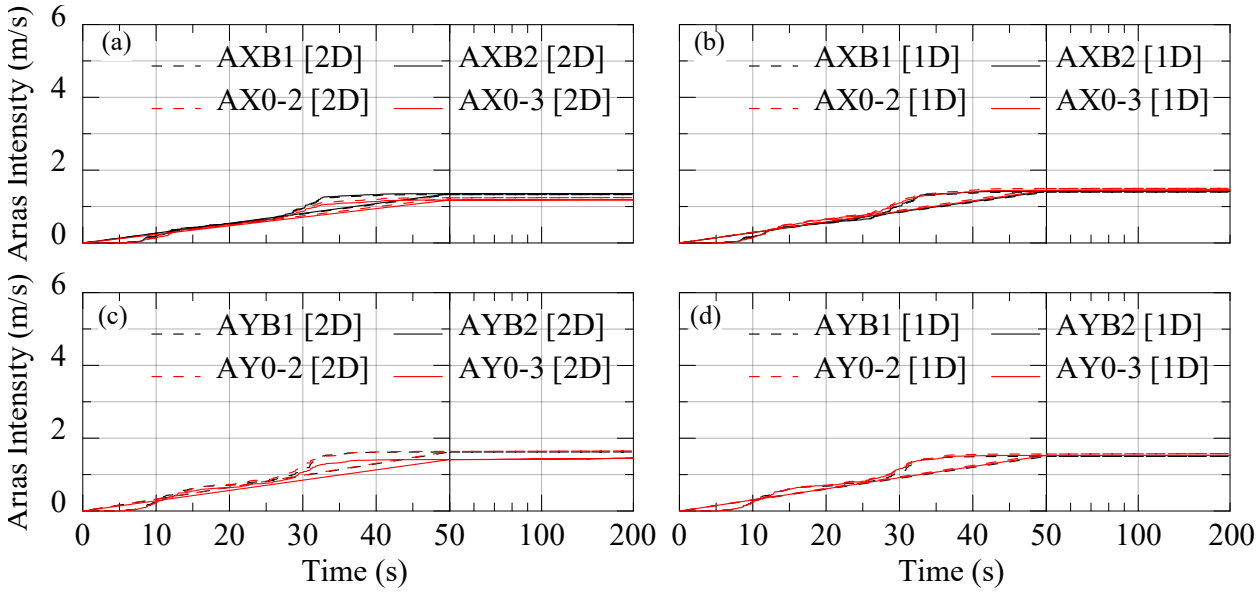

Figure C-429 Comparison of Arias Intensity of 2D laminar container table and within model base input motion for motions (a) M3-2D [X]; (b) M3-2D [Y]; (c) M3-1D [X] and (d) M3-1D [Y]

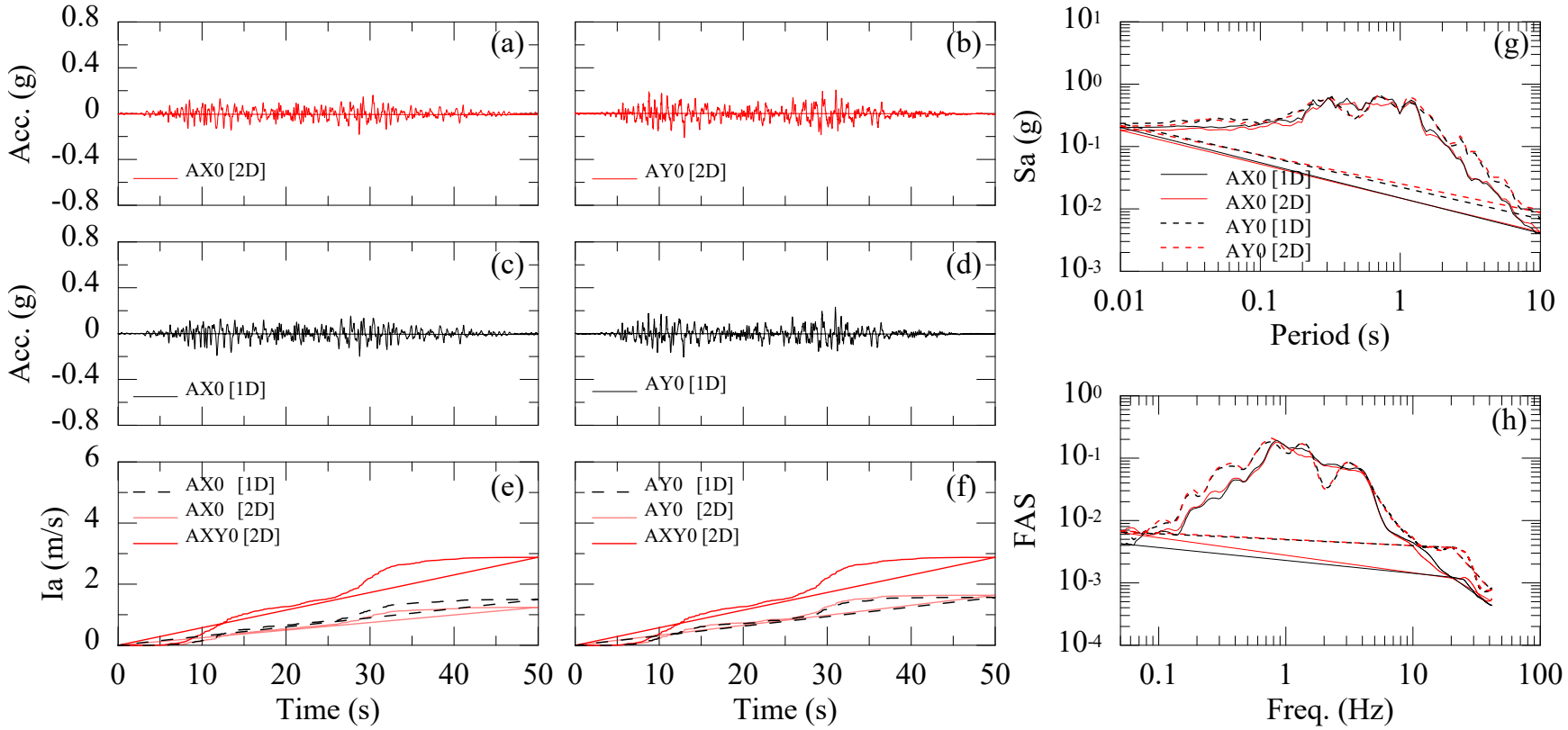

Figure C-430 Recorded input (2D) and 1D (X or Y) ground motions for: (a) M3-2D [X]; (b) M3-2D [Y]; (c) M3-1D [X]; and (d) M3-1D [Y]. Arias Intensity M3 (1D and 2D) for: (e) X direction; and (f) Y direction. Response Spectra (g) M3-2D [X]; M3-2D [Y]; M3-1D [X]; and M3-1D [Y]. Smoothed Fourier amplitude spectra (FAS) (h) M3-2D [X]; M3-2D [Y]; M3-1D [X]; and M3-1D [Y].

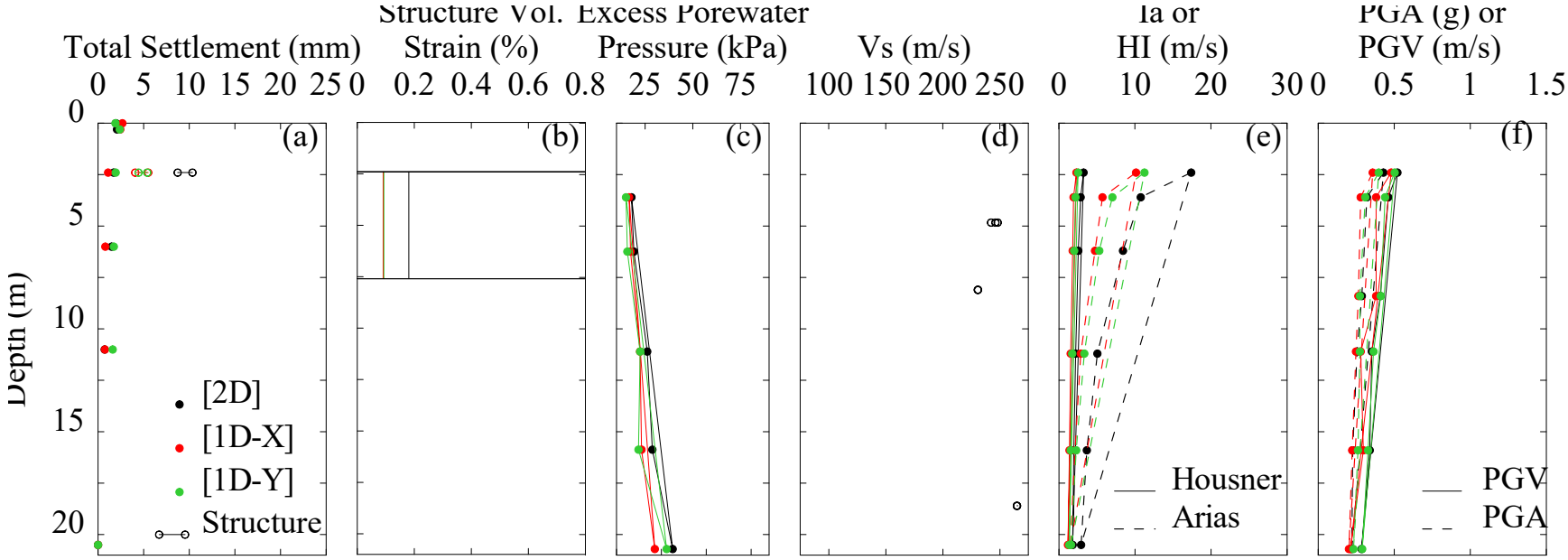

Figure C-431 Recorded or computed profiles for input motion M3-X, Y, and 2D. (a) Total settlement; (b) structure volumetric strain; (c) excess pore water pressure; (d) shear wave velocity; (e) Arias and Housner intensities; and (f) PGA and PGV.

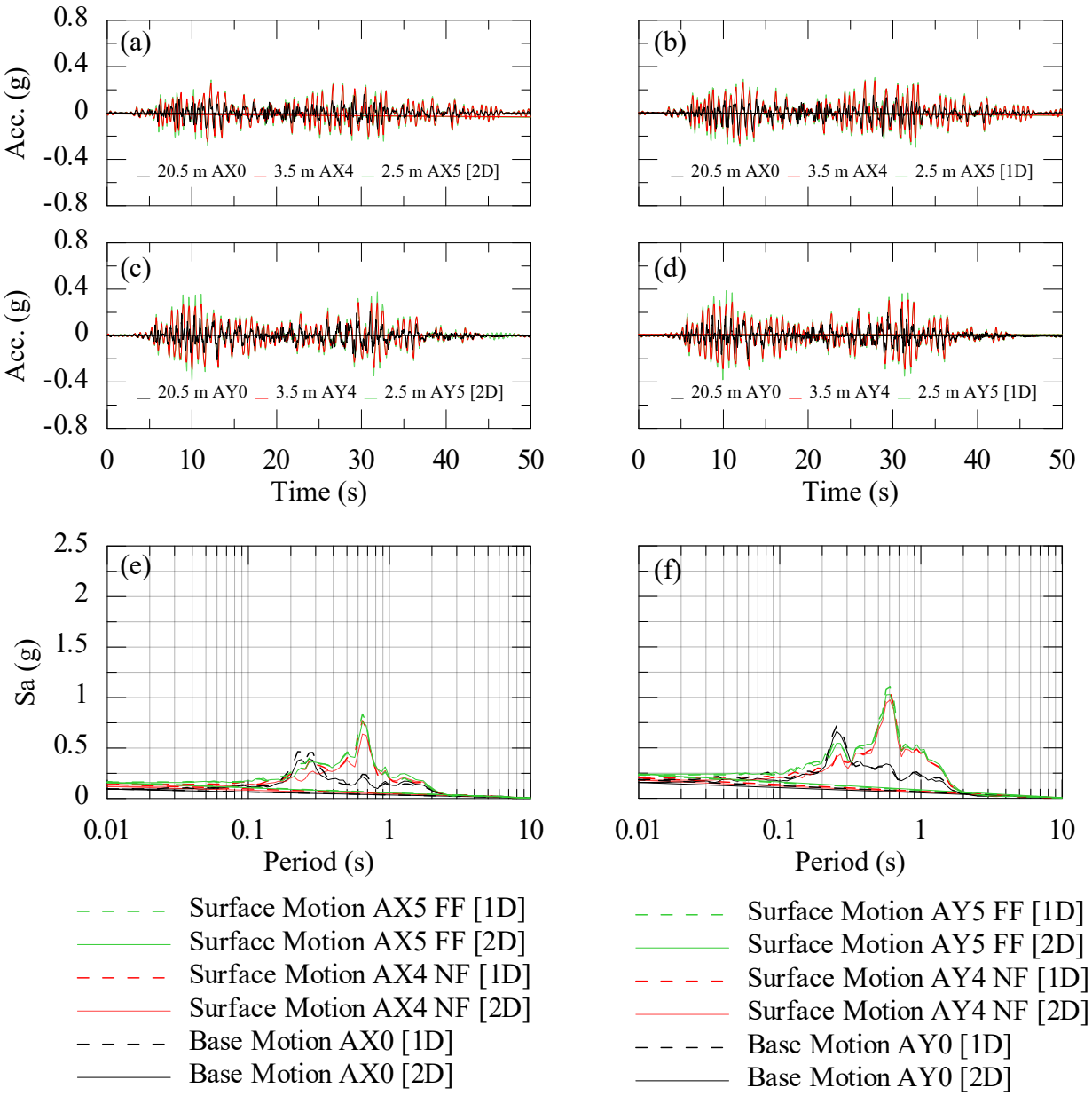

Figure C-432 Recorded input and near surface ground motions: (a) M3-2D [X]; (b) M3-1D [X]; (c) M3-2D [Y]; and (d) M3-1D [Y]. Computed response spectra from Near Field Test [PT3] for motions M3 (1D and 2D) for: (e) X direction; and (f) Y direction.

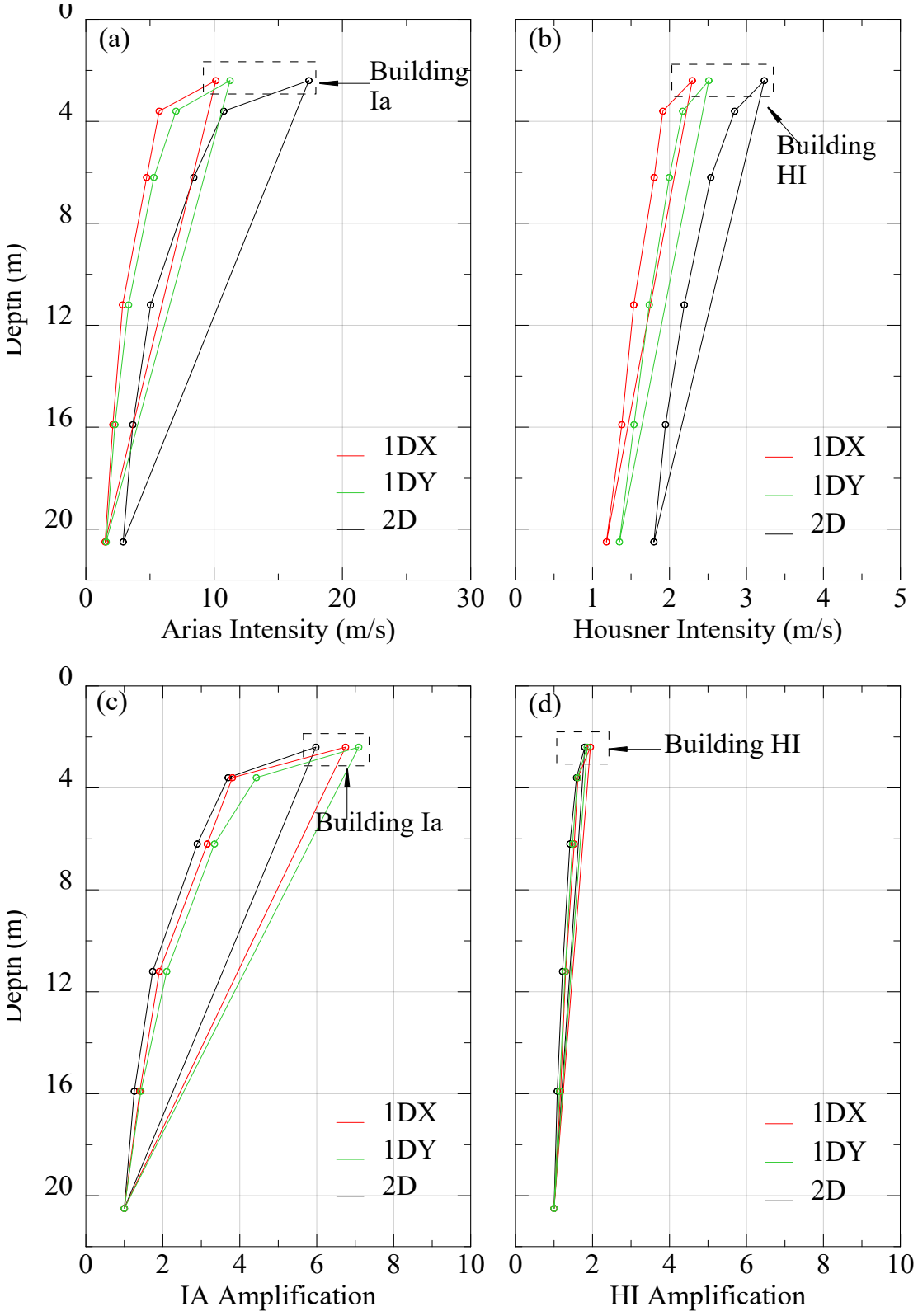

Figure C-433 Variation of total (a) Arias Intensity (M3-X,Y and 2D) ; (b) Housner Intensity (M3-X,Y and 2D) (c) Arias Intensity Amplification Factor (M3-X,Y and 2D); and (d) Housner Intensity Amplification Factor (M3-X,Y and 2D).

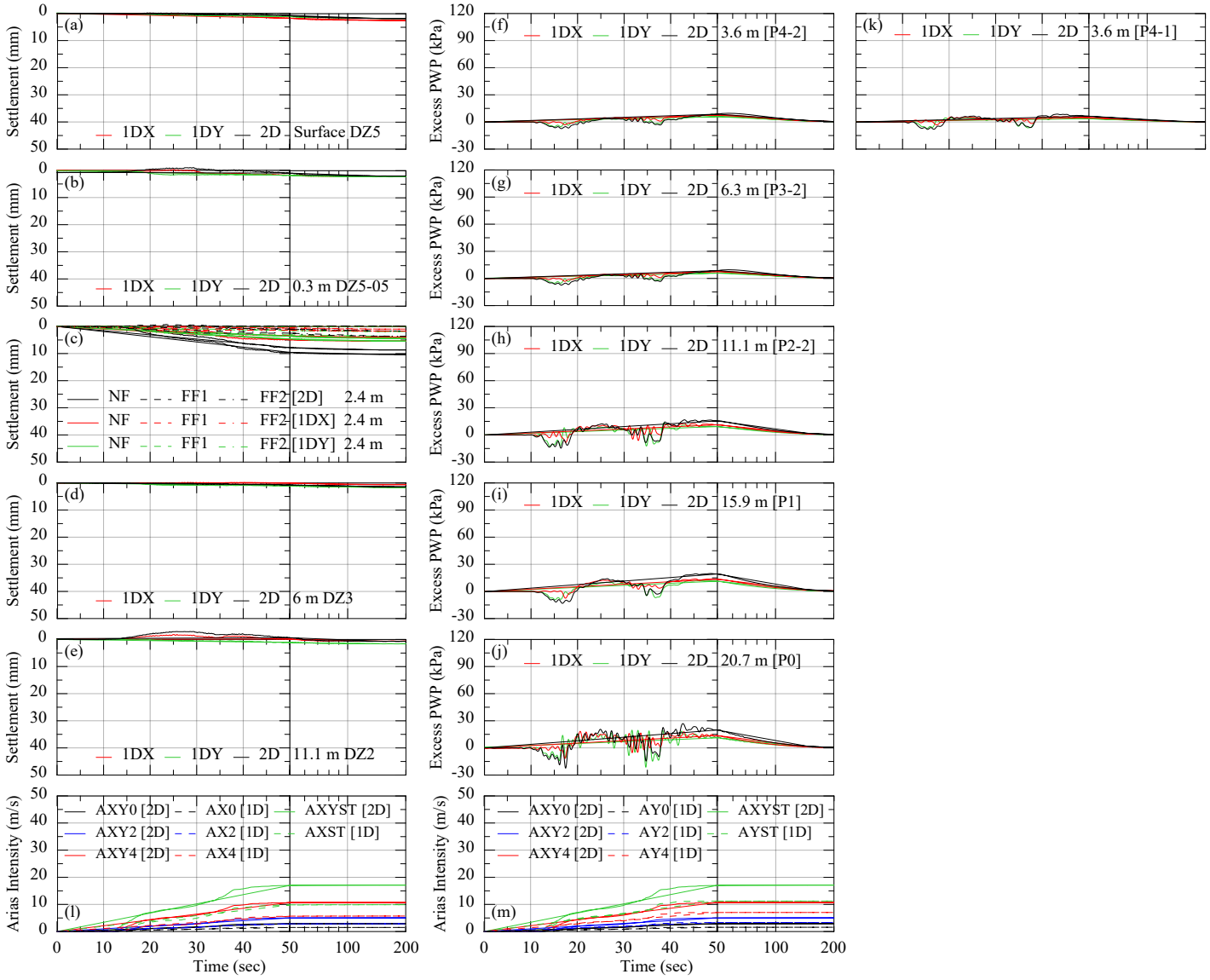

Figure C-434 Variation of total (a) to (e) Settlement with depth (M3-X,Y and 2D) ; (f) to (k) Excess pore water pressure (M3-X,Y and 2D) (l) and (m) Arias Intensity along model (M3-X,Y and 2D).

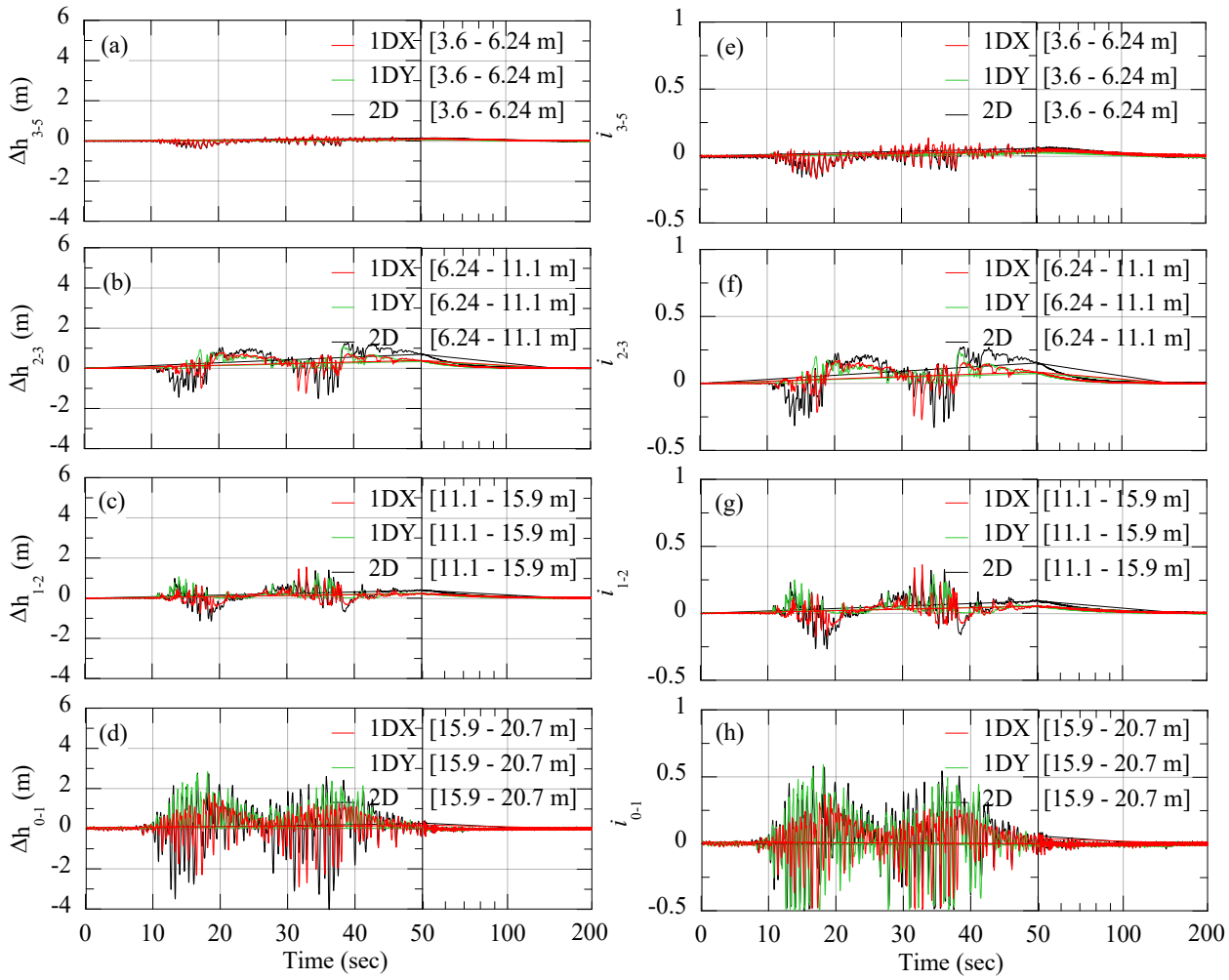

Figure C-435 Variation of total (a) to (d) Total Head Loss with depth (M3-X, Y and 2D); (e) to (h) Shaking induced Hydraulic Gradient (M3-X, Y and 2D)

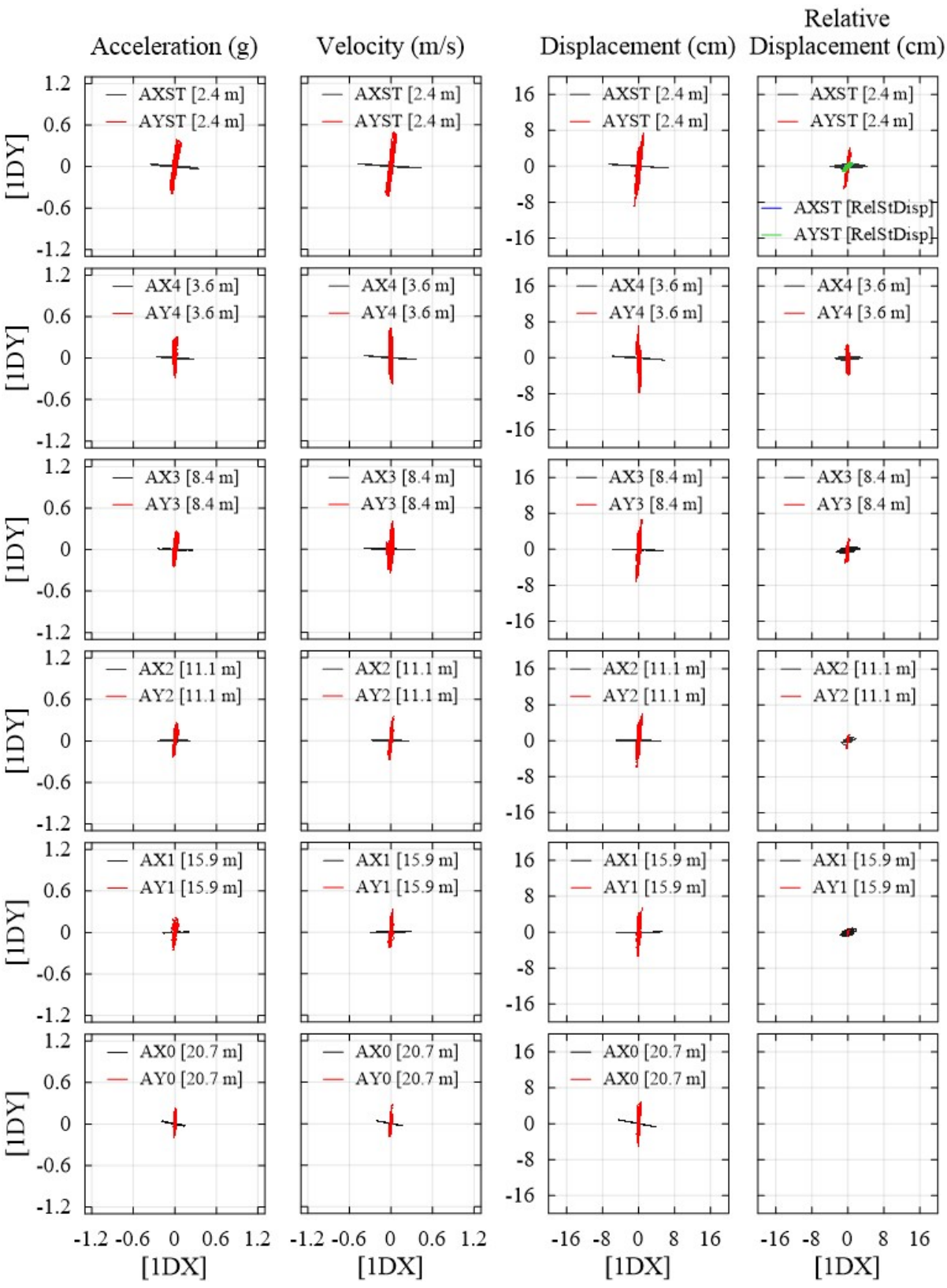

Figure C-436 Recorded input and within model ground motions for acceleration, velocity, displacement and relative displacement for M3-1D [X] and M3-1D [Y]

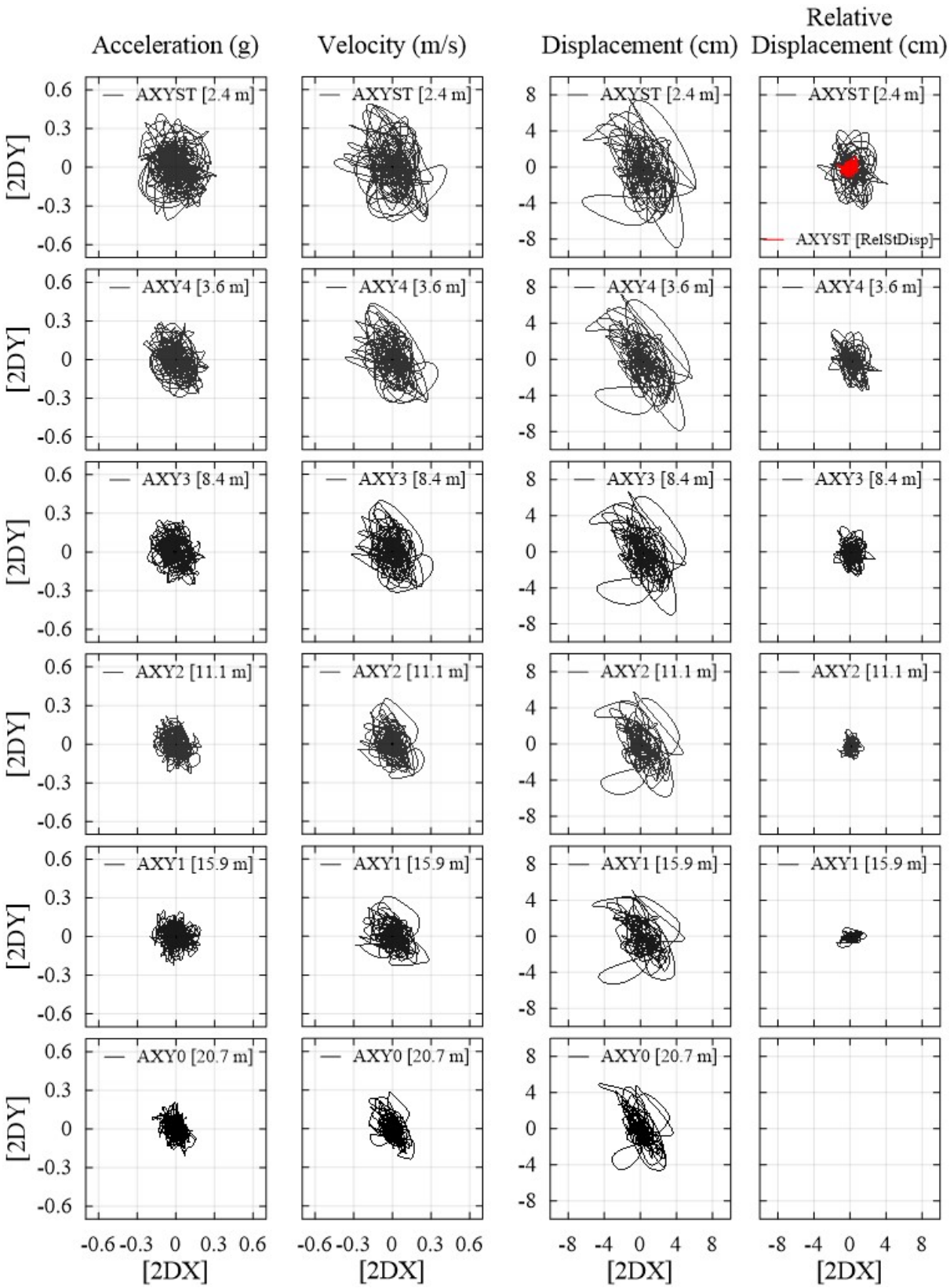

Figure C-437 Recorded input and within model ground motions for acceleration, velocity, displacement and relative displacement for M3-2D

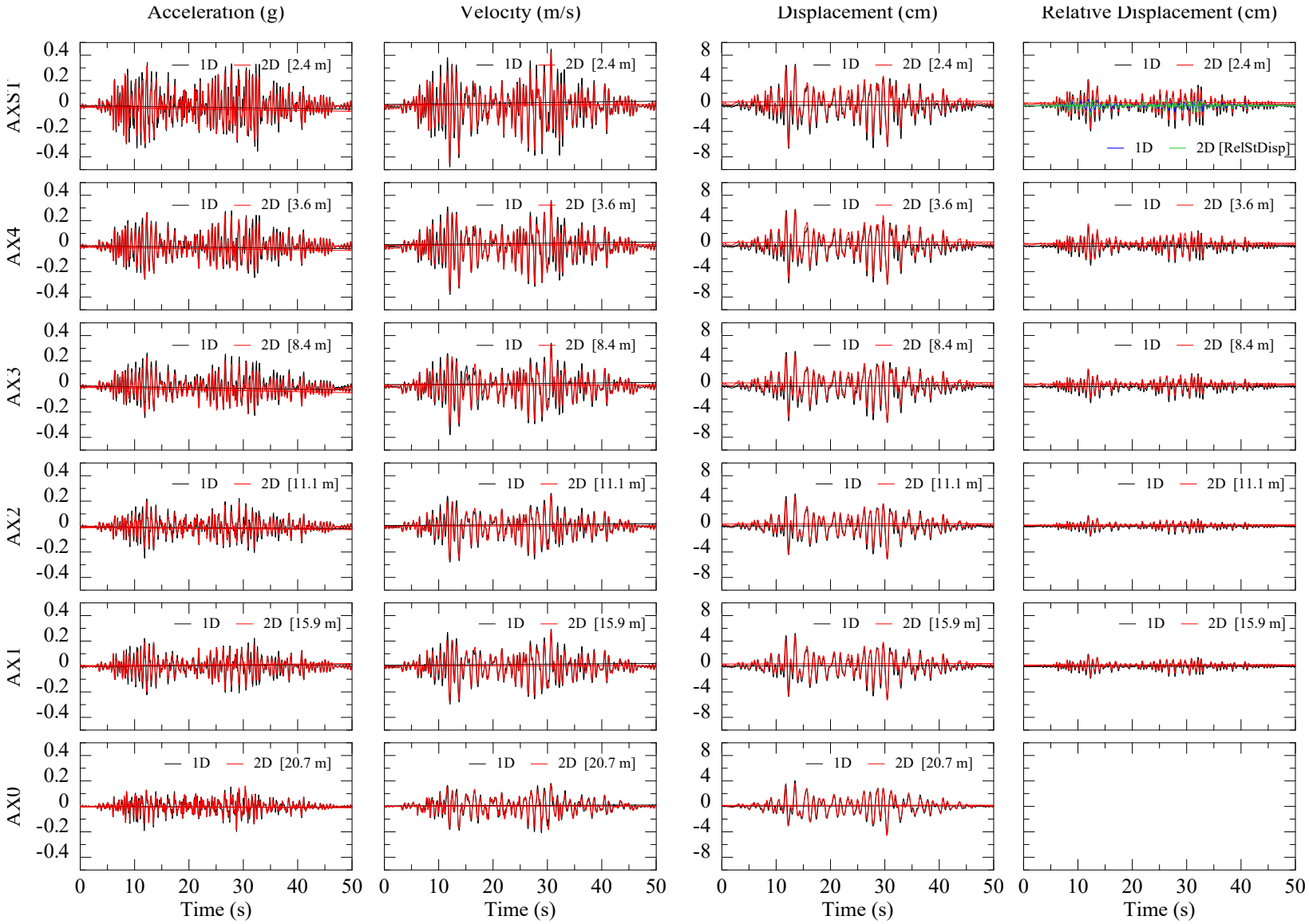

Figure C-438 Recorded input and within model ground motions time histories for acceleration, velocity, displacement and relative displacement for M3-2D [X] and M3-1D [X]

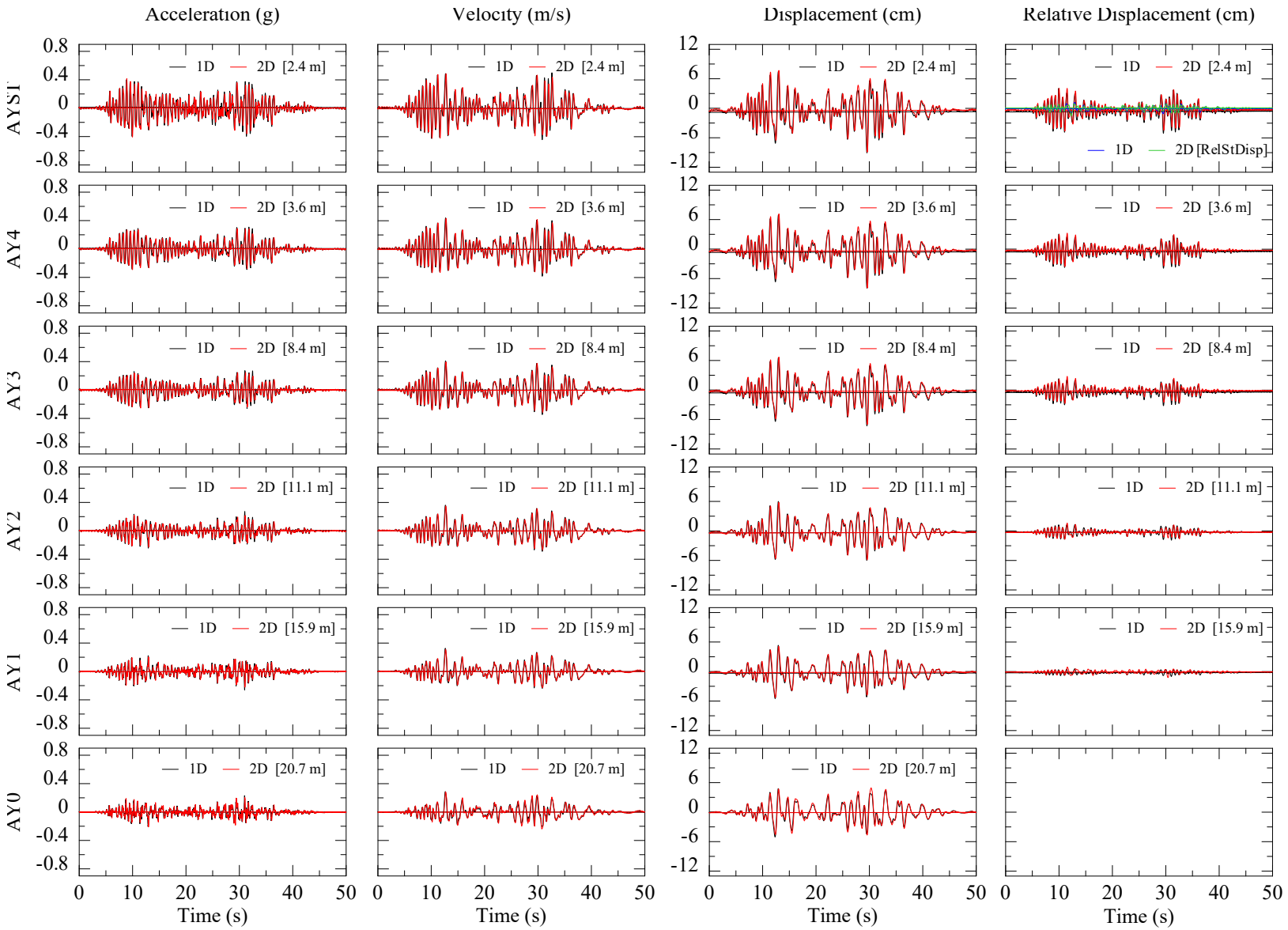

Figure C-439 Recorded input and within model ground motions time histories for acceleration, velocity, displacement and relative displacement for M3-2D [Y] and M3-1D [Y]

1.6.7 Motion 5 (M5)

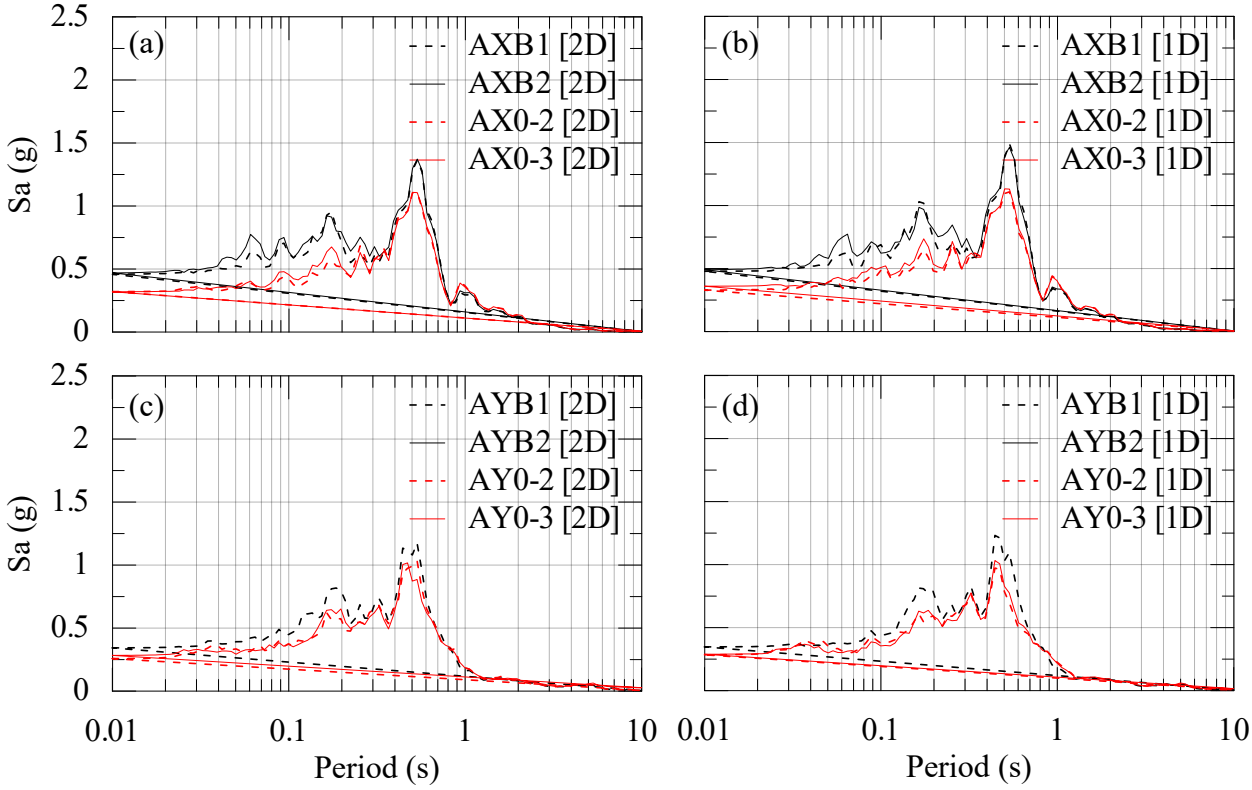

Figure C-440 Comparison of response spectra of 2D laminar container table and within model base input motion for motions (M5-X, Y and 2D).

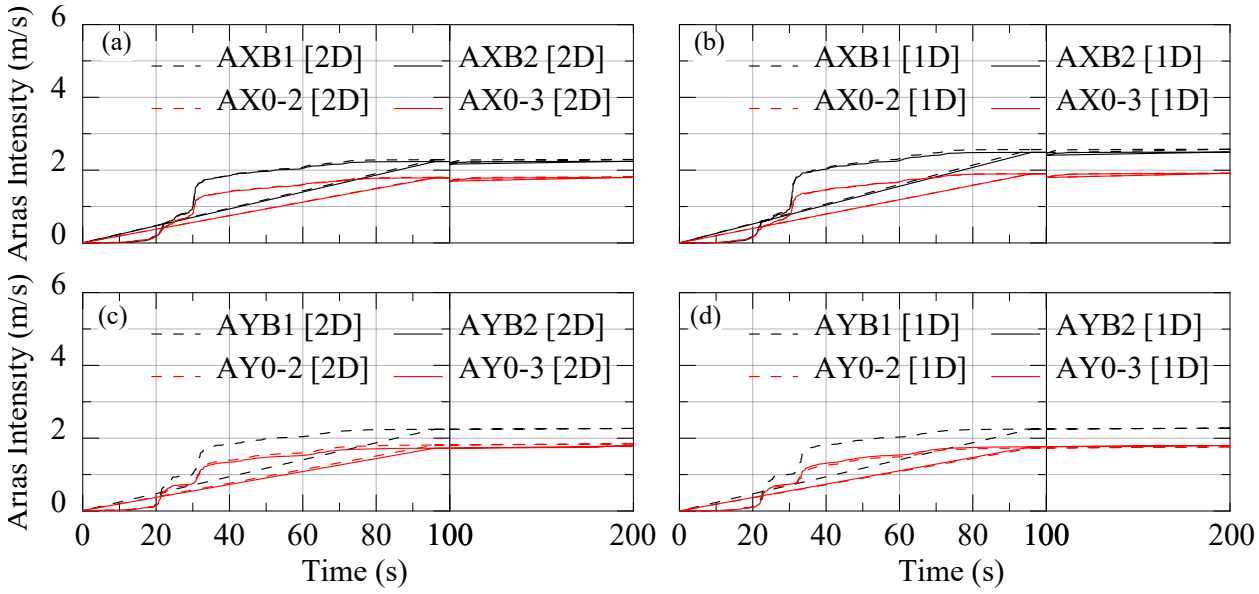

Figure C-441 Comparison of Arias Intensity of 2D laminar container table and within model base input motion for motions (a) M5-2D [X]; (b) M5-2D [Y]; (c) M5-1D [X] and (d) M5-1D [Y]

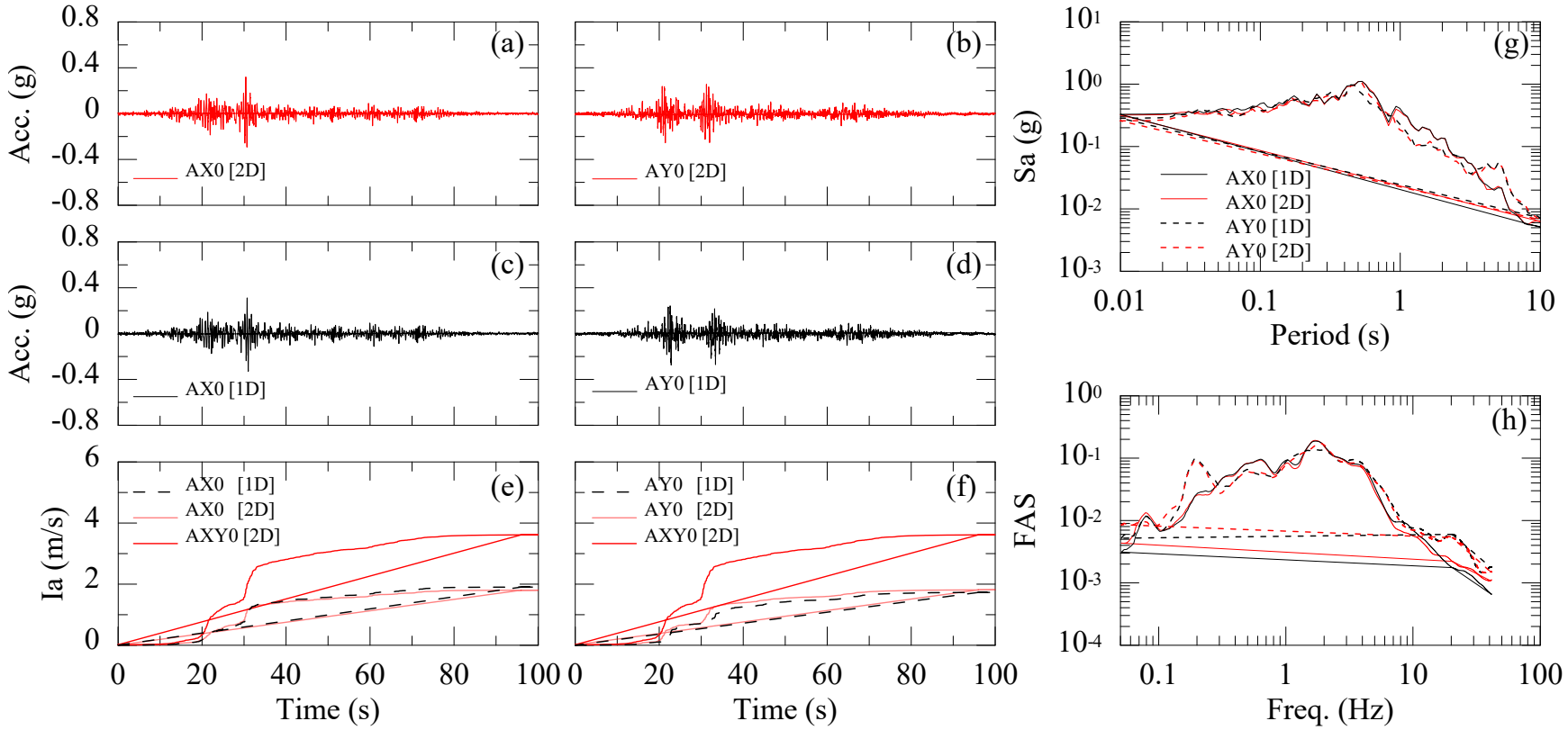

Figure C-442 Recorded input (2D) and 1D (X or Y) ground motions for: (a) M5-2D [X]; (b) M5-2D [Y]; (c) M5-1D [X]; and (d) M5-1D [Y]. Arias Intensity M5 (1D and 2D) for: (e) X direction; and (f) Y direction. Response Spectra (g) M5-2D [X]; M5-2D [Y]; M5-1D [X]; and M5-1D [Y]. Smoothed Fourier amplitude spectra (FAS) (h) M5-2D [X]; M5-2D [Y]; M5-1D [X]; and M5-1D [Y].

Figure C-443 Recorded or computed profiles for input motion M5-X, Y, and 2D. (a) Total settlement; (b) structure volumetric strain; (c) excess pore water pressure; (d) shear wave velocity; (e) Arias and Housner intensities; and (f) PGA and PGV.

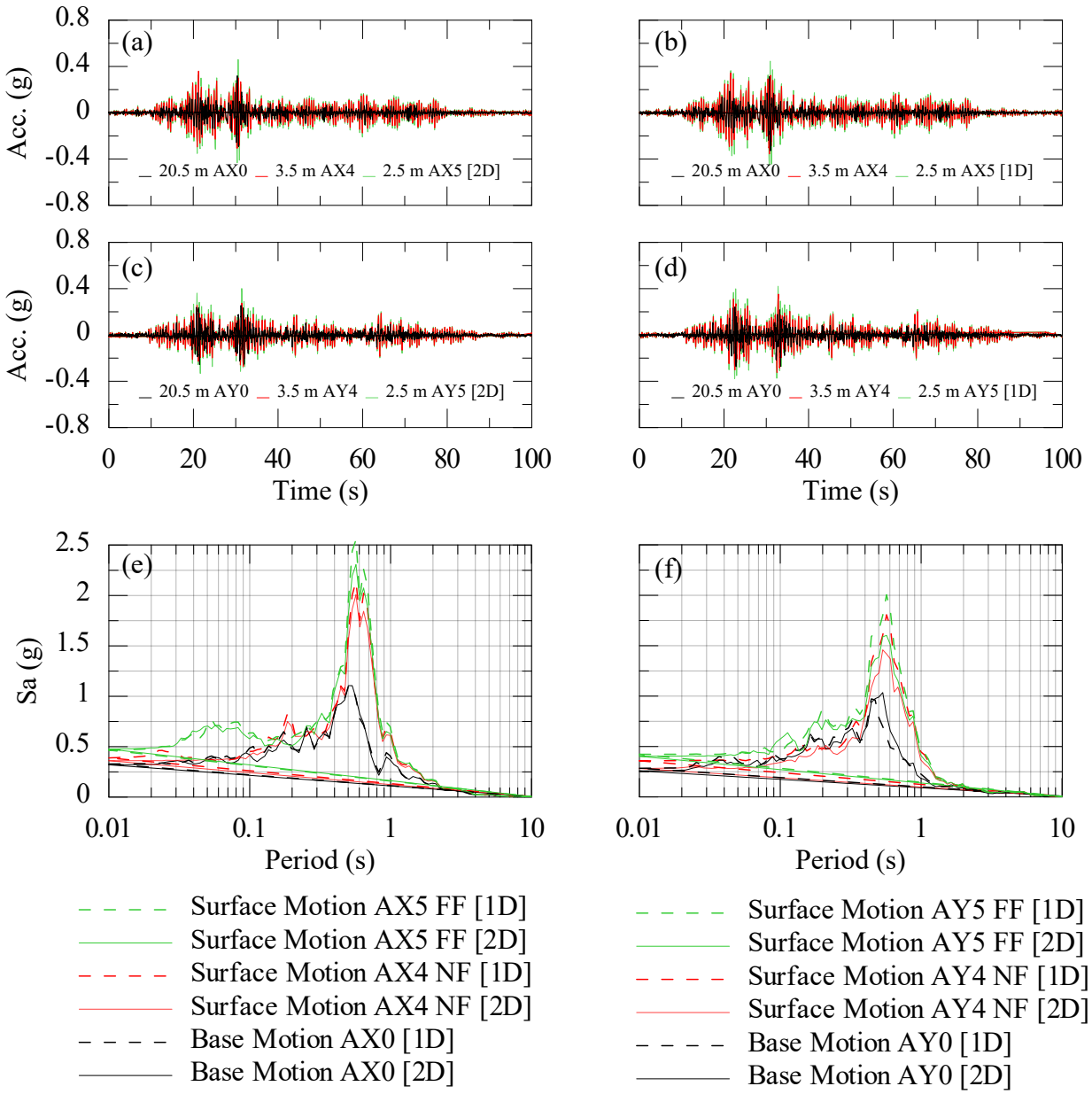

Figure C-444 Recorded input and near surface ground motions: (a) M5-2D [X]; (b) M5-1D [X]; (c) M5-2D [Y]; and (d) M5-1D [Y]. Computed response spectra from Near Field Test [PT3] for motions M5 (1D and 2D) for: (e) X direction; and (f) Y direction.

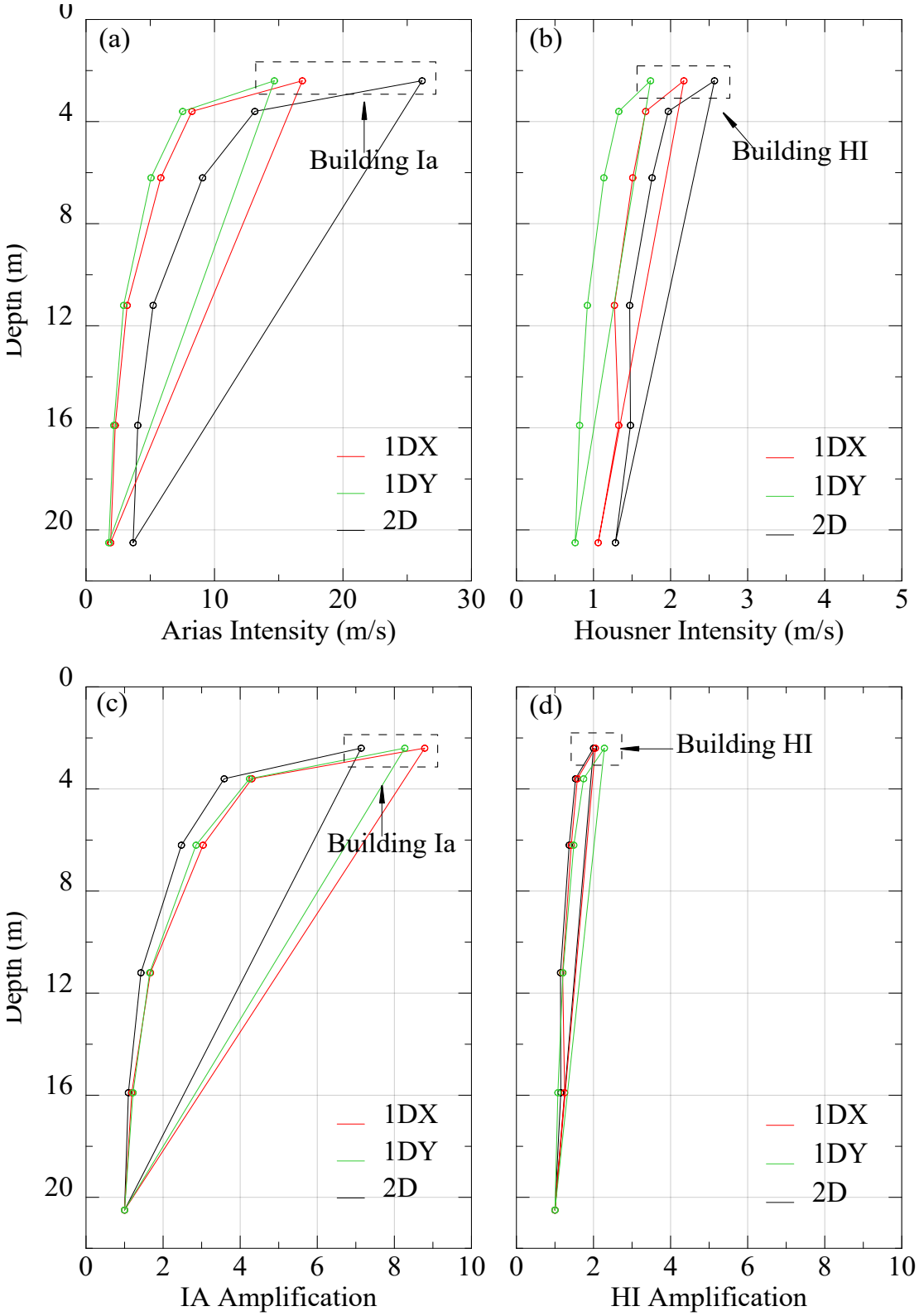

Figure C-445 Variation of total (a) Arias Intensity (M5-X,Y and 2D) ; (b) Housner Intensity (M5-X,Y and 2D) (c) Arias Intensity Amplification Factor (M5-X,Y and 2D); and (d) Housner Intensity Amplification Factor (M5-X,Y and 2D).

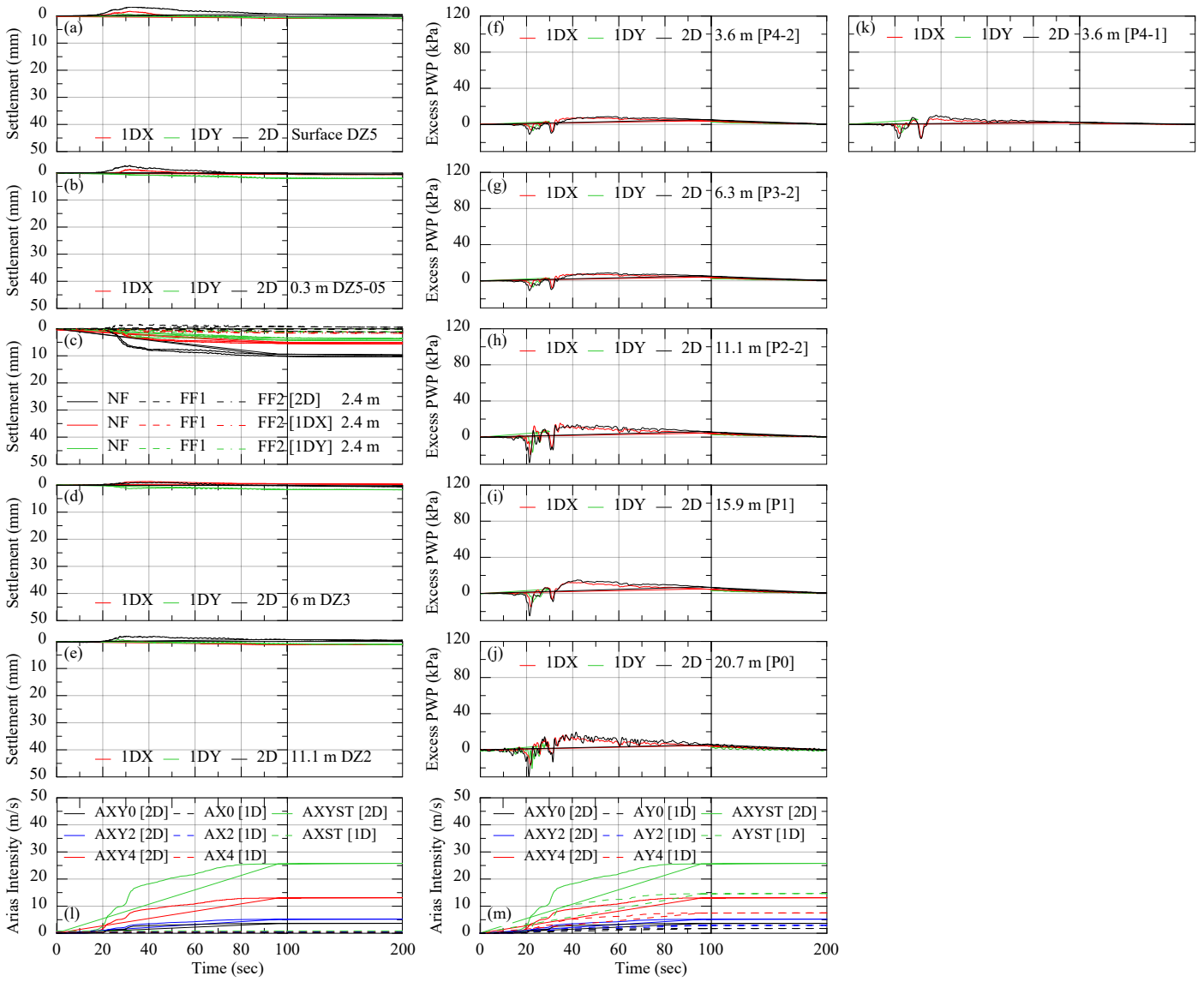

Figure C-446 Variation of total (a) to (e) Settlement with depth (M5-X,Y and 2D) ; (f) to (k) Excess pore water pressure ratio (M5-X,Y and 2D) (l) and (m) Arias Intensity along model (M5-X,Y and 2D).

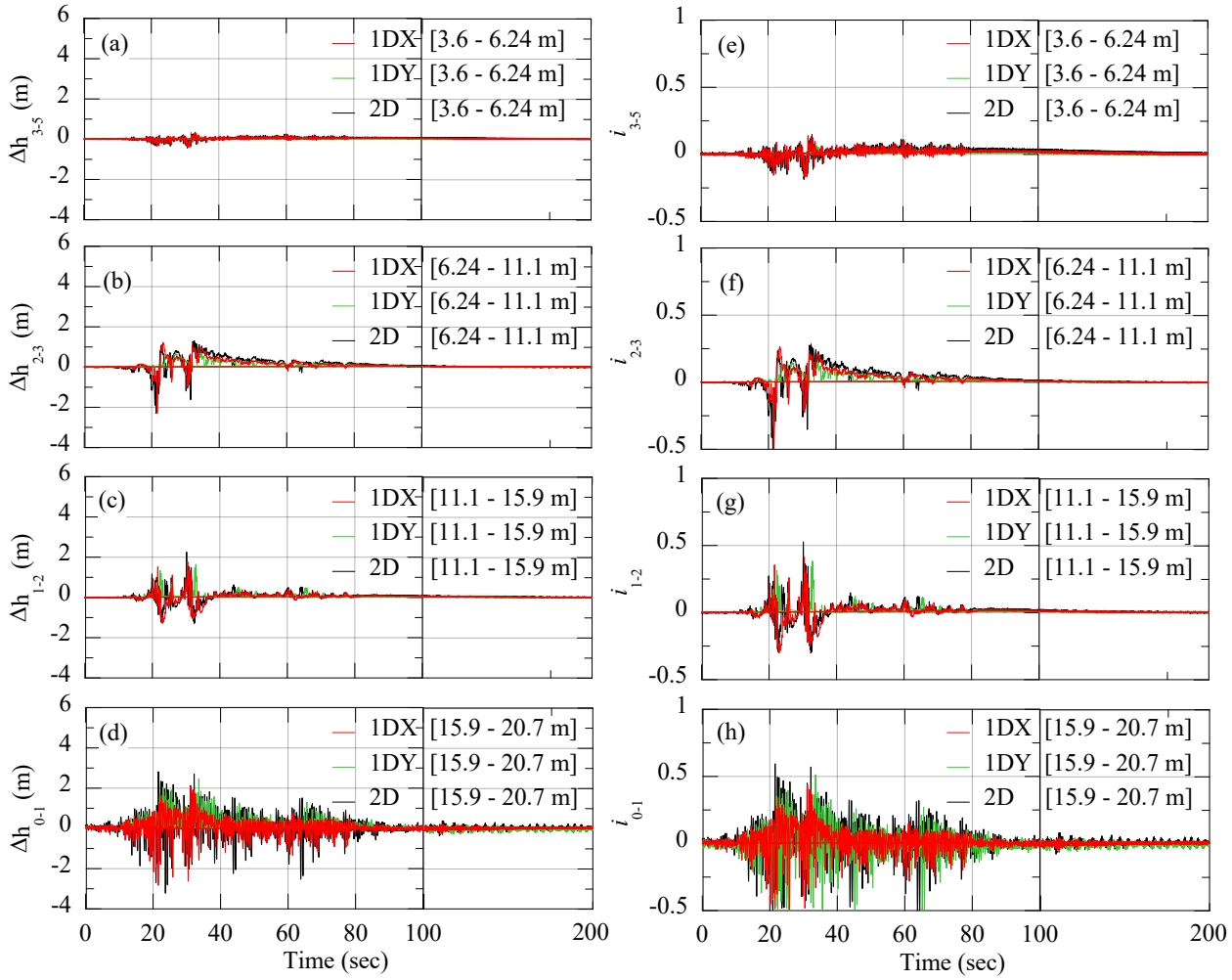

Figure C-447 Variation of total (a) to (d) Total Head Loss with depth (M5-X, Y and 2D); (e) to (h) Shaking induced Hydraulic Gradient (M5-X, Y and 2D)

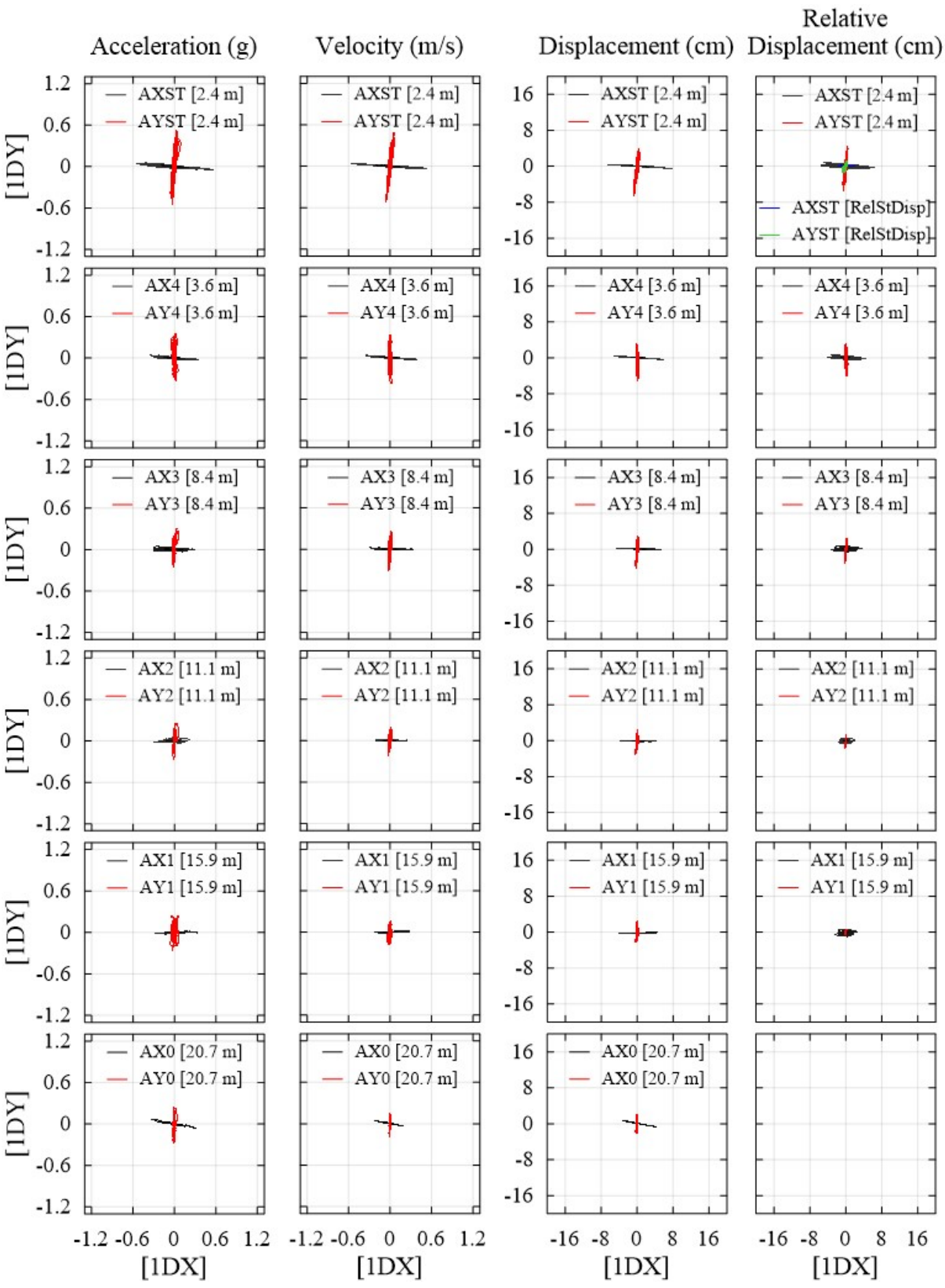

Figure C-448 Recorded input and within model ground motions for acceleration, velocity, displacement and relative displacement for M5-1D [X] and M5-1D [Y]

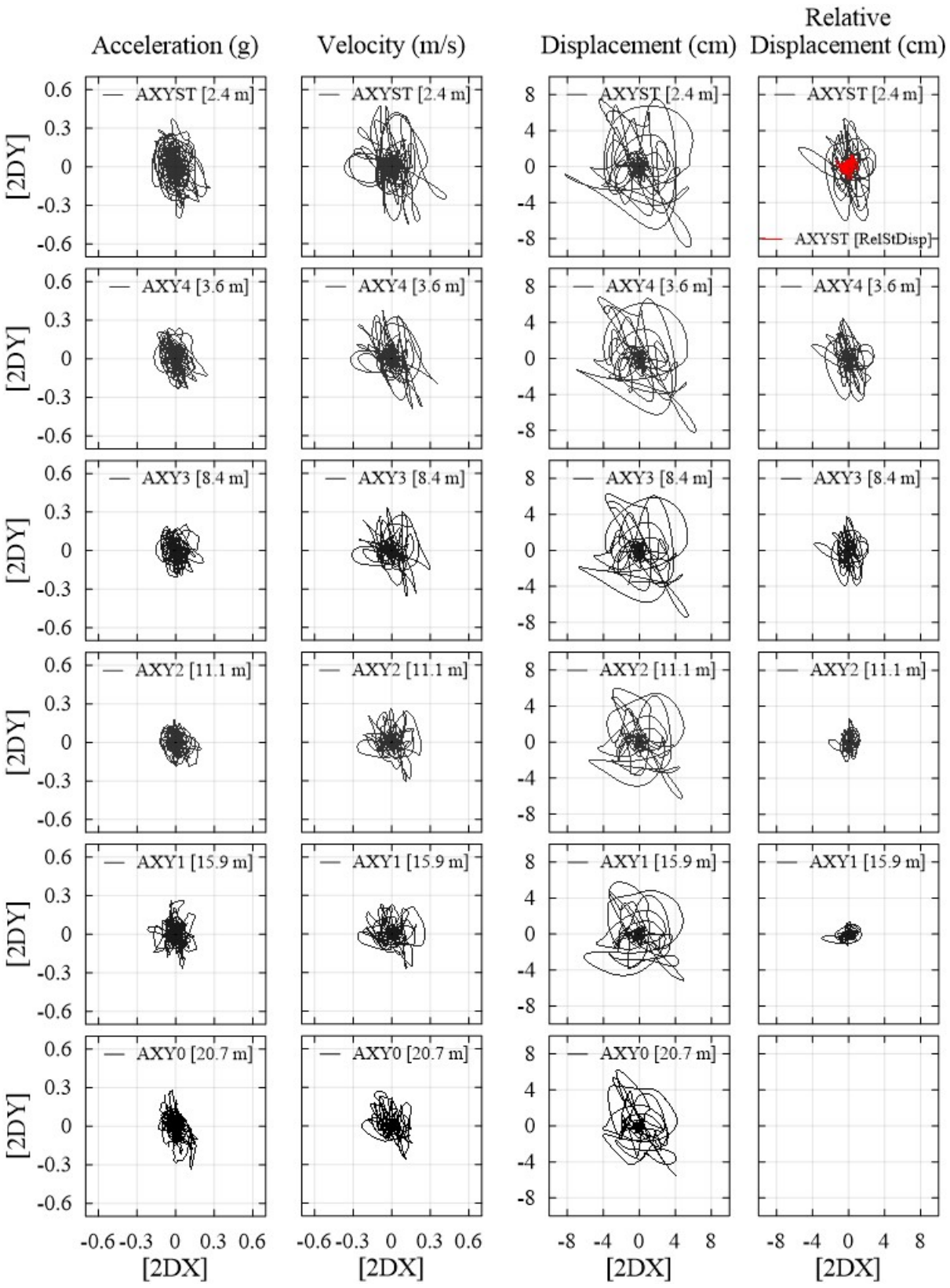

Figure C-449 Recorded input and within model ground motions for acceleration, velocity, displacement and relative displacement for M5-2D

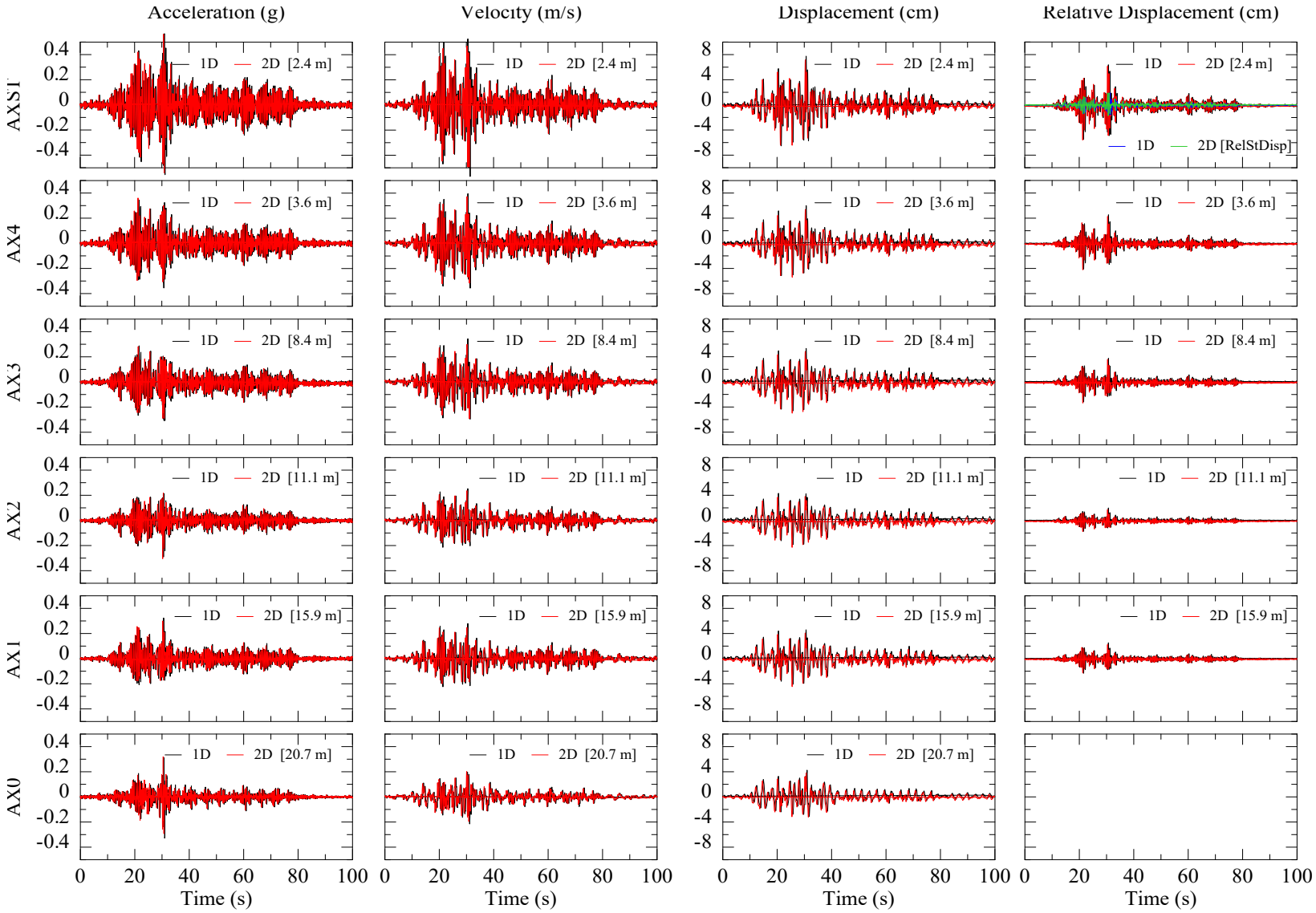

Figure C-450 Recorded input and within model ground motions time histories for acceleration, velocity, displacement and relative displacement for M5-2D [X] and M5-1D [X]

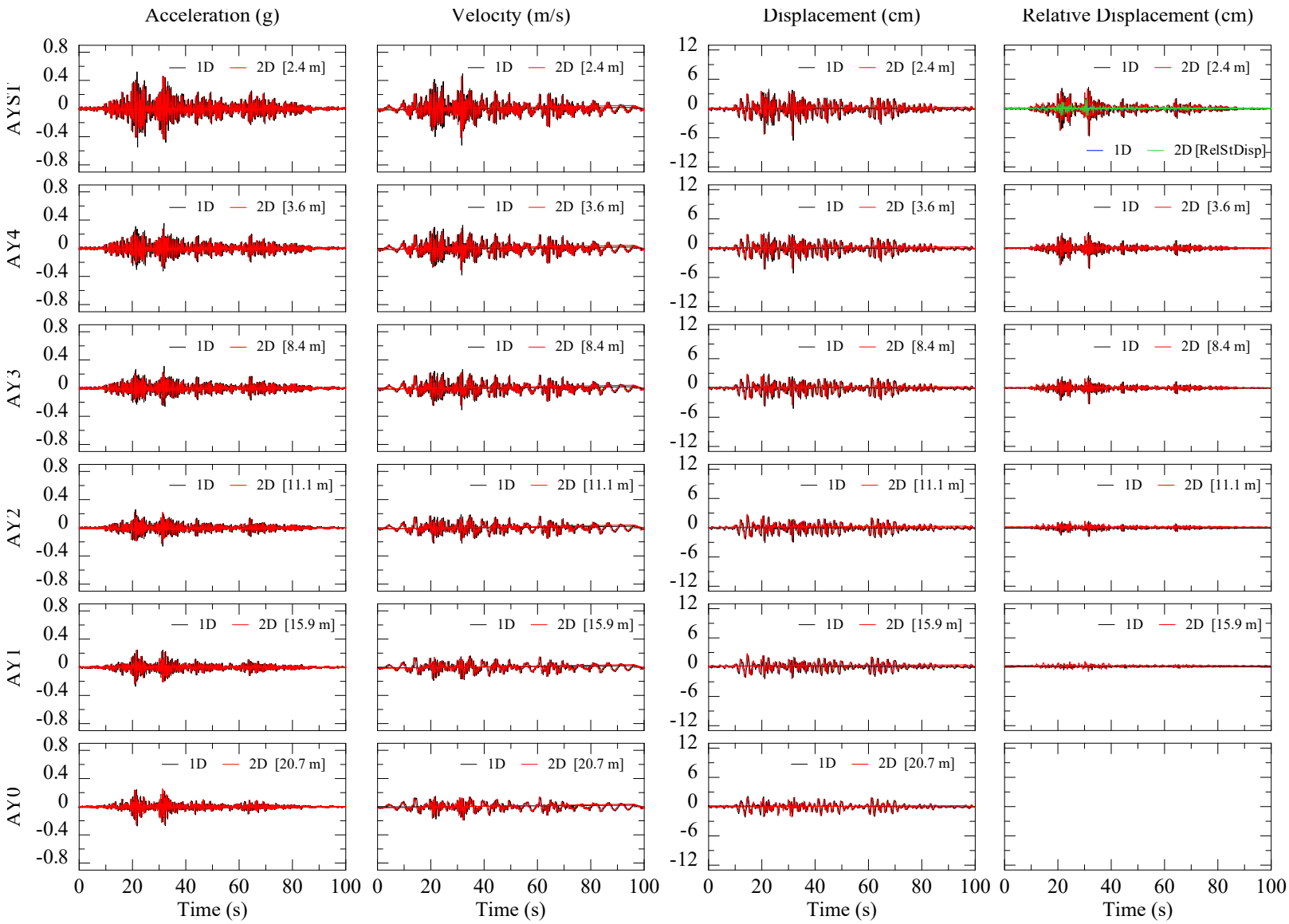

Figure C-451 Recorded input and within model ground motions time histories for acceleration, velocity, displacement and relative displacement for M5-2D [Y] and M5-1D [Y]

1.6.8 Motion 6 (M6)

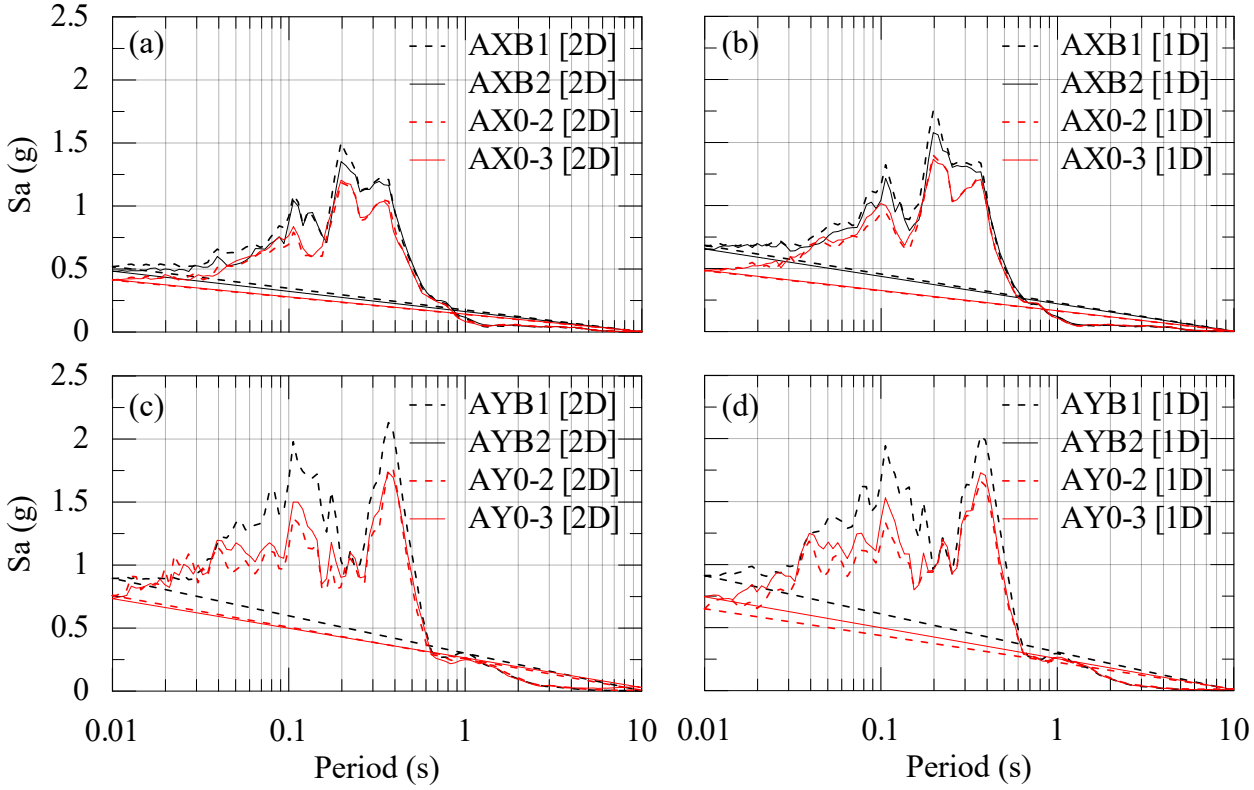

Figure C-452 Comparison of response spectra of 2D laminar container table and within model base input motion for motions (M6-X, Y and 2D).

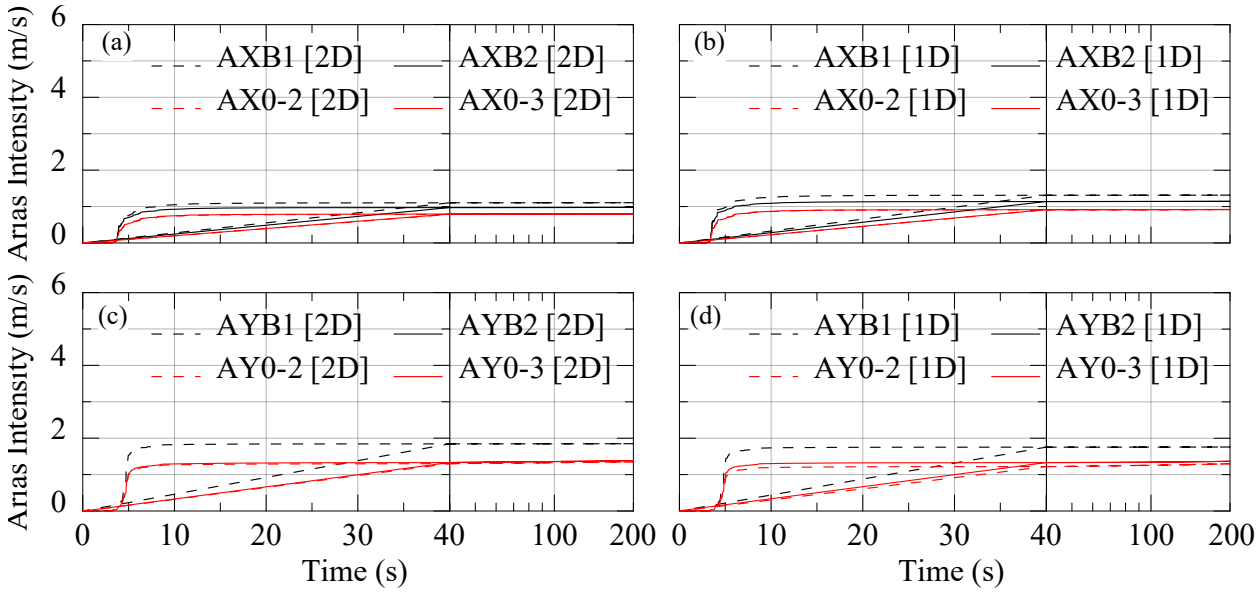

Figure C-453 Comparison of Arias Intensity of 2D laminar container table and within model base input motion for motions (a) M6-2D [X]; (b) M6-2D [Y]; (c) M6-1D [X] and (d) M6-1D [Y]

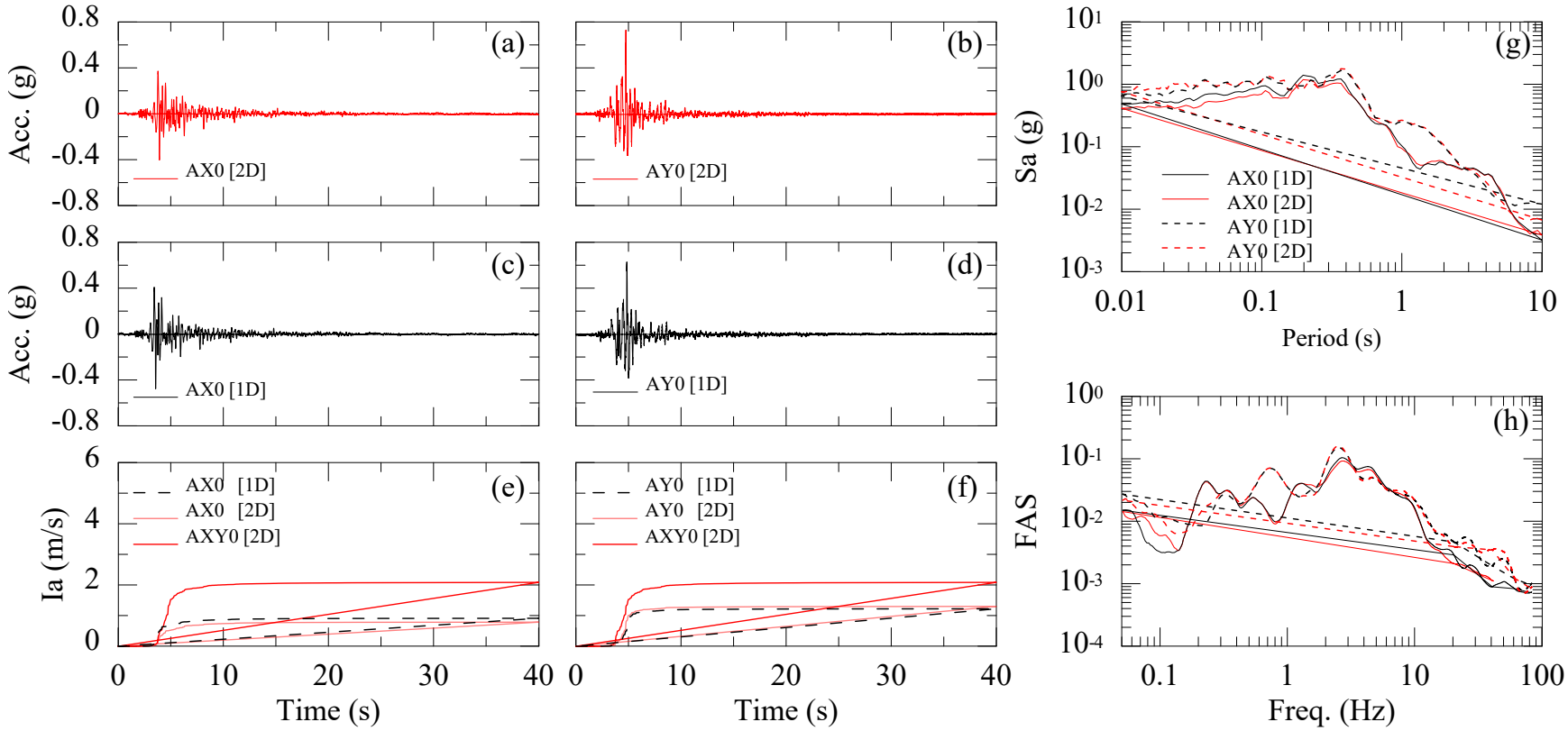

Figure C-454 Recorded input (2D) and 1D (X or Y) ground motions for: (a) M6-2D [X]; (b) M6-2D [Y]; (c) M6-1D [X]; and (d) M6-1D [Y]. Arias Intensity M6 (1D and 2D) for: (e) X direction; and (f) Y direction. Response Spectra (g) M6-2D [X]; M6-2D [Y]; M6-1D [X]; and M6-1D [Y]. Smoothed Fourier amplitude spectra (FAS) (h) M6-2D [X]; M6-2D [Y]; M6-1D [X]; and M6-1D [Y].

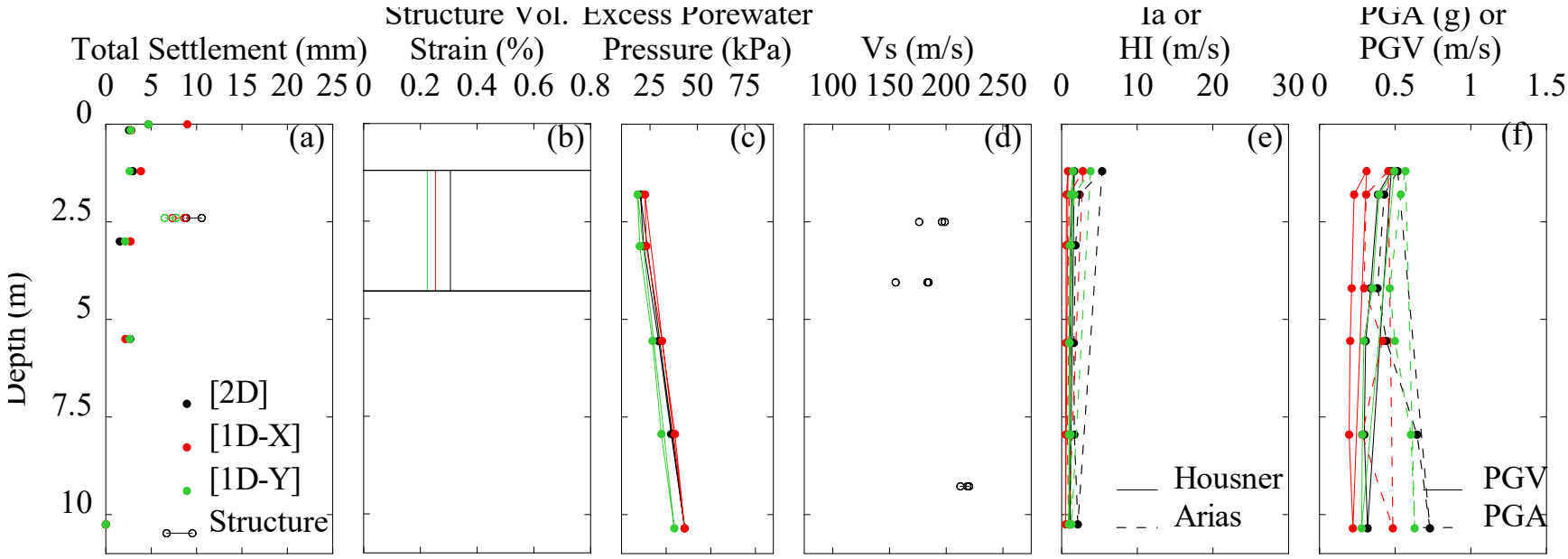

Figure C-455 Recorded or computed profiles for input motion M6-X, Y, and 2D. (a) Total settlement; (b) structure volumetric strain; (c) excess pore water pressure; (d) shear wave velocity; (e) Arias and Housner intensities; and (f) PGA and PGV.

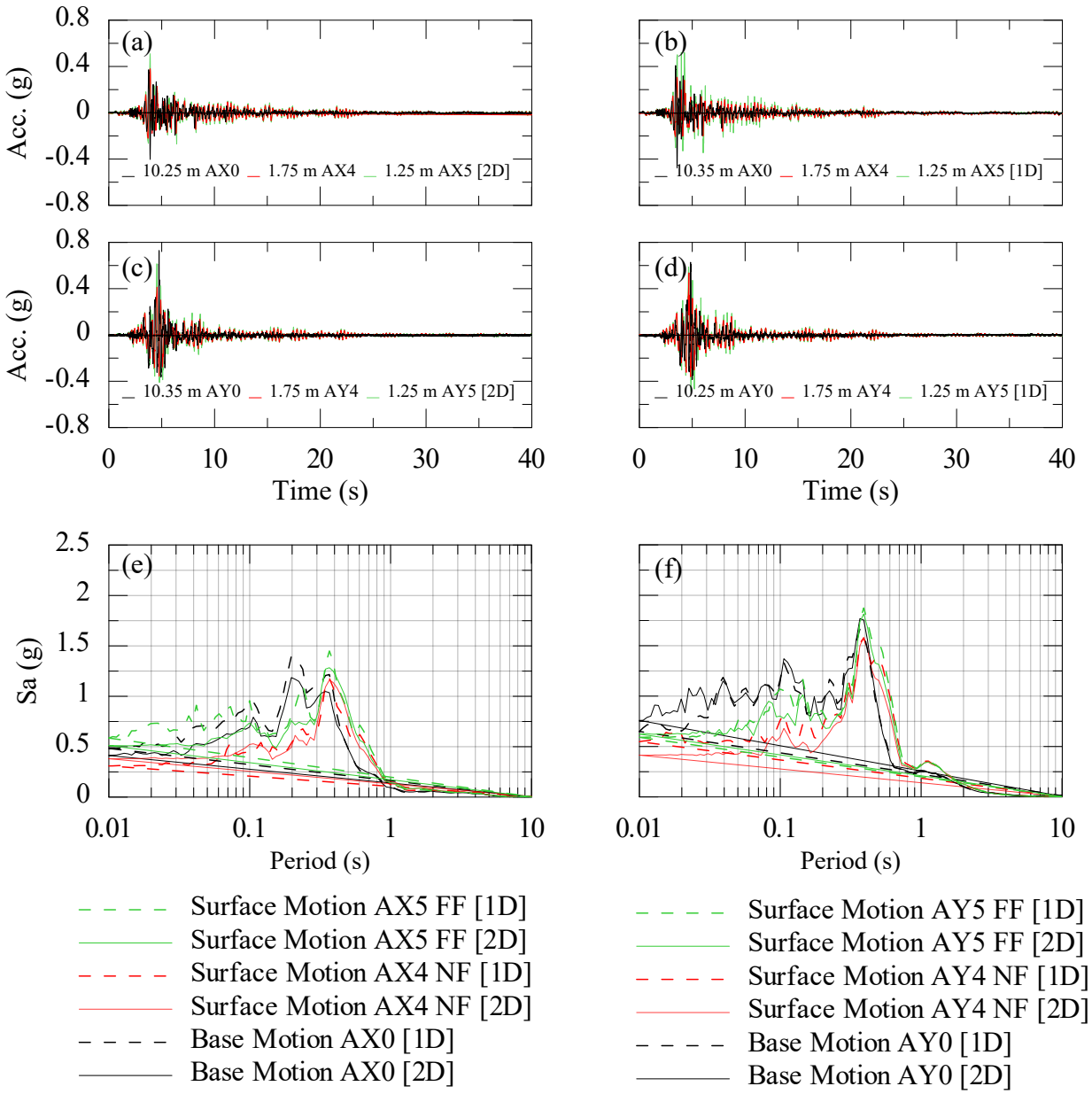

Figure C-456 Recorded input and near surface ground motions: (a) M6-2D [X]; (b) M6-1D [X]; (c) M6-2D [Y]; and (d) M6-1D [Y]. Computed response spectra from Near Field Test [PT3] for motions M6 (1D and 2D) for: (e) X direction; and (f) Y direction.

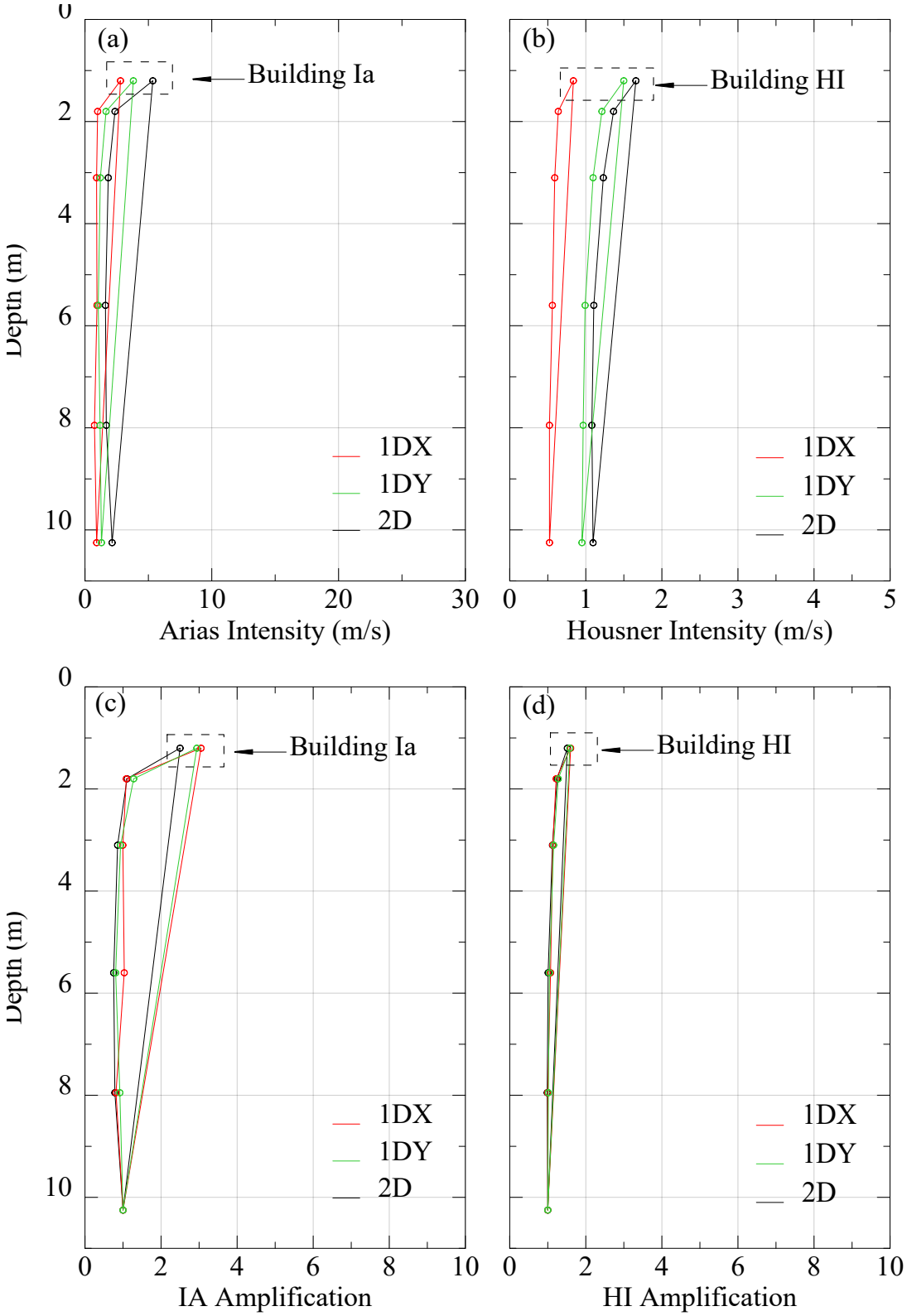

Figure C-457 Variation of total (a) Arias Intensity (M6-X,Y and 2D) ; (b) Housner Intensity (M6-X,Y and 2D) (c) Arias Intensity Amplification Factor (M6-X,Y and 2D); and (d) Housner Intensity Amplification Factor (M6-X,Y and 2D).

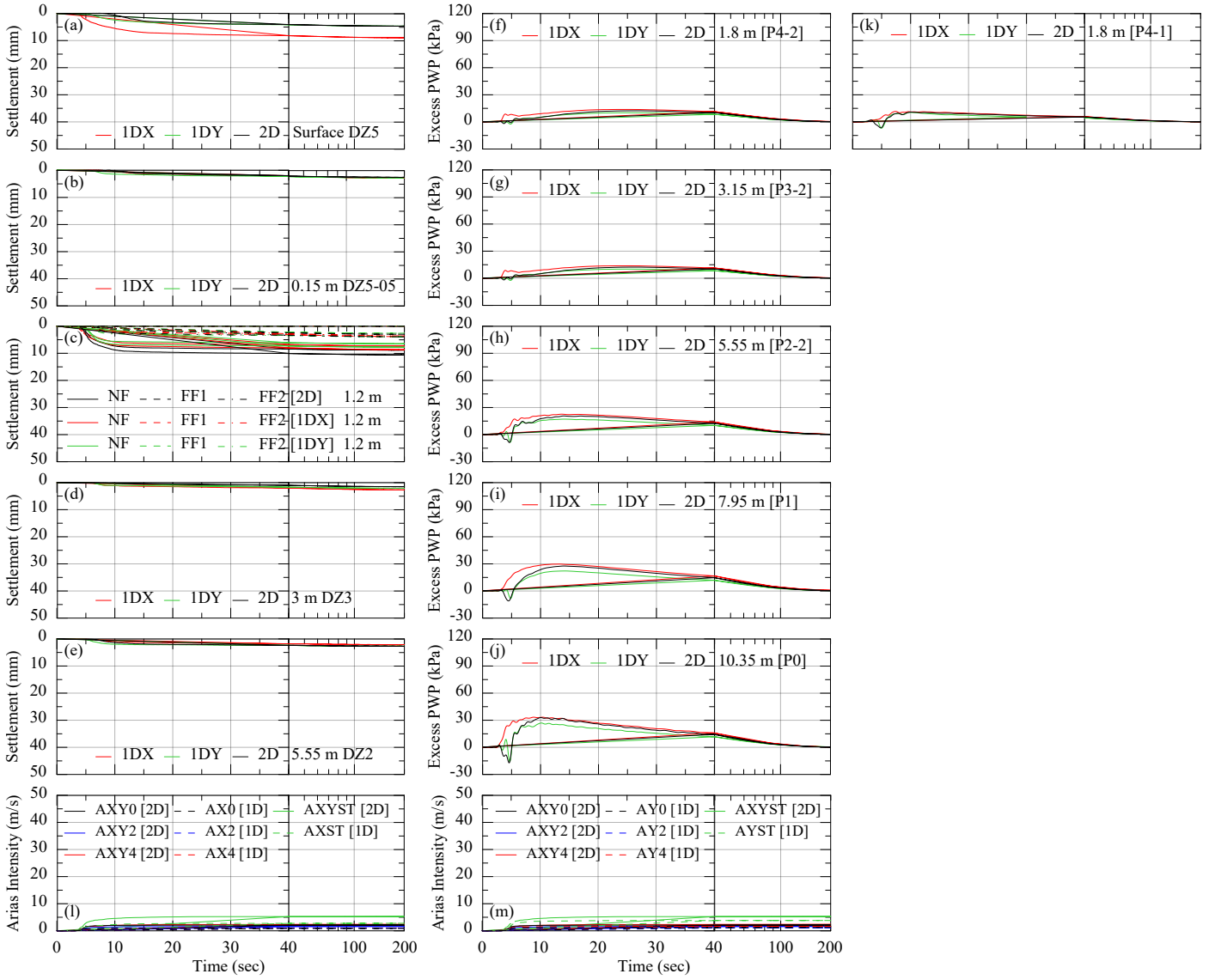

Figure C-458 Variation of total (a) to (e) Settlement with depth (M6-X,Y and 2D) ; (f) to (k) Excess pore water pressure (M6-X,Y and 2D) (l) and (m) Arias Intensity along model (M6-X,Y and 2D).

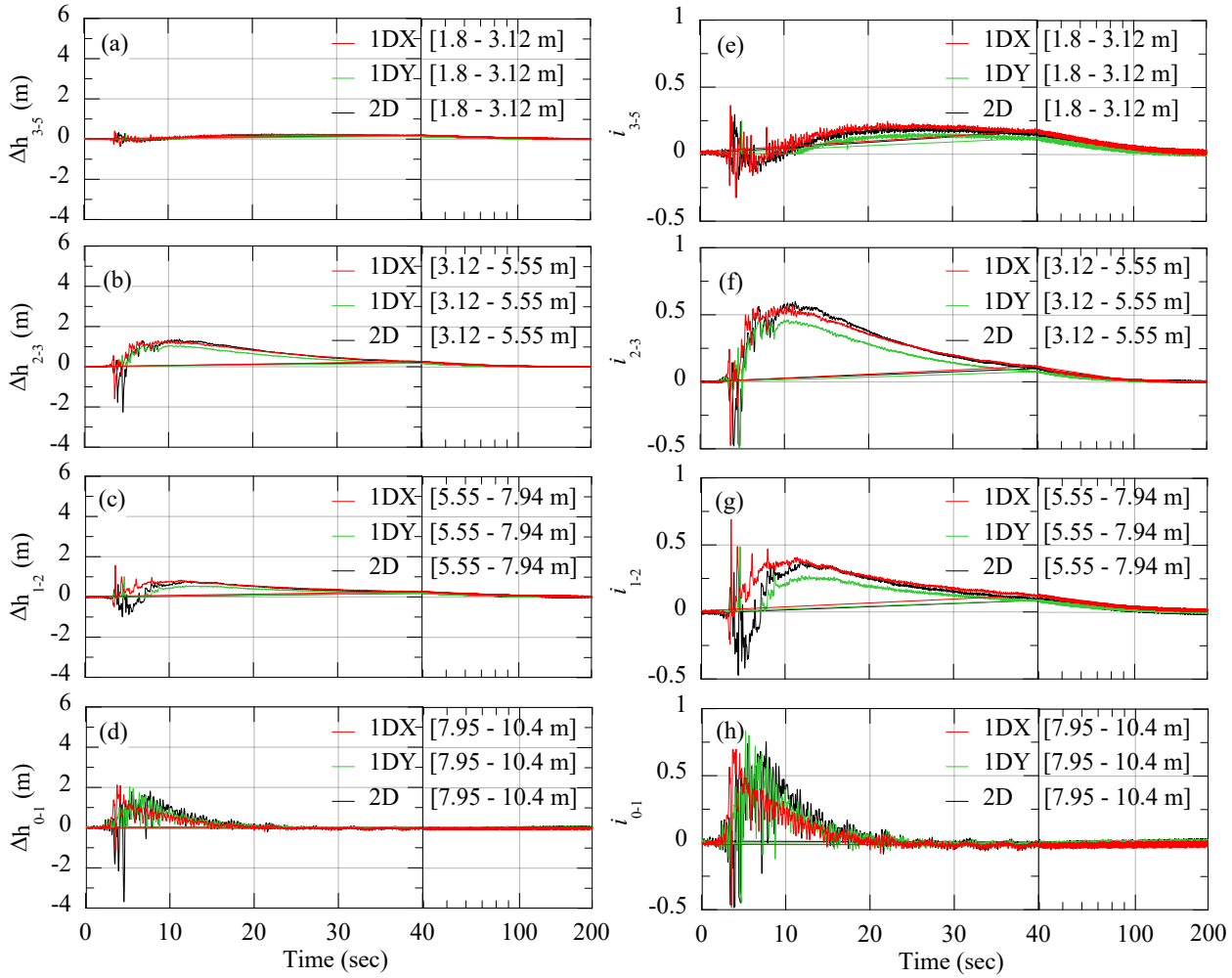

Figure C-459 Variation of total (a) to (d) Total Head Loss with depth (M6-X, Y and 2D); (e) to (h) Shaking induced Hydraulic Gradient (M6-X, Y and 2D)

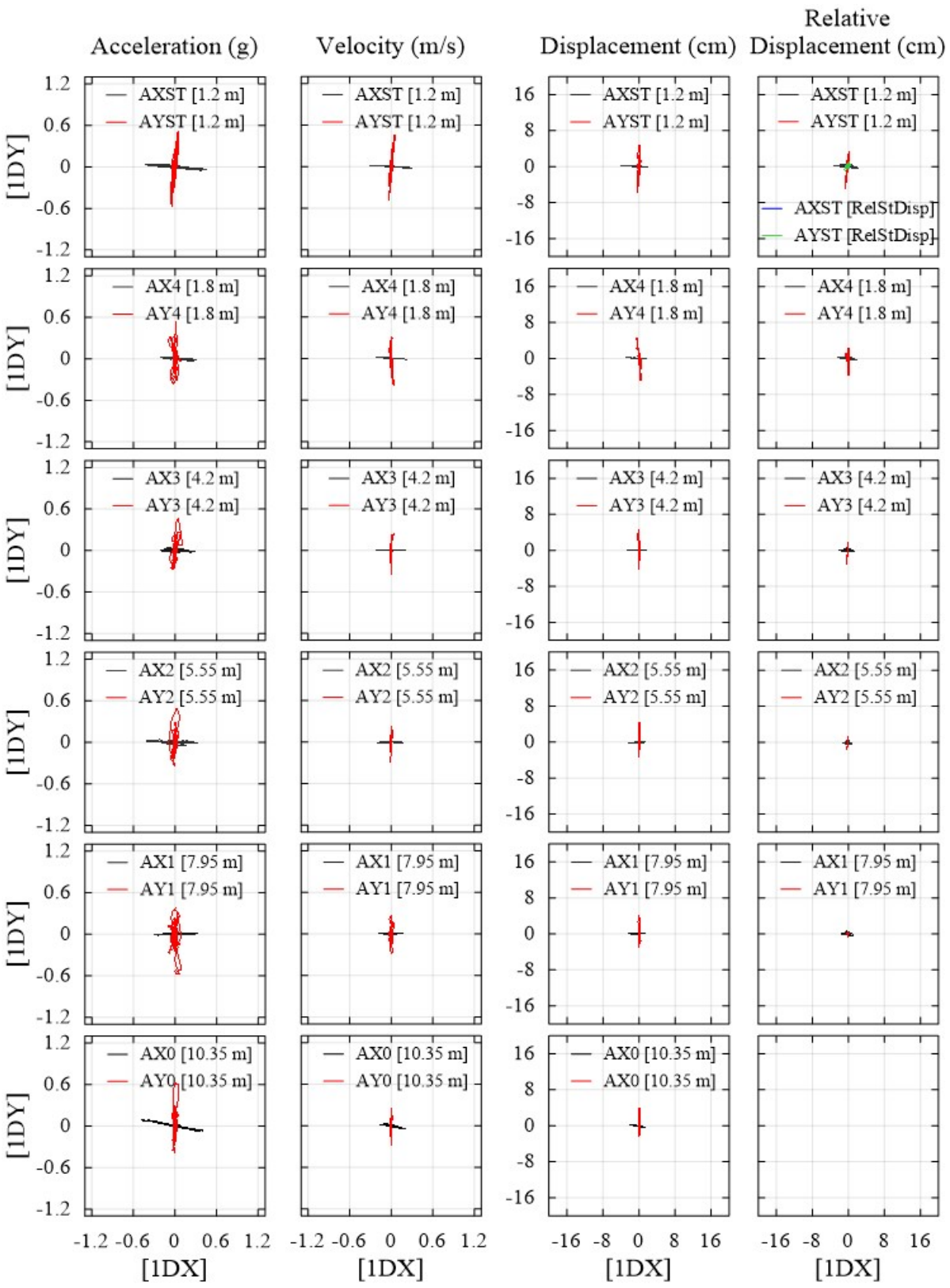

Figure C-460 Recorded input and within model ground motions for acceleration, velocity, displacement and relative displacement for M6-1D [X] and M6-1D [Y]

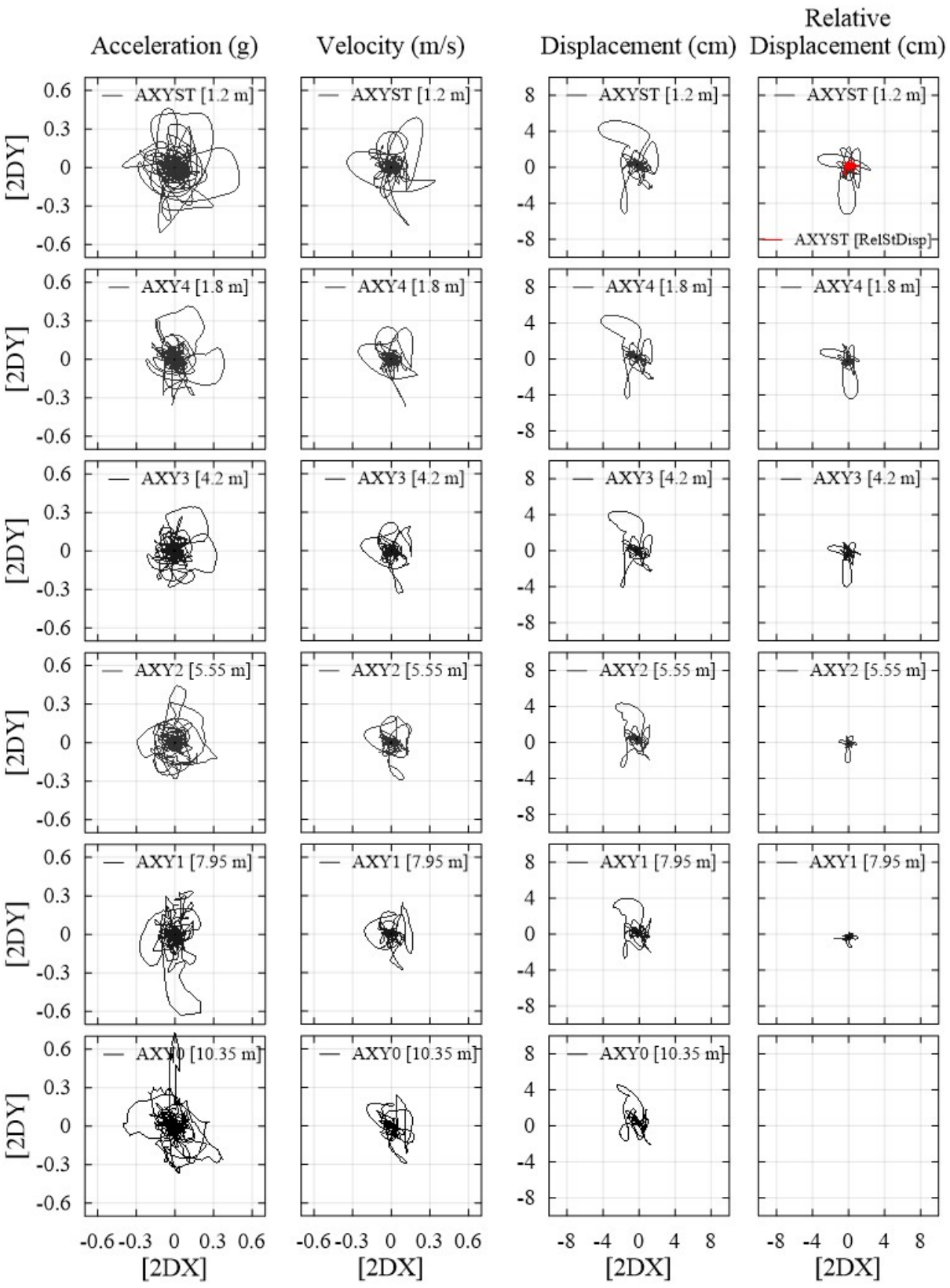

Figure C-461 Recorded input and within model ground motions for acceleration, velocity, displacement and relative displacement for M6-2D

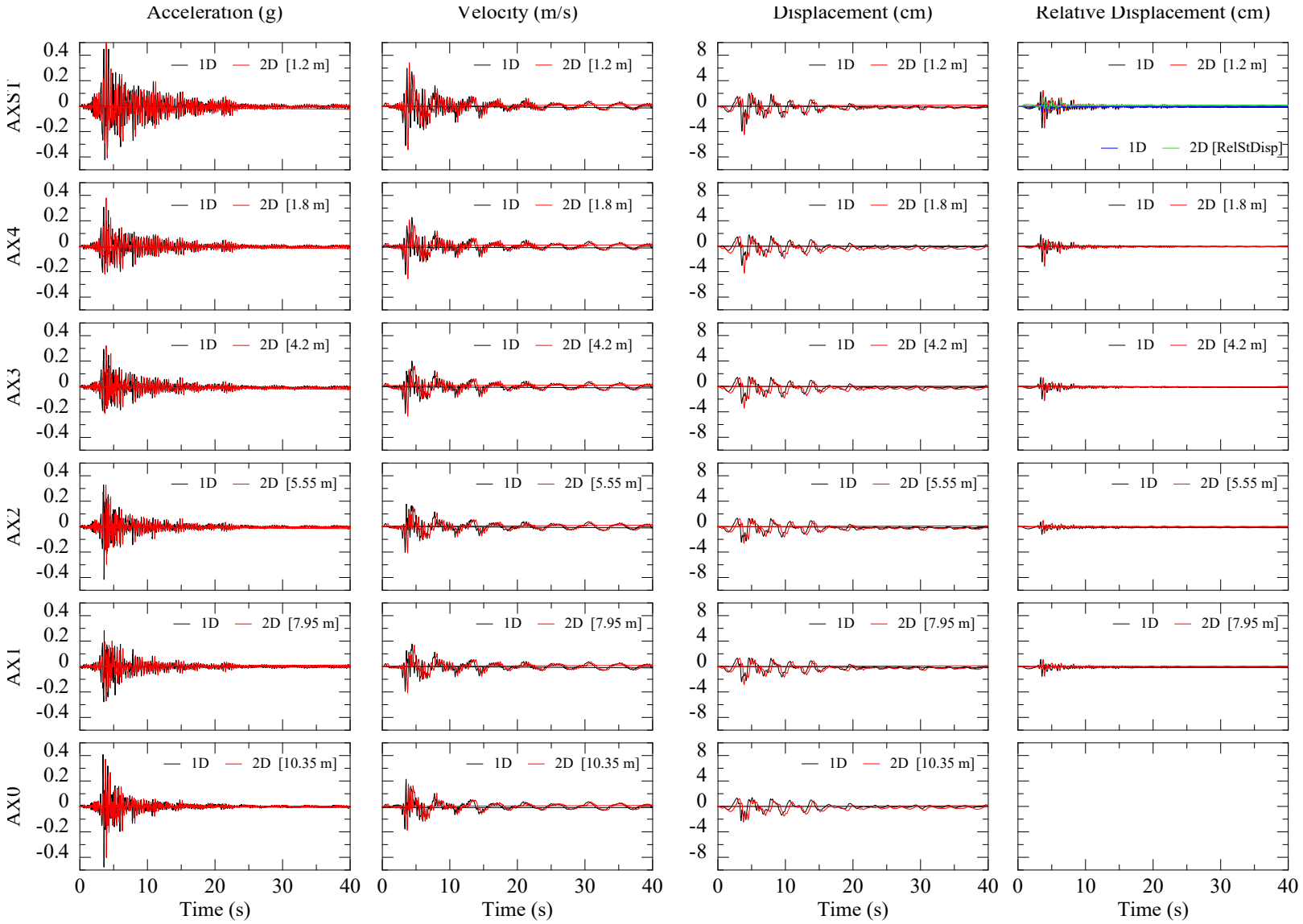

Figure C-462 Recorded input and within model ground motions time histories for acceleration, velocity, displacement and relative displacement for M6-2D [X] and M6-1D [X]

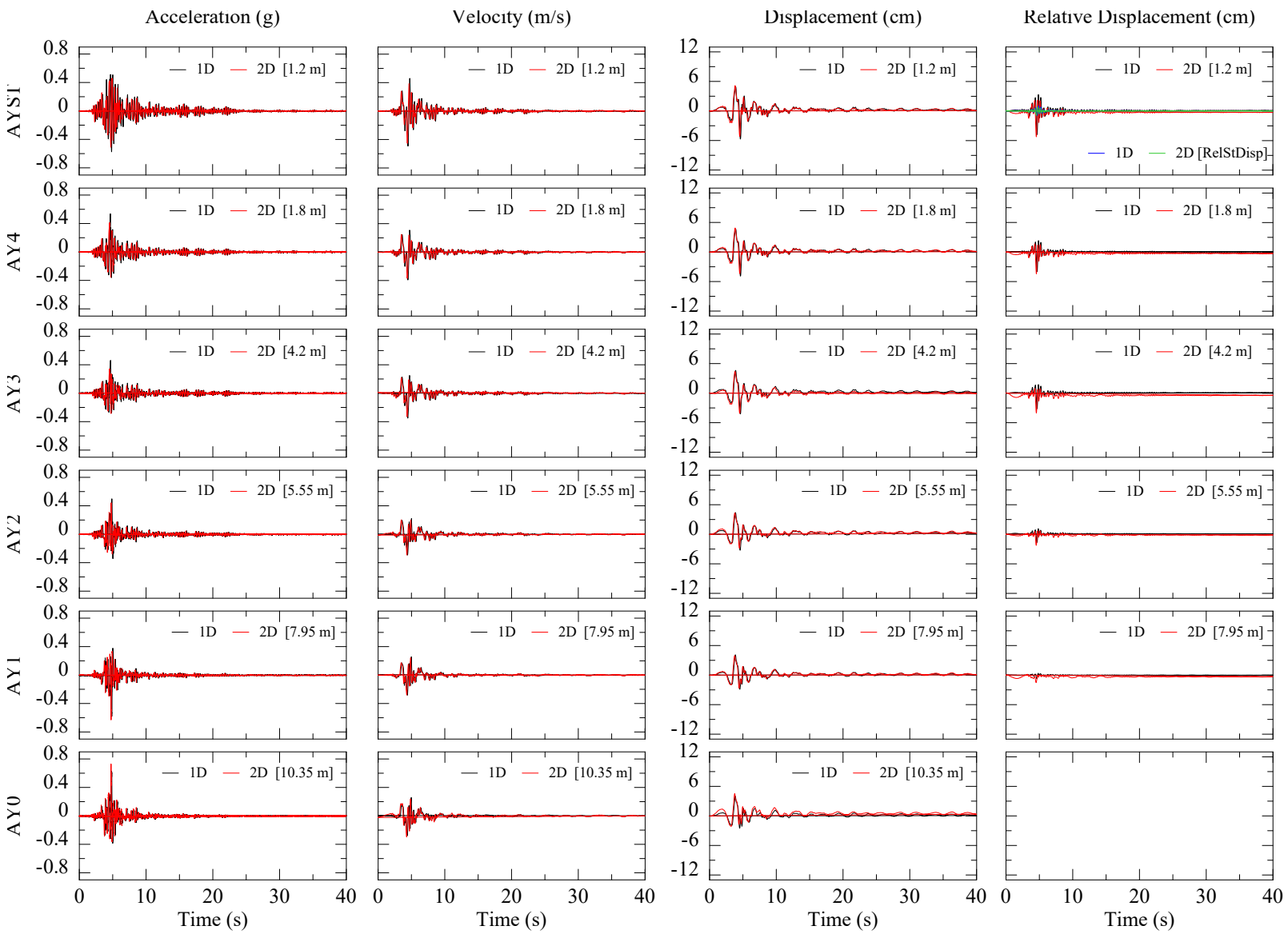

Figure C-463 Recorded input and within model ground motions time histories for acceleration, velocity, displacement and relative displacement for M6-2D [Y] and M6-1D [Y]

1.6.9 Motion 7 (M7)

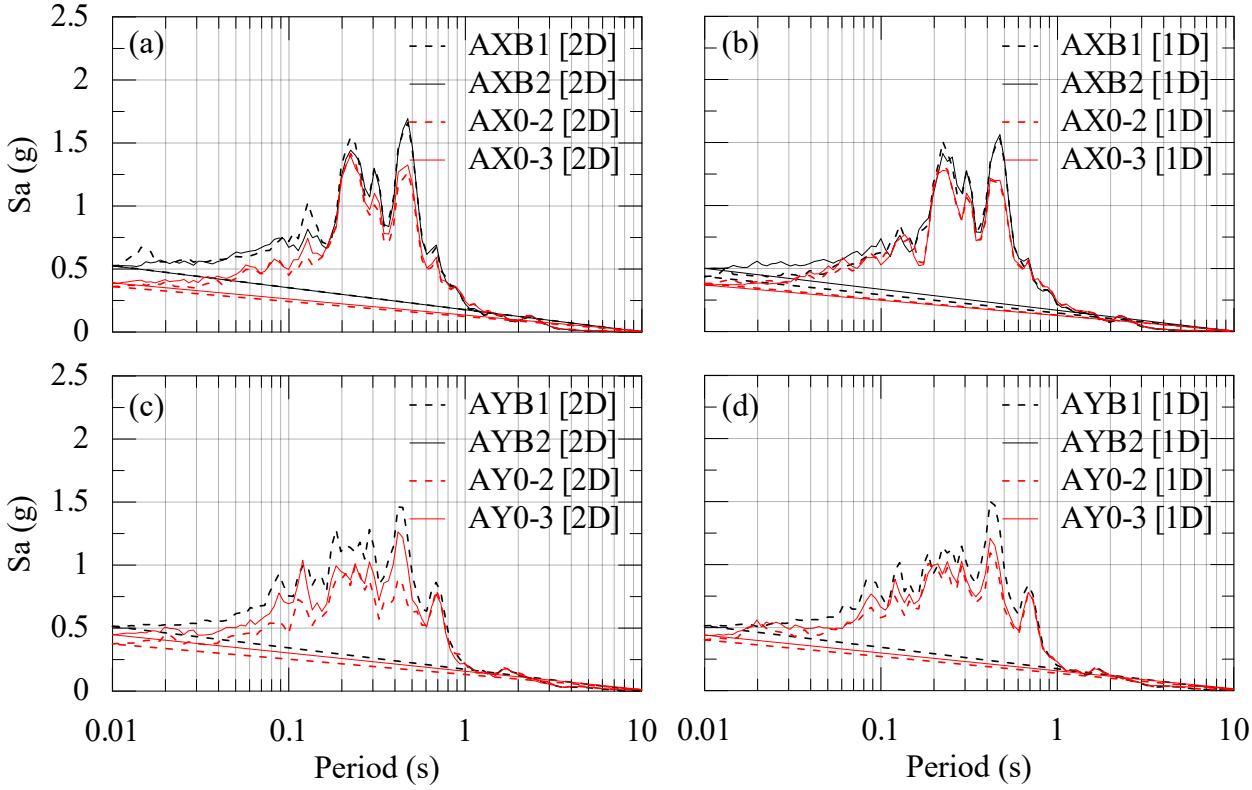

Figure C-464 Comparison of response spectra of 2D laminar container table and within model base input motion for motions (M7-X, Y and 2D).

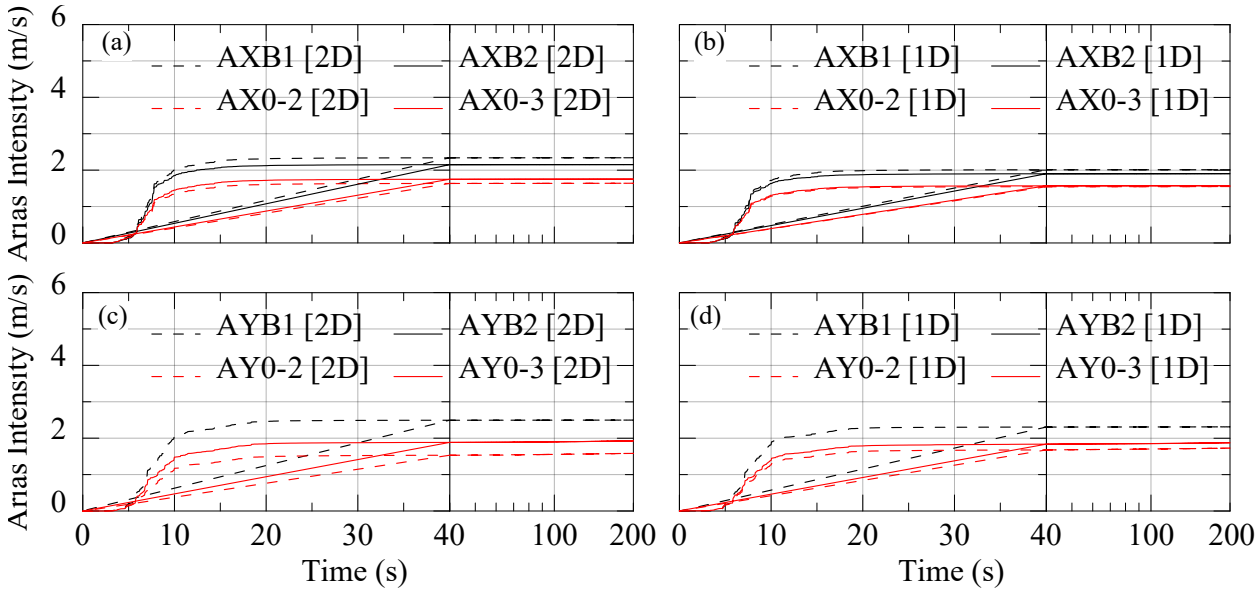

Figure C-465 Comparison of Arias Intensity of 2D laminar container table and within model base input motion for motions (a) M7-2D [X]; (b) M7-2D [Y]; (c) M7-1D [X] and (d) M7-1D [Y]

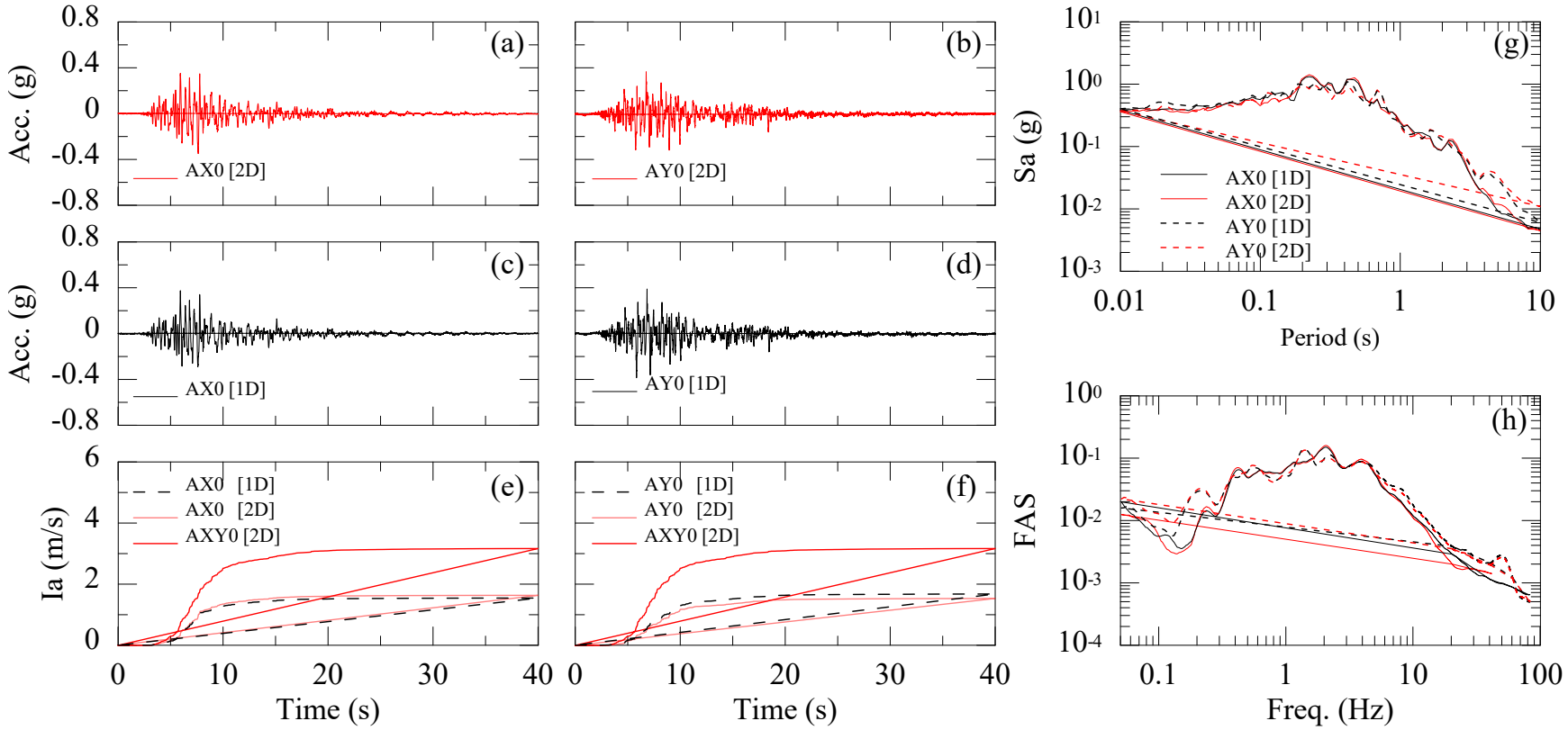

Figure C-466 Recorded input (2D) and 1D (X or Y) ground motions for: (a) M7-2D [X]; (b) M7-2D [Y]; (c) M7-1D [X]; and (d) M7-1D [Y]. Arias Intensity M7 (1D and 2D) for: (e) X direction; and (f) Y direction. Response Spectra (g) M7-2D [X]; M7-2D [Y]; M7-1D [X]; and M7-1D [Y]. Smoothed Fourier amplitude spectra (FAS) (h) M7-2D [X]; M7-2D [Y]; M7-1D [X]; and M7-1D [Y].

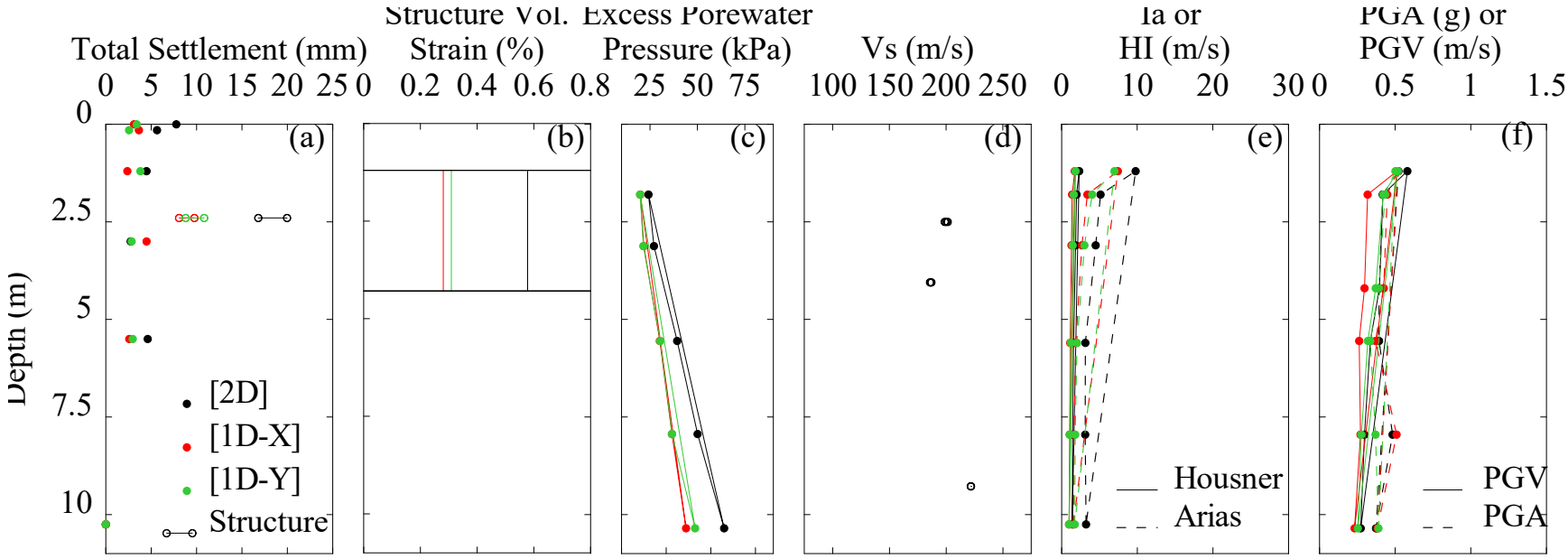

Figure C-467 Recorded or computed profiles for input motion M7-X, Y, and 2D. (a) Total settlement; (b) structure volumetric strain; (c) excess pore water pressure; (d) shear wave velocity; (e) Arias and Housner intensities; and (f) PGA and PGV.

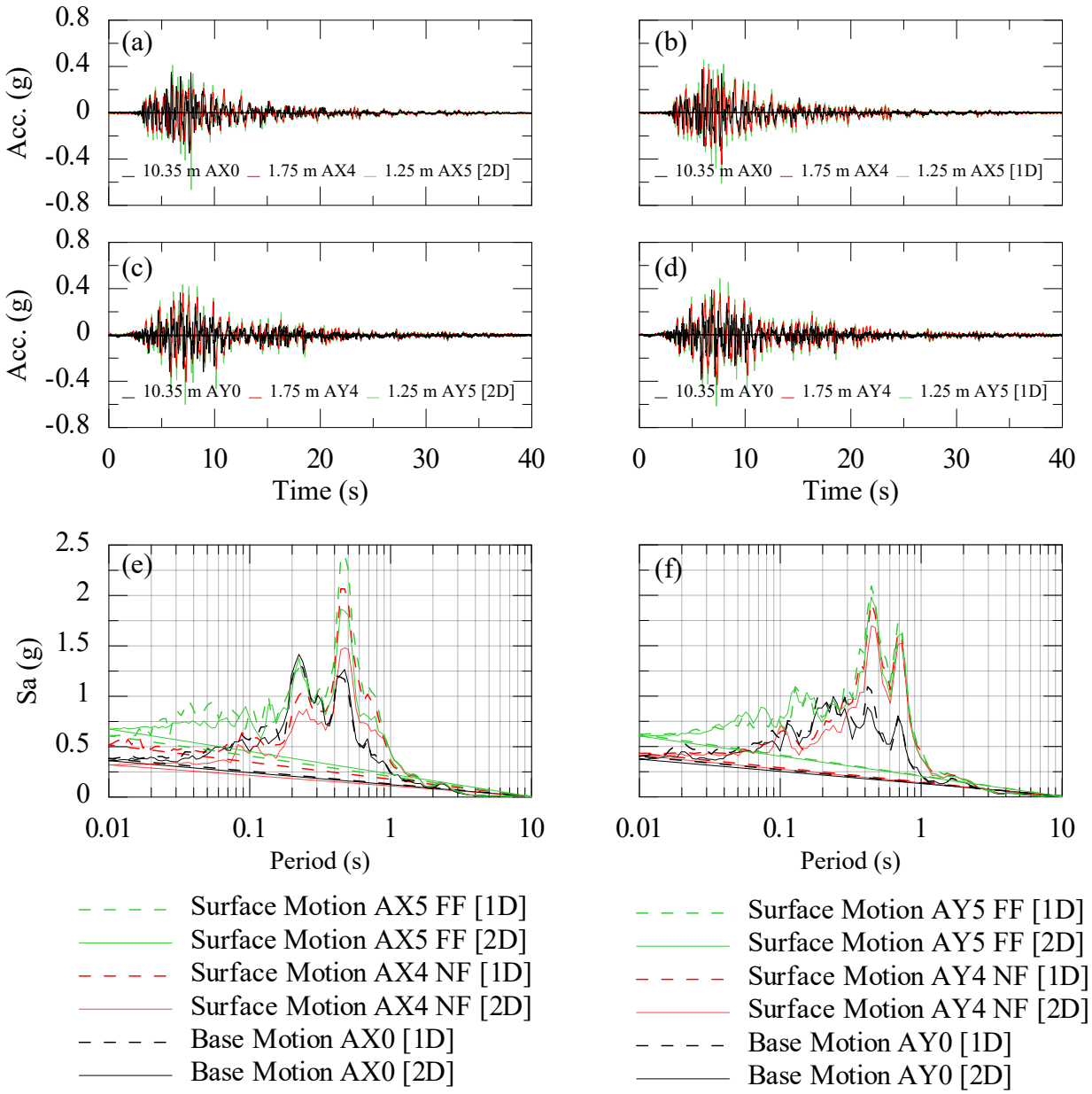

Figure C-468 Recorded input and near surface ground motions: (a) M7-2D [X]; (b) M7-1D [X]; (c) M7-2D [Y]; and (d) M7-1D [Y]. Computed response spectra from Near Field Test [PT3] for motions M7 (1D and 2D) for: (e) X direction; and (f) Y direction.

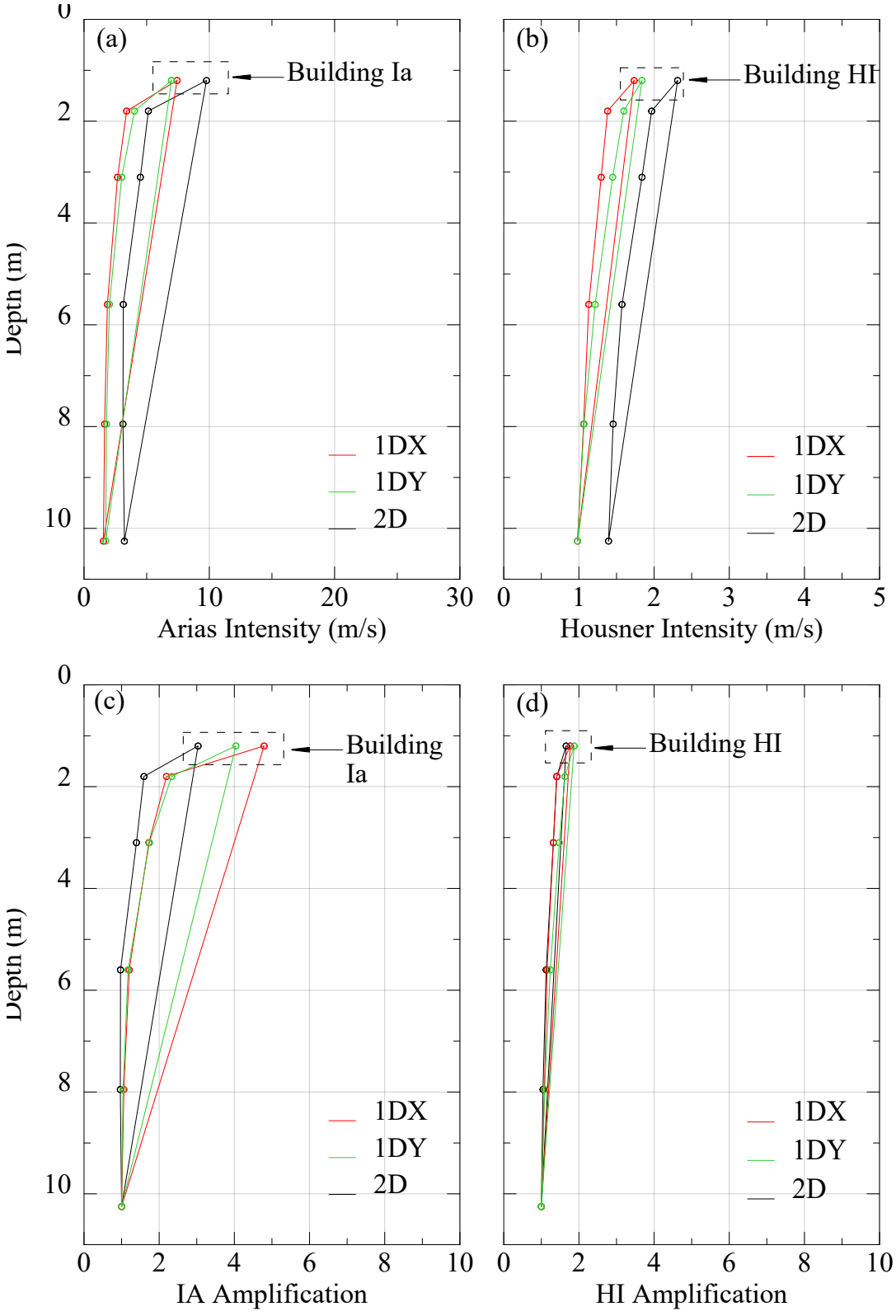

Figure C-469 Variation of total (a) Arias Intensity (M7-X,Y and 2D) ; (b) Housner Intensity (M7-X,Y and 2D) (c) Arias Intensity Amplification Factor (M7-X,Y and 2D); and (d) Housner Intensity Amplification Factor (M7-X,Y and 2D).

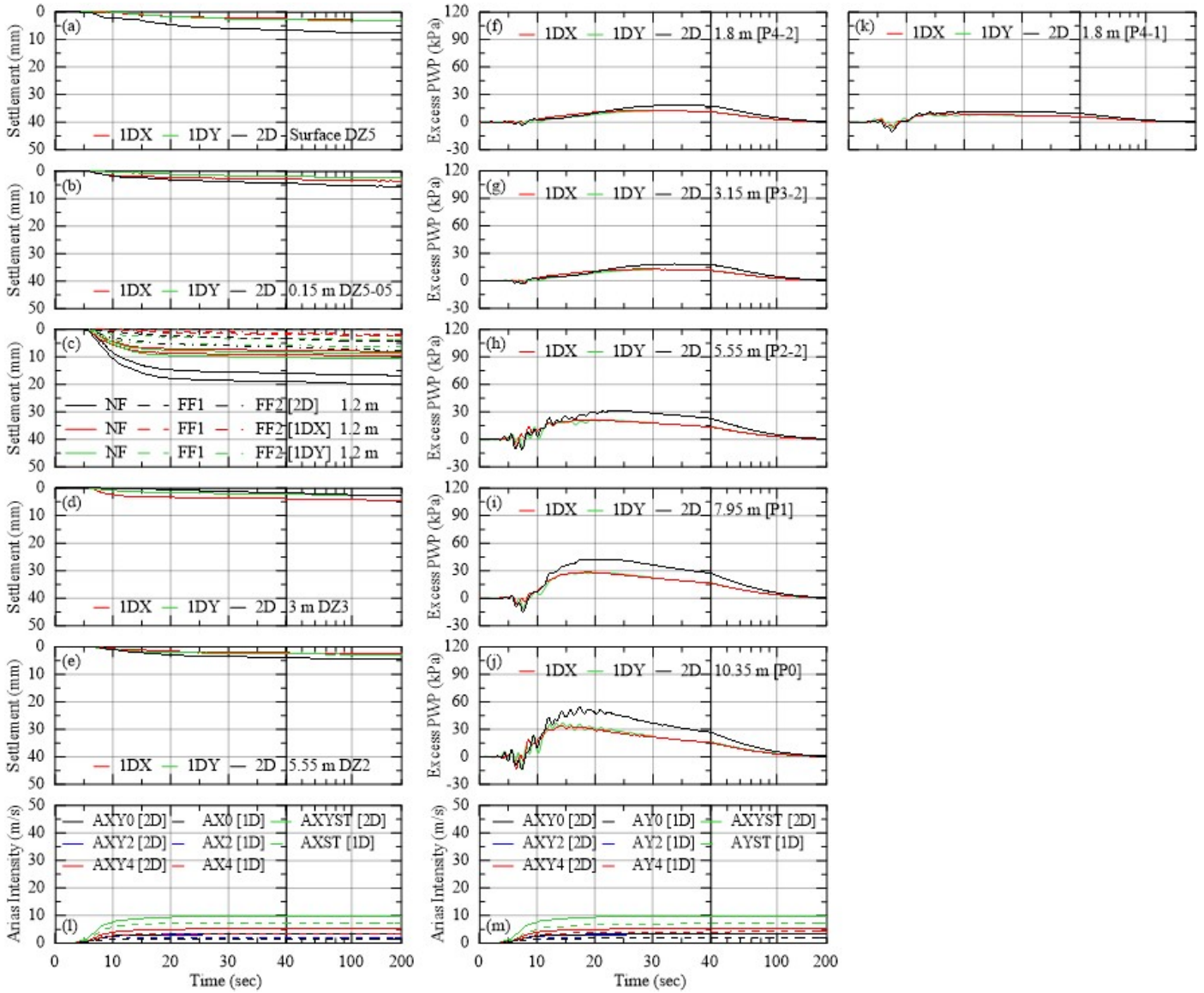

Figure C-470 Variation of total (a) to (e) Settlement with depth (M7-X,Y and 2D) ; (f) to (k) Excess pore water pressure (M7-X,Y and 2D) (l) and (m) Arias Intensity along model (M7-X,Y and 2D).

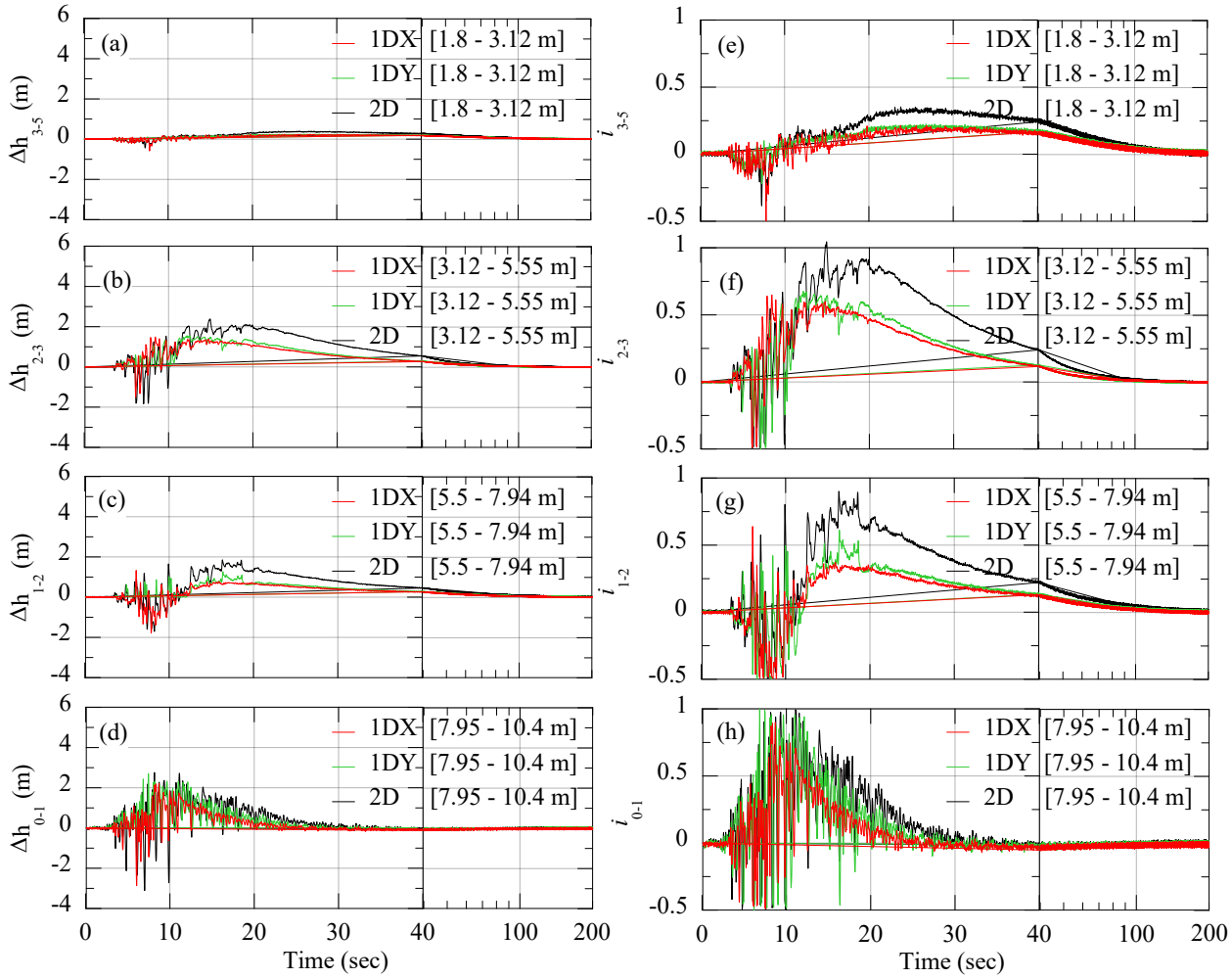

Figure C-471 Variation of total (a) to (d) Total Head Loss with depth (M7-X, Y and 2D); (e) to (h) Shaking induced Hydraulic Gradient (M7-X, Y and 2D)

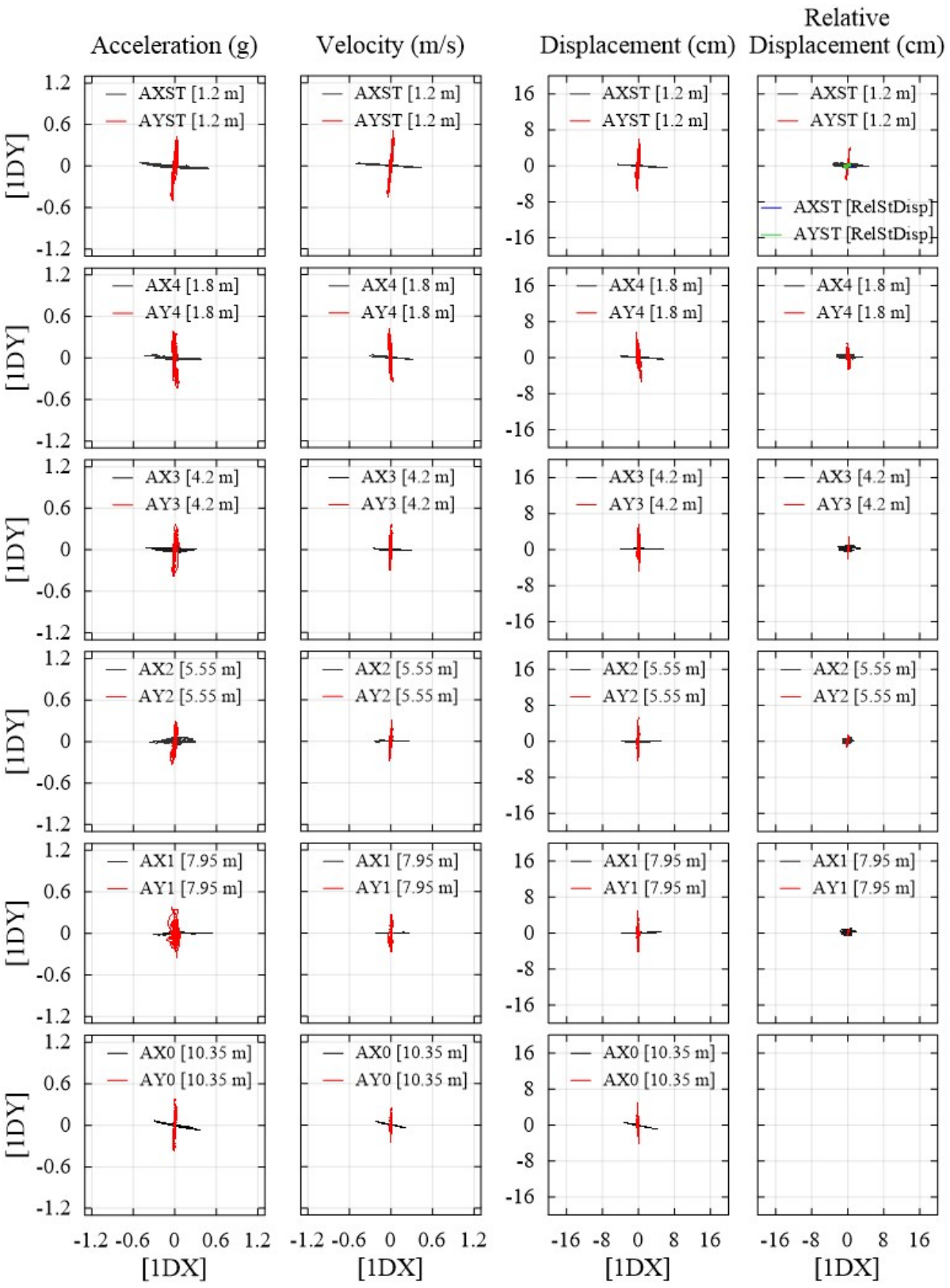

Figure C-472 Recorded input and within model ground motions for acceleration, velocity, displacement and relative displacement for M7-1D [X] and M7-1D [Y]

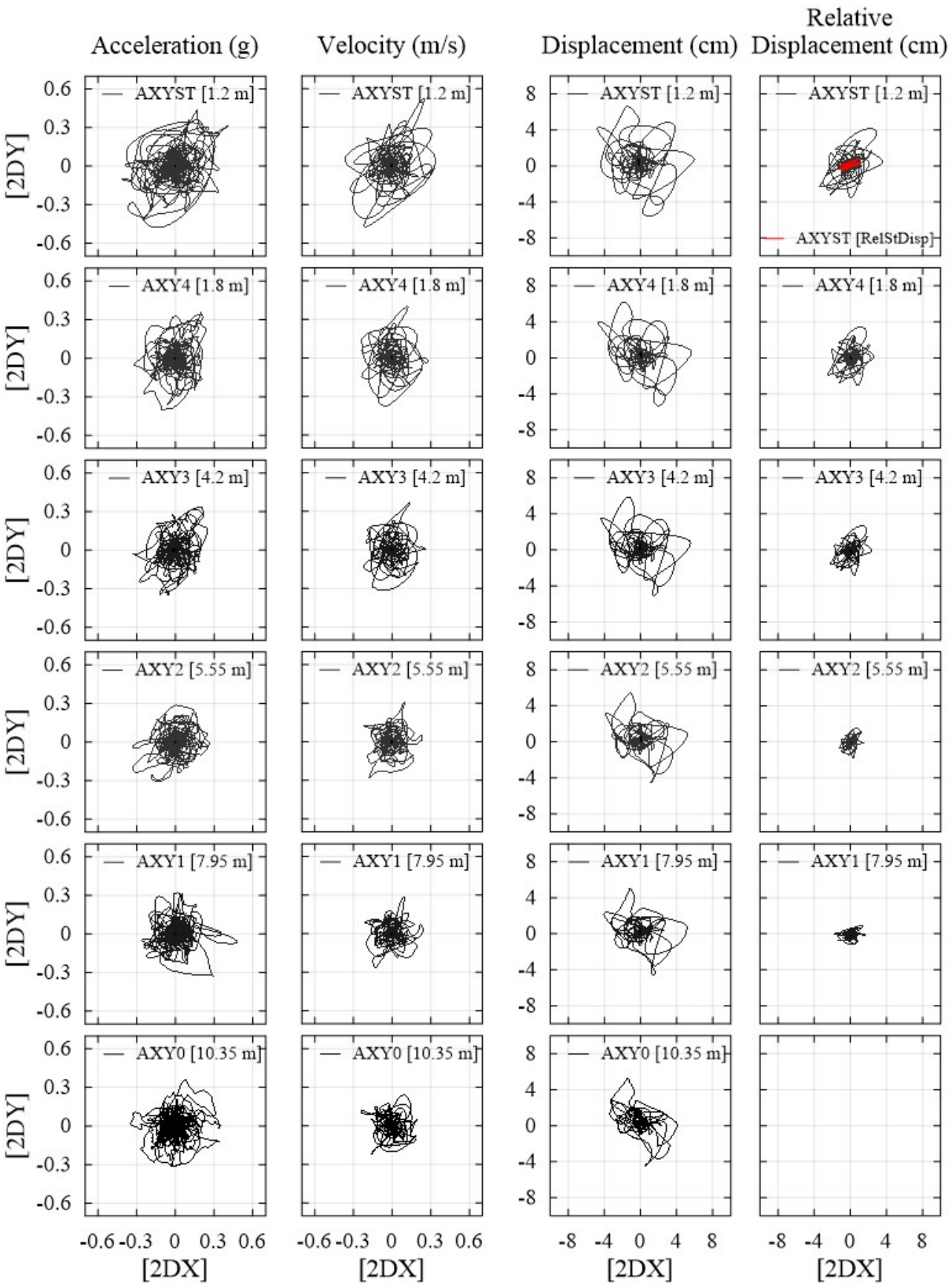

Figure C-473 Recorded input and within model ground motions for acceleration, velocity, displacement and relative displacement for M7-2D

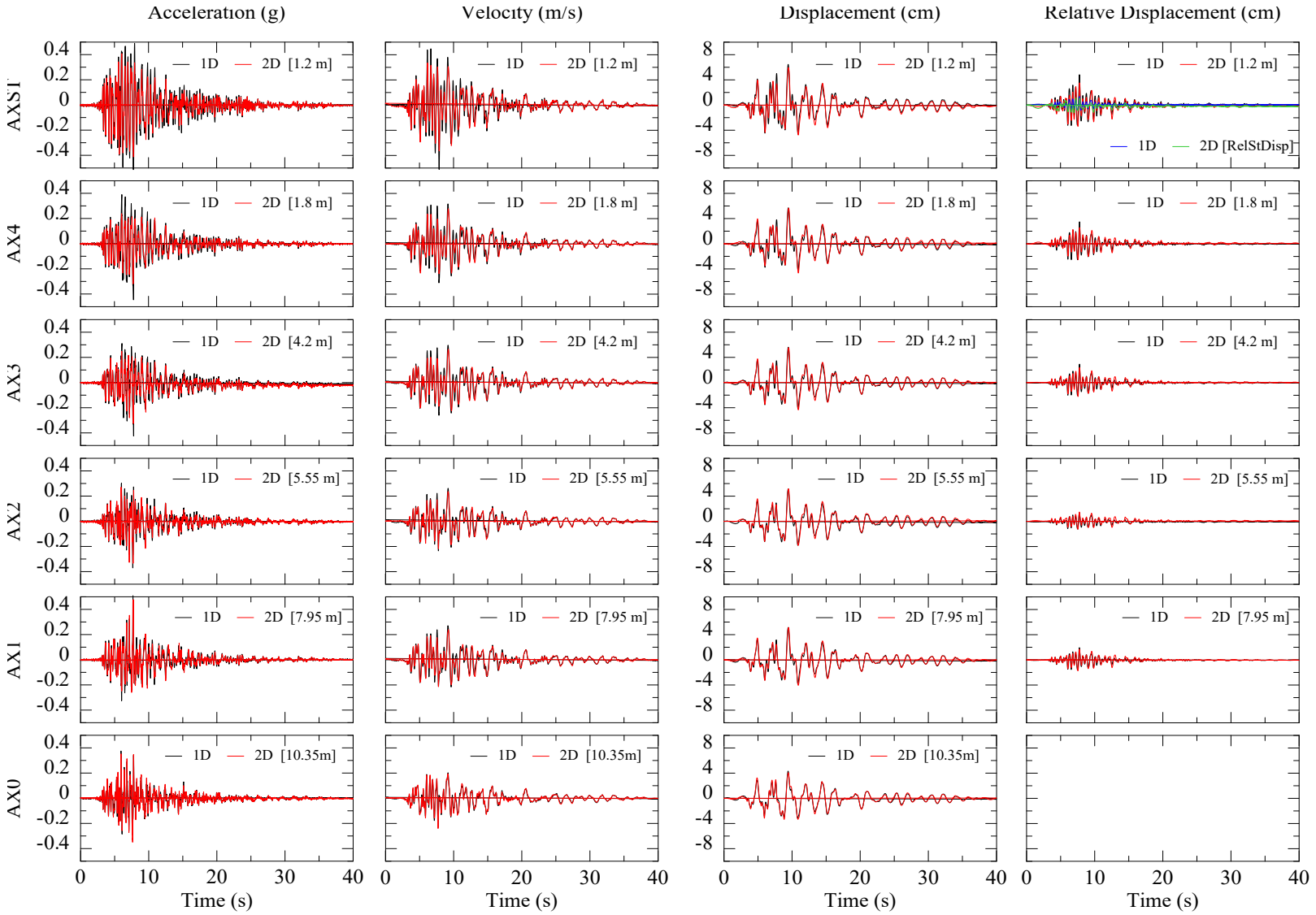

Figure C-474 Recorded input and within model ground motions time histories for acceleration, velocity, displacement and relative displacement for M7-2D [X] and M7-1D [X]

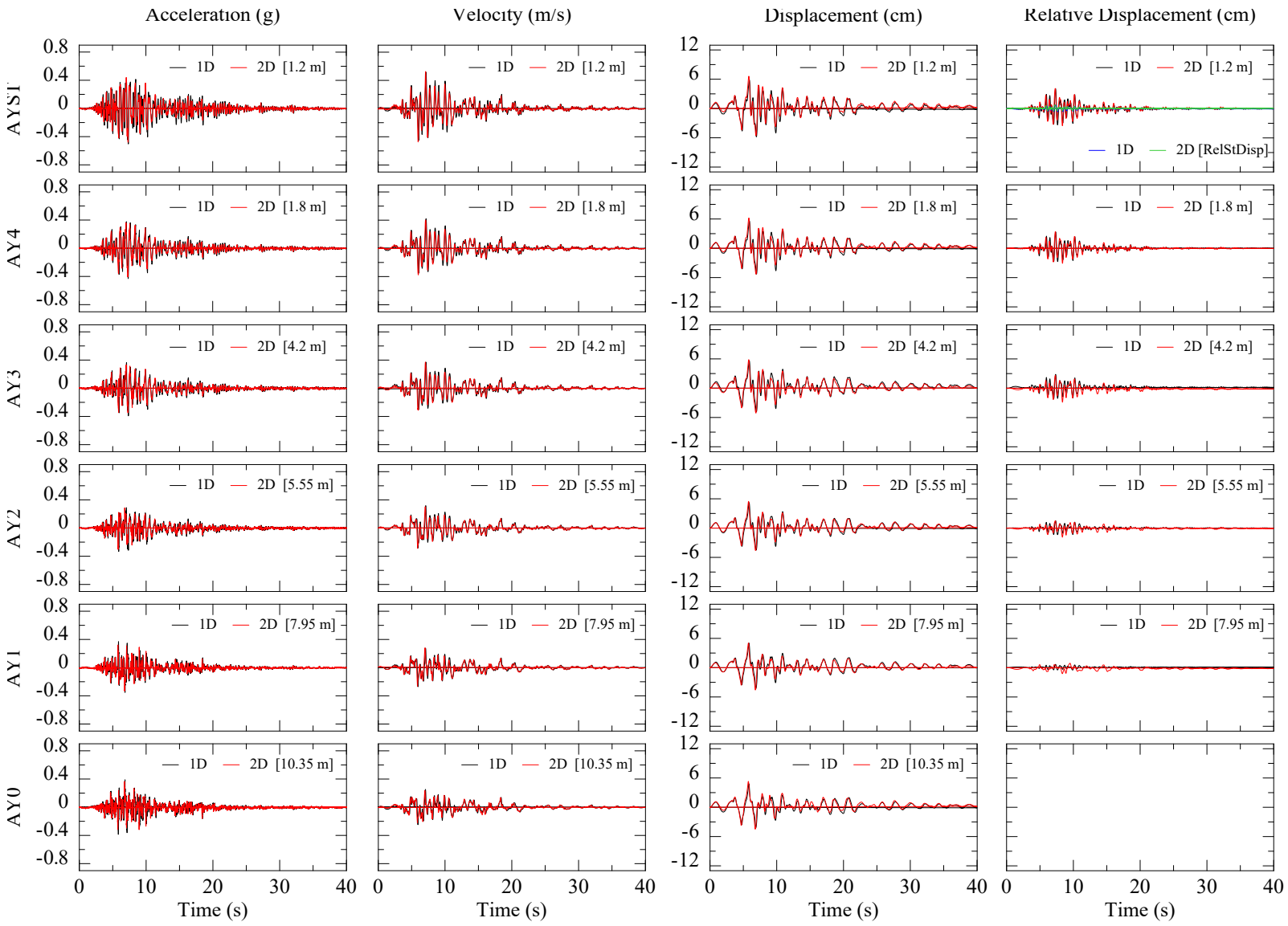

Figure C-475 Recorded input and within model ground motions time histories for acceleration, velocity, displacement and relative displacement for M7-2D [Y] and M7-1D [Y]

1.7 Test: Dr95NF (PT2) - Bender Elements Measurements

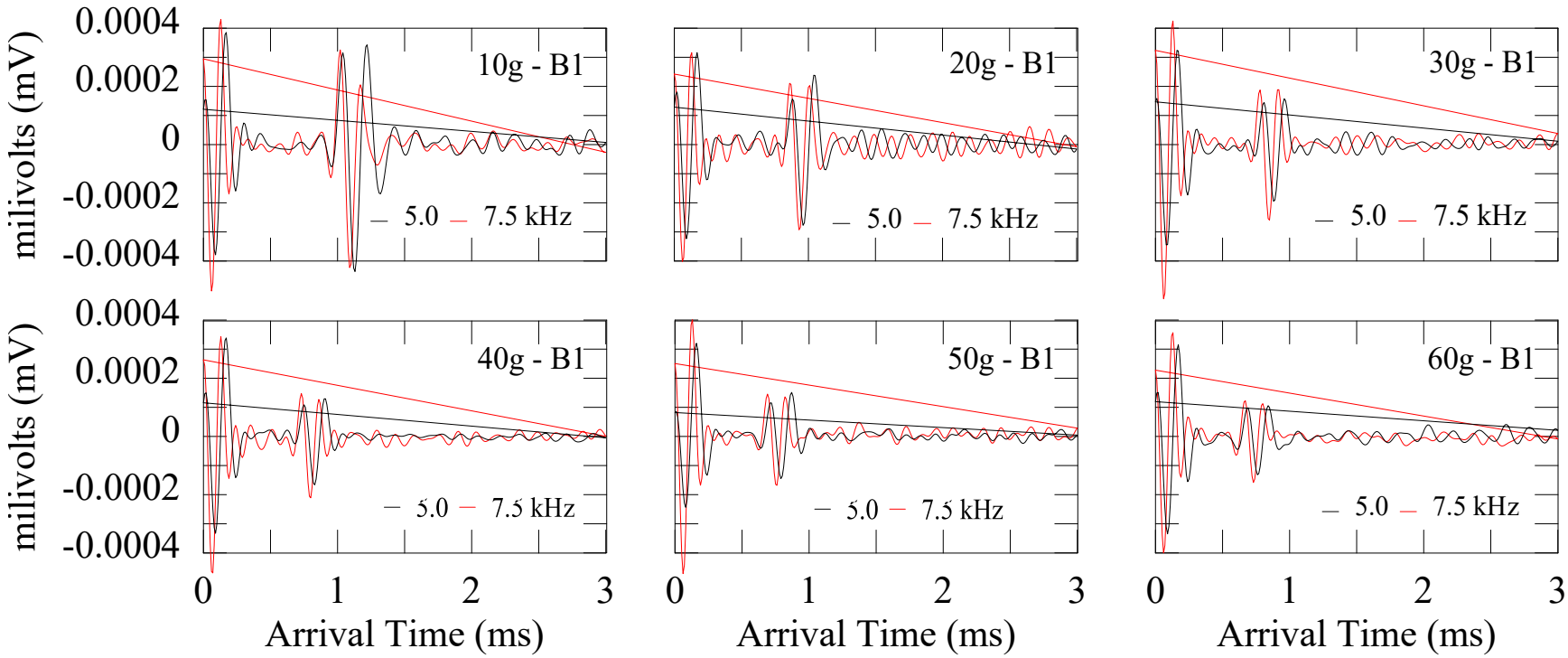

Figure C-476 Bender elements (B1) arrival times at various 'g' levels during spin-up for test Dr95NF.

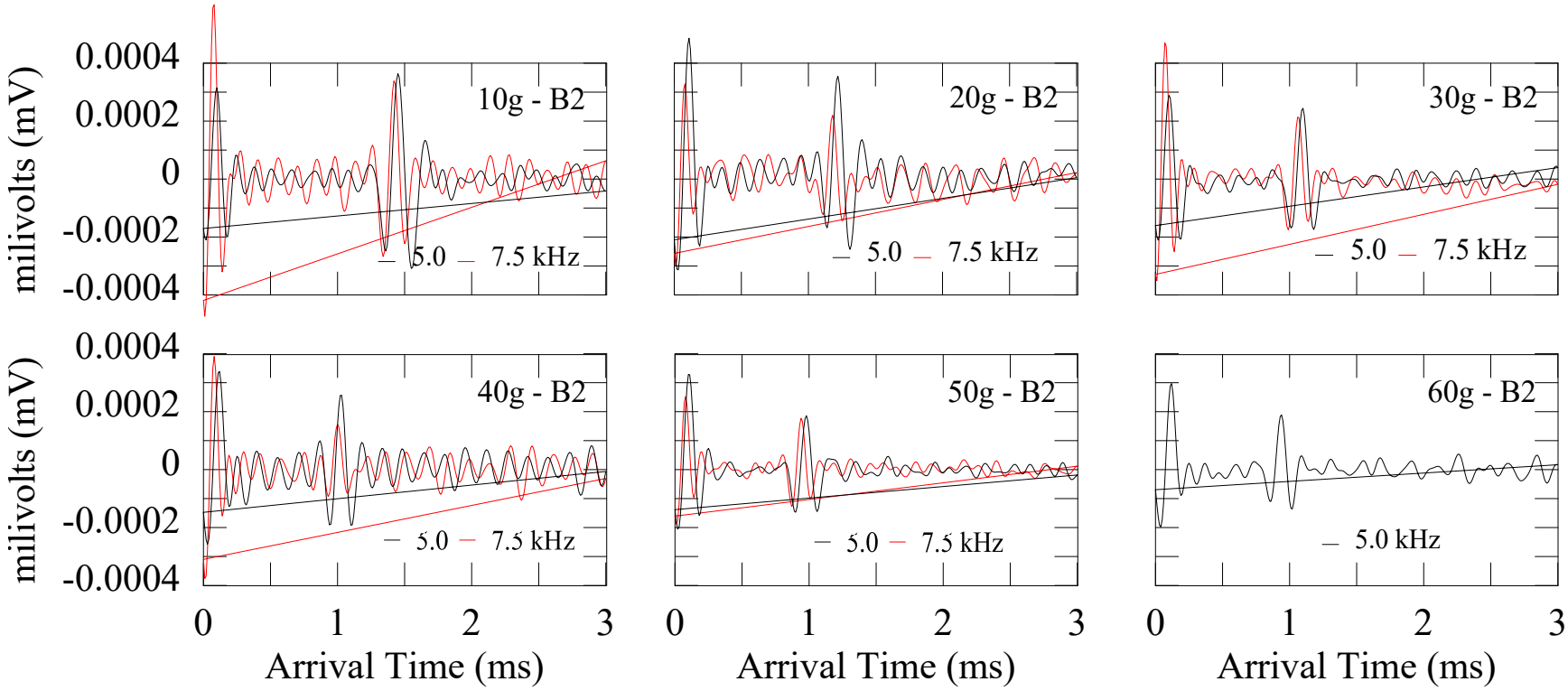

Figure C-477 Bender elements (B2) arrival times at various 'g' levels during spin-up for test Dr95NF.

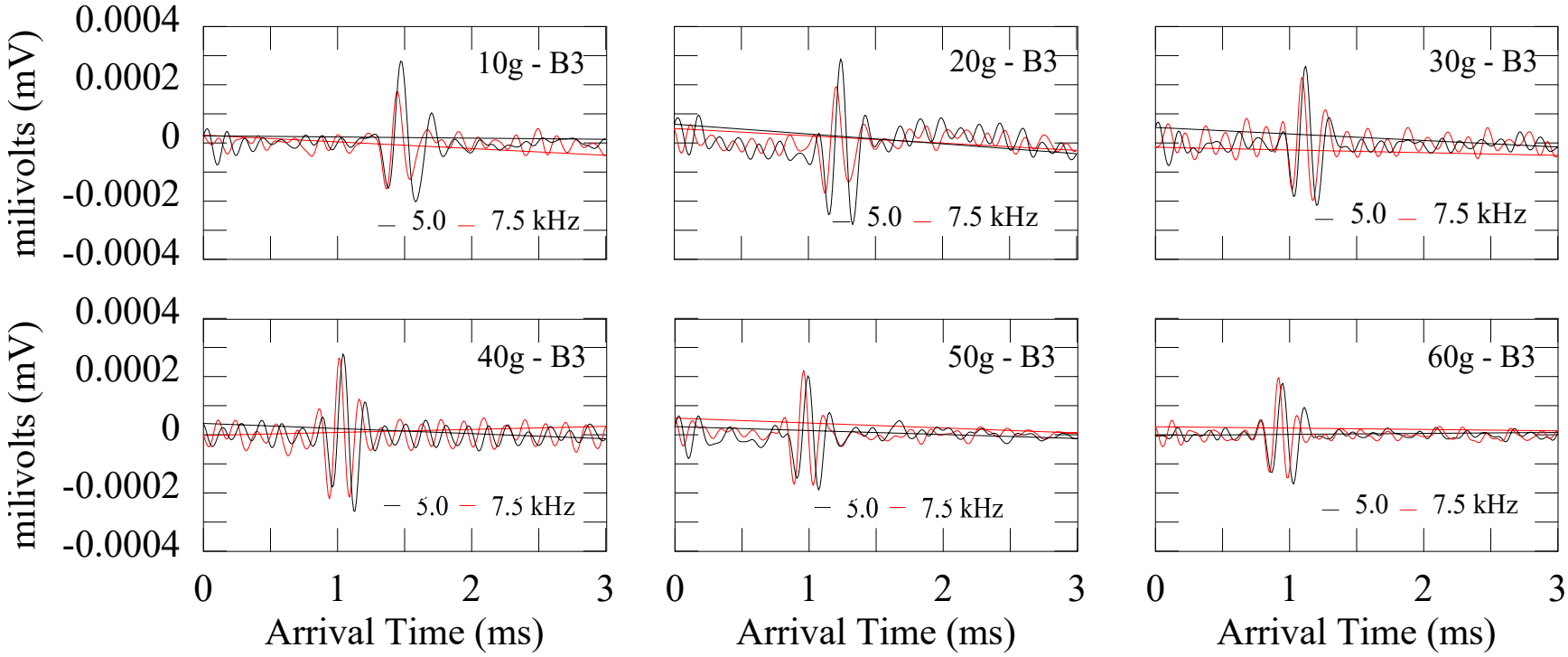

Figure C-478 Bender elements (B3) arrival times at various 'g' levels during spin-up for test Dr95NF.

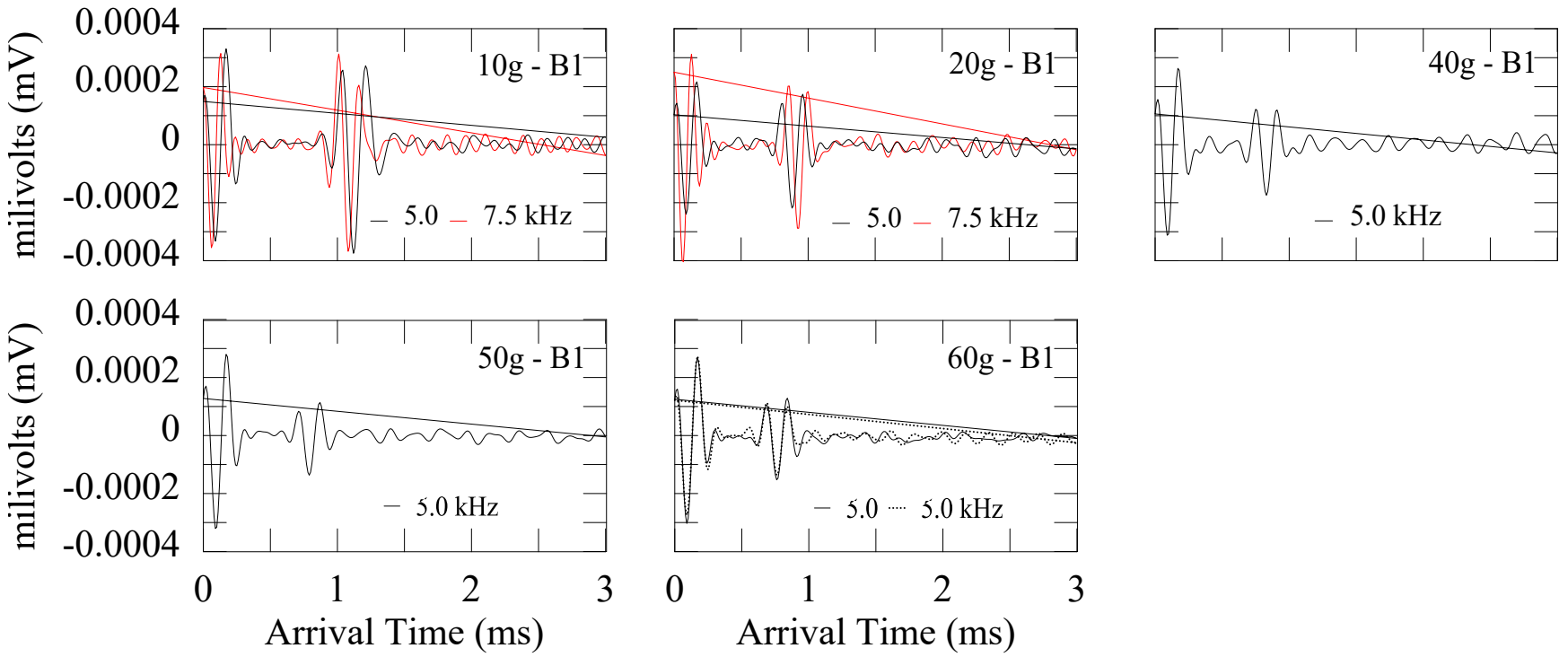

Figure C-479 Bender elements (B1) arrival times at various 'g' levels during spin-up 2 for test Dr95NF.

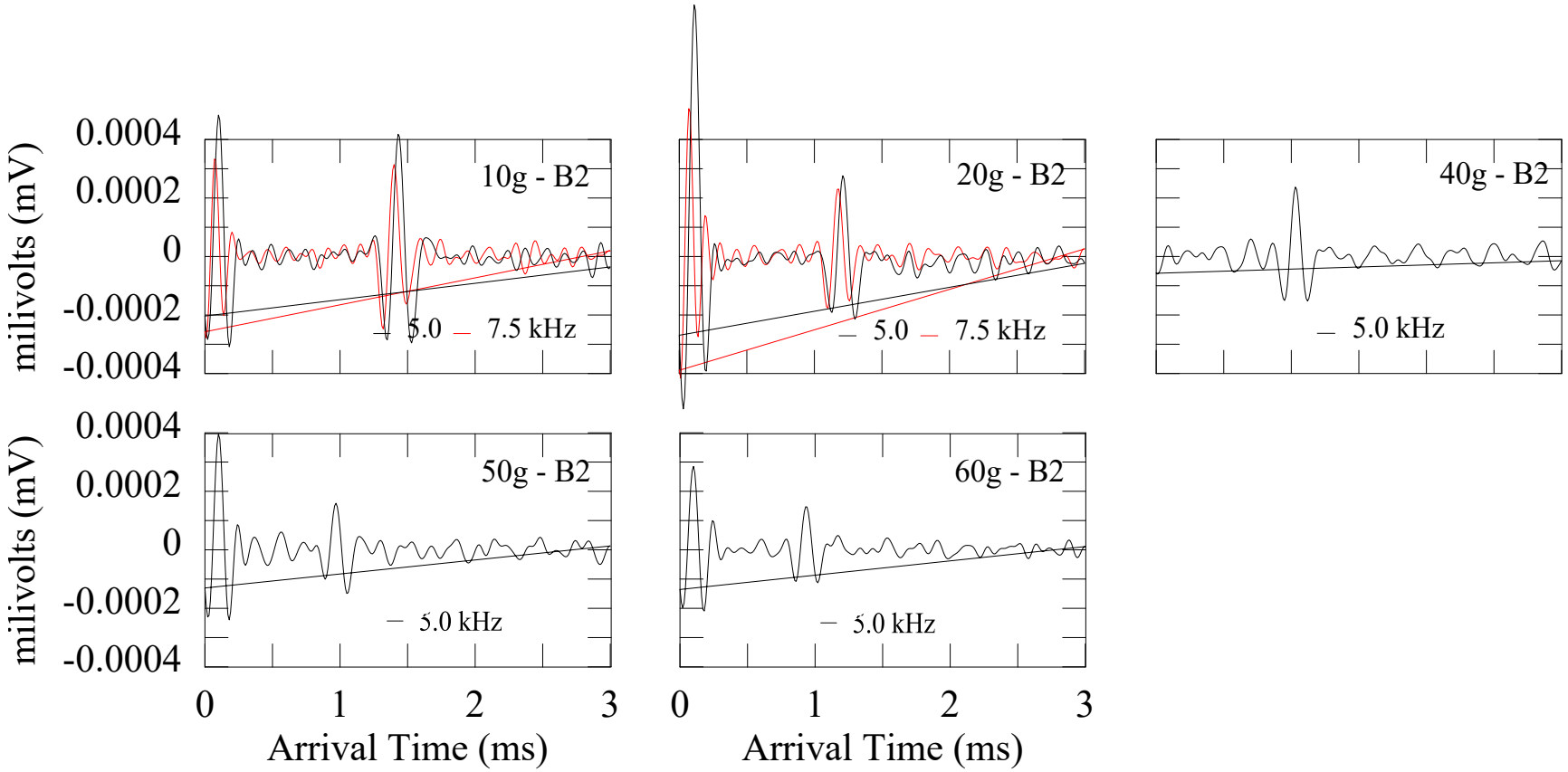

Figure C-480 Bender elements (B2) arrival times at various 'g' levels during spin-up 2 for test Dr95NF.

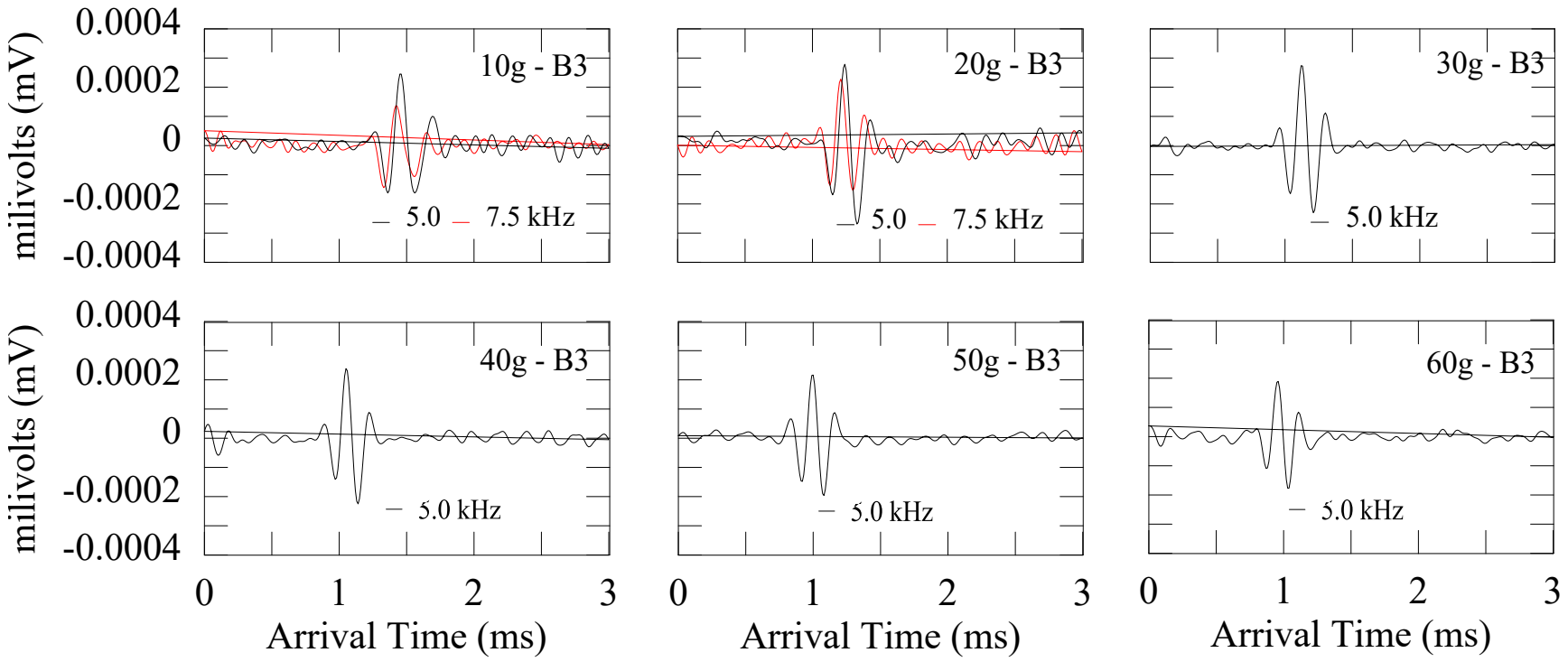

Figure C-481 Bender elements (B3) arrival times at various 'g' levels during spin-up 2 for test Dr95NF.

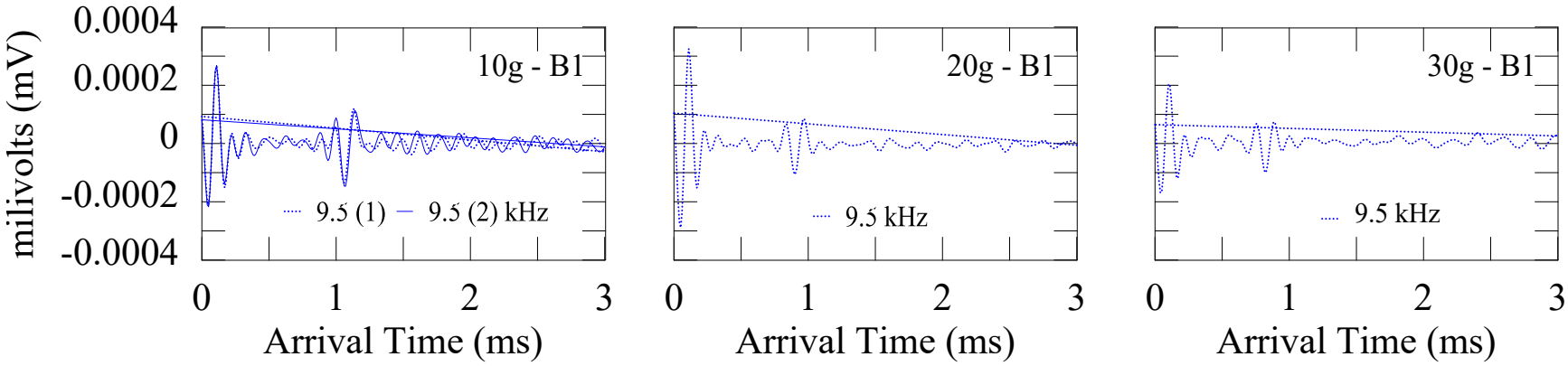

Figure C-482 Bender elements (B1) arrival times at various 'g' levels during spin-up 3 for test Dr95NF.

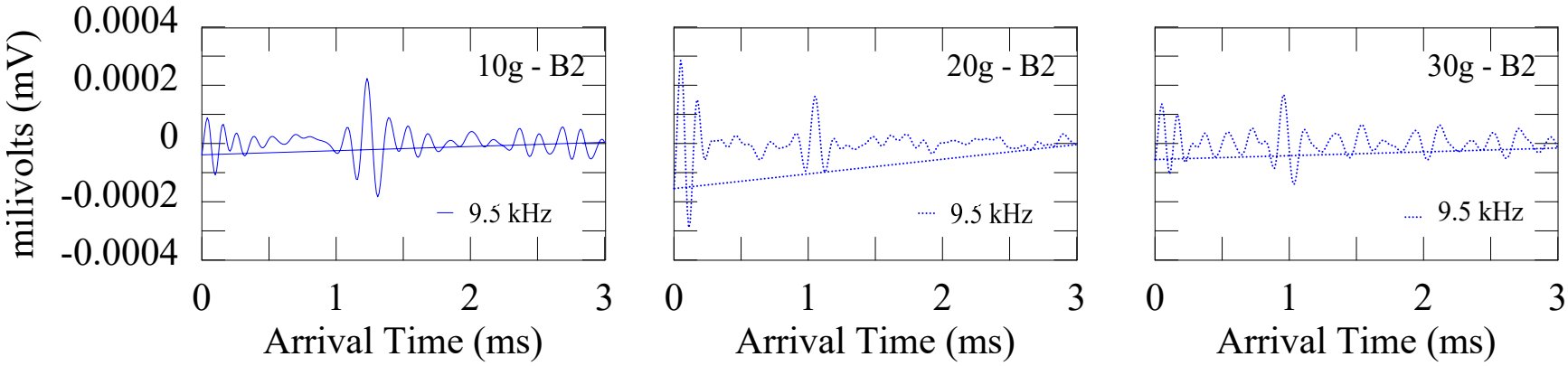

Figure C-483 Bender elements (B2) arrival times at various 'g' levels during spin-up 3 for test Dr95NF.

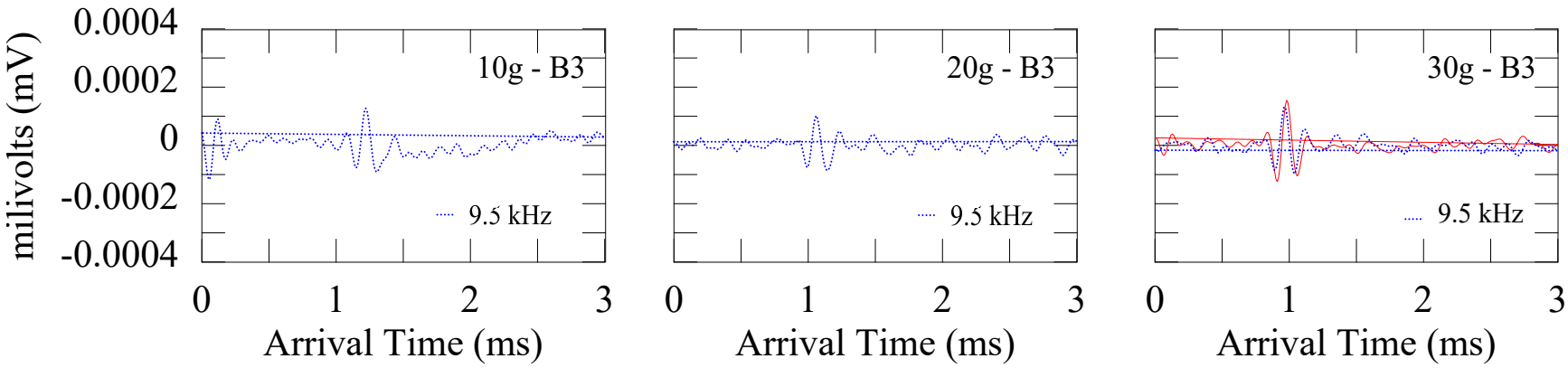

Figure C-484 Bender elements (B3) arrival times at various 'g' levels during spin-up 3 for test Dr95NF.

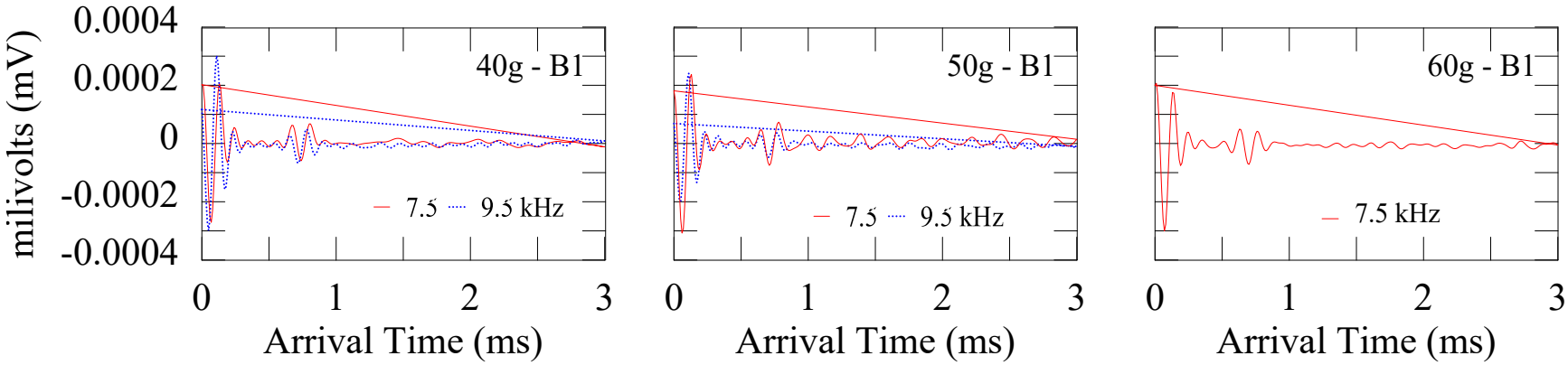

Figure C-485 Bender elements (B1) arrival times at various 'g' levels during spin-up 4 for test Dr95NF.

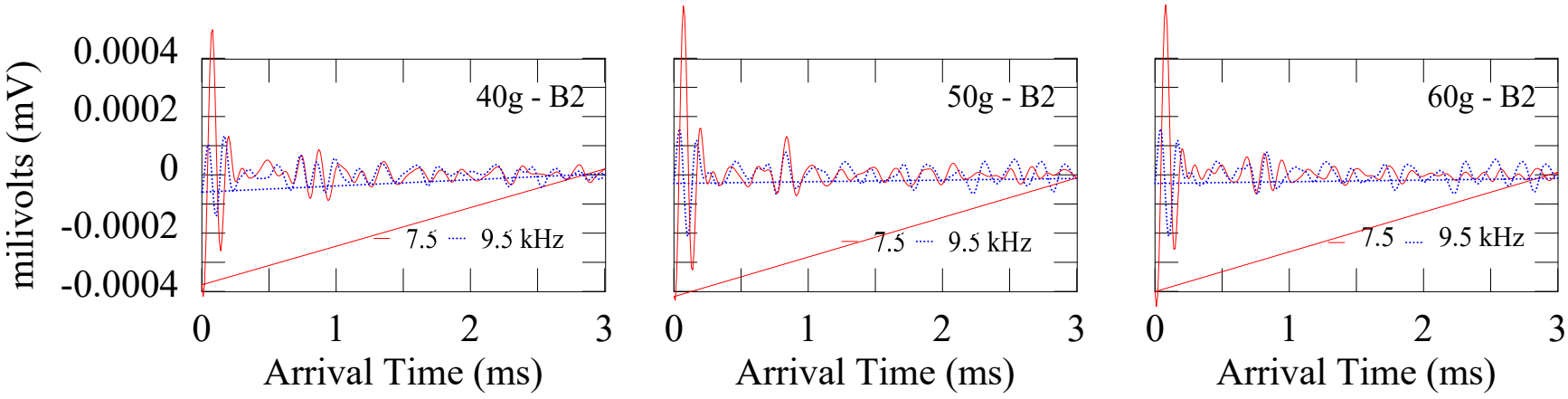

Figure C-486 Bender elements (B2) arrival times at various 'g' levels during spin-up 4 for test Dr95NF.

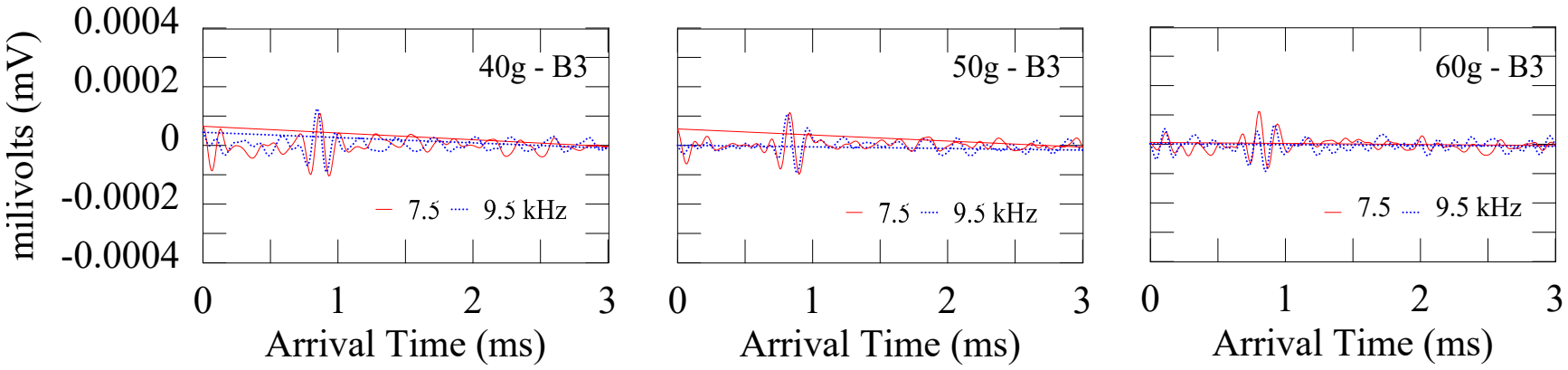

Figure C-487 Bender elements (B3) arrival times at various 'g' levels during spin-up 4 for test Dr95NF.

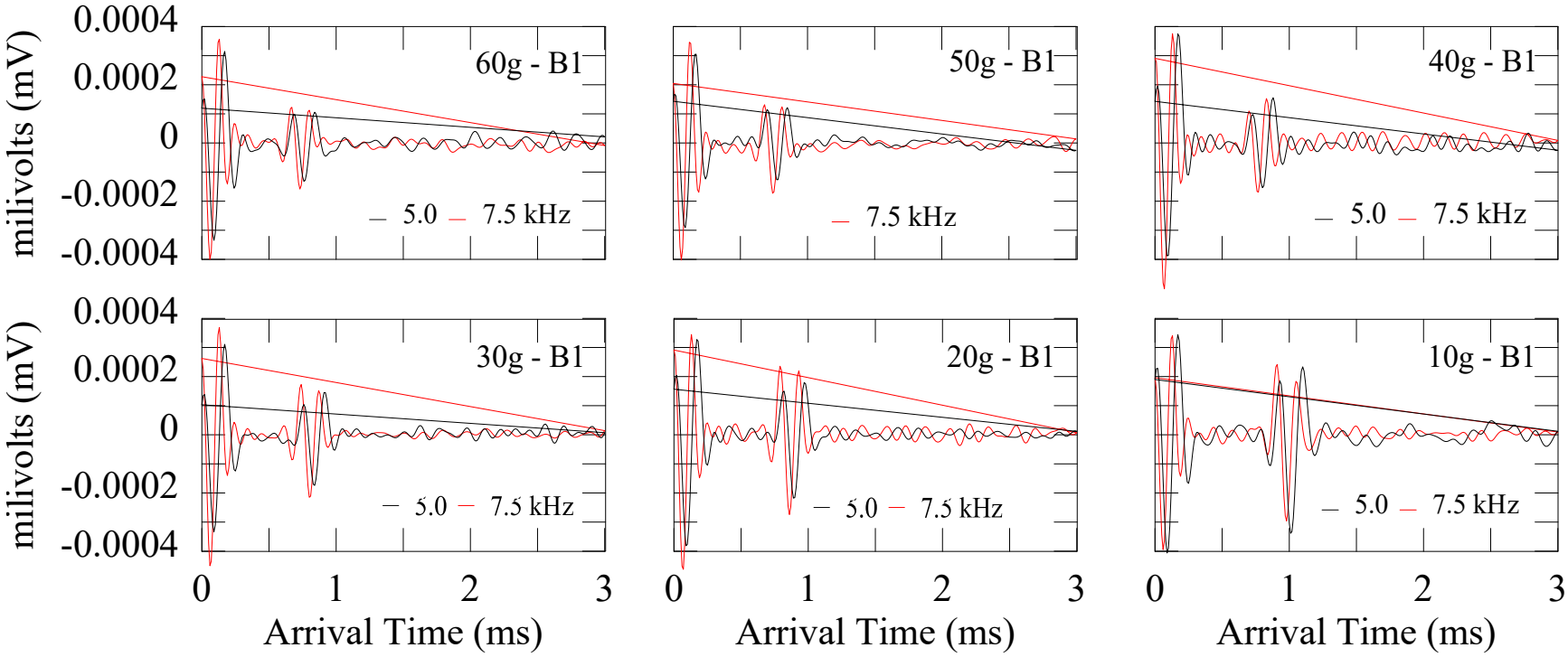

Figure C-488 Bender elements (B3) arrival times at various 'g' levels during spin-down 1 for test Dr95NF.

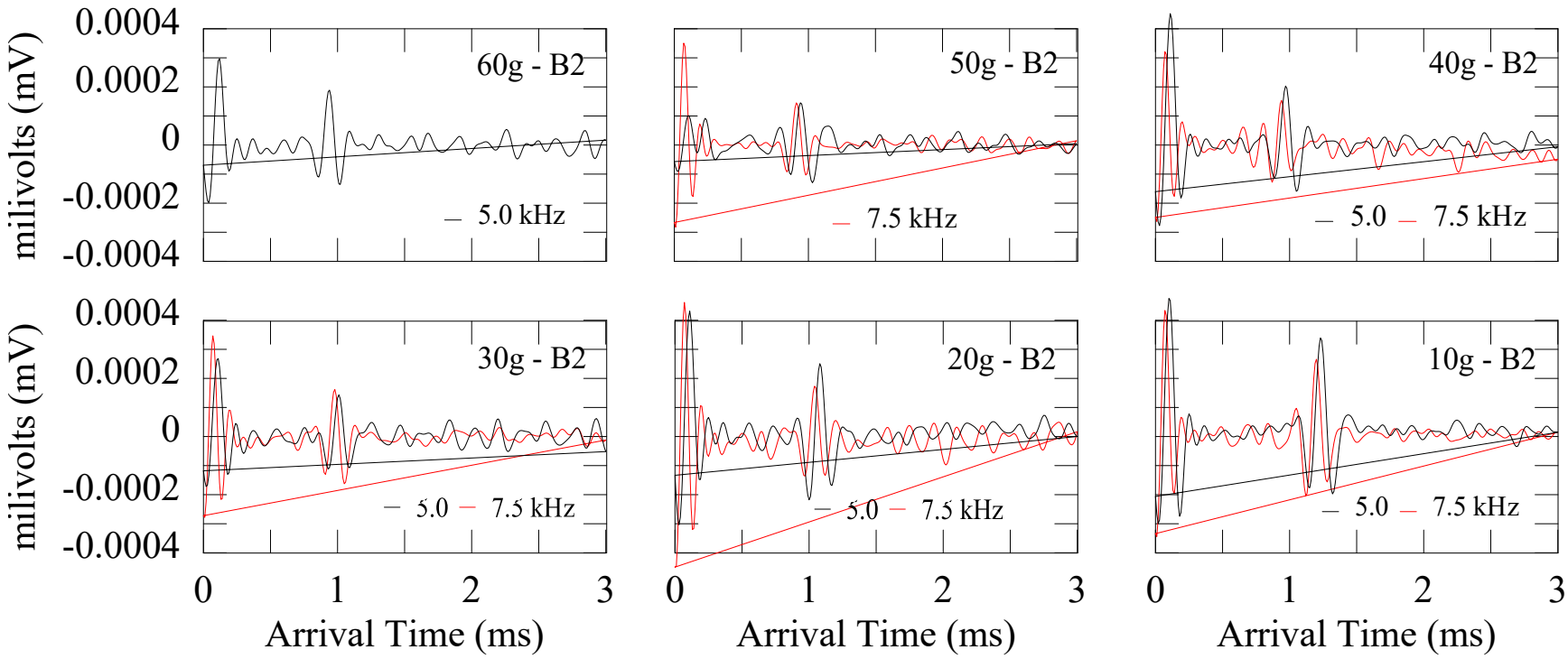

Figure C-489 Bender elements (B2) arrival times at various 'g' levels during spin-down 1 for test Dr95NF.

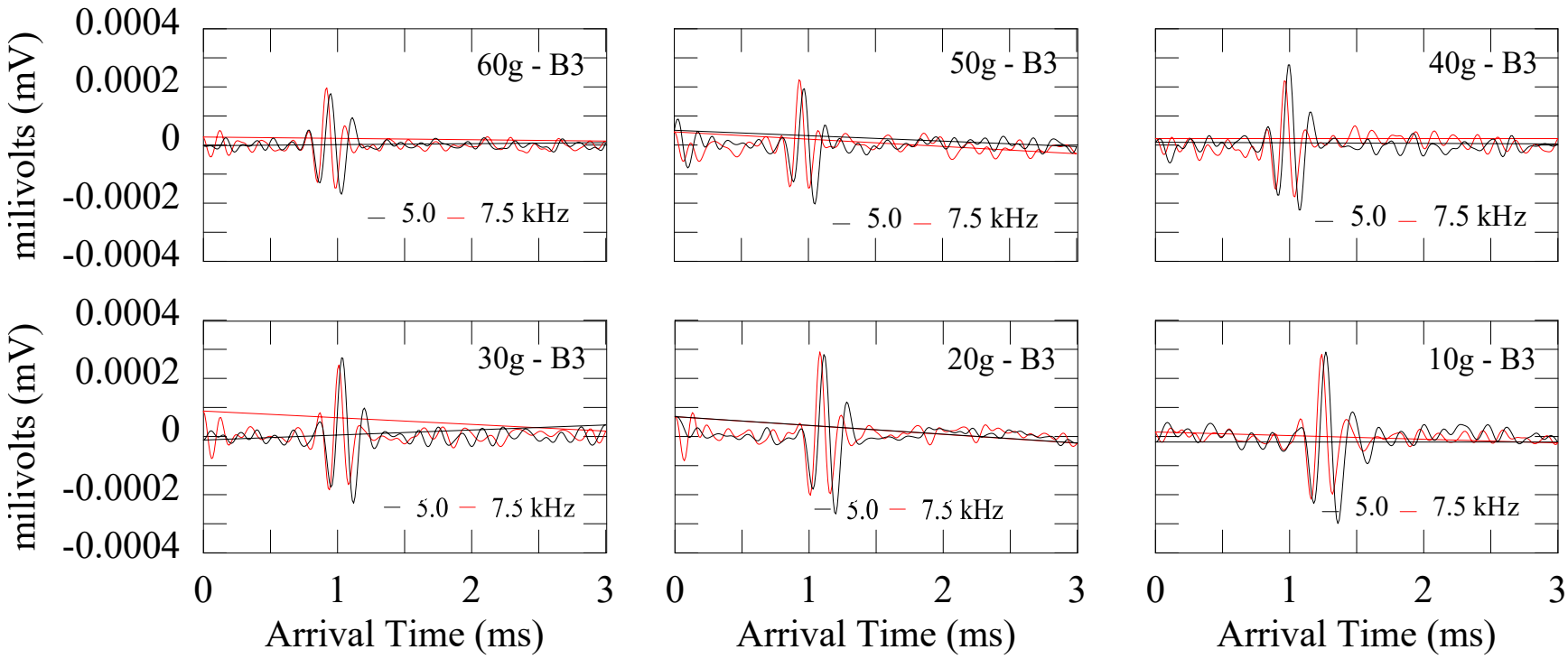

Figure C-490 Bender elements (B3) arrival times at various 'g' levels during spin-down 1 for test Dr95NF.

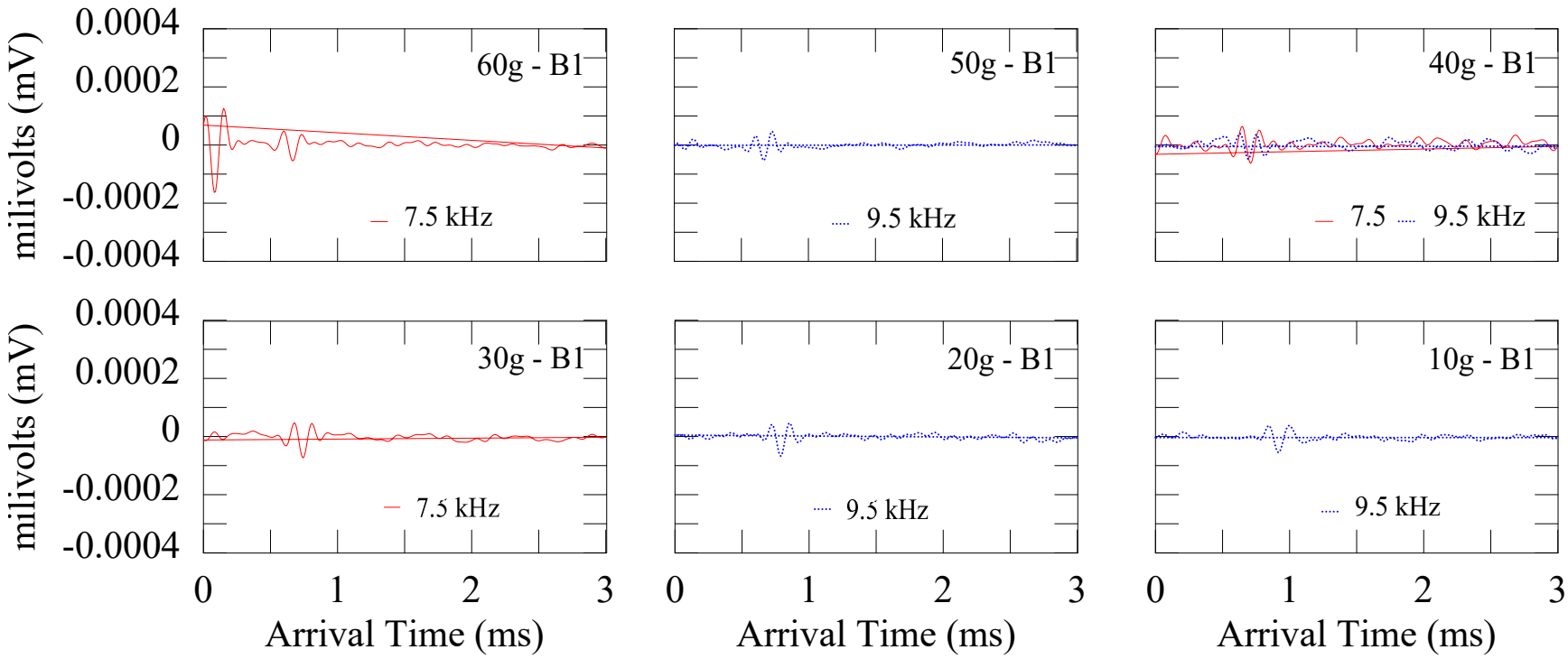

Figure C-491 Bender elements (B1) arrival times at various 'g' levels during spin-down 2 for test Dr95NF.

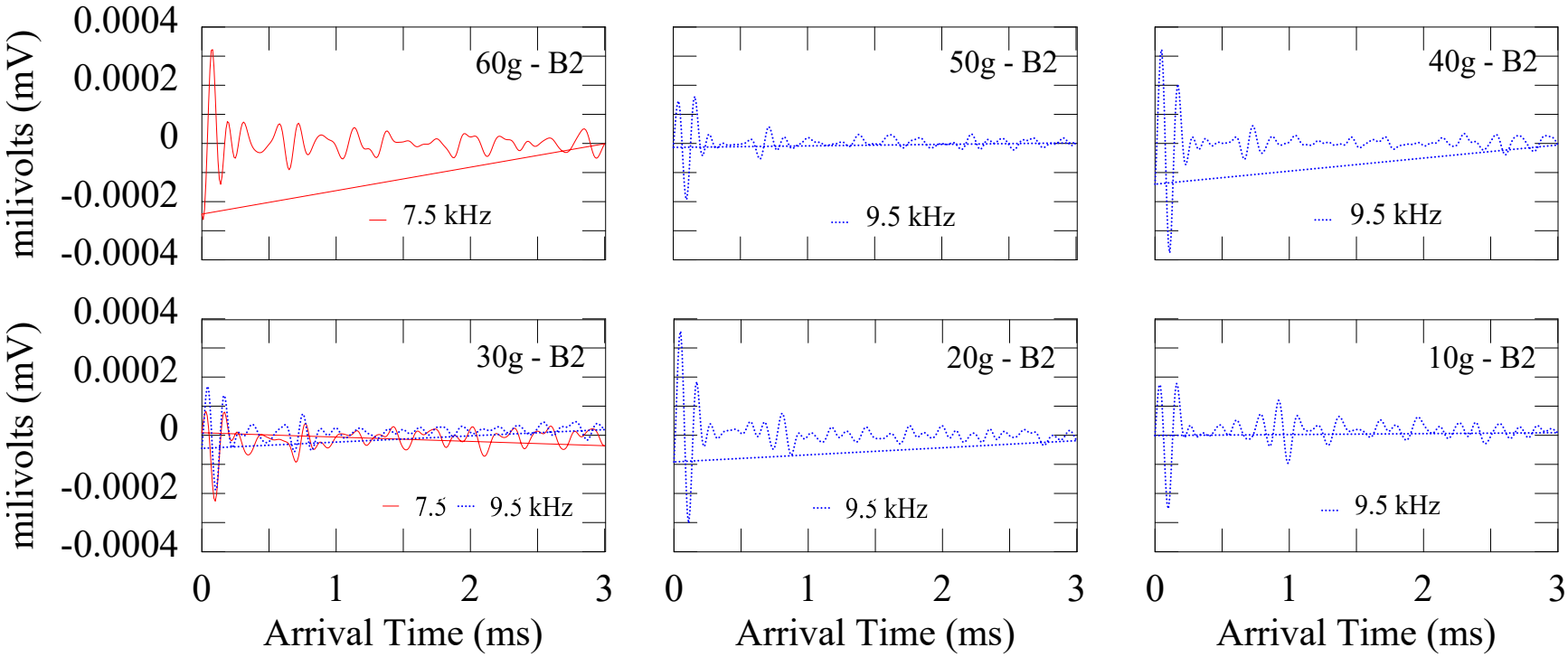

Figure C-492 Bender elements (B2) arrival times at various 'g' levels during spin-down 2 for test Dr95NF.

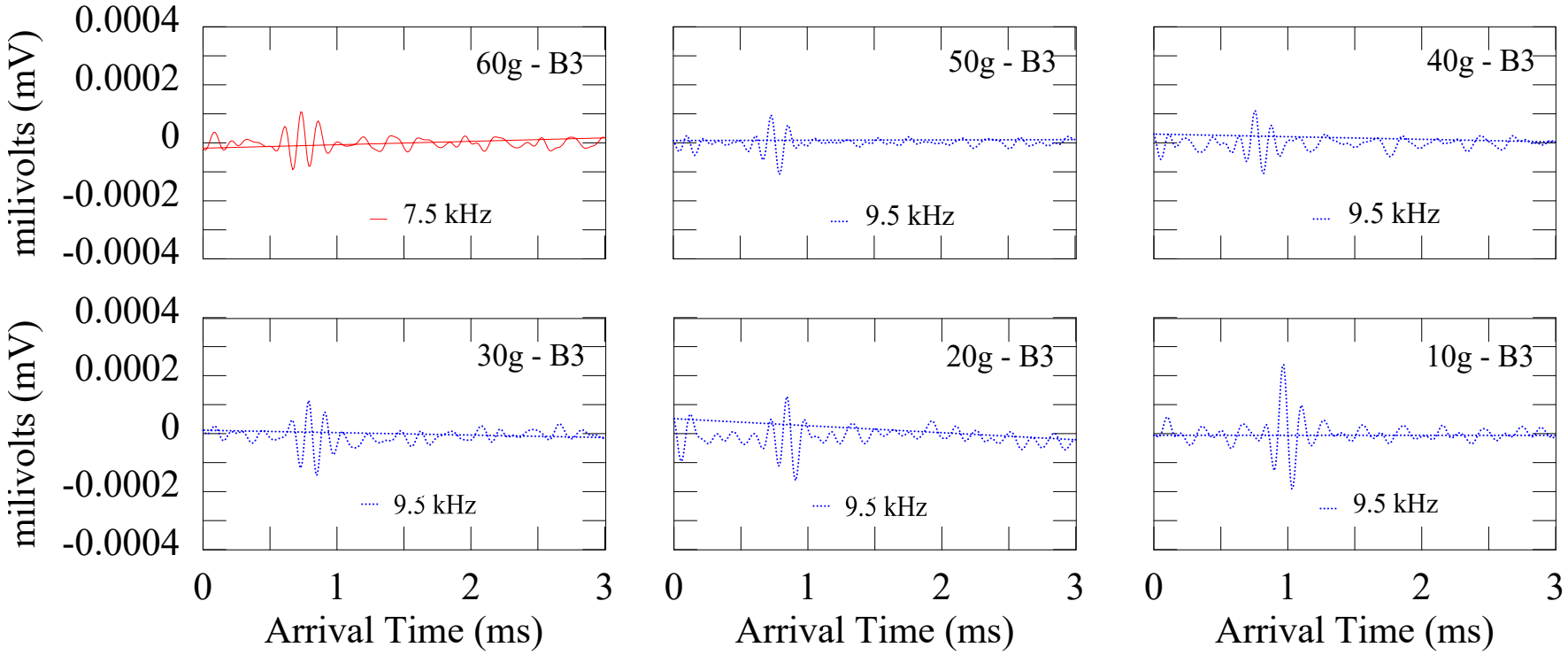

Figure C-493 Bender elements (B3) arrival times at various 'g' levels during spin-down 2 for test Dr95NF.

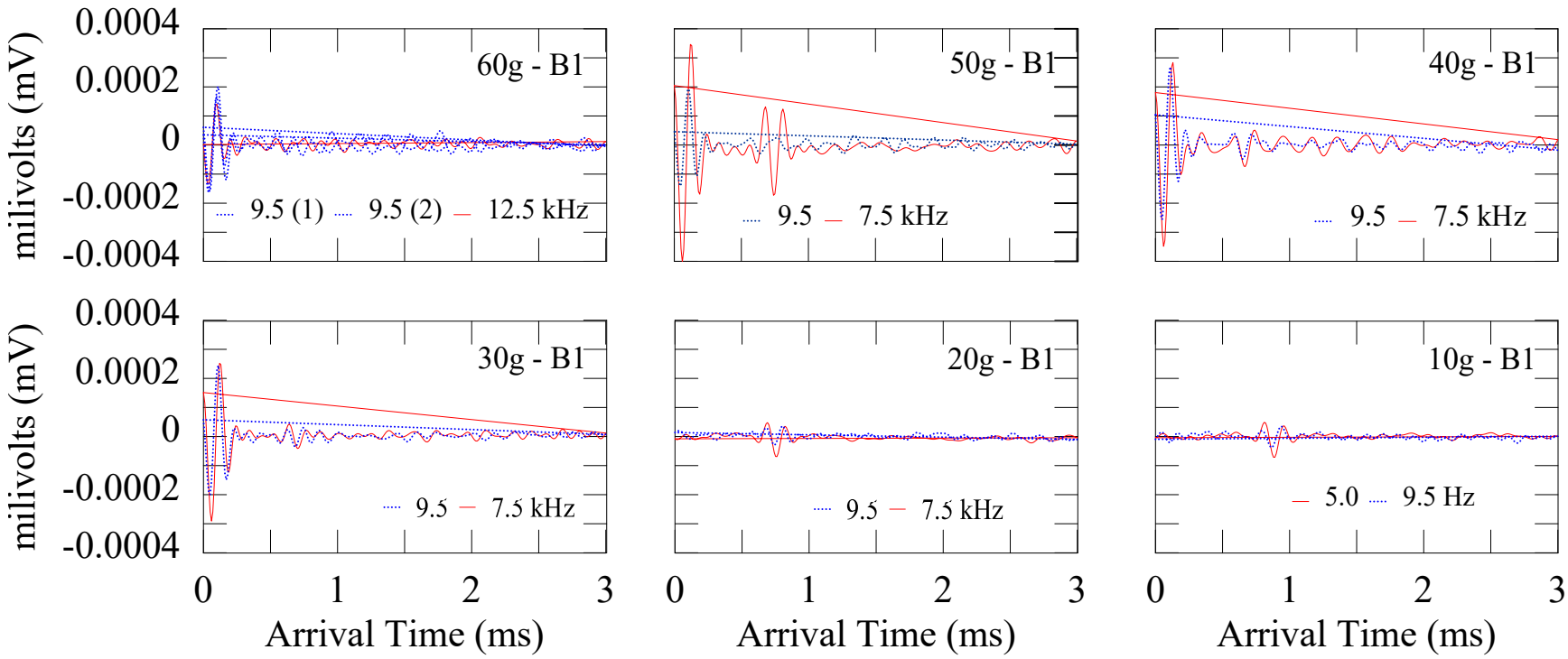

Figure C-494 Bender elements (B1) arrival times at various 'g' levels during spin-down final for test Dr95NF.

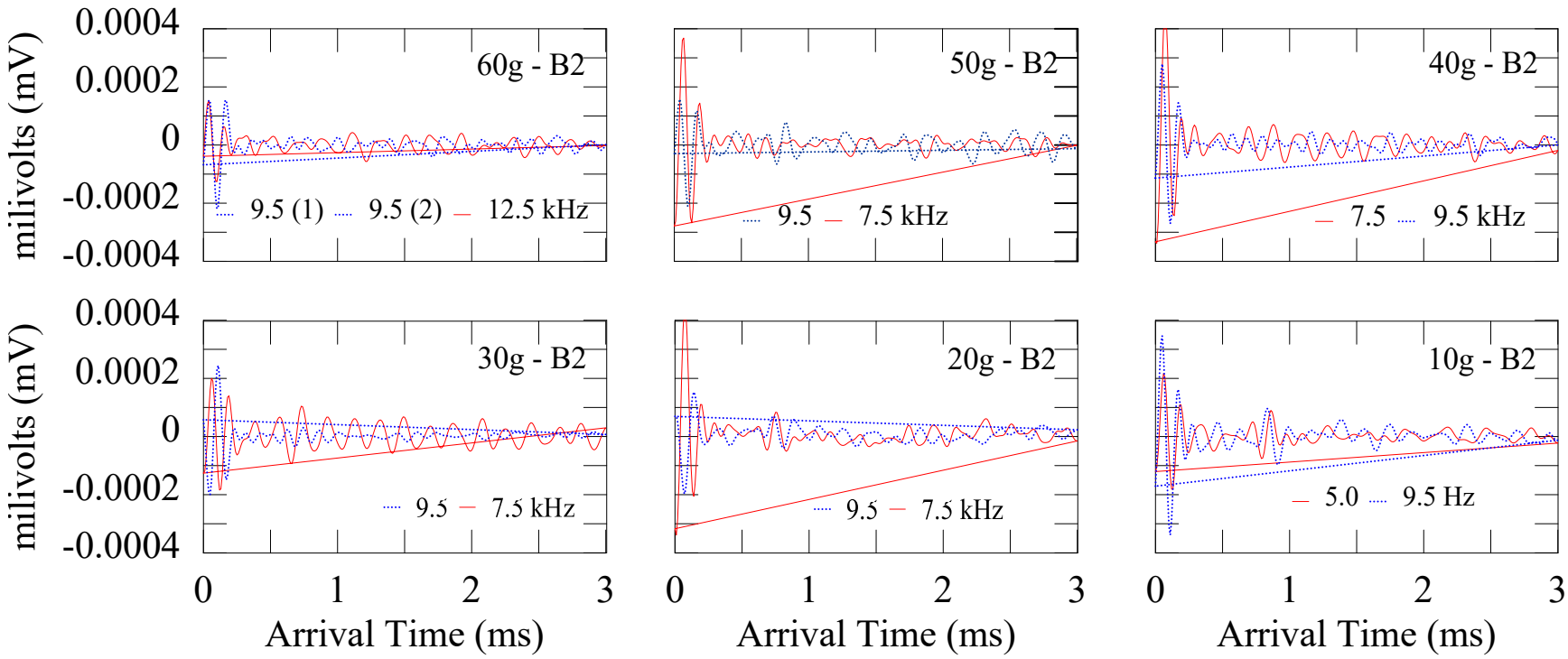

Figure C-495 Bender elements (B2) arrival times at various 'g' levels during spin-down final for test Dr95NF.

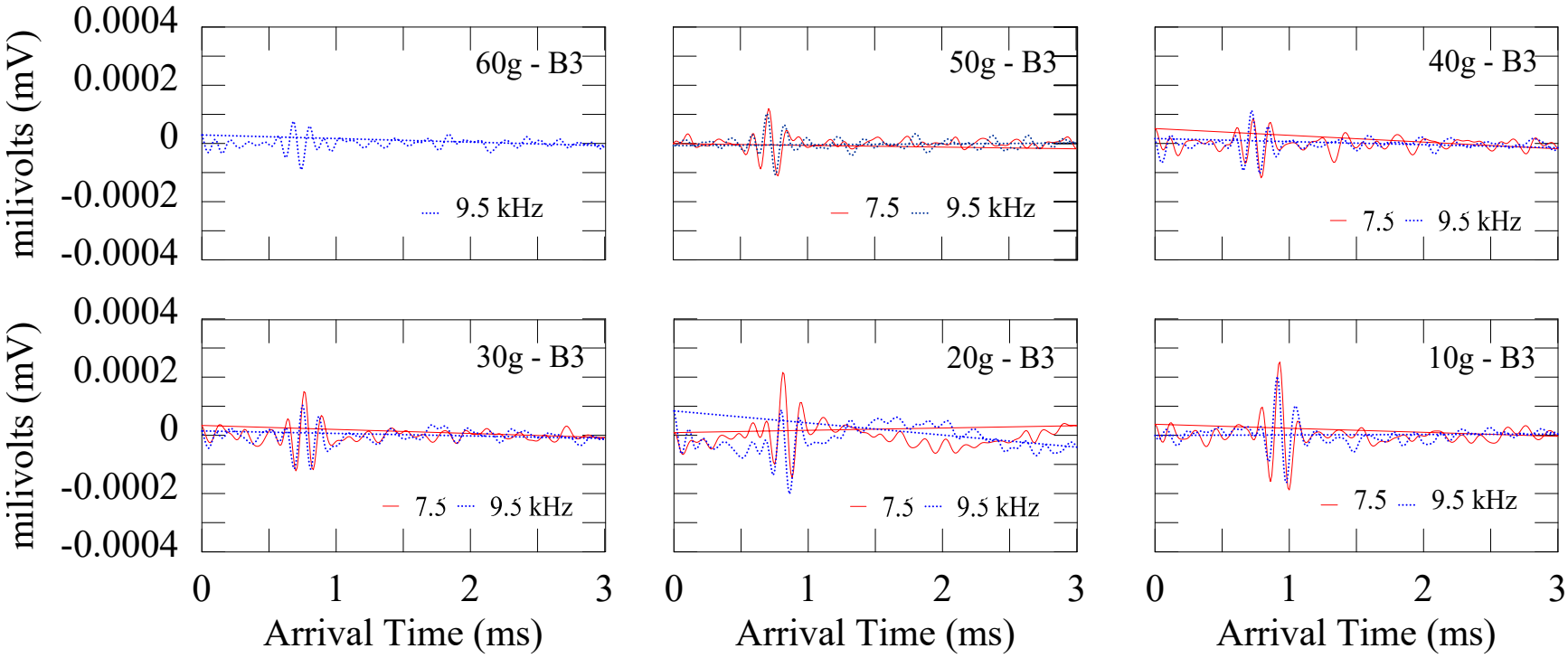

Figure C-496 Bender elements (B3) arrival times at various 'g' levels during spin-down final for test Dr95NF.

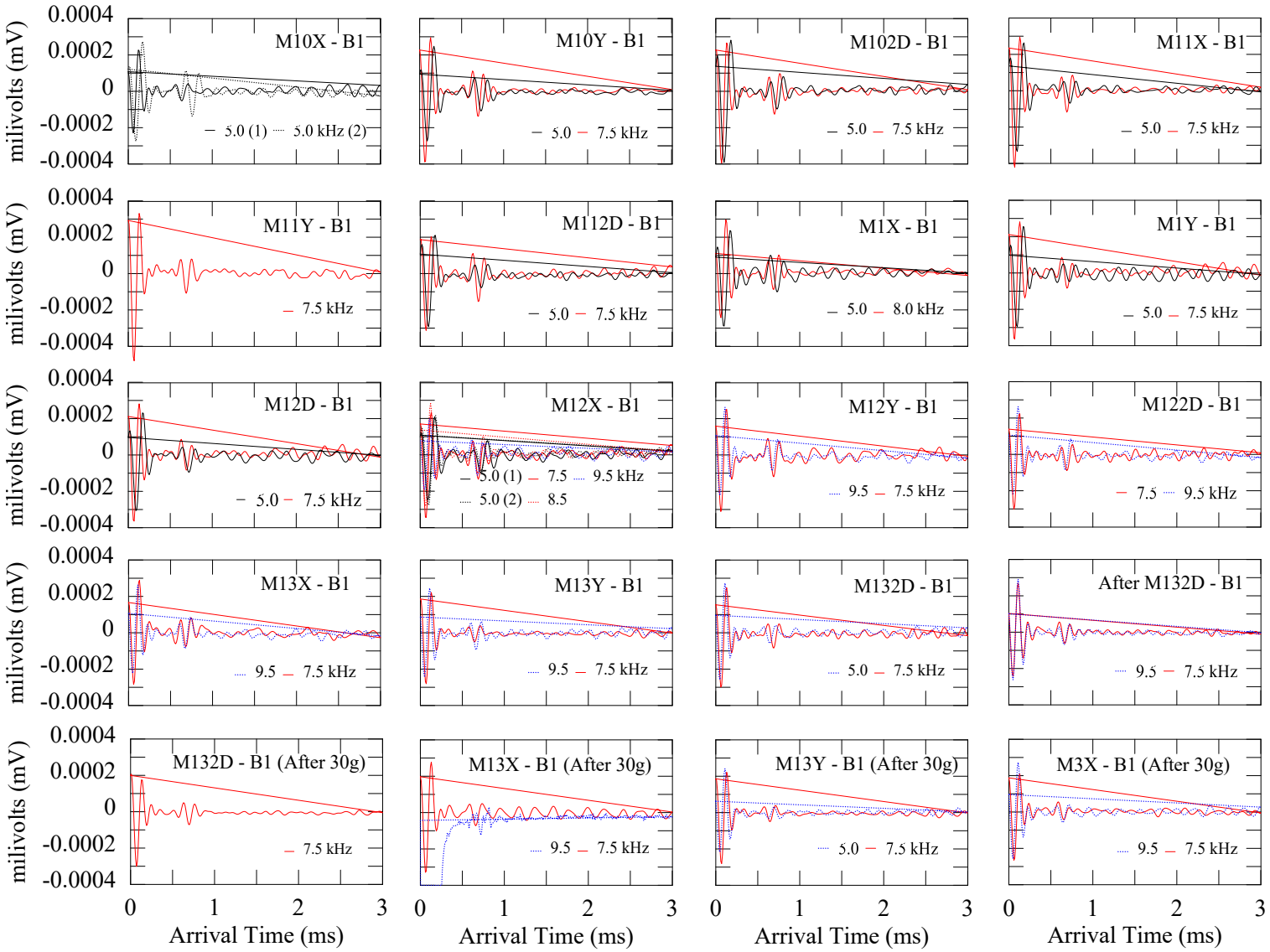

Figure C-497 Bender elements (B1) arrival times in between 60g motions Dr95NF.

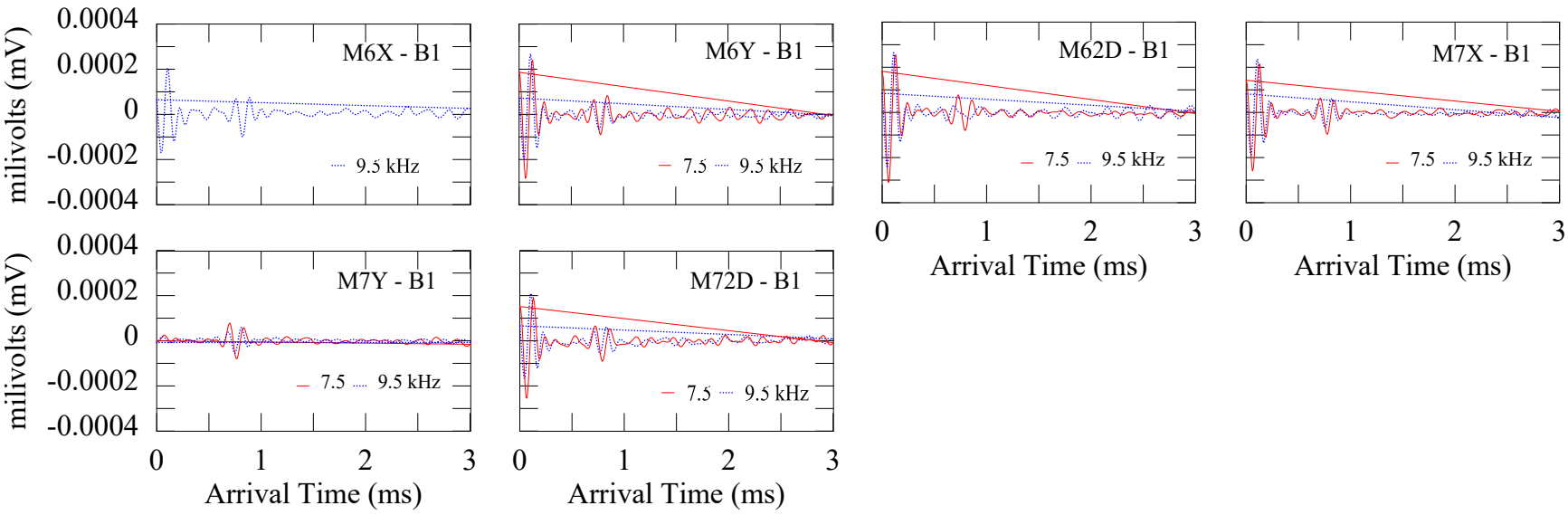

Figure C-498 Bender elements (B1) arrival times in between 30g motions Dr95NF.

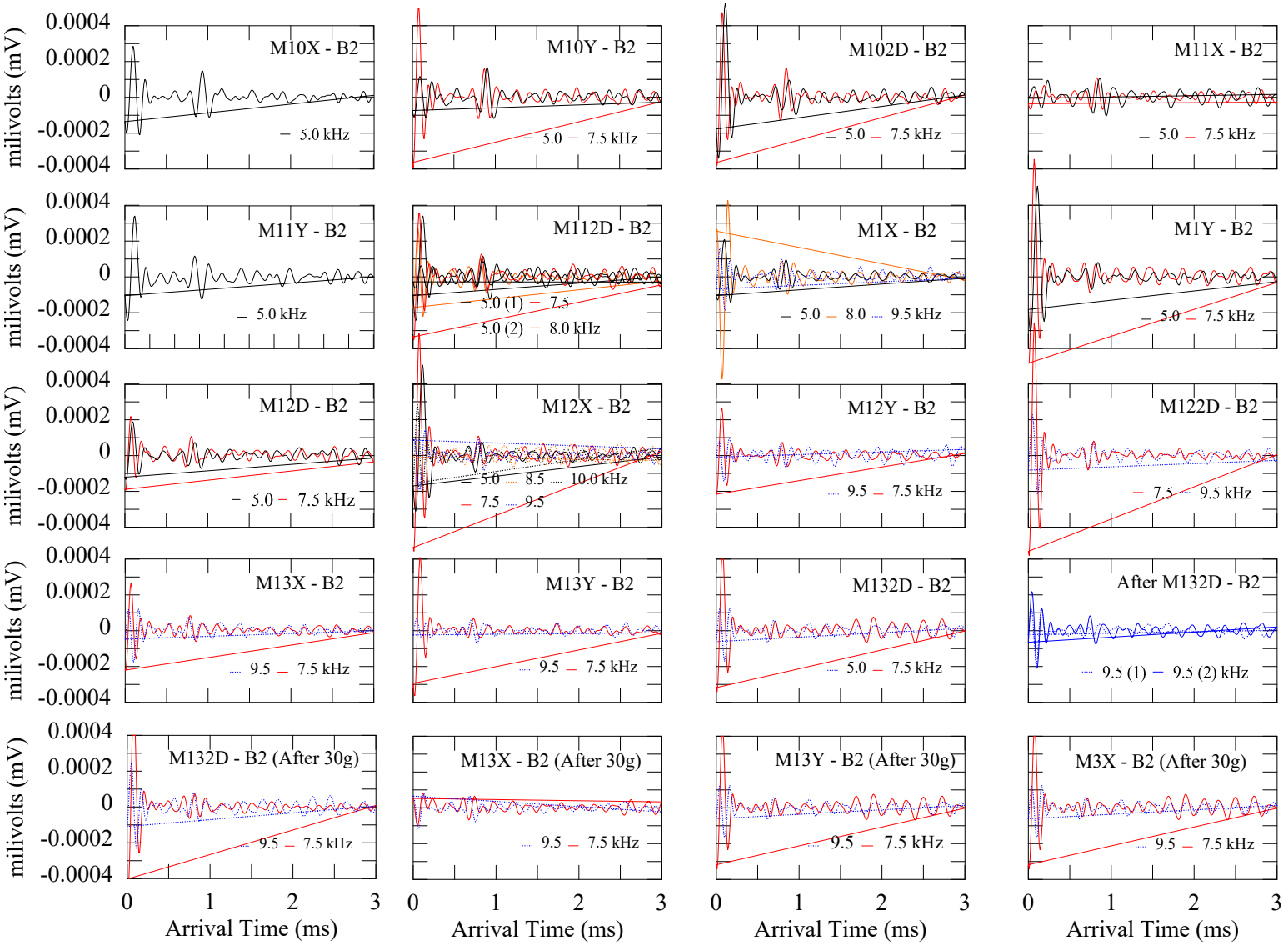

Figure C-499 Bender elements (B2) arrival times in between 60g motions Dr95NF.

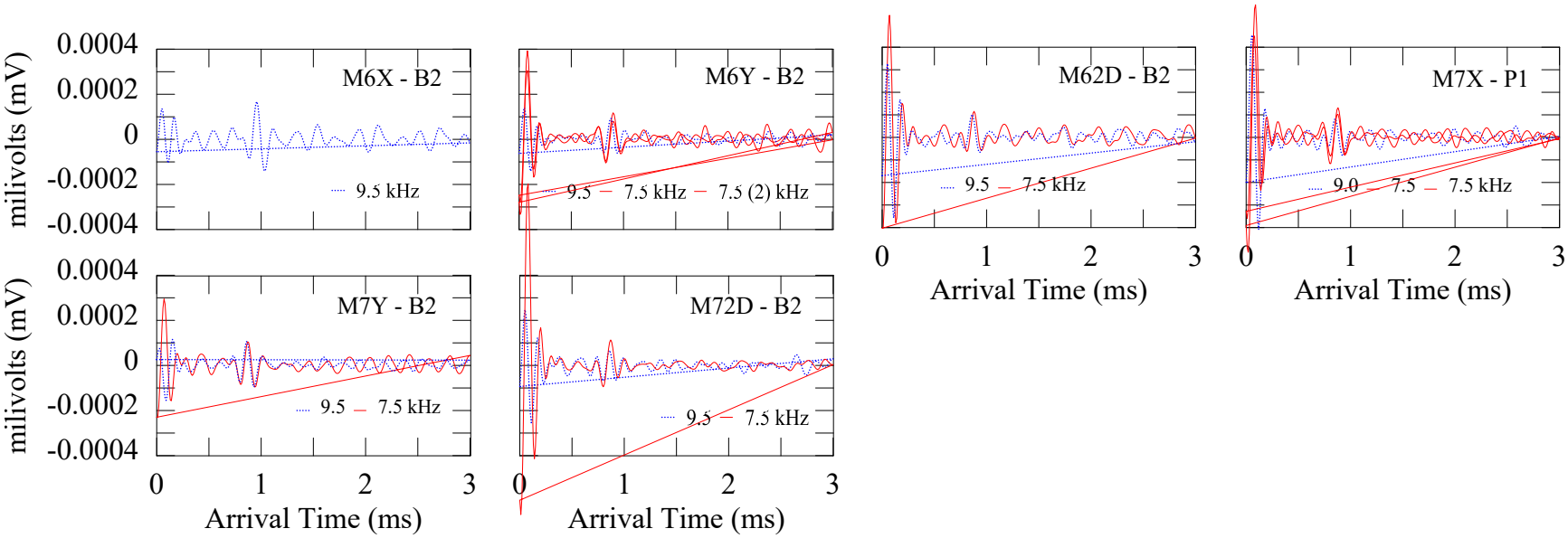

Figure C-500 Bender elements (B2) arrival times in between 30g motions Dr95NF.

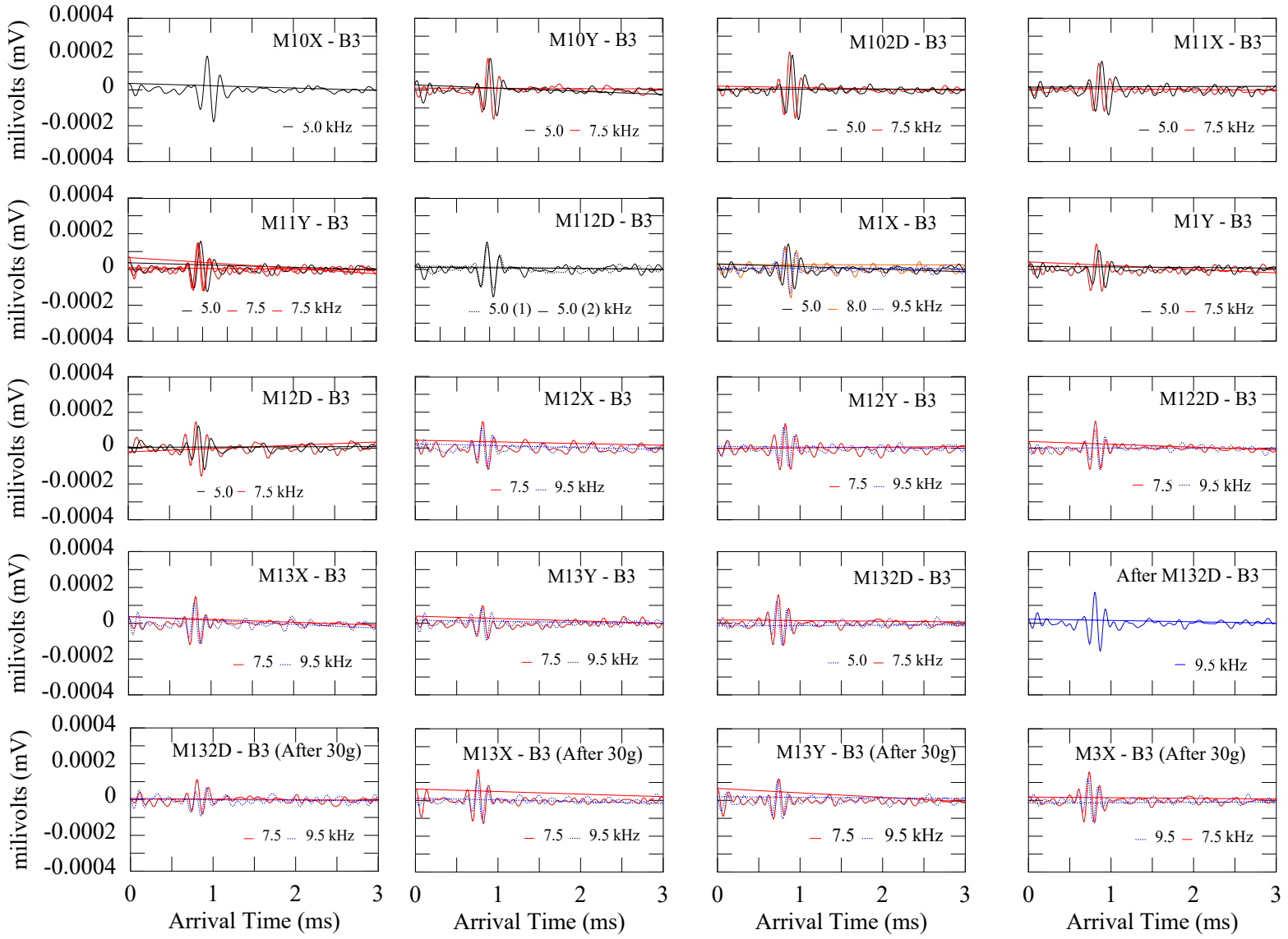

Figure C-501 Bender elements (B3) arrival times in between 60g motions Dr95NF.

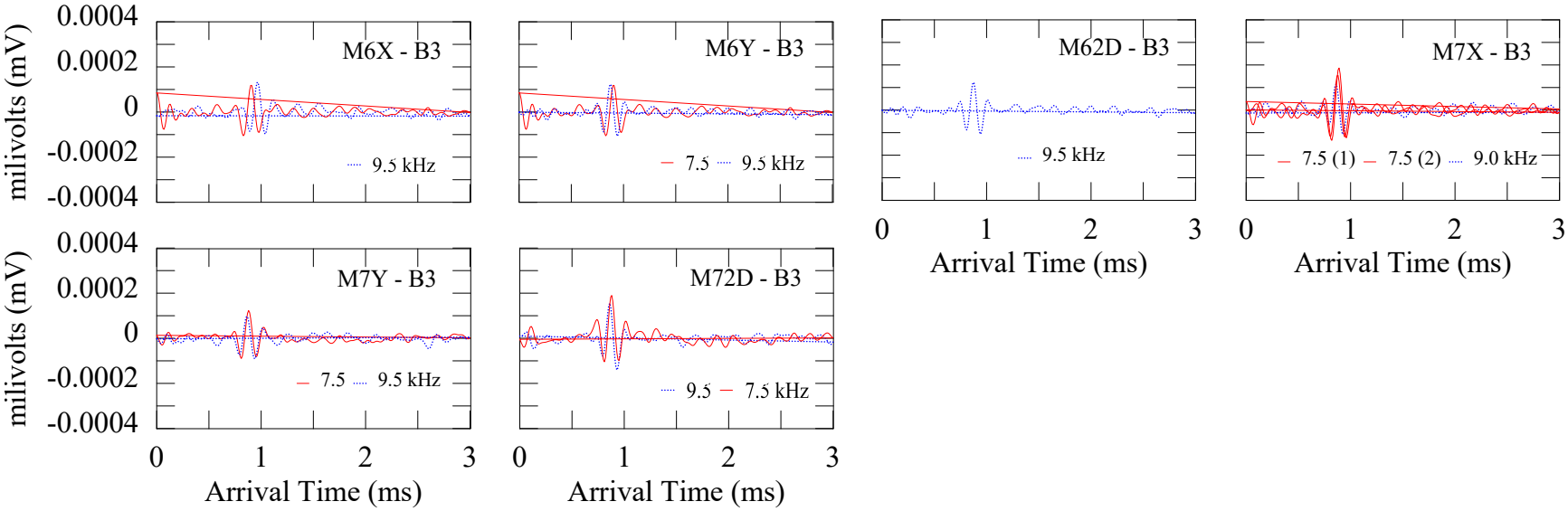

Figure C-502 Bender elements (B3) arrival times in between 30g motions Dr95NF.